

- (I) Zinc complexes as synthetic analogues for carbonic anhydrase and
as catalysts for H₂ production and CO₂ functionalization**
- (II) Application of lithium silylamides in the synthesis of transition metal
isocyanide compounds from their carbonyl derivatives**
- (III) Structural and spectroscopic studies of thimerosal and its derivatives**

Wesley Sattler

Submitted in partial fulfillment of the
requirements for the degree
of Doctor of Philosophy
in the Graduate School of Arts and Sciences

Columbia University

2012

© 2012

Wesley Sattler
All rights reserved

ABSTRACT

(I) Zinc complexes as synthetic analogues for carbonic anhydrase and as catalysts for H₂ production and CO₂ functionalization

(II) Application of lithium silylamides in the synthesis of transition metal isocyanide compounds from their carbonyl derivatives

(III) Structural and spectroscopic studies of thimerosal and its derivatives

Wesley Sattler

The multidentate alkyl ligand, [Tptm] ([Tptm] = *tris*(2-pyridylthio)methyl), provides an organometallic counterpart to the more common tripodal ligands, [Tp] ([Tp] = *tris*(pyrazolyl)hydroborato) and [Tm] ([Tm] = *tris*(2-mercaptoimidazolyl)hydroborato). A wide range of [Tptm] zinc complexes have been synthesized, enabling a diverse range of both stoichiometric and catalytic chemical transformations including the production of H₂ and the functionalization of CO₂.

The [Tptm] ligand has been used to isolate the first mononuclear alkyl zinc hydride complex, [κ³-Tptm]ZnH. The hydride complex may be easily synthesized on a multigram scale *via* reaction of the trimethylsiloxide complex, [κ⁴-Tptm]ZnOSiMe₃, with PhSiH₃. The hydride complex, [κ³-Tptm]ZnH, provides access to a variety of other [Tptm]ZnX derivatives. For example, [κ³-Tptm]ZnH reacts with (i) R₃SiOH (R = Me, Ph) to give [κ⁴-Tptm]ZnOSiR₃, (ii) Me₃SiX (X = Cl, Br, I) to give [κ⁴-Tptm]ZnX and (iii) CO₂ to give the formate complex, [κ⁴-Tptm]ZnO₂CH. [κ³-Tptm]ZnH is hydrolyzed to give the dimeric hydroxide complex, {[κ³-Tptm]Zn(μ-OH)}₂, which when treated with

CO₂, results in the bicarbonate complex, [κ⁴-Tptm]ZnOCO₂H. The halide complexes, [κ⁴-Tptm]ZnX (X = Cl, Br, I), can be used to synthesize the fluoride complex, [κ⁴-Tptm]ZnF, *via* treatment with tetrabutylammonium fluoride (TBAF).

The *bis*(trimethylsilyl)amide complex, [κ³-Tptm]ZnN(SiMe₃)₂, which has been prepared directly *via* the reaction of [Tptm]H with [ZnN(SiMe₃)₂]₂, reacts with CO₂ to give the isocyanate complex, [κ⁴-Tptm]ZnNCO. The formation of the isocyanate complex results from a multistep sequence in which the initial step is insertion of CO₂ into the Zn-N(SiMe₃)₂ bond to give the carbamate derivative, [Tptm]Zn[O₂CN(SiMe₃)₂], followed by rearrangement to [κ⁴-Tptm]ZnOSiMe₃ with the expulsion of Me₃SiNCO, which further reacts to give [κ⁴-Tptm]ZnNCO. An important discovery is that the rate of the final metathesis step, to give [κ⁴-Tptm]ZnNCO, is enhanced by CO₂. Specifically, insertion of CO₂ into the Zn-O bond of [κ⁴-Tptm]ZnOSiMe₃ gives the carbonate complex [κ⁴-Tptm]Zn[O₂COSiMe₃], which is more susceptible towards metathesis than is the siloxide derivative.

The [Tptm] ligand has also been effective for other metals, such as magnesium and nickel. While [Tptm] complexes of magnesium exhibit chemistry that is similar to that of zinc, the linear nickel nitrosyl complex, [κ³-Tptm]NiNO, shows diverse reactivity involving its nitrosyl ligand. For example, oxygenation of [κ³-Tptm]NiNO is reversible. The reaction of [κ³-Tptm]NiNO with air gives the paramagnetic nitrite complex, [κ⁴-Tptm]Ni[κ²-O₂N], the latter which may be deoxygenated *via* reaction with trimethylphosphine.

Additionally, the tetradentate alkyl ligand, *tris*(1-methyl-imidazol-2-ylthio)methyl, [Titm^{Me}], has been studied as a comparison to the [Tptm] system. The *bis*(trimethylsilyl)amide complex, [κ³-Titm^{Me}]ZnN(SiMe₃)₂ has been synthesized, and it also reacts with CO₂ to give the isocyanate complex, [κ⁴-Titm^{Me}]ZnNCO.

The hydroxide complexes, [Tp^{Bu^t,Me}]ZnOH ([Tp^{Bu^t,Me}] = *tris*(3-*t*-butyl-5-methylpyrazolyl)hydroborato), and {[κ³-Tptm]Zn(μ-OH)}₂, were used to model

transformations with CO₂ that are of relevance to the mechanism of action of carbonic anhydrase. Low temperature ¹H and ¹³C NMR spectroscopic studies on solutions of the hydroxide complex, [Tp^{Bu^t,Me}]ZnOH, in the presence of 1 atmosphere of CO₂ have allowed for the identification of the bicarbonate complex, [Tp^{Bu^t,Me}]ZnOCO₂H. In the presence of less than 1 atmosphere of CO₂, both [Tp^{Bu^t,Me}]ZnOH and [Tp^{Bu^t,Me}]ZnOCO₂H may be observed in equilibrium, thereby allowing for the measurement of the equilibrium constant for insertion of CO₂ into the Zn–OH bond. At 217 K, the equilibrium constant is $6 \pm 2 \times 10^3 \text{ M}^{-1}$, corresponding to a value of $\Delta G = -3.8 \pm 0.2 \text{ kcal mol}^{-1}$. In addition to the solution-state spectroscopic studies, [Tp^{Bu^t,Me}]ZnOCO₂H and [κ^4 -Tptm]ZnOCO₂H have been structurally characterized by X-ray diffraction, thereby providing the first examples of structurally characterized terminal zinc bicarbonate complexes. The bicarbonate complexes afford important metrical data of importance to the critical bicarbonate intermediate of the mechanism of action of carbonic anhydrase. The dimeric hydroxide complex, {[κ^3 -Tptm]Zn(μ -OH)}₂, is sufficiently reactive towards CO₂ that it is able to abstract CO₂ directly from air to form the bridging carbonate complex, [Tptm]Zn(μ -CO₃)Zn[Tptm]. Both the bicarbonate and carbonate complexes are reduced by silanes to give the formate derivative, [κ^4 -Tptm]ZnO₂CH, a transformation that is significant for the functionalization of CO₂.

The alkyl zinc hydride complex, [κ^3 -Tptm]ZnH, has also proven to be an effective and robust catalyst for a variety of transformations including (i) the rapid generation of hydrogen on demand, (ii) the hydrosilylation of aldehydes and ketones producing siloxanes and (iii) the functionalization of CO₂ to produce a useful formylating agent, (EtO)₃SiO₂CH. The trimethylsiloxide complex, [κ^4 -Tptm]ZnOSiMe₃, may also be used as an effective precatalyst for these reactions. For example, in the [κ^4 -Tptm]ZnOSiMe₃ catalyzed hydrolysis and methanolysis of PhSiH₃, three equivalents of H₂ are released, with the methanolysis reaction achieving 10⁵ turnovers and turnover frequencies surpassing 10⁶ h⁻¹.

Additionally, $[\kappa^3\text{-Bptm}^*]\text{ZnO}_2\text{CH}$ ($\text{Bptm}^* = \text{bis}(2\text{-pyridylthio})(p\text{-tolylthio})\text{methyl}$) has been synthesized using the tridentate $[\text{Bptm}^*]$ ligand, which has only two chelating pyridyl arms, forbidding a κ^4 -coordination. It serves as a room temperature catalyst for the hydrosilylation of CO_2 , resulting in more rapid CO_2 functionalization compared to the $[\text{Tptm}]$ system. $[\kappa^3\text{-Tptm}]\text{ZnH}$ and $[\kappa^3\text{-Bptm}^*]\text{ZnO}_2\text{CH}$ provide the first two examples of zinc complexes that catalyze the hydrosilylation of CO_2 . These results provide evidence that, in suitable ligand environments, inexpensive and abundant non-transition metals can perform reactions that are typically catalyzed by precious metal-containing compounds.

The use of $\text{Li}[\text{Me}_3\text{SiNR}]$ in order to generate an isocyanide complex from its carbonyl precursor provides a novel, convenient synthetic method that circumvents the use of the free isocyanide as a reagent. Metal isocyanide compounds are most commonly synthesized using the free isocyanide. By contrast, the reaction of transition metal carbonyl compounds, L_nMCO , with $\text{Li}[\text{Me}_3\text{SiNR}]$ yields the corresponding isocyanide derivative, L_nMCNR . This reaction is driven by the cleavage of a weak silicon-nitrogen bond with concomitant formation of a stronger silicon-oxygen bond. Both sterically hindered and enantiopure isocyanide complexes have been synthesized.

Thimerosal, $[(\text{Ar}^{\text{CO}_2})\text{SHgEt}]\text{Na}$, an organomercurial utilized since the 1930s as a topical antiseptic, and more recently as a vaccine preservative, previously was not structurally characterized. Therefore, the molecular structures have been determined for thimerosal, its protonated derivative, $(\text{Ar}^{\text{CO}_2\text{H}})\text{SHgEt}$, and its mercurated derivative, $[(\text{Ar}^{\text{CO}_2\text{HgEt}})\text{SHgEt}]_2$, using single crystal X-ray diffraction. ^1H NMR spectroscopic studies indicate that the appearance of the ^{199}Hg mercury satellites of the ethyl groups is highly dependent on the magnetic field and the viscosity of the solvent; this observation is attributed to relaxation caused by chemical shift anisotropy. The relative signs of the Hg-H coupling constants (*i.e.* $^2J_{\text{Hg-H}}$ and $^3J_{\text{Hg-H}}$) have been determined by virtue of the fact that the inner pair of satellites appears as a singlet at 400 MHz. Reactivity studies

involving $(\text{Ar}^{\text{CO}_2\text{H}})\text{SHgEt}$ provide evidence that the Hg-C bond is kinetically stable with respect to protolytic cleavage. Finally, a series of known dithiol compounds have been synthesized for use as mercury chelating agents.

TABLE OF CONTENTS

Acknowledgements	ii
Dedication	ix
Chapter 1. Applications of Nitrogen-Rich Tetradentate Ligands: Organozinc-Hydride Chemistry	1
Chapter 2. Zinc Synthetic Analogues of Carbonic Anhydrase	116
Chapter 3. Zinc Catalysts for On Demand Hydrogen Generation and the Hydrosilylation of Aldehydes, Ketones and CO ₂	181
Chapter 4. Synthesis of Transition Metal Isocyanide Compounds from Carbonyl Complexes <i>via</i> Reaction with Li[Me ₃ SiNR]	257
Chapter 5. Structure and Reactivity of Thimerosal: Studies Towards Mercury Detoxification	308

ACKNOWLEDGMENTS

First, I would like to thank my advisor, Ged (G), for giving me the opportunity to do research in his group for the past five years and for his consistent support. I feel fortunate to have this opportunity. Thank you for teaching me how to be a synthetic chemist, especially teaching me the many physical techniques that are necessary to work with air and moisture sensitive compounds. I am also grateful for how you have taught me *(i)* to be an X-ray crystallographer, *(ii)* to use multinuclear NMR spectroscopy to not only determine the structure of a molecule, but also to analyze dynamic processes occurring in solution, and *(iii)* to think about bonding, structure and reactivity. All in all, you have taught me how to think about chemistry, and how to scrutinize every result before making a definitive conclusion, so thank you. Additionally, I would also like to thank you for having me as a teaching assistant for many semesters, both at the undergraduate and graduate level. I was fortunate enough to not only enjoy my teaching experience, but to learn from one of the best. Overall, graduate school was amazing, and in large part that is because of you. I am very indebted to have you as my PhD advisor, and more importantly, as my very good friend – this means the most to me. Thanks also to Ged's family - Rita, Lia and Catherine - for being so nice and warm to me; it is always great to see you guys and spend time with you. I am confident that we will all have a lifelong friendship.

Next, I would like to thank the members of my graduate committee: Professor Jack Norton and Professor Scott Snyder. Thank you both for your support and advice concerning chemistry and life over the past five years. Specifically, thank you, Jack, for our discussions regarding kinetics, polymerization and IR spectroscopy and also for teaching me about organometallic chemistry, kinetics and group theory. I have greatly enjoyed our discussions; each time I speak to you I feel like I learn something new and

interesting. Scott, thank you for your help with organic chemistry, and for your help and support during my postdoctoral search. You have been so supportive throughout my graduate school experience, which I very much appreciate.

Also, thanks to Professor James Canary (New York University), Professor John Magyar (Barnard College) and Professor Jon Owen (Columbia University) for taking the time to read my thesis and serve on my thesis defense committee. I would also like to thank Jon for his advice over the past couple of years concerning materials chemistry, semiconductors and my postdoctoral search. Also, thank you for your help with the distillation of $(\text{EtO})_3\text{SiH}$. I am moreover very grateful for your continued support as I venture into new areas of chemistry.

Professor Daniela Buccella, "Deeb," deserves a tremendous acknowledgment (she earned it!!). As a fifth year graduate student, Daniela was preparing to defend her thesis, finishing up her own research projects and getting ready for a post-doc at MIT. Even while dealing with the completion of her PhD, she still spent so much of her time to teach me (and Aaron) about chemistry; Deeb literally answered hundreds of questions from both Aaron and myself, and this was each day!! Not only did Daniela teach me how to manipulate a Schlenk line, work with air sensitive chemicals (e.g. PMe_3 and NaK) and perform X-ray crystallography, she also taught me how to approach chemistry and how to think about solving problems. Even after Daniela left for MIT, she continued to help. We would often skype with each other, talk on the phone, and visit each other. Her advice was and still is always insightful. Daniela was the graduate student that I emulated; I often thought to myself, "What would Daniela do?" Finally, I must also point out, and thank Daniela, for being one of my very good friends, pretty much like a big sister! A big thank you also goes to Dr. Collin Chan, for your consistent support. Thank you for all of your advice concerning chemistry, graduate school and life in general. Thank you for being so generous to both Aaron and me.

Next, I would like to thank my brother, Aaron. Not only does he clean our apartment more than I do, but he also has been instrumental in my research. He quickly became the lab-guru of X-ray crystallography. My competitive nature made it hard for me to ask Aaron for help with a crystal structure, but when I did, it was always worth it. While Aaron and I think a lot alike, our discussions about chemistry have still benefited me substantially. Besides the chemistry discussions, I want to thank you for being a great brother and a great friend. You have always been there for me and I feel extremely lucky to have you as my brother!

Ahmed Al-Harbi, a.k.a “Ack the doc,” needs a big thanks as well. Besides our chemistry conversations, and his valuable chemistry advice to me over the past few years, thank you for being such a great friend and labmate. Thanks for making sure I did the control experiments!! You have taught me a lot about life: how not to stress and worry so much, how to take life as it comes, and how to enjoy the present. You always have a gentle perspective, and this has been instrumental to my growth as a person. You have been able to really keep me grounded over the past few years. I am looking forward to seeing more great chemistry from you, and I am sure we will have a life-long relationship. Thank you so much for all of this!

I would also like to thank the other members of the Parkin Group. First, thank you, Yi Rong! Yi, you *always* bring a smile to my face. I appreciate our conversations about life, the future, relationships and diamonds! It has been great to spend four whole years with you; you are like a little sister to me. I will miss saying, “Yiiiiiiii” everyday, and of course, I will miss you a lot!

Thanks also to Ava Kreider-Mueller, Ashley Zuzek and Neena Chakrabarti. Ava, thanks for being a great desk-mate and my friend, for translating some German papers, and for being so supportive all of these years. Ashley, thanks for your support, for your good cooking, and for being a good friend to me over the past couple of years. Neena, thanks for always providing the needed joke, and for your support and

friendship. Serge Ruccolo, it has been nice working with you in lab, and enjoyable to often get a couple of beers with you after lab. I am happy I was able to show you how American football is played, the “real” football! I need to give a big thanks to Julia Oktawiec, a superstar undergraduate in the Parkin Group. It has been amazing to work with you and has been to my benefit to mentor you; you have taught me a lot. Thank you for your detailed editing of this entire thesis. I anticipate great things from you in the future, so keep up the good work! I would also like to thank our new postdoc, Dr. Joshua Palmer, for his advice concerning Caltech, and his discussions regarding spectroscopy. Thank you to all of the aforementioned group members for reading part of my thesis. I would also like to thank the other Parkin Group members that I have had the privilege to work with: Joseph Ulichny, Ben Kriegel, Victoria Landry, Keliang Pang, Michelle Neary, Kevin Yurkerwich, Ariel Schaap, Douglas Villalta and Greg Theophall. I would like to additionally thank Joseph for being so helpful and welcoming when first arriving at Columbia, and then when joining the Parkin Group. I wish the best for everyone in the Parkin Group in their future endeavors.

A big thanks goes to my best friends, Johnny Gartiser (a.k.a Dream) and Eric Harris (a.k.a. E). For many years, you both have been family to me, always supportive, and always there for me. I am lucky to have you guys as my friends (thanks for the guide to the galaxy)!! You both know how to deal with Aaron and me; you always have good advice, and I appreciate you both very much. You both have made graduate school much easier compared to if I did not see you guys so often. Our many trips have always provided a relief that was needed, and I look forward to continuing this trend. Good luck to you both in your teaching and coaching careers.

I would also like to thank my friends in the chemistry department. Dr. Dan Treitler, thanks for organizing the Wungsten Warrior football team (the best chemistry football team that I have ever seen), thanks for your help with organic chemistry, and thanks for being a great friend. A warm thanks goes to Jessie Jousot, who most

commonly, I call Jejo. You are an amazing friend, and have taught me a lot about life, the world and food (e.g. fruit). Thanks for preparing my trip to France, and thanks for your constant support and friendship, I greatly appreciate it; you mean a lot to me. I would also like to thank Dr. Adel Elsohly, Alex Brucks and Nate Wright for being such good friends during graduate school, and for the many good memories. Adel, thanks for the great chemistry conversations, and I wish you and your family the best in California. Alex, thanks for being so awesome. I've really enjoyed hanging out with you, it was always a lot of fun! Nate, thanks for your consistent support, it was always cool to have a baseball catch or watch a football game with you. Additionally, I would like to thank Dr. Brandi Cossairt, Stephen Thomas, James Eagen, Jeff Bandar, Alex Buitrago Santanilla, Dr. Chris Plummer, Steven Breazzano, Dr. Wes Chalifoux, Carrie Yozwiak, Dan Griffith, Alex Beecher, Dr. Abe Wolcott and Myles Smith for your friendship over the past several years. Additionally, I would like to thank Dr. Jeffrey Lancaster for his support and help with using Microsoft Word when writing this thesis, for his assistance in finding research articles in the library, and always for being nice and helpful.

Thank you to Dr. John Decatur and Michael Appel for your expertise and support with NMR. Specifically, thanks a lot to John for setting up a number of special NMR experiments that were crucial to my research, and for always answering my questions regarding NMR spectroscopy. Thank you, Dr. Yasuhiro Itagaki, for your help with Mass Spectrometry, and our discussions regarding baseball and beer. Thank you, Dr. Calman Lobel, for your assistance in running DFT calculations. Thank you, Deven Estes, for your assistance with obtaining IR spectra and also for your help with using a Fischer-Porter bottle. Thank you, Song Yu, for helping me find research articles that were not readily accessible through the Columbia library services.

I would also like to thank Professor Gilbert Stork, for his advice in the syntheses of a series of organic compounds. Our interactions and discussions have been

extraordinary; I feel fortunate to be able to hear your wisdom. Also, thank you, Professor Stork and Dr. Ayako Yamashita, for your support, advice, and kindness. Thank you, Professor Nicholas Turro and Dr. Steffen Jockush, for allowing me to use their photoreactors and for discussions about photochemistry. Thank you, Professor Bruce Bursten, for discussions about DFT calculations, charge distributions, group theory, and molecular orbitals, and for your support during my postdoctoral search. Thank you, Professor Breslow, for your advice concerning the synthesis of a carbene compound.

I would like to thank the entire chemistry department, for making Columbia such a great and special place to do my graduate research. Socky Lugo and Daisy Melendez, you both made teaching much easier than it could have been. You both are consistent with providing a smile and support; it was always nice to stop in your office for some small talk, so thank you very much. Carlos Garcia and Emilia Warlinski-Tokiwa, thanks for making sure I always got paid! Thanks also for the great conversations, most often at happy hour. Alix Lamia and Dani Farrell, thanks for keeping everything in check and always booking a room when I needed one. Jay Kirschenbaum, Robert Rutherford, Chris Cecilio and Bill Reynolds (and Felix Rosado), this place would crumble without you guys. Thanks so much for all of your help, always making sure everything is running smoothly, and the good conversations. Dr. Louis Avila, you provided a warm welcome when I arrived for the STAT program. You are always friendly, helpful and supportive; thanks so much. Maria Gomez and Noris Wallace, thank you both for always keeping everything clean, and for your friendship over the past five years. You all keep Columbia chemistry alive and moving forward!

I would also like to thank the teachers and professors who sparked my interest in science and chemistry before graduate school. Mr. Walsh of Ardsley Middle School, thanks for being an amazing teacher. I still remember how you inspired me to love science; you really sparked my interest in the physical world around me, so thanks for

that initial push in the “right” direction. Moving onto Binghamton University, I would like to thank Professor Wayne E. Jones. As my advisor for three years, in addition to my professor for many classes, you really drove me to love chemistry. It was your inorganic chemistry class my sophomore year that led me to not only choose chemistry as my major, but specifically inspired me to perform research on the subject of inorganic chemistry. Thanks also to Professor James Dix, who taught me physical chemistry. You allowed me to ask all of the questions I wanted (and there were a lot of them), and always provided great discussion. Thank you both for your support during my time at Binghamton University, and also when applying to graduate school.

Last, but definitely not least, I need to give the biggest thanks to my parents. Without them, I would obviously not be here, and I would not be the person I am today without you both. Since the day we (Aaron and I) were born, you have been the most supportive and loving people in my life. Your love means the world to me and always reminds me what truly is important. Our family, the family you both have created, is sacred to me, and always will be. Mom and dad, you have been to two biggest guides in my life, always providing the encouragement, direction and driving force. So thank you very much!

For my parents with love

CHAPTER 1

Applications of Nitrogen-Rich Tetradentate Ligands: Organozinc-Hydride Chemistry

Table of Contents

1.1	Introduction	5
1.1.1	Zinc Hydrides	5
1.1.2	<i>Tris</i> (2-pyridylthio)methane: [Tptm]H	6
1.2	Metalation of [Tptm]	9
1.3	[κ^3 -Tptm]ZnH	11
1.3.1	Synthesis and structural characterization of [κ^3 -Tptm]ZnH	11
1.3.2	Reactivity of [κ^3 -Tptm]ZnH and related compounds	22
1.4	Reactivity of [κ^3 -Tptm]ZnN(SiMe ₃) ₂ towards CO ₂ and the CO ₂ promoted displacement of siloxide ligands.	35
1.5	Ligand kapticity: A Density Functional Theory Investigation	43
1.6	Synthesis of a bulky [Tptm] ligand: [Tptm ^{Ph,Me}]H	45
1.7	[κ^4 -Tptm]MgN(SiMe ₃) ₂ chemistry	48
1.8	[κ^3 -Tptm]NiNO chemistry	50
1.9	Utilization of [Titm ^{Me}]H as a tetradentate ligand	56
1.10	Summary and conclusions	60
1.11	Experimental details	61
1.11.1	General considerations	61
1.11.2	Computational details	62
1.11.3	X-ray structure determinations	62
1.11.4	Synthesis of Zn[N(SiMe ₃) ₂] ₂	63
1.11.5	Synthesis of [Tptm]H	63
1.11.6	Synthesis of [κ^3 -Tptm]ZnMe	64

1.11.7	Synthesis of $[\kappa^3\text{-Tptm}]\text{ZnN}(\text{SiMe}_3)_2$	65
1.11.8	Synthesis of $[\kappa^4\text{-Tptm}]\text{ZnOSiMe}_3$	65
1.11.9	Synthesis of $[\kappa^4\text{-Tptm}]\text{ZnOSiPh}_3$	66
1.11.10	Synthesis of $[\kappa^3\text{-Tptm}]\text{ZnH}$	67
1.11.11	Synthesis of $[\kappa^3\text{-Tptm}]\text{ZnD}$	68
1.11.12	Synthesis of $[\kappa^4\text{-Tptm}]\text{ZnO}_2\text{CH}$	69
1.11.13	Synthesis of $[\kappa^4\text{-Tptm}]\text{Li}$	71
1.11.14	Synthesis of $\{[\kappa^4\text{-Tptm}]\text{MgBr}\}_2$	71
1.11.15	Synthesis of $[\text{Tptm}]\text{MgCl}$	72
1.11.16	Synthesis of $[\kappa^4\text{-Tptm}]\text{ZnCl}$	72
1.11.17	Reaction of $[\kappa^4\text{-Tptm}]\text{ZnOSiMe}_3$ with Me_3SiCl : Formation of $[\kappa^4\text{-Tptm}]\text{ZnCl}$	73
1.11.18	Reaction of $[\kappa^4\text{-Tptm}]\text{ZnOSiPh}_3$ with Me_3SiCl : Formation of $[\kappa^4\text{-Tptm}]\text{ZnCl}$	73
1.11.19	Reaction of $[\kappa^4\text{-Tptm}]\text{ZnO}_2\text{CH}$ with Me_3SiCl : Formation of $[\kappa^4\text{-Tptm}]\text{ZnCl}$	73
1.11.20	Reaction of $[\kappa^3\text{-Tptm}]\text{ZnH}$ with Me_3SiCl : Formation of $[\kappa^4\text{-Tptm}]\text{ZnCl}$	73
1.11.21	Reaction of $[\kappa^4\text{-Tptm}]\text{ZnOSiMe}_3$ with Me_3SiBr : Formation of $[\kappa^4\text{-Tptm}]\text{ZnBr}$	74
1.11.22	Reaction of $[\kappa^4\text{-Tptm}]\text{ZnOSiPh}_3$ with Me_3SiBr : Formation of $[\kappa^4\text{-Tptm}]\text{ZnBr}$	74
1.11.23	Reaction of $[\kappa^4\text{-Tptm}]\text{ZnO}_2\text{CH}$ with Me_3SiBr : Formation of $[\kappa^4\text{-Tptm}]\text{ZnBr}$	74
1.11.24	Reaction of $[\kappa^3\text{-Tptm}]\text{ZnH}$ with Me_3SiBr : Formation of $[\kappa^4\text{-Tptm}]\text{ZnBr}$	75
1.11.25	Synthesis of $[\kappa^4\text{-Tptm}]\text{ZnI}$	75
1.11.26	Reaction of $[\kappa^4\text{-Tptm}]\text{ZnOSiPh}_3$ with Me_3SiI : Formation of $[\kappa^4\text{-Tptm}]\text{ZnI}$	76
1.11.27	Reaction of $[\kappa^4\text{-Tptm}]\text{ZnO}_2\text{CH}$ with Me_3SiI : Formation of $[\kappa^4\text{-Tptm}]\text{ZnI}$	76
1.11.28	Reaction of $[\kappa^3\text{-Tptm}]\text{ZnH}$ with Me_3SiI : Formation of $[\kappa^4\text{-Tptm}]\text{ZnI}$	76
1.11.29	Reaction of $[\kappa^4\text{-Tptm}]\text{ZnOSiMe}_3$ with Me_3SiI : Formation of $[\kappa^4\text{-Tptm}]\text{ZnI}$	76
1.11.30	Reaction of $[\kappa^4\text{-Tptm}]\text{ZnOSiMe}_3$ with Me_3SiN_3 : Synthesis of $[\kappa^4\text{-Tptm}]\text{ZnN}_3$	77
1.11.31	Reaction of $[\kappa^4\text{-Tptm}]\text{ZnO}_2\text{CH}$ with Me_3SiN_3 : Formation of $[\kappa^4\text{-Tptm}]\text{ZnN}_3$	77
1.11.32	Reaction of $[\kappa^4\text{-Tptm}]\text{ZnOSiPh}_3$ with Me_3SiN_3 : Formation of $[\kappa^4\text{-Tptm}]\text{ZnN}_3$	78
1.11.33	Reaction of $[\kappa^4\text{-Tptm}]\text{ZnOSiMe}_3$ with Me_3SiOAc : Synthesis of $[\kappa^4\text{-Tptm}]\text{ZnOAc}$	78

1.11.34	Reaction of $[\kappa^4\text{-Tptm}]\text{ZnOSiPh}_3$ with Me_3SiOAc : Formation of $[\kappa^4\text{-Tptm}]\text{ZnOAc}$	79
1.11.35	Reaction of $[\kappa^4\text{-Tptm}]\text{ZnO}_2\text{CH}$ with Me_3SiOAc : Formation of $[\kappa^4\text{-Tptm}]\text{ZnOAc}$	79
1.11.36	Reaction of $[\kappa^3\text{-Tptm}]\text{ZnH}$ with HOAc : Formation of $[\kappa^4\text{-Tptm}]\text{ZnOAc}$	80
1.11.37	Reaction of $[\kappa^3\text{-Tptm}]\text{ZnN}(\text{SiMe}_3)_2$ with CO_2 : Synthesis of $[\kappa^4\text{-Tptm}]\text{ZnNCO}$	80
1.11.38	Reaction of $[\kappa^4\text{-Tptm}]\text{ZnO}_2\text{CH}$ with Me_3SiNCO : Synthesis of $[\kappa^4\text{-Tptm}]\text{ZnNCO}$	81
1.11.39	Synthesis of $[\kappa^4\text{-Tptm}]\text{ZnNCO}$ <i>via</i> the CO_2 Promoted Reaction of $[\kappa^4\text{-Tptm}]\text{ZnOSiMe}_3$ with Me_3SiNCO	82
1.11.40	Reaction of $[\kappa^4\text{-Tptm}]\text{ZnOSiMe}_3$ with $^{13}\text{CO}_2$: ^{13}C NMR Spectroscopic Characterization of $[\kappa^4\text{-Tptm}]\text{ZnOC}(\text{O})\text{OSiMe}_3$	82
1.11.41	Reaction of $[\kappa^4\text{-Tptm}]\text{ZnOSiPh}_3$ with $^{13}\text{CO}_2$: ^{13}C NMR Spectroscopic Characterization of $[\kappa^4\text{-Tptm}]\text{ZnOC}(\text{O})\text{OSiPh}_3$	83
1.11.42	Synthesis of $[\kappa^4\text{-Tptm}]\text{ZnCl}$ <i>via</i> the CO_2 Promoted Reaction of $[\kappa^4\text{-Tptm}]\text{ZnOSiMe}_3$ with Me_3SiCl	83
1.11.43	Synthesis of $[\kappa^4\text{-Tptm}]\text{ZnBr}$ <i>via</i> the CO_2 Promoted Reaction of $[\kappa^4\text{-Tptm}]\text{ZnOSiPh}_3$ with Me_3SiBr	83
1.11.44	Synthesis of $[\kappa^4\text{-Tptm}]\text{ZnF}$	84
1.11.45	Reaction of $[\kappa^4\text{-Tptm}]\text{ZnF}$ with PhSiH_3 : Synthesis of $[\kappa^3\text{-Tptm}]\text{ZnH}$	84
1.11.46	Reaction of $[\kappa^4\text{-Tptm}]\text{ZnF}$ with Me_3SiCl : Synthesis of $[\kappa^4\text{-Tptm}]\text{ZnCl}$	85
1.11.47	Synthesis of $[\kappa^3\text{-Titm}^{\text{Me}}]\text{ZnN}(\text{SiMe}_3)_2$	85
1.11.48	Synthesis of $[\kappa^4\text{-Titm}^{\text{Me}}]\text{ZnNCO}$	85
1.11.49	Synthesis of $[\kappa^4\text{-Tptm}]\text{MgN}(\text{SiMe}_3)_2$	86
1.11.50	Synthesis of $[\kappa^3\text{-Tptm}]\text{NiNO}$	86
1.11.51	Synthesis of 6-phenyl,4-methyl,2-pyridone	87
1.11.52	Synthesis of 6-Phenyl,4-Methyl,2-thiopyridone	88
1.11.53	Synthesis of $[\text{Tptm}^{\text{Ph,Me}}]\text{H}$	89
1.11.54	Synthesis of $[\text{Bptm}^{\text{Ph,Me}}]\text{H}_2$	89

1.11.55	Synthesis of the trithiocarbonate, (6-Phenyl,4-Methyl,2-thiopyridyl) ₂ CS	90
1.12	Crystallographic data	91
1.13	References and notes	108

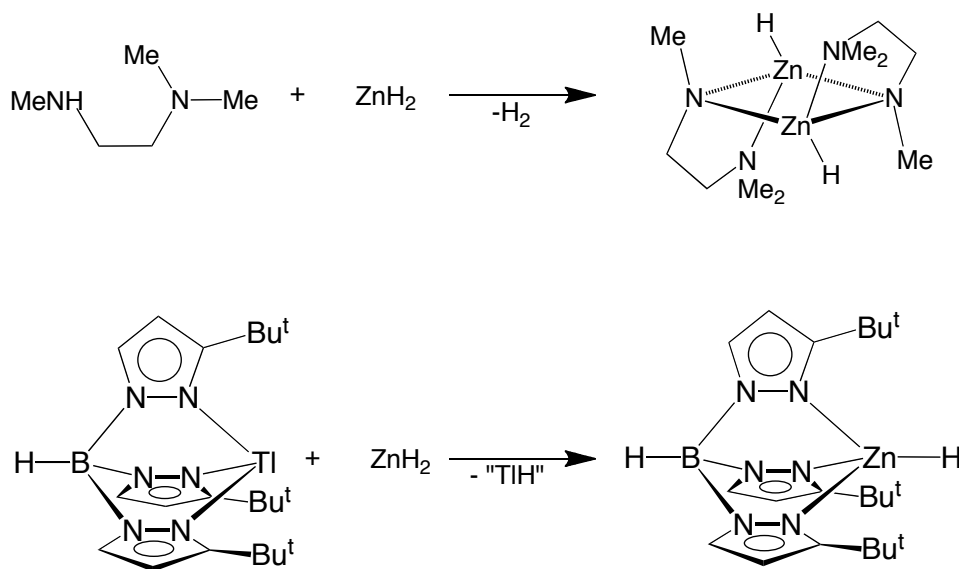
Reproduced in part from:

W. Sattler and G. Parkin *J. Am. Chem. Soc.* **2011**, *133*, 9708-9711.

1.1 Introduction

1.1.1 Zinc Hydrides

Zinc hydride, ZnH_2 , a polymeric, insoluble binary compound, was first prepared in 1947 by the reaction of LiAlH_4 with Me_2Zn .¹ Twenty one years later, the first terminal zinc hydride complex was prepared *via* the reaction of ZnH_2 with trimethylethylenediamine to give 2-dimethylaminoethyl(methyl)amidozinc hydride (Scheme 1).² In 1991, the sterically demanding *tris*(3-*tert*-butylpyrazolyl)hydroborato ligand, $[\text{Tp}^{\text{Bu}^t}]$, was used by the Parkin Group to synthesize the first monomeric, terminal zinc hydride, namely, $[\text{Tp}^{\text{Bu}^t}]\text{ZnH}$, *via* the reaction of ZnH_2 with $[\text{Tp}^{\text{Bu}^t}]\text{Ti}$ (Scheme 1).³



Scheme 1. Synthesis of first terminal zinc hydride compound (top) and the first monomeric, terminal zinc hydride compound (bottom).

According to the Cambridge Structural Database, there are currently 64 structurally characterized zinc hydride compounds, 18 of which contain terminal hydride moieties.⁴ It is evident that zinc hydride compounds are not prevalent, and

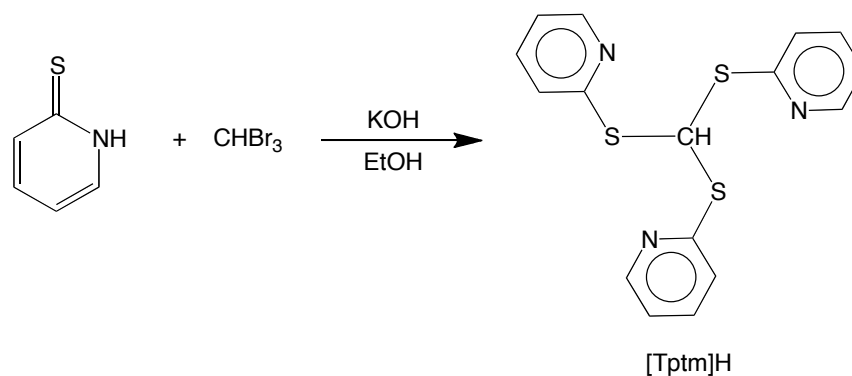
that well-defined mononuclear zinc complexes featuring terminal hydride ligands are rare.^{5,6,7} The latter is presumably due to the proclivity of the hydride ligand to bridge two or more zinc centers.⁸ Monomeric, terminal zinc hydrides are of greatest interest in terms of detailed mechanistic studies because they are well-defined species.

Zinc hydride species are of considerable interest due to their intrinsic reactivity as a hydride transfer agent and also because the moiety has been little studied. For example, they have been used in organic transformations, usually as chemoselective reductants.⁹ Additionally, zinc hydrides have a significant role in the Cu/ZnO catalyzed synthesis of methanol from a mixture of CO, CO₂ and H₂.¹⁰ Specifically, zinc hydride and zinc formate species (resulting from CO₂ insertion into a zinc hydride bond) are proposed intermediates in methanol synthesis and therefore are of interest in the catalytic conversion of CO₂ to reduced products (*i.e.* for the production of useful chemicals and/or fuels). Zinc hydrides are nucleophilic (transfers H⁻), and are often reactive towards numerous functionalities, such as (i) alcohols to produce H₂ and the corresponding zinc alkoxide compound, (ii) alkyl halides resulting in reduction to the corresponding alkane and (iii) heterocumulenes, such as carbon dioxide and carbon disulfide, resulting in a reduced species *via* an insertion reaction.³ However, progress in utilizing zinc hydrides has been hampered mainly due to the difficulty in preparing zinc hydride compounds. In this chapter, the synthesis and reactivity of a monomeric zinc hydride based on the alkyl ligand derived from *tris*(2-pyridylthio)methane, [Tptm]H (*vide infra*),¹¹ will be described. The hydride complex, namely [κ³-Tptm]ZnH, is the first example of a monomeric alkyl zinc hydride complex.

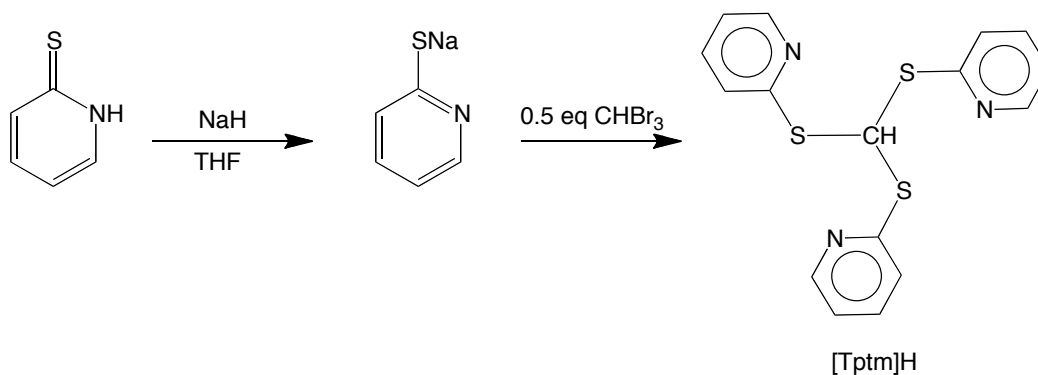
1.1.2 *Tris*(2-pyridylthio)methane: [Tptm]H

Tris(2-pyridylthio)methane, [Tptm]H,¹¹ was synthesized in 2002 in a manner depicted in Scheme 2. We have developed a new synthesis for [Tptm]H (Scheme 3) that produces [Tptm]H in much higher yields and proceeds at room temperature as

opposed to *ca.* 80 °C. The molecular structure of [Tptm]H was determined by single crystal X-ray diffraction, which is depicted in Figure 1. One aspect of the molecular structure of [Tptm]H that is worth noting is the intramolecular hydrogen bonding between the pyridyl nitrogen atoms and the methine hydrogen atom. If a metal replaces the hydrogen atom, an atrane structural motif results (Figure 2);¹² there is a central covalent bond between the carbon atom of [Tptm] and a metal atom that forms a caged structure. In 2008, the first two zinc containing compounds of [Tptm] were synthesized, namely $[\kappa^4\text{-Tptm}]\text{ZnCl}$ and $[\kappa^4\text{-Tptm}]\text{ZnBr}$.¹³ These organozinc compounds were prepared by reaction of [Tptm]H with ZnX_2 ($\text{X} = \text{Cl}, \text{Br}$) in the presence of K_2CO_3 .¹³ The one-electron oxidation of these compounds was studied, and was described as a ligand based oxidation resulting in the compounds' decomposition.¹³



Scheme 2. Synthesis of [Tptm]H.



Scheme 3. New method for the synthesis of [Tptm]H.

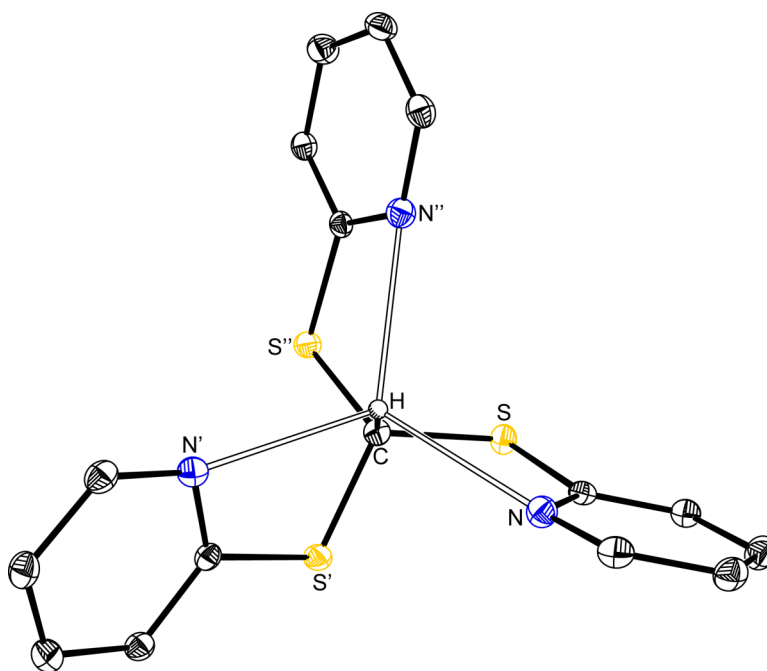


Figure 1. Molecular Structure of [Tptm]H.¹⁴

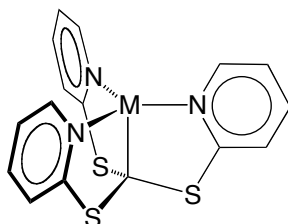


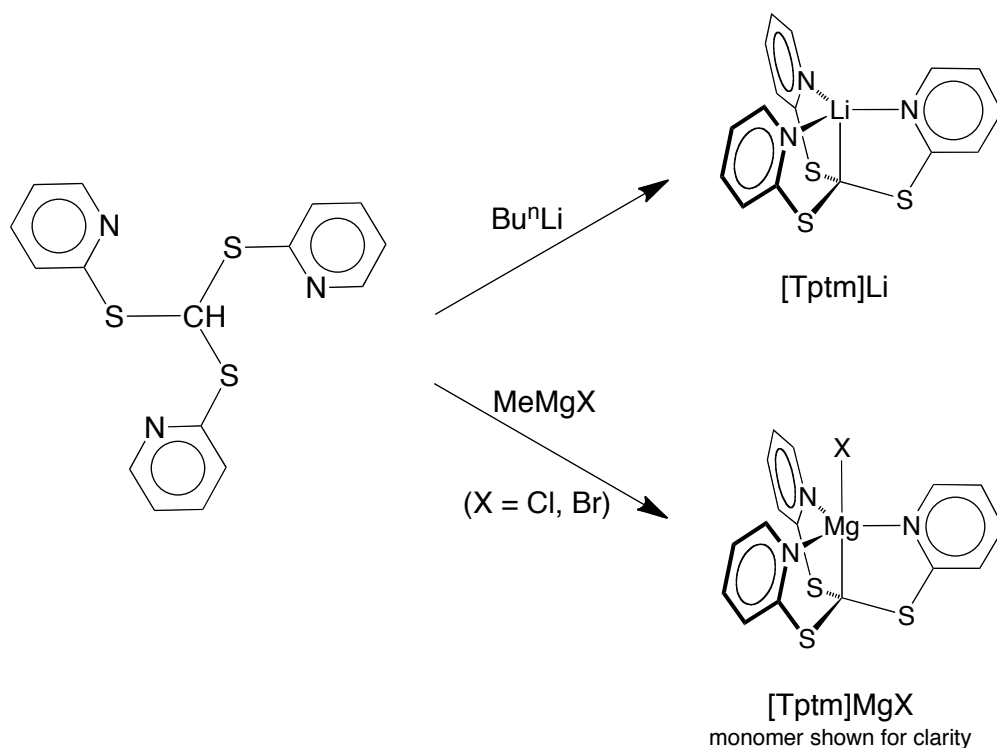
Figure 2. Atrane structural motif using the [Tptm] ligand.

While [Tptm] has been utilized with other metals, such as Fe¹⁵, Ni¹⁶, Sn¹⁷ and Cu¹⁸, there has been little research performed using this ligand compared to similar ligands, such as the tripodal ligands, [Tp] and [Tm]. A key difference between [Tptm] and the [Tp] and [Tm] ligands is the L₃X nature of the [Tptm] ligand. It should be noted that the [Tptm] ligand can bind *via* 2 or 3 of its pyridyl arms, resulting in a L₂X and L₃X ligand, respectively (*vide infra*). The tripodal ligands, [Tp] and [Tm] are L₂X in nature, with the X-type ligand being delocalized over the majority of the ligand. On the other

hand, the [Tptm] ligand binds through its central carbon atom in a specific X-type manner, and the L-type pyridyl donors provide additional chelation to the metal center. One final distinction is that the [Tptm] ligand is an organometallic ligand, due to there being a direct metal-carbon bond.

1.2 Metalation of [Tptm]

There has been no report in the literature of synthesizing a lithium or magnesium complex of [Tptm]. Therefore, in order to have a [Tptm] anionic synthon, [Tptm] was metalated with with (i) Bu^nLi to give $[\kappa^4\text{-Tptm}]\text{Li}$ and (ii) MeMgX to give $\{[\kappa^4\text{-Tptm}]\text{MgX}\}_2$ ($\text{X} = \text{Cl}, \text{Br}$) which is depicted in Scheme 4.¹⁹



Scheme 4. Metalation of [Tptm]H to give $[\kappa^4\text{-Tptm}]\text{Li}$ and $\{[\kappa^4\text{-Tptm}]\text{MgX}\}_2$.

$[\kappa^4\text{-Tptm}]\text{Li}$ is a thermally sensitive solid and is therefore prepared and stored at low temperature. On the other hand, the $[\text{Tptm}]\text{MgX}$ compounds are thermally robust and may be stored at room temperature. The molecular structures of $[\kappa^4\text{-Tptm}]\text{Li}$ and $\{[\kappa^4\text{-Tptm}]\text{MgBr}\}_2$ are depicted in Figure 3 and Figure 4, respectively. Both the lithium and magnesium complexes proved to be amenable for salt elimination reactions (*i.e.* elimination of LiX or MgX_2 where $\text{X} = \text{halide}$) with other metal compounds of interest (*vide infra*). $[\kappa^4\text{-Tptm}]\text{Li}$ is the more reactive source of $[\text{Tptm}]^-$, and importantly, it does not contain any halide. The $[\text{Tptm}]\text{MgX}$ compounds are easier to handle, but are less reactive and do contain a halide. The latter can cause problems when performing reactions with other metal compounds containing halides due to halide exchange, therefore producing a mixture of compounds.

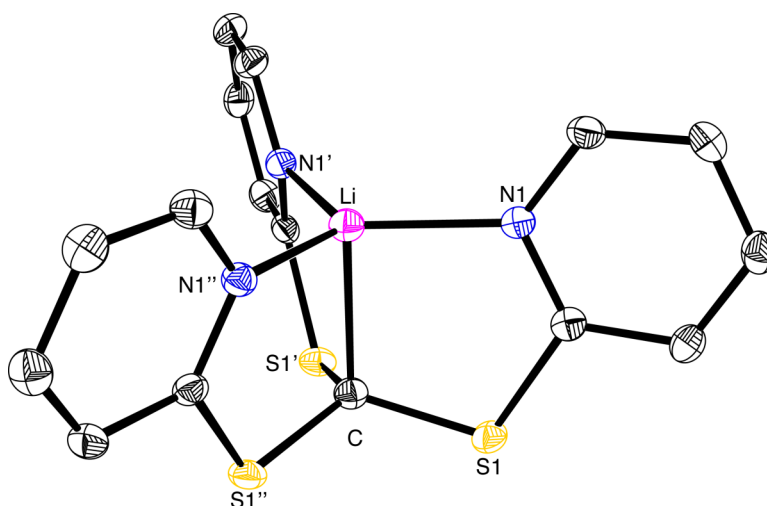


Figure 3. Molecular Structure of $[\kappa^4\text{-Tptm}]\text{Li}$.

As shown in Figure 3, $[\kappa^4\text{-Tptm}]\text{Li}$ adopts an atrane structural motif, where the lithium is coordinated by all three pyridyl donors to make a trigonal mono-pyramid around lithium. On the other hand, $\{[\kappa^4\text{-Tptm}]\text{MgBr}\}_2$ forms a dimeric compound with bridging bromide ligands. In the magnesium structure, each magnesium atom is in a

pseudo-octahedral geometry as depicted in Figure 4. The $[\text{Tptm}]\text{MgX}$ compounds are, in fact, Grignard reagents, as they are of the generic formula RMgX , where R is an alkyl and X is a halide. However, due to the intramolecular chelation by the pyridyl rings, there is little possibility of a Schlenk equilibrium occurring, unless $[\text{Tptm}]_2\text{Mg}$ were to be formed, which has not been observed to date. These compounds could provide well-defined reactivity of the Mg-X bond in a Grignard reagent.

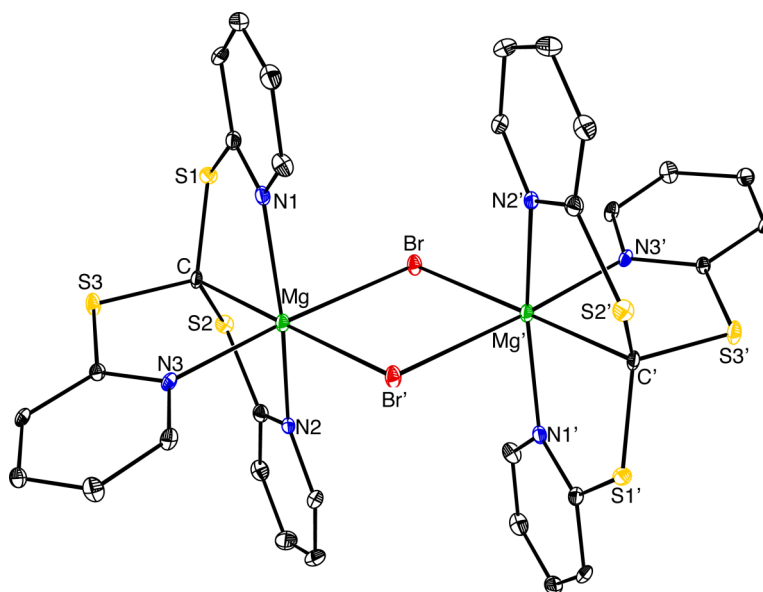


Figure 4. Molecular Structure of $\{[\kappa^4\text{-Tptm}]\text{MgBr}\}_2$.

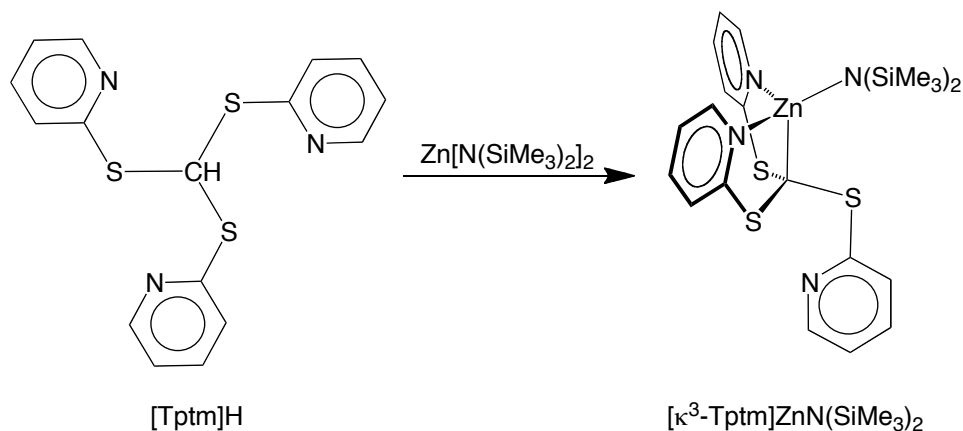
1.3 $[\kappa^3\text{-Tptm}]\text{ZnH}$

1.3.1 Synthesis and structural characterization of $[\kappa^3\text{-Tptm}]\text{ZnH}$

As mentioned earlier, $[\text{Tptm}]\text{H}$ has been deprotonated using a weak base (K_2CO_3) in the presence of ZnX_2 ($\text{X} = \text{Cl}, \text{Br}$)⁹ and additionally, there have been reports about the low pK_a of orthothioformates.²⁰ Therefore, basic ligands on zinc were attempted to perform an intermolecular deprotonation of the methine proton in order to form a zinc complex. In this vein, many zinc hydride compounds have already been synthesized using ZnH_2 as the hydride source, and additionally, hydride ligands on

zinc are known to be basic. As such, ZnH_2 appeared to be an appropriate reagent to metallate $[\text{Tptm}]\text{H}$, where one of the hydride ligands on ZnH_2 would deprotonate the methine proton to give H_2 , leading to the desired organozinc hydride compound, $[\text{Tptm}]\text{ZnH}$. However, the reaction between ZnH_2 and $[\text{Tptm}]\text{H}$ gave undesired products, with no sign of $[\text{Tptm}]\text{ZnH}$.

Another zinc compound with basic ligands is $\text{Zn}[\text{N}(\text{SiMe}_3)_2]_2$.²¹ Not only are the amide ligands basic, but the amine byproduct, $\text{HN}(\text{SiMe}_3)_2$ (hexamethyldisilazane) should be easy to remove because it is a volatile liquid (b.p. = 126 °C). In this regard, the reaction of $[\text{Tptm}]\text{H}$ with $\text{Zn}[\text{N}(\text{SiMe}_3)_2]_2$ cleanly produces the *bis*(trimethylsilyl)amide derivative, $[\kappa^3\text{-Tptm}]\text{ZnN}(\text{SiMe}_3)_2$ which is illustrated in Scheme 5. $[\kappa^3\text{-Tptm}]\text{ZnN}(\text{SiMe}_3)_2$ is easily prepared on multigram scale at room temperature, and the desired compound is obtained as a pure off-white powder after lyophilization of the reaction mixture.



Scheme 5. Synthesis of $[\kappa^3\text{-Tptm}]\text{ZnN}(\text{SiMe}_3)_2$.

Although the molecular structure of $[\kappa^3\text{-Tptm}]\text{ZnN}(\text{SiMe}_3)_2$ has not been determined by single crystal X-ray diffraction, variable temperature ^1H NMR spectroscopy provides evidence for the κ^3 -coordination of the $[\text{Tptm}]$ ligand. Specifically, a 2:1 ratio of pyridyl groups in the ^1H NMR spectrum at $\leq -10^\circ\text{C}$ is

consistent with κ^3 -coordination (Figure 5). At room temperature, only three broad resonances are observed in the aromatic region. Analysis of the variable temperature ^1H NMR spectra (Table 1) allows for the determination of the activation parameters for the exchange process occurring in solution. Specifically, an Eyring plot, which is depicted in Figure 6, gives $\Delta H^\ddagger = 15.9 \text{ kcal mol}^{-1}$ and $\Delta S^\ddagger = 12.0 \text{ e.u}$ (Table 2). The positive value obtained for the entropy of activation implies that there is a decrease of order in the transition state, suggesting a dissociative mechanism. One possible mechanism involves dissociation of one of the pyridyl moieties and formation of $[\kappa^2\text{-Tptm}]\text{ZnN}(\text{SiMe}_3)_2$, prior to coordination of a different pyridyl arm.

$[\kappa^3\text{-Tptm}]\text{ZnN}(\text{SiMe}_3)_2$ may be stored at room temperature under an inert atmosphere with no sign of decomposition after several months. We attempted to synthesize the hydride complex directly from $[\kappa^3\text{-Tptm}]\text{ZnN}(\text{SiMe}_3)_2$ but no clean reactivity was observed. However, due to the basic nature of the $\text{N}(\text{SiMe}_3)_2$ ligand, we were able to use protic reagents for the synthesis of other $[\text{Tptm}]\text{Zn}$ compounds.

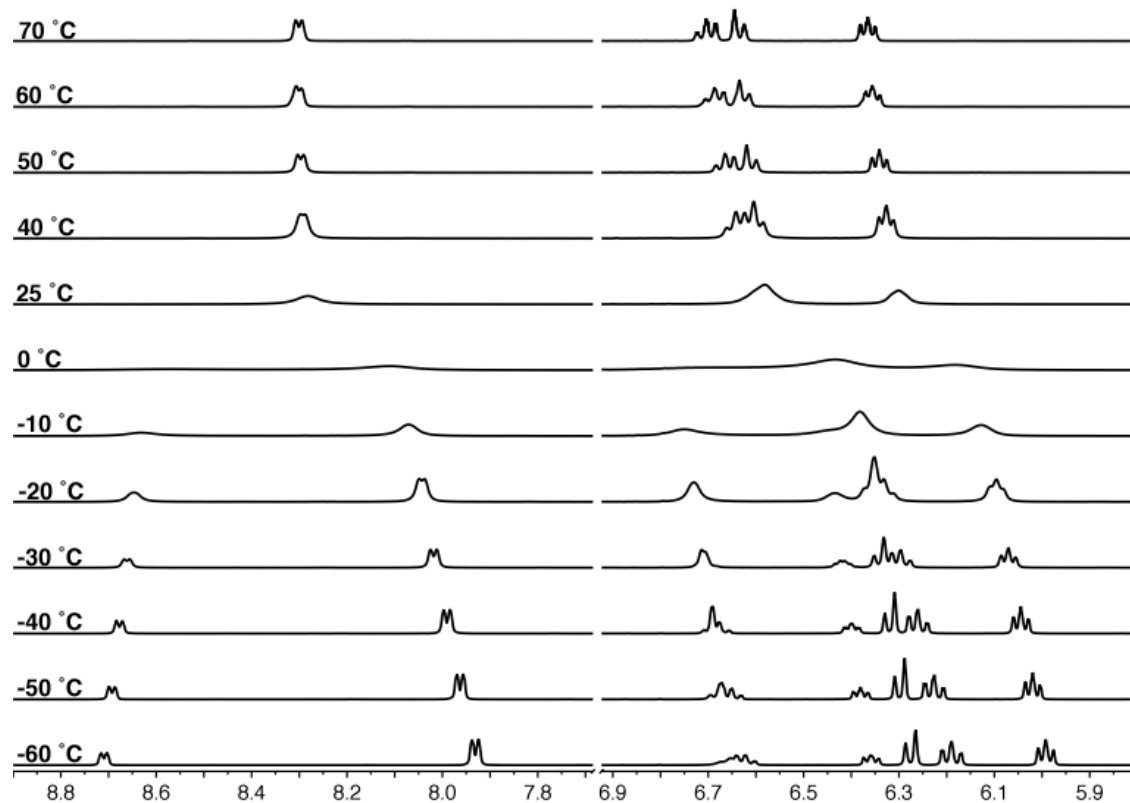


Figure 5. Variable temperature ^1H NMR spectroscopy of $[\kappa^3\text{-Tptm}]\text{ZnN}(\text{SiMe}_3)_2$ (only aromatic region shown for clarity).

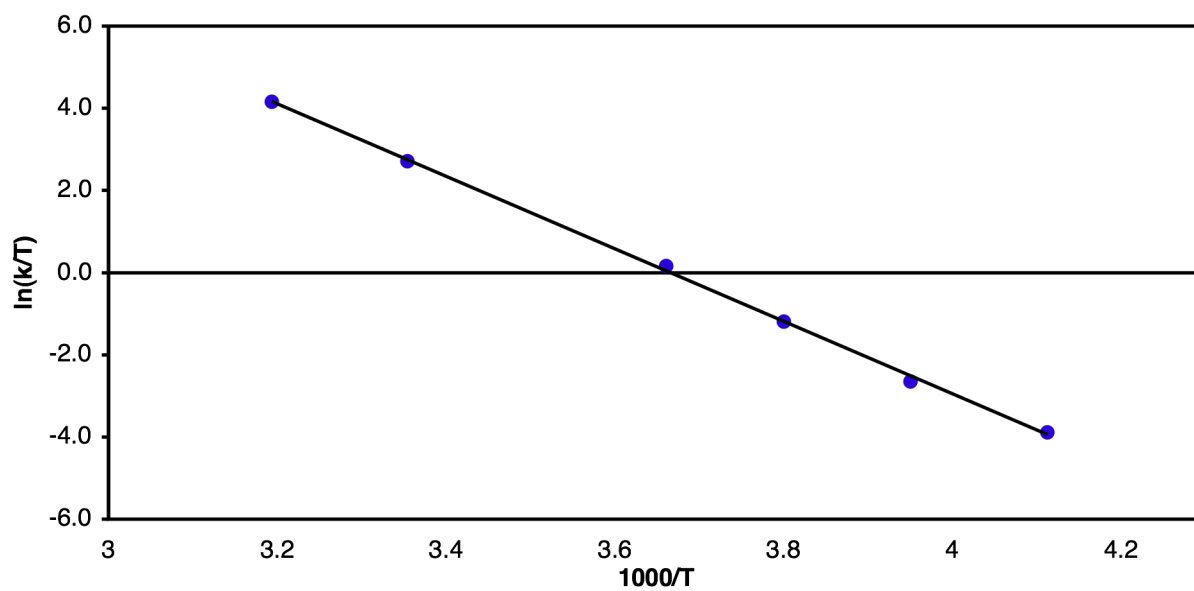


Figure 6. Eyring plot for the exchange process occurring in toluene for $[\kappa^3\text{-Tptm}]\text{ZnN}(\text{SiMe}_3)_2$.

For example, treatment of $[\kappa^3\text{-Tp}^{\text{R}}]\text{ZnN}(\text{SiMe}_3)_2$ with the commercially available silanol, trimethylsilanol (Me_3SiOH), yields the siloxide complex, $[\kappa^4\text{-Tp}^{\text{R}}]\text{ZnOSiMe}_3$. This reaction proceeds cleanly and pure $[\kappa^4\text{-Tp}^{\text{R}}]\text{ZnOSiMe}_3$ can be prepared on multigram scale with quantitative conversion occurring in less than 5 minutes. Lyophilization of the reaction mixture provides the trimethylsiloxide complex, $[\kappa^4\text{-Tp}^{\text{R}}]\text{ZnOSiMe}_3$, as a pure yellow powder, which can be recrystallized from benzene. Trimethylsiloxide complexes of zinc are not common, and the only structurally characterized compound listed in the Cambridge Structural Database is $[\text{Tp}^{\text{R,R}}]\text{ZnOSiMe}_3$.²²

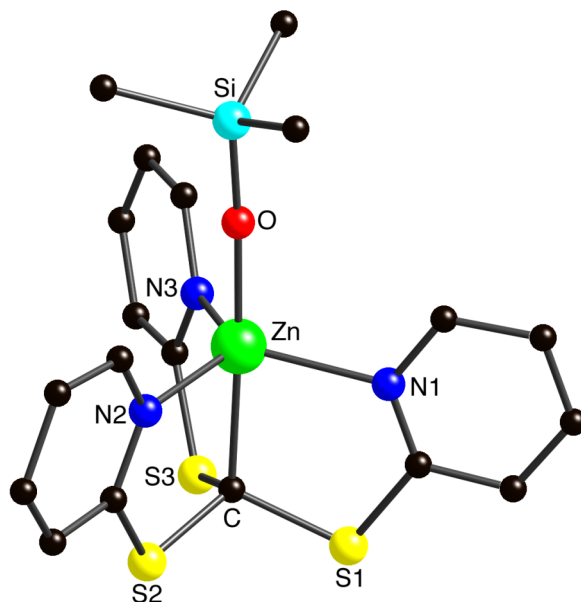


Figure 7. Molecular structure of $[\kappa^4\text{-Tp}^{\text{m}}]\text{ZnOSiMe}_3$.

The molecular structure of $[\kappa^4\text{-Tp}^{\text{m}}]\text{ZnOSiMe}_3$ has been determined by single crystal X-ray diffraction, thereby confirming the κ^4 -coordination mode of the $[\text{Tp}^{\text{m}}]$ ligand. However, there are six independent molecules in the asymmetric unit (space

group is $P2_1/n$, with a unit cell volume equal to 13618(3)) and the data quality is very poor. Therefore, a ball and stick model is shown in Figure 7.

With the aim to synthesize the hydride complex, silanes were selected to perform a metathesis reaction with $[\kappa^4\text{-Tptm}]\text{ZnOSiMe}_3$; the strength of the Si–O bond would provide the necessary driving force. Specifically, $[\kappa^4\text{-Tptm}]\text{ZnOSiMe}_3$ reacts immediately with phenylsilane (PhSiH_3) to deposit colorless crystals of the hydride complex, $[\kappa^3\text{-Tptm}]\text{ZnH}$ (Figure 8).

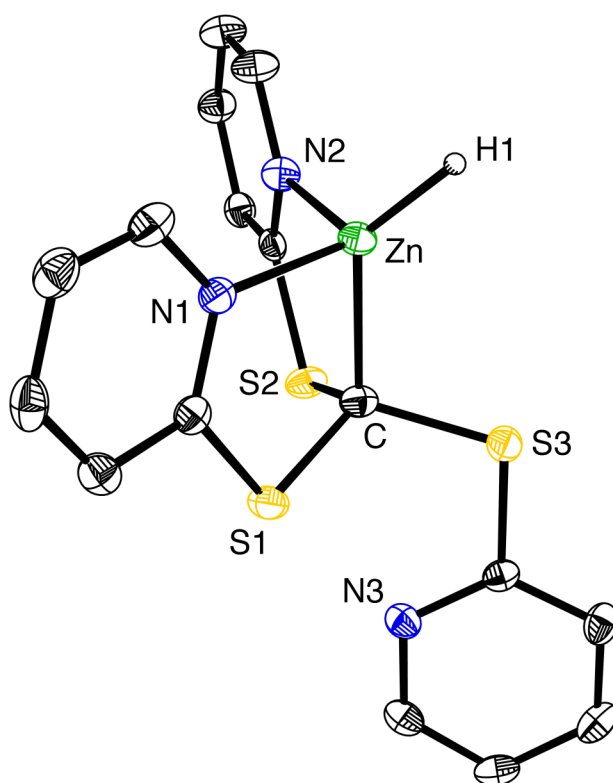
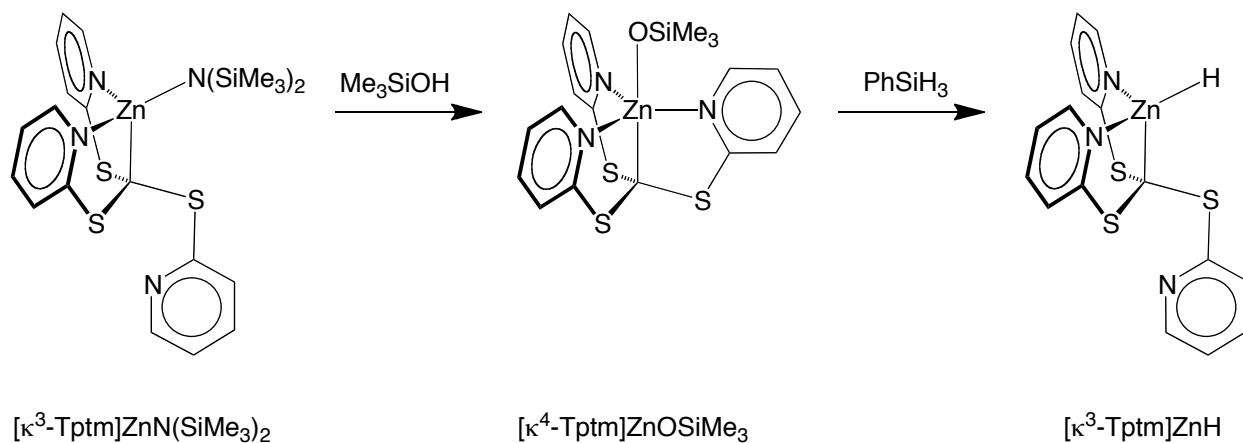


Figure 8. Molecular structure of $[\kappa^3\text{-Tptm}]\text{ZnH}$.

$[\kappa^3\text{-Tptm}]\text{ZnH}$ is obtained in high yield and purity after decantation of the mother liquor, followed by evaporation of the mixture *in vacuo*. $[\kappa^3\text{-Tptm}]\text{ZnH}$ should be stored at low temperature as it decomposes slowly at room temperature. To summarize, multigram quantities of $[\kappa^3\text{-Tptm}]\text{ZnH}$ can be obtained in three steps

starting with [Tptm]H and $\text{Zn}[\text{N}(\text{SiMe}_3)_2]_2$ as depicted in Scheme 5 and Scheme 6. Two attractive features of this synthetic route are (i) the ease of purification of the products and (ii) the high yield of each step (89% overall yield beginning with [Tptm]H).



Scheme 6. Synthesis of $[\kappa^3\text{-Tptm}]\text{ZnH}$.

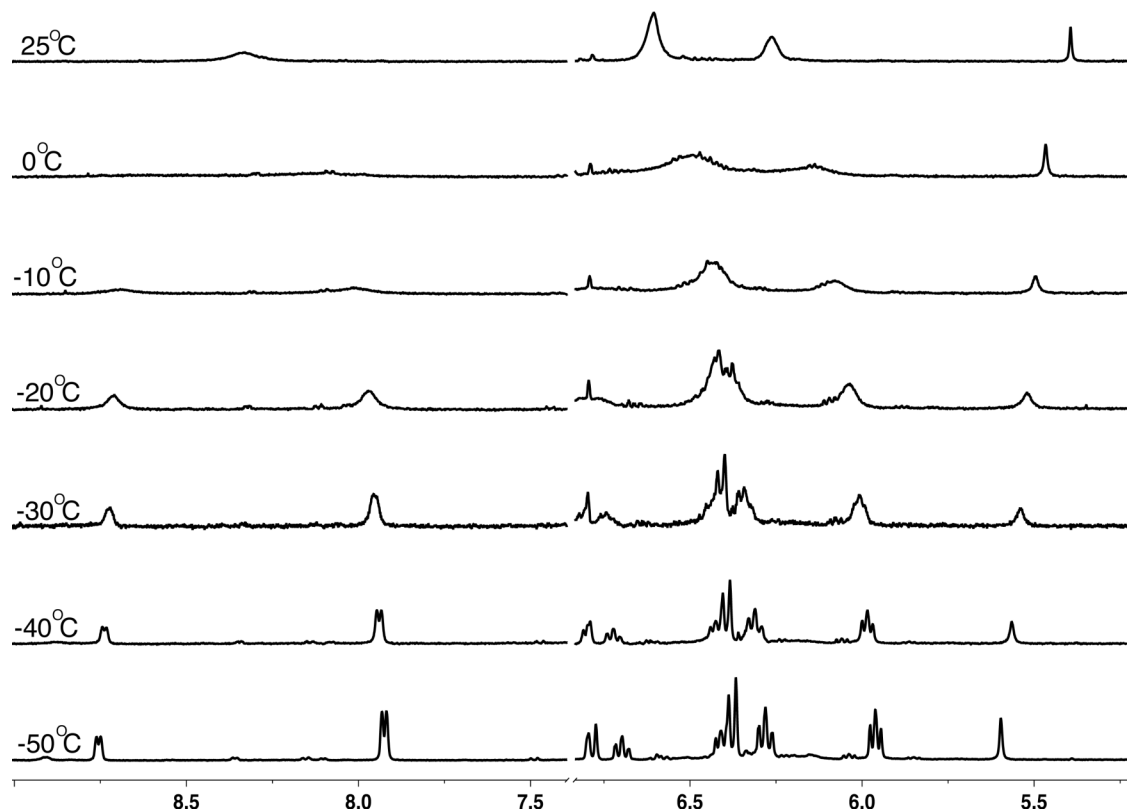


Figure 9. Variable temperature ^1H NMR spectroscopy of $[\kappa^3\text{-Tptm}]\text{ZnH}$. It should be noted that $[\kappa^3\text{-Tptm}]\text{ZnH}$ has very limited solubility in toluene, the solvent used to acquire the spectra above.

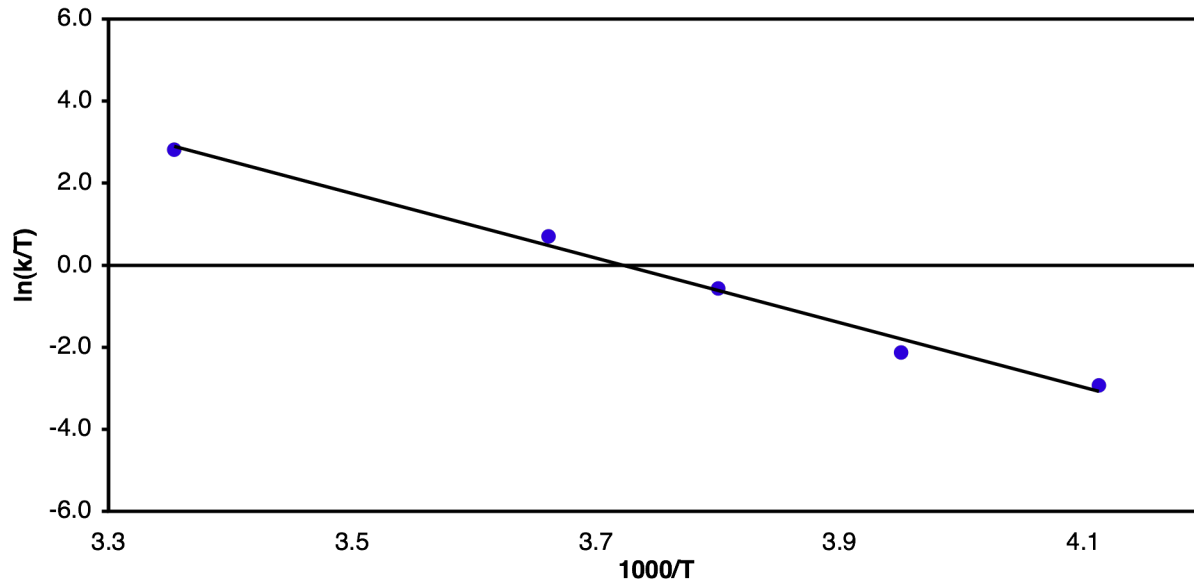
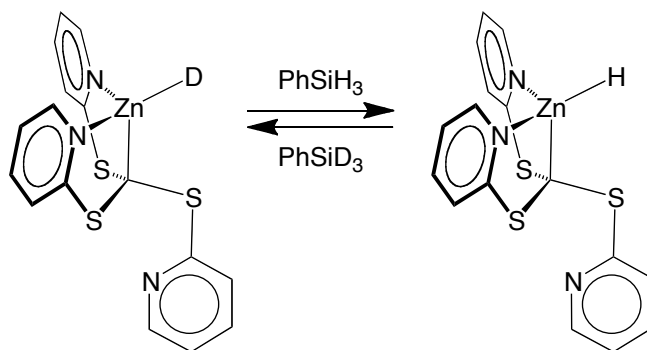


Figure 10. Eyring plot for the exchange process occurring in toluene for $[\kappa^3\text{-Tptm}]\text{ZnH}$.

The Zn-H moiety of $[\kappa^3\text{-Tptm}]\text{ZnH}$ is characterized by (i) a Zn-H bond length of 1.51(3) Å, which compares favorably with the mean Zn-H bond length for terminal hydride compounds listed in the Cambridge Structural Database (1.55 Å), (ii) a singlet at δ 5.60 in the ^1H NMR spectrum and (iii) an absorption at 1729 cm^{-1} in the IR spectrum, which shifts to 1242 cm^{-1} for the zinc deuteride isotopologue $[\kappa^3\text{-Tptm}]\text{ZnD}$ [$\nu_{\text{H}}/\nu_{\text{D}} = 1.39$]. The zinc deuteride, $[\kappa^3\text{-Tptm}]\text{ZnD}$, is easily prepared using PhSiD_3 in place of PhSiH_3 . It should also be noted that H/D exchange is observed when mixing $[\kappa^3\text{-Tptm}]\text{ZnD}$ with PhSiH_3 or visa versa (Scheme 7).



Scheme 7. H/D exchange between $[\kappa^3\text{-Tptm}]\text{ZnD}$ with PhSiH_3 .

The zinc methyl counterpart, $[\kappa^3\text{-Tptm}]\text{ZnMe}$ (Figure 11), has also been synthesized using the same methodology as the $\text{Zn}[\text{N}(\text{SiMe}_3)_2]_2$ reaction, *via* the reaction of $[\text{Tptm}]\text{H}$ with dimethylzinc, Me_2Zn . $[\kappa^3\text{-Tptm}]\text{ZnMe}$ has a distorted tetrahedral geometry similar to that of $[\kappa^3\text{-Tptm}]\text{ZnH}$. For example, the C-Zn-H bond angle is $132(1)^\circ$ while the C-Zn-CH₃ bond angle is $135.8(1)^\circ$ and $134.1(1)^\circ$ for two different crystalline forms that is noticeably greater than the tetrahedral value of 109.5° . $[\kappa^3\text{-Tptm}]\text{ZnH}$ and $[\kappa^3\text{-Tptm}]\text{ZnMe}$ both retain their κ^3 -coordination in solution as observed by using variable temperature ^1H NMR spectroscopy (Figure 9 and Figure 12). Analysis of the spectra gives the kinetics data listed in Table 1, from which the Eyring plots for $[\kappa^3\text{-Tptm}]\text{ZnH}$ and $[\kappa^3\text{-Tptm}]\text{ZnMe}$ (Figure 10 and Figure 13, respectively) give the activation parameters listed in Table 2. As mentioned for $[\kappa^3\text{-Tptm}]\text{ZnN}(\text{SiMe}_3)_2$, the positive entropy of activation suggests a transition state with more disorder, implying a dissociative mechanism. At this point, it is worth noting that the $[\text{Tptm}]$ ligand can have two coordination modes; two or three pyridyl arms can coordinate to the metal center, namely κ^3 - of κ^4 - coordination, respectively (see section 1.5).

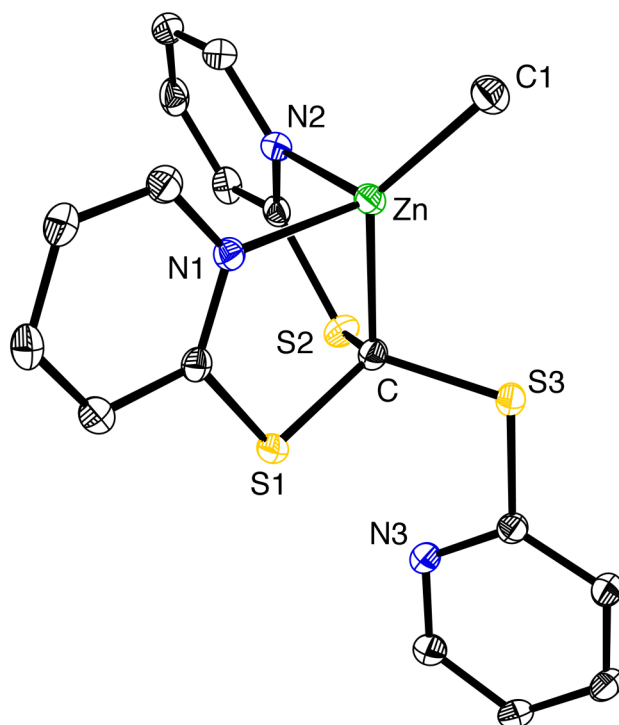


Figure 11. Molecular structure of $[\kappa^3\text{-Tptm}]\text{ZnMe}$.

While $[\kappa^3\text{-Tptm}]\text{ZnMe}$ is easily prepared, it has not been utilized much as a precursor to other compounds due to its lack of selective reactivity; the Zn-Me moiety and the carbon-zinc bond of the [Tptm] ligand both react with electrophiles. As such, $[\kappa^3\text{-Tptm}]\text{ZnH}$ and $[\kappa^3\text{-Tptm}]\text{ZnN}(\text{SiMe}_3)_2$ have been utilized to a much greater extent for the synthesis of a variety of [Tptm]ZnX compounds (*vide infra*).

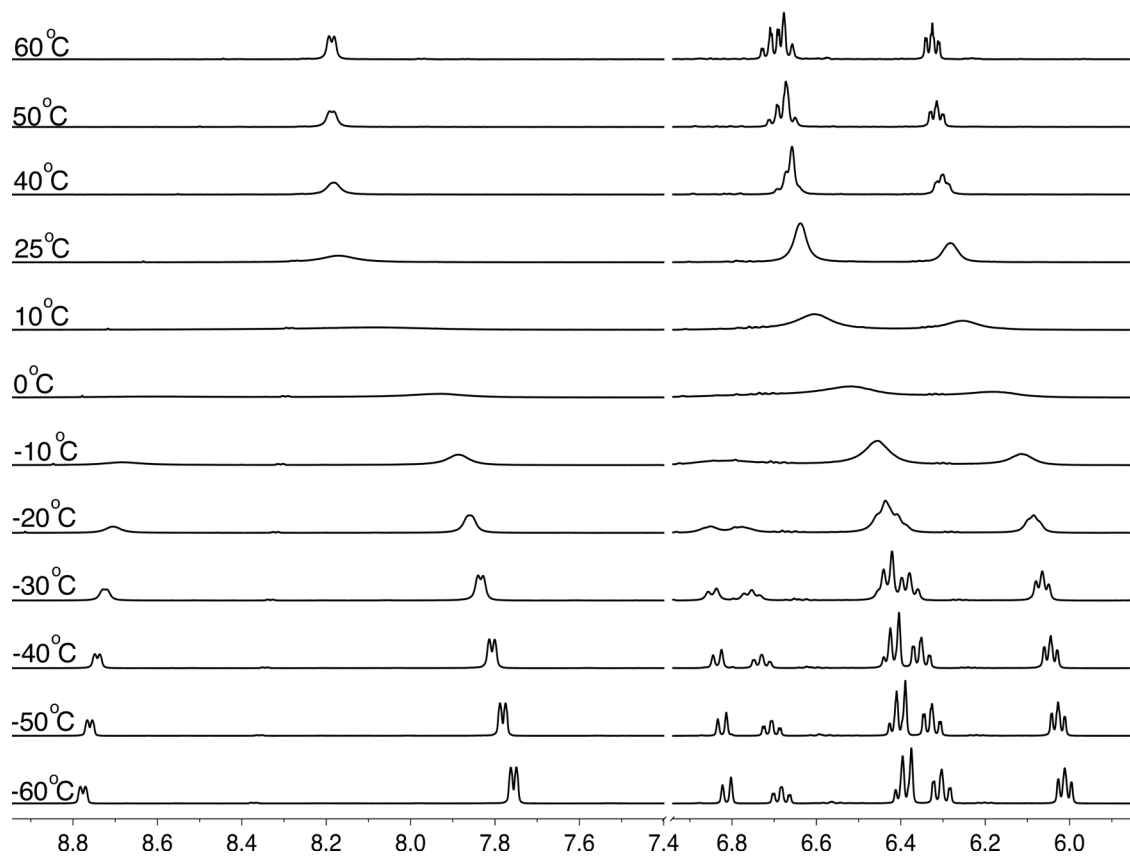


Figure 12. Variable temperature ¹H NMR spectroscopy of [κ³-Tptm]ZnMe (only aromatic region shown for clarity).

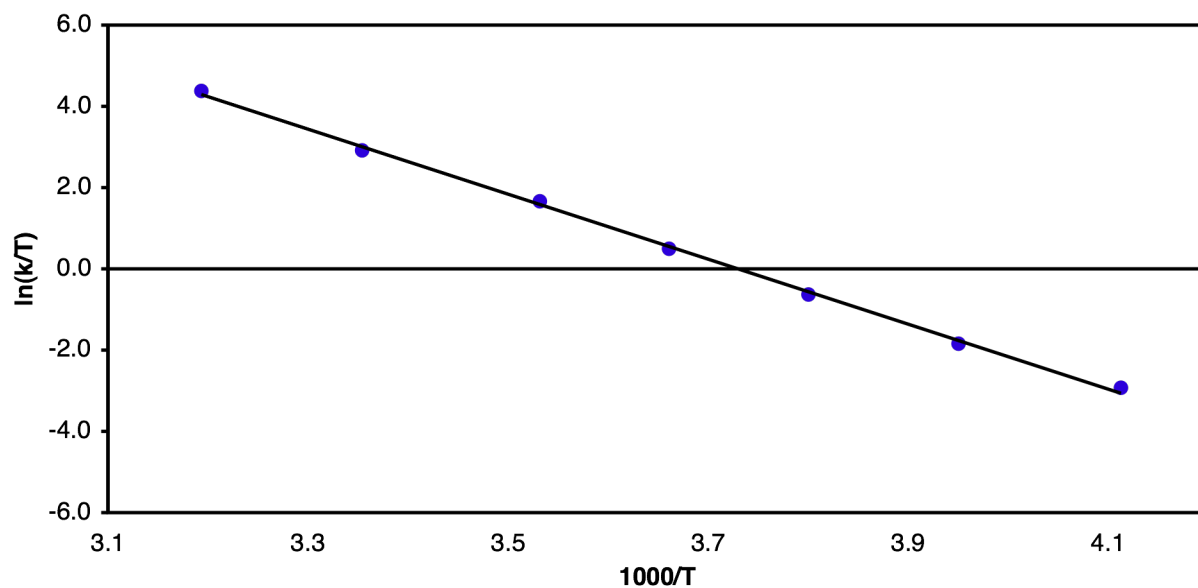


Figure 13. Eyring plot for the exchange process occurring in toluene for [κ³-Tptm]ZnMe.

Table 1. Rate constants (s^{-1}) at various temperatures derived from gNMR²³ for the exchange process occurring in toluene.

Temperature	Rate constants (s^{-1})		
	$[\kappa^3\text{-Tptm}]\text{ZnN}(\text{SiMe}_3)_2$	$[\kappa^3\text{-Tptm}]\text{ZnH}$	$[\kappa^3\text{-Tptm}]\text{ZnMe}$
+40°C	20,000	–	25,000
+25°C	4,500	5,000	5,500
+10°C	–	–	1,500
0°C	320	550	450
-10°C	80	150	140
-20°C	18	30	40
-30°C	5	13	13

Table 2. Activation parameters determined from Eyring plots for the exchange process occurring in toluene.^a

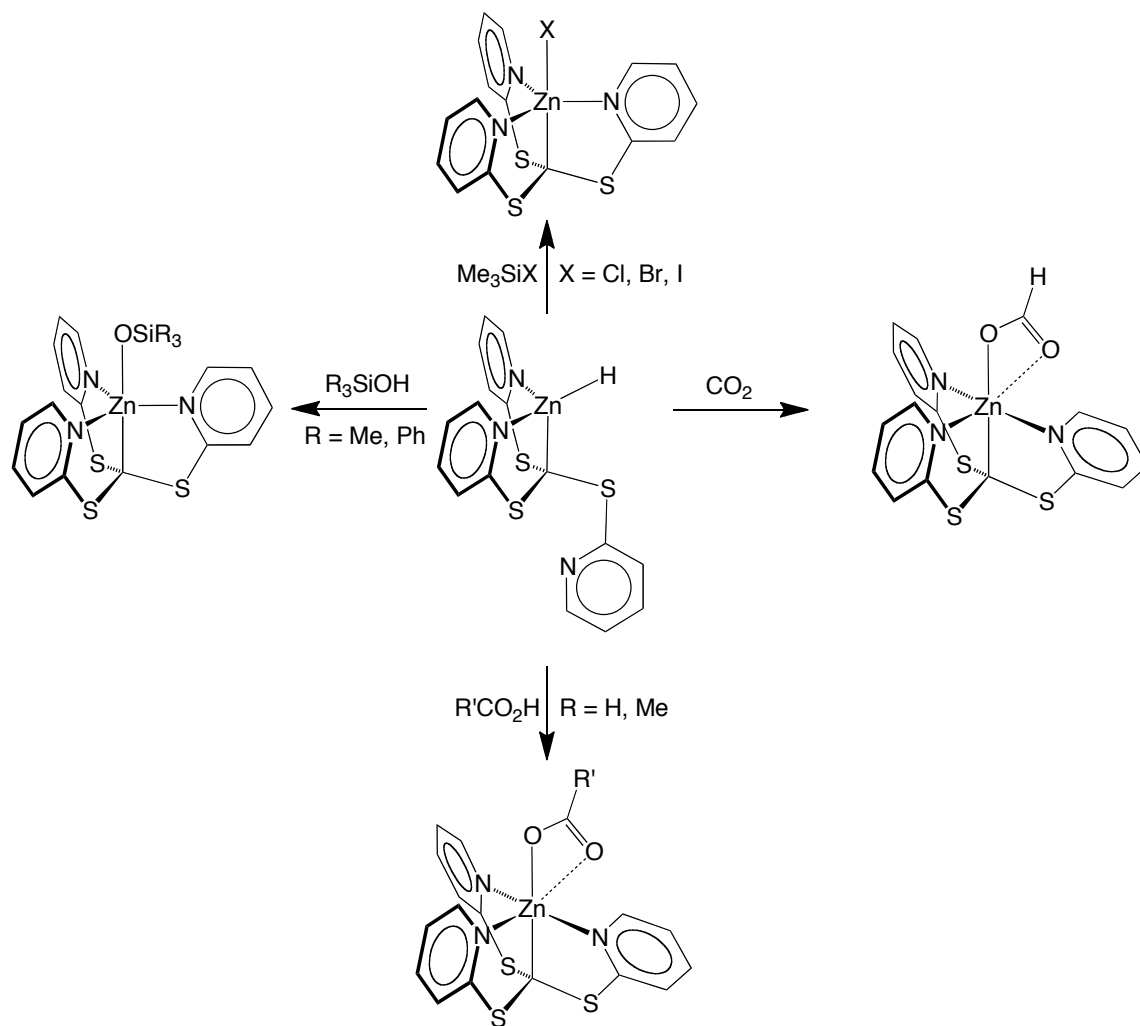
Compound	ΔH^\ddagger (kcal mol ⁻¹)	ΔS^\ddagger e.u.	$\Delta G^\ddagger_{298\text{K}}$ (kcal mol ⁻¹)
$[\kappa^3\text{-Tptm}]\text{ZnN}(\text{SiMe}_3)_2$	17.5 ± 0.7	17.0 ± 3	12.5
$[\kappa^3\text{-Tptm}]\text{ZnH}$	15.7 ± 2.8	11.0 ± 10	12.4
$[\kappa^3\text{-Tptm}]\text{ZnMe}$	15.9 ± 0.7	12.0 ± 3	12.3

^a Least-squares error limits associated with the analysis are within a 95% confidence interval.

1.3.2 Reactivity of $[\kappa^3\text{-Tptm}]\text{ZnH}$ and related compounds

$[\kappa^3\text{-Tptm}]\text{ZnH}$ serves as a precursor to a variety of other $[\text{Tptm}]\text{ZnX}$ derivatives, as illustrated in Scheme 8. For example, the zinc hydride bond of $[\kappa^3\text{-Tptm}]\text{ZnH}$ (*i*) is protolytically cleaved by R_3SiOH ($\text{R} = \text{Me}, \text{Ph}$) to give $[\kappa^4\text{-Tptm}]\text{ZnOSiR}_3$, (*ii*) is

protolytically cleaved by $R'CO_2H$ to give $[\kappa^4\text{-Tp}tm]\text{ZnO}_2\text{CR}'$ ($R' = \text{H, Me}$), and (iii) undergoes metathesis with Me_3SiX ($X = \text{Cl, Br, I}$) to give $[\kappa^4\text{-Tp}tm]\text{ZnX}$.¹³ Depicted in Figure 14 is the molecular structure of $[\kappa^4\text{-Tp}tm]\text{ZnO}_2\text{CMe}$.



Scheme 8. Reactivity of $[\kappa^3\text{-Tp}tm]\text{ZnH}$.

Of most note, $[\kappa^3\text{-Tp}tm]\text{ZnH}$ reacts rapidly with CO_2 *via* an insertion reaction to give the formate complex, $[\kappa^4\text{-Tp}tm]\text{ZnO}_2\text{CH}$ ²⁴ (Figure 15). The facile reactivity of $[\kappa^3\text{-Tp}tm]\text{ZnH}$ towards CO_2 is in contrast to the $[\text{Tp}^{\text{Bu}t}]\text{ZnH}$ complex, which only reacts with CO_2 at 50 °C. Such reactivity towards CO_2 is of specific interest in view of the fact

that formate species, which presumably arise from zinc hydride species, are proposed intermediates in the ZnO and Cu/ZnO catalyzed synthesis of methanol.¹⁰ It is important to note that the insertion of CO₂ into zinc-hydride bonds is not well preceded. The only other examples involving monomeric zinc hydride complexes pertain to [Tp^R]ZnH derivatives. It should be noted that regeneration of [κ³-Tptm]ZnH from [κ⁴-Tptm]ZnO₂CH would result in catalytic CO₂ functionalization (See chapter 5). Furthermore, if reduction of the formate group to formaldehyde, methanol or methane could be achieved, this would be useful for (i) chemical transformations and (ii) fuel.

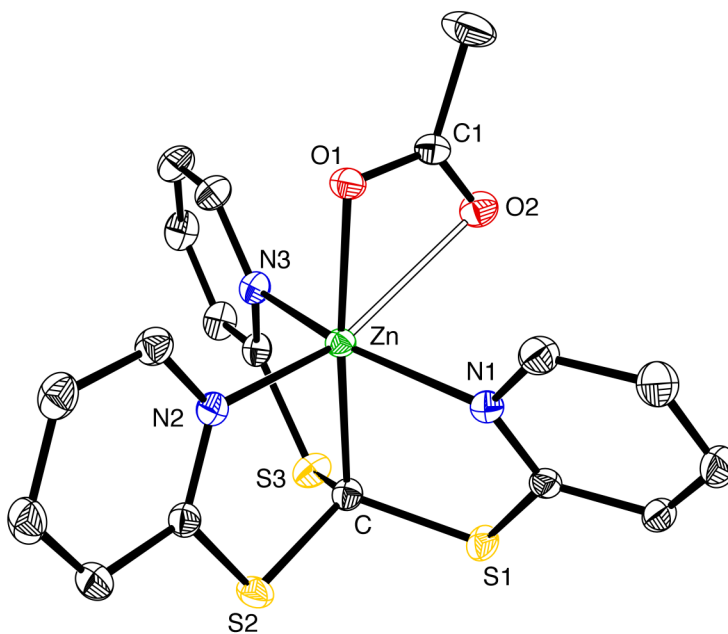


Figure 14. Molecular structure of [κ⁴-Tptm]ZnO₂CMe.

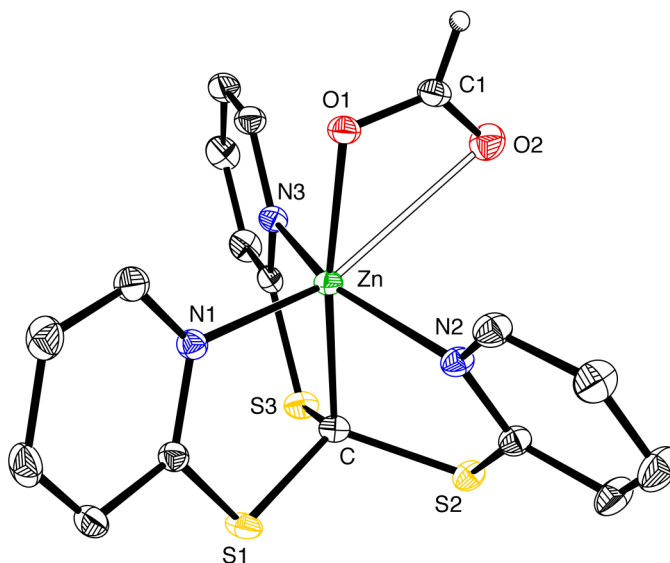
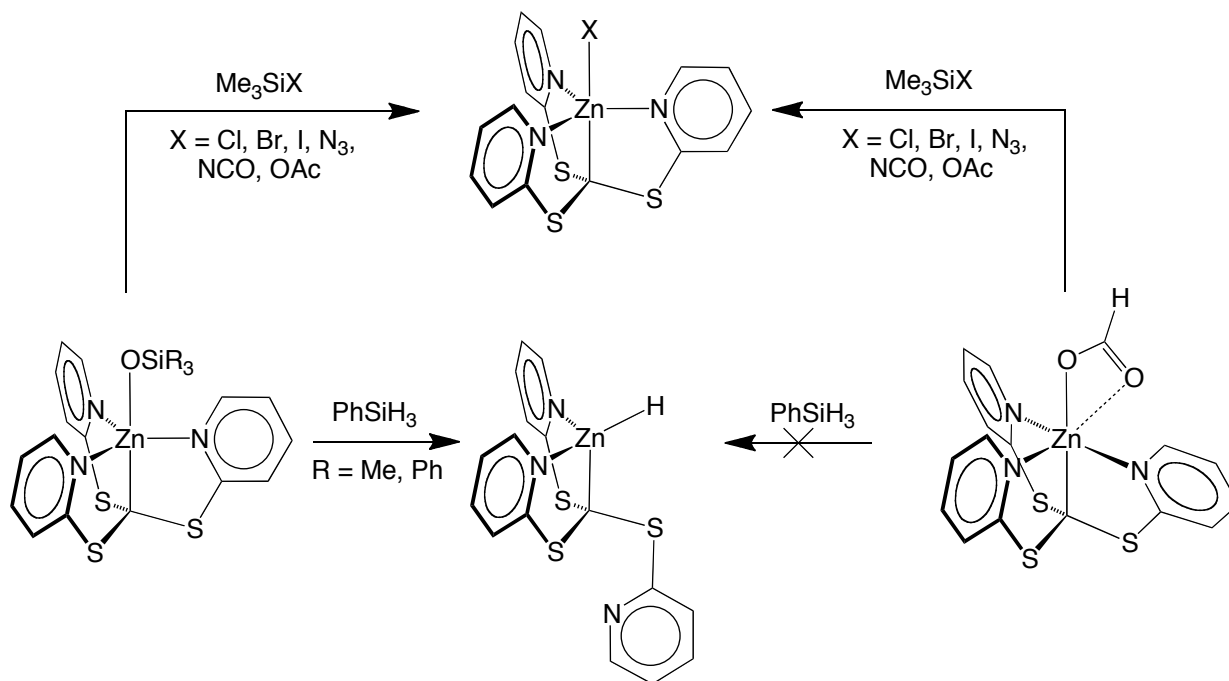


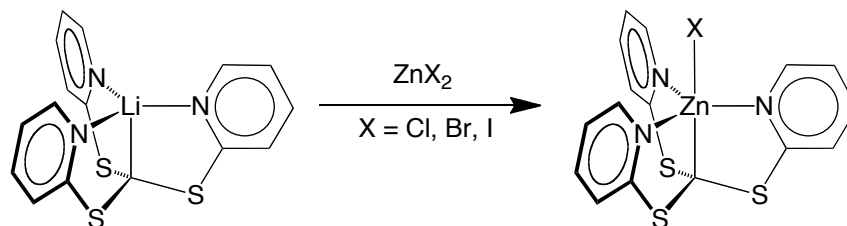
Figure 15. Molecular structure of $[\kappa^4\text{-Tptm}]\text{ZnO}_2\text{CH}$.

Both the formate and siloxide derivatives, $[\kappa^4\text{-Tptm}]\text{ZnO}_2\text{CH}$ and $[\kappa^4\text{-Tptm}]\text{ZnOSiR}_3$ ($\text{R} = \text{Me}, \text{Ph}$), can be converted to a variety of other $[\kappa^4\text{-Tptm}]\text{ZnX}$ derivatives upon treatment with Me_3SiX ($\text{X} = \text{Cl}, \text{Br}, \text{I}, \text{N}_3, \text{NCO}, \text{OAc}$), as illustrated in Scheme 9. The halide compounds, $[\kappa^4\text{-Tptm}]\text{ZnX}$ ($\text{X} = \text{Cl}, \text{Br}, \text{I}$) may also be synthesized *via* the reaction of $[\kappa^4\text{-Tptm}]\text{Li}$ with ZnX_2 (Scheme 10), however, the former reaction with Me_3SiX is preferred due to ease of preparation. The halides are produced rapidly when employing Me_3SiX ($\text{X} = \text{Cl}, \text{Br}, \text{I}$), with all byproducts being volatile liquids which are easily removed. On the other hand, the reaction between $[\kappa^4\text{-Tptm}]\text{Li}$ with ZnX_2 results in a mixture of $[\text{Tptm}]\text{H}$, $[\kappa^4\text{-Tptm}]\text{ZnX}$ and LiX .



Scheme 9. Reactivity of $[\kappa^4\text{-Tptm}]\text{ZnOSiMe}_3$ and $[\kappa^4\text{-Tptm}]\text{ZnO}_2\text{CH}$.

It should be noted that the reaction of $[\kappa^4\text{-Tptm}]\text{ZnO}_2\text{CH}$ with Me_3SiOAc to give $[\kappa^4\text{-Tptm}]\text{ZnOAc}$ and $\text{Me}_3\text{SiO}_2\text{CH}$ does not go to completion due to the establishment of an equilibrium which has been studied using ^1H NMR spectroscopy. However, both $[\kappa^4\text{-Tptm}]\text{ZnO}_2\text{CH}$ and $[\kappa^4\text{-Tptm}]\text{ZnOAc}$ may be prepared in pure form *via* the reaction of $[\kappa^3\text{-Tptm}]\text{ZnMe}$ or $[\kappa^3\text{-Tptm}]\text{ZnH}$ with formic acid and acetic acid, respectively (Scheme 11).



Scheme 10. Reaction of $[\kappa^4\text{-Tptm}]\text{Li}$ with ZnX_2 to give $[\kappa^4\text{-Tptm}]\text{ZnX}$ ($\text{X} = \text{Cl, Br, I}$).

While there is a reaction between $[\kappa^4\text{-Tptm}]\text{ZnOSiR}_3$ ($R = \text{Me, Ph}$) and PhSiH_3 to produce the hydride complex, $[\kappa^3\text{-Tptm}]\text{ZnH}$, there is no reaction between $[\kappa^4\text{-Tptm}]\text{ZnO}_2\text{CH}$ or $[\kappa^4\text{-Tptm}]\text{ZnOAc}$ with PhSiH_3 . A catalytic cycle can be envisioned for the reaction between PhSiH_3 and R_3SiOH to generate a siloxane and H_2 , where the two catalytic intermediates are $[\kappa^3\text{-Tptm}]\text{ZnH}$ and $[\kappa^4\text{-Tptm}]\text{ZnOSiR}_3$ (see Chapter 5). Catalysts that are able to perform silane-alcohol coupling are of interest for H_2 production.

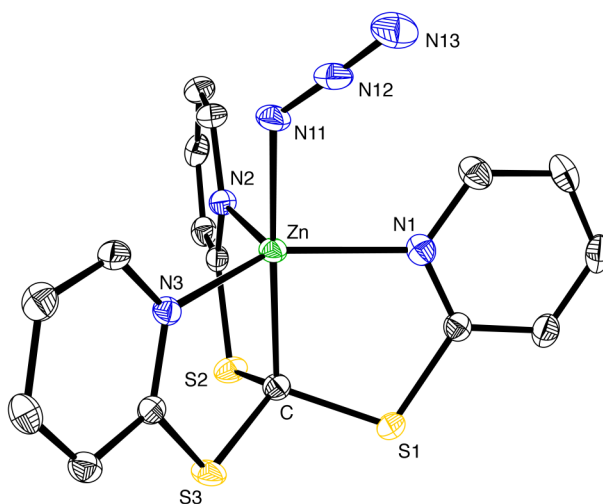
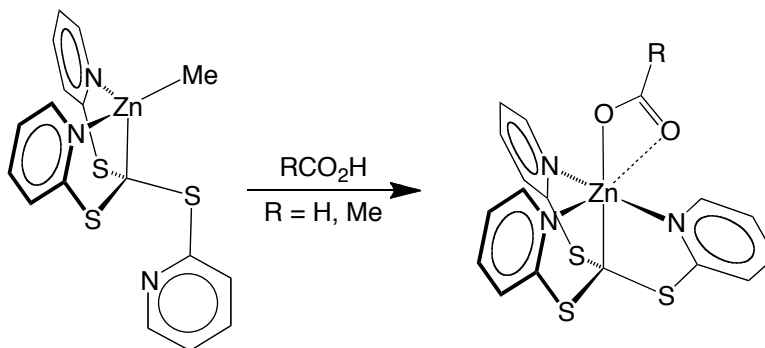


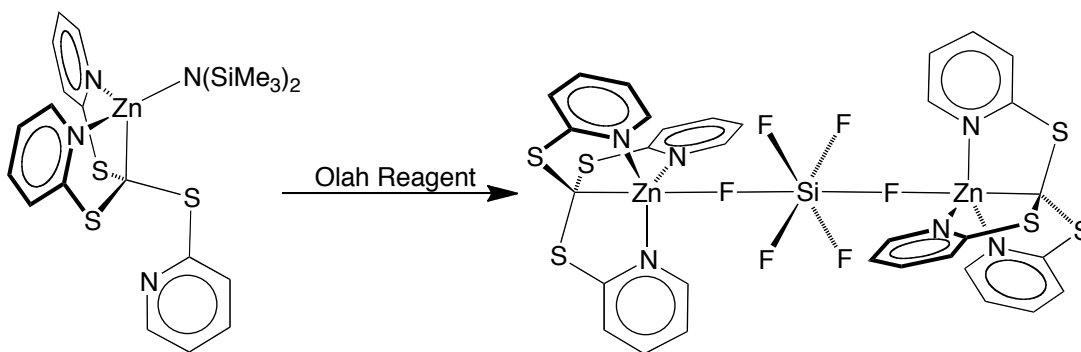
Figure 16. Molecular structure of $[\kappa^4\text{-Tptm}]\text{ZnN}_3$.

$[\kappa^3\text{-Tptm}]\text{ZnH}$ cannot be converted directly to $[\kappa^4\text{-Tptm}]\text{ZnN}_3$ or $[\kappa^4\text{-Tptm}]\text{ZnNCO}$ using the respective Me_3SiX reagents due to a competing insertion reaction, which results in a mixture of products. However, conversion of $[\kappa^3\text{-Tptm}]\text{ZnH}$ to either $[\kappa^4\text{-Tptm}]\text{ZnOSiR}_3$ ($R = \text{Me, Ph}$) or $[\kappa^4\text{-Tptm}]\text{ZnO}_2\text{CH}$ followed by reaction with Me_3SiN_3 or Me_3SiNCO allows for the conversion of $[\kappa^3\text{-Tptm}]\text{ZnH}$ to $[\kappa^4\text{-Tptm}]\text{ZnN}_3$ or $[\kappa^4\text{-Tptm}]\text{ZnNCO}$, respectively, in two steps.



Scheme 11. Production of $[\kappa^4\text{-Tptm}]\text{ZnO}_2\text{CH}$ and $[\kappa^4\text{-Tptm}]\text{ZnOAc}$ from $[\kappa^3\text{-Tptm}]\text{ZnMe}$.

In order to complete the halide series, several attempts were made to synthesize the fluoride complex, $[\text{Tptm}]\text{ZnF}$. ZnF_2 did not react with $[\text{Tptm}]\text{Li}$ or $[\text{Tptm}]\text{MgX}$ ($\text{X} = \text{Br}, \text{I}$) to give $[\text{Tptm}]\text{ZnF}$, which is presumably due to the insolubility of ZnF_2 . Silane reagents were not attempted due to the strong Si-F bond. Treatment of $[\kappa^3\text{-Tptm}]\text{ZnN}(\text{SiMe}_3)_2$ with hydrofluoric acid-pyridine (Olah Reagent), was then attempted to produce the fluoride complex. While this reaction did result in the cleavage of the Zn-N bond to give a Zn-F bond, concomitant reaction with the Lewis acid, SiF_4 (presumably generated from reaction of HF with the glassware) resulted in the formation of $\{[\kappa^4\text{-Tptm}]\text{ZnF}\}_2\text{SiF}_4$ (Scheme 12 and Figure 17).



Scheme 12. Reaction of $[\kappa^3\text{-Tptm}]\text{ZnN}(\text{SiMe}_3)_2$ with $\text{HF}\cdot\text{pyridine}$.

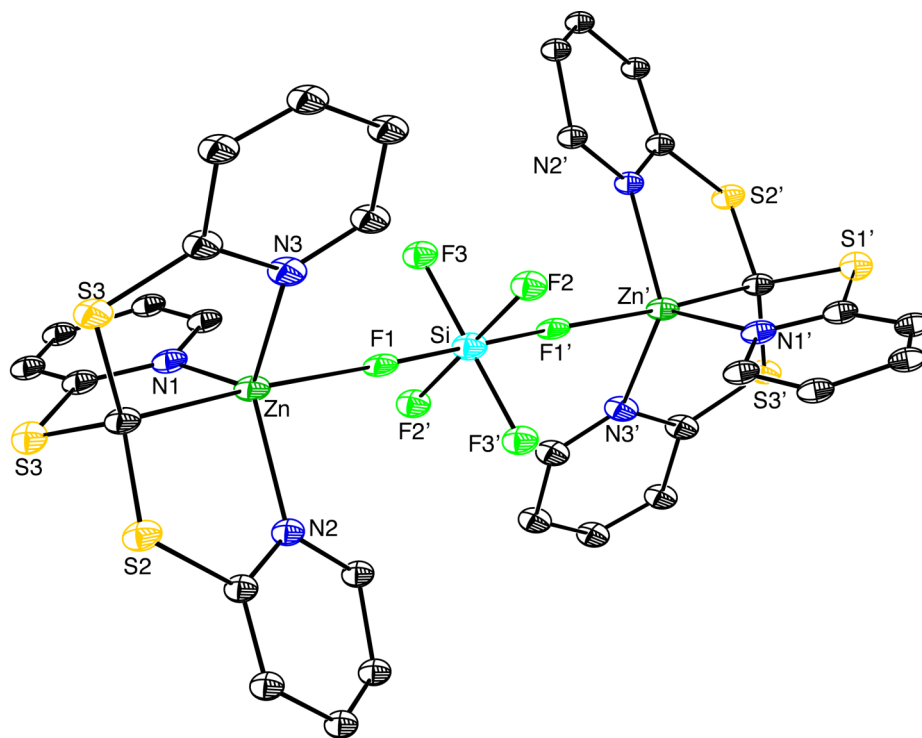
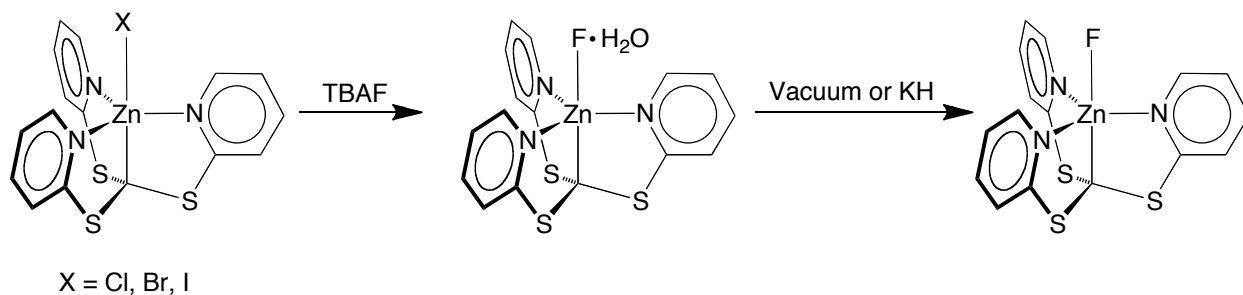


Figure 17. Molecular structure of $\{[\kappa^4\text{-Tptm}]\text{ZnF}\}_2\text{SiF}_4$.

Halide exchange between $[\kappa^4\text{-Tptm}]\text{ZnX}$ ($X = \text{Cl}, \text{Br}, \text{I}$) and tetrabutylammonium fluoride (TBAF) worked well to give $[\kappa^4\text{-Tptm}]\text{ZnF}\cdot\text{H}_2\text{O}$ as a crystalline solid. The water molecule, which is derived from the wet TBAF, is hydrogen bonded to the fluoride ligand as shown in Figure 18. $[\kappa^4\text{-Tptm}]\text{ZnF}\cdot\text{H}_2\text{O}$ may be converted to $[\kappa^4\text{-Tptm}]\text{ZnF}$ by either (i) treatment with KH or (ii) by removal of the water from $[\kappa^4\text{-Tptm}]\text{ZnF}\cdot\text{H}_2\text{O}$ by evaporation *in vacuo* (Scheme 13).



Scheme 13. Synthesis of $[\kappa^4\text{-Tptm}]\text{ZnF}$.

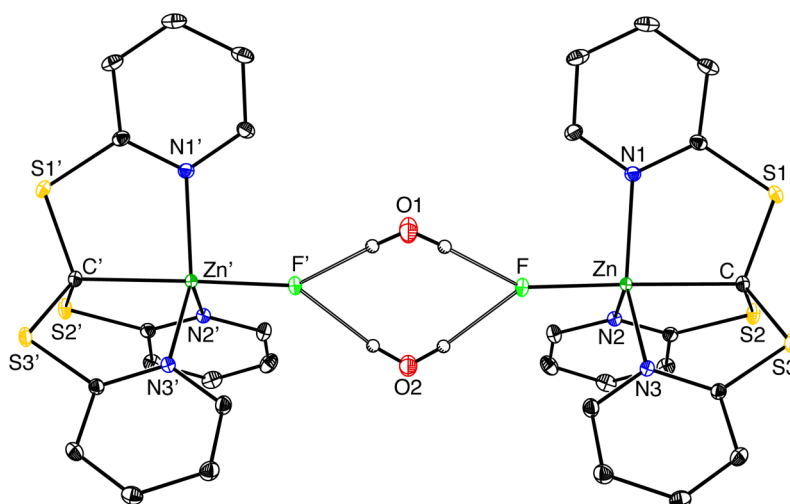


Figure 18. Molecular structure of $[\kappa^4\text{-Tptm}]\text{ZnF}\cdot\text{H}_2\text{O}$ (hydrogen bonded dimer shown).

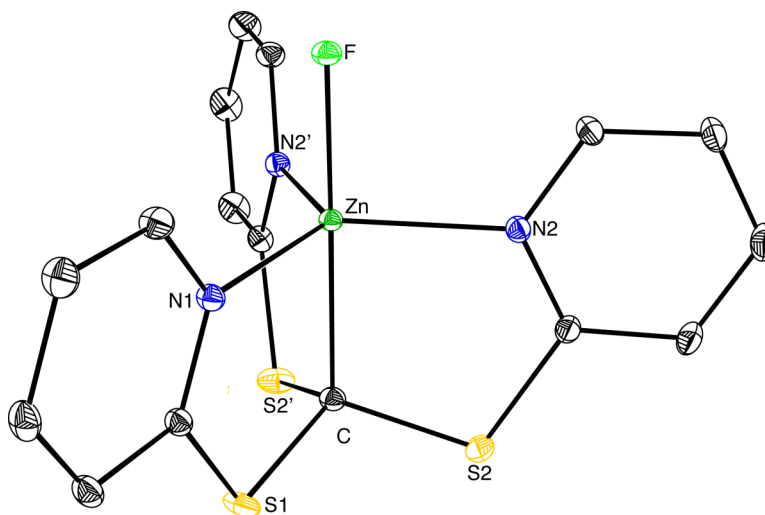
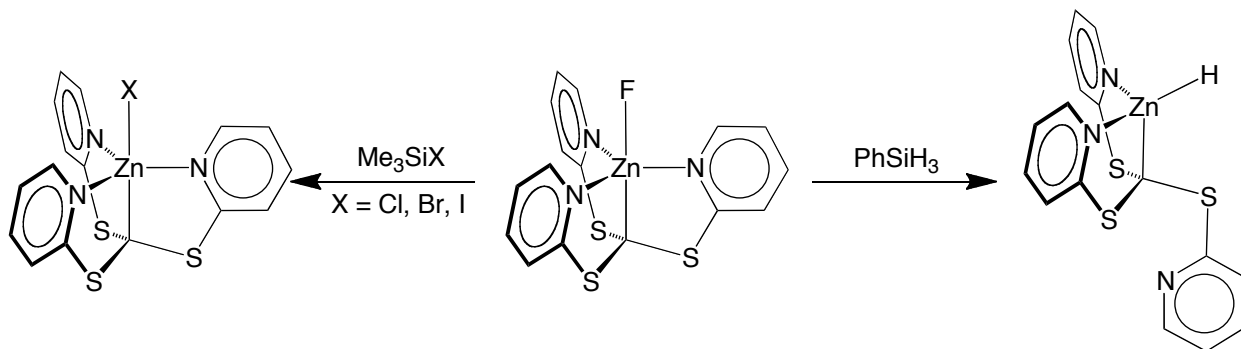


Figure 19. Molecular structure of $[\kappa^4\text{-Tptm}]\text{ZnF}$.

The molecular structure of $[\kappa^4\text{-Tptm}]\text{ZnF}$ has also been determined by X-ray diffraction (Figure 19). ^{19}F NMR spectroscopy provides evidence for hydrogen bonding for the hydrated compound in solution. Specifically, whereas $[\kappa^4\text{-Tptm}]\text{ZnF}$ has a ^{19}F signal at δ -216.7 ppm, $[\kappa^4\text{-Tptm}]\text{ZnF}\cdot\text{H}_2\text{O}$ has a deshielded resonance at δ -204.2 ppm. $[\kappa^4\text{-Tptm}]\text{ZnF}$ and $[\kappa^4\text{-Tptm}]\text{ZnF}\cdot\text{H}_2\text{O}$ provide two well-defined examples of

monomeric zinc fluoride compounds, which are not common due to the propensity of the fluoride ligand to bridge multiple zinc centers,²⁵ the same tendency that has been observed with hydride ligands. There are only four terminal zinc fluoride compounds listed in the CSD.²⁶

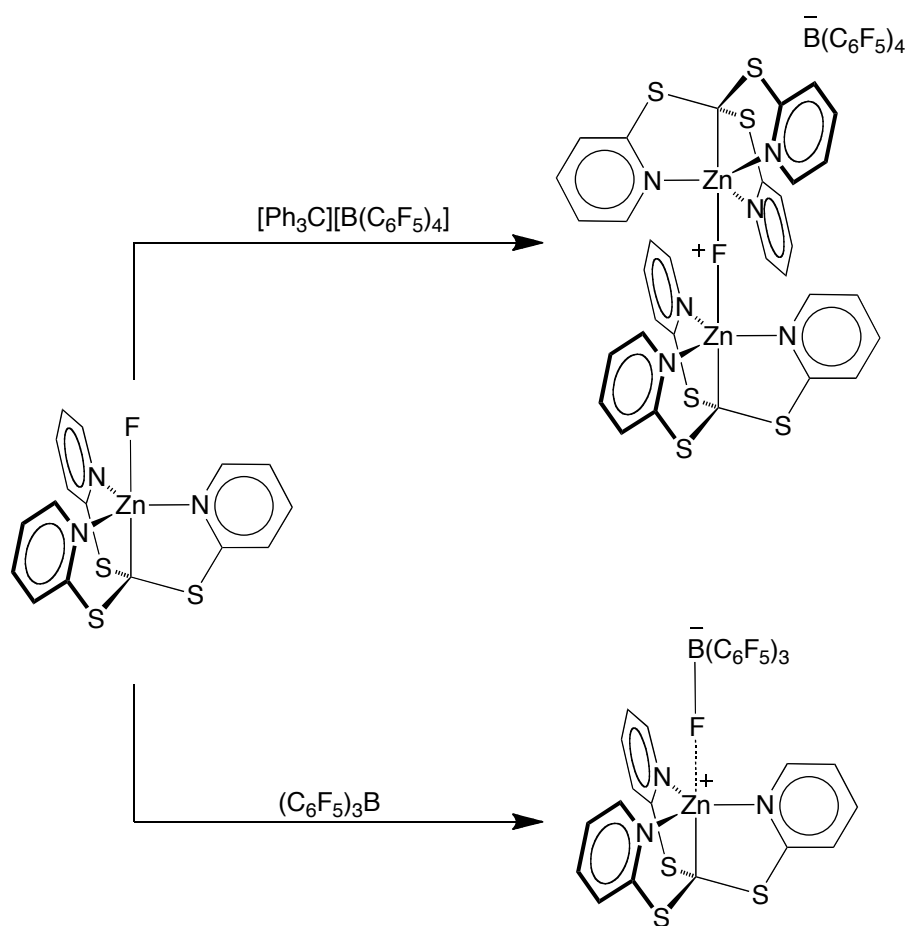
$[\kappa^4\text{-Tptm}]\text{ZnF}$, like $[\kappa^3\text{-Tptm}]\text{ZnH}$, also exhibits diverse reactivity with silane reagents, which might be expected as the formation of the Si-F bond provides a strong thermodynamic driving force. For example, $[\kappa^4\text{-Tptm}]\text{ZnF}$ reacts with (i) Me_3SiX ($\text{X} = \text{Cl, Br, I}$) to form $[\kappa^4\text{-Tptm}]\text{ZnX}$ and (ii) PhSiH_3 to form $[\kappa^3\text{-Tptm}]\text{ZnH}$. This reactivity is summarized in Scheme 14.



Scheme 14. Reactivity of $[\kappa^4\text{-Tptm}]\text{ZnF}$ with silane reagents.

We also explored the reactivity of $[\kappa^4\text{-Tptm}]\text{ZnF}$ with strong Lewis acids in order to generate a cationic $[\text{Tptm}]\text{Zn}^+$ compound *via* fluoride abstraction. For example, $[\kappa^4\text{-Tptm}]\text{ZnF}$ was treated with the powerful Lewis acids, $(\text{C}_6\text{F}_5)_3\text{B}$ and $[\text{Ph}_3\text{C}^+][(\text{C}_6\text{F}_5)_4\text{B}^-]$, resulting in fluoride abstraction and generating two distinct compounds, as depicted in Scheme 15. Specifically, application of $(\text{C}_6\text{F}_5)_3\text{B}$ to $[\kappa^4\text{-Tptm}]\text{ZnF}$ results in coordination of the boron atom to the fluorine atom but does not completely abstract the fluoride ion from $[\kappa^4\text{-Tptm}]\text{ZnF}$; instead, there is a lengthening of the Zn-F bond. In $[\kappa^4\text{-Tptm}]\text{ZnF}$, the Zn-F bond length is 1.9443(10) Å, which is considerably shorter than the Zn-F bond length in $[\kappa^4\text{-Tptm}]\text{Zn}\cdots\text{FB}(\text{C}_6\text{F}_5)_3$,

which is 2.262(3) Å. The molecular structure of $[\kappa^4\text{-Tptm}]\text{Zn}\cdots\text{FB}(\text{C}_6\text{F}_5)_3$ is presented in Figure 20. This is the first example of an adduct between $\text{B}(\text{C}_6\text{F}_5)_3$ and a zinc fluoride complex. Treatment of $[\kappa^4\text{-Tptm}]\text{ZnF}$ with $[\text{Ph}_3\text{C}^+][(\text{C}_6\text{F}_5)_4\text{B}^-]$ results in complete fluoride abstraction. However, presumably due to the high Lewis acidity of the resulting zinc cation, $[\kappa^4\text{-Tptm}]\text{Zn}^+$, an additional molecule of $[\kappa^4\text{-Tptm}]\text{ZnF}$ traps $[\kappa^4\text{-Tptm}]\text{Zn}^+$ to make the dinuclear zinc cation, namely, $\{[\kappa^4\text{-Tptm}]\text{ZnFZn}[\kappa^4\text{-Tptm}]^+\}[(\text{C}_6\text{F}_5)_4\text{B}^-]$ (Scheme 15). The Zn–F bond lengths (2.0450(6) and 2.0358(6) Å) are moderately lengthened in this complex, presumably due to the multi-center bonding. The molecular structure of $\{[\kappa^4\text{-Tptm}]\text{ZnFZn}[\kappa^4\text{-Tptm}]^+\}[(\text{C}_6\text{F}_5)_4\text{B}^-]$ is shown in Figure 21. This is the first example of a linear, two coordinate fluoride ligand between two zinc centers, where the two zinc atoms are only connected by the bridging fluoride ligand.²⁷



Scheme 15. Fluoride abstraction from [κ⁴-Tptm]ZnF using strong Lewis acids.

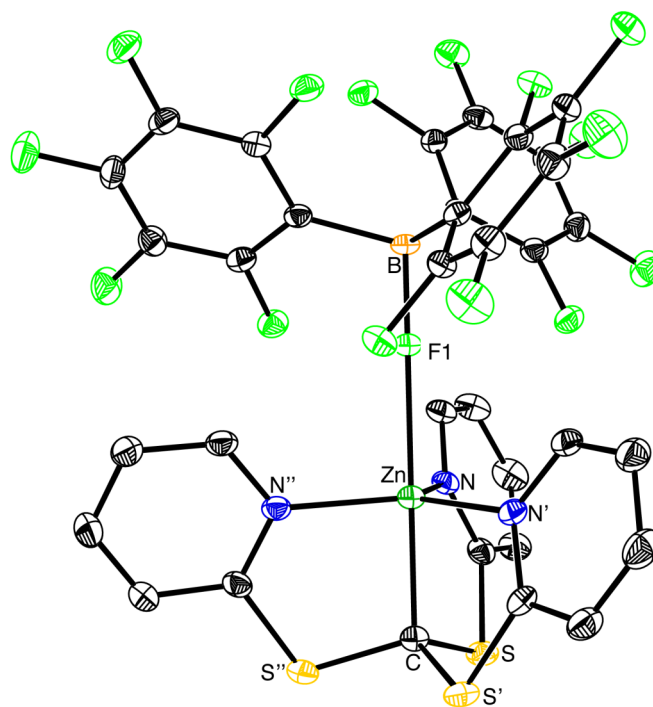


Figure 20. Molecular structure of $[\kappa^4\text{-Tptm}]\text{ZnF}\cdots\text{B}(\text{C}_6\text{F}_5)_3$ (Fluorine atoms on $\text{B}(\text{C}_6\text{F}_5)_3$ not labeled for clarity).

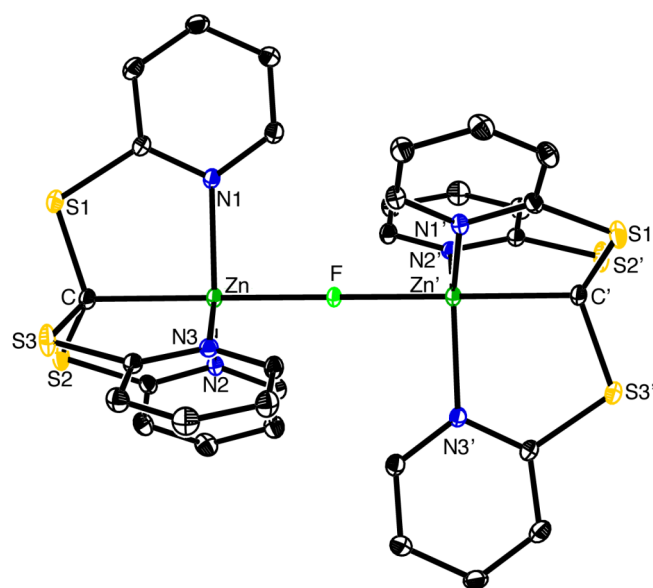
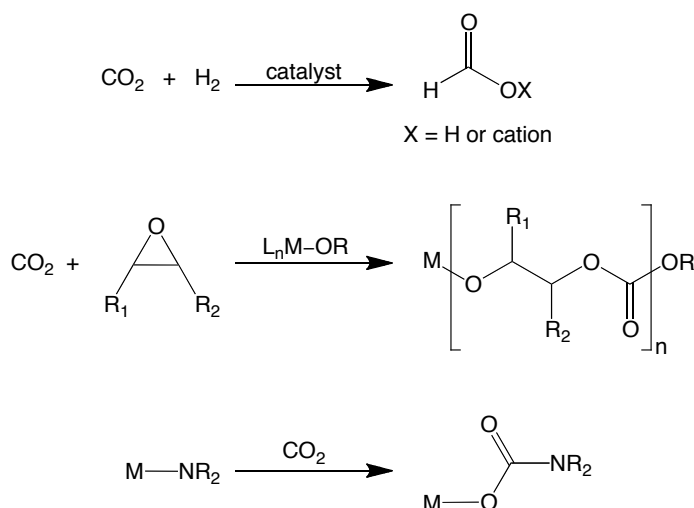


Figure 21. Molecular structure of $\{[\kappa^4\text{-Tptm}]\text{ZnFZn}[\kappa^4\text{-Tptm}]^+\}\{(\text{C}_6\text{F}_5)_4\text{B}^-\}$. Anion not shown for clarity.

In summary, the alkyl zinc hydride compound, $[\kappa^3\text{-Tptm}]\text{ZnH}$, is reactive, and is able to generate numerous other zinc compounds such as $[\kappa^4\text{-Tptm}]\text{ZnOSiR}_3$ ($R = \text{Me, Ph}$), $[\kappa^4\text{-Tptm}]\text{ZnX}$ ($X = \text{Cl, Br, I}$), and the formate complex, $[\kappa^4\text{-Tptm}]\text{ZnO}_2\text{CH}$. Additionally, $[\kappa^3\text{-Tptm}]\text{ZnH}$ is novel, as it is the first example where zinc incorporates an alkyl ligand and a hydride ligand.

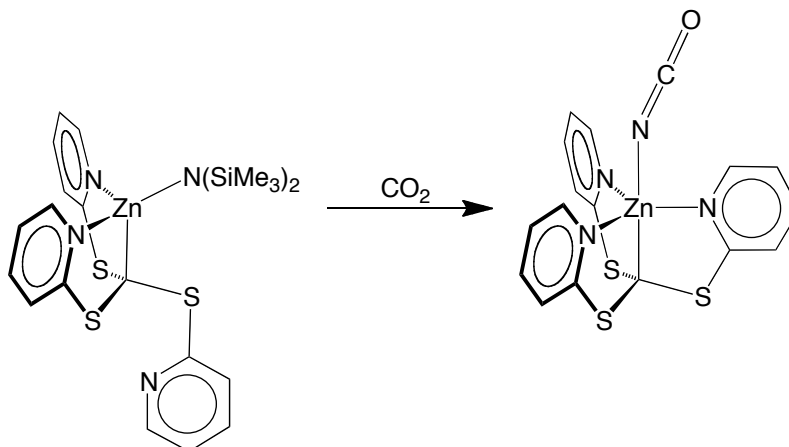
1.4 Reactivity of $[\kappa^3\text{-Tptm}]\text{ZnN}(\text{SiMe}_3)_2$ towards CO_2 and the CO_2 promoted displacement of siloxide ligands.

In addition to its role in methanol synthesis,¹⁰ there are efforts to discover other synthetic methods that employ CO_2 as a C_1 building block.²⁸ This is exemplified by (i) the metal-catalyzed hydrogenation to formic acid and formates,²⁹ and (ii) the formation of polycarbonates by copolymerization with epoxides (Scheme 16).³⁰ The reactivity of CO_2 towards transition metal compounds has, therefore, been the focus of much attention.^{28,31} For example, the insertion of CO_2 into metal amide bonds (M-NR_2) bonds to give carbamato ($\text{M-O}_2\text{CNR}_2$) derivatives has been widely studied (Scheme 16).³²



Scheme 16. CO_2 hydrogenation to formic acid or formates (top), CO_2 co-polymerization with epoxides (middle) and CO_2 insertion into metal amide bonds (bottom).

In contrast, however, there are few reports concerned with the reactivity of CO_2 towards main group amides, and even fewer reports concerned with *bis*(trimethylsilyl)amido complexes.³³ In this context, the reactivity of $[\kappa^3\text{-Tptm}]\text{ZnN}(\text{SiMe}_3)_2$ towards CO_2 was investigated. While one might expect the carbamate product, namely $[\text{Tptm}]\text{Zn}[\text{O}_2\text{CN}(\text{SiMe}_3)_2]$, formed *via* insertion of CO_2 into the Zn-N bond, the carbamate intermediate has not been observed or isolated. Instead, the final product of the reaction is the isocyanate complex, $[\kappa^4\text{-Tptm}]\text{ZnNCO}$, which has been structurally characterized by X-ray diffraction (Figure 22 and Scheme 17).



Scheme 17. Reaction of $[\kappa^3\text{-Tptm}]\text{ZnN}(\text{SiMe}_3)_2$ with CO_2 to give $[\kappa^4\text{-Tptm}]\text{ZnNCO}$.

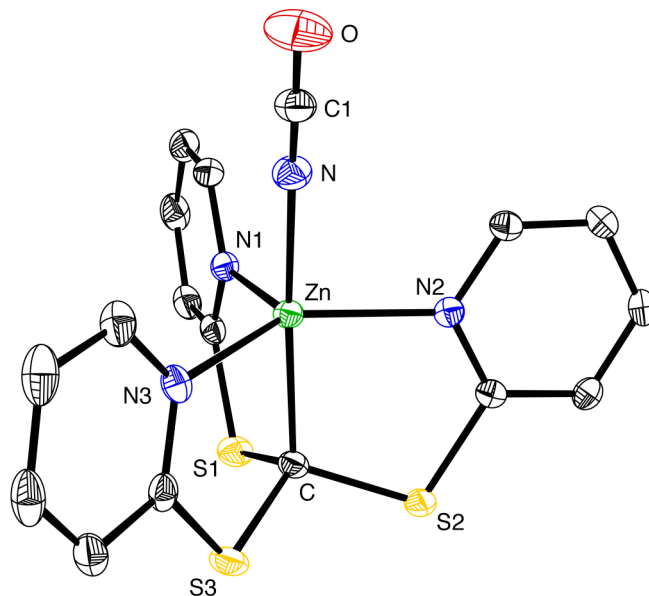
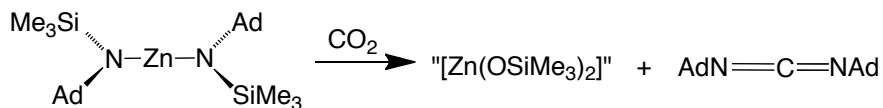


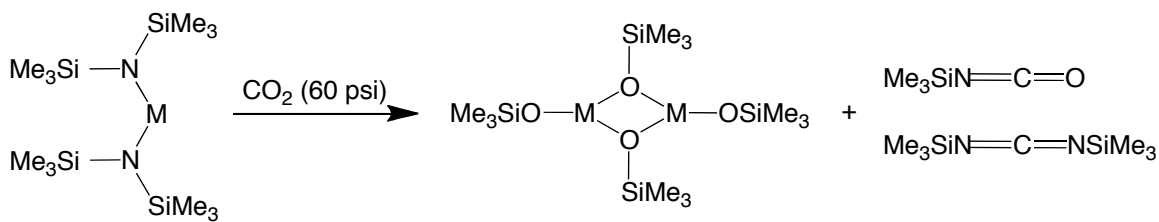
Figure 22. Molecular structure of $[\kappa^4\text{-Tptm}]\text{ZnNCO}$.

It is evident that, rather than undergoing only a simple insertion reaction of the type that is observed for many metal amide complexes,³² the reaction proceeds to deoxygenate CO_2 , a transformation that is made feasible by the formation of a strong Si-O bond.^{34,35} The formation of the isocyanate complex $[\kappa^4\text{-Tptm}]\text{ZnNCO}$ differs compared to the analogous reaction of $\text{Zn}[\text{N}(\text{SiMe}_3)(\text{Ad})]_2$ (Ad = adamantyl) with CO_2 which gives the symmetrical carbodiimide, $\text{AdN}=\text{C}=\text{NAd}$ and unidentified zinc trimethylsiloxide species.³⁶ $\text{AdN}=\text{C}=\text{NAd}$, presumably results from the reaction of the generated isocyanate, AdNCO , with $\text{Zn}[\text{N}(\text{SiMe}_3)(\text{Ad})]_2$ through a mechanism involving insertion, followed by Me_3Si migration (*i.e.* the equivalent mechanism as the CO_2 reaction, where one oxygen atom has been replaced by AdN).



Scheme 18. Reaction of $\text{Zn}[\text{N}(\text{SiMe}_3)(\text{Ad})]_2$ (Ad = adamantyl) with CO_2 .

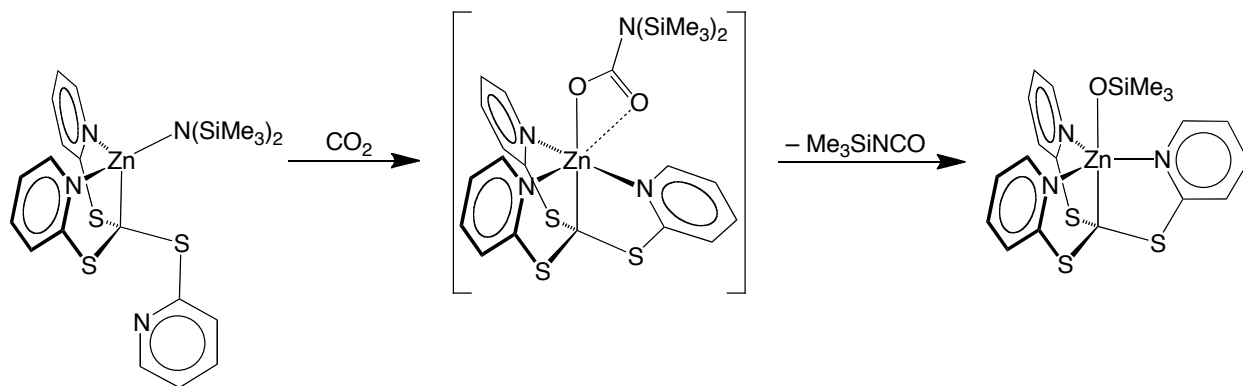
Similar reactivity with CO_2 was also observed for the *bis*(trimethylsilyl)amido complexes of tin(II) and germanium(II), namely $\text{Sn}[\text{N}(\text{SiMe}_3)_2]_2$ and $\text{Ge}[\text{N}(\text{SiMe}_3)_2]_2$, respectively. These group 14 amide complexes react with CO_2 , resulting in the formation of $\text{M}_2(\text{OSiMe}_3)_4$ ($\text{M} = \text{Sn}$ and Ge) with the generation of both the isocyanate and carbodiimide products, namely Me_3SiNCO and $\text{Me}_3\text{SiN}=\text{C}=\text{NSiMe}_3$ (Scheme 19).³⁷



Scheme 19. Reactivity of $\text{Sn}[\text{N}(\text{SiMe}_3)_2]_2$ and $\text{Ge}[\text{N}(\text{SiMe}_3)_2]_2$ with CO_2 .

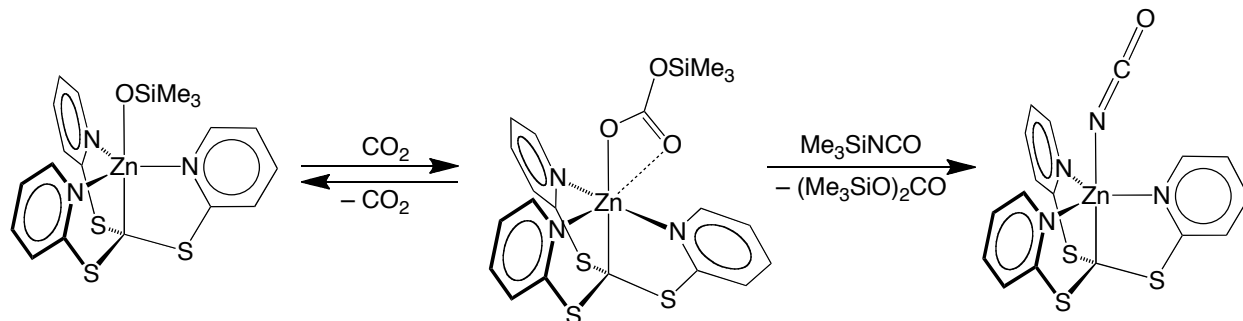
The reaction of $\text{Zn}[\text{N}(\text{SiMe}_3)_2]_2$ with CO_2 results in the formation of Me_3SiNCO and unidentified zinc trimethylsiloxide compounds, which provides evidence that the formation of $[\kappa^4\text{-Tptm}]\text{ZnNCO}$ is permitted to occur due to the incorporation of an additional ancillary ligand, namely $[\text{Tptm}]$.

The generation of $[\kappa^4\text{-Tptm}]\text{ZnNCO}$ must be a multistep reaction in which the initial step is proposed to be the insertion of CO_2 into the Zn-N bond to give $[\text{Tptm}]\text{Zn}[\text{O}_2\text{CN}(\text{SiMe}_3)_2]$. As mentioned above, this proposed intermediate has not been observed due a rapid rearrangement to the trimethylsiloxide derivative $[\kappa^4\text{-Tptm}]\text{ZnOSiMe}_3$ with the expulsion of Me_3SiNCO (Scheme 20). In support of this proposal, both $[\kappa^4\text{-Tptm}]\text{ZnOSiMe}_3$ and Me_3SiNCO are observed by ^1H NMR spectroscopy as the initial products, which decrease during the course of the reaction.



Scheme 20. Reaction of $[\kappa^3\text{-Tptm}]\text{ZnN}(\text{SiMe}_3)_2$ with CO_2 to initially generate $[\kappa^4\text{-Tptm}]\text{ZnOSiMe}_3$ and Me_3SiNCO .

Interestingly, while the simplest explanation for the formation of $[\kappa^4\text{-Tptm}]\text{ZnNCO}$ from $[\kappa^4\text{-Tptm}]\text{ZnOSiMe}_3$ and Me_3SiNCO involves direct metathesis to give hexamethyldisiloxane, $(\text{Me}_3\text{Si})_2\text{O}$, additional experiments suggest that this is *not* the operative mechanism. Specifically, independent experiments indicate that while $[\kappa^4\text{-Tptm}]\text{ZnNCO}$ is formed upon treatment of $[\kappa^4\text{-Tptm}]\text{ZnOSiMe}_3$ with Me_3SiNCO , the reaction is extremely slow by comparison to the formation of $[\text{Tptm}]\text{ZnNCO}$ upon treatment of $[\kappa^3\text{-Tptm}]\text{ZnN}(\text{SiMe}_3)_2$ with CO_2 . The formation of the isocyanate complex, $[\text{Tptm}]\text{ZnNCO}$ is, however, accelerated if CO_2 is added to a mixture of $[\kappa^4\text{-Tptm}]\text{ZnOSiMe}_3$ and Me_3SiNCO . On this basis, we propose that the formation of $[\kappa^4\text{-Tptm}]\text{ZnNCO}$ is promoted by insertion of CO_2 into the Zn-OSiMe_3 bond to give the trimethylsilyl carbonate derivative, $[\kappa^4\text{-Tptm}]\text{Zn}[\text{O}_2\text{COSiMe}_3]$, that is more susceptible towards metathesis with Me_3SiNCO compared to $[\kappa^4\text{-Tptm}]\text{ZnOSiMe}_3$ (Scheme 21).



Scheme 21. Proposed mechanism of CO_2 accelerated metathesis.

Evidence for the facile and reversible insertion of CO_2 into the Zn-OSiMe_3 bond is provided by variable temperature $^{13}\text{C}\{^1\text{H}\}$ NMR spectroscopic studies. Specifically, $[\kappa^4\text{-Tptm}]\text{Zn}[\text{O}_2\text{COSiMe}_3]$ is observed at temperatures $\leq ca. 5^\circ\text{C}$, as illustrated by a signal at $\delta 157.9$ ppm in the $^{13}\text{C}\{^1\text{H}\}$ NMR spectrum attributable to the carbonate moiety (Figure 23).

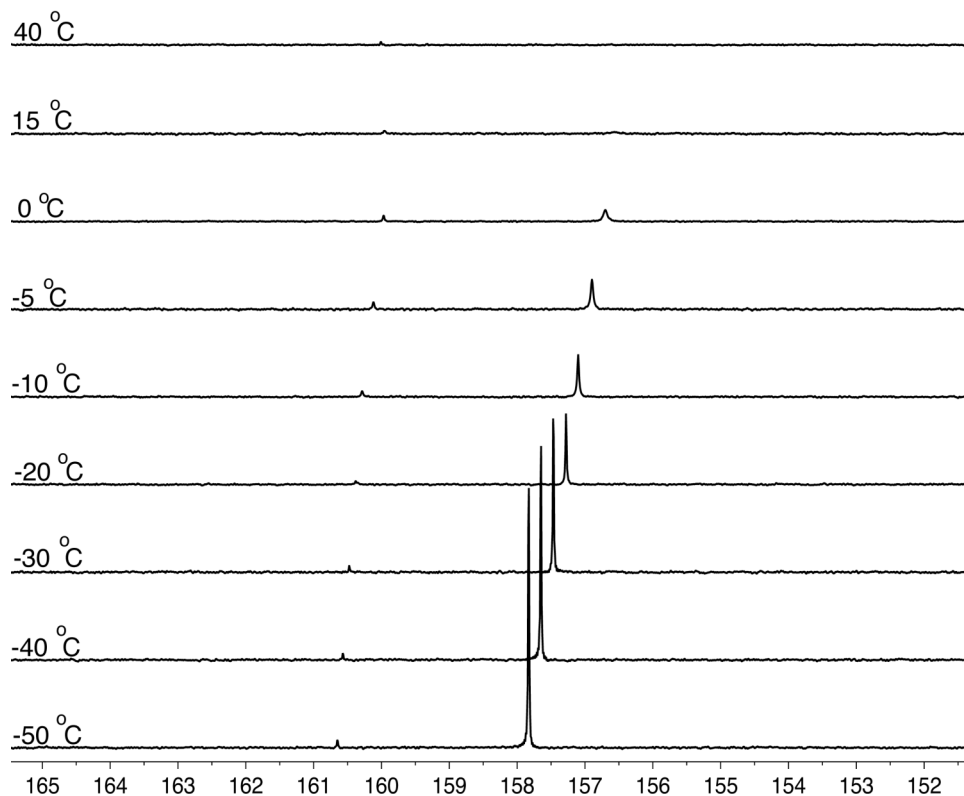
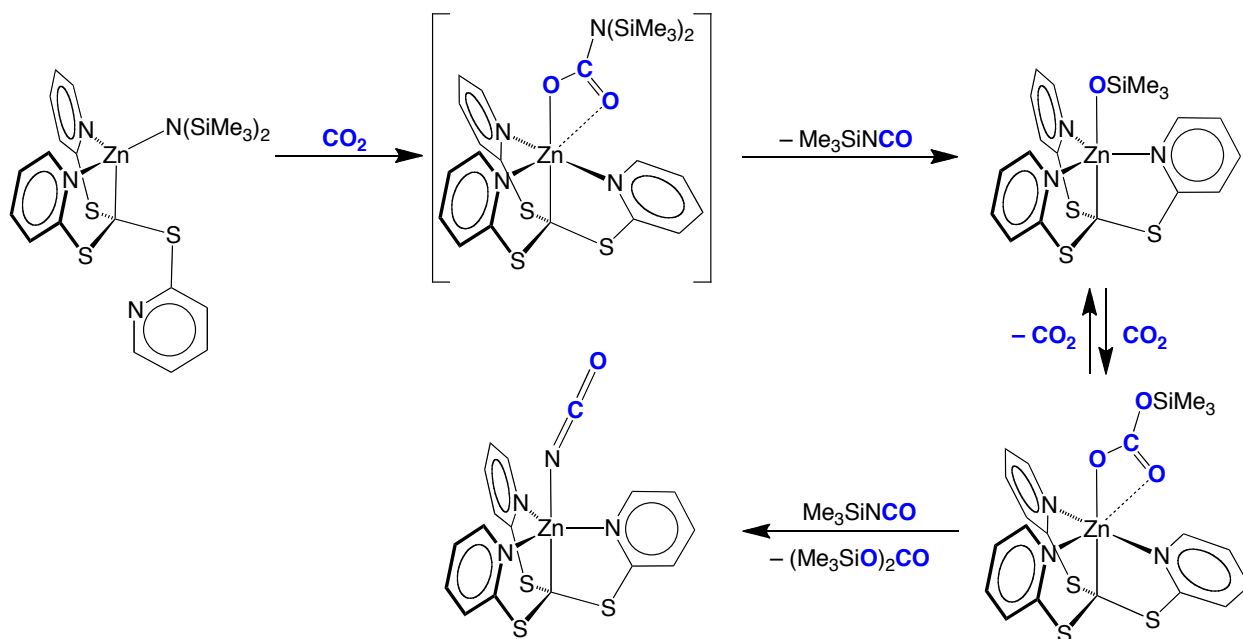


Figure 23. Variable ^{13}C NMR spectroscopic evidence for $[\kappa^4\text{-Tptm}]\text{Zn}[\text{O}_2\text{COSiMe}_3]$ using $^{13}\text{CO}_2$.

Additionally, broadening of the OSiMe₃ group is observed in the ¹H NMR spectrum at room temperature, suggesting fluxionality on the NMR timescale. Metathesis occurring between [κ⁴-Tptm]Zn[O₂COSiMe₃] and Me₃SiNCO should produce the byproduct *bis*(trimethylsilyl) carbonate, (Me₃SiO)₂CO, which has been verified by ¹H and ¹³C NMR spectroscopy, as well as mass spectrometry. Importantly, this observation is in accord with Me₃SiNCO undergoing metathesis with [κ⁴-Tptm]Zn[O₂COSiMe₃] and *not* with [κ⁴-Tptm]ZnOSiMe₃. The overall proposed mechanistic scheme is depicted in Scheme 22.



Scheme 22. Proposed mechanism for the reaction of [κ³-Tptm]ZnN(SiMe₃)₂ with CO₂. Atoms derived from CO₂ are bolded and in blue.

Depicted in Figure 24 are the ¹³C{¹H} NMR spectra of the reaction between [κ³-Tptm]ZnN(SiMe₃)₂ and ¹³CO₂. The initial spectrum shows mostly Me₃SiN¹³CO, which decreases over time as (Me₃SiO)₂¹³CO and [κ⁴-Tptm]ZnN¹³CO are formed.

$(\text{Me}_3\text{SiO})_2^{13}\text{CO}$ decomposes over time to form $(\text{Me}_3\text{Si})_2\text{O}$ and $^{13}\text{CO}_2$, which is why the $(\text{Me}_3\text{SiO})_2^{13}\text{CO}$ signal disappears.

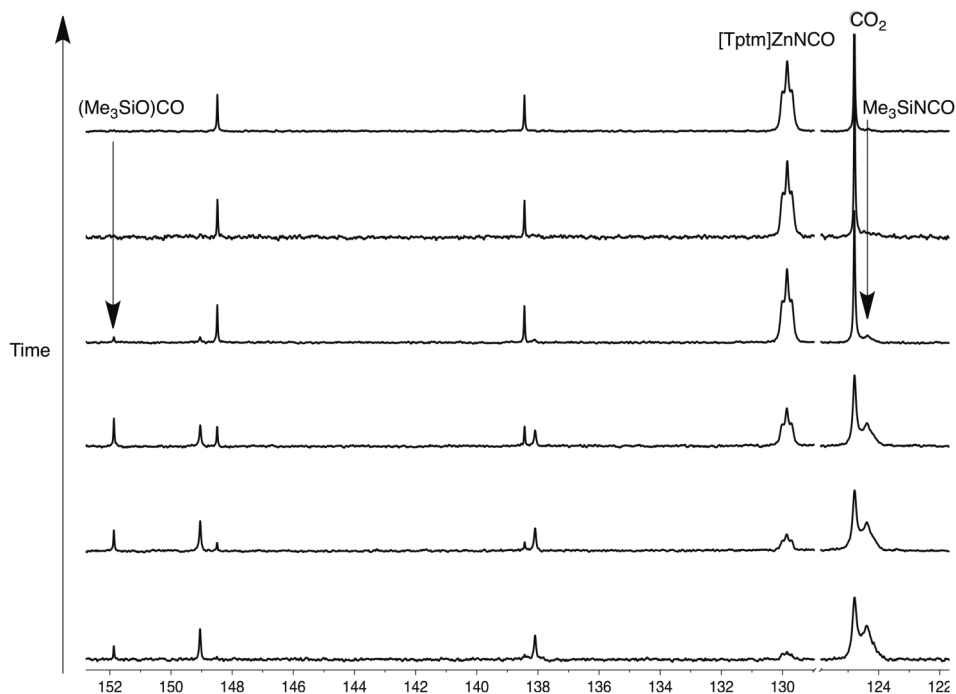


Figure 24. $^{13}\text{C}\{^1\text{H}\}$ NMR spectra of the reaction between $[\kappa^3\text{-Tptm}]\text{ZnN}(\text{SiMe}_3)_2$ and $^{13}\text{CO}_2$. The peaks that are not labeled are due to $[\text{Tptm}]$.

Two factors that may contribute to the more facile cleavage of the Zn-OC(O)OSiMe_3 bond compared to the Zn-OSiMe_3 bond are (i) insertion of the CO_2 group displaces the OSiMe_3 group from the metal center such that there is less steric hindrance around the metal center, and (ii) the presence of the C(O) group allows for a six-membered transition state differing from a four-membered transition state, which is depicted in Figure 25. In view of the ability for CO_2 to accelerate the reaction between $[\kappa^4\text{-Tptm}]\text{ZnOSiMe}_3$ and Me_3SiNCO , a variety of other Me_3SiX compounds were explored for the same type of rate enhancement. Consistent with the proposed

mechanism, a variety of Me_3SiX ($\text{X} = \text{Cl}, \text{Br}, \text{I}, \text{N}_3$) showed enhanced reactivity in the presence of CO_2 with $[\kappa^4\text{-Tptm}]\text{ZnOSiMe}_3$ to give the corresponding $[\kappa^4\text{-Tptm}]\text{ZnX}$ compound. Additionally, CO_2 -accelerated rate enhancement is also observed for the reactions of $[\kappa^4\text{-Tptm}]\text{ZnOSiPh}_3$ with Me_3SiX ($\text{X} = \text{Cl}, \text{Br}, \text{I}, \text{N}_3$).

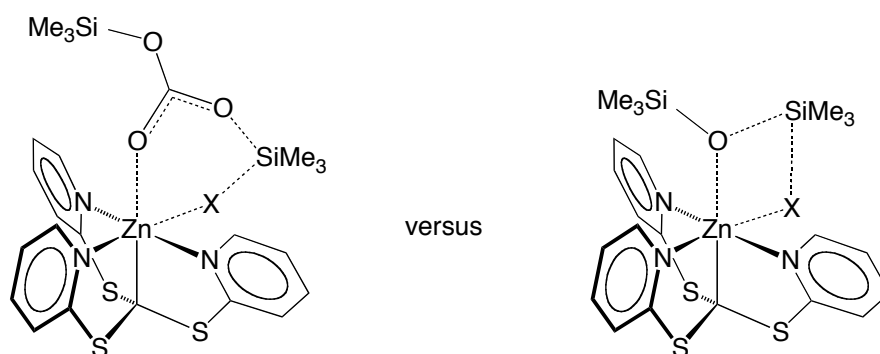


Figure 25. CO_2 accelerated metathesis (left) compared to metathesis in the absence of CO_2 (right).

The ability of CO_2 to promote the overall displacement of a siloxide ligand has implications with respect to the fact that siloxides find frequent use as ancillary ligands.³⁸ Thus, while the insertion of CO_2 into M-OSiR_3 bonds has been little investigated,^{39,40} it is evident from the above studies that the presence of CO_2 could provide a general means to enhance the reactivity of compounds with M-OSiR_3 bonds.⁴¹ In this respect, it also suggests that the presence of CO_2 could be disadvantageous for situations in which the siloxide ligand is intended to play the role of a spectator (*i.e.* as an ancillary ligand).

1.5 Ligand kapticity: A Density Functional Theory Investigation

The [Tptm] ligand has the ability to coordinate to zinc *via* two or three of its pyridyl groups, namely in a κ^3 - or κ^4 -manner, generating two structural classes of [Tptm]ZnX compounds. Specifically, κ^4 -coordination is observed in the solid state for $[\kappa^4\text{-Tptm}]\text{ZnF}$, $[\kappa^4\text{-Tptm}]\text{ZnF}\cdot\text{H}_2\text{O}$, $[\kappa^4\text{-Tptm}]\text{ZnCl}$, $[\kappa^4\text{-Tptm}]\text{ZnBr}$, $[\kappa^4\text{-Tptm}]\text{ZnI}$,

$[\kappa^4\text{-Tptm}]\text{ZnNCO}$, $[\kappa^4\text{-Tptm}]\text{ZnN}_3$, $[\kappa^4\text{-Tptm}]\text{ZnOSiMe}_3$, $[\kappa^4\text{-Tptm}]\text{ZnOSiPh}_3$, $[\kappa^4\text{-Tptm}]\text{ZnO}_2\text{CH}$ and $[\kappa^4\text{-Tptm}]\text{ZnO}_2\text{CMe}$, while κ^3 -coordination is observed for $[\kappa^3\text{-Tptm}]\text{ZnH}$ and $[\kappa^3\text{-Tptm}]\text{ZnMe}$. Low temperature ^1H NMR spectroscopic studies suggest that these coordination modes are also preserved in solution. Although all $[\text{Tptm}]\text{ZnX}$ complexes exhibit three chemically equivalent pyridyl groups at room temperature, a 2:1 pattern of peaks in the ^1H NMR emerges for $[\kappa^3\text{-Tptm}]\text{ZnH}$, $[\kappa^3\text{-Tptm}]\text{ZnMe}$ and $[\kappa^3\text{-Tptm}]\text{ZnN}(\text{SiMe}_3)_2$ at *ca.* -10°C , consistent with κ^3 -coordination (Figure 5, Figure 9 and Figure 12). In contrast, the low temperature ^1H NMR spectra of $[\kappa^4\text{-Tptm}]\text{ZnX}$ [$X = \text{F}, \text{Cl}, \text{Br}, \text{I}, \text{NCO}, \text{N}_3, \text{OSiR}_3$ ($\text{R} = \text{Me}, \text{Ph}$), $\text{O}_2\text{CMe}, \text{O}_2\text{CH}$] exhibit chemically equivalent pyridyl groups indicative of κ^4 -coordination.⁴²

While density functional theory (DFT) calculations predict that the κ^4 isomer is always more stable than the κ^3 isomer, the preference for κ^4 -coordination for monodentate X ligands increases in the sequence $\text{Me} < \text{N}(\text{SiMe}_3)_2 < \text{H} < \text{I} < \text{OSiMe}_3 < \text{Br} < \text{Cl} < \text{N}_3 < \text{NCO} < \text{F}$, as summarized in Table 3. Also listed in Table 3 is the calculated natural bond orbital (NBO) charge on zinc for the $[\kappa^3\text{-Tptm}]\text{ZnX}$ complexes.

In view of the fact that the hydride derivative adopts a κ^3 -coordination mode while the bulky triphenylsiloxide derivative adopts a κ^4 -coordination mode, it is evident that steric factors do not dominate in determining the differences in coordination. However, a consideration of $[\text{Tptm}]\text{ZnX}$ derivatives in which X is monoatomic ($X = \text{F}, \text{Cl}, \text{Br}, \text{I},$ and H), indicates that the preference for κ^4 -coordination correlates well with the electronegativity of X, a trend which suggests that κ^4 -coordination becomes more favored with increasing charge on the zinc center.⁴³ Additionally, the κ^4 -isomer becomes more stable when the NBO charge increases on zinc in the κ^3 -isomer, (Table 3).

X	$[E(\kappa^3) - E(\kappa^4)]/\text{kcal mol}^{-1}$	NBO Charge on Zn in [κ^3 -Tptm]ZnX
Me	1.382	1.516
N(SiMe ₃) ₂	2.796	1.647
H	4.329	1.441
I	6.812	1.492
OSiMe ₃	7.415	1.657
Br	9.271	1.523
Cl	9.814	1.575
N ₃	10.028	1.612
NCO	10.152	1.643
F	13.627	1.646

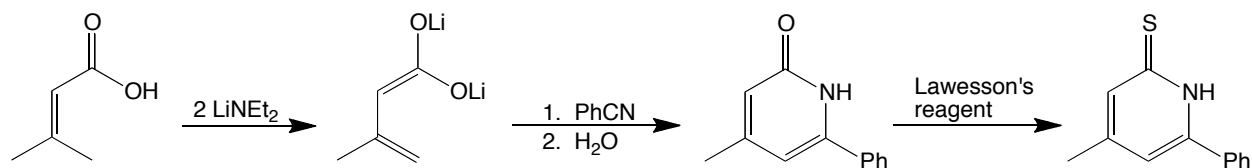
Table 3. Relative energies of κ^3 - and κ^4 -isomers and the charge on zinc in [κ^3 -Tptm]ZnX (cc-pVTZ(-f) and LACV3P** basis sets).

When the [Tptm] ligand coordinates in a κ^4 manner, the Zn-C_{Tptm} bond is *trans* to the X ligand in [κ^4 -Tptm]ZnX compounds. Thus, there is a resulting 3-center-4-electron hypervalent ω interaction⁴⁴, which we believe causes the Zn-X bond to weaken, and therefore lengthen, in comparison to a conventional 2-center-2-electron bond.⁴⁵

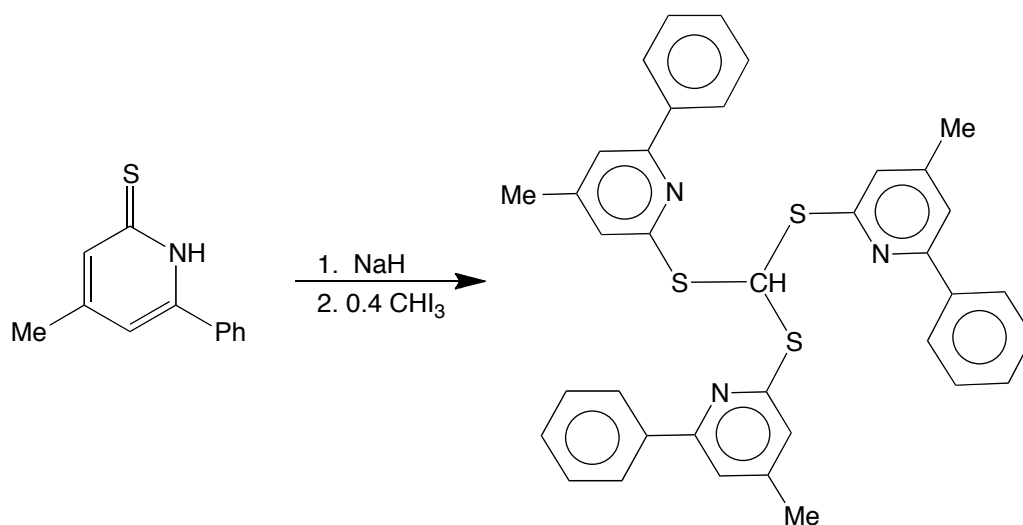
1.6 Synthesis of a bulky [Tptm] ligand: [Tptm^{Ph,Me}]H

There has been much interest in developing ligands that provide steric bulk around a metal center. Having a substituent at the 6-position of the 2-mercaptopyridine ring would create a protective cage around the metal center, potentially allowing for small molecule activation. An example of this methodology is provided by Holland

and co-workers;⁴⁶ using a sterically demanding β -diketiminato ligand, dinitrogen activation was achieved upon reduction of the low coordinate, bulky iron complex.



Scheme 23. Synthesis of 6-phenyl,4-methyl,2-thiopyridone.



Scheme 24. Synthesis of $[\text{Tptm}^{\text{Ph,Me}}]\text{H}$.

Therefore, we synthesized 6-phenyl,4-methyl,2-thiopyridone as a bulky analogue of 2-mercaptopyridine (Scheme 23). 6-phenyl,4-methyl,2-thiopyridone was transformed into $[\text{Tptm}^{\text{Ph,Me}}]\text{H}$ *via* a sequence involving deprotonation to generate the thiolate anion, followed by reaction with iodoform (CHI_3) to form the tripodal ligand, which is summarized in Scheme 24.

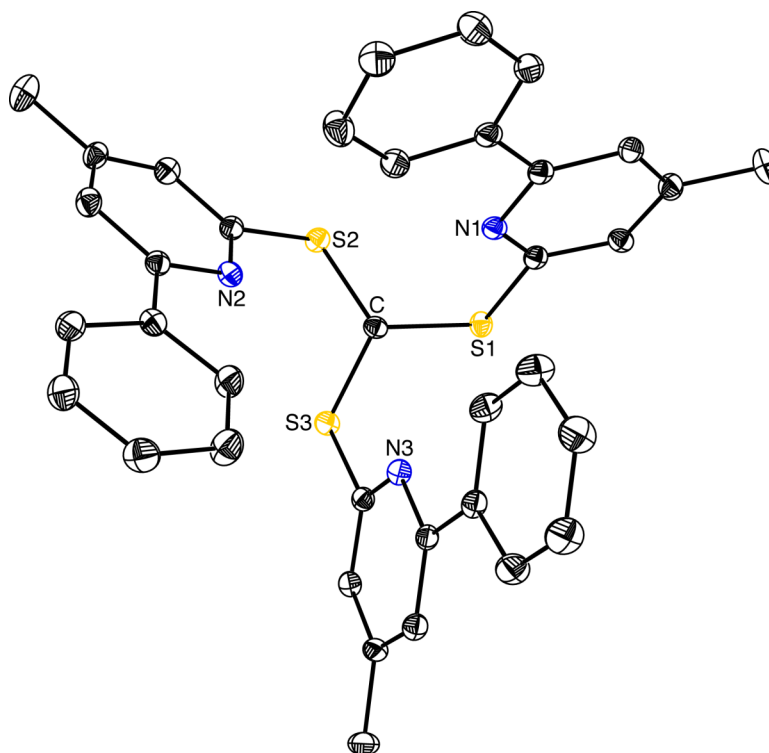


Figure 26. Molecular structure of $[\text{Tptm}^{\text{Ph,Me}}]\text{H}$ (hydrogen atoms not shown for clarity).

The molecular structure of $[\text{Tptm}^{\text{Ph,Me}}]\text{H}$ is depicted in Figure 26. Unfortunately, to date, not much reactivity with $[\text{Tptm}^{\text{Ph,Me}}]\text{H}$ has been observed. One reaction that has been achieved is the lithiation reaction using MeLi at cold temperatures. The molecular structure of $[\text{Tptm}^{\text{Ph,Me}}]\text{Li}$ can be seen in Figure 27, which demonstrates the bulky nature of the $[\text{Tptm}^{\text{Ph,Me}}]$ ligand.

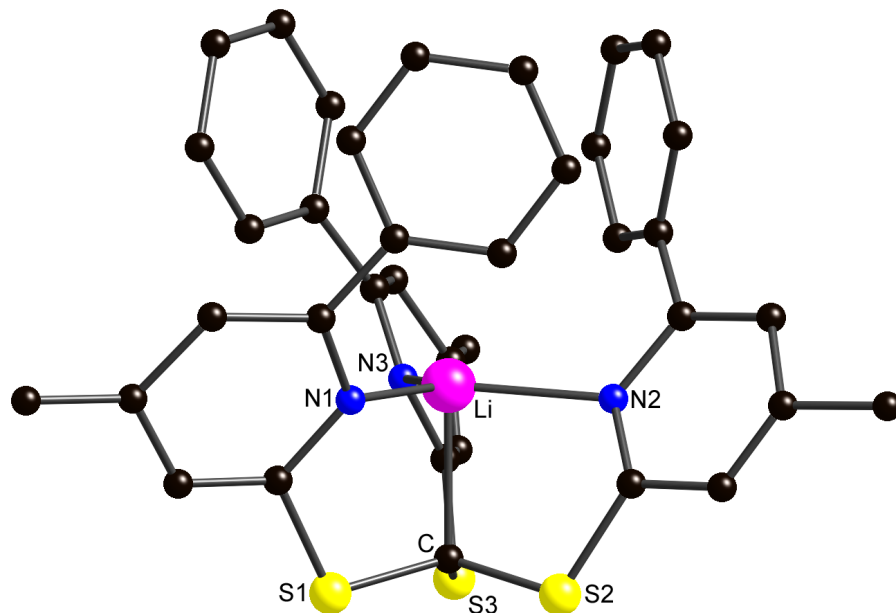


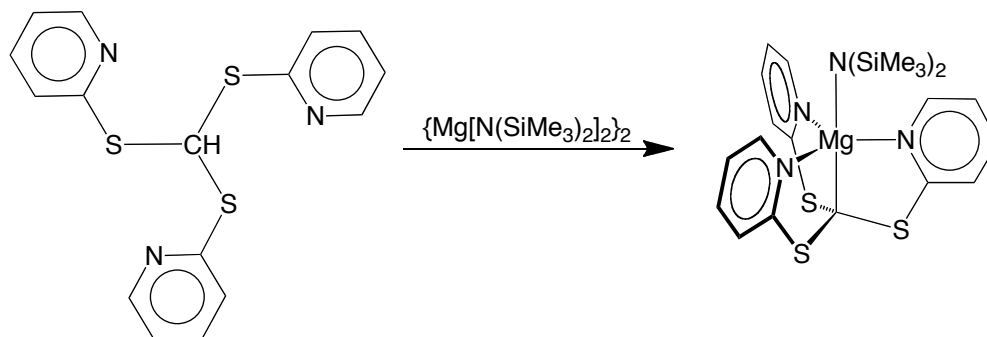
Figure 27. Molecular structure of $[\text{Tptm}^{\text{Ph,Me}}]\text{Li}$.

1.7 $[\kappa^4\text{-Tptm}]\text{MgN}(\text{SiMe}_3)_2$ chemistry

Magnesium, a group 2 metal, is similar to zinc in many aspects. For example, as Sir Edward Frankland demonstrated in 1848, ethylzinc iodide (EtZnI) and diethylzinc (Et_2Zn) are produced when heating ethyl iodide with zinc metal at high temperatures.⁴⁷ This is very similar to the more common, well-known Grignard reagent, prepared more than 50 years later by Victor Grignard in 1900.⁴⁸ As described above, we have prepared the Grignard reagent with the alkyl group $[\text{Tptm}]$ (see Scheme 4 and Figure 4). Additionally, we were interested to see if magnesium showed similar reactivity to zinc, with respect to its CO_2 chemistry.

As depicted in Scheme 25, $[\text{Tptm}]\text{H}$ can be directly metalated by $\{\text{Mg}[\text{N}(\text{SiMe}_3)_2]_2\}_2$ to give $[\kappa^4\text{-Tptm}]\text{MgN}(\text{SiMe}_3)_2$. It is important to note two distinctions between the magnesium and zinc systems. Firstly, $\{\text{Mg}[\text{N}(\text{SiMe}_3)_2]_2\}_2$ ⁴⁹ exists as a dimeric solid, contrasting $\text{Zn}[\text{N}(\text{SiMe}_3)_2]_2$, which exists as monomeric, free-flowing liquid. Secondly, the *bis*(trimethylsilylamide) complex, $[\kappa^4\text{-Tptm}]\text{MgN}(\text{SiMe}_3)_2$,

is structurally different from $[\kappa^3\text{-Tptm}]\text{ZnN}(\text{SiMe}_3)_2$, as the [Tptm] ligand binds in a κ^4 fashion for the magnesium compound, as shown in Figure 28.



Scheme 25. Synthesis of $[\kappa^4\text{-Tptm}]\text{MgN}(\text{SiMe}_3)_2$.

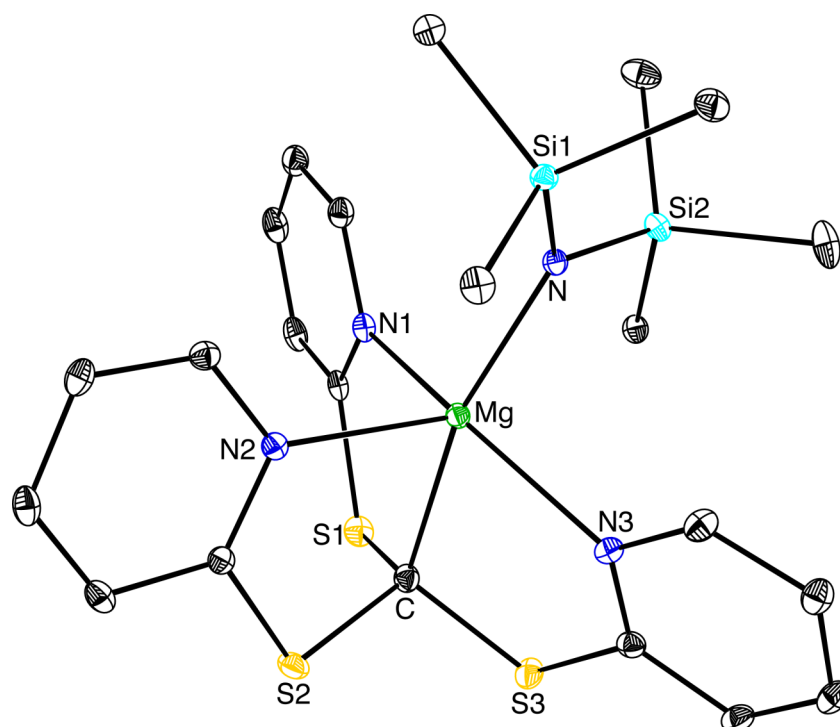


Figure 28. Molecular structure of $[\kappa^4\text{-Tptm}]\text{MgN}(\text{SiMe}_3)_2$.

The reactivity of the *bis*(trimethylsilylamide) complex, $[\kappa^4\text{-Tptm}]\text{MgN}(\text{SiMe}_3)_2$, with CO_2 was explored to see if the magnesium complex showed similar reactivity as compared to the zinc complex. Addition of CO_2 to a solution of $[\kappa^4\text{-Tptm}]\text{MgN}(\text{SiMe}_3)_2$

results in an immediate reaction and the deposition of crystals of $\{[\kappa^4\text{-Tptm}]\text{Mg}(\text{NCO})\}_2$ at room temperature. The molecular structure of $\{[\kappa^4\text{-Tptm}]\text{Mg}(\text{NCO})\}_2$ has been determined by single crystal X-ray diffraction, which is shown in Figure 29. The isocyanate ligands bridge the magnesium centers using both their nitrogen and oxygen atoms, such that each magnesium center is six coordinate with a pseudo-octahedral geometry. The dimeric structure is in contrast to the zinc complex, $[\kappa^4\text{-Tptm}]\text{ZnNCO}$, which exists as a five coordinate monomer.

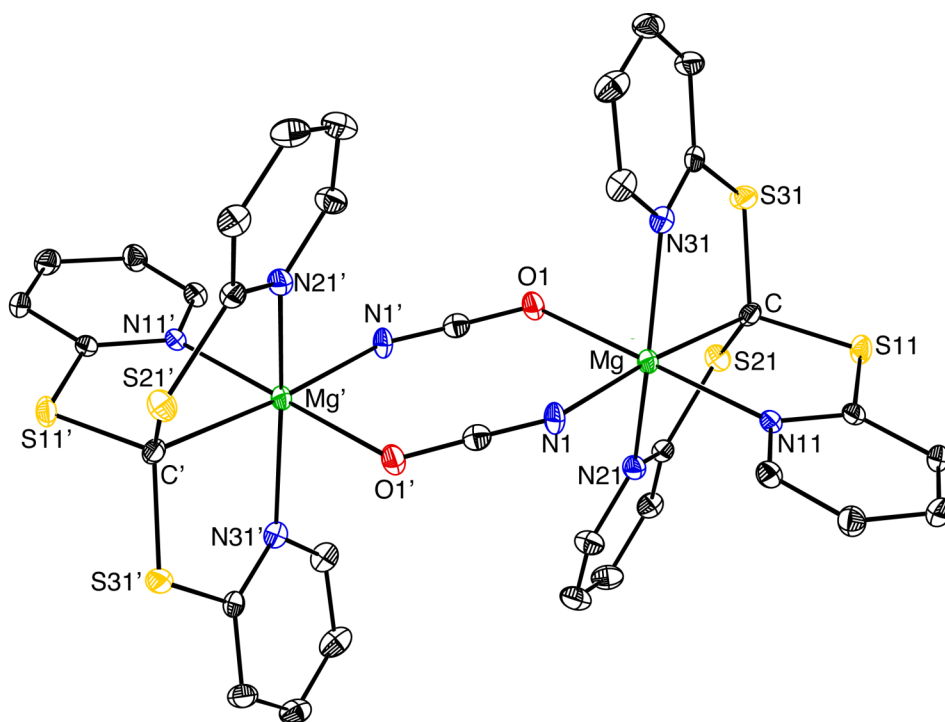
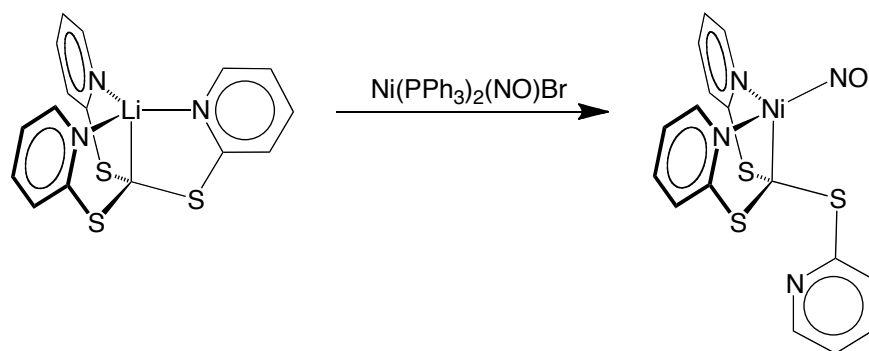


Figure 29. Molecular structure of $\{[\kappa^4\text{-Tptm}]\text{Mg}(\text{NCO})\}_2$.

1.8 $[\kappa^3\text{-Tptm}]\text{NiNO}$ chemistry

In addition to the main group chemistry described above, some transition metal chemistry was explored, specifically with nickel. The nickel nitrosyl complex, namely $[\kappa^3\text{-Tptm}]\text{NiNO}$ may be readily prepared *via* the reaction of $\text{Ni}(\text{PPh}_3)_2(\text{NO})\text{Br}$ with $[\kappa^4\text{-Tptm}]\text{Li}$ as depicted in Scheme 26. The molecular structure of $[\kappa^3\text{-Tptm}]\text{NiNO}$ has

been determined by single crystal X-ray diffraction, demonstrating the κ^3 nature of the [Tptm] ligand, and the linear nature of the nitrosyl ligand ($170.6(2)^\circ$); the molecular structure is depicted in Figure 30. $[\kappa^3\text{-Tptm}]\text{NiNO}$ exists as a purple, diamagnetic solid that has limited solubility in hydrocarbon solvents. It is, however, soluble in chlorinated solvents (CHCl_3 and CH_2Cl_2), although the nitrosyl complex slowly decomposes to, *inter alia*, the chloride complex $\{[\kappa^4\text{-Tptm}]\text{Ni}(\mu\text{-Cl})\}_2$, which exists as a chloride bridged dimer (Figure 31).



Scheme 26. Synthesis of $[\kappa^3\text{-Tptm}]\text{NiNO}$.

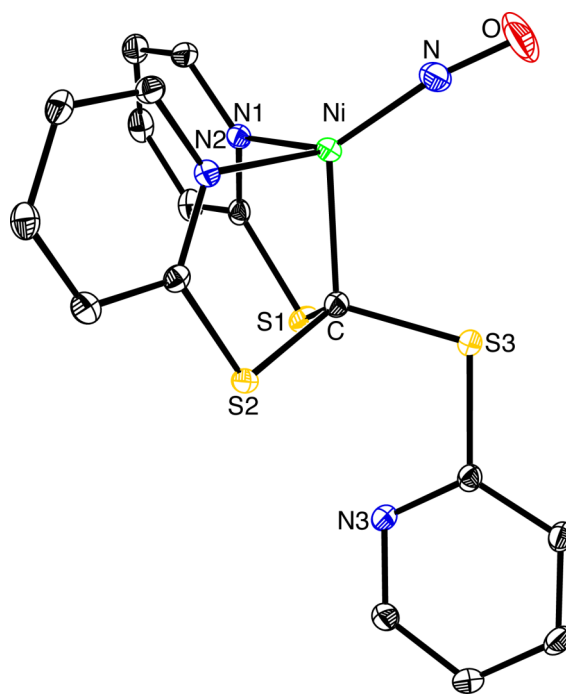


Figure 30. Molecular structure of $[\kappa^3\text{-Tptm}]\text{NiNO}$.

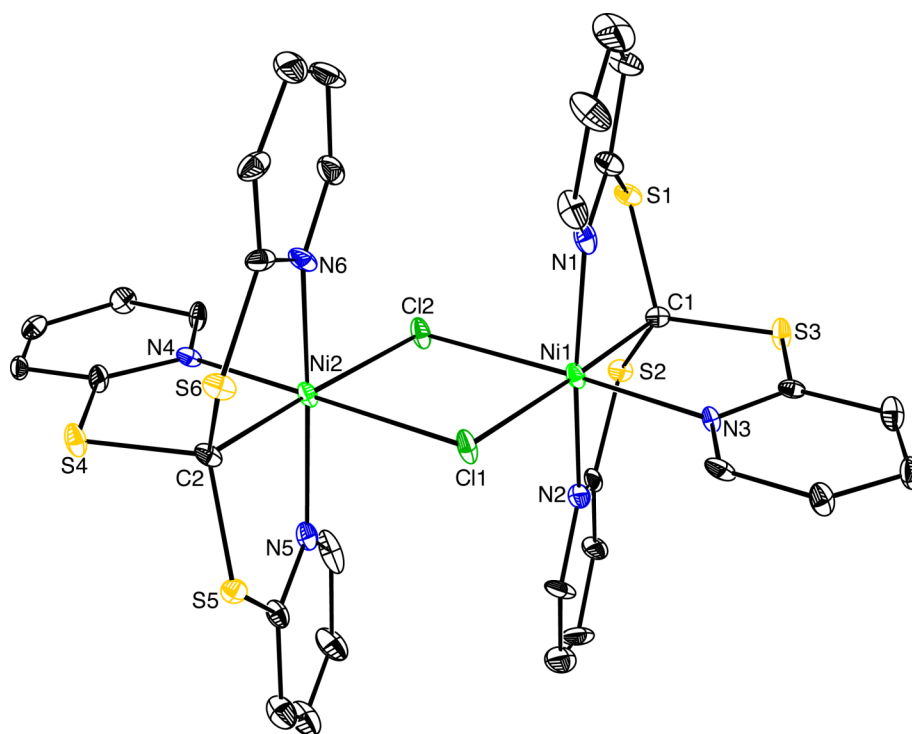
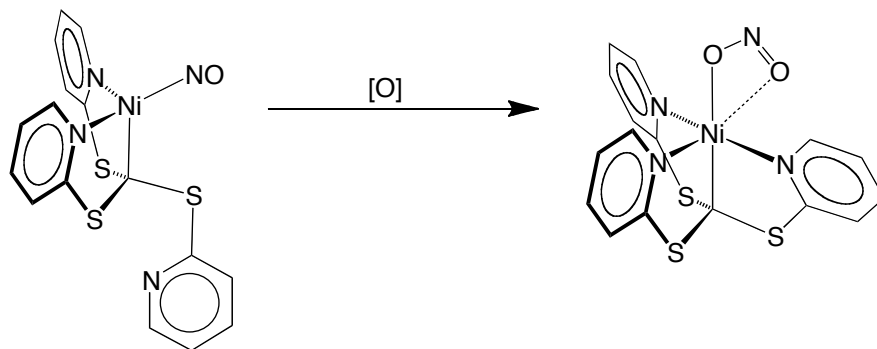


Figure 31. Molecular structure of $\{[\kappa^4\text{-Tptm}]\text{Ni}(\mu\text{-Cl})\}_2$.

We were interested in the reactivity of $[\kappa^3\text{-Tptm}]\text{NiNO}$ with small molecules, with the overall goal of catalysis. One small molecule of interest to activate is dioxygen, O_2 . Specifically, using O_2 as an oxidant is highly desirable, because O_2 is abundant, non-toxic, cheap and atom-economical.⁵⁰ In this regard, $[\kappa^3\text{-Tptm}]\text{NiNO}$ reacts with O_2 ⁵¹ to produce the mono-oxygenated nitrite complex, namely, $[\kappa^4\text{-Tptm}]\text{Ni}[\kappa^2\text{-O}_2\text{N}]$, whose molecular structure has been determined by single crystal X-ray diffraction (Figure 32). The same complex can be produced *via* treatment of $[\kappa^3\text{-Tptm}]\text{NiNO}$ with air. Interestingly, $[\kappa^4\text{-Tptm}]\text{Ni}[\kappa^2\text{-O}_2\text{N}]$ may be deoxygenated to the nitrosyl complex with PMe_3 to produce OPMe_3 (Scheme 28).⁵² Thus, the oxygenation of $[\kappa^3\text{-Tptm}]\text{NiNO}$ is reversible, and could possibly be used to catalyze oxygen atom transfer reactions using O_2 . For example, transition metal nitro complexes have been shown to

stoichiometrically and catalytically transfer an oxygen atom to a variety of substrates including olefins, phosphines, alcohols and nitric oxide.^{53,54}



Scheme 27. Oxygenation of $[\kappa^3\text{-Tptm}]\text{NiNO}$ to $[\kappa^4\text{-Tptm}]\text{Ni}[\kappa^2\text{-O}_2\text{N}]$.

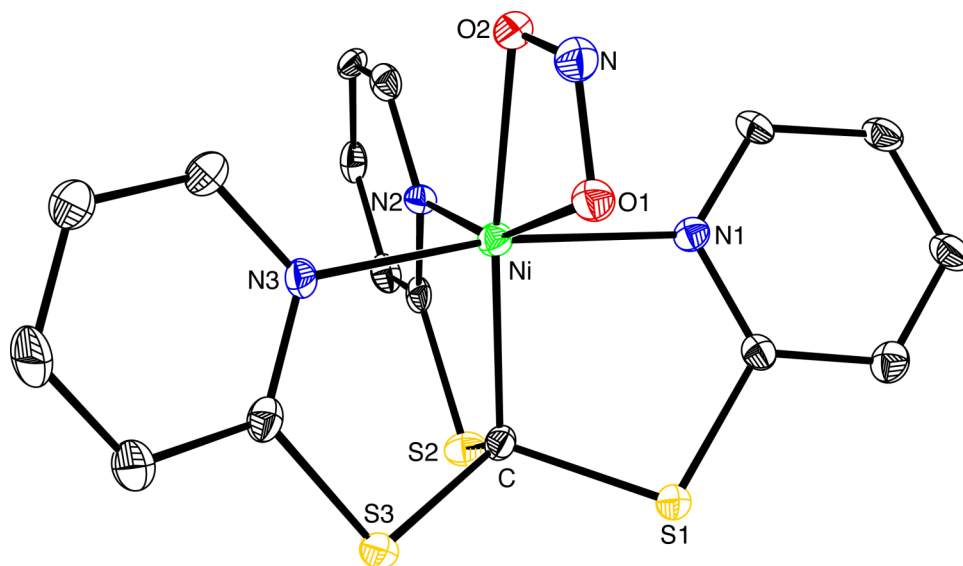
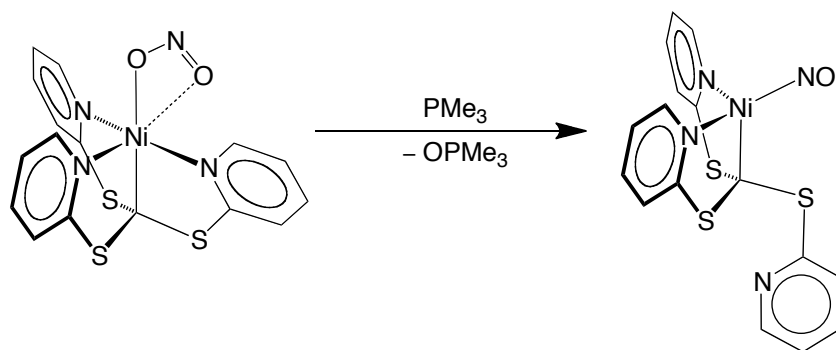
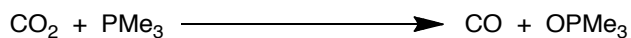


Figure 32. Molecular structure of $[\kappa^4\text{-Tptm}]\text{Ni}[\kappa^2\text{-O}_2\text{N}]$.

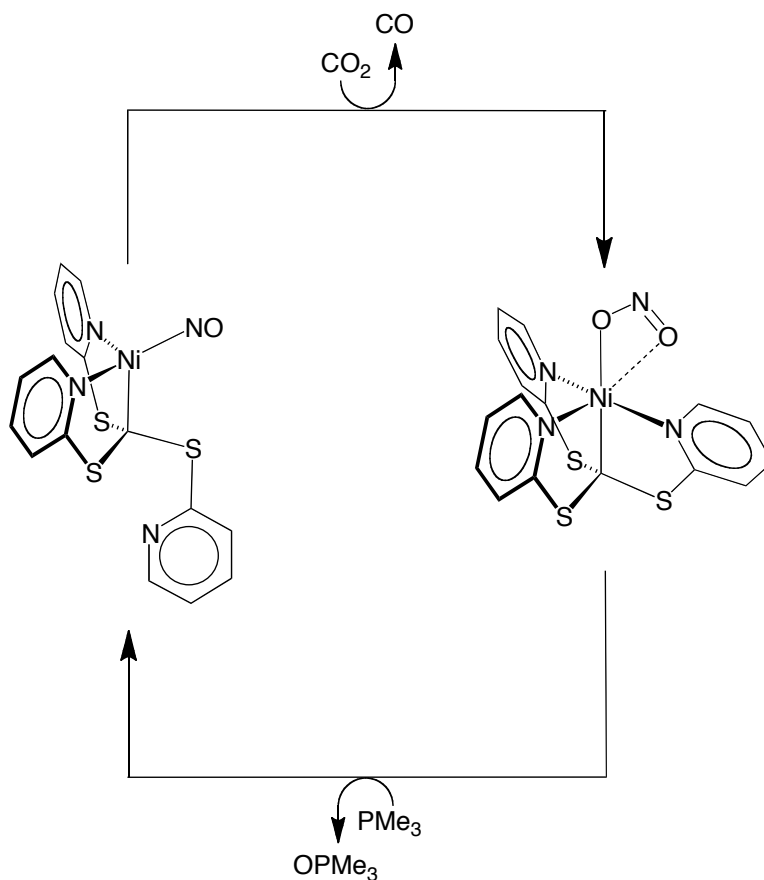


Scheme 28. Deoxygenation of $[\kappa^4\text{-Tptm}]\text{Ni}[\kappa^2\text{-O}_2\text{N}]$ to $[\kappa^3\text{-Tptm}]\text{NiNO}$ using PMe_3 .

In addition to O_2 , CO_2 is an attractive oxygen atom source. In this vein, if $[\kappa^3\text{-Tptm}]\text{NiNO}$ were to react with CO_2 to produce the nitrite complex and CO , the resulting nitrite complex could then transfer the oxygen atom to an oxygen acceptor, such as PMe_3 or PPh_3 . The overall reaction described in Scheme 29 is predicted to be enthalpically favored by $12.1 \text{ kcal mol}^{-1}$ according to gas-phase thermodynamic data compiled by Holm and Donahue.^{55,56} This reaction is formally an oxygen transfer from CO_2 to PMe_3 , however, this reaction does not occur without a catalyst present. A catalytic cycle using $[\kappa^3\text{-Tptm}]\text{NiNO}$ for the oxygen transfer from CO_2 to PMe_3 (or other suitable oxygen atom acceptors) can be envisioned and is depicted in Scheme 30. To date, this has not yet been observed.

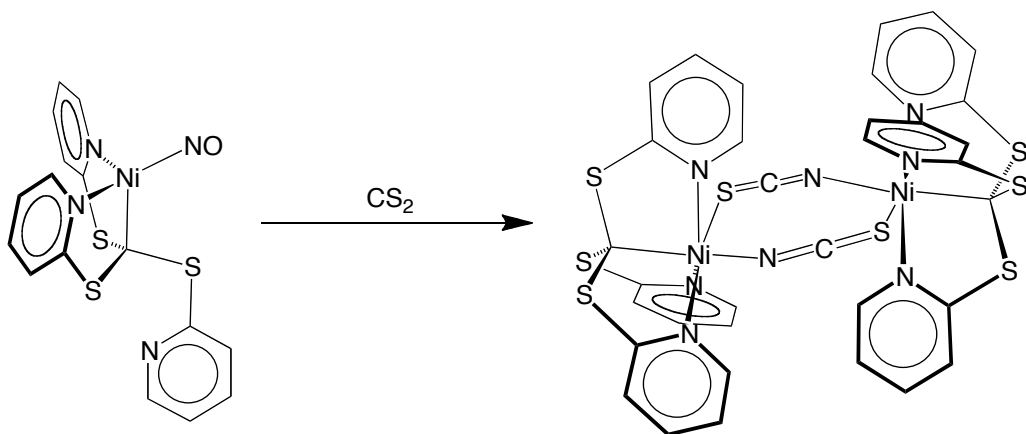


Scheme 29. Reaction of CO_2 with PMe_3 to give CO and OPMe_3 .



Scheme 30. Possible catalytic cycle for the $[\kappa^3\text{-Tptm}]\text{NiNO}$ catalyzed deoxygenation of CO_2 by PMe_3 .

The reaction between $[\kappa^3\text{-Tptm}]\text{NiNO}$ and carbon disulfide (CS_2) has also been explored. This reaction does not result in the transfer of a sulfur atom to the nickel complex. Instead, a CS group is transfer with loss of an oxygen atom to form the dimeric isothiocyanate complex, $\{[\kappa^4\text{-Tptm}]\text{NiNCS}\}_2$ (Scheme 31). At this point, the fate of the missing oxygen and sulfur atoms is unknown. The molecular structure of $\{[\kappa^4\text{-Tptm}]\text{NiNCS}\}_2$ is depicted in Figure 33.



Scheme 31. Reaction of $[\kappa^3\text{-Tptm}]\text{NiNO}$ with CS_2 to give $\{[\kappa^4\text{-Tptm}]\text{NiNCS}\}_2$.

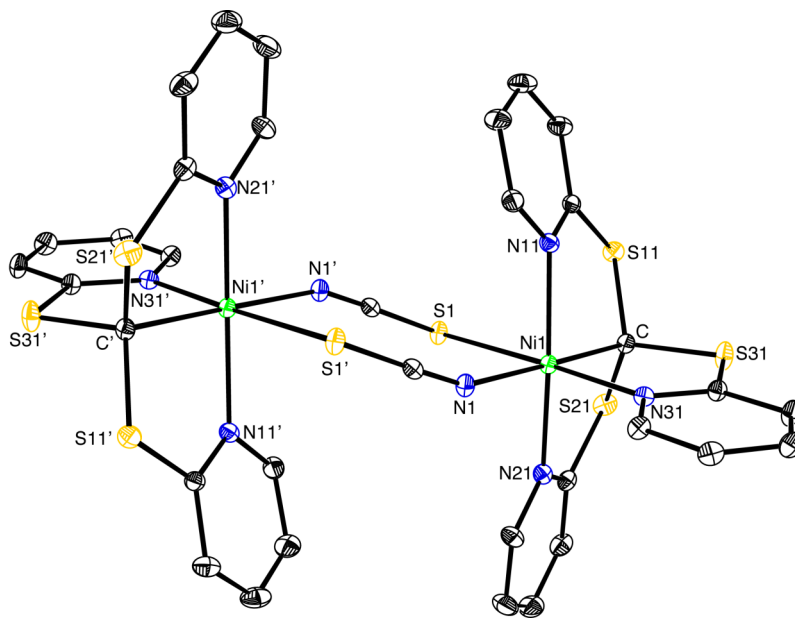
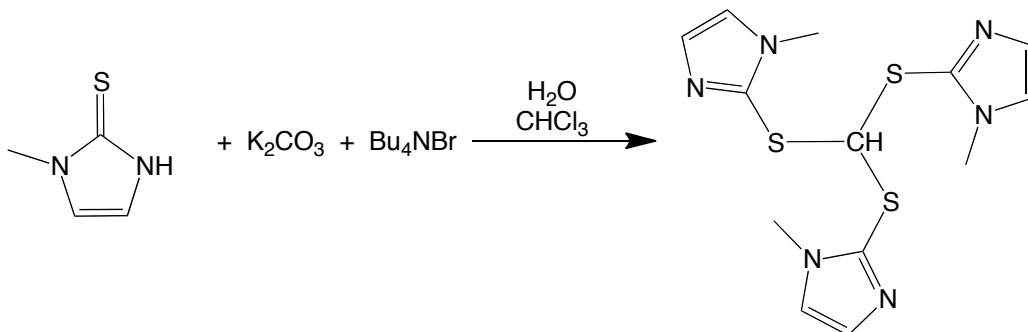


Figure 33. Molecular structure of $\{[\kappa^4\text{-Tptm}]\text{NiNCS}\}_2$.

1.9 Utilization of $[\text{Titm}^{\text{Me}}]\text{H}$ as a tetradentate ligand

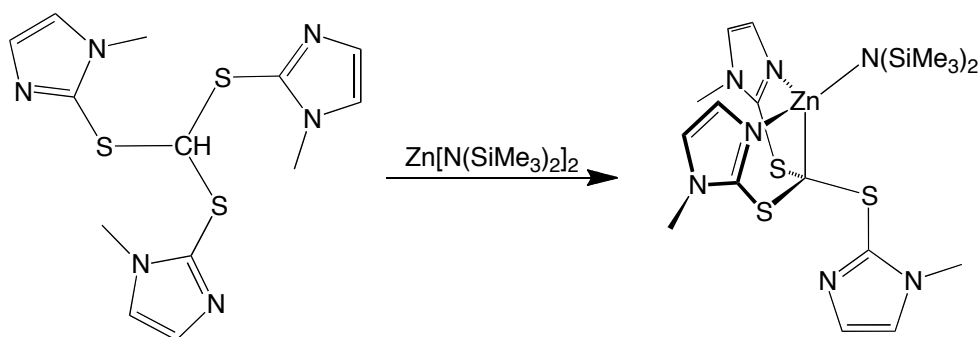
Similar to $[\text{Tptm}]\text{H}$, *tris*(1-methyl-imidazol-2-ylthio)methane, $[\text{Titm}^{\text{Me}}]\text{H}$, (Scheme 32) has also been utilized as a tetradentate alkyl ligand for zinc.⁵⁷ $[\text{Titm}^{\text{Me}}]\text{H}$ was prepared by Gwengo and co-workers as depicted in Scheme 32, using a triphasic reaction, with tetrabutylammonium bromide as the phase-transfer agent. However, in

the original report, $[\text{Titm}^{\text{Me}}]\text{H}$ was not metalated to form any $[\text{Titm}^{\text{Me}}]\text{M}$ compounds. Therefore, we explored the reactivity of $[\text{Titm}^{\text{Me}}]\text{H}$ for a comparative study with $[\text{Tptm}]\text{H}$.



Scheme 32. Synthesis of $[\text{Titm}^{\text{Me}}]\text{H}$.

$[\text{Titm}^{\text{Me}}]\text{H}$ was treated with $\text{Zn}[\text{N}(\text{SiMe}_3)_2]_2$ which reacts cleanly to give $[\kappa^3\text{-Titm}^{\text{Me}}]\text{ZnN}(\text{SiMe}_3)_2$ in high yield (Scheme 33), very similar to the synthesis of $[\kappa^3\text{-Tptm}]\text{ZnN}(\text{SiMe}_3)_2$. In the case of $[\kappa^3\text{-Titm}^{\text{Me}}]\text{ZnN}(\text{SiMe}_3)_2$, the molecular structure has been determined by single crystal X-ray diffraction, which demonstrates the κ^3 nature of the $[\text{Titm}^{\text{Me}}]$ ligand, as depicted in Figure 34.



Scheme 33. Synthesis of $[\kappa^3\text{-Titm}^{\text{Me}}]\text{ZnN}(\text{SiMe}_3)_2$.

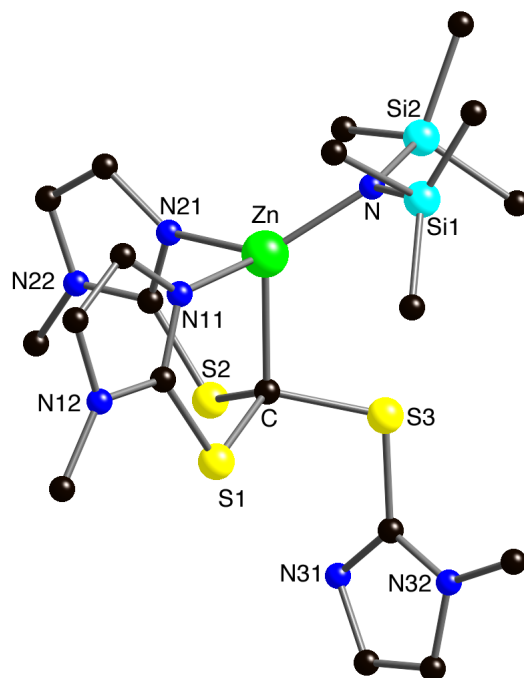
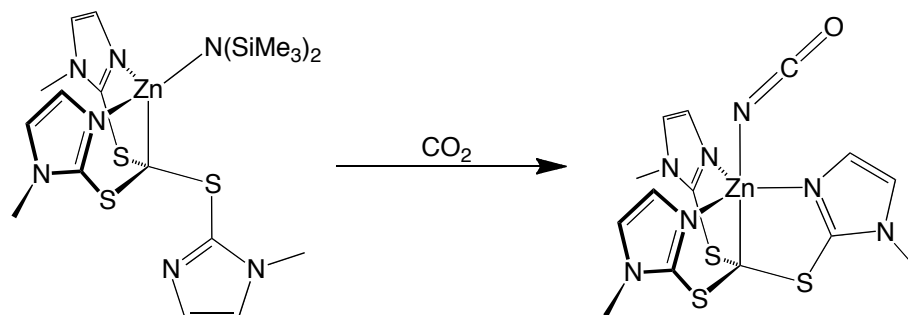


Figure 34. Molecular structure of $[\kappa^3\text{-Titm}^{\text{Me}}]\text{ZnN}(\text{SiMe}_3)_2$.

Like $[\kappa^3\text{-Tptm}]\text{ZnN}(\text{SiMe}_3)_2$, $[\kappa^3\text{-Titm}^{\text{Me}}]\text{ZnN}(\text{SiMe}_3)_2$ reacts with CO_2 to immediately form Me_3SiNCO and $[\text{Titm}^{\text{Me}}]\text{ZnOSiMe}_3$ which converts to $[\kappa^4\text{-Titm}^{\text{Me}}]\text{ZnNCO}$ at room temperature (Scheme 34). This reaction is similar compared to the [Tptm] system; however, preliminary results suggests that the metathesis step to give $[\kappa^4\text{-Titm}^{\text{Me}}]\text{ZnNCO}$ is faster for the $[\text{Titm}^{\text{Me}}]$ system. The molecular structure of $[\kappa^4\text{-Titm}^{\text{Me}}]\text{ZnNCO}$ has been determined by single crystal X-ray diffraction, which verifies the κ^4 nature of the $[\text{Titm}^{\text{Me}}]$ ligand, as depicted in Figure 35.



Scheme 34. Synthesis of $[\kappa^4\text{-Titm}^{\text{Me}}]\text{ZnNCO}$.

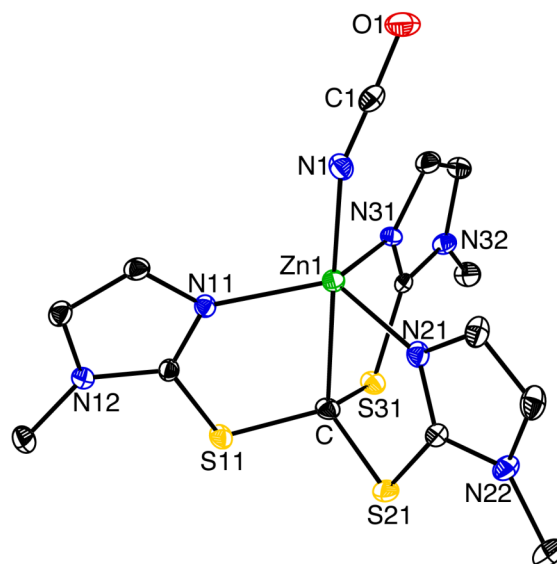
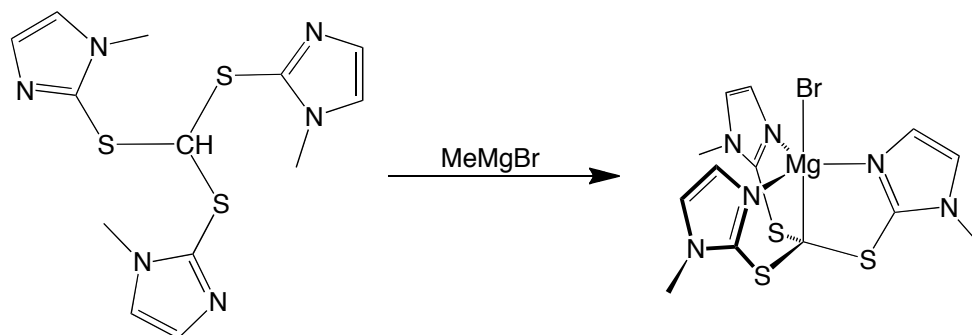


Figure 35. Molecular structure of $[\kappa^4\text{-Titm}^{\text{Me}}]\text{ZnNCO}$.

Finally, in addition to the zinc compounds described above, the Grignard reagent has also been prepared by addition of MeMgBr to $[\text{Titm}^{\text{Me}}]\text{H}$ as depicted in Scheme 35. The molecular structure of $[\kappa^4\text{-Titm}^{\text{Me}}]\text{MgBr}$ is presented in Figure 36, which shows that the $[\text{Titm}^{\text{Me}}]$ ligand binds in a κ^4 -coordination mode. It is interesting to note that the Mg-C bond length, which is $2.401(5)$ Å, is exceptionally long. For example, in the analogous $[\text{Tptm}]$ structure, namely $\{[\kappa^4\text{-Tptm}]\text{MgBr}\}_2$, has a Mg-C bond length of $2.243(6)$ Å. Additionally, the average Mg-C bond length listed in the CSD⁴ is 2.206 Å.

This lengthening is presumably due to a constraint by placed by the ligand, which holds the magnesium atom further away from the carbon than is ideal.



Scheme 35. Synthesis of $[\kappa^4\text{-Titm}^{\text{Me}}]\text{MgBr}$.

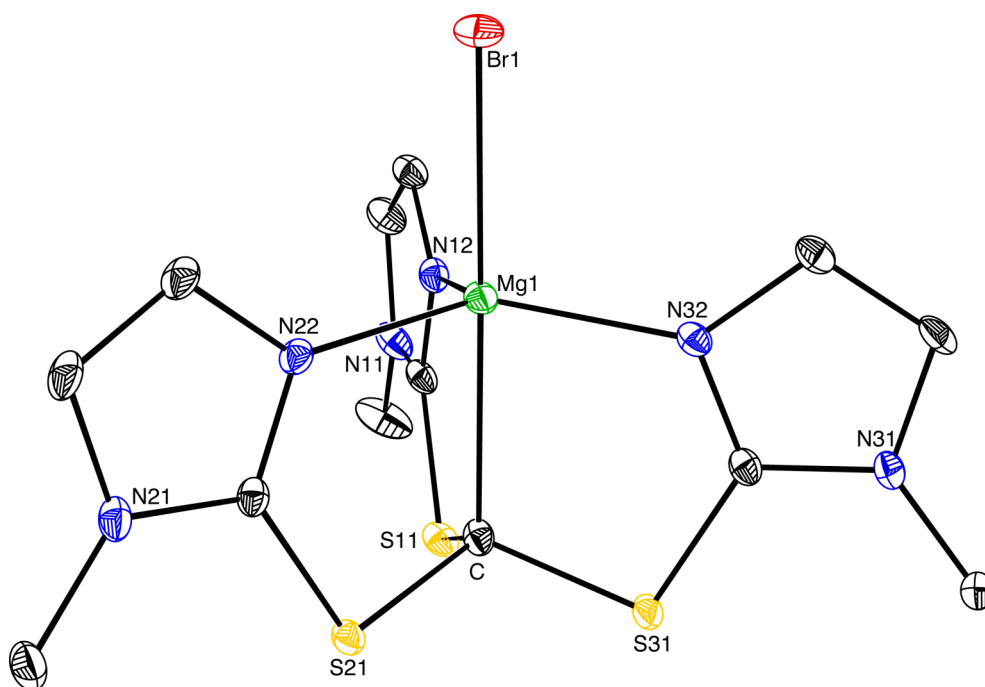


Figure 36. Molecular structure of $[\kappa^4\text{-Titm}^{\text{Me}}]\text{MgBr}$.

1.10 Summary and conclusions

In summary, the mononuclear alkyl zinc hydride complex, $[\kappa^3\text{-Tptm}]\text{ZnH}$, may be synthesized on multigram scale *via* treatment of $[\kappa^4\text{-Tptm}]\text{ZnOSiMe}_3$ with PhSiH_3 .

$[\kappa^3\text{-Tptm}]\text{ZnH}$ exhibits diverse reactivity, including insertion of CO_2 to give the formate complex, $[\kappa^4\text{-Tptm}]\text{ZnO}_2\text{CH}$. A variety of $[\text{Tptm}]\text{ZnX}$ compounds can be synthesized from $[\kappa^3\text{-Tptm}]\text{ZnH}$. The *bis*(trimethylsilyl)amide complex, $[\kappa^3\text{-Tptm}]\text{ZnN}(\text{SiMe}_3)_2$, reacts with CO_2 , but the product obtained is the isocyanate complex, $[\kappa^4\text{-Tptm}]\text{ZnNCO}$, that results from a multistep sequence in which the initial step is insertion of CO_2 into the $\text{Zn-N}(\text{SiMe}_3)_2$ bond, followed by rearrangement to $[\kappa^4\text{-Tptm}]\text{ZnOSiMe}_3$ and Me_3SiNCO . An important discovery is that the final metathesis step to give $[\kappa^4\text{-Tptm}]\text{ZnNCO}$ is promoted by CO_2 , an observation that indicates that the carbonate complex, $[\kappa^4\text{-Tptm}]\text{Zn}[\text{O}_2\text{COSiMe}_3]$, is more susceptible towards metathesis than is the siloxide derivative, $[\kappa^4\text{-Tptm}]\text{ZnOSiMe}_3$. As such, this finding has ramifications with respect to inducing reactivity of other siloxide compounds. Additionally, the $[\text{Tptm}]$ ligand has been utilized with respect to some magnesium and nickel chemistry. The $[\text{Tptm}]$ system is an organometallic counterpart to the more common tripodal ligands, $[\text{Tp}]$ and $[\text{Tm}]$. Finally, the $[\text{Titm}^{\text{Me}}]$ ligand, another tetradentate, alkyl ligand has been utilized for zinc and magnesium chemistry.

1.11 Experimental details

1.11.1 General considerations

All manipulations were performed using a combination of glovebox, high vacuum, and Schlenk techniques under a nitrogen or argon atmosphere,⁵⁸ with the exception of the synthesis of $[\text{Tptm}]\text{H}$. Solvents were purified and degassed by standard procedures. ^1H NMR spectra were measured on Bruker 300 DRX, Bruker 400 DRX, and Bruker Avance 500 DMX spectrometers. ^1H NMR chemical shifts are reported in ppm relative to SiMe_4 ($\delta = 0$) and were referenced internally with respect to the protio solvent impurity ($\delta 7.16$ for $\text{C}_6\text{D}_5\text{H}$).⁵⁹ Coupling constants are given in hertz. Infrared spectra

were recorded on Nicolet Avatar 370 DTGS spectrometer and are reported in cm^{-1} . Mass spectra were obtained on a Micromass Quadrupole-Time-of-Flight mass spectrometer using fast atom bombardment (FAB). All chemicals were obtained from Aldrich, with the exception of 2-mercaptopyridine (Acros Organics), bromoform (Fisher Scientific), phenylsilane (Alfa Aesar), trimethylsilyl isocyanate (Alfa Aesar), and dimethylzinc (Strem Chemicals). Trimethylsilanol was obtained by the literature method.⁶⁰ PhSiD_3 was prepared by using a method analogous to that reported in the literature method for PhSiH_3 ,⁶¹ but employing LiAlD_4 (Aldrich) in place of LiAlH_4 .

1.11.2 Computational details

Calculations were carried out using DFT as implemented in the Jaguar 7.5 (release 207) suite of *ab initio* quantum chemistry programs.⁶² Geometry optimizations were performed with the B3LYP density functional⁶³ using the 6-31G** (C, H, N, O, Si, S, F, Cl) and LAV3P (Br, I and Zn) basis sets.⁶⁴ The energies of the optimized structures were reevaluated by additional single point calculations on each optimized geometry using cc-pVTZ(-f)⁶⁵ correlation consistent triple- ζ (C, H, N, O, Si, S, F, Cl) and LAV3P (Br, I, Zn) basis sets.

1.11.3 X-ray structure determinations

X-ray diffraction data were collected on a Bruker Apex II diffractometer. Crystal data, data collection and refinement parameters are summarized in Table 4. The structures were solved using direct methods and standard difference map techniques, and were refined by full-matrix least-squares procedures on F^2 with SHELXTL (Version 6.1).⁶⁶

1.11.4 Synthesis of $\text{Zn}[\text{N}(\text{SiMe}_3)_2]_2$

$\text{Zn}[\text{N}(\text{SiMe}_3)_2]_2$ was prepared by a modification of a literature method.²¹ A solution of $\text{NaN}(\text{SiMe}_3)_2$ (18.00 g, 98.16 mmol) in Et_2O (ca. 100 mL) was cooled to $-78\text{ }^\circ\text{C}$, where it became a white suspension. Solid ZnCl_2 (5.75 g, 42.19 mmol) was added in three portions over a period of 10 minutes. The mixture was then allowed to warm to room temperature, and was stirred overnight. The next morning, the suspension was filtered, and the filtrate was evacuated *in vacuo* to remove the volatile components. The residue was then distilled under dynamic vacuum at ca. $100\text{ }^\circ\text{C}$ using a heat gun to give $\text{Zn}[\text{N}(\text{SiMe}_3)_2]_2$ as a colorless liquid (8.27 g, 51%).

1.11.5 Synthesis of [Tptm]H

[Tptm]H was prepared by a modification of a literature method.⁶⁷ A yellow solution of KOH (37.6 g, 670.1 mmol), 2-mercaptopyridine (50.0 g, 449.8 mmol), and EtOH (ca. 500 mL) in a 1 L round bottom flask was treated in a dropwise manner with bromoform (13.1 mL, 150.3 mmol) over a period of 30 minutes, during which period the solution became a darker yellow and a yellow precipitate formed. A reflux condenser was then connected, and the suspension was refluxed for ca. 5 hours by using a heating mantle. At the end of this period, the reaction vessel contained an off-white precipitate in a dark supernatant. The mixture was allowed to cool to room temperature and then filtered. The precipitate was extracted into EtOH ($2 \times 100\text{ mL}$) and the combined extract was evaporated *in vacuo* to give a viscous brown residue. The residue was extracted into benzene (ca. 500 mL) and filtered through a frit. The filtrate was then passed through a short plug of silica gel (ca. 50 mL in a 9cm diameter frit) and the volatile components were removed *in vacuo*. The residue obtained was dissolved in EtOH (ca. 150 mL) and allowed to crystallize at room temperature in an open vessel over a period of 3 days. The yellow crystals were isolated *via* decantation and washed with cold EtOH to give

pure [Tptm]H (9.76 g, 19 %). A second batch of crystals was isolated after a week of evaporation at room temperature from the previous mother liquor (1.37 g, total yield 22 %).

^1H NMR (C_6D_6): 6.31 [m, 3H, $\text{HC}(\text{SC}_5\text{H}_4\text{N})_3$], 6.71 [m, 3H, $\text{HC}(\text{SC}_5\text{H}_4\text{N})_3$], 6.83 [d, $^3\text{J}_{\text{H-H}} = 8$ Hz, 3H, $\text{HC}(\text{SC}_5\text{H}_4\text{N})_3$], 8.32 [d, $^3\text{J}_{\text{H-H}} = 4$ Hz, 3H, $\text{HC}(\text{SC}_5\text{H}_4\text{N})_3$], 8.82 [s, 1H, $\text{HC}(\text{SC}_5\text{H}_4\text{N})_3$]. ^{13}C NMR (C_6D_6): 49.3 [d, $^1\text{J}_{\text{C-H}} = 169$ Hz, 1C, $\text{HC}(\text{SC}_5\text{H}_4\text{N})_3$], 119.8 [dt, $^1\text{J}_{\text{C-H}} = 164$ Hz, $^2\text{J}_{\text{C-H}} = 7$ Hz, 3C, $\text{HC}(\text{SC}_5\text{H}_4\text{N})_3$], 121.9 [dd, $^1\text{J}_{\text{C-H}} = 166$ Hz, $^2\text{J}_{\text{C-H}} = 7$ Hz, 3C, $\text{HC}(\text{SC}_5\text{H}_4\text{N})_3$], 136.1 [dd, $^1\text{J}_{\text{C-H}} = 163$ Hz, $^2\text{J}_{\text{C-H}} = 7$ Hz, 3C, $\text{HC}(\text{SC}_5\text{H}_4\text{N})_3$], 149.9 [ddd, $^1\text{J}_{\text{C-H}} = 180$ Hz, $^2\text{J}_{\text{C-H}} = 7$ Hz, $^2\text{J}_{\text{C-H}} = 4$ Hz, 3C, $\text{HC}(\text{SC}_5\text{H}_4\text{N})_3$], 158.6 [s, 3C, $\text{HC}(\text{SC}_5\text{H}_4\text{N})_3$].

IR Data (KBr disk, cm^{-1}): 3071 (w), 3062 (w), 3047 (w), 3018 (w), 2993 (w), 2945(w), 1572 (s), 1554 (s), 1449 (s), 1408 (s), 1279 (m), 1241 (w), 1176 (w), 1147 (m), 1126 (s), 1104 (s), 1084 (s), 1043 (s), 985 (s), 957 (w), 872 (w), 757 (s), 720 (m), 617 (m), 483 (m), 452 (m).

1.11.6 Synthesis of $[\kappa^3\text{-Tptm}]\text{ZnMe}$

A frozen suspension of [Tptm]H (800 mg, 2.33 mmol) in toluene (*ca.* 4 mL) was treated with Me_2Zn (0.30 mL, 4.35 mmol) *via* vacuum transfer. The mixture was allowed to warm room temperature, thereby resulting in the evolution of methane and colorless crystals of $[\kappa^3\text{-Tptm}]\text{ZnMe}$ started to deposit after a period of 1.5 hours. The mixture was allowed to stand at room temperature overnight, after which period the mother liquor was decanted to give colorless crystals of $[\kappa^3\text{-Tptm}]\text{ZnMe}$ that were dried *in vacuo* (919 mg, 93 %). Anal. Calcd. for $[\kappa^3\text{-Tptm}]\text{ZnMe}$: C, 48.3%; H, 3.6%; N, 9.9%. Found: C, 48.4%; H, 3.6%; N, 9.8%.

^1H NMR (C_6D_6): 0.14 [s, 3H, $\text{H}_3\text{CZnC}(\text{SC}_5\text{H}_4\text{N})_3$], 6.23 [br, 3H, $\text{MeZnC}(\text{SC}_5\text{H}_4\text{N})_3$], 6.58 [br, 3H, $\text{MeZnC}(\text{SC}_5\text{H}_4\text{N})_3$], 6.68 [br, 3H, $\text{MeZnC}(\text{SC}_5\text{H}_4\text{N})_3$], 8.19 [br, 3H, $\text{MeZnC}(\text{SC}_5\text{H}_4\text{N})_3$]. $^{13}\text{C}\{^1\text{H}\}$ NMR (60 °C, C_6D_6): -15.5 [s, 1C, $\text{MeZnC}(\text{SC}_5\text{H}_4\text{N})_3$], not

observed [MeZnC(SC₅H₄N)₃], 118.8 [s, 3C, MeZnC(SC₅H₄N)₃], 120.9 [s, 3C, MeZnC(SC₅H₄N)₃], 136.8 [s, 3C, MeZnC(SC₅H₄N)₃], 147.5 [s, 3C, MeZnC(SC₅H₄N)₃], 165.4 [s, 3C, MeZnC(SC₅H₄N)₃].

IR Data (KBr disk, cm⁻¹): 3081 (w), 3055 (w), 3009 (w), 2944 (w), 2900 (w), 2831 (w), 1590 (s), 1553 (s), 1455 (s), 1413 (s), 1281 (m), 1130 (m), 1091 (w), 1044 (m), 1008 (m), 758 (s), 720 (m), 650 (m), 531 (m), 486 (w).

1.11.7 Synthesis of [κ³-Tptm]ZnN(SiMe₃)₂

A light yellow solution of [Tptm]H (2.934 mg, 8.54 mmol) in benzene (*ca.* 20 mL) was treated with Zn[N(SiMe₃)₂]₂ (3.627 mg, 9.392 mmol) *via* pipette. The reaction mixture was allowed to stand at room temperature overnight and then lyophilized overnight to give [κ³-Tptm]ZnN(SiMe₃)₂ (4.847 g, 99%) as an off white solid.

¹H NMR (C₆D₆): 0.47 [s, 18H, [(H₃C)₃Si]₂NZnC(SC₅H₄N)₃], 6.22 [br, 3H, (Me₃Si)₂NZnC(SC₅H₄N)₃], 6.50 [br, 3H, (Me₃Si)₂NZnC(SC₅H₄N)₃], 6.60 [br, 3H, (Me₃Si)₂NZnC(SC₅H₄N)₃], 8.30 [br, 3H, (Me₃Si)₂NZnC(SC₅H₄N)₃]. ¹³C{¹H} NMR (60 °C, C₆D₆): 6.6 [s, 6C, (Me₃Si)₂N ZnC(SC₅H₄N)₃], not observed [(Me₃Si)₂NZnC(SC₅H₄N)₃], 119.0 [s, 3C, (Me₃Si)₂NZnC(SC₅H₄N)₃], 121.5 [s, 3C, (Me₃Si)₂NZnC(SC₅H₄N)₃], 137.1 [s, 3C, (Me₃Si)₂NZnC(SC₅H₄N)₃], 147.5 [s, 3C, (Me₃Si)₂NZnC(SC₅H₄N)₃], 165.2 [s, 3C, (Me₃Si)₂NZnC(SC₅H₄N)₃].

IR Data (KBr disk, cm⁻¹): 3083 (w), 3048 (w), 3015 (w), 2991 (w), 2954 (w), 2893 (w), 1588 (s), 1557 (s), 1454 (s), 1416 (s), 1281 (m), 1251 (m), 1178 (w), 1131 (m), 1092 (w), 1044 (m), 1006 (m), 932 (m), 879 (w), 845 (m), 757 (s), 722 (m), 639 (w), 614 (w).

1.11.8 Synthesis of [κ⁴-Tptm]ZnOSiMe₃

(i) A solution of [κ³-Tptm]ZnN(SiMe₃)₂ (1.315 g, 2.31 mmol) in benzene (*ca.* 8 mL) was treated with trimethylsilanol (385 mg, 4.27 mmol). The reaction mixture was allowed to stand at room temperature for 5 minutes and then lyophilized to give

$[\kappa^4\text{-Tptm}]\text{ZnOSiMe}_3$ as a light yellow powder (1.095 g, 95 %) Crystals suitable for X-ray diffraction were obtained *via* slow evaporation from benzene. Anal. Calcd. for $[\kappa^4\text{-Tptm}]\text{ZnOSiMe}_3$: C, 45.9%; H, 4.3%; N, 8.5%. Found: C, 46.1%; H, 3.9%; N, 8.4%.

^1H NMR (C_6D_6): 0.59 [s, 9H, $(\text{H}_3\text{C})_3\text{SiOZnC}(\text{SC}_5\text{H}_4\text{N})_3$], 6.34 [t, $^3J_{\text{H-H}} = 6$ Hz, 3H, $\text{Me}_3\text{SiOZnC}(\text{SC}_5\text{H}_4\text{N})_3$], 6.48 [d, $^3J_{\text{H-H}} = 8$ Hz, 3H, $\text{Me}_3\text{SiOZnC}(\text{SC}_5\text{H}_4\text{N})_3$], 6.54 [t, $^3J_{\text{H-H}} = 8$ Hz, 3H, $\text{Me}_3\text{SiOZnC}(\text{SC}_5\text{H}_4\text{N})_3$], 9.23 [d, $^3J_{\text{H-H}} = 5$ Hz, 3H, $\text{SiMe}_3\text{OZnC}(\text{SC}_5\text{H}_4\text{N})_3$]. $^{13}\text{C}\{^1\text{H}\}$ NMR (C_6D_6): 5.5 [s, 3C, $\text{Me}_3\text{SiOZnC}(\text{SC}_5\text{H}_4\text{N})_3$], not observed [$\text{Me}_3\text{SiOZnC}(\text{SC}_5\text{H}_4\text{N})_3$], 118.9 [s, 3C, $\text{Me}_3\text{SiOZnC}(\text{SC}_5\text{H}_4\text{N})_3$], 120.5 [s, 3C, $\text{Me}_3\text{SiOZnC}(\text{SC}_5\text{H}_4\text{N})_3$], 138.0 [s, 3C, $\text{Me}_3\text{SiOZnC}(\text{SC}_5\text{H}_4\text{N})_3$], 149.0 [s, 3C, $\text{Me}_3\text{SiOZnC}(\text{SC}_5\text{H}_4\text{N})_3$], 161.4 [s, 3C, $\text{Me}_3\text{SiOZnC}(\text{SC}_5\text{H}_4\text{N})_3$].

IR Data (KBr disk, cm^{-1}): 3087 (w), 3067 (w), 3013 (w), 2942 (m), 2888 (w), 1589 (s), 1557 (s), 1453 (s), 1416 (s), 1277 (m), 1252 (m), 1239 (m), 1130 (s), 1093 (w), 1033 (s), 1003 (s), 820 (s), 756 (s), 732 (w), 661 (w), 640 (w), 595 (w), 488 (w).

(ii) A suspension of $[\kappa^3\text{-Tptm}]\text{ZnH}$ (7 mg, 0.02 mmol) in C_6D_6 (*ca.* 0.7 mL) was treated with trimethylsilanol (11 mg, 0.12 mmol). The reaction was monitored by ^1H NMR spectroscopy, thereby demonstrating the formation of $[\kappa^4\text{-Tptm}]\text{ZnOSiMe}_3$ and H_2 over a period of 5 minutes at room temperature. The molecular structure of $[\kappa^4\text{-Tptm}]\text{ZnOSiMe}_3$ was determined by X-ray diffraction, thereby confirming the κ^4 -coordination mode, but the presence of six independent molecules and the low quality of the data prevents further discussion of the structure.

1.11.9 Synthesis of $[\kappa^4\text{-Tptm}]\text{ZnOSiPh}_3$

(i) A mixture of triphenylsilanol (58 mg, 0.21 mmol) and $[\kappa^3\text{-Tptm}]\text{ZnN}(\text{SiMe}_3)_2$ (100 mg, 0.18 mmol) was treated with benzene (*ca.* 3 mL) and the resulting solution was allowed to stand at room temperature for 5 minutes and then lyophilized. The resulting

residue was washed with MeCN (2 × 3 mL) and dried *in vacuo*, thereby giving $[\kappa^4\text{-Tptm}]\text{ZnOSiPh}_3$ as a light yellow powder (95 mg, 79 %). Crystals suitable for X-ray diffraction were obtained *via* slow evaporation from benzene. Anal. Calcd. for $[\kappa^4\text{-Tptm}]\text{ZnOSiPh}_3$: C, 59.8%; H, 4.0%; N, 6.2%. Found: C, 59.4%; H, 4.2%; N, 6.0%.

^1H NMR (C_6D_6): 6.02 [m, 3H, $\text{Ph}_3\text{SiOZnC}(\text{SC}_5\text{H}_4\text{N})_3$], 6.46 [br, 6H, $\text{Ph}_3\text{SiOZnC}(\text{SC}_5\text{H}_4\text{N})_3$], 7.26 [m, 9H, $\text{Ph}_3\text{SiOZnC}(\text{SC}_5\text{H}_4\text{N})_3$], 8.06 [br, 6H, $\text{Ph}_3\text{SiOZnC}(\text{SC}_5\text{H}_4\text{N})_3$], 9.31 [d, $^3J_{\text{H-H}} = 5$ Hz, 3H, $\text{Ph}_3\text{SiOZnC}(\text{SC}_5\text{H}_4\text{N})_3$]. $^{13}\text{C}\{^1\text{H}\}$ NMR (C_6D_6): not observed [$\text{Ph}_3\text{SiOZnC}(\text{SC}_5\text{H}_4\text{N})_3$], 119.0 [s, 3C, $\text{Ph}_3\text{SiOZnC}(\text{SC}_5\text{H}_4\text{N})_3$], 120.5 [s, 3C, $\text{Ph}_3\text{SiOZnC}(\text{SC}_5\text{H}_4\text{N})_3$], 127.9 [s, 6C, $\text{Ph}_3\text{SiOZnC}(\text{SC}_5\text{H}_4\text{N})_3$], 128.8 [s, 3C, $\text{Ph}_3\text{SiOZnC}(\text{SC}_5\text{H}_4\text{N})_3$], 136.1 [s, 6C, $\text{Ph}_3\text{SiOZnC}(\text{SC}_5\text{H}_4\text{N})_3$], 138.2 [s, 3C, $\text{Ph}_3\text{SiOZnC}(\text{SC}_5\text{H}_4\text{N})_3$], 143.3 [s, 3C, $\text{Ph}_3\text{SiOZnC}(\text{SC}_5\text{H}_4\text{N})_3$], 149.9 [s, 3C, $\text{Ph}_3\text{SiOZnC}(\text{SC}_5\text{H}_4\text{N})_3$], 161.5 [s, 3C, $\text{Ph}_3\text{SiOZnC}(\text{SC}_5\text{H}_4\text{N})_3$].

IR Data (KBr disk, cm^{-1}): 3086 (w), 3065 (w), 3047 (w), 3018 (w), 2993 (w), 1589 (s), 1559 (s), 1454 (s), 1417 (s), 1279 (m), 1131 (m), 1106 (s), 1040 (m), 1023 (w), 1004 (m), 759 (m), 721 (w), 703 (s), 640 (w), 515 (m).

(ii) A suspension of $[\kappa^3\text{-Tptm}]\text{ZnH}$ (10 mg, 0.02 mmol) in C_6D_6 (*ca.* 0.7 mL) was treated with triphenylsilanol (7 mg, 0.02 mmol). The reaction was monitored by ^1H NMR spectroscopy, thereby demonstrating the formation of $[\kappa^4\text{-Tptm}]\text{ZnOSiPh}_3$ and H_2 over a period of 5 minutes at room temperature. The κ^4 -coordination mode within $[\kappa^4\text{-Tptm}]\text{ZnOSiPh}_3$ was confirmed by X-ray diffraction, but disorder prevents further discussion of the structure.

1.11.10 Synthesis of $[\kappa^3\text{-Tptm}]\text{ZnH}$

(i) A solution of $[\kappa^4\text{-Tptm}]\text{ZnOSiMe}_3$ (1.865 g, 3.75 mmol) in C_6D_6 (*ca.* 5 mL) was treated with phenylsilane (530 mg, 4.88 mmol), thereby resulting in the rapid deposition of

colorless crystals. The mixture was allowed to stand at room temperature for 30 minutes. After this period, the mixture was filtered and the crystals obtained were dried *in vacuo* to give $[\kappa^3\text{-Tptm}]\text{ZnH}\cdot\text{C}_6\text{D}_6$ (1.755 g, 95 %).

(ii) A solution of $[\kappa^4\text{-Tptm}]\text{ZnOSiMe}_3$ (520 mg, 1.05 mmol) in benzene (*ca.* 5 mL) was treated with phenylsilane (165 mg, 1.53 mmol), thereby resulting in the rapid deposition of colorless crystals. The mixture was allowed to stand at room temperature for 1 day. After this period, the mixture was filtered and the crystals obtained were washed with benzene (2 × 2 mL) and dried *in vacuo* to give $[\kappa^3\text{-Tptm}]\text{ZnH}\cdot\text{C}_6\text{H}_6$ (421 mg, 83 %). Anal. Calcd. for $[\kappa^3\text{-Tptm}]\text{ZnH}\cdot 0.65(\text{C}_6\text{H}_6)$: C, 52.0%; H, 3.7%; N, 9.1%. Found: C, 51.8%; H, 3.9%; N, 8.8%.

$^1\text{H NMR}$ (C_6D_6): 5.60 [s, 1H, $\underline{\text{H}}\text{ZnC}(\text{SC}_5\text{H}_4\text{N})_3$], 6.21 [br, 3H, $\text{HZnC}(\text{SC}_5\underline{\text{H}}_4\text{N})_3$], 6.55 [br, 3H, $\text{HZnC}(\text{SC}_5\underline{\text{H}}_4\text{N})_3$], 6.64 [br, 3H, $\text{HZnC}(\text{SC}_5\underline{\text{H}}_4\text{N})_3$], 8.37 [br, 3H, $\text{HZnC}(\text{SC}_5\underline{\text{H}}_4\text{N})_3$].

IR Data (KBr disk, cm^{-1}): 3089 (w), 3067 (w), 3035 (w), 3013 (w), 2989 (w), 2963 (w), 1729 (m) [$\nu(\text{ZnH})$], 1592 (s), 1554 (s), 1460 (s), 1415 (s), 1284 (m), 1131 (m), 1091 (w), 1046 (w), 1010 (w), 758 (s), 721 (m), 686 (m), 518 (m), 484 (w), 463 (w).

1.11.11 Synthesis of $[\kappa^3\text{-Tptm}]\text{ZnD}$

A solution of $[\kappa^4\text{-Tptm}]\text{ZnOSiMe}_3$ (26 mg, 0.05 mmol) in benzene (*ca.* 5 mL) was treated with PhSiD_3 (6 mg, 0.05 mmol), thereby resulting in the rapid deposition of colorless crystals. The mixture was allowed to stand at room temperature for 3 hours. After this period, the mixture was filtered and the crystals obtained were washed with benzene (0.5 mL) and dried *in vacuo* to give $[\kappa^3\text{-Tptm}]\text{ZnD}\cdot\text{C}_6\text{H}_6$ (10 mg, 40 %).

^1H NMR (C_6D_6): 6.21 [br, 3H, $\text{DZnC}(\text{SC}_5\text{H}_4\text{N})_3$], 6.55 [br, 3H, $\text{DZnC}(\text{SC}_5\text{H}_4\text{N})_3$], 6.64 [br, 3H, $\text{DZnC}(\text{SC}_5\text{H}_4\text{N})_3$], 8.38 [br, 3H, $\text{DZnC}(\text{SC}_5\text{H}_4\text{N})_3$]. ^2H NMR (C_6H_6): 5.60 [br, 1D, $\text{DZnC}(\text{SC}_5\text{H}_4\text{N})_3$].

IR Data (KBr disk, cm^{-1}): 3087 (w), 3068 (w), 3037 (w), 3013 (w), 2988 (w), 2956 (w), 2930 (w), 1592 (s), 1574 (m), 1554 (s), 1460 (s), 1415 (s), 1284 (m), 1242 (m) [$\nu(\text{ZnD})$], 1133 (m), 1091 (w), 1046 (w), 1010 (w), 758 (s), 721 (m), 686 (s), 662 (w), 643 (w), 484 (w), 415 (w).

1.11.12 Synthesis of $[\kappa^4\text{-Tptm}]\text{ZnO}_2\text{CH}$

(i) A suspension of $[\kappa^3\text{-Tptm}]\text{ZnH}$ (14 mg, 0.03 mmol) in C_6D_6 (*ca.* 0.7 mL) in an NMR tube equipped with a J. Young valve was treated with CO_2 (1 atm) resulting in the dissolution of the $[\kappa^3\text{-Tptm}]\text{ZnH}$ and the formation of a pale yellow solution over a period of *ca.* 20 minutes. The reaction was monitored by ^1H NMR spectroscopy, thereby indicating the quantitative conversion to $[\kappa^4\text{-Tptm}]\text{ZnO}_2\text{CH}$. The solution was lyophilized, giving $[\kappa^4\text{-Tptm}]\text{ZnO}_2\text{CH}$ as a white powder (10 mg, 65%; the isolated yield is < 100% due to difficulties removing the sample from the tube). Anal. Calcd. for $[\kappa^4\text{-Tptm}]\text{Zn}(\kappa^2\text{-O}_2\text{CH})$: C, 45.1%; H, 2.9%; N, 9.3%. Found: C, 45.4%; H, 3.0%; N, 9.1%.

^1H NMR (C_6D_6): 6.25 [m, 3H, $\text{H}(\text{O})\text{COZnC}(\text{SC}_5\text{H}_4\text{N})_3$], 6.43 - 6.51 [m, 6H, $\text{H}(\text{O})\text{COZnC}(\text{SC}_5\text{H}_4\text{N})_3$], 9.16 [d, $^3J_{\text{H-H}} = 5$ Hz, 3H, $\text{H}(\text{O})\text{COZnC}(\text{SC}_5\text{H}_4\text{N})_3$], 9.53 [s, 1H, $\text{H}(\text{O})\text{COZnC}(\text{SC}_5\text{H}_4\text{N})_3$].

IR Data (KBr disk, cm^{-1}): 3085 (w), 3059 (w), 3016 (w), 2797 (w) [$\nu(\text{O-H})$], 2704 (w), 1621 (m) [$\nu_{\text{asym}}(\text{CO}_2)$], 1589 (s), 1557 (s), 1456 (s), 1417 (s), 1317 (m) [$\nu_{\text{sym}}(\text{CO}_2)$], 1283 (m), 1131 (m), 1093 (w), 1046 (w), 1006 (w), 760 (s), 723 (m), 640 (w), 486 (w).

(ii) $[\kappa^4\text{-Tptm}]\text{Zn}(\kappa^2\text{-O}_2^{13}\text{CH})$ was prepared in an analogous manner from the reaction of $[\kappa^3\text{-Tptm}]\text{ZnH}$ with $^{13}\text{CO}_2$.

^1H NMR (C_6D_6): 6.28 [m, 3H, $\text{H}(\text{O})\text{COZnC}(\text{SC}_5\text{H}_4\text{N})_3$], 6.46 - 6.55 [m, 6H, $\text{H}(\text{O})\text{COZnC}(\text{SC}_5\text{H}_4\text{N})_3$], 9.14 [d, $^3J_{\text{H-H}} = 5$ Hz, 3H, $\text{H}(\text{O})\text{COZnC}(\text{SC}_5\text{H}_4\text{N})_3$], 9.51 [d, $^1J_{\text{C-H}} = 192$ Hz, 1H, $\text{H}(\text{O})\text{COZnC}(\text{SC}_5\text{H}_4\text{N})_3$]. $^{13}\text{C}\{^1\text{H}\}$ NMR (C_6D_6): not observed
 $[\text{H}(\text{O})\text{COZnC}(\text{SC}_5\text{H}_4\text{N})_3]$, 119.6 [s, 3C, $\text{H}(\text{O})\text{COZnC}(\text{SC}_5\text{H}_4\text{N})_3$], 120.7 [s, 3C, $\text{H}(\text{O})\text{COZnC}(\text{SC}_5\text{H}_4\text{N})_3$], 138.2 [s, 3C, $\text{H}(\text{O})\text{COZnC}(\text{SC}_5\text{H}_4\text{N})_3$], 149.1 [s, 3C, $\text{H}(\text{O})\text{COZnC}(\text{SC}_5\text{H}_4\text{N})_3$], 161.4 [s, 3C, $\text{H}(\text{O})\text{COZnC}(\text{SC}_5\text{H}_4\text{N})_3$], 167.8 [s, 1C, $\text{H}(\text{O})\text{COZnC}(\text{SC}_5\text{H}_4\text{N})_3$].

IR Data (KBr disk, cm^{-1}): 3087 (w), 3067 (w), 3015 (w), 2951 (w), 2790 (w), [$\nu(^{13}\text{CO-H})$], 2686 (w), 1590 (s) [$\nu_{\text{asym}}(^{13}\text{CO}_2)$], 1554 (s), 1458 (s), 1417 (s), 1300 (m) [$\nu_{\text{sym}}(^{13}\text{CO}_2)$], 1277 (m), 1132 (m), 1093 (w), 1046 (w), 1007 (w), 759 (s), 722 (m), 681 (w), 641 (w), 610 (w), 486 (w).

(iii) A mixture of $[\kappa^3\text{-Tptm}]\text{ZnMe}$ (43 mg, 0.10 mmol) and C_6D_6 (ca. 1.0 mL) was treated with formic acid (10 μL , 0.27 mmol). The reaction was monitored by ^1H NMR spectroscopy, thereby demonstrating the formation of $[\kappa^4\text{-Tptm}]\text{Zn}(\kappa^2\text{-O}_2\text{CH})$ and methane. The solution was lyophilized and then the solid obtained was extracted into benzene (ca. 1.0 mL). Colorless crystals of $[\kappa^4\text{-Tptm}]\text{Zn}(\kappa^2\text{-O}_2\text{CH})$ (33 mg, 72%) were obtained by vapor diffusion of pentane into the benzene solution and were isolated by decanting the mother liquor and dried *in vacuo*.

(iv) A suspension of $[\kappa^3\text{-Tptm}]\text{ZnH}$ (13 mg, 0.03 mmol) in C_6D_6 (ca. 0.7 mL) in an NMR tube equipped with a J. Young valve was treated with formic acid (10 μL , 0.32 mmol). The reaction was monitored by NMR spectroscopy, thereby demonstrating the conversion to $[\kappa^4\text{-Tptm}]\text{Zn}(\kappa^2\text{-O}_2\text{CH})$ over a period of 5 minutes at room temperature.

1.11.13 Synthesis of $[\kappa^4\text{-Tptm}]\text{Li}$

A suspension of finely powdered $[\text{Tptm}]\text{H}$ (769 mg, 2.24 mmol) in Et_2O (ca. 10 mL, *via* vacuum transfer from LiAlH_4) was placed in an ice-water bath and treated dropwise with a solution of Bu^nLi in hexanes (2.5 M, 0.99 mL, 2.48 mmol). The mixture was stirred at 0 °C for 1.5 hours and then filtered at this temperature. The precipitate obtained was dried *in vacuo* to give $[\kappa^4\text{-Tptm}]\text{Li}$ (530 mg, 67.8 %) as an off-white solid. Colorless crystals were obtained by slow evaporation from benzene. Anal. Calcd. for $[\kappa^4\text{-Tptm}]\text{Li}$: C, 55.0%; H, 3.5%; N, 12.0%. Found: C, 55.3%; H, 3.7%; N, 11.3%.

^1H NMR (C_6D_6): 6.25 [m, 3H, $\text{LiC}(\text{SC}_5\text{H}_4\text{N})_3$], 6.61 [m, 3H, $\text{LiC}(\text{SC}_5\text{H}_4\text{N})_3$], 6.77 [d, $^3J_{\text{H-H}} = 8$ Hz, 3H, $\text{LiC}(\text{SC}_5\text{H}_4\text{N})_3$], 7.89 [d, $^3J_{\text{H-H}} = 5$ Hz, 3H, $\text{LiC}(\text{SC}_5\text{H}_4\text{N})_3$]. $^{13}\text{C}\{^1\text{H}\}$ NMR (C_6D_6): not observed [$\text{LiC}(\text{SC}_5\text{H}_4\text{N})_3$], 118.0 [s, 3C, $\text{LiC}(\text{SC}_5\text{H}_4\text{N})_3$], 120.1 [s, 3C, $\text{LiC}(\text{SC}_5\text{H}_4\text{N})_3$], 136.2 [s, 3C, $\text{LiC}(\text{SC}_5\text{H}_4\text{N})_3$], 147.2 [s, 3C, $\text{LiC}(\text{SC}_5\text{H}_4\text{N})_3$], 173.4 [s, 3C, $\text{LiC}(\text{SC}_5\text{H}_4\text{N})_3$]. ^7Li NMR (C_6D_6): 7.23 [s, 1Li, $\text{LiC}(\text{SC}_5\text{H}_4\text{N})_3$].

IR Data (KBr disk, cm^{-1}): 3070 (w), 3041 (w), 2982 (w), 2937 (w), 1573 (s), 1557 (s), 1453 (s), 1414 (s), 1279 (m), 1241 (w), 1174 (w), 1148 (m), 1125 (s), 1104 (s), 1082 (m), 1043 (m), 986 (m), 953 (w), 872 (w), 754 (s), 722 (m), 618 (w), 595 (w), 481 (m), 451 (m).

1.11.14 Synthesis of $\{[\kappa^4\text{-Tptm}]\text{MgBr}\}_2$

In a small Schlenk tube, $\text{H}[\text{Tptm}]$ (184 mg, 0.54 mmol) was suspended in Et_2O (ca. 8 mL, vacuum transferred from LiAlH_4) and put at 0 °C using an ice-water bath. MeMgBr (3.0 M in Et_2O , 0.38 mL, 1.14 mmol) was added *via* syringe, and the suspension was stirred at 0 °C for 3 hours. The precipitate was allowed to settle, filtered at 0 °C, and then dried *in vacuo* giving $\{[\kappa^4\text{-Tptm}]\text{MgBr}\}_2$ with 1 equivalent of Et_2O per magnesium determined by NMR spectroscopy (239 mg, 85.7%). Colorless crystals suitable for X-ray diffraction were obtained by slow evaporation from benzene.

^1H NMR (C_6D_6): 6.17 [m, 3H, $\text{BrMgC}(\text{SC}_5\text{H}_4\text{N})_3$], 6.41 - 6.46 [m, 6H, $\text{BrMgC}(\text{SC}_5\text{H}_4\text{N})_3$], 9.76 [m, 3H, $\text{BrMgC}(\text{SC}_5\text{H}_4\text{N})_3$].

1.11.15 Synthesis of [Tptm]MgCl

In a small Schlenk tube, $\text{H}[\text{Tptm}]$ (221 mg, 0.64 mmol) was suspended in Et_2O (*ca.* 8 mL, vacuum transferred from LiAlH_4) and put at 0°C using an ice-water bath. MeMgCl (3.0 M in THF, 0.26 mL, 0.77 mmol) was added *via* syringe, and the suspension was stirred at 0°C for 10 minutes, and then room temperature for 30 minutes. The precipitate was allowed to settle, filtered, and then dried *in vacuo* giving [Tptm]MgCl with Et_2O and THF as the only contaminants (290 mg including solvents).

^1H NMR (C_6D_6): 6.20 [t, $^3J_{\text{H-H}} = 5$ Hz, 3H, $\text{ClMgC}(\text{SC}_5\text{H}_4\text{N})_3$], 6.44 - 6.51 [m, 6H, $\text{ClMgC}(\text{SC}_5\text{H}_4\text{N})_3$], 9.64 [d, $^3J_{\text{H-H}} = 6$ Hz, 3H, $\text{ClMgC}(\text{SC}_5\text{H}_4\text{N})_3$].

1.11.16 Synthesis of [κ^4 -Tptm]ZnCl

A mixture of [κ^4 -Tptm]Li (125 mg, 0.36 mmol) and ZnCl_2 (59 mg, 0.43 mmol) was treated with Et_2O (*ca.* 5 mL *via* vacuum transfer from LiAlH_4). The frozen mixture was allowed to warm to room temperature and the thick white suspension was stirred overnight. After this period, the volatile components were removed *in vacuo* and the solid was extracted into benzene (*ca.* 5 mL). The extract was lyophilized and the solid obtained was washed with acetonitrile (*ca.* 5 mL) and dried *in vacuo* giving [κ^4 -Tptm]ZnCl as an off white powder (65 mg, 41%). Anal. Calcd. for [κ^4 -Tptm]ZnCl \cdot 0.30 C_6H_6 (sample obtained by crystallization from benzene): C, 45.8%; H, 3.0%; N, 9.0%. Found: C, 45.8%; H, 2.6%; N, 9.8%.

^1H NMR (C_6D_6): 6.24 [m, 3H, $\text{ClZnC}(\text{SC}_5\text{H}_4\text{N})_3$], 6.44 - 6.52 [m, 6H, $\text{ClZnC}(\text{SC}_5\text{H}_4\text{N})_3$], 9.82 [d, $^3J_{\text{H-H}} = 6$ Hz, 3H, $\text{ClZnC}(\text{SC}_5\text{H}_4\text{N})_3$].

IR Data (KBr disk, cm^{-1}): 3084 (w), 3059 (w), 3013 (w), 2963 (w), 1589 (s), 1556 (s),

1454 (s), 1415 (s), 1282 (m), 1259 (w), 1131 (m), 1094 (w), 1046 (m), 1004 (m), 877 (w), 803 (w), 761 (s), 723 (m), 639 (m), 614 (m), 490 (m).

1.11.17 Reaction of $[\kappa^4\text{-Tptm}]\text{ZnOSiMe}_3$ with Me_3SiCl : Formation of $[\kappa^4\text{-Tptm}]\text{ZnCl}$

A solution of $[\kappa^4\text{-Tptm}]\text{ZnOSiMe}_3$ (6 mg, 0.01 mmol) in C_6D_6 (ca. 0.7 mL) in an NMR tube equipped with a J. Young valve was treated with Me_3SiCl (20 μL , 0.16 mmol). The reaction was monitored by NMR spectroscopy, thereby demonstrating the conversion to $[\kappa^4\text{-Tptm}]\text{ZnCl}$ over a period of 2 days at room temperature.

1.11.18 Reaction of $[\kappa^4\text{-Tptm}]\text{ZnOSiPh}_3$ with Me_3SiCl : Formation of $[\kappa^4\text{-Tptm}]\text{ZnCl}$

A solution of $[\kappa^4\text{-Tptm}]\text{ZnOSiPh}_3$ (5 mg, 0.01 mmol) in C_6D_6 (ca. 0.7 mL) in an NMR tube equipped with a J. Young valve was treated with Me_3SiCl (20 μL , 0.16 mmol). The reaction was monitored by NMR spectroscopy, thereby demonstrating very slow conversion to $[\kappa^4\text{-Tptm}]\text{ZnCl}$ at room temperature. Complete conversion to $[\kappa^4\text{-Tptm}]\text{ZnCl}$ was achieved by heating the sample at 60 °C for 3 days.

1.11.19 Reaction of $[\kappa^4\text{-Tptm}]\text{ZnO}_2\text{CH}$ with Me_3SiCl : Formation of $[\kappa^4\text{-Tptm}]\text{ZnCl}$

A solution of $[\kappa^4\text{-Tptm}]\text{ZnO}_2\text{CH}$ (2 mg, 0.004 mmol) in C_6D_6 (ca. 0.7 mL) in an NMR tube equipped with a J. Young valve was treated with Me_3SiCl (20 μL , 0.16 mmol). The reaction was monitored by NMR spectroscopy, thereby demonstrating the conversion to $[\kappa^4\text{-Tptm}]\text{ZnCl}$ over a period of 15 minutes at room temperature.

1.11.20 Reaction of $[\kappa^3\text{-Tptm}]\text{ZnH}$ with Me_3SiCl : Formation of $[\kappa^4\text{-Tptm}]\text{ZnCl}$

A suspension of $[\kappa^3\text{-Tptm}]\text{ZnH}$ (8 mg, 0.02 mmol) in C_6D_6 (ca. 0.7 mL) in an NMR tube equipped with a J. Young valve was treated with Me_3SiCl (20 μL , 0.16 mmol). The reaction was monitored by NMR spectroscopy, thereby demonstrating the conversion

to $[\kappa^4\text{-Tptm}]\text{ZnCl}$ over a period of 16 hours at room temperature.

1.11.21 Reaction of $[\kappa^4\text{-Tptm}]\text{ZnOSiMe}_3$ with Me_3SiBr : Formation of $[\kappa^4\text{-Tptm}]\text{ZnBr}$

A solution of $[\kappa^4\text{-Tptm}]\text{ZnOSiMe}_3$ (24 mg, 0.05 mmol) in C_6D_6 (ca. 0.7 mL) in an NMR tube equipped with a J. Young valve was treated with Me_3SiBr (10 μL , 0.08 mmol). The reaction was monitored by ^1H NMR spectroscopy, thereby demonstrating the conversion to $[\kappa^4\text{-Tptm}]\text{ZnBr}$ over a period of 20 minutes at room temperature. The reaction was then lyophilized to give $[\kappa^4\text{-Tptm}]\text{ZnBr}$ as an off-white solid (17 mg, 72%).

^1H NMR (C_6D_6): 6.23 [m, 3H, $\text{BrZnC}(\text{SC}_5\text{H}_4\text{N})_3$], 6.42 - 6.49 [m, 6H, $\text{BrZnC}(\text{SC}_5\text{H}_4\text{N})_3$], 9.86 [d, $^3J_{\text{H-H}} = 5$ Hz, 3H, $\text{BrZnC}(\text{SC}_5\text{H}_4\text{N})_3$]. $^{13}\text{C}\{^1\text{H}\}$ NMR (C_6D_6): not observed [$\text{BrZnC}(\text{SC}_5\text{H}_4\text{N})_3$], 119.3 [s, 3C, $\text{BrZnC}(\text{SC}_5\text{H}_4\text{N})_3$], 120.7 [s, 3C, $\text{Br}(\text{SC}_5\text{H}_4\text{N})_3$], 138.3 [s, 3C, $\text{BrZnC}(\text{SC}_5\text{H}_4\text{N})_3$], 150.2 [s, 3C, $\text{BrZnC}(\text{SC}_5\text{H}_4\text{N})_3$], 161.0 [s, 3C, $\text{BrZnC}(\text{SC}_5\text{H}_4\text{N})_3$].

IR Data (KBr disk, cm^{-1}): 3082 (w), 3059 (w), 3015 (w), 2346 (w), 1590 (s), 1557 (s), 1457 (s), 1416 (s), 1283 (m), 1254 (w), 1132 (m), 1090 (w), 1048 (m), 1004 (m), 875 (w), 761 (s), 724 (m), 639 (m), 623 (m), 409 (w).

1.11.22 Reaction of $[\kappa^4\text{-Tptm}]\text{ZnOSiPh}_3$ with Me_3SiBr : Formation of $[\kappa^4\text{-Tptm}]\text{ZnBr}$

A solution of $[\kappa^4\text{-Tptm}]\text{ZnOSiPh}_3$ (3 mg, 0.004 mmol) in C_6D_6 (ca. 0.7 mL) in an NMR tube equipped with a J. Young valve was treated with Me_3SiBr (10 μL , 0.08 mmol). The reaction was monitored by ^1H NMR spectroscopy, thereby demonstrating conversion to $[\kappa^4\text{-Tptm}]\text{ZnBr}$ over a period of 20 hours at room temperature.

1.11.23 Reaction of $[\kappa^4\text{-Tptm}]\text{ZnO}_2\text{CH}$ with Me_3SiBr : Formation of $[\kappa^4\text{-Tptm}]\text{ZnBr}$

A solution of $[\kappa^4\text{-Tptm}]\text{ZnO}_2\text{CH}$ (4 mg, 0.01 mmol) in C_6D_6 (ca. 0.7 mL) in an NMR tube equipped with a J. Young valve was treated with Me_3SiBr (3 μL , 0.02 mmol). The

reaction was monitored by ^1H NMR spectroscopy, thereby demonstrating the conversion to $[\kappa^4\text{-Tptm}]\text{ZnBr}$ over a period of 30 minutes at room temperature.

1.11.24 Reaction of $[\kappa^3\text{-Tptm}]\text{ZnH}$ with Me_3SiBr : Formation of $[\kappa^4\text{-Tptm}]\text{ZnBr}$

A suspension of $[\kappa^3\text{-Tptm}]\text{ZnH}$ (4 mg, 0.01 mmol) in C_6D_6 (*ca.* 0.7 mL) in an NMR tube equipped with a J. Young valve was treated with Me_3SiBr (10 μL , 0.08 mmol). The reaction was monitored by ^1H NMR spectroscopy, thereby demonstrating the conversion to $[\kappa^4\text{-Tptm}]\text{ZnBr}$ over a period of 20 minutes at room temperature.

1.11.25 Synthesis of $[\kappa^4\text{-Tptm}]\text{ZnI}$

A mixture of $[\kappa^4\text{-Tptm}]\text{Li}$ (500 mg, 1.43 mmol) and ZnI_2 (580 mg, 1.82 mmol) was treated with Et_2O (*ca.* 10 mL, *via* vacuum transferred from LiAlH_4). The frozen mixture was allowed to warm to room temperature and the thick white suspension was stirred overnight. After this period, the volatile components were removed *in vacuo* and the solid was extracted into benzene (*ca.* 10 mL). The extract was lyophilized and the solid obtained was washed with acetonitrile (*ca.* 8 mL) and dried *in vacuo* to give $[\kappa^4\text{-Tptm}]\text{ZnI}$ (454 mg, 59 %) as a yellow powder. Colorless crystals of $[\kappa^4\text{-Tptm}]\text{ZnI}$ suitable for X-ray diffraction were obtained by slow evaporation from benzene. Anal. Calcd. for $[\kappa^4\text{-Tptm}]\text{ZnI}$: C, 35.9%; H, 2.3 %; N, 7.9%. Found: C, 34.0%; H, 2.0%; N, 7.2%.

^1H NMR (C_6D_6): 6.22 [m, 3H, $\text{IZnC}(\text{SC}_5\text{H}_4\text{N})_3$], 6.40 - 6.48 [m, 6H, $\text{IZnC}(\text{SC}_5\text{H}_4\text{N})_3$], 9.70 [br, 3H, $\text{IZnC}(\text{SC}_5\text{H}_4\text{N})_3$]. $^{13}\text{C}\{^1\text{H}\}$ NMR (C_6D_6): not observed [$\text{IZn}\underline{\text{C}}(\text{SC}_5\text{H}_4\text{N})_3$], 119.2 [s, 3C, $\text{IZnC}(\text{SC}_5\text{H}_4\text{N})_3$], 121.0 [s, 3C, $\text{IZnC}(\text{SC}_5\text{H}_4\text{N})_3$], 138.3 [s, 3C, $\text{IZnC}(\text{SC}_5\text{H}_4\text{N})_3$], 150.0 [s, 3C, $\text{IZnC}(\text{SC}_5\text{H}_4\text{N})_3$], 160.8 [s, 3C, $\text{IZnC}(\text{SC}_5\text{H}_4\text{N})_3$].

IR Data (KBr disk, cm^{-1}): 3079 (w), 3056 (w), 3013 (w), 2963 (w), 2906 (w), 1589 (s), 1554 (s), 1457 (s), 1414 (s), 1282 (m), 1262 (s), 1130 (w), 1093 (w), 1045 (w), 875 (s), 801 (s), 759 (s), 723 (m), 637 (m).

The κ^4 -coordination mode within $[\kappa^4\text{-Tptm}]\text{ZnI}$ was confirmed by X-ray diffraction, but disorder prevents further discussion of the structure. $[\kappa^4\text{-Tptm}]\text{ZnI}$ is monoclinic, Cc ($Z = 4$), $a = 15.7489(17)$ Å, $b = 9.2982(17)$ Å, $c = 14.137(2)$ Å, $\alpha = 90$, $\beta = 117.813(3)^\circ$, $\gamma = 90^\circ$, $V = 1831.1(5)$ Å³, $T = 125$ K.

1.11.26 Reaction of $[\kappa^4\text{-Tptm}]\text{ZnOSiPh}_3$ with Me_3SiI : Formation of $[\kappa^4\text{-Tptm}]\text{ZnI}$

A solution of $[\kappa^4\text{-Tptm}]\text{ZnOSiPh}_3$ (3 mg, 0.004 mmol) in C_6D_6 (*ca.* 0.7 mL) in an NMR tube equipped with a J. Young valve was treated with Me_3SiI (10 mg, 0.05 mmol). The reaction was monitored by NMR spectroscopy, thereby demonstrating the conversion to $[\kappa^4\text{-Tptm}]\text{ZnI}$ over a period of 22 hours at room temperature.

1.11.27 Reaction of $[\kappa^4\text{-Tptm}]\text{ZnO}_2\text{CH}$ with Me_3SiI : Formation of $[\kappa^4\text{-Tptm}]\text{ZnI}$

A solution of $[\kappa^4\text{-Tptm}]\text{ZnO}_2\text{CH}$ (2 mg, 0.004 mmol) in C_6D_6 (*ca.* 0.7 mL) in an NMR tube equipped with a J. Young valve was treated with Me_3SiI (10 mg, 0.05 mmol). The reaction was monitored by NMR spectroscopy, thereby demonstrating the conversion to $[\kappa^4\text{-Tptm}]\text{ZnI}$ over a period of 15 minutes at room temperature.

1.11.28 Reaction of $[\kappa^3\text{-Tptm}]\text{ZnH}$ with Me_3SiI : Formation of $[\kappa^4\text{-Tptm}]\text{ZnI}$

A suspension of $[\kappa^3\text{-Tptm}]\text{ZnH}$ (4 mg, 0.01 mmol) in C_6D_6 (*ca.* 0.7 mL) in an NMR tube equipped with a J. Young valve was treated with Me_3SiI (3 mg, 0.02 mmol). The reaction was monitored by NMR spectroscopy, thereby demonstrating the conversion to $[\kappa^4\text{-Tptm}]\text{ZnI}$ over a period of 15 minutes at room temperature.

1.11.29 Reaction of $[\kappa^4\text{-Tptm}]\text{ZnOSiMe}_3$ with Me_3SiI : Formation of $[\kappa^4\text{-Tptm}]\text{ZnI}$

A solution of $[\kappa^4\text{-Tptm}]\text{ZnOSiMe}_3$ (65 mg, 0.13 mmol) in C_6D_6 (*ca.* 0.7 mL) in an NMR tube equipped with a J. Young valve was treated with Me_3SiI (*ca.* 0.3 mL, 2.1 mmol) *via*

vacuum transfer. The reaction was monitored by ^1H NMR spectroscopy, thereby demonstrating the conversion to $[\kappa^4\text{-Tptm}]\text{ZnI}$ over a period of 15 minutes at room temperature. The sample was then lyophilized to give $[\kappa^4\text{-Tptm}]\text{ZnI}$ as a yellow powder (57 mg, 82%).

1.11.30 Reaction of $[\kappa^4\text{-Tptm}]\text{ZnOSiMe}_3$ with Me_3SiN_3 : Synthesis of $[\kappa^4\text{-Tptm}]\text{ZnN}_3$

A solution of $[\kappa^4\text{-Tptm}]\text{ZnOSiMe}_3$ (5 mg, 0.01 mmol) in C_6D_6 (ca. 0.7 mL) in an NMR tube equipped with a J. Young valve was treated with Me_3SiN_3 (20 μL , 0.15 mmol). The reaction was monitored by NMR spectroscopy, thereby demonstrating the quantitative conversion to $[\kappa^4\text{-Tptm}]\text{ZnN}_3$ over a period of 2 days at room temperature. The solution was lyophilized to give $[\kappa^4\text{-Tptm}]\text{ZnN}_3$ as a yellow powder (4 mg, 89%; the isolated yield is < 100% due to difficulties removing the sample from the tube). Anal. Calcd. for $[\kappa^4\text{-Tptm}]\text{ZnN}_3 \cdot 0.25(\text{C}_6\text{H}_6)$: C, 44.8%; H, 2.9 %; N, 17.9%. Found: C, 44.3%; H, 2.6%; N, 17.5%.

^1H NMR (C_6D_6): 6.24 [m, 3H, $\text{N}_3\text{Zn C}(\text{SC}_5\text{H}_4\text{N})_3$], 6.40 [m, 3H, $\text{N}_3\text{Zn C}(\text{SC}_5\text{H}_4\text{N})_3$], 6.46 [m, 3H, $\text{N}_3\text{ZnC}(\text{SC}_5\text{H}_4\text{N})_3$], 9.12 [d, $^3J_{\text{HH}} = 5$ Hz, 3H, $\text{N}_3\text{ZnC}(\text{SC}_5\text{H}_4\text{N})_3$]. $^{13}\text{C}\{^1\text{H}\}$ NMR (C_6D_6): not observed [$\text{N}_3\text{ZnC}(\text{SC}_5\text{H}_4\text{N})_3$], 119.8 [s, 3C, $\text{N}_3\text{ZnC}(\text{SC}_5\text{H}_4\text{N})_3$], 120.7 [s, 3C, $\text{N}_3\text{ZnC}(\text{SC}_5\text{H}_4\text{N})_3$], 138.5 [s, 3C, $\text{N}_3\text{ZnC}(\text{SC}_5\text{H}_4\text{N})_3$], 148.8 [s, 3C, $\text{N}_3\text{ZnC}(\text{SC}_5\text{H}_4\text{N})_3$], 161.2 [s, 3C, $\text{N}_3\text{ZnC}(\text{SC}_5\text{H}_4\text{N})_3$].

IR Data (KBr disk, cm^{-1}): 3083 (w), 3069 (w), 3057 (w), 3016 (w), 2964 (w), 2066 (m) [$\nu(\text{N}_3)$], 1591 (s), 1555 (s), 1458 (s), 1412 (s), 1263 (m), 1132 (s), 1089 (w), 1049 (w), 1012 (w), 763 (s).

1.11.31 Reaction of $[\kappa^4\text{-Tptm}]\text{ZnO}_2\text{CH}$ with Me_3SiN_3 : Formation of $[\kappa^4\text{-Tptm}]\text{ZnN}_3$

A solution of $[\kappa^4\text{-Tptm}]\text{ZnO}_2\text{CH}$ (2 mg, 0.004 mmol) in C_6D_6 (ca. 0.7 mL) in an NMR tube equipped with a J. Young valve was treated with Me_3SiN_3 (20 μL , 0.15 mmol). The

reaction was monitored by NMR spectroscopy, thereby demonstrating the conversion to $[\kappa^4\text{-Tptm}]\text{ZnN}_3$ over a period of 1 hour at room temperature.

1.11.32 Reaction of $[\kappa^4\text{-Tptm}]\text{ZnOSiPh}_3$ with Me_3SiN_3 : Formation of $[\kappa^4\text{-Tptm}]\text{ZnN}_3$

A solution of $[\kappa^4\text{-Tptm}]\text{ZnOSiPh}_3$ (4 mg, 0.006 mmol) in C_6D_6 (ca. 0.7 mL) in an NMR tube equipped with a J. Young valve was treated with Me_3SiN_3 (20 μL , 0.15 mmol). The reaction was monitored by NMR spectroscopy, thereby demonstrating the conversion to $[\kappa^4\text{-Tptm}]\text{ZnN}_3$ over a period of 1 hour at room temperature.

1.11.33 Reaction of $[\kappa^4\text{-Tptm}]\text{ZnOSiMe}_3$ with Me_3SiOAc : Synthesis of $[\kappa^4\text{-Tptm}]\text{ZnOAc}$

Me_3SiOAc (20 μL , 0.13 mmol) was added to a solution of $[\kappa^4\text{-Tptm}]\text{ZnOSiMe}_3$ (18 mg, 0.04 mmol) in C_6D_6 (ca. 0.7 mL) in an NMR tube equipped with a J. Young valve. The reaction was monitored by NMR, thereby demonstrating the clean conversion to $[\kappa^4\text{-Tptm}]\text{ZnOAc}$ over a period of 30 minutes at room temperature. The solution was then lyophilized, giving $[\kappa^4\text{-Tptm}]\text{ZnOAc}$ (14 mg, 83%) as an off-white powder. Mass spectrum: $m/z = 465.0$ {M}+.

^1H NMR (C_6D_6): 2.35 [s, 3H, $\text{H}_3\text{CC}(\text{O})\text{OZnC}(\text{SC}_5\text{H}_4\text{N})_3$], 6.29 [bt, $^3J_{\text{H-H}} = 5$ Hz, 3H, $\text{AcOZnC}(\text{SC}_5\text{H}_4\text{N})_3$], 6.45 - 6.52 [m, 6H, $\text{AcOZnC}(\text{SC}_5\text{H}_4\text{N})_3$], 9.09 [d, $^3J_{\text{H-H}} = 5$ Hz, 3H, $\text{AcOZnC}(\text{SC}_5\text{H}_4\text{N})_3$]. $^{13}\text{C}\{^1\text{H}\}$ NMR (C_6D_6): 23.7 [s, 1C, $\text{Me}(\text{O})\text{COZnC}(\text{SC}_5\text{H}_4\text{N})_3$], not observed [$\text{AcOZnC}(\text{SC}_5\text{H}_4\text{N})_3$], 119.5 [s, 3C, $\text{AcOZnC}(\text{SC}_5\text{H}_4\text{N})_3$], 120.8 [s, 3C, $\text{AcOZnC}(\text{SC}_5\text{H}_4\text{N})_3$], 137.9 [s, 3C, $\text{AcOZnC}(\text{SC}_5\text{H}_4\text{N})_3$], 148.7 [s, 3C, $\text{AcOZnC}(\text{SC}_5\text{H}_4\text{N})_3$], 161.5 [s, 3C, $\text{AcOZnC}(\text{SC}_5\text{H}_4\text{N})_3$], 177.8 [s, 1C, $\text{Me}(\text{O})\text{COZnC}(\text{SC}_5\text{H}_4\text{N})_3$].

IR Data (KBr disk, cm^{-1}): 3084 (w), 3059 (w), 3014 (w), 2964 (w), 2919 (w), 2850 (w), 2370 (w), 2348 (w), $\nu_{\text{OAc}} = 1613$ (s), 1590 (s), 1558 (s), 1459 (s), 1418 (s), 1388 (s) [$\nu(\text{OAc})$], 1333 (m) [$\nu(\text{OAc})$], 1281 (m), 1131 (m), 1086 (w), 1046 (w), 1005 (w), 769 (s), 722

(m).

1.11.34 Reaction of $[\kappa^4\text{-Tptm}]\text{ZnOSiPh}_3$ with Me_3SiOAc : Formation of $[\kappa^4\text{-Tptm}]\text{ZnOAc}$

A solution of $[\kappa^4\text{-Tptm}]\text{ZnOSiPh}_3$ (5 mg, 0.007 mmol) in C_6D_6 (*ca.* 0.7 mL) in an NMR tube equipped with a J. Young valve was treated with Me_3SiOAc (20 μL , 0.13 mmol). The reaction was monitored by NMR spectroscopy, thereby demonstrating the conversion to $[\kappa^4\text{-Tptm}]\text{ZnOAc}$ over a period of 2 hours at room temperature.

1.11.35 Reaction of $[\kappa^4\text{-Tptm}]\text{ZnO}_2\text{CH}$ with Me_3SiOAc : Formation of $[\kappa^4\text{-Tptm}]\text{ZnOAc}$

A solution of $[\kappa^4\text{-Tptm}]\text{ZnO}_2\text{CH}$ (3 mg, 0.007 mmol) in C_6D_6 (*ca.* 0.7 mL) in an NMR tube equipped with a J. Young valve was treated with Me_3SiOAc (10 μL , 0.07 mmol). The reaction was monitored by ^1H NMR spectroscopy, thereby demonstrating the partial formation of $[\kappa^4\text{-Tptm}]\text{ZnOAc}$ over a period of 10 minutes. The sample was lyophilized, dissolved in C_6D_6 (*ca.* 0.7 mL), and shown to be a *ca.* 0.5:1 mixture of $[\kappa^4\text{-Tptm}]\text{ZnOAc}$: $[\kappa^4\text{-Tptm}]\text{ZnO}_2\text{CH}$ by ^1H NMR spectroscopy. A further quantity of Me_3SiOAc (30 μL , 0.20 mmol) was added and the sample lyophilized to give 1.7:1 mixture of $[\kappa^4\text{-Tptm}]\text{ZnOAc}$: $[\kappa^4\text{-Tptm}]\text{ZnO}_2\text{CH}$. The process was repeated sequentially with (i) additional Me_3SiOAc (60 μL , 0.40 mmol) to give a 4.4:1 mixture of $[\kappa^4\text{-Tptm}]\text{ZnOAc}$: $[\kappa^4\text{-Tptm}]\text{ZnO}_2\text{CH}$ and (ii) additional Me_3SiOAc (60 μL , 0.40 mmol) to give a 13.4:1 mixture of $[\kappa^4\text{-Tptm}]\text{ZnOAc}$: $[\kappa^4\text{-Tptm}]\text{ZnO}_2\text{CH}$. The observation that excess Me_3SiOAc does not produce $[\kappa^4\text{-Tptm}]\text{ZnOAc}$ in a quantitative manner suggests an equilibrium situation.

1.11.36 Reaction of $[\kappa^3\text{-Tptm}]\text{ZnH}$ with HOAc: Formation of $[\kappa^4\text{-Tptm}]\text{ZnOAc}$

A suspension of $[\kappa^3\text{-Tptm}]\text{ZnH}$ (3 mg, 0.01 mmol) in C_6D_6 (ca. 0.7 mL) in an NMR tube equipped with a J. Young valve was treated with acetic acid (20 μL , 0.35 mmol). The reaction was monitored by NMR spectroscopy, thereby demonstrating the conversion to $[\kappa^4\text{-Tptm}]\text{ZnOAc}$ over a period of 10 minutes at room temperature.

1.11.37 Reaction of $[\kappa^3\text{-Tptm}]\text{ZnN}(\text{SiMe}_3)_2$ with CO_2 : Synthesis of $[\kappa^4\text{-Tptm}]\text{ZnNCO}$

A solution of $[\kappa^3\text{-Tptm}]\text{ZnN}(\text{SiMe}_3)_2$ (28 mg, 0.05 mmol) in C_6D_6 (ca. 1 mL) in a flame-dried ampoule was treated with CO_2 (1 atm.) for a period of 4 days. After this period, the solution was lyophilized and the solid obtained was dissolved in C_6D_6 (ca. 1 mL) and analyzed by NMR spectroscopy, thereby demonstrating quantitative conversion to $[\kappa^4\text{-Tptm}]\text{ZnNCO}$. The solution was allowed to evaporate and deposit colorless crystals of $[\kappa^4\text{-Tptm}]\text{ZnNCO}$ suitable for X-ray diffraction (13 mg, 59 %). Evidence for the formation of $(\text{Me}_3\text{SiO})_2\text{CO}^{68}$ as a byproduct is provided by mass spectrometry [$m/z = 207.03$ { $\text{M}+\text{H}^+$ }] and ^1H [δ 0.21] and ^{13}C [δ 151.9] NMR spectroscopy. Anal. Calcd. for $[\kappa^4\text{-Tptm}]\text{ZnNCO}\cdot 0.50 \text{C}_6\text{H}_6$: C, 49.1%; H, 3.1%; N, 11.5%. Found: C, 48.7%; H, 2.5%; N, 11.4%.

^1H NMR (C_6D_6): 6.20 [m, 3H, $\text{OCN}\text{ZnC}(\text{SC}_5\text{H}_4\text{N})_3$], 6.42 [d, $^3J_{\text{H-H}} = 8$ Hz, 3H, $\text{OCN}\text{ZnC}(\text{SC}_5\text{H}_4\text{N})_3$], 6.50 [m, 3H, $\text{OCN}\text{ZnC}(\text{SC}_5\text{H}_4\text{N})_3$], 9.11 [d, $^3J_{\text{H-H}} = 5$ Hz, 3H, $\text{OCN}\text{ZnC}(\text{SC}_5\text{H}_4\text{N})_3$].

IR Data (KBr disk, cm^{-1}): 3087 (w), 3072 (w), 3056 (w), 3015 (w), 2223 (m) [ν_{asym} (NCO)], 1589 (s), 1554 (s), 1455 (s), 1417 (s), 1339 (w) [ν_{sym} (NCO)], 1280 (m), 1131 (m), 1092 (w), 1046 (m), 1004 (w), 875 (w), 763 (s), 722 (m), 641 (w), 622 (m), 521 (m), 489 (m).

(ii) *Mass Spectrometric Characterization of $(\text{Me}_3\text{SiO})_2\text{CO}$ in the reaction of $[\kappa^4\text{-Tptm}]\text{ZnN}(\text{SiMe}_3)_2$ and CO_2 .*

A solution of $[\kappa^3\text{-Tptm}]\text{ZnN}(\text{SiMe}_3)_2$ (8 mg, 0.01 mmol) in C_6H_6 (ca. 0.7 mL) in an NMR tube equipped with a J. Young valve was treated with CO_2 (1 atm). The sample was left overnight at room temperature, and then analyzed by mass spectrometry which provided evidence for $(\text{Me}_3\text{SiO})_2\text{CO}$ $m/z = 207.03$ $\{\text{M}+\text{H}\}^+$.

(iii) Reaction of $[\kappa^3\text{-Tptm}]\text{ZnN}(\text{SiMe}_3)_2$ with $^{13}\text{CO}_2$.

A solution of $[\kappa^3\text{-Tptm}]\text{ZnN}(\text{SiMe}_3)_2$ (36 mg, 0.06 mmol) in C_6D_6 (ca. 1 mL) in an NMR tube equipped with a J. Young valve was treated with $^{13}\text{CO}_2$ (1 atm). The reaction was monitored by ^1H and ^{13}C NMR spectroscopy, thereby demonstrating the initial formation of $[\text{Tptm}]\text{ZnOSiMe}_3$ and $\text{Me}_3\text{SiN}^{13}\text{CO}$, which subsequently converts to $[\kappa^4\text{-Tptm}]\text{ZnN}^{13}\text{CO}$ ($^{13}\text{C}\{^1\text{H}\}$ δ 124.4) and $\text{Me}_3\text{SiO}^{13}\text{C}(\text{O})\text{OSiMe}_3$ ($^{13}\text{C}\{^1\text{H}\}$ δ 151.9)⁶⁸ in the presence of $^{13}\text{CO}_2$.

$^{13}\text{C}\{^1\text{H}\}$ NMR (C_6D_6): not observed $[\text{O}^{13}\text{CNZnC}(\text{SC}_5\text{H}_4\text{N})_3]$, 119.7 [s, 3C, $\text{O}^{13}\text{CNZnC}(\text{SC}_5\text{H}_4\text{N})_3]$, 120.6 [s, 3C, $\text{O}^{13}\text{CNZnC}(\text{SC}_5\text{H}_4\text{N})_3]$, 129.9 [t, $^1\text{J}_{\text{N-C}} = 16$, 1C, $\text{O}^{13}\text{CNZnC}(\text{SC}_5\text{H}_4\text{N})_3]$, 138.4 [s, 3C, $\text{O}^{13}\text{CNZnC}(\text{SC}_5\text{H}_4\text{N})_3]$, 148.5 [s, 3C, $\text{O}^{13}\text{CNZnC}(\text{SC}_5\text{H}_4\text{N})_3]$, 161.1 [s, 3C, $\text{O}^{13}\text{CNZnC}(\text{SC}_5\text{H}_4\text{N})_3]$.

IR Data (KBr disk, cm^{-1}): 3087 (w), 3069 (w), 3016 (w), 2153 (s) [$\nu_{\text{asym}}(\text{N}^{13}\text{CO})$], 1590 (s), 1559 (s), 1457 (s), 1417 (s), 1325 (w) [$\nu_{\text{sym}}(\text{N}^{13}\text{CO})$], 1280 (m), 1132 (m), 1089 (w), 1047 (m), 1007 (w), 758 (s), 723 (m), 641 (w), 606(m), 486 (w), 410 (w).

1.11.38 Reaction of $[\kappa^4\text{-Tptm}]\text{ZnO}_2\text{CH}$ with Me_3SiNCO : Synthesis of $[\kappa^4\text{-Tptm}]\text{ZnNCO}$

A solution of $[\kappa^4\text{-Tptm}]\text{ZnO}_2\text{CH}$ (2 mg, 0.004 mmol) in benzene (ca. 0.7 mL) in an NMR tube equipped with a J. Young valve was treated with Me_3SiNCO (10 mg, 0.09 mmol). The reaction was monitored by NMR spectroscopy, thereby demonstrating the conversion to $[\kappa^4\text{-Tptm}]\text{ZnNCO}$ over a period of 24 days at room temperature.

1.11.39 Synthesis of $[\kappa^4\text{-Tptm}]\text{ZnNCO}$ via the CO_2 Promoted Reaction of $[\kappa^4\text{-Tptm}]\text{ZnOSiMe}_3$ with Me_3SiNCO

(i) A solution of $[\kappa^4\text{-Tptm}]\text{ZnOSiMe}_3$ in C_6D_6 (ca. 2 mL) in a vial was treated with excess Me_3SiNCO and was divided equally into two NMR tubes equipped with J. Young valves. One sample was saturated with CO_2 (1 atm) and the other was left under an argon atmosphere. The reactions were monitored by ^1H NMR spectroscopy, thereby demonstrating the clean conversion to $[\kappa^4\text{-Tptm}]\text{ZnNCO}$ in the presence of CO_2 over a period of 4 days. In the absence of CO_2 , there was little conversion to $[\kappa^4\text{-Tptm}]\text{ZnNCO}$ at room temperature over this period and heating to $60\text{ }^\circ\text{C}$ resulted in the formation of several species. A separate experiment employing $[\kappa^4\text{-Tptm}]\text{ZnOSiMe}_3$ (6 mg, 0.01 mmol) and Me_3SiNCO (72 mg, 0.62 mmol) in C_6D_6 (ca. 0.7 mL), in which the sample was kept at room temperature, required 49 days for the formation of $[\kappa^4\text{-Tptm}]\text{ZnNCO}$ to proceed to completion.

(ii) Reaction of $[\kappa^3\text{-Tptm}]\text{ZnOSiMe}_3$ with $^{13}\text{CO}_2$ and Me_3SiNCO .

A solution of $[\kappa^3\text{-Tptm}]\text{ZnOSiMe}_3$ (27 mg, 0.05 mmol) in C_6D_6 (ca. 1 mL) in an NMR tube equipped with a J. Young valve was treated with Me_3SiNCO (148 mg, 1.28 mmol). The solution was then treated with $^{13}\text{CO}_2$ (1 atm). The reaction was monitored by ^1H and ^{13}C NMR spectroscopy, thereby demonstrating the formation of $[\kappa^4\text{-Tptm}]\text{ZnNCO}$ and $\text{Me}_3\text{SiO}^{13}\text{C}(\text{O})\text{OSiMe}_3$ (C^{13} signal at 151.7 ppm) over a period of 52 hours.

1.11.40 Reaction of $[\kappa^4\text{-Tptm}]\text{ZnOSiMe}_3$ with $^{13}\text{CO}_2$: ^{13}C NMR Spectroscopic Characterization of $[\kappa^4\text{-Tptm}]\text{ZnOC}(\text{O})\text{OSiMe}_3$

A solution of $[\kappa^3\text{-Tptm}]\text{ZnOSiMe}_3$ (8 mg, 0.02 mmol) in C_7D_8 (ca. 1 mL) in an NMR tube equipped with a J. Young valve was treated with $^{13}\text{CO}_2$ (0.6 atm). The reaction was monitored by ^1H and ^{13}C NMR spectroscopy and a signal attributable to

$[\kappa^4\text{-Tptm}]\text{ZnO}^{13}\underline{\text{C}}(\text{O})\text{OSiMe}_3$ is observed at *ca.* 157.9 ppm (5 °C to – 50 °C).

1.11.41 Reaction of $[\kappa^4\text{-Tptm}]\text{ZnOSiPh}_3$ with $^{13}\text{CO}_2$: ^{13}C NMR Spectroscopic Characterization of $[\kappa^4\text{-Tptm}]\text{ZnOC}(\text{O})\text{OSiPh}_3$

A solution of $[\kappa^3\text{-Tptm}]\text{ZnOSiPh}_3$ (5 mg, 0.01 mmol) in C_7D_8 (*ca.* 1 mL) in an NMR tube equipped with a J. Young valve was treated with $^{13}\text{CO}_2$ (0.6 atm). The reaction was monitored by ^1H and ^{13}C NMR spectroscopy. Although no signal assignable to $[\kappa^4\text{-Tptm}]\text{ZnO}^{13}\underline{\text{C}}(\text{O})\text{OSiPh}_3$ was observed at room temperature, a signal at *ca.* 160.7 is observed at low temperature –70 °C.

1.11.42 Synthesis of $[\kappa^4\text{-Tptm}]\text{ZnCl}$ via the CO_2 Promoted Reaction of $[\kappa^4\text{-Tptm}]\text{ZnOSiMe}_3$ with Me_3SiCl

A solution of $[\kappa^4\text{-Tptm}]\text{ZnOSiMe}_3$ (14 mg, 0.03 mmol) in C_6D_6 (*ca.* 2 mL) was treated with Me_3SiCl (20 μL , 0.16 mmol). This solution was shaken and then separated equally into two NMR tubes equipped with J. Young valves. One sample was saturated with CO_2 (1 atm) while the other sample was left under an atmosphere of N_2 . The reactions were monitored by ^1H NMR spectroscopy, thereby demonstrating the quantitative conversion of the sample prepared under CO_2 to $[\kappa^4\text{-Tptm}]\text{ZnCl}$ within 15 minutes. In contrast, the sample prepared under N_2 was only 28% complete after 15 minutes but proceeded to completion within 16 hours.

1.11.43 Synthesis of $[\kappa^4\text{-Tptm}]\text{ZnBr}$ via the CO_2 Promoted Reaction of $[\kappa^4\text{-Tptm}]\text{ZnOSiPh}_3$ with Me_3SiBr

A solution of $[\kappa^4\text{-Tptm}]\text{ZnOSiPh}_3$ (10 mg, 0.01 mmol) in C_6D_6 (*ca.* 2 mL) was treated with Me_3SiBr (15 μL , 0.11 mmol). This solution was shaken and then separated equally into two NMR tubes equipped with J. Young valves. One sample was saturated with CO_2 (1

atm) while the other sample was left under an atmosphere of N₂. The reactions were monitored by ¹H NMR spectroscopy, thereby demonstrating the quantitative conversion of the sample prepared under CO₂ to [κ⁴-Tptm]ZnBr within 1 hour. In contrast, the sample prepared under N₂ was only 45 % complete after 1 hour but proceeded to completion within 44 hours.

1.11.44 Synthesis of [κ⁴-Tptm]ZnF

A yellow mixture of [κ⁴-Tptm]ZnI (211 mg, 0.39 mmol) and benzene (*ca.* 3 mL) was treated dropwise with a solution of tetrabutylammonium fluoride (TBAF) in tetrahydrofuran (1.0M, *ca.* 5 wt. %H₂O, 0.51 mL, 0.51 mmol). The mixture becomes a lighter yellow color, and colorless crystals of [κ⁴-Tptm]ZnF•H₂O deposit. The mixture was allowed to sit at room temperature for 3 hours. The mother liquor was then decanted, and the precipitate was washed with benzene (*ca.* 1 mL), followed by H₂O (10 × 1.5 mL, 2 × 5 mL), followed by acetonitrile (2 × 1 mL). The solid was then dried *in vacuo* to give [κ⁴-Tptm]ZnF (90 mg, 53.4%) as a colorless powder. Colorless crystals of [κ⁴-Tptm]ZnF suitable for X-ray diffraction were obtained by slow evaporation from benzene. %). ¹H NMR (C₆D₆): 6.25 [broad m, 3H, FZnC(SC₅H₄N)₃], 6.50 [broad m, 6H, FZnC(SC₅H₄N)₃], 9.69 [broad, 3H, FZnC(SC₅H₄N)₃]. ¹⁹F{¹H} NMR (C₆D₆): -216.70 [s, 1F, FZnC(SC₅H₄N)₃]. IR Data (KBr disk, cm⁻¹): 3082 (w), 3059 (w), 3015 (w), 2346 (w), 1590 (s), 1557 (s), 1457 (s), 1416 (s), 1283 (m), 1254 (w), 1132 (m), 1090 (w), 1048 (m), 1004 (m), 875 (w), 761 (s), 724 (m), 639 (m), 623 (m), 409 (w).

1.11.45 Reaction of [κ⁴-Tptm]ZnF with PhSiH₃: Synthesis of [κ³-Tptm]ZnH

A solution of [κ⁴-Tptm]ZnF (3 mg, 0.01 mmol) in C₆D₆ (*ca.* 0.7 mL) in an NMR tube equipped with a J. Young valve was treated with PhSiH₃ (10 mg, 0.09 mmol) resulting in the formation of colorless crystals. The reaction was monitored by ¹H NMR

spectroscopy, thereby demonstrating the conversion to $[\kappa^3\text{-Tptm}]\text{ZnH}$ over a period of 10 minutes at room temperature.

1.11.46 Reaction of $[\kappa^4\text{-Tptm}]\text{ZnF}$ with Me_3SiCl : Synthesis of $[\kappa^4\text{-Tptm}]\text{ZnCl}$

A solution of $[\kappa^4\text{-Tptm}]\text{ZnF}$ (3 mg, 0.01 mmol) in C_6D_6 (ca. 0.7 mL) in an NMR tube equipped with a J. Young valve was treated with Me_3SiCl (15 μL , 0.12 mmol) resulting in the formation of a colorless precipitate. The reaction was monitored by ^1H NMR spectroscopy, thereby demonstrating the conversion to $[\kappa^4\text{-Tptm}]\text{ZnCl}$ over a period of 10 minutes at room temperature.

1.11.47 Synthesis of $[\kappa^3\text{-Titm}^{\text{Me}}]\text{ZnN}(\text{SiMe}_3)_2$

$[\text{Titm}^{\text{Me}}]\text{H}$ (165 mg, 0.47 mmol) was placed in an NMR tube equipped with a J. Young valve and treated with C_6D_6 (ca. 1.5 mL). To the heterogenous mixture, $\text{Zn}[\text{N}(\text{SiMe}_3)_2]_2$ (220 mg, 0.57 mmol) was added *via* pipette. The sample was then sealed, shaken periodically, and monitored by ^1H NMR spectroscopy, thereby indicating the formation of $[\kappa^3\text{-Titm}^{\text{Me}}]\text{ZnN}(\text{SiMe}_3)_2$ after a period of ca. 3 hours. The sample was allowed to sit at room temperature overnight (16 hours total), and then filtered. The precipitate was extracted with benzene (ca. 1 mL), and the combined filtrates were then lyophilized, giving a light beige powder (226 mg, 83.6%). ^1H NMR (C_6D_6): 0.59 [s, 18H, $[(\underline{\text{H}}_3\text{C})_3\text{Si}]_2\text{NZnC}(\text{SC}_3\text{H}_2\text{N}_2\text{Me})_3$], 2.34 [s, 9H, $(\text{SiMe}_3)_2\text{NZnC}(\text{SC}_3\text{H}_2\text{N}_2\underline{\text{C}}\text{H}_3)_3$], 5.99 [s, 3H, $(\text{SiMe}_3)_2\text{NZnC}(\text{SC}_3\underline{\text{H}}_2\text{N}_2\text{Me})_3$], 7.07 [s, 3H, $(\text{SiMe}_3)_2\text{NZnC}(\text{SC}_3\underline{\text{H}}_2\text{N}_2\text{Me})_3$].

1.11.48 Synthesis of $[\kappa^4\text{-Titm}^{\text{Me}}]\text{ZnNCO}$

$[\kappa^3\text{-Titm}^{\text{Me}}]\text{ZnN}(\text{SiMe}_3)_2$ (11 mg, 0.02 mmol) was placed in an NMR tube equipped with a J. Young valve and treated with C_6D_6 (ca. 0.7 mL). The atmosphere was removed, and CO_2 (ca. 1 atm) was added. The reaction was monitored by NMR spectroscopy,

indicating the immediate formation of Me_3SiNCO . After *ca.* 3 hours, all the Me_3SiNCO was consumed, with the formation of $[\kappa^4\text{-Titm}^{\text{Me}}]\text{ZnNCO}$. The sample was lyophilized, and redissolved in C_6D_6 , which showed almost pure $[\kappa^4\text{-Titm}^{\text{Me}}]\text{ZnNCO}$ (4 mg, 47.0%). Single crystals for X-ray diffraction can be obtained from slow evaporation from benzene.

1.11.49 Synthesis of $[\kappa^4\text{-Tptm}]\text{MgN}(\text{SiMe}_3)_2$

Crystals of $\text{H}[\text{Tptm}]$ (310 mg, 0.90 mmol) were ground into a fine powder and $\{\text{Mg}[\text{N}(\text{SiMe}_3)_2]_2\}_2$ (330 mg, 0.48 mmol) were placed in an NMR tube equipped with a J. Young valve and treated with C_6D_6 (*ca.* 3.0 mL). The yellow heterogeneous mixture was shaken, where colorless crystals began to form within 10 minutes. The reaction was monitored by NMR spectroscopy, and after 2 hours, the mother liquor was decanted from the colorless crystals that formed in the reaction. The colorless crystals were washed with pentane, and then dried *in vacuo* giving pure $[\kappa^4\text{-Tptm}]\text{MgN}(\text{SiMe}_3)_2$ (41 mg). The mother liquor was lyophilized, washed with pentane, and dried *in vacuo* giving $[\kappa^4\text{-Tptm}]\text{MgN}(\text{SiMe}_3)_2$ (188 mg, total yield: 48.1%) with a small impurity. Though this material was typically utilized without further purification, analytically pure material could be obtained by crystallization from benzene. ^1H NMR (C_6D_6): 0.40 [s, 18H, $[(\text{H}_3\text{C})_3\text{Si}]_2\text{N-Mg-C}(\text{SC}_5\text{H}_4\text{N})_3$], 6.31 [m, 3H, $(\text{SiMe}_3)_2\text{N-Mg-C}(\text{SC}_5\text{H}_4\text{N})_3$], 6.48 - 6.55 [m, 6H, $(\text{SiMe}_3)_2\text{N-Mg-C}(\text{SC}_5\text{H}_4\text{N})_3$], 9.00 [d, $^3J_{\text{H-H}} = 5$ Hz, 3H, $(\text{SiMe}_3)_2\text{N-Mg-C}(\text{SC}_5\text{H}_4\text{N})_3$].

1.11.50 Synthesis of $[\kappa^3\text{-Tptm}]\text{NiNO}$

$\text{Ni}(\text{NO})\text{Br}(\text{PPh}_3)_2$ (992 mg, 1.43 mmol) was added to a suspension of $[\kappa^4\text{-Tptm}]\text{Li}$ (500 mg, 1.43 mmol) in benzene (*ca.* 10 mL). The resulting dark purple suspension was

stirred for 2 hours, and then allowed to settle for 2 hours. The suspension was then filtered, and the precipitate was washed with benzene (*ca.* 3 × 5 mL). The purple precipitate was then extracted into DCM (*ca.* 15 mL, then 10 mL), leaving behind a white precipitate. The purple extract was evaporated *in vacuo* to give [κ^3 -Tptm]NiNO (355 mg, 57.5%). ¹H NMR (CDCl₃): 7.09 [t, ³J_{H-H} = 5 Hz, 3H, ONNiC(SC₅H₄N)₃], 7.12 [d, ³J_{H-H} = 8 Hz, 3H, ONNiC(SC₅H₄N)₃], 7.50 [m, 3H, ONNiC(SC₅H₄N)₃], 9.39 [bs, 3H, ONNiC(SC₅H₄N)₃].

1.11.51 Synthesis of 6-phenyl,4-methyl,2-pyridone⁶⁹

THF (*ca.* 400 mL) and diethylamine (73.14 g, 1.0 mol) were added to a large round bottom-Schlenk flask. The solution was cooled to -78 °C, and then BuⁿLi (100 mL, 10.0M in hexanes, 1.0 mol) was added *via* cannula slowly over a period of three hours. The resulting cloudy yellow suspension was stirred at -78 °C for an additional hour, at which point it was allowed to warm to 0 °C and then stirred for one hour. The suspension was then cooled back to -78 °C, and then a solution of 3,3-dimethylacrylic acid (50.06 g, 0.5 mol) in THF (*ca.* 400 mL) was added dropwise over a period of four hours. After the addition, the resulting yellow-orange suspension was allowed to warm to 0 °C and stirred for one hour, where the color dissipates and becomes a thick slurry. The slurry was then cooled to -78 °C, and a solution of benzonitrile (51.56 g, 0.5 mol) in THF (*ca.* 400 mL) was added dropwise *via* cannula over a period of 1.5 hours. The suspension was allowed to warm to room temperature, and was stirred overnight. After stirring at room temperature for 27 hours, H₂O (*ca.* 2.5 L) was slowly added, followed by the addition of aqueous HCl (1500 mL, 1.0 M) resulting in the formation of colorless crystals. The crystals were isolated by filtration, washed with H₂O (*ca.* 500 mL), Et₂O (*ca.* 100 mL) and then CH₂Cl₂ (*ca.* 100 mL). The sample was evaporated *in vacuo* overnight, and allowed to sit for two days, giving 6-phenyl,4-methyl,2-pyridone

(59 g, 64%).

^1H NMR (CDCl_3): 2.25 (s, 3H of methyl), 6.32 (s, 1H of pyridone), 6.34 (s, 1H of pyridone), 7.48 (m, 3H of phenyl), 7.69 (d, $^3J_{\text{H-H}} = 7$ Hz, 2H of phenyl), 11.95 (bs, NH).

1.11.52 Synthesis of 6-Phenyl,4-Methyl,2-thiopyridone

6-Phenyl,4-methyl,2-pyridone (16.3 g, 88.0 mmol) and Lawesson's Reagent (28.7 g, 71.0 mmol) were added to a 500 mL round bottom flask. The solids were degassed *in vacuo* for 1 hour. Toluene (*ca.* 200 mL) was then added, and a reflux condenser fit with a nitrogen inlet was attached. The reaction vessel was degassed, and filled with nitrogen. At this point, the white suspension was heated to reflux, where a yellow color develops quickly, and the suspension was refluxed for 25 hours. The reaction was then allowed to cool to room temperature, at which point H_2O (*ca.* 175 mL, sparged with nitrogen with 10 minutes) was added, and the mixture was stirred for 1 hour. The layers were separated, and the yellow thick residue which was left in the round bottom flask was taken into CH_2Cl_2 (*ca.* 500 mL), and washed with H_2O (*ca.* 200 mL). The organic layers were combined, and put through silica (100 mL) on top of a medium frit, and extracted with CH_2Cl_2 (*ca.* 100 mL). The combined filtrate was evaporated *in vacuo*, and to this residue, CH_2Cl_2 (*ca.* 200 mL) was added. The resulting suspension was filtered, where the precipitate was placed into a medium Schlenk, dried *in vacuo*, washed with MeCN (4×10 mL), and then dried *in vacuo* to give 6-phenyl,4-methyl,2-thiopyridone (2.17 g, 12.2%). The filtrate was placed in the freezer (-15 °C) for 24 hours, and the yellow crystals that deposited were filtered, washed with benzene (4×5 mL), and dried *in vacuo* to give more 6-Phenyl,4-methyl,2-thiopyridone (4.63 g, 26.1%, total yield: 38.3%).

^1H NMR (C_6D_6): 1.48 (s, 3H of methyl), 5.86 (s, 1H of thiopyridone), 6.88 (m, 2H of phenyl), 6.99 (m, 3H of phenyl), 7.20 (s, 1H of thiopyridone), 10.60 (bs, NH).

1.11.53 Synthesis of [Tptm^{Ph,Me}]H

6-Phenyl,4-Methyl,2-thiopyridone (500 mg, 2.48 mmol) and NaH (112 mg, 4.67 mmol) were added to a small Schlenk. THF (10 mL vac. transferred from LiAlH₄) was added *via* vapor transfer. The yellow suspension was allowed to warm to room temperature, where the evolution of H₂ was observed over a period of *ca.* 5 minutes. The suspension was stirred for 20 minutes, at which point iodoform (424 mg, 1.08 mmol) was added, where a deep orange-red color develops immediately. The suspension becomes brown, and was stirred for 30 minutes, allowed to sit for 30 minutes, and then the volatiles were evacuated *in vacuo*. The solid was washed with benzene (3 × 3 mL), and the precipitate was extracted into CH₂Cl₂ (3 × 20 mL). The extract was evaporated *in vacuo* to give [Tptm^{Ph,Me}]H (375 mg, 73.8%) as an off-white powder. Colorless crystals of [Tptm^{Ph,Me}]H can be obtained from hot toluene.

¹H NMR (C₆D₆): 1.66 (s, 9H of methyl), 6.55 (s, 3H of thiopyridyl), 6.94-7.04 (m, 12H), 8.28 (d, ³J_{H-H} = 7 Hz, 6H of phenyl), 9.56 (s, 1H, methine CH).

1.11.54 Synthesis of [Bptm^{Ph,Me}]H₂

6-Phenyl,4-Methyl,2-thiopyridone (1.01 g, 5.02 mmol) and NaH (150 mg, 6.25 mmol) were added to a small Schlenk. THF (10 mL vac. transferred from LiAlH₄) was added *via* vapor transfer. The yellow suspension was allowed to warm to room temperature, where the evolution of H₂ was observed over a period of *ca.* 5 minutes. The suspension was stirred for 2 hours, at which point dibromomethane (175 μL, 2.49 mmol) was added with a microsyringe. The mixture was allowed to stir for 12 hours, where it became a white suspension. The volatiles were evacuated *in vacuo*, and the residue was extracted with benzene (*ca.* 10 mL then 5 mL, 15 mL total). The benzene extract was lyophilized to give [Bptm^{Ph,Me}]H₂ (826 mg, 80%).

¹H NMR (C₆D₆): 1.71 (s, 6H of methyl), 5.53 (s, 2H of methylene), 6.62 (s, 2H of

thiopyridyl), 6.93 (s, 2H of thiopyridyl), 7.20 (m, 2H of phenyl), 7.30 (t, $^3J_{\text{H-H}} = 7$ Hz, 4H of phenyl), 8.18 (d, $^3J_{\text{H-H}} = 7$ Hz, 4H of phenyl).

1.11.55 Synthesis of the trithiocarbonate, (6-Phenyl,4-Methyl,2-thiopyridyl)₂CS

6-Phenyl,4-Methyl,2-thiopyridone (261 mg, 1.30 mmol), NaH (62 mg, 2.59 mmol) and 1,1'-thiocarbonyldiimidazole (110 mg, 0.62 mmol) were added to a small ampoule. THF (6 mL vacuum transferred from LiAlH₄) was added *via* vapor transfer. The mixture was allowed to reach room temperature, and allowed to stir for 2 hours. The reaction was then heated overnight at 60 °C, and then allowed to cool to room temperature. The mixture was allowed to settle for two hours, and then was filtered. The precipitate was extracted with THF (*ca.* 2 mL), and the combined filtrates were evaporated *in vacuo*. The resulting red solid was washed with Et₂O (10 mL, then 2 mL, 12 mL total), and then dried *in vacuo* giving 6-Phenyl,4-Methyl,2-thiopyridyl)₂CS as a red solid (203 mg, 35%).

¹H NMR (CD₃CN): 2.14 (s, 6H of methyl), 6.80 (s, 2H of thiopyridyl), 7.08 (s, 2H of thiopyridyl), 7.33 (m, 6H of phenyl), 7.78 (d, $^3J_{\text{H-H}} = 7$ Hz, 4H of phenyl). ¹³C{¹H} NMR (CD₃CN): 20.8 (2C of methyl), 114.0 (2C of pyridone), 128.0 (4C of phenyl), 128.6 (2C of pyridone), 128.7 (2C), 129.3 (4C of phenyl), 142.2 (2C), 146.0 (2C), 156.7 (2C), 179.8 (1C of CS).

1.12 Crystallographic data

Table 4. Crystal, intensity collection and refinement data.

	$[\kappa^3\text{-Tptm}]\text{ZnMe}\cdot(\text{C}_6\text{H}_6)$	$[\kappa^3\text{-Tptm}]\text{ZnMe}$
lattice	Triclinic	Orthorhombic
formula	$\text{C}_{23}\text{H}_{21}\text{N}_3\text{S}_3\text{Zn}$	$\text{C}_{17}\text{H}_{15}\text{N}_3\text{S}_3\text{Zn}$
formula weight	500.98	422.87
space group	<i>P</i> -1	<i>Pbca</i>
<i>a</i> /Å	8.4946(15)	9.174(7)
<i>b</i> /Å	9.3522(16)	14.901(11)
<i>c</i> /Å	14.843(3)	27.65(2)
α /°	87.096(2)	90
β /°	83.984(2)	90
γ /°	75.395(2)	90
<i>V</i> /Å ³	1134.4(3)	3780(5)
<i>Z</i>	2	8
temperature (K)	125(2)	123(2)
radiation (λ , Å)	0.71073	0.71073
ρ (calcd.), g cm ⁻³	1.467	1.486
μ (Mo K α), mm ⁻¹	1.374	1.634
θ max, deg.	30.50	32.38
no. of data collected	18448	37371
no. of data used	6891	6552
no. of parameters	272	218
R_1 [$I > 2\sigma(I)$]	0.0371	0.0415
wR_2 [$I > 2\sigma(I)$]	0.0750	0.0884
R_1 [all data]	0.0599	0.0829
wR_2 [all data]	0.0838	0.1022
GOF	1.028	1.018

Table 4(cont). Crystal, intensity collection and refinement data.

	$[\kappa^4\text{-Tptm}]\text{ZnNCO}$ $\cdot 0.5(\text{C}_6\text{H}_6)$	$[\kappa^4\text{-Tptm}]\text{Zn}(\kappa^2\text{-O}_2\text{CH})$
lattice	Monoclinic	Monoclinic
formula	$\text{C}_{20}\text{H}_{15}\text{N}_4\text{O}_5\text{S}_3\text{Zn}$	$\text{C}_{17}\text{H}_{13}\text{N}_3\text{O}_2\text{S}_3\text{Zn}$
formula weight	488.91	452.85
space group	$C2/c$	$P2_1/c$
$a/\text{\AA}$	32.946(3)	14.0412(9)
$b/\text{\AA}$	9.1119(9)	14.5162(10)
$c/\text{\AA}$	13.9160(14)	9.1317(6)
$\alpha/^\circ$	90	90
$\beta/^\circ$	101.273(2)	96.0850(10)
$\gamma/^\circ$	90	90
$V/\text{\AA}^3$	4096.9(7)	1850.8(2)
Z	8	4
temperature (K)	125(2)	296(2)
radiation (λ , \AA)	0.71073	0.71073
ρ (calcd.), g cm^{-3}	1.585	1.625
μ (Mo $K\alpha$), mm^{-1}	1.524	1.682
θ max, deg.	30.63	31.77
no. of data collected	31939	31437
no. of data used	6292	6280
no. of parameters	250	235
$R_1 [I > 2\sigma(I)]$	0.0504	0.0321
$wR_2 [I > 2\sigma(I)]$	0.1204	0.0754
R_1 [all data]	0.0875	0.0476
wR_2 [all data]	0.1356	0.0819
GOF	1.188	1.030

Table 4(cont). Crystal, intensity collection and refinement data.

	[κ^4 -Tptm]ZnN ₃	[κ^4 -Tptm]ZnOAc·(C ₆ H ₆)
lattice	Monoclinic	Triclinic
formula	C ₁₆ H ₁₂ N ₆ S ₃ Zn	C ₂₄ H ₂₁ N ₃ O ₂ S ₃ Zn
formula weight	449.87	544.99
space group	<i>Pna</i> 2 ₁	<i>P</i> -1
<i>a</i> /Å	13.598(3)	9.3780(6)
<i>b</i> /Å	9.344(2)	10.1829(6)
<i>c</i> /Å	13.935(3)	13.4332(8)
α /°	90	70.7700(10)
β /°	90	84.2960(10)
γ /°	90	83.6070(10)
<i>V</i> /Å ³	1770.6(7)	1201.01(13)
<i>Z</i>	4	2
temperature (K)	150(2)	150(2)
radiation (λ , Å)	0.71073	0.71073
ρ (calcd.), g cm ⁻³	1.688	1.507
μ (Mo K α), mm ⁻¹	1.754	1.310
θ max, deg.	31.15	30.50
no. of data collected	28178	19439
no. of data used	5698	7299
no. of parameters	236	299
R_1 [$I > 2\sigma(I)$]	0.0367	0.0239
wR_2 [$I > 2\sigma(I)$]	0.0697	0.0651
R_1 [all data]	0.0577	0.0266
wR_2 [all data]	0.0769	0.0668
GOF	1.010	1.057

Table 4(cont). Crystal, intensity collection and refinement data.

	$[\kappa^3\text{-Tptm}]\text{ZnH}\cdot 0.5(\text{C}_6\text{H}_6)$	$\text{H}[\text{Tptm}]$
lattice	Monoclinic	Monoclinic
formula	$\text{C}_{19}\text{H}_{16}\text{N}_3\text{S}_3\text{Zn}$	$\text{C}_{16}\text{H}_{13}\text{N}_3\text{S}_3$
formula weight	447.90	343.47
space group	<i>Pbca</i>	<i>P2₁/c</i>
<i>a</i> /Å	8.607(2)	10.317(5)
<i>b</i> /Å	14.655(4)	9.503(5)
<i>c</i> /Å	30.490(8)	17.703(9)
α /°	90	90
β /°	90	106.121(8)
γ /°	90	90
<i>V</i> /Å ³	3845.6(18)	1667.4(15)
<i>Z</i>	8	4
temperature (K)	150(2)	200(2)
radiation (λ , Å)	0.71073	0.71073
ρ (calcd.), g cm ⁻³	1.547	1.368
μ (Mo K α), mm ⁻¹	1.611	0.443
θ max, deg.	30.56	30.51
no. of data collected	58670	26298
no. of data used	5896	5072
no. of parameters	239	199
$R_1 [I > 2\sigma(I)]$	0.0465	0.0845
$wR_2 [I > 2\sigma(I)]$	0.0834	0.0762
R_1 [all data]	0.1075	0.3680
wR_2 [all data]	0.1024	0.1270
GOF	1.001	0.879

Table 4 (cont). Crystal, intensity collection and refinement data.

	H[Tptm]	H[Tptm]
lattice	Rhombohedral	Monoclinic
formula	$C_{16}H_{13}N_3S_3$	$C_{16}H_{13}N_3S_3$
formula weight	343.47	343.47
space group	$R-3c$	$P2_1/c$
$a/\text{\AA}$	11.7989(8)	8.853(3)
$b/\text{\AA}$	11.7989(8)	14.198(4)
$c/\text{\AA}$	39.078(3)	13.204(4)
$\alpha/^\circ$	90	90
$\beta/^\circ$	90	105.605(4)
$\gamma/^\circ$	120	90
$V/\text{\AA}^3$	4711.3(5)	1598.5(8)
Z	12	4
temperature (K)	125(2)	125(2)
radiation (λ , \AA)	0.71073	0.71073
ρ (calcd.), g cm^{-3}	1.453	1.427
μ (Mo $K\alpha$), mm^{-1}	0.470	0.462
θ max, deg.	30.59	30.63
no. of data collected	11954	25261
no. of data used	1617	4908
no. of parameters	67	199
$R_1 [I > 2\sigma(I)]$	0.0439	0.0497
$wR_2 [I > 2\sigma(I)]$	0.0970	0.0944
R_1 [all data]	0.0646	0.1033
wR_2 [all data]	0.1055	0.1123
GOF	1.067	1.033

Table 4(cont). Crystal, intensity collection and refinement data.

	$[\kappa^4\text{-Tptm}]\text{Li}$	$[\kappa^4\text{-Tptm}]\text{ZnF}$
lattice	Trigonal	Orthorhombic
formula	$\text{C}_{19}\text{H}_{15}\text{LiN}_3\text{S}_3$	$\text{C}_{16}\text{H}_{12}\text{N}_3\text{S}_3\text{ZnF}$
formula weight	388.46	426.84
space group	<i>P-3c1</i>	<i>Pnma</i>
<i>a</i> /Å	12.670(2)	14.3162(9)
<i>b</i> /Å	12.670(2)	13.2855(8)
<i>c</i> /Å	13.663(2)	9.0351(6)
α /°	90	90
β /°	90	90
γ /°	120	90
<i>V</i> /Å ³	1899.5(6)	1718.46(19)
<i>Z</i>	4	4
temperature (K)	123(2)	296(2)
radiation (λ , Å)	0.71073	0.71073
ρ (calcd.), g cm ⁻³	1.358	1.650
μ (Mo K α), mm ⁻¹	0.397	1.806
θ max, deg.	32.62	32.67
no. of data collected	32530	28202
no. of data used	2273	3151
no. of parameters	78	124
R_1 [$I > 2\sigma(I)$]	0.0343	0.0230
wR_2 [$I > 2\sigma(I)$]	0.0789	0.0602
R_1 [all data]	0.0454	0.0284
wR_2 [all data]	0.0844	0.0623
GOF	1.049	1.056

Table 4(cont). Crystal, intensity collection and refinement data.

	$[\kappa^4\text{-Tptm}]\text{ZnF}\cdot\text{H}_2\text{O}$	$\{[\kappa^4\text{-Tptm}]\text{ZnF}\}_2\text{SiF}_4$
lattice	Orthorhombic	Monoclinic
formula	$\text{C}_{19}\text{H}_{17}\text{N}_3\text{S}_3\text{ZnFO}$	$\text{C}_{44}\text{H}_{36}\text{F}_6\text{N}_6\text{S}_6\text{SiZn}_2$
formula weight	483.91	1113.98
space group	<i>Pnma</i>	<i>P-1</i>
<i>a</i> /Å	14.2716(11)	8.627(13)
<i>b</i> /Å	31.714(2)	10.617(15)
<i>c</i> /Å	8.8844(7)	12.900(19)
α /°	90	92.47(2)
β /°	90	93.78(2)
γ /°	90	101.987(19)
<i>V</i> /Å ³	4021.1(5)	1151(3)
<i>Z</i>	8	1
temperature (K)	150(2)	150(2)
radiation (λ , Å)	0.71073	0.71073
ρ (calcd.), g cm ⁻³	1.599	1.607
μ (Mo K α), mm ⁻¹	1.557	1.405
θ max, deg.	32.80	30.36
no. of data collected	66823	16113
no. of data used	7314	6659
no. of parameters	273	295
R_1 [$I > 2\sigma(I)$]	0.0291	0.1067
wR_2 [$I > 2\sigma(I)$]	0.0683	0.2150
R_1 [all data]	0.0400	0.4306
wR_2 [all data]	0.0727	0.3904
GOF	1.041	0.651

Table 4(cont). Crystal, intensity collection and refinement data.

	$[\kappa^4\text{-Tptm}]\text{Zn}\bullet\bullet\bullet\text{FBCF}$	$\{[\kappa^4\text{-Tptm}]\text{Zn}\}_2\text{F BARF}$
lattice	Trigonal	Monoclinic
formula	$\text{C}_{37}\text{H}_{15}\text{N}_3\text{S}_3\text{ZnBF}_{16}$	$\text{C}_{92}\text{H}_{60}\text{N}_6\text{S}_6\text{BF}_{21}\text{Zn}_2$
formula weight	977.88	1982.37
space group	<i>P</i> -3	<i>C</i> 2/ <i>m</i>
<i>a</i> /Å	13.735(2)	25.528(6)
<i>b</i> /Å	13.735(2)	53.143(13)
<i>c</i> /Å	11.4476(17)	12.752(3)
α /°	90	90
β /°	90	91.097(4)
γ /°	120	90
<i>V</i> /Å ³	1870.2(5)	17297(7)
<i>Z</i>	2	8
temperature (K)	150(2)	150(2)
radiation (λ , Å)	0.71073	0.71073
ρ (calcd.), g cm ⁻³	1.736	1.523
μ (Mo K α), mm ⁻¹	0.939	0.796
θ max, deg.	30.64	30.57
no. of data collected	29416	140465
no. of data used	3856	26739
no. of parameters	187	1186
R_1 [$I > 2\sigma(I)$]	0.0399	0.0543
wR_2 [$I > 2\sigma(I)$]	0.0698	0.1041
R_1 [all data]	0.1362	0.1338
wR_2 [all data]	0.1015	0.1313
GOF	1.120	1.010

Table 4 (cont). Crystal, intensity collection and refinement data.

	[Tptm ^{Ph,Me}]H • PhH	[Tptm ^{Ph,Me}]H • PhMe
lattice	Triclinic	Triclinic
formula	C ₄₀ H ₃₄ N ₃ S ₃	C ₈₁ H ₇₀ N ₆ S ₆
formula weight	652.88	1319.79
space group	<i>P</i> -1	<i>P</i> -1
<i>a</i> /Å	11.773(3)	11.7971(9)
<i>b</i> /Å	11.906(3)	11.9388(10)
<i>c</i> /Å	12.087(3)	12.2719(10)
α /°	81.041(4)	81.4970(10)
β /°	80.041(4)	78.9110(10)
γ /°	81.858(4)	81.5590(10)
<i>V</i> /Å ³	1636.9(7)	1665.0(2)
<i>Z</i>	2	1
temperature (K)	150(2)	150(2)
radiation (λ , Å)	0.71073	0.71073
ρ (calcd.), g cm ⁻³	1.325	1.316
μ (Mo K α), mm ⁻¹	0.261	0.257
θ max, deg.	30.55	32.17
no. of data collected	26170	29174
no. of data used	9924	11347
no. of parameters	418	442
R_1 [$I > 2\sigma(I)$]	0.0799	0.0503
wR_2 [$I > 2\sigma(I)$]	0.1582	0.1130
R_1 [all data]	0.1923	0.0910
wR_2 [all data]	0.1975	0.1299
GOF	1.009	1.033

Table 4 (cont). Crystal, intensity collection and refinement data.

	6-Phenyl,4-Methyl,2- pyridone	6-Phenyl,4-Methyl,2- thiopyridone
lattice	Triclinic	Monoclinic
formula	C ₁₂ H ₁₁ NO	C ₁₂ H ₁₁ NS
formula weight	185.22	201.28
space group	<i>P</i> -1	<i>P</i> 2 ₁ / <i>n</i>
<i>a</i> /Å	6.7463(19)	10.6925(6)
<i>b</i> /Å	7.605(2)	7.6190(4)
<i>c</i> /Å	10.067(3)	12.7478(7)
α /°	110.389(4)	90
β /°	96.916(4)	105.9080(10)
γ /°	94.303(4)	90
<i>V</i> /Å ³	476.8(2)	998.74(9)
<i>Z</i>	2	4
temperature (K)	150(2)	149(2)
radiation (λ , Å)	0.71073	0.71073
ρ (calcd.), g cm ⁻³	1.290	1.339
μ (Mo K α), mm ⁻¹	0.083	0.279
θ max, deg.	28.28	30.51
no. of data collected	4966	15521
no. of data used	2343	3037
no. of parameters	128	128
R_1 [$I > 2\sigma(I)$]	0.0434	0.0319
wR_2 [$I > 2\sigma(I)$]	0.1068	0.0863
R_1 [all data]	0.0612	0.0355
wR_2 [all data]	0.1179	0.0889
GOF	1046	1.032

Table 4 (cont). Crystal, intensity collection and refinement data.

	[Tptm ^{Ph,Me}] ₃ Li	HC(SPy ^{Ph,Me}) ₂ Spy "Bis-bulky"
lattice	Monoclinic	Triclinic
formula	C ₄₃ H ₃₆ N ₃ S ₃ Li	C ₃₀ H ₂₅ N ₃ S ₃
formula weight	697.87	523.71
space group	<i>P</i> 2 ₁ / <i>c</i>	<i>P</i> -1
<i>a</i> /Å	9.740(2)	9.5467(7)
<i>b</i> /Å	19.703(4)	11.9537(9)
<i>c</i> /Å	19.805(5)	12.4516(9)
α /°	90	75.2140(10)
β /°	104.064(4)	76.0900(10)
γ /°	90	74.6380(10)
<i>V</i> /Å ³	3686.9(14)	1301.87(17)
<i>Z</i>	4	2
temperature (K)	150(2)	150(2)
radiation (λ , Å)	0.71073	0.71073
ρ (calcd.), g cm ⁻³	1.257	1.336
μ (Mo K α), mm ⁻¹	0.236	0.310
θ max, deg.	30.69	30.61
no. of data collected	59070	21171
no. of data used	11362	7962
no. of parameters	416	327
R_1 [$I > 2\sigma(I)$]	0.1809	0.0391
wR_2 [$I > 2\sigma(I)$]	0.3900	0.0969
R_1 [all data]	0.3589	0.0538
wR_2 [all data]	0.4348	0.1055
GOF	1.585	1.026

Table 4 (cont). Crystal, intensity collection and refinement data.

	[Bptm ^{Ph,Me}]H	(SPy ^{Ph,Me}) ₂ "Disulfide"
lattice	Monoclinic	Monoclinic
formula	C ₂₅ H ₂₂ N ₂ S ₂	C ₂₄ H ₂₀ N ₂ S ₂
formula weight	414.57	400.54
space group	<i>P</i> 2 ₁ / <i>n</i>	<i>P</i> 2 ₁ / <i>c</i>
<i>a</i> /Å	17.1662(12)	12.0587(13)
<i>b</i> /Å	5.0903(4)	9.2175(10)
<i>c</i> /Å	24.1268(17)	19.184(2)
α /°	90	90
β /°	94.2650(10)	107.5430(10)
γ /°	90	90
<i>V</i> /Å ³	2102.4(3)	2033.2(4)
<i>Z</i>	4	4
temperature (K)	150(2)	150(2)
radiation (λ , Å)	0.71073	0.71073
ρ (calcd.), g cm ⁻³	1.310	1.309
μ (Mo K α), mm ⁻¹	0.267	0.274
θ max, deg.	31.18	30.59
no. of data collected	33188	32313
no. of data used	6752	6238
no. of parameters	264	246
R_1 [$I > 2\sigma(I)$]	0.0490	0.1864
wR_2 [$I > 2\sigma(I)$]	0.1056	0.3911
R_1 [all data]	0.1117	0.2165
wR_2 [all data]	0.1311	0.4035
GOF	1.006	1.141

Table 4 (cont). Crystal, intensity collection and refinement data.

	$[\kappa^3\text{-Titm}^{\text{Me}}]\text{ZnN}(\text{SiMe}_3)_2$	$[\kappa^4\text{-Titm}^{\text{Me}}]\text{ZnNCO}$
lattice	Triclinic	Triclinic
formula	$\text{C}_{19}\text{H}_{33}\text{N}_7\text{S}_3\text{Si}_2\text{Zn}$	$\text{C}_{14}\text{H}_{15}\text{N}_7\text{S}_3\text{ZnO}$
formula weight	577.25	458.88
space group	<i>P</i> -1	<i>P</i> -1
<i>a</i> /Å	9.106(9)	11.307(4)
<i>b</i> /Å	9.311(13)	13.657(4)
<i>c</i> /Å	18.04(20)	13.962(4)
α /°	92.20(2)	68.636(4)
β /°	92.113(13)	69.584(5)
γ /°	118.769(12)	70.758(5)
<i>V</i> /Å ³	1337(3)	1830.5(10)
<i>Z</i>	2	4
temperature (K)	150(2)	200(2)
radiation (λ , Å)	0.71073	0.71073
ρ (calcd.), g cm ⁻³	1.434	1.665
μ (Mo K α), mm ⁻¹	1.264	1.704
θ max, deg.	30.78	26.37
no. of data collected	11848	22285
no. of data used	7763	7484
no. of parameters	130	475
R_1 [$I > 2\sigma(I)$]	0.1726	0.0513
wR_2 [$I > 2\sigma(I)$]	0.3474	0.0759
R_1 [all data]	0.3445	0.1234
wR_2 [all data]	0.3893	0.0933
GOF	1.337	1.001

Table 4 (cont). Crystal, intensity collection and refinement data.

	$[\kappa^4\text{-Titm}^{\text{Me}}]\text{MgBr}$	$[\kappa^4\text{-Titm}^{\text{Me}}]\text{MgN}(\text{SiMe}_3)_2$
lattice	Triclinic	Triclinic
formula	$\text{C}_{14}\text{H}_6\text{N}_6\text{S}_3\text{BrCl}_3\text{Mg}$	$\text{C}_{19}\text{H}_{33}\text{N}_7\text{S}_3\text{Si}_2\text{Mg}$
formula weight	575.08	527.17
space group	<i>P</i> -1	<i>P</i> -1
<i>a</i> /Å	9.467(3)	10.556(3)
<i>b</i> /Å	11.503(3)	10.837(3)
<i>c</i> /Å	12.276(4)	13.441(4)
α /°	66.438(4)	83.027(4)
β /°	68.512(4)	83.342(4)
γ /°	78.926(4)	60.903(4)
<i>V</i> /Å ³	1138.6(6)	1330.7(6)
<i>Z</i>	2	2
temperature (K)	125(2)	125(2)
radiation (λ , Å)	0.71073	0.71073
ρ (calcd.), g cm ⁻³	1.677	1.316
μ (Mo K α), mm ⁻¹	2.474	0.410
θ max, deg.	30.76	28.28
no. of data collected	18554	18615
no. of data used	7032	6597
no. of parameters	256	295
R_1 [$I > 2\sigma(I)$]	0.0695	0.0423
wR_2 [$I > 2\sigma(I)$]	0.1727	0.0879
R_1 [all data]	0.1262	0.0737
wR_2 [all data]	0.2023	0.0987
GOF	1.049	1.014

Table 4 (cont). Crystal, intensity collection and refinement data.

	$\{[\kappa^4\text{-Tp}^{\text{tm}}]\text{MgNCO}\}_2$	$\{[\kappa^4\text{-Tp}^{\text{tm}}]\text{MgBr}\}_2$
lattice	Monoclinic	Monoclinic
formula	$\text{C}_{40}\text{H}_{30}\text{N}_8\text{S}_6\text{O}_2\text{Mg}_2$	$\text{C}_{38}\text{H}_{30}\text{N}_6\text{S}_6\text{Mg}_2\text{Br}_2$
formula weight	895.70	971.48
space group	$C2/c$	$P2_1/c$
$a/\text{\AA}$	30.405(8)	12.757(4)
$b/\text{\AA}$	10.021(3)	9.675(3)
$c/\text{\AA}$	14.221(4)	16.740(6)
$\alpha/^\circ$	90	90
$\beta/^\circ$	110.762(4)	107.121(5)
$\gamma/^\circ$	90	90
$V/\text{\AA}^3$	4051.5(18)	1974.6(11)
Z	4	2
temperature (K)	150(2)	123(2)
radiation (λ , \AA)	0.71073	0.71073
ρ (calcd.), g cm^{-3}	1.468	1.634
μ (Mo $K\alpha$), mm^{-1}	0.417	2.440
θ max, deg.	27.88	27.87
no. of data collected	26699	22691
no. of data used	4831	4709
no. of parameters	263	244
$R_1 [I > 2\sigma(I)]$	0.0563	0.0624
$wR_2 [I > 2\sigma(I)]$	0.0987	0.0937
R_1 [all data]	0.1447	0.1491
wR_2 [all data]	0.1257	0.1170
GOF	1.003	1.000

Table 4 (cont). Crystal, intensity collection and refinement data.

	[κ^3 -Tptm]NiNO	[κ^4 -Tptm]NiNO ₂
lattice	Triclinic	Triclinic
formula	C ₂₂ H ₁₈ N ₄ S ₃ NiO	C ₂₂ H ₁₈ N ₄ S ₃ NiO ₂
formula weight	509.29	525.29
space group	<i>P</i> -1	<i>P</i> -1
<i>a</i> /Å	8.535(2)	8.6699(19)
<i>b</i> /Å	9.308(3)	9.215(2)
<i>c</i> /Å	14.712(4)	14.653(3)
α /°	87.437(4)	99.273(3)
β /°	83.898(4)	93.403(4)
γ /°	72.848(4)	95.113(3)
<i>V</i> /Å ³	1110.2(5)	1147.6(4)
<i>Z</i>	2	2
temperature (K)	125(2)	125(2)
radiation (λ , Å)	0.71073	0.71073
ρ (calcd.), g cm ⁻³	1.523	1.520
μ (Mo K α), mm ⁻¹	1.178	1.146
θ max, deg.	30.60	26.37
no. of data collected	18158	13968
no. of data used	6794	4696
no. of parameters	280	289
R_1 [$I > 2\sigma(I)$]	0.0484	0.0572
wR_2 [$I > 2\sigma(I)$]	0.0838	0.0851
R_1 [all data]	0.0935	0.1405
wR_2 [all data]	0.0961	0.1091
GOF	1.000	0.953

Table 4 (cont). Crystal, intensity collection and refinement data.

$\{[\kappa^4\text{-Tp}^{\text{tm}}]\text{NiNCS}\}_2$	
lattice	Triclinic
formula	$\text{C}_{36}\text{H}_{26}\text{N}_8\text{S}_8\text{Ni}_2\text{Cl}_6$
formula weight	1157.25
space group	<i>P</i> -1
<i>a</i> /Å	9.8558(13)
<i>b</i> /Å	13.5582(18)
<i>c</i> /Å	18.335(3)
α /°	82.123(2)
β /°	74.533(2)
γ /°	76.342(2)
<i>V</i> /Å ³	2287.4(5)
<i>Z</i>	2
temperature (K)	150(2)
radiation (λ , Å)	0.71073
ρ (calcd.), g cm ⁻³	1.680
μ (Mo K α), mm ⁻¹	1.578
θ max, deg.	30.68
no. of data collected	36756
no. of data used	14038
no. of parameters	541
R_1 [$I > 2\sigma(I)$]	0.0501
wR_2 [$I > 2\sigma(I)$]	0.0943
R_1 [all data]	0.1084
wR_2 [all data]	0.1125
GOF	1.002

1.13 References and notes

- (1) Finholt, A. E.; Bond Jr., A. C.; Schlesinger, H. I. *J. Am. Chem. Soc.* **1947**, *69*, 1199-1203.
- (2) (a) Bell, N. A.; Coates, G. E. *J. Chem. Soc. A* **1968**, 823–826.
(b) Bell, N. A.; Moseley, P. T.; Shearer, H. M. M.; Spencer, C. B. *Acta Crystallogr.* **1980**, *B36*, 2950–2954.
- (3) Han, R.; Gorrell, I. B.; Looney, A. G.; Parkin, G. J. *Chem. Soc. Chem. Commun.* **1991**, 717-719.
- (4) Cambridge Structural Database (Version 5.32). 3D Search and Research Using the Cambridge Structural Database, Allen, F. H.; Kennard, O. *Chemical Design Automation News* **1993**, *8* (1), pp 1 & 31-37.
- (5) (a) Han, R.; Gorrell, I. B.; Looney, A. G.; Parkin, G. J. *Chem. Soc. Chem. Commun.* **1991**, 717-719.
(b) Looney, A.; Han, R.; Gorrell, I. B.; Cornebise, M.; Yoon, K.; Parkin, G.; Rheingold, A. L. *Organometallics* **1995**, *14*, 274-288.
- (6) For more recent [Tp^{RR'}]ZnH derivatives^{a-d} and other well defined mononuclear zinc hydride complexes,^{e,f} see:
(a) Bergquist, C.; Parkin, G. *Inorg. Chem.* **1999**, *38*, 422-423.
(b) Bergquist, C.; Koutcher, L.; Vaught, A. L.; Parkin, G. *Inorg. Chem.* **2002**, *41*, 625-627.
(c) Kläui, W.; Schilde, U.; Schmidt, M. *Inorg. Chem.* **1997**, *36*, 1598-1601.

- (d) Rombach, M.; Brombacher, H.; Vahrenkamp, H. *Eur. J. Inorg. Chem.* **2002**, 153-159.
- (e) Mukherjee, D.; Ellern, A.; Sadow, A. D. *J. Am. Chem. Soc.* **2010**, *132*, 7582-7583.
- (f) Spielmann, J.; Piesik, D.; Wittkamp, B.; Jansen, G.; Harder, S. *Chem. Commun.* **2009**, 3455-3456.
- (7) Aldridge, S.; Downs, A. *J. Chem. Rev.* **2001**, *101*, 3305-3365.
- (8) For examples of complexes with Zn–H–Zn bridges, see:
- (a) Zhu, Z., Fettinger, J. C.; Olmstead, M. M.; Power, P. P. *Organometallics* **2009**, *28*, 2091-2095.
- (b) Hao, H.; Cui, C.; Roesky, H. W.; Bai, G.; Schmidt, H.-G.; Noltemeyer, M. *Chem. Commun.* **2001**, 1118-1119.
- (c) Coles, M. P.; El-Hamruni, S. M.; Smith, J. D.; Hitchcock, P. B. *Angew. Chem. Int. Edit.* **2008**, *47*, 10147-10150.
- (d) Fedushkin, I. L.; Eremenko, O. V.; Skatova, A. A.; Piskunov, A. V.; Fukin, G. K.; Ketkov, S. Y.; Irran, E.; Schumann, H. *Organometallics* **2009**, *28*, 3863-3868.
- (e) Zhu, Z.; Wright, R. J.; Olmstead, M. M.; Rivard, E.; Brynda, M.; Power, P. P. *Angew. Chem. Int. Edit.* **2006**, *45*, 5807-5810.
- (9) (a) Uchiyama, M.; Furumoto, S.; Saito, M.; Kondo, Y.; Sakamoto, T. *J. Am. Chem. Soc.* **1997**, *119*, 11425-11433.
- (b) Gao, Y.; Harada, K.; Hata, T.; Urabe, H.; Sato, F. *J. Org. Chem.* **1995**, *60*, 290-291.

- (c) de Koning, A. J.; Boersma, J.; van der Kerk, G. J. M. *J. Organomet. Chem.* **1980**, *186*, 159-172.
- (d) de Koning, A. J.; Boersma, J.; van der Kerk, G. J. M. *J. Organomet. Chem.* **1980**, *195*, 1-12.
- (10) (a) Strunk, J.; Kähler, K.; Xia, X.; Muhler, M. *Surf. Sci.* **2009**, *603*, 1776-1783.
- (b) Spencer, M. S. *Top. Catal.* **1999**, *8*, 259-266.
- (c) Waugh, K. C. *Catal. Today* **1992**, *15*, 51-75. (d) Spencer, M. S. *Catal. Lett.* **1998**, *50*, 37-40.
- (d) Chinchin, G. C.; Mansfield, K.; Spencer, M. S. *Chemtech* **1990**, *20*, 692-699.
- (e) Chinchin, G. C.; Denny, P. J.; Parker, D. G.; Spencer, M. S.; Whan, D. A. *Appl. Catal.* **1987**, *30*, 333-338.
- (f) Kurtz, M.; Strunk, J.; Hinrichsen, O.; Muhler, M.; Fink, K.; Meyer, B.; Wöll, C. *Angew. Chem. Int. Edit.* **2005**, *44*, 2790-2794. (g) French, S. A.; Sokol, A. A.; Bromley, S. T.; Catlow, C. R. A.; Sherwood, P. *Top. Catal.* **2003**, *24*, 161-172.
- (11) de Castro, V. D.; de Lima, G. M.; Filgueiras, C. A. L.; Gambardella, M. T. P. *J. Mol. Struct.* **2002**, *609*, 199-203.
- (12) Verkade, J. G. *Coord. Chem. Rev.* **1994**, *137*, 233-295.
- (13) Kitano, K.; Kuwamura, N.; Tanaka, R.; Santo, R.; Nishioka, T.; Ichimura, A.; Kinoshita, I. *Chem. Commun.* **2008**, 1314-1316.
- (14) The ortep diagram shown in Figure 1 is from the crystal structure obtained by me; it has the same structure as published in reference 11.

- (15) Kuwamura, N.; Kato, R.; Kitano, K.; Hirotsu, M.; Nishioka, T.; Hashimoto, H.; Kinoshita, I. *Dalton Trans.* **2010**, 39, 9988-9993.
- (16) Viera, F. T.; de Lima, G. M.; Wardell, J. L.; Wardell, S. M. S. V.; Krambrock, K.; Alcântara, A. F. d. C. *J. Organomet. Chem.* **2008**, 693, 1986-1990.
- (17) Pellei, M.; Lobbia, G. G.; Mancini, M.; Spagna, R.; Santini, C. *J. Organomet. Chem.* **2006**, 691, 1615-1621.
- (18) Miyamoto, R.; Santo, R.; Matsushita, T.; Nishioka, T.; Ichimura, A.; Teki, Y.; Kinoshita, I. *Dalton Trans.* **2005**, 3179-3186.
- (19) The molecular structure for [Tptm]MgCl has not yet been determined.
- (20) For example, triphenyl orthothioformate has a pKa of 22.8 in cyclohexylamine. See references:
- (a) Tupitsyn, I. F.; Zatssepina, N. N. *Russ. J. Gen. Chem.* **2002**, 72, 405-417.
- (b) Streitwieser, A.J., Jurasti, E., and Nebenzahl, L.L., *Comprehensive Carbanion Chemistry*, New York: Elsevier, **1980**, p. 324.
- (21) Bochmann, M.; Bwembya, G.; Webb, K. J. *Inorganic Syntheses* **1997**, 31, 19-24.
- (22) Chisholm, M. H.; Eilerts, N. W.; Huffman, J. C.; Iyer, S. S.; Pacold, M.; Phomphrai, K. *J. Am. Chem. Soc.* **2000**, 122, 11845-11854.
- (23) gNMR. Cherwell Scientific Publishing, The Magdalen Centre, Oxford Science Park, Oxford OX4 4GA, Great Britain, +44 (0)1865 784800 E-mail: info@cherwell.com; WWW: <http://www.cherwell.com>. In the U.S.: 744 San Antonio Road Suite 27A, Palo Alto, CA 94303, 650 / 852-0720.
- (24) [κ^4 -Tptm]ZnO₂CH can also be obtained *via* the reaction of [κ^4 -Tptm]ZnMe with HCO₂H.

- (25) There are 13 examples in the CSD of bridging fluoride ligands between two zinc centers.
- (26) (a) Hahn, F. E.; Jocher, C.; Lugger, T.; Pape, T. *Z. Anorg. Allg. Chem.* **2003**, *629*, 2341-2347.
- (b) Ambrosi, G.; Formica, M.; Fusi, V.; Giorgi, L.; Macedi, E.; Micheloni, M.; Paoli, P.; Pontellini, R.; Rossi, P. *Chem. Eur. J.* **2011**, *17*, 1670-1682.
- (c) Tesmer, M. Shu, M.; Vahrenkamp, H. *Inorg. Chem.* **2001**, *40*, 4022-4029.
- (d) Kläui, W.; Schilde, U.; Schmidt, M. *Inorg. Chem.* **1997**, *36*, 1598-1601.
- (27) For an example of a two coordinate fluoride ligand between two zinc centers assembled by only one ligand, see:
- Reger, D. L.; Watson, R. P.; Gardinier, J. R.; Smith, M. D.; Pellechia, P. J. *Inorg. Chem.* **2006**, *45*, 10088-10097.
- (28) (a) Aresta, M.; Dibenedetto, A. *Dalton Trans.* **2007**, 2975-2992.
- (b) Mikkelsen, M.; Jorgensen, M.; Krebs, F. C. *Energy Environ. Sci.* **2010**, *3*, 43-81.
- (c) Arakawa, H. et al; Aresta, M.; Armor, J. N.; Barteau, M. A.; Beckman, E. J.; Bell, A. T.; Bercaw, J. E.; Creutz, C.; Dinjus, E.; Dixon, D. A.; Domen, K.; DuBois, D. L.; Eckert, J.; Fujita, E.; Gibson, D. H.; Goddard, W. A.; Goodman, D. W.; Keller, J.; Kubas, G. J.; Kung, H. H.; Lyons, J. E.; Manzer, L. E.; Marks, T. J.; Morokuma, K.; Nicholas, K. M.; Periana, R.; Que, L.; Rostrup-Nielson, J.; Sachtler, W. M. H.; Schmidt, L. D.; Sen, A.; Somorjai, G. A.; Stair, P. C.; Stults, B. R.; Tumas, W. *Chem. Rev.* **2001**, *101*, 953-996.
- (d) Sakakura, T.; Choi, J.-C.; Yasuda, H. *Chem. Rev.* **2007**, *107*, 2365-2387.

- (e) Aresta, M.; Dibenedetto, A. *Catal. Today* **2004**, *98*, 455-462.
- (f) Louie, J. *Curr. Org. Chem.* **2005**, *9*, 605-623.
- (g) Jiang, Z.; Xiao, T.; Kuznetsov, V. L.; Edwards, P. P. *Philos. Trans. R. Soc. A-Math. Phys. Eng. Sci.* **2010**, *368*, 3343-3364.
- (h) Darensbourg, D. J. *Inorg. Chem.* **2010**, *49*, 10765-10780.
- (29) (a) Jessop, P. G.; Joó, F.; Tai, C.-C. *Coord. Chem. Rev.* **2004**, *248*, 2425-2442.
- (b) Himeda, Y. *Eur. J. Inorg. Chem.* **2007**, 3927-3941.
- (c) Enthaler, S.; von Langermann, J.; Schmidt, T. *Energy Environ. Sci.* **2010**, *3*, 1207-1217.
- (30) (a) Darensbourg, D. J.; Mackiewicz, R. M.; Phelps, A. L.; Billodeaux, D. R. *Accounts Chem. Res.* **2004**, *37*, 836-844.
- (b) Coates, G. W.; Moore, D. R. *Angew. Chem. Int. Edit.* **2004**, *43*, 6618-6639.
- (c) Darensbourg, D. J.; Holtcamp, M. W. *Coord. Chem. Rev.* **1996**, *153*, 155-174.
- (d) Chisholm, M. H.; Zhou, Z. *J. Mater. Chem.* **2004**, *14*, 3081-3092.
- (31) (a) Yin, X.; Moss, J. R. *Coord. Chem. Rev.* **1999**, *181*, 27-59.
- (b) Leitner, W. *Coord. Chem. Rev.* **1996**, *153*, 257-284.
- (32) Dell'Amico, D. B.; Calderazzo, F.; Labella, L.; Marchetti, F.; Pampaloni, G. *Chem. Rev.* **2003**, *103*, 3857-3897.
- (33) (a) Tsuda, T.; Washita, H.; Saegusa, T. *J. Chem. Soc. Chem. Commun.* **1977**, 468-469.

- (b) Sita, L. R.; Babcock, J. R.; Xi, R. *J. Am. Chem. Soc.* **1996**, *118*, 10912-10913.
- (c) Wannagat, U.; Kuckertz, H.; Kruger, C.; Pump, J. *Z. Anorg. Allg. Chem.* **1964**, *333*, 54-61.
- (d) Cheng, M.; Moore, D. R.; Reczek, J. J.; Chamberlain, B. M.; Lobkovsky, E. B.; Coates, G. W. *J. Am. Chem. Soc.* **2001**, *123*, 8738-8749.
- (e) Andersen, R. A. *Inorg. Chem.* **1979**, *18*, 2928-2932.
- (f) Phull, H.; Alberti, D.; Korobkov, I.; Gambarotta, S.; Budzelaar, P. H. M. *Angew. Chem.-Int. Edit.* **2006**, *45*, 5331-5334.
- (34) For a recent example of isocyanate formation from the reaction of a cyclic disilylamide derivative with CO₂, see: Stewart, C. A.; Dickie, D. A.; Parkes, M. V.; Saria, J. A.; Kemp, R. A. *Inorg. Chem.* **2010**, *49*, 11133-11141.
- (35) The formation of strong Si-O bonds has also been proposed to be a driving force for the conversion of CO ligands to CNR ligands by treatment with Li[Me₃SiNR]. See: Sattler, W.; Parkin, G. *Chem. Commun.* **2009**, 7566-7568.
- (36) Tang, Y.; Felix, A. M.; Boro, B. J.; Zakharov, L. N.; Rheingold, A. L.; Kemp, R. A. *Polyhedron* **2005**, *24*, 1093-1100.
- (37) Sita, L. R.; Babcock, J. R.; Rimo X. *J. Am. Chem. Soc.* **1996**, *118*, 10912-10913.
- (38) (a) Marciniak, B.; Maciejewski, H. *Coord. Chem. Rev.* **2001**, *223*, 301-335.
- (b) Boyle, T. J.; Ottley, L. A. M. *Chem. Rev.* **2008**, *108*, 1896-1917.
- (c) Wolczanski, P. T. *Chem. Commun.* **2009**, 740-757.

- (39) (a) Fedotova, Y. V.; Zhezlova, E. V.; Mushtina, T. G.; Kornev, A. N.; Chesnokova, T. A.; Fukin, G. K.; Zakharov, L. N.; Domrachev, G. A. *Russ. Chem. Bull.* **2003**, *52*, 414-420.
- (b) Kornev, A. N.; Chesnokova, T. A.; Zhezlova, E. V.; Zakharov, L. N.; Fukin, G. K.; Kursky, Y. A.; Domrachev, G. A.; Lickiss, P. D. *J. Organomet. Chem.* **1999**, *587*, 113-121.
- (c) Radkov, Y. F.; Fedorova, E. A.; Khorshev, S. Y.; Kalinina, G. S.; Bochkarev, M. N.; Razuvaev, G. A. *Zhurnal Obshchei Khimii* **1986**, *56*, 386-389.
- (d) Kornev, A. N.; Chesnokova, T. A.; Zhezlova, E. V.; Fukin, G. K.; Zakharov, L. N.; Domrachev, G. A. *Dokl. Chem.* **1999**, *369*, 274-277.
- (40) For examples of reversible insertion of CO₂ into M-OR bonds, see:
- (a) Tam, E. C. Y.; Johnstone, N. C.; Ferro, L.; Hitchcock, P. B.; Fulton, J. R. *Inorg. Chem.* **2009**, *48*, 8971-8976.
- (b) Simpson, R. D.; Bergman, R. G. *Organometallics* **1992**, *11*, 4306-4315.
- (c) Tsuda, T.; Saegusa, T. *Inorg. Chem.* **1972**, *11*, 2561-2563.
- (d) Aresta, M.; Dibenedetto, A.; Pastore, C. *Inorg. Chem.* **2003**, *42*, 3256-3261.
- (e) Mandal, S. K.; Ho, D. M.; Orchin, M. *Organometallics* **1993**, *12*, 1714-1719.
- (f) Ballivet-Tkatchenko, D.; Chermette, H.; Plasseraud, L.; Walter, O. *Dalton Trans.* **2006**, 5167-5175.
- (41) In this regard, we have also observed that CO₂ promotes the formation of [κ⁴-Tptm]ZnX (X = Cl, Br) upon treatment of [κ⁴-Tptm]ZnOSiR₃ (R = Me, Ph) with Me₃SiX.

- (42) The observation of equivalent pyridyl groups for $[\kappa^4\text{-Tptm}]\text{Zn}(\kappa^2\text{-O}_2\text{CR})$ (R = H, Me) implies that access to the $\kappa^1\text{-O}_2\text{CR}$ isomer is facile.
- (43) Accordingly, DFT studies indicate that the difference in energies between $[\kappa^3\text{-Tptm}]\text{ZnX}$ and $[\kappa^4\text{-Tptm}]\text{ZnX}$ (X = F, Cl, Br, I, H) correlate well with the NBO charges on zinc (see Supporting Information).
- (44) (a) Weinhold, F.; Landis, C. *Valency and Bonding*, Cambridge University Press, New York, **2005**; pp. 275-306.
- (b) Ramsden, C. A. *Chem. Soc. Rev.* **1994**, *23*, 111-118.
- (45) It is possible that the $[\kappa^3\text{-Tptm}]\text{ZnX}$ compounds can react *via* either a $[\kappa^4\text{-Tptm}]$ coordination (and *visa versa*), or that coordination of an incoming nucleophile to a $[\kappa^3\text{-Tptm}]\text{ZnX}$ complex could result in the carbon bond being *trans* to the X ligand, therefore enhancing its reactivity.
- (46) Smith, J. M.; Lachicotte, R. J.; Pittard, K. A.; Cundari, T. R.; Lukat-Rodgers, G.; Rodgers, K. R.; Holland, P. L. *J. Am. Chem. Soc.* **2001**, *123*, 9222-9223.
- (47) (a) Frankland, E. *Ann.* **1849**, *71*, 171.
- (b) For a very nice cover essay on Sir Edward Frankland concerning his work with preparing the first main-group organometallic compound, see: Seyferth, D. *Organometallics*, **2001**,*20*, 2940-2955.
- (48) (a) Grignard, V. *Compt. rend. Hebd. Séances Acad. Sci.* **1900**, *130*, 1322.
- (b) For a very nice cover essay on the Grignard reagents, see: Seyferth, D. *Organometallics*, **2009**,*28*, 1598-1605.
- (49) Westerhausen, M. *Inorg. Chem.* **1991**,*30*, 96-101.
- (50) Campbell, A. N.; Stahl, S. S. *Acc. Chem. Res.* **2012**, DOI: 10.1021/ar2002045.

- (51) For an example of a nickel nitrosyl complex reacting with O₂ to produce the corresponding nitrite complex, see:

Ugo, R.; Bhaduri, S.; Johnson, B. F. G.; Khair, A.; Pickard, A.; Benn-Raarit, B. J. C. *S. Chem. Comm.* **1976**, 694-695.

- (52) For an example of a nickel nitrite complex transferring an oxygen atom to CO to produce the corresponding nitrosyl complex, see:

Doughty, D. T.; Gordon, G.; Stewart, Jr. R. P. *J. Am. Chem. Soc.* **1979**, *101*, 2645-2648.

- (53) Andrews, M. A.; Chang, T. C.-T.; Cheng, C.-W. F. *Organometallics*, **1985**, *4*, 268-274 and references therein.

- (54) Khan, M. M. T.; Chatterjee, D.; Shirin, Z.; Bajaj, H. C.; Siddiqui, M. R. H.; Venkatasubramanian, K.; Bhadchade, M. M. *J. Mol Catal.* **1992**, *72*, 271-282.

- (55) Holm, R. H.; Donahue, J. P. *Polyhedron*, **1993**, *12*, 571-589.

- (56) According to reference 55, the oxygenation using O₂ of CO is enthalpically favored by 67.6 kcal mol⁻¹ while the oxygenation using O₂ of Me₃P is enthalpically favored by 79.7 kcal mol⁻¹.

- (57) Gwengo, C.; Silva, R. M.; Smith, M. D.; Lindeman S. V.; Gardinier, J. R. *Inorg. Chim. Acta* **2009**, *362*, 4127-4136.

- (58) (a) McNally, J. P.; Leong, V. S.; Cooper, N. J. in *Experimental Organometallic Chemistry*, Wayda, A. L.; Darensbourg, M. Y., Eds.; American Chemical Society: Washington, DC, 1987; Chapter 2, pp 6-23.

(b) Burger, B.J.; Bercaw, J. E. in *Experimental Organometallic Chemistry*; Wayda, A.

- L.; Darensbourg, M. Y., Eds.; American Chemical Society: Washington, DC, 1987; Chapter 4, pp 79-98.
- (c) Shriver, D. F.; Drezdron, M. A.; *The Manipulation of Air-Sensitive Compounds*, 2nd Edition; Wiley-Interscience: New York, 1986.
- (59) Gottlieb, H. E.; Kotlyar, V.; Nudelman, A. *J. Org. Chem.* **1997**, *62*, 7512-7515.
- (60) Cella, J. A.; Carpenter, J. C. *J. Organomet. Chem.* **1994**, *480*, 23-26.
- (61) Banovetz, J. P.; Suzuki, H.; Waymouth, R. M. *Organometallics* **1993**, *12*, 4700-4703.
- (62) Jaguar 7.5, Schrödinger, LLC, New York, NY 2008.
- (63) (a) Becke, A. D. *J. Chem. Phys.* **1993**, *98*, 5648-5652.
- (b) Becke, A. D. *Phys. Rev. A* **1988**, *38*, 3098-3100.
- (c) Lee, C. T.; Yang, W. T.; Parr, R. G. *Phys. Rev. B* **1988**, *37*, 785-789.
- (d) Vosko, S. H.; Wilk, L.; Nusair, M. *Can. J. Phys.* **1980**, *58*, 1200-1211.
- (e) Slater, J. C. *Quantum Theory of Molecules and Solids, Vol. 4: The Self-Consistent Field for Molecules and Solids*; McGraw-Hill: New York, 1974.
- (64) (a) Hay, P. J.; Wadt, W. R. *J. Chem. Phys.* **1985**, *82*, 270-283.
- (b) Wadt, W. R.; Hay, P. J. *J. Chem. Phys.* **1985**, *82*, 284-298.
- (c) Hay, P. J.; Wadt, W. R. *J. Chem. Phys.* **1985**, *82*, 299-310.
- (65) Dunning, T. H. *J. Chem. Phys.* **1989**, *90*, 1007-1023.

- (66) (a) Sheldrick, G. M. SHELXTL, An Integrated System for Solving, Refining and Displaying Crystal Structures from Diffraction Data; University of Göttingen, Göttingen, Federal Republic of Germany, 1981.
- (b) Sheldrick, G. M. *Acta Cryst.* **2008**, *A64*, 112-122.
- (67) de Castro, V. D.; de Lima, G. M.; Filgueiras, C. A. L.; Gambardella, M. T. P. *J. Mol. Struct.* **2002**, *609*, 199-203.
- (68) $(\text{Me}_3\text{SiO})_2\text{CO}$ was identified by comparison with an authentic sample prepared by an adaptation of the literature method (Yamamoto, Y.; Tarbell, D. S.; Fehlner, J. R.; Pope, B. M. *J. Org. Chem.*, **1973**, *38*, 2521-2525).
- (69) *Synthesis*, **2000**, *2*, 273-280.

CHAPTER 2

Zinc Synthetic Analogues of Carbonic Anhydrase

Table of Contents

2.1	Introduction	123
2.2	Previous studies using $[\text{Tp}^{\text{Bu}^t, \text{Me}}]\text{ZnOH}$	124
2.3	Low temperature ^1H and $^{13}\text{C}\{^1\text{H}\}$ NMR spectroscopic characterization of $[\text{Tp}^{\text{Bu}^t, \text{Me}}]\text{ZnOCO}_2\text{H}$.	127
2.4	DFT calculations concerning the reaction of $[\text{Tp}^{\text{Bu}^t, \text{Me}}]\text{ZnOH}$ with CO_2 to give $[\text{Tp}^{\text{Bu}^t, \text{Me}}]\text{ZnOCO}_2\text{H}$.	134
2.5	Structural characterization of $[\text{Tp}^{\text{Bu}^t, \text{Me}}]\text{ZnOCO}_2\text{H}$ and $[\text{Tptm}]\text{ZnOCO}_2\text{H}$	135
2.6	DFT calculations concerning bonding modes of $[\text{Tp}^{\text{Bu}^t, \text{Me}}]\text{ZnOCO}_2\text{H}$ and $[\text{Tp}^{\text{Bu}^t, \text{Me}}]\text{ZnNO}_3$.	144
2.7	CO_2 reduction <i>via</i> reactivity of $[\kappa^4\text{-Tptm}]\text{ZnOCO}_2\text{H}$ and $[\text{Tptm}]\text{Zn}(\mu\text{-CO}_3)\text{Zn}[\text{Tptm}]$ with silanes.	152
2.8	Conclusions	154
2.9	Experimental details	155
2.9.1	General considerations	155
2.9.2	Computational details	156
2.9.3	X-ray structure determinations	156
2.9.4	Synthesis of $[\text{Tp}^{\text{Bu}^t, \text{Me}}]\text{ZnNO}_3$	156
2.9.5	Measurement of the equilibrium constant for the formation of $[\text{Tp}^{\text{Bu}^t, \text{Me}}]\text{ZnOCO}_2\text{H}$ <i>via</i> reaction of $[\text{Tp}^{\text{Bu}^t, \text{Me}}]\text{ZnOH}$ with CO_2	156
2.9.6	Synthesis of $[\text{Tp}^{\text{Bu}^t, \text{Me}}]\text{ZnOH}$	157
2.9.7	Structural characterization of $[\text{Tp}^{\text{Bu}^t, \text{Me}}]\text{ZnOCO}_2\text{H}$	158
2.9.8	Synthesis of $\{[\kappa^3\text{-Tptm}]\text{Zn}(\mu\text{-OH})\}_2$	158

	121
2.9.9 Synthesis of $[\kappa^4\text{-Tptm}]\text{ZnOCO}_2\text{H}$	159
2.9.10 Synthesis of $[\kappa^4\text{-Tptm}]\text{ZnO}^{13}\text{CO}_2\text{H}$	160
2.9.11 Synthesis of $[\kappa^4\text{-Tptm}]\text{ZnO}^{13}\text{CO}_2\text{D}$	160
2.9.12 Synthesis of $[\text{Tptm}]\text{Zn}(\mu\text{-CO}_3)\text{Zn}[\text{Tptm}]$	161
2.9.13 Synthesis of $[\text{Tptm}]\text{Zn}(\mu\text{-}^{13}\text{CO}_3)\text{Zn}[\text{Tptm}]$	162
2.9.14 Synthesis of $[\kappa^4\text{-Tptm}]\text{ZnO}_2\text{CH}$ by reduction of $[\kappa^4\text{-Tptm}]\text{ZnOCO}_2\text{H}$ with PhSiH_3	162
2.9.15 Synthesis of $[\kappa^4\text{-Tptm}]\text{ZnO}_2^{13}\text{CH}$ by reduction of $[\kappa^4\text{-Tptm}]\text{ZnO}^{13}\text{CO}_2\text{H}$ with PhSiH_3	163
2.9.16 Reduction of $[\kappa^4\text{-Tptm}]\text{ZnO}^{13}\text{CO}_2\text{H}$ with PhSiH_3 in the presence of CO_2	163
2.9.17 Reduction of $[\kappa^4\text{-Tptm}]\text{ZnO}^{13}\text{CO}_2\text{D}$ with PhSiH_3	163
2.9.18 H/D Exchange in the reaction of $[\kappa^4\text{-Tptm}]\text{ZnD}$ with PhSiH_3	163
2.9.19 H/D Exchange in the reaction of $[\kappa^4\text{-Tptm}]\text{ZnH}$ with PhSiD_3	164
2.9.20 Reaction of $[\kappa^4\text{-Tptm}]\text{ZnO}^{13}\text{CO}_2\text{H}$ with Me_3SiCl : Formation of $[\kappa^4\text{-Tptm}]\text{ZnCl}$	164
2.9.21 Reaction of $[\text{Tptm}]\text{Zn}(\mu\text{-CO}_3)\text{Zn}[\text{Tptm}]$ with PhSiH_3 : Formation of $[\kappa^3\text{-Tptm}]\text{ZnH}$ and $[\kappa^4\text{-Tptm}]\text{ZnO}_2\text{CH}$	164
2.9.22 Reaction of $[\text{Tptm}]\text{Zn}(\mu\text{-CO}_3)\text{Zn}[\text{Tptm}]$ with PhSiH_3 in the presence of CO_2 : Formation of $[\kappa^4\text{-Tptm}]\text{ZnO}_2\text{CH}$	165
2.9.23 Reaction of $[\kappa^4\text{-Tptm}]\text{ZnO}_2^{13}\text{CH}$ with CO_2 : Exchange of CO_2	165
2.9.24 Synthesis of $[\kappa^4\text{-Tptm}]\text{ZnO}_2\text{CH}$ by reduction of $[\kappa^4\text{-Tptm}]\text{ZnOCO}_2\text{H}$ with Et_2SiH_2	165
2.9.25 Absence of H/D Exchange in the reaction of $[\kappa^4\text{-Tptm}]\text{ZnD}$ with Et_2SiH_2	165
2.9.26 Synthesis of $[\kappa^4\text{-Tptm}]\text{ZnO}_2\text{CD}$ by reduction of $[\kappa^4\text{-Tptm}]\text{ZnOCO}_2\text{H}$ with Et_2SiH_2	166
2.10 Crystallographic data	167
2.11 References and notes	171

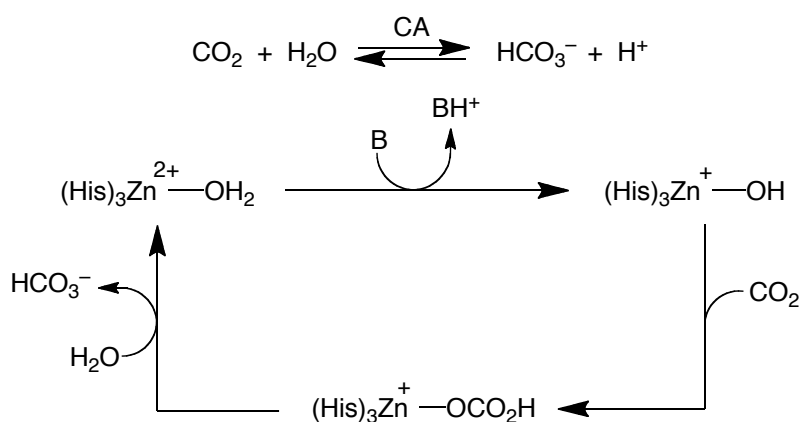
Reproduced in part from:

W. Sattler and G. Parkin *Polyhedron* **2012**, 32, 41-48.

W. Sattler and G. Parkin *Chem. Sci.* **2012**, 133, 9708-9711.

2.1 Introduction

Carbonic anhydrase (CA) is the enzyme that is responsible for catalyzing the reversible hydration of carbon dioxide (Scheme 1) and, as such, plays important roles in respiration and in buffering the pH of blood.¹ CA was the first enzyme recognized to contain zinc² and it has had a pivotal role in the development of enzymology.¹ It is one of the most efficient enzymes known, with rates limited by the diffusion of its substrates. As such, carbonic anhydrase plays a critical function in respiration, where it transports CO₂ between metabolizing tissues and the lungs,¹ and it is also responsible for providing an effective intracellular pH buffer *via* CO₂/HCO₃⁻ equilibration.³ The latter is very important in maintaining the narrow physiological pH range, where very small changes can have severely detrimental effects (*i.e.* below *ca.* 7.35, the blood becomes too acidic due to an excess of CO₂ and above *ca.* 7.45 is too basic). The active site of carbonic anhydrase consists of a tetrahedral zinc center that is coordinated to the protein by the imidazole groups of three histidine (His) residues, with the fourth site being occupied by a water molecule (Figure 1).¹



Scheme 1. Proposed mechanism of action of carbonic anhydrase.

Essential features of the mechanism of action are postulated to involve (i) deprotonation of the coordinated water to give the active zinc hydroxide derivative

$[(\text{His})_3\text{Zn-OH}]^+$, (ii) nucleophilic attack of the zinc-bound hydroxide upon carbon dioxide to give a bicarbonate intermediate $[(\text{His})_3\text{Zn-OCO}_2\text{H}]^+$, and (iii) displacement of the bicarbonate anion by H_2O to complete the catalytic cycle, as illustrated in Scheme 1.

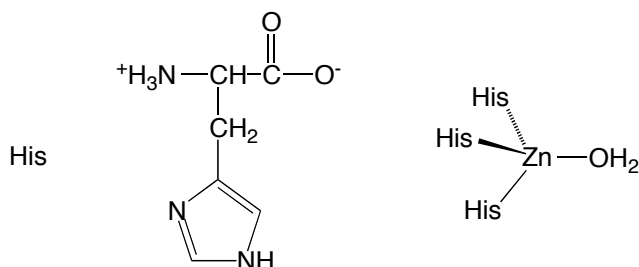


Figure 1. Histidine amino acid (left) and the active site of carbonic anhydrase (right).

The mechanism of action of carbonic anhydrase has been the subject of many investigations, both experimental^{1,4} and theoretical.⁵ Furthermore, synthetic analogues, also known as small molecule mimics, of carbonic anhydrase have also received much attention with respect to providing information concerning the individual steps of the catalytic transformations.⁶ While many of these synthetic analogues have provided valuable information, there has been no experimental measurement of an equilibrium constant for the CO_2 insertion step, or has there been any structural characterization of the bicarbonate intermediate. This chapter will detail our studies to provide (i) the application of low temperature ^1H and ^{13}C NMR spectroscopies to provide details concerned with the formation of a bicarbonate complex *via* insertion of CO_2 into a zinc hydroxide bond and (ii) structural characterization of two zinc bicarbonate complexes, which are of relevance to the mechanism of action of carbonic anhydrase.

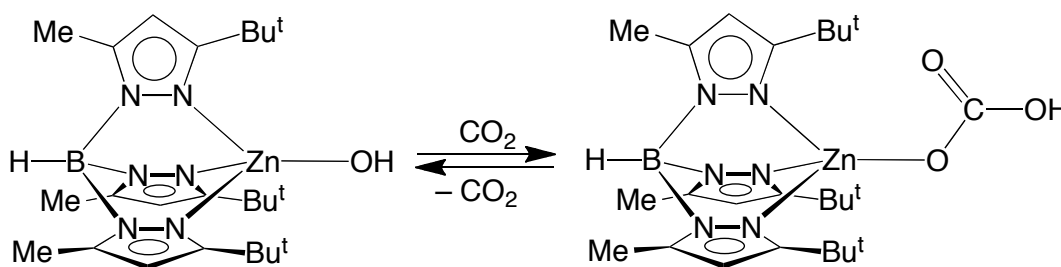
2.2 Previous studies using $[\text{Tp}^{\text{Bu}^t, \text{Me}}]\text{ZnOH}$

Much effort has been directed towards an investigation of synthetic analogues to provide details concerned with the nature of the fundamental transformations of

carbonic anhydrases.^{7,8,9,10,11,12} For example, sterically demanding *tris*(pyrazolyl)hydroborato ligands, [Tp^{RR'}], have been previously utilized to synthesize monomeric tetrahedral zinc hydroxide complexes of the type [Tp^{RR'}]ZnOH, that serve as synthetic analogues of carbonic anhydrase.¹³

In this regard, the Parkin group has previously demonstrated that the *tris*(3-*t*-butyl-5-methylpyrazolyl)hydroborato derivative, [Tp^{Bu^t,Me}]ZnOH, reacts rapidly with carbon dioxide to generate a bicarbonate compound [Tp^{Bu^t,Me}]ZnOCO₂H (Scheme 2) that was identified by absorptions at 1675 cm⁻¹ and 1302 cm⁻¹ in the IR spectrum (Figure 2).^{13c,14} Not only do the IR absorptions provide evidence for the formation of the bicarbonate ligand, but also impart information regarding the mode in which the bicarbonate ligand binds to zinc. In this vein, carboxylate ligands have been analyzed using IR spectroscopy to determine whether they bind in a unidentate or bidentate manner.¹⁵ Specifically, a large separation (*i.e.* $\Delta\nu > 200$ cm⁻¹) between the symmetric ($\nu_{\text{sym}}\text{CO}_2$) and asymmetric ($\nu_{\text{asym}}\text{CO}_2$) CO₂ stretching bands indicates unidentate coordination (*i.e.* the CO₂ group has increased isolated single and double bond character, approaching that of an organic carbonyl compound).¹⁶ In the case of [Tp^{Bu^t,Me}]ZnOCO₂H, $\Delta\nu = 373$ cm⁻¹ which therefore indicates unidentate coordination of the bicarbonate ligand. Unidentate coordination has implications with respect to carbonic anhydrase and it has been suggested that unidentate bicarbonate ligands would be displaced more readily than bidentate ligands (*vide infra*). However, due to the lack of structurally characterized metal bicarbonate complexes, it is difficult to correlate the binding mode of the bicarbonate ligand to that of carbonic anhydrase activity. On the other hand, many nitrate complexes have been studied with respect to their coordination modes. In this regard, the metal complexes [Tp^{Bu^t}]M(NO₃) (M = Zn, Co, Ni and Cu) have been structurally characterized, and show increased bidentate coordination in the series Zn < Co < Ni and Cu.^{13c} Studies on metal-substituted carbonic anhydrases have revealed that there is decreased activity in the series Zn > Co

> Ni and Cu. The decreased activity correlates well with increased bidentate coordination of the corresponding nitrate complexes. The correlation of nitrate coordination mode with carbonic anhydrase activity provides support for the suggestion that unidentate bicarbonate coordination results in the more rapid displacement by H₂O.



Scheme 2. Reaction of [Tp^{Bu^t,Me}]ZnOH with CO₂ to give [Tp^{Bu^t,Me}]ZnOCO₂H.

Additional evidence for the formation of the bicarbonate intermediate was provided by ¹H NMR spectroscopy. Specifically, treatment of [Tp^{Bu^t,Me}]ZnOH with CO₂ resulted in the disappearance of the hydroxide signal, which was rapidly regenerated upon removal of the CO₂ atmosphere. The reversible insertion of CO₂ into the Zn-OH bond provided an excellent model for carbonic anhydrase, however, no signal for the bicarbonate proton or carbon was observed in these previous studies, rendering them incomplete.

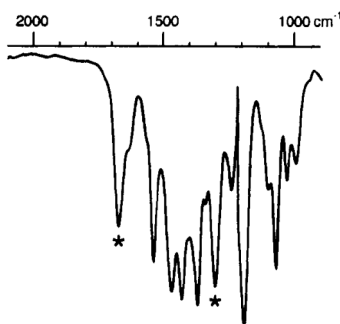
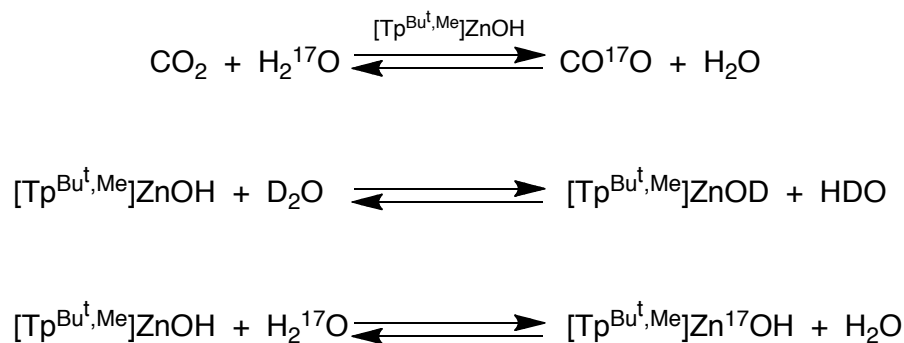


Figure 2. IR spectrum of the bicarbonate complex [Tp^{Bu^t,Me}]ZnOCO₂H. Absorptions marked with a * are due to the bicarbonate ligand. Figure taken from reference 13c.

$[\text{Tp}^{\text{Bu}^\dagger, \text{Me}}]\text{ZnOH}$ also catalyzes a variety of exchange reactions that are required for the catalytic activity in accord with the enzyme, carbonic anhydrase. Specifically, the exchange reaction between CO_2 and H_2^{17}O to give CO^{17}O and H_2O (Scheme 3) is catalyzed by $[\text{Tp}^{\text{Bu}^\dagger, \text{Me}}]\text{ZnOH}$. This exchange reaction shows that $[\text{Tp}^{\text{Bu}^\dagger, \text{Me}}]\text{ZnOH}$ is a functional model for CA, as the enzyme naturally catalyzes this reaction. Moreover, H/D exchange is also observed in the reaction of $[\text{Tp}^{\text{Bu}^\dagger, \text{Me}}]\text{ZnOH}$ with D_2O (Scheme 3), while labeled oxygen exchange is observed in the reaction of $[\text{Tp}^{\text{Bu}^\dagger, \text{Me}}]\text{ZnOH}$ with H_2^{17}O (Scheme 3). These previous studies provided the first well-defined example of a synthetic analog for carbonic anhydrase.



Scheme 3. Exchange reactions catalyzed by $[\text{Tp}^{\text{Bu}^\dagger, \text{Me}}]\text{ZnOH}$.

2.3 Low temperature ^1H and $^{13}\text{C}\{^1\text{H}\}$ NMR spectroscopic characterization of $[\text{Tp}^{\text{Bu}^\dagger, \text{Me}}]\text{ZnOCO}_2\text{H}$.

Due to the facile, reversible reaction between $[\text{Tp}^{\text{Bu}^\dagger, \text{Me}}]\text{ZnOH}$ and CO_2 , $[\text{Tp}^{\text{Bu}^\dagger, \text{Me}}]\text{ZnOCO}_2\text{H}$ was not previously observed using NMR spectroscopy. Therefore, we have used low temperature NMR spectroscopy in order to slow down the exchange between $[\text{Tp}^{\text{Bu}^\dagger, \text{Me}}]\text{ZnOH}$ and $[\text{Tp}^{\text{Bu}^\dagger, \text{Me}}]\text{ZnOCO}_2\text{H}$, such that $[\text{Tp}^{\text{Bu}^\dagger, \text{Me}}]\text{ZnOCO}_2\text{H}$ could be observed. In agreement with previous studies in C_6D_6 , ^{13}C addition of CO_2 (1 atm) to a solution of $[\text{Tp}^{\text{Bu}^\dagger, \text{Me}}]\text{ZnOH}$ in CD_2Cl_2 at 25°C results in the immediate disappearance of the ^1H NMR spectroscopic signal attributed to the hydroxide ligand, but without the

appearance of a corresponding signal for the bicarbonate group (Figure 3). However, upon cooling to 189 K, a sharp signal (singlet) attributed to the bicarbonate ligand appears at 13.2 ppm.

In addition to the ^1H signal for the bicarbonate ligand, we also employed ^{13}C NMR spectroscopy to characterize the bicarbonate ligand. A signal is clearly evident in the $^{13}\text{C}\{^1\text{H}\}$ NMR spectrum at 161.9 ppm, which has been confirmed to be the bicarbonate ligand by the use of labeled $^{13}\text{CO}_2$,^{17,18} whereas it is not discernible at room temperature (Figure 4).¹⁹ It is important to note that a value of 157.9 ppm has been previously reported for the chemical shift of the bicarbonate ligand of $[\text{Tp}^{\text{Bu}^t, \text{Me}}]\text{ZnOCO}_2\text{H}$ in CDCl_3 at room temperature,^{13b} which we have not observed in our own studies. However, we have observed that solutions of $[\text{Tp}^{\text{Bu}^t, \text{Me}}]\text{ZnOCO}_2\text{H}$ in CDCl_3 decompose slightly when left at room temperature for several days, and these solutions exhibit a $^{13}\text{C}\{^1\text{H}\}$ NMR signal at 166.2 ppm that is derived from CO_2 confirmed by the use of $^{13}\text{CO}_2$. The signal at 166.2 ppm does not correspond to either a bicarbonate or carbonate species, as it is a doublet in the ^{13}C NMR spectrum, with $^1J_{\text{C-H}} = 200$ Hz, implying that this proton signal corresponds to a CH moiety. The magnitude of this coupling constant implies that it is an sp^2 hybridized carbon, and most likely a formate species. Additionally, the hydrogen that is coupling to the carbon is observed at 8.70 ppm in the ^1H NMR spectrum. While we are unsure of the exact nature of this species, it has been previously observed that *bis*(pyrazolyl)hydroborato zinc complexes are known to react with CO_2 to give formate derivatives. Similar low temperature NMR spectra are observed in d_8 -toluene and CDCl_3 , as summarized in **Table 1**.

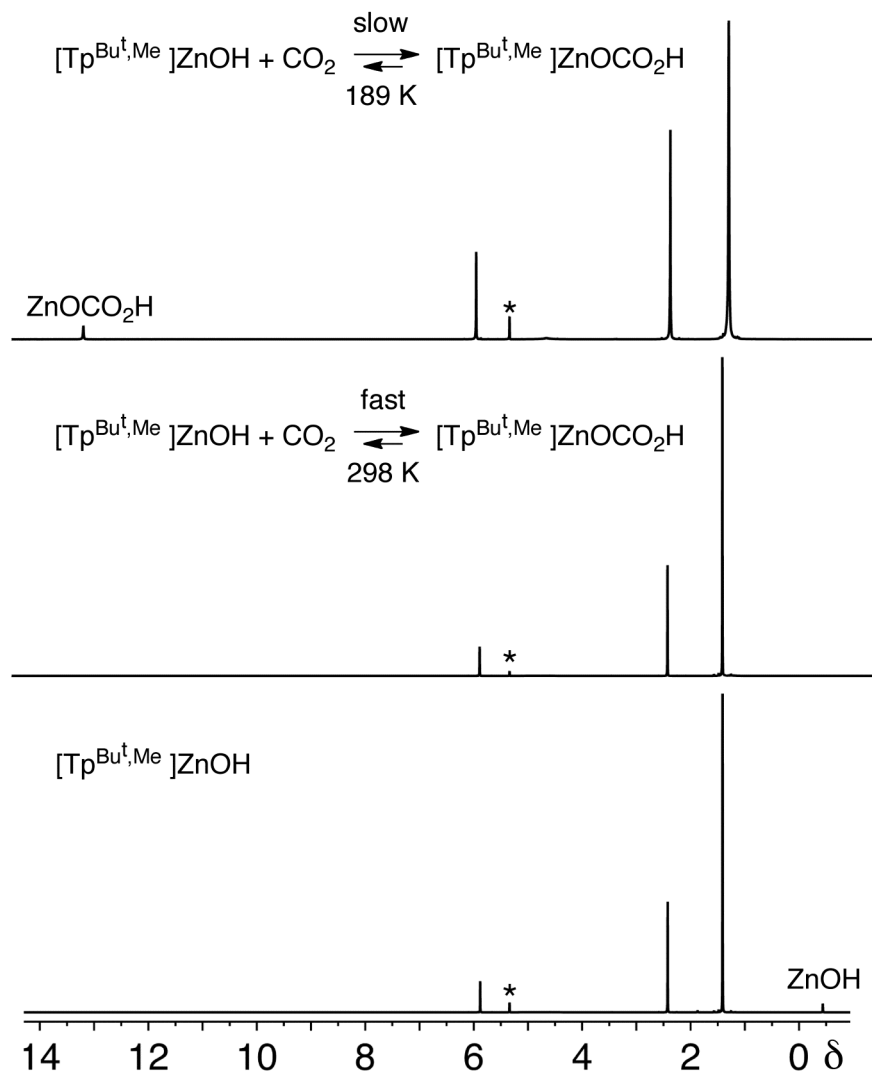


Figure 3. ^1H NMR spectra of $[\text{Tp}^{\text{Bu}^t, \text{Me}}]\text{ZnOH}$ in CD_2Cl_2 at 298 K (bottom), $[\text{Tp}^{\text{Bu}^t, \text{Me}}]\text{ZnOH}$ in the presence of CO_2 (1 atm) at 298 K (middle) and $[\text{Tp}^{\text{Bu}^t, \text{Me}}]\text{ZnOH}$ in the presence of CO_2 (1 atm) at 189 K (top). Although no signals due to either the zinc hydroxide or bicarbonate ligands are evident at room temperature in the presence of CO_2 , a signal due to the bicarbonate ligand emerges at 189 K. The residual protio signal of the solvent is marked with an asterisk (*).

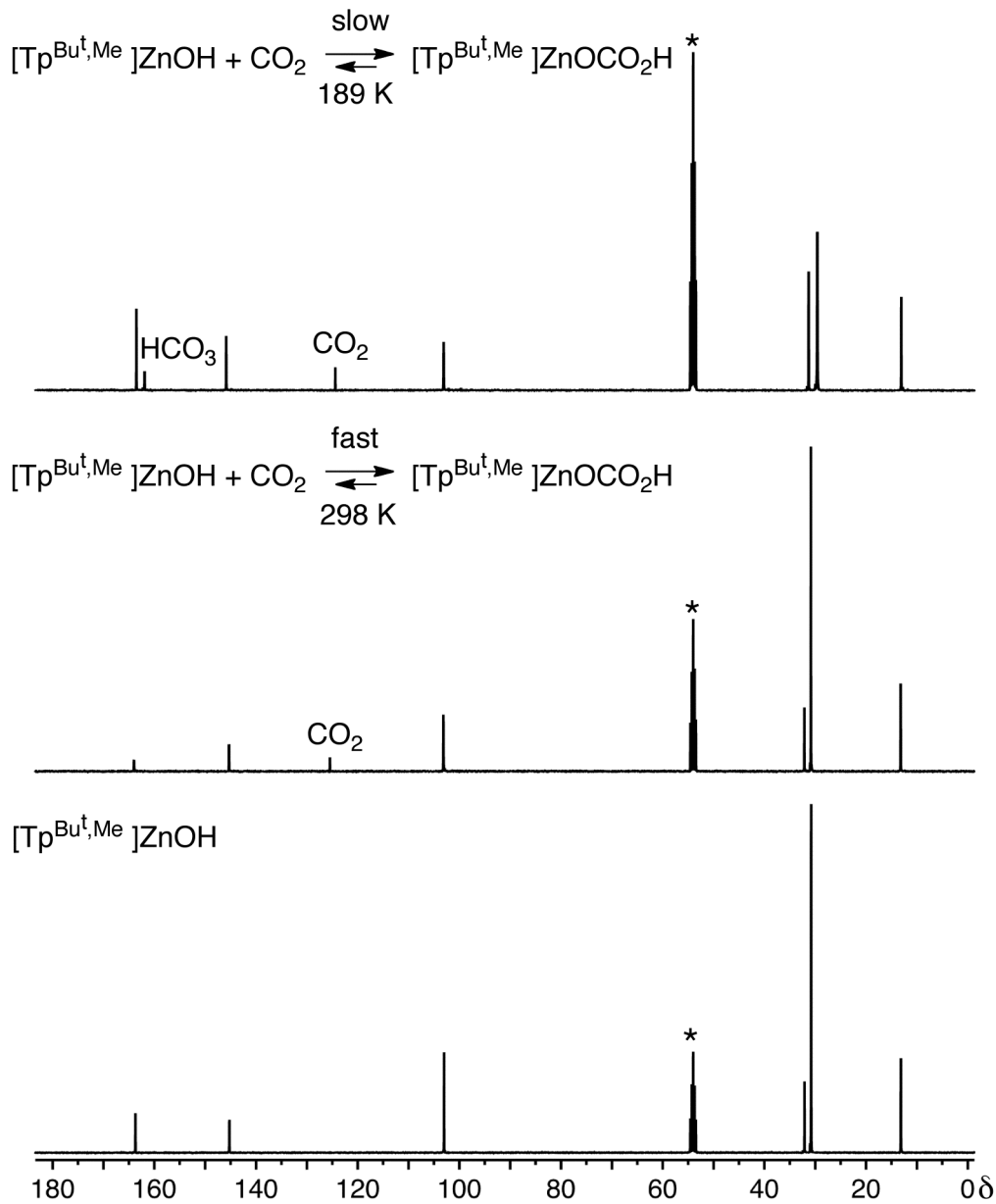


Figure 4. $^{13}\text{C}\{^1\text{H}\}$ NMR spectra of $[\text{Tp}^{\text{Bu}^t, \text{Me}}]\text{ZnOH}$ in CD_2Cl_2 at 298 K (bottom), $[\text{Tp}^{\text{Bu}^t, \text{Me}}]\text{ZnOH}$ in the presence of CO_2 (1 atm) at 298 K (middle) and $[\text{Tp}^{\text{Bu}^t, \text{Me}}]\text{ZnOH}$ in the presence of CO_2 (1 atm) at 189 K (top). Although no signals due to the zinc bicarbonate ligand are evident at 25°C in the presence of CO_2 , a signal due to the bicarbonate ligand emerges at 189 K. The signal of the solvent is marked with an asterisk (*).

Table 1. ^1H and ^{13}C NMR spectroscopic data for bicarbonate moieties.

Compound	δ (^1H)	δ (^{13}C)	Reference
$[\text{Tp}^{\text{Bu}^t, \text{Me}}]\text{Zn}(\kappa^1\text{-OCO}_2\text{H})$	13.2 (CD_2Cl_2) ^a	161.9 (CD_2Cl_2) ^a	this work
	13.4 (CDCl_3) ^b	161.4 (CDCl_3) ^b	
	14.0 (C_7D_8) ^c	163.1 (C_7D_8) ^c	
$\{[\text{N}(\text{CH}_2\text{BIM})_3]\text{Zn}(\kappa^1\text{-OCO}_2\text{H})\}^+$	– ^d	167	20
$[\text{Zn}(\text{tnpa})(\text{HCO}_3)]^+$	– ^d	160.8	22
$\text{PhPt}(\kappa^1\text{-OCO}_2\text{H})(\text{PEt}_3)_2$	11.2	161.4	23
$[\kappa^3\text{-}(\text{C}_6\text{H}_2)(\text{CH}_2\text{P}^t\text{Bu}^t)_2]\text{Pd}(\kappa^1\text{-OCO}_2\text{H})$	– ^d	162.5	24
$\text{Ru}(\text{IMes})_2(\text{CO})(\kappa^2\text{-O}_2\text{COH})\text{H}$	8.8	160.3	25
$[\text{Et}_4\text{N}][\text{W}(\text{CO})_5(\kappa^1\text{-OCO}_2\text{H})]$	11.9	160.4	18

^a 189 K

^b 217 K;

^c 220 K;

^d data not reported.

For comparison purposes, ^1H and ^{13}C NMR spectroscopic data for bicarbonate complexes from the literature are also presented in **Table 1**. The ^1H NMR chemical shifts span the range 8.8 – 14.0 ppm, while the ^{13}C NMR chemical shifts span the range 160 – 167 ppm.^{18,20,21,22,23,24,25,26} It is also worth noting that the bridging carbonate complexes $\{[\text{Tp}^{\text{Bu}^t, \text{Me}}]\text{Zn}\}_2(\mu\text{-}\kappa^1, \kappa^1\text{-CO}_3)$ and $\{[\text{Tp}^{\text{Pr}^i}_2]\text{Zn}\}_2(\mu\text{-}\kappa^1, \kappa^2\text{-CO}_3)$ exhibit signals close to that of $[\text{Tp}^{\text{Bu}^t, \text{Me}}]\text{ZnOCO}_2\text{H}$, specifically 164.0 ppm and 171.5 ppm, respectively.^{13c} Other carbonate complexes from the literature also exhibit comparable chemical shifts.²⁷ Due to the similar ^{13}C NMR chemical shifts of bicarbonate and carbonate complexes, it appears that ^{13}C NMR spectroscopy is not a good indicator of whether a particular compound is a bicarbonate or carbonate complex. On the other hand, definitive evidence for the formation of a bicarbonate ligand, as opposed to a bridging carbonate,

is provided by the observation of a signal in the range $\approx 9 - 14$ ppm of the ^1H NMR spectrum.

Solutions of $[\text{Tp}^{\text{Bu}^t, \text{Me}}]\text{ZnOH}$ in CD_2Cl_2 saturated with 1 atmosphere of CO_2 reveal only signals associated with $[\text{Tp}^{\text{Bu}^t, \text{Me}}]\text{ZnOCO}_2\text{H}$ and CO_2 when cooled to 189 K in the probe of the NMR spectrometer (Figure 3 and Figure 4). However, this is *not* the case when a lower CO_2 pressure is applied to $[\text{Tp}^{\text{Bu}^t, \text{Me}}]\text{ZnOH}$ in CD_2Cl_2 . In particular, $[\text{Tp}^{\text{Bu}^t, \text{Me}}]\text{ZnOH}$ may also be observed with lower pressures of CO_2 . For example, a sample of $[\text{Tp}^{\text{Bu}^t, \text{Me}}]\text{ZnOH}$ in CD_2Cl_2 treated with 500 mmHg of $^{13}\text{CO}_2$ and then cooled to 212 K exhibits the ^1H and $^{13}\text{C}\{^1\text{H}\}$ NMR spectra illustrated in Figure 5 and Figure 6, thereby indicating the presence of $[\text{Tp}^{\text{Bu}^t, \text{Me}}]\text{ZnOH}$, $[\text{Tp}^{\text{Bu}^t, \text{Me}}]\text{ZnOCO}_2\text{H}$ and CO_2 . Similar spectra are also observed at 217 K in the presence of 600 mmHg $^{13}\text{CO}_2$.²⁸ Monitoring the latter sample in the probe of the NMR spectrometer at 217 K shows the change in concentrations of all three compounds ($[\text{Tp}^{\text{Bu}^t, \text{Me}}]\text{ZnOH}$, $[\text{Tp}^{\text{Bu}^t, \text{Me}}]\text{ZnO}^{13}\text{CO}_2\text{H}$ and $^{13}\text{CO}_2$) reaching equilibrium after several hours. Once the equilibrium is established, quantitative $^{13}\text{C}\{^1\text{H}\}$ NMR spectra have been obtained, which confirms the establishment of an equilibrium situation. Specifically, integration of the $^{13}\text{C}\{^1\text{H}\}$ NMR spectra allows for the determination of the equilibrium constant, namely $K = 6 \pm 2 \times 10^3 \text{ M}^{-1}$, which corresponds to the thermodynamic value, $\Delta G_{217\text{K}} = -3.8 \pm 0.2 \text{ kcal mol}^{-1}$. This spectrum is shown in Figure 6, in which the ^{13}C signals for $[\text{Tp}^{\text{Bu}^t, \text{Me}}]\text{ZnOH}$, $[\text{Tp}^{\text{Bu}^t, \text{Me}}]\text{ZnO}^{13}\text{CO}_2\text{H}$ and $^{13}\text{CO}_2$ are observed. These NMR studies provide the first direct measurement of an equilibrium constant for the reaction of CO_2 with a zinc hydroxide complex to form the bicarbonate derivative.

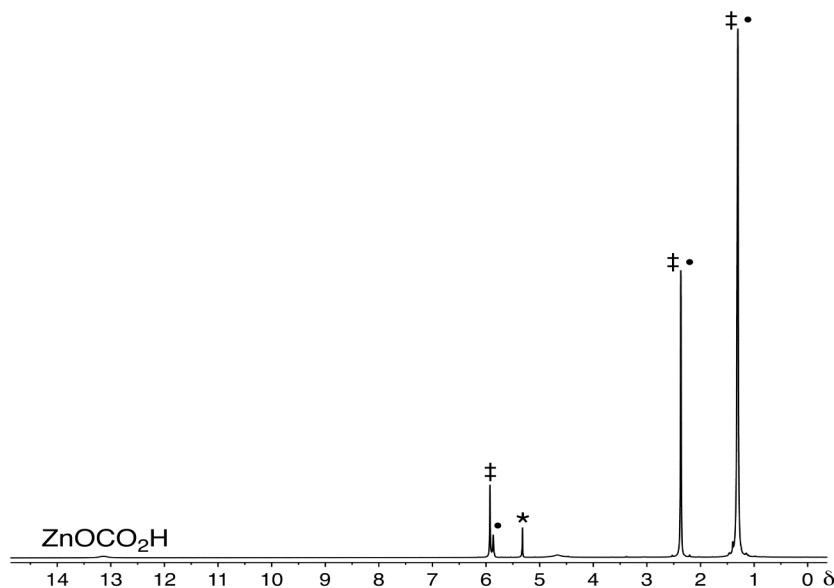


Figure 5. ^1H NMR spectrum of $[\text{Tp}^{\text{Bu}^t, \text{Me}}]\text{ZnOH}$ in CD_2Cl_2 (marked *) in the presence of $^{13}\text{CO}_2$ (500 mm Hg) at 212 K, indicating the presence of both $[\text{Tp}^{\text{Bu}^t, \text{Me}}]\text{ZnOH}$ (as indicated by the pyrazolyl hydrogens marked •) and $[\text{Tp}^{\text{Bu}^t, \text{Me}}]\text{ZnOCO}_2\text{H}$ (as indicated by the pyrazolyl hydrogens marked †). The methyl and t-butyl signals of $[\text{Tp}^{\text{Bu}^t, \text{Me}}]\text{ZnOH}$ and $[\text{Tp}^{\text{Bu}^t, \text{Me}}]\text{ZnOCO}_2\text{H}$ are coincident.

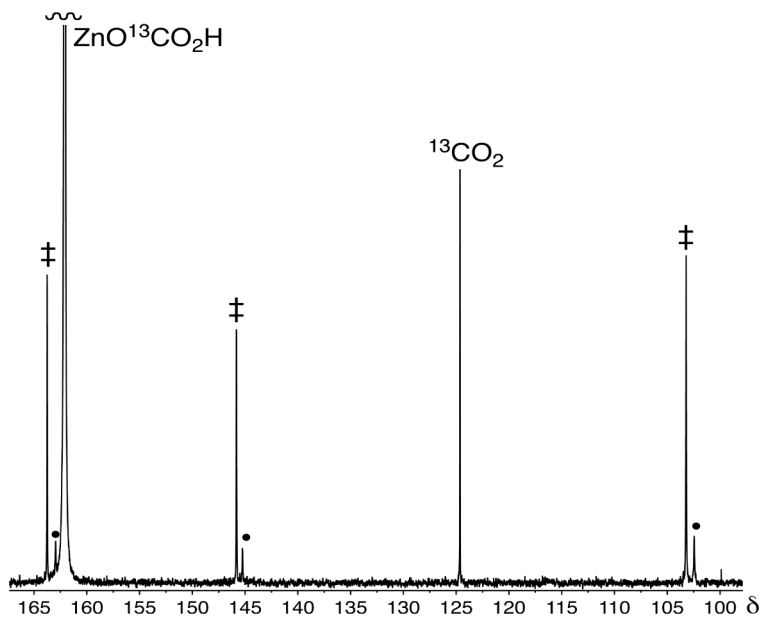


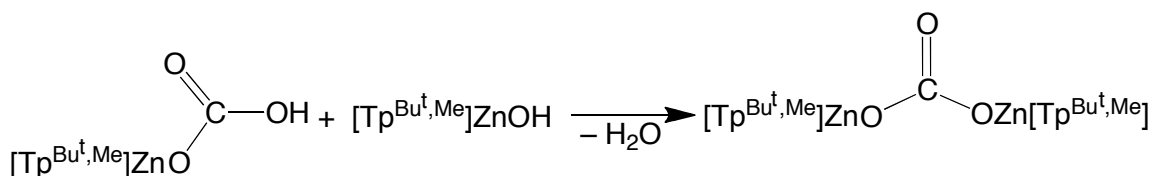
Figure 6. $^{13}\text{C}\{^1\text{H}\}$ NMR spectrum of $[\text{Tp}^{\text{Bu}^t, \text{Me}}]\text{ZnOH}$ in CD_2Cl_2 in the presence of $^{13}\text{CO}_2$ (500 mm Hg) at 212 K, indicating the presence of $[\text{Tp}^{\text{Bu}^t, \text{Me}}]\text{ZnOH}$ (as indicated by the pyrazolyl carbons marked •), $[\text{Tp}^{\text{Bu}^t, \text{Me}}]\text{ZnOCO}_2\text{H}$ (as indicated by the pyrazolyl carbons marked †) and CO_2 (the signals due to the methyl and t-butyl groups are not shown). The bicarbonate signal is off-scale due to the ^{13}C isotope enrichment level.

2.4 DFT calculations concerning the reaction of $[\text{Tp}^{\text{Bu}^t, \text{Me}}]\text{ZnOH}$ with CO_2 to give $[\text{Tp}^{\text{Bu}^t, \text{Me}}]\text{ZnOCO}_2\text{H}$.

We have also evaluated the thermodynamics associated with insertion of CO_2 into the Zn–OH bond computationally. Specifically, Density Functional Theory (DFT) with the B3LYP density functional using the 6-31G** (C, H, N, O, B) and LAV3P (Zn) basis sets has been applied. The DFT calculated ΔG at 217 K is $-2.7 \text{ kcal mol}^{-1}$ with $\Delta H_{217\text{K}} = -12.07 \text{ kcal mol}^{-1}$ and $\Delta S_{217\text{K}} = -42.94 \text{ e.u.}$ ²⁹ It is important to note that this value of ΔG is close to the experimentally obtained value of $-3.8 \text{ kcal mol}^{-1}$ at the same temperature. ΔG is strongly temperature dependent, as a result of the significant entropy term. This entropy term is largely associated with $\text{CO}_2(\text{g})$ ($S = 51.1 \text{ e.u.}$), where release of CO_2 decreases the Gibbs free energy due to an increase in the entropy.³⁰ As such increasing the temperature to 298 K results in a calculated ΔG value of $0.8 \text{ kcal mol}^{-1}$ with $\Delta H_{298\text{K}} = -12.18 \text{ kcal mol}^{-1}$ and $\Delta S_{298\text{K}} = -43.38 \text{ e.u.}$, which is consistent with the T ΔS term becoming larger at higher temperatures (*i.e.* there is no substantial change in the value of ΔH or ΔS). Thus, at room temperature, the insertion of CO_2 into the Zn–OH bond is calculated to be slightly endergonic (nearly thermoneutral), which is consistent with the fact that CO_2 is released from a solution of $[\text{Tp}^{\text{Bu}^t, \text{Me}}]\text{ZnOCO}_2\text{H}$ in benzene in a sealed NMR tube at room temperature. This observation is of relevance to carbonic anhydrase. In order to be an effective catalytic system, the intermediates must not be too thermodynamically stable. The thermodynamic data pertaining to the reaction of $[\text{Tp}^{\text{Bu}^t, \text{Me}}]\text{ZnOH}$ with CO_2 , therefore, reinforces the description that $[\text{Tp}^{\text{Bu}^t, \text{Me}}]\text{ZnOH}$ is a respectable synthetic analogue of carbonic anhydrase.

2.5 Structural characterization of $[\text{Tp}^{\text{Bu}^t, \text{Me}}]\text{ZnOCO}_2\text{H}$ and $[\text{Tptm}]\text{ZnOCO}_2\text{H}$

The facile reversibility of CO_2 insertion into $[\text{Tp}^{\text{Bu}^t, \text{Me}}]\text{ZnOH}$ originally impeded the characterization of $[\text{Tp}^{\text{Bu}^t, \text{Me}}]\text{ZnOCO}_2\text{H}$ by X-ray diffraction. In particular, efforts to obtain crystals of $[\text{Tp}^{\text{Bu}^t, \text{Me}}]\text{ZnOCO}_2\text{H}$ by employing slow evaporation of a benzene solution in a CO_2 atmosphere resulted in the formation of the carbonate complex $\{[\text{Tp}^{\text{Bu}^t, \text{Me}}]\text{Zn}\}_2(\mu\text{-CO}_3)$, due to the condensation of $[\text{Tp}^{\text{Bu}^t, \text{Me}}]\text{ZnOCO}_2\text{H}$ with $[\text{Tp}^{\text{Bu}^t, \text{Me}}]\text{ZnOH}$ over long periods of time (Scheme 4).



Scheme 4. Condensation between $[\text{Tp}^{\text{Bu}^t, \text{Me}}]\text{ZnOCO}_2\text{H}$ and $[\text{Tp}^{\text{Bu}^t, \text{Me}}]\text{ZnOH}$ to give $\{[\text{Tp}^{\text{Bu}^t, \text{Me}}]\text{Zn}\}_2(\mu\text{-CO}_3)$.

However, employing a new crystallization technique, we have now succeeded in isolating crystals of $[\text{Tp}^{\text{Bu}^t, \text{Me}}]\text{ZnOCO}_2\text{H}$ suitable for single crystal X-ray diffraction. Specifically, pentane diffusion into a benzene solution of $[\text{Tp}^{\text{Bu}^t, \text{Me}}]\text{ZnOCO}_2\text{H}$ under a CO_2 atmosphere provides a more rapid means to deposit crystals of the bicarbonate complex, thereby minimizing the possibility of forming the carbonate complex $\{[\text{Tp}^{\text{Bu}^t, \text{Me}}]\text{Zn}\}_2(\mu\text{-CO}_3)$.

The molecular structure of $[\text{Tp}^{\text{Bu}^t, \text{Me}}]\text{ZnOCO}_2\text{H}$, as determined by X-ray diffraction, is illustrated in Figure 7. The most important structural feature of $[\text{Tp}^{\text{Bu}^t, \text{Me}}]\text{ZnOCO}_2\text{H}$ is that the bicarbonate ligand is a terminal ligand and binds *via* a distinct unidentate coordination mode,³¹ with Zn–O distances of 1.872(3) Å and 3.451(3) Å, and $\Delta d(\text{Zn-O}) = 1.579$ Å (Table 2).³² This binding mode is in accord with the notion that in carbonic anhydrase, the bicarbonate ligand binds to zinc in a unidentate fashion, which is necessary for rapid displacement by H_2O .^{13c} It should be emphasized that this

is the first structurally characterized example of a terminal, monomeric zinc bicarbonate complex.

Table 2. Bond lengths (Å) and angles (°) for bicarbonate coordination to zinc.

Compound	$d(\text{Zn-O}_1)/\text{Å}$	$d(\text{Zn-O}_2)/\text{Å}$	$\text{Zn-O}_1\text{-C}/^\circ$	$\text{Zn-O}_2\text{-C}/^\circ$	$\Delta(\text{Zn-O})/\text{Å}$
$[\text{Tp}^{\text{Bu}^\dagger, \text{Me}}]\text{ZnOCO}_2\text{H}$	1.872(3)	3.451(3)	140.4(3)	57.0(2)	1.579
$[\kappa^4\text{-Tptm}]\text{ZnOCO}_2\text{H}$	2.039(2)	3.406(2)	132.6(2)	61.5(1)	1.367

Although structurally characterized metal bicarbonate complexes are not common, they are known for other metals. Analysis of bicarbonate complexes in the Cambridge Structural Database³³ indicates that the bicarbonate ligand is flexible, exhibiting both bidentate and unidentate coordination,^{34,35} with $\Delta d(\text{M-O})$ values ranging from 0.006 Å³⁶ to 2.094 Å.³⁷ A similar variation in coordination mode exists for the structures of a variety of carbonic anhydrases and their mutants in the presence of bicarbonate,⁴ among which that of human carbonic anhydrase I, with Zn–O distances of 1.8 and 3.1 Å,^{4a} corresponds most closely to that of $[\text{Tp}^{\text{Bu}^\dagger, \text{Me}}]\text{ZnOCO}_2\text{H}$.³⁸ Also of note is the fact that $[\text{Tp}^{\text{Bu}^\dagger, \text{Me}}]\text{ZnOCO}_2\text{H}$ exists as a hydrogen-bonded dimer, common for carboxylic acid groups. While the carbonic anhydrase does not exist as a hydrogen-bonded dimer, the bicarbonate ligand has hydrogen bonding interactions to other amino acid residues or to water.

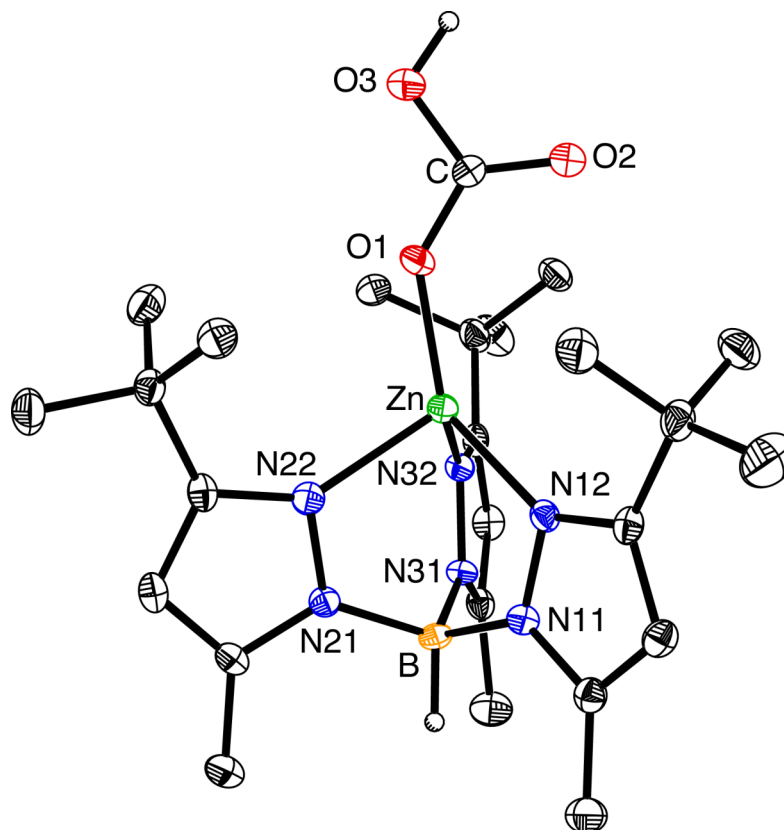
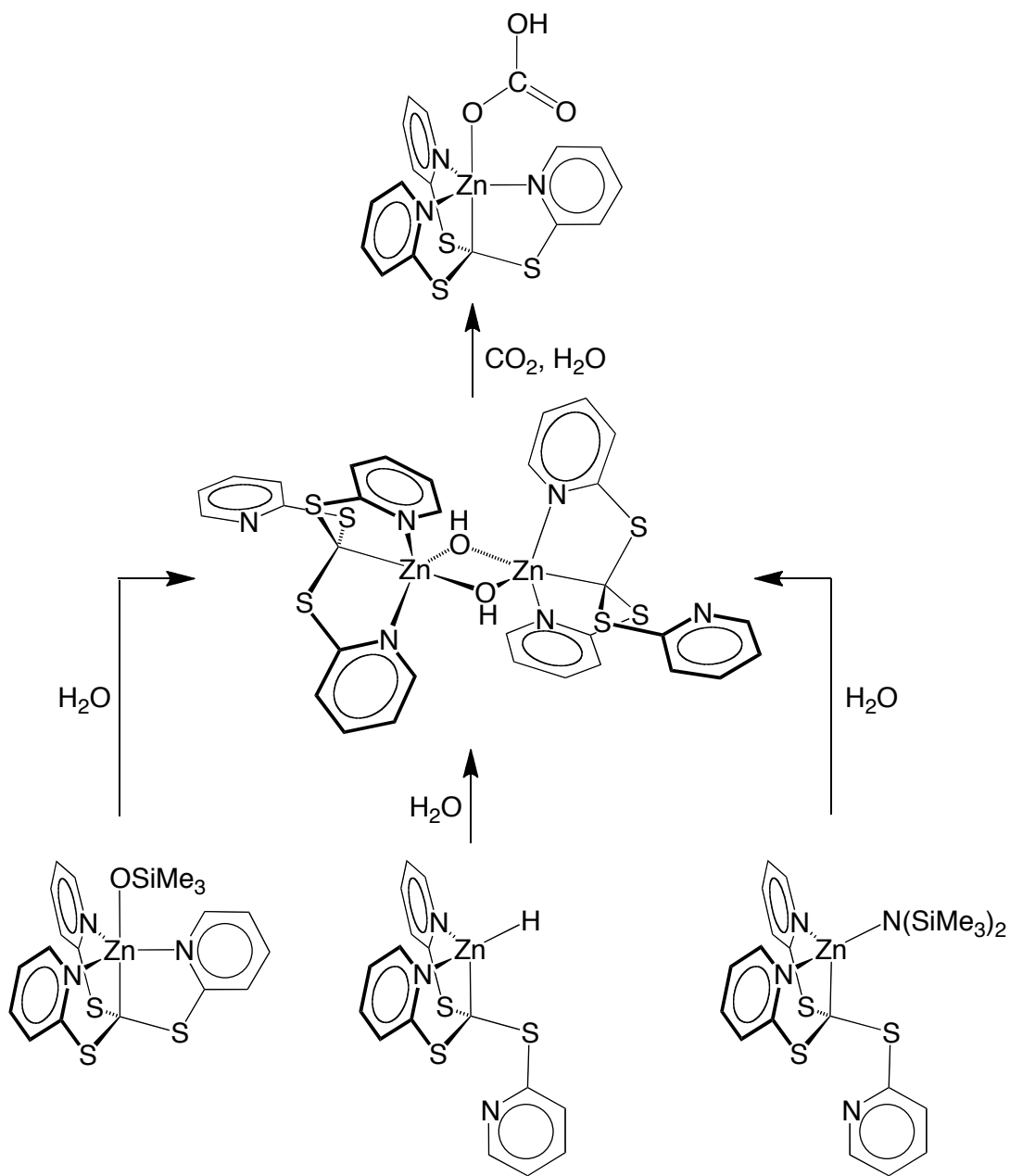


Figure 7. Molecular structure of $[\text{Tp}^{\text{Bu}^t, \text{Me}}]\text{ZnOCO}_2\text{H}$.

In addition to using the tridentate $[\text{Tp}^{\text{Bu}^t, \text{Me}}]$ ligand in a synthetic analogue of carbonic anhydrase, we have also utilized the tetradentate tripodal *tris*(2-pyridylthio)methyl ligand, $[\text{Tptm}]$. The zinc bicarbonate complex, namely $[\kappa^4\text{-Tptm}]\text{ZnOCO}_2\text{H}$, has also been synthesized and has been structurally characterized by single crystal X-ray diffraction. Treatment of either $[\kappa^3\text{-Tptm}]\text{ZnH}$, $[\kappa^3\text{-Tptm}]\text{ZnN}(\text{SiMe}_3)_2$ or $[\kappa^4\text{-Tptm}]\text{ZnOSiMe}_3$ ³⁹ with H_2O generates the hydroxide complex, $\{[\kappa^3\text{-Tptm}]\text{Zn}(\mu\text{-OH})\}_2$, which reacts with CO_2 in the presence of water (*vide infra*) to give the bicarbonate complex, $[\kappa^4\text{-Tptm}]\text{ZnOCO}_2\text{H}$ (Scheme 5). The isolated hydroxide dimer, $\{[\kappa^3\text{-Tptm}]\text{Zn}(\mu\text{-OH})\}_2$, also reacts with CO_2 in the presence of H_2O to give the bicarbonate complex. However, due to difficulty in the preparation of $\{[\kappa^3\text{-Tptm}]\text{Zn}(\mu\text{-OH})\}_2$, this is not the preferred method for synthesizing

$[\kappa^4\text{-Tptm}]\text{ZnOCO}_2\text{H}$. Crystals of $\{[\kappa^3\text{-Tptm}]\text{Zn}(\mu\text{-OH})\}_2$ have also been obtained from room temperature benzene solutions and cold toluene solutions, allowing for the determination of the molecular structure by using single crystal X-ray diffraction (Figure 8).



Scheme 5. Synthesis of $[\kappa^4\text{-Tptm}]\text{ZnOCO}_2\text{H}$.

It is important to emphasize that the reaction of $[\kappa^3\text{-Tptm}]\text{ZnH}$ and $[\kappa^3\text{-Tptm}]\text{ZnN}(\text{SiMe}_3)_2$ with H_2O and CO_2 needs to be done in that order (*i.e.* first H_2O , followed by addition of CO_2). If CO_2 is added first, the hydride complex will produce the formate complex, $[\kappa^4\text{-Tptm}]\text{ZnO}_2\text{CH}$, and the *bis*(trimethylsilyl)amide complex will begin to generate the isocyanate complex, $[\kappa^4\text{-Tptm}]\text{ZnNCO}$ (see chapter 3). Therefore, it is important to hydrolyze both of these compounds followed by addition of CO_2 . On the other hand, the order of addition of H_2O and CO_2 to $[\kappa^4\text{-Tptm}]\text{ZnOSiMe}_3$ does not matter, as $[\kappa^4\text{-Tptm}]\text{ZnOSiMe}_3$ reacts reversibly with CO_2 to generate the carbonate complex.

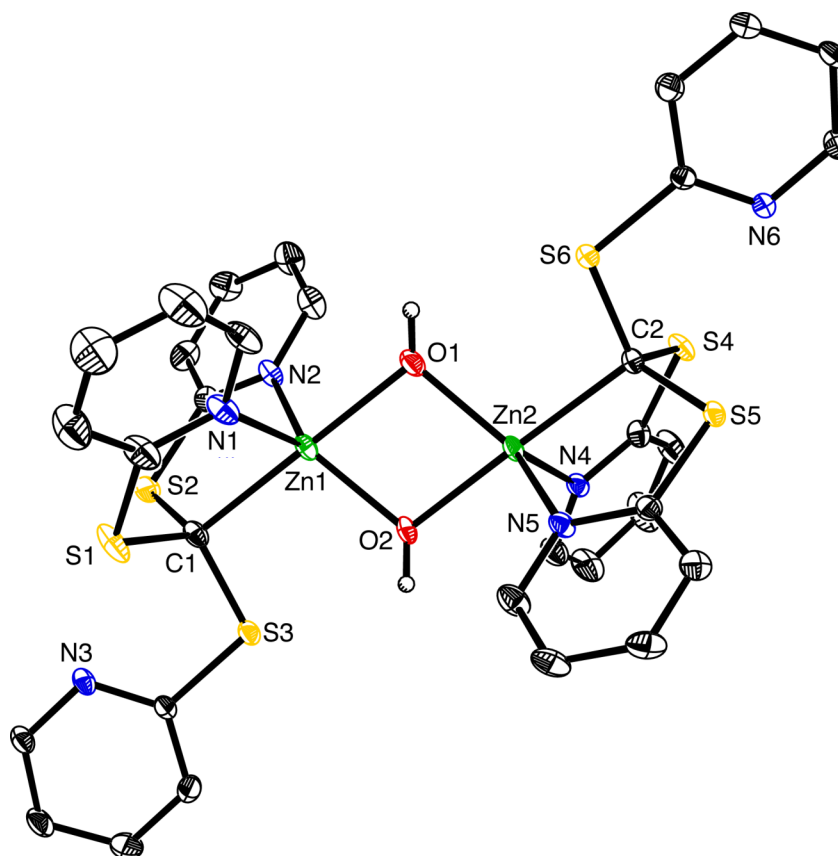


Figure 8. Molecular structure of $\{[\kappa^3\text{-Tptm}]\text{Zn}(\mu\text{-OH})\}_2$.

The molecular structure of $[\kappa^4\text{-Tptm}]\text{ZnOCO}_2\text{H}$ has been determined by X-ray diffraction (Figure 9) and the most noteworthy feature is that the bicarbonate ligand of $[\kappa^4\text{-Tptm}]\text{ZnOCO}_2\text{H}$ is less asymmetric than that of $[\text{Tp}^{\text{Bu}^\dagger, \text{Me}}]\text{ZnOCO}_2\text{H}$ (Table 2). For example, $\Delta d(\text{Zn}-\text{O})$ for $[\kappa^4\text{-Tptm}]\text{ZnOCO}_2\text{H}$ is 0.212 Å smaller than that for $[\text{Tp}^{\text{Bu}^\dagger, \text{Me}}]\text{ZnOCO}_2\text{H}$.

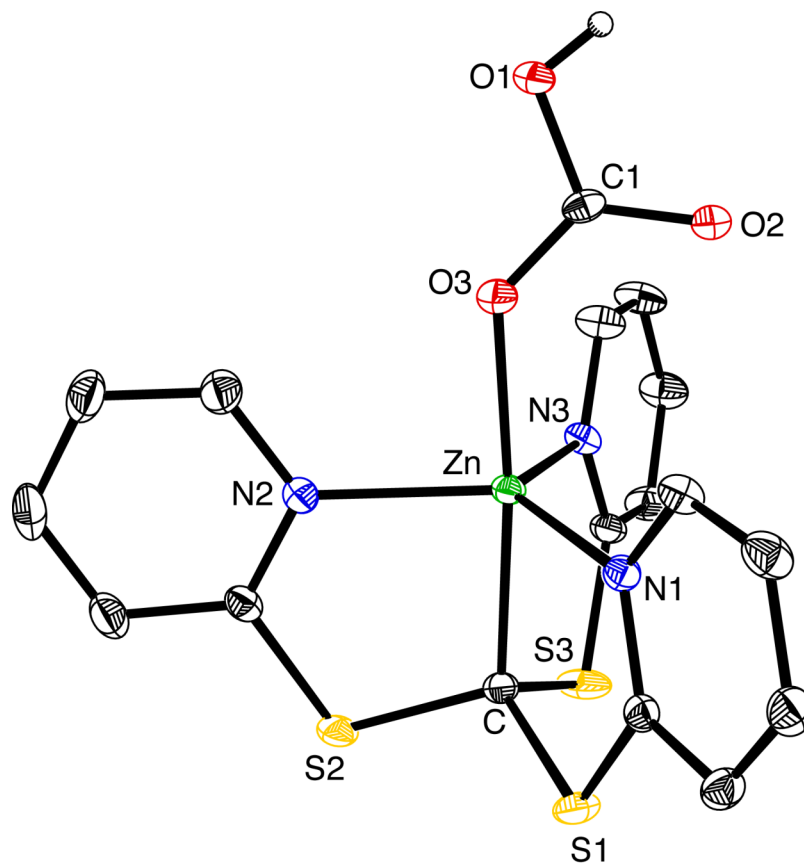


Figure 9. Molecular structure of $[\kappa^4\text{-Tptm}]\text{ZnOCO}_2\text{H}$.

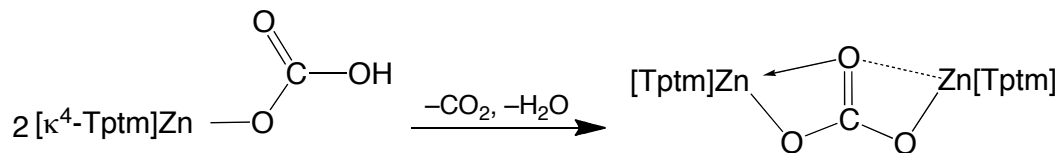
The reduced asymmetry of the bicarbonate ligand in $[\kappa^4\text{-Tptm}]\text{ZnOCO}_2\text{H}$ is due to two factors. First, there is a shorter secondary $\text{Zn}\cdots\text{O}$ interaction⁴⁰ of 3.406(2) in $[\kappa^4\text{-Tptm}]\text{ZnOCO}_2\text{H}$, and second, $[\kappa^4\text{-Tptm}]\text{ZnOCO}_2\text{H}$ has a longer primary $\text{Zn}-\text{O}$ bond of 2.039(2). Specifically, the $\text{Zn}-\text{O}$ bond in $[\kappa^4\text{-Tptm}]\text{ZnOCO}_2\text{H}$ is 0.167 Å longer than that in $[\text{Tp}^{\text{Bu}^\dagger, \text{Me}}]\text{ZnOCO}_2\text{H}$. We attribute the longer $\text{Zn}-\text{O}$ bond in $[\kappa^4\text{-Tptm}]\text{ZnOCO}_2\text{H}$

to it being a component of a 3-center-4-electron hypervalent ω interaction⁴¹ involving the *trans* carbon atom of the [κ^4 -Tptm] ligand. This is in comparison to a conventional 2-center-2-electron bond in [Tp^{Bu^t,Me}]ZnOCO₂H. Further evidence for the longer Zn–O bond in [κ^4 -Tptm]ZnOCO₂H being attributed to a 3-center-4-electron hypervalent ω interaction is the absence of lengthening of the Zn–N bonds in [κ^4 -Tptm]ZnOCO₂H. The average Zn–N bond length in [κ^4 -Tptm]ZnOCO₂H is 2.103 Å which is only 0.070 Å longer than the corresponding value for [Tp^{Bu^t,Me}]ZnOCO₂H (2.033 Å). Thus, the lengthening observed for the Zn–O bond (0.167 Å) is exceptional and is not a consequence of an increased coordination number. Rather, it is associated with the fact that the bicarbonate ligand is in a *trans* disposition with respect to the carbon atom and is a component of a 3-center-4-electron interaction. It should be noted that the bicarbonate ligand in [κ^4 -Tptm]ZnOCO₂H binds *via* a distinct unidentate coordination and also exists as a hydrogen-bonded dimer.

[κ^4 -Tptm]ZnOCO₂H is not stable in solution, as it rapidly loses CO₂. As such, we were not able to obtain a ¹³C NMR in solution to characterize the bicarbonate ligand. We therefore used solid state ¹³C{¹H} NMR to characterize the bicarbonate moiety of ¹³C enriched [κ^4 -Tptm]ZnO¹³CO₂H which displays a signal at 165.0 ppm. Additionally, the bicarbonate ligand has characteristic absorptions at 1628/1621 cm⁻¹ and 1363 cm⁻¹ in the IR spectrum, the assignments of which have been confirmed by comparison with the ¹³C isotopologue, [κ^4 -Tptm]ZnO¹³CO₂H (1580 and 1352 cm⁻¹). These IR absorptions are comparable to those of [Tp^{Bu^t,Me}]ZnOCO₂H (1675 and 1302 cm⁻¹) and are consistent with a unidentate coordination mode,⁴² while the isotope shifts, $\nu(^{12}\text{C}/^{13}\text{C})$, are comparable to values that are observed for other systems.⁴³

As described above, [κ^4 -Tptm]ZnOCO₂H exhibits limited stability in solution such that when dissolved in dichloromethane, it rapidly releases CO₂ and forms the bridging carbonate complex, [Tptm]Zn(μ -CO₃)Zn[Tptm]. Presumably, this is a result of

a condensation reaction between $[\kappa^4\text{-Tptm}]\text{ZnOCO}_2\text{H}$ and the incipient hydroxide species, $\{[\text{Tptm}]\text{ZnOH}\}$ (Scheme 6).⁴⁴



Scheme 6. Generation of $[\text{Tptm}]\text{Zn}(\mu\text{-CO}_3)\text{Zn}[\text{Tptm}]$.

The carbonate complex $[\text{Tptm}]\text{Zn}(\mu\text{-CO}_3)\text{Zn}[\text{Tptm}]$ can also be obtained directly by treatment of solutions of $\{[\kappa^3\text{-Tptm}]\text{Zn}(\mu\text{-OH})\}_2$ with CO_2 . $\{[\kappa^3\text{-Tptm}]\text{Zn}(\mu\text{-OH})\}_2$ is so reactive towards CO_2 that it actually fixes CO_2 from the atmosphere to form the carbonate complex $[\text{Tptm}]\text{Zn}(\mu\text{-CO}_3)\text{Zn}[\text{Tptm}]$.⁴⁵

An interesting aspect of the carbonate complex $[\text{Tptm}]\text{Zn}(\mu\text{-CO}_3)\text{Zn}[\text{Tptm}]$ is that it has been isolated in two isomeric forms (Figure 10). In one form, each zinc is six-coordinate with a $[\kappa^4\text{-Tptm}]$ ligand and a symmetric $\mu\text{-}\kappa^2,\kappa^2$ -carbonate ligand, namely $[\kappa^4\text{-Tptm}]\text{Zn}(\mu\text{-}\kappa^2,\kappa^2\text{-OCO}_2)\text{Zn}[\kappa^4\text{-Tptm}]$, and in another form, one zinc is five-coordinate with a $[\kappa^3\text{-Tptm}]$ ligand and a κ^2 -carbonate ligand, and the other zinc is five-coordinate with a $[\kappa^4\text{-Tptm}]$ ligand and a κ^1 -carbonate ligand asymmetric $[\kappa^3\text{-Tptm}]\text{Zn}(\mu\text{-}\kappa^2,\kappa^1\text{-OCO}_2)\text{Zn}[\kappa^4\text{-Tptm}]$.⁴⁶ The Zn–O distances of the bridging oxygen of symmetric $[\kappa^4\text{-Tptm}]\text{Zn}(\mu\text{-}\kappa^2,\kappa^2\text{-OCO}_2)\text{Zn}[\kappa^4\text{-Tptm}]$ are 2.303(3) and 2.277(3) Å, whereas the values are more disparate for asymmetric $[\kappa^3\text{-Tptm}]\text{Zn}(\mu\text{-}\kappa^2,\kappa^1\text{-OCO}_2)\text{Zn}[\kappa^4\text{-Tptm}]$, with 2.636(4) and 2.224(4) Å for one crystalline form, and 2.658(2) and 2.245(2) Å for a second crystalline form. Evidence for the existence of two isomers of $[\text{Tptm}]\text{Zn}(\mu\text{-CO}_3)\text{Zn}[\text{Tptm}]$ in solution is provided by variable temperature $^{13}\text{C}\{^1\text{H}\}$ NMR spectroscopy. Although a single resonance at 170.7 ppm is observed for the carbonate carbon in the $^{13}\text{C}\{^1\text{H}\}$ NMR spectrum at room temperature, two signals in a *ca.* 1:1 ratio

are observed at 168.6 and 170.3 ppm at 228 K. Furthermore, two carbonate signals at 171.6 and 172.1 ppm are also observed in the solid state $^{13}\text{C}\{^1\text{H}\}$ NMR spectrum.

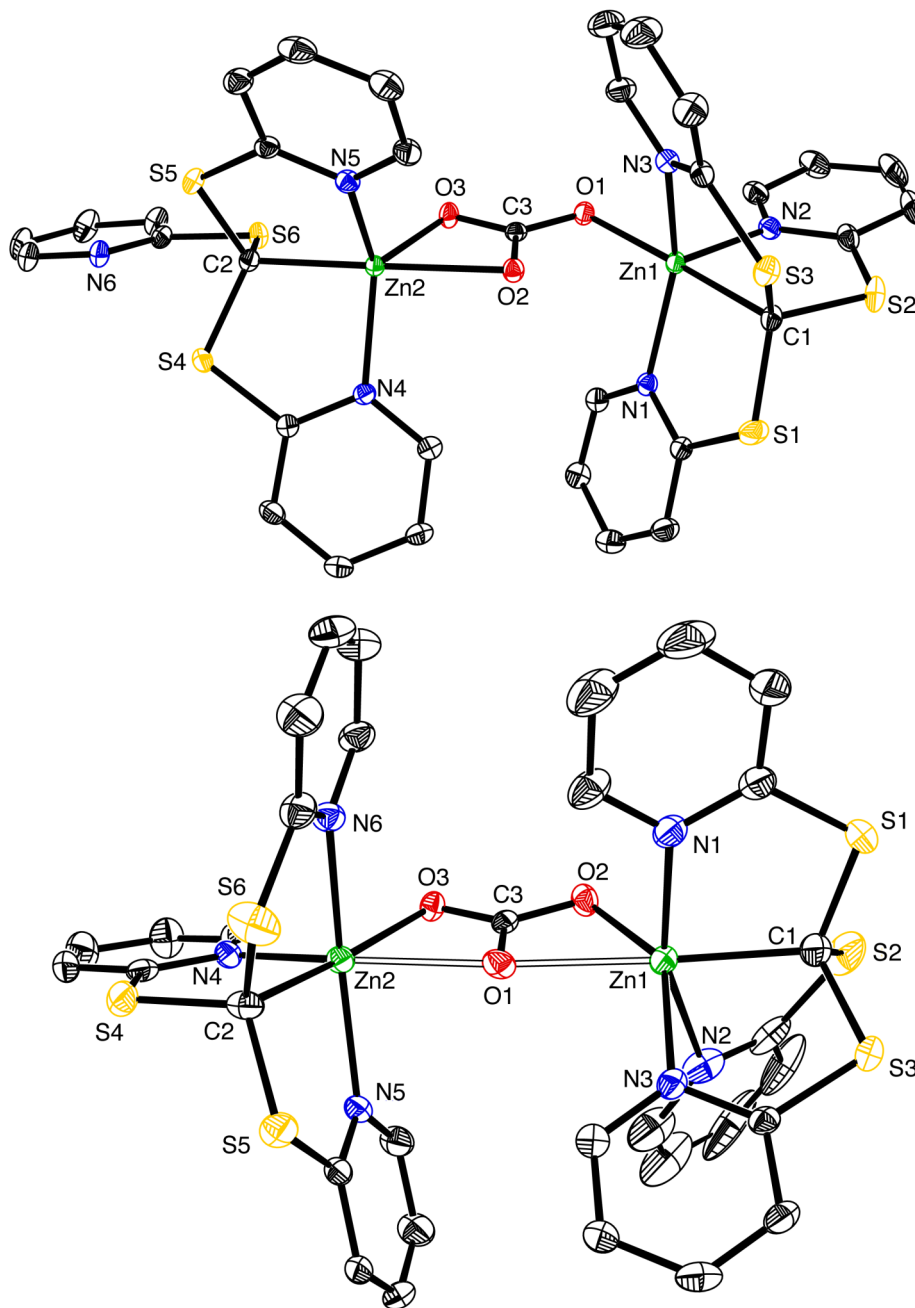


Figure 10. Molecular structures of $[\kappa^3\text{-Tptm}]\text{Zn}(\mu\text{-}\kappa^2, \kappa^1\text{-OCO}_2)\text{Zn}[\kappa^4\text{-Tptm}]$ (top) and $[\kappa^4\text{-Tptm}]\text{Zn}(\mu\text{-}\kappa^2, \kappa^2\text{-OCO}_2)\text{Zn}[\kappa^4\text{-Tptm}]$ (bottom).

2.6 DFT calculations concerning bonding modes of $[\text{Tp}^{\text{Bu}^t, \text{Me}}]\text{ZnOCO}_2\text{H}$ and $[\text{Tp}^{\text{Bu}^t, \text{Me}}]\text{ZnNO}_3$.

The nature of the bicarbonate ligand in $[\text{Tp}^{\text{Bu}^t, \text{Me}}]\text{ZnOCO}_2\text{H}$ and $[\kappa^4\text{-Tp}^{\text{tm}}]\text{ZnOCO}_2\text{H}$ is of significance in light of the fact that both unidentate⁴⁷ and bidentate⁴⁸ structures of the bicarbonate intermediate of the carbonic anhydrase catalytic cycle have been identified by X-ray diffraction and studied computationally.^{49,50,51} Therefore, we have employed density functional theory (DFT) calculations (B3LYP with 6-31G** and LAV3P basis sets) to obtain insight into the structure of $[\text{Tp}^{\text{Bu}^t, \text{Me}}]\text{ZnOCO}_2\text{H}$. Significantly, the geometry optimized structure features a bicarbonate ligand that coordinates in an asymmetric manner, with Zn–O bond lengths of 2.066 Å and 2.316 Å (Figure 11, left). It should be noted that this is much more symmetric than that in the experimental crystal structure. Furthermore, since the hydrogen is attached to the oxygen atom that does not coordinate to zinc, the binding mode corresponds to the so-called “Lipscomb-like structure,”⁴⁹ a species that is considered to be formed prior to displacement of the bicarbonate ligand by water. The initial insertion of CO_2 into the Zn–OH bond, nevertheless, is believed to give an isomeric species in which the OH group interacts with the zinc, the so-called “Lindskog-like structure” (Figure 11, right).⁴⁹ Geometry optimization of the “Lindskog-like structure” results in a species that is 4.2 kcal mol⁻¹ higher in energy and is significantly more asymmetric, with Zn–O distances of 1.940 Å and 3.092 Å (Figure 11, right).⁵² The large difference in energy implies that the bicarbonate OH group shows little tendency to coordinate to zinc. In this regard, calculations on carbonic anhydrase II also indicate that the Lindskog-like structure is unstable relative to the Lipscomb-like structure.⁴⁹ These DFT calculations are in accord with a Lipscomb-like structure being the species that is ultimately displaced by water in the catalytic cycle.

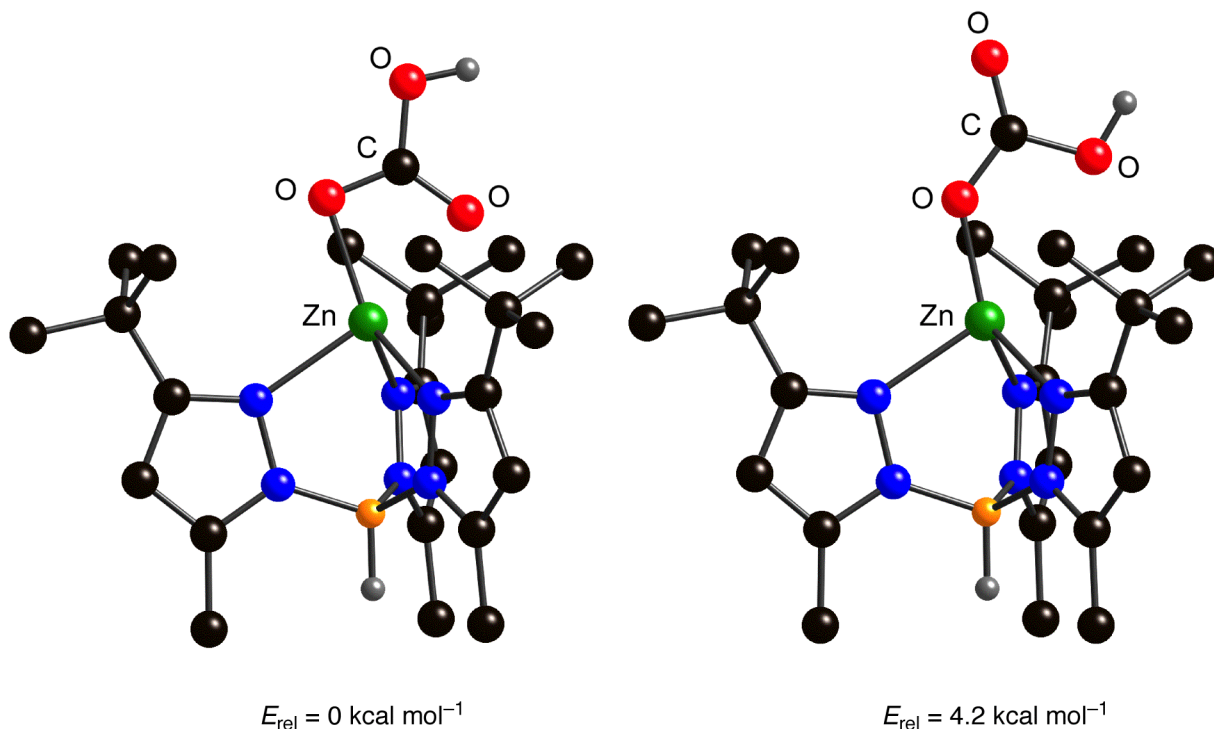


Figure 11. Geometry optimized structures of $[\text{Tp}^{\text{Bu}^t, \text{Me}}]\text{ZnOCO}_2\text{H}$ that corresponds to a “Lipscomb-like” structure (left) and a higher energy “Lindskog-like” isomer (right). Hydrogen atoms on carbon atoms of the $[\text{Tp}^{\text{Bu}^t, \text{Me}}]$ ligand are omitted for clarity.

While geometry optimization predicts an asymmetric coordination mode for the bicarbonate ligand, it is not as asymmetric as would have been expected by comparison to the methylcarbonate complex, $[\text{Tp}^{\text{Bu}^t, \text{Me}}]\text{ZnOCO}_2\text{Me}$, which has been shown by X-ray diffraction to possess a unidentate coordination mode,^{13b} albeit disordered.⁵³ Geometry optimization of the methylcarbonate, $[\text{Tp}^{\text{Bu}^t, \text{Me}}]\text{ZnOCO}_2\text{Me}$, however, results in a structure with a Zn–O–C angle of 95.3° (Figure 12) that corresponds closely to that of the geometry optimized bicarbonate, $[\text{Tp}^{\text{Bu}^t, \text{Me}}]\text{ZnOCO}_2\text{H}$. It appears that the calculations may overemphasize the importance of the secondary Zn–O interactions in this system, being that both $[\text{Tp}^{\text{Bu}^t, \text{Me}}]\text{ZnOCO}_2\text{H}$ and $[\text{Tp}^{\text{Bu}^t, \text{Me}}]\text{ZnOCO}_2\text{Me}$ are significantly more asymmetric.

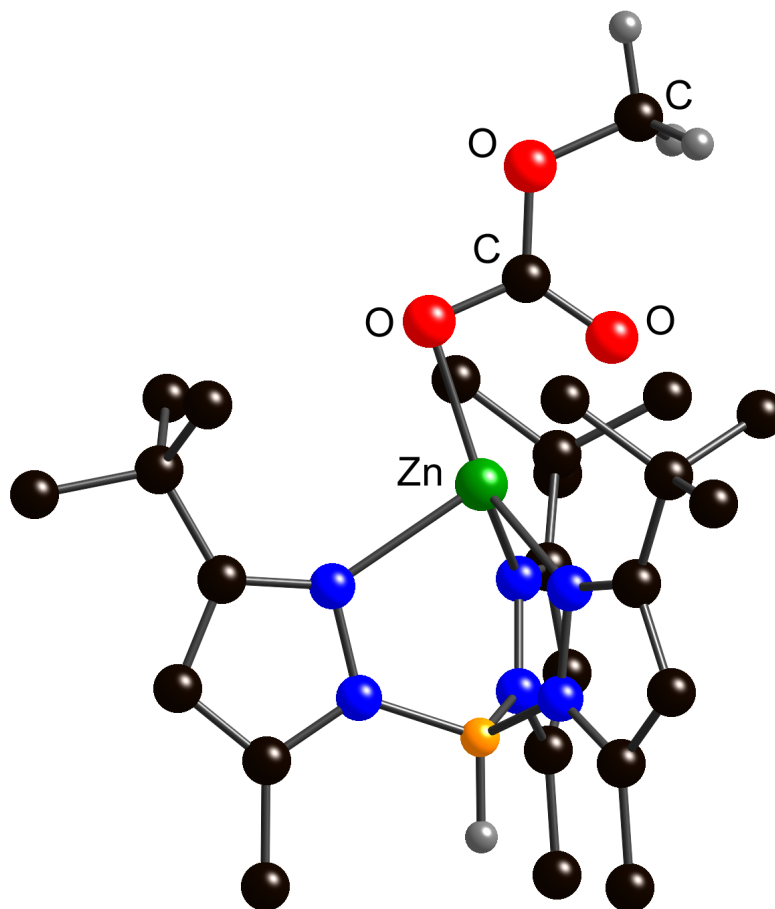
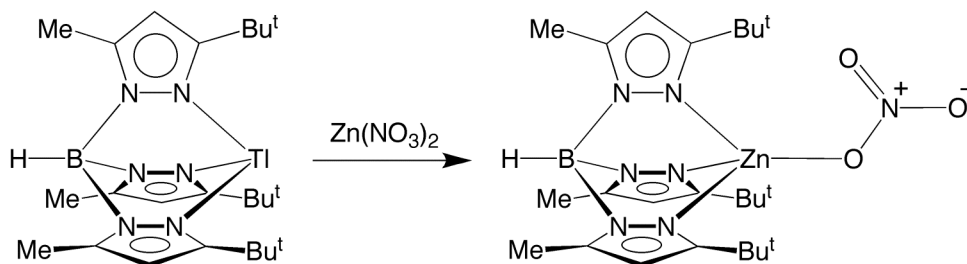


Figure 12. Geometry optimized structures of $[\text{Tp}^{\text{Bu}^t, \text{Me}}]\text{ZnOCO}_2\text{Me}$. Hydrogen atoms on carbon atoms of the $[\text{Tp}^{\text{Bu}^t, \text{Me}}]$ ligand are not shown for clarity.

In order to evaluate further the possibility that the DFT calculations overestimate secondary Zn–O interactions, we investigated the nitrate counterpart, $[\text{Tp}^{\text{Bu}^t, \text{Me}}]\text{ZnNO}_3$ (Scheme 7), which has been structurally characterized by X-ray diffraction (Figure 13). Selected bond lengths for the two crystallographically independent molecules of $[\text{Tp}^{\text{Bu}^t, \text{Me}}]\text{ZnNO}_3$ are listed in Table 3. Nitrate ligand coordination modes may be classified as bidentate, anisobidentate or unidentate, as summarized in Figure 14 and Table 4 according to the asymmetry of the interaction.^{54,55,56} On this basis, the coordination mode in $[\text{Tp}^{\text{Bu}^t, \text{Me}}]\text{ZnNO}_3$ can be classified as unidentate, as the difference in Zn–O distances (Δd) are 0.53 Å and 0.68 Å for the two crystallographically

independent molecules. $[\text{Tp}^{\text{RR}'}]\text{ZnNO}_3$ complexes that have been structurally characterized have similar coordination modes, indicating that the asymmetric coordination mode is common, with the difference in Zn–O distances ranging from 0.38 Å to 0.68 Å (Table 5),^{57,58,59,60,61,62,63} such that the nitrate ligands are classified as either anisobidentate or unidentate.⁶⁴



Scheme 7. Synthesis of $[\text{Tp}^{\text{Bu}^t, \text{Me}}]\text{ZnNO}_3$.

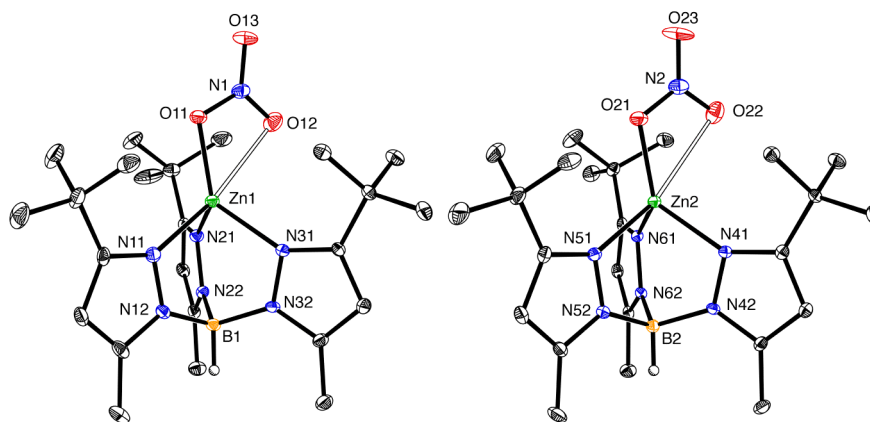
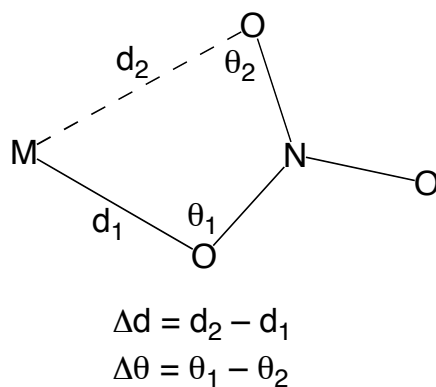


Figure 13. Molecular structure of the two crystallographically independent molecules of $[\text{Tp}^{\text{Bu}^t, \text{Me}}]\text{ZnNO}_3$.

Table 3. Selected bond lengths (Å) and angles (°) for [Tp^{But,Me}]ZnNO₃.

Molecule #1		Molecule #2	
Zn1–O11 / Å	1.9842(19)	Zn2–O21 / Å	1.962(2)
Zn1–O12 / Å	2.516(2)	Zn2–O22 / Å	2.640(2)
Zn1–N11 / Å	2.049(2)	Zn2–N41 / Å	2.036(2)
Zn1–N21 / Å	2.033(2)	Zn2–N51 / Å	2.043(2)
Zn1–N31 / Å	2.039(2)	Zn2–N61 / Å	2.037(2)
Zn1–O11–N1 / °	105.36(16)	Zn2–O21–N2 / °	110.43(17)
Zn1–O12–N1 / °	82.09(16)	Zn2–O22–N2 / °	79.25(16)

**Figure 14.** Parameters used for assigning nitrate coordination modes.**Table 4.** Criteria for Assigning Nitrate Coordination Modes.^a

	unidentate	anisobidentate	bidentate
$\Delta d / \text{Å}$	> 0.6	0.3 – 0.6	< 0.3
$\Delta\theta / ^\circ$	> 28	14 – 28	< 14

^a Reference 55.

Table 5. Summary of nitrate coordination in [Tp^{RR'}]ZnNO₃ complexes.^a

	$d_1/\text{\AA}$	$d_2/\text{\AA}$	$\theta_1/^\circ$	$\theta_2/^\circ$	$\Delta d/\text{\AA}$	$\Delta\theta/^\circ$	Reference
[Tp ^{Bu^t,Me}]ZnNO ₃ ^b	1.962	2.640	110.4	79.3	0.678	31.1	this work
[Tp ^{Bu^t,Me}]ZnNO ₃ ^b	1.984	2.516	105.4	82.1	0.532	23.3	this work
[Tp ^{Bu^t}]ZnNO ₃	1.978	2.581	109.4	79.8	0.603	29.6	57
[Tp ^{Ph,Me}]ZnNO ₃	1.945	2.480	104.6	81.0	0.535	23.6	58
[Tp ^{CO₂Et,Me}]ZnNO ₃	1.934	2.457	108.5	75.3	0.523	33.2	59
[Tp ^{Prⁱ₂}]ZnNO ₃	1.954	2.488	106.2	81.2	0.534	25.0	60
[Tp ^{Ph}]ZnNO ₃	1.947	2.475	104.3	81.9	0.528	22.4	61
[Tp]ZnNO ₃	1.981	2.399	102.2	83.5	0.418	18.7	62
[Tp ^{C₃F₇,Me}]ZnNO ₃	1.972	2.347	100.9	84.5	0.377	16.4	63

^a See Figure 14 for the definition of d_1 , d_2 , θ_1 and θ_2 .

^b values for two crystallographically independent molecules.

In contrast to the distinctly asymmetric experimental structure, however, geometry optimization of [Tp^{Bu^t,Me}]ZnNO₃ converged to a bidentate structure with very similar Zn–O bond lengths and Zn–O–N bond angles, such that $\Delta d = 0.14 \text{ \AA}$ and $\Delta\theta = 5.6^\circ$ (Figure 15). This again implies that DFT overemphasizes the secondary Zn–O interaction.

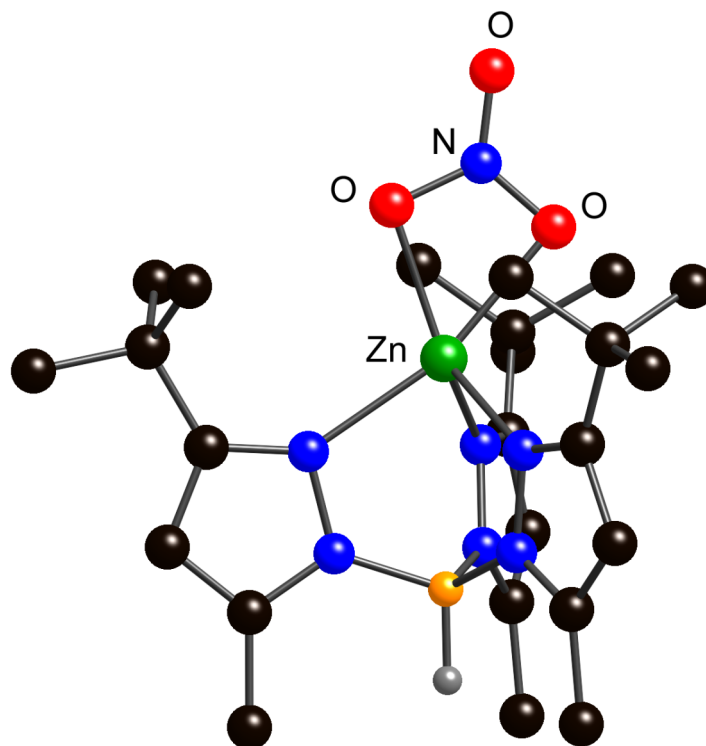


Figure 15. Geometry optimized structure of $[\text{Tp}^{\text{Bu,t,Me}}]\text{ZnNO}_3$. Hydrogen atoms on carbon atoms of the $[\text{Tp}^{\text{Bu,t,Me}}]$ ligand are not shown for clarity.

In order to determine the extent to which the secondary Zn–O interaction influences the energy of the molecule in these geometry optimizations, we have evaluated the energies for a series geometry optimizations in which the secondary Zn–O bond length is varied while the primary Zn–O bond length remains fixed. The calculations indicate that the energy of the molecule is not strongly dependent on geometry of the nitrate or bicarbonate ligand (Figure 16).⁶⁵

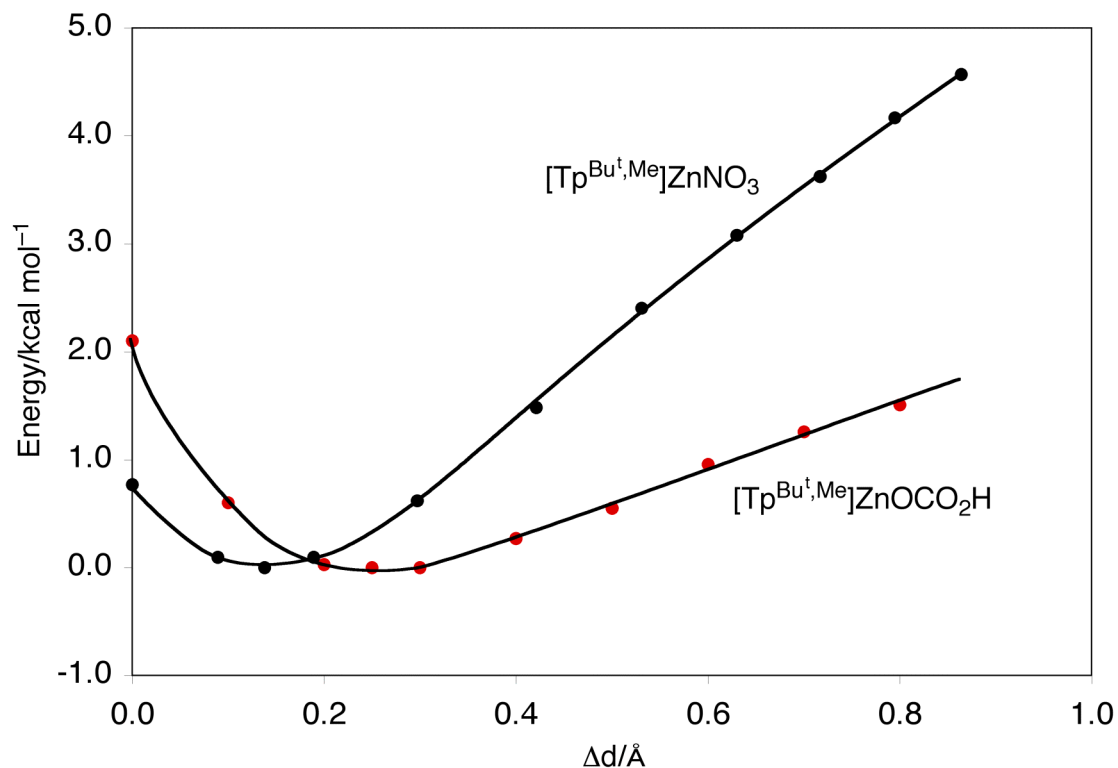
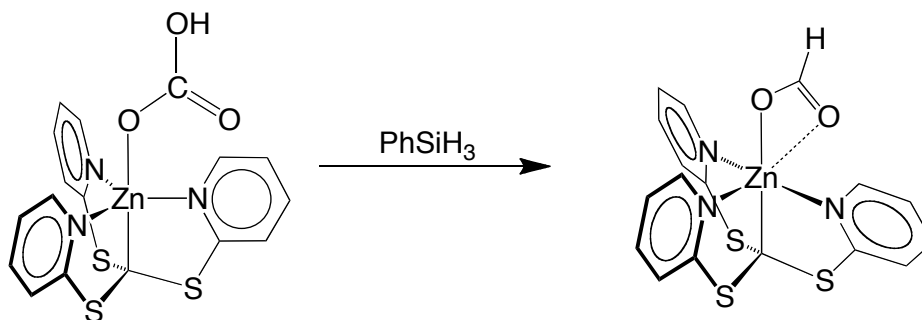


Figure 16. Linear transit geometry optimization calculations for $[\text{Tp}^{\text{Bu}^t, \text{Me}}]\text{ZnOCO}_2\text{H}$ and $[\text{Tp}^{\text{Bu}^t, \text{Me}}]\text{ZnNO}_3$ as a function of Δd .

As can be seen in Figure 16, increasing the asymmetry to a value of $\Delta d = 0.61 \text{ \AA}$ (the average value of the two crystallographically independent molecules) increases the energy by only $\approx 2 \text{ kcal mol}^{-1}$. It is not surprising that the geometry optimization procedure does not converge to the experimental structure of $[\text{Tp}^{\text{Bu}^t, \text{Me}}]\text{ZnNO}_3$ given the soft nature of the energy surface. Similar linear transit geometry optimization calculations on the bicarbonate complex $[\text{Tp}^{\text{Bu}^t, \text{Me}}]\text{ZnOCO}_2\text{H}$ indicate that it is also easy to perturb the coordination mode in this molecule (Figure 16). It should be noted that the energy surface for distorting the bicarbonate interaction is even softer than that for the nitrate ligand.

2.7 CO₂ reduction *via* reactivity of [κ⁴-Tptm]ZnOCO₂H and [Tptm]Zn(μ-CO₃)Zn[Tptm] with silanes.

There is currently a great deal of interest in the reduction of CO₂ to C₁ chemicals, such as formic acid. In this vein, a particularly noteworthy observation is that [κ⁴-Tptm]ZnOCO₂H reacts with PhSiH₃ to give the formate complex, [κ⁴-Tptm]ZnO₂CH (Scheme 8).^{66,67}



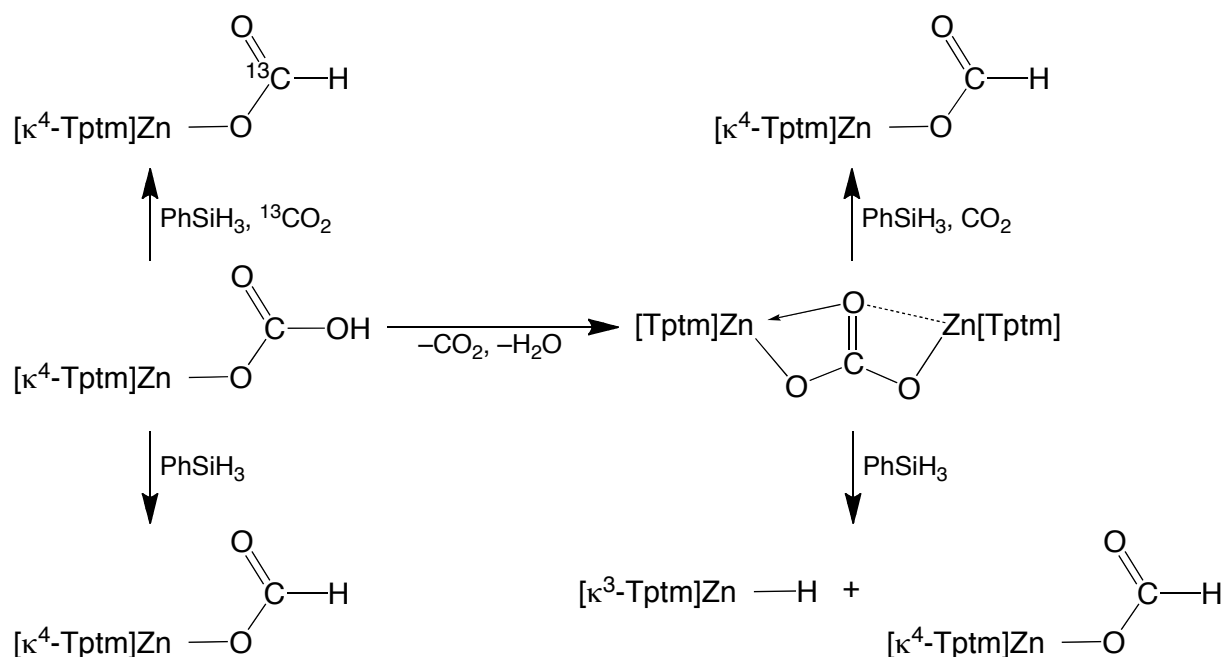
Scheme 8. Reaction of [κ⁴-Tptm]ZnOCO₂H with PhSiH₃ to give [κ⁴-Tptm]ZnO₂CH.

Since bicarbonates are easier to handle than CO₂, the conversion of bicarbonate to formate is of relevance as an alternative means of using CO₂ as a C₁ feedstock. There are, however, few reports concerned with the reduction of bicarbonate to formate in homogeneous systems⁶⁷ and so the formation of [κ⁴-Tptm]ZnO₂CH from [κ⁴-Tptm]ZnOCO₂H is of interest, especially because PhSiH₃ does not react directly with CO₂ under these conditions.

While the mechanism of this transformation is unknown, the formation of [κ⁴-Tptm]ZnOCO₂H does not necessarily require a direct transfer of hydride from silicon to carbon. An alternative pathway involves the generation of a zinc hydride intermediate that can be generated by metathesis with PhSiH₃, which then reacts with CO₂ that has been generated by dissociation of the silylbicarbonate.⁶⁸ In support of this mechanism, when the reaction of [κ⁴-Tptm]ZnOCO₂H with PhSiH₃ is performed in the

presence of $^{13}\text{CO}_2$ (1 atm), $[\kappa^4\text{-Tptm}]\text{ZnO}_2^{13}\text{CH}$ is the resulting product. Exchange between $[\kappa^4\text{-Tptm}]\text{ZnOCO}_2\text{H}$ and $^{13}\text{CO}_2$ or $[\kappa^4\text{-Tptm}]\text{ZnO}_2\text{CH}$ and $^{13}\text{CO}_2$ does not occur on the timescale of the reaction.

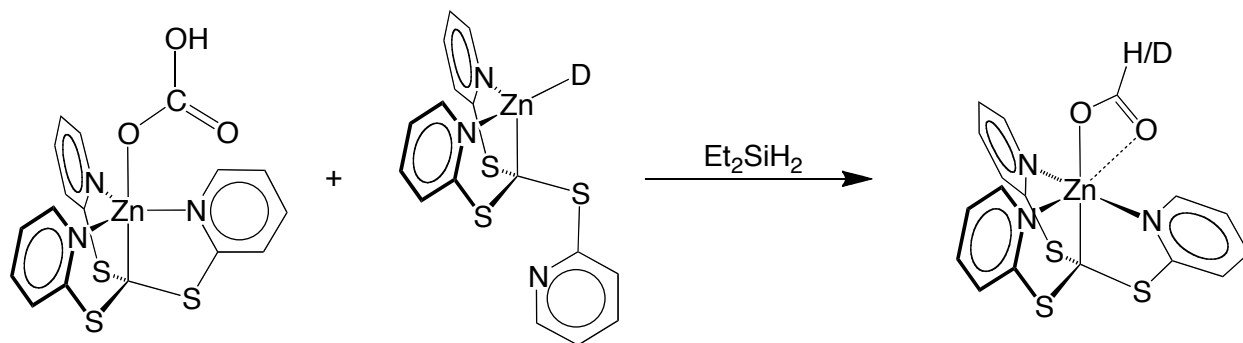
The carbonate complex $[\text{Tptm}]\text{Zn}(\mu\text{-CO}_3)\text{Zn}[\text{Tptm}]$ is also reduced by PhSiH_3 to give the formate $[\kappa^4\text{-Tptm}]\text{ZnO}_2\text{CH}$ (Scheme 9). However, because there are two zinc centers per carbonate ligand, only one equivalent of $[\kappa^4\text{-Tptm}]\text{ZnO}_2\text{CH}$ is formed, with the second zinc center forming the hydride complex, $[\kappa^3\text{-Tptm}]\text{ZnH}$. Since $[\kappa^3\text{-Tptm}]\text{ZnH}$ reacts with CO_2 to give $[\kappa^4\text{-Tptm}]\text{ZnO}_2\text{CH}$,³⁹ the formate becomes the exclusive zinc-containing product if the reaction between $[\text{Tptm}]\text{Zn}(\mu\text{-CO}_3)\text{Zn}[\text{Tptm}]$ and PhSiH_3 is performed in the presence of CO_2 (Scheme 9).



Scheme 9. Reactivity of $[\kappa^4\text{-Tptm}]\text{ZnOCO}_2\text{H}$ and $[\text{Tptm}]\text{Zn}(\mu\text{-CO}_3)\text{Zn}[\text{Tptm}]$ with PhSiH_3 .

In order to provide more evidence for the proposed mechanism involving the zinc hydride intermediate, a suspension of $[\kappa^4\text{-Tptm}]\text{ZnOCO}_2\text{H}$ and $[\kappa^3\text{-Tptm}]\text{ZnD}$ in C_6D_6 was treated with Et_2SiH_2 resulting in the generation of both $[\kappa^4\text{-Tptm}]\text{ZnO}_2\text{CH}$ and

$[\kappa^4\text{-Tptm}]\text{ZnO}_2\text{CD}$ (Scheme 10). Et_2SiH_2 was used as this silane because it does not undergo HD exchange with $[\kappa^3\text{-Tptm}]\text{ZnD}$, while PhSiH_3 does. The production of $[\kappa^4\text{-Tptm}]\text{ZnO}_2\text{CD}$ implies that there is free CO_2 produced in the reaction, which then reacts with the zinc deuteride complex, $[\kappa^3\text{-Tptm}]\text{ZnD}$, to make the deuterated formate complex, $[\kappa^4\text{-Tptm}]\text{ZnO}_2\text{CD}$.



Scheme 10. Reactivity of $[\kappa^4\text{-Tptm}]\text{ZnOCO}_2\text{H}$ with Et_2SiH_2 in the presence of $[\kappa^3\text{-Tptm}]\text{ZnD}$.

2.8 Conclusions

In summary, low temperature ^1H and ^{13}C NMR spectroscopic studies on solutions of $[\text{Tp}^{\text{Bu}^t, \text{Me}}]\text{ZnOH}$ in the presence of CO_2 have allowed identification of the bicarbonate moiety of $[\text{Tp}^{\text{Bu}^t, \text{Me}}]\text{ZnOCO}_2\text{H}$. Furthermore, in the presence of less than 1 atmosphere of CO_2 , both $[\text{Tp}^{\text{Bu}^t, \text{Me}}]\text{ZnOH}$ and $[\text{Tp}^{\text{Bu}^t, \text{Me}}]\text{ZnOCO}_2\text{H}$ may be observed in equilibrium, thereby allowing measurement of the equilibrium constant for insertion of CO_2 into the $\text{Zn}-\text{OH}$ bond. At 217 K, the equilibrium constant is $6 \pm 2 \times 10^3 \text{ M}^{-1}$, corresponding to a value of $\Delta G = -3.8 \pm 0.2 \text{ kcal mol}^{-1}$ for insertion of CO_2 into the $\text{Zn}-\text{OH}$ bond of $[\text{Tp}^{\text{Bu}^t, \text{Me}}]\text{ZnOH}$. Additionally, both $[\text{Tp}^{\text{Bu}^t, \text{Me}}]\text{ZnOCO}_2\text{H}$ and $[\kappa^4\text{-Tptm}]\text{ZnOCO}_2\text{H}$ have been structurally characterized by X-ray diffraction, and they are the first structurally characterized examples of terminal zinc bicarbonate complexes. As a result, they provide important metrical data of relevance to the critical intermediate of the mechanism of action of carbonic anhydrase. $[\text{Tptm}]\text{Zn}(\mu\text{-CO}_3)\text{Zn}[\text{Tptm}]$, which may

be obtained *via* reaction of the hydroxide $\{[\kappa^3\text{-Tptm}]\text{Zn}(\mu\text{-OH})\}_2$ with atmospheric CO_2 , and $[\kappa^4\text{-Tptm}]\text{ZnOCO}_2\text{H}$ can be reduced by silanes to give the formate derivative, $[\kappa^4\text{-Tptm}]\text{ZnO}_2\text{CH}$, a transformation that is of significance with respect to the functionalization of CO_2 , especially because the silanes used do not exhibit such reactivity towards CO_2 by themselves.

2.9 Experimental details

2.9.1 General considerations

All manipulations were performed using a combination of glovebox, high vacuum, and Schlenk techniques under a nitrogen or argon atmosphere,⁶⁹ with the exception of the synthesis of $[\text{Tptm}]\text{H}$. Solvents were purified and degassed by standard procedures. ^1H NMR spectra were measured on Bruker 300 DRX, Bruker 400 DRX, and Bruker Avance 500 DMX spectrometers. ^1H NMR chemical shifts are reported in ppm relative to SiMe_4 ($\delta = 0$) and were referenced internally with respect to the protio solvent impurity ($\delta 7.16$ for $\text{C}_6\text{D}_5\text{H}$).⁷⁰ Coupling constants are given in hertz. Infrared spectra were recorded on Nicolet Avatar 370 DTGS spectrometer and are reported in cm^{-1} . Mass spectra were obtained on a Micromass Quadrupole-Time-of-Flight mass spectrometer using fast atom bombardment (FAB). All chemicals were obtained from Aldrich, with the exception of 2-mercaptopyridine (Acros Organics), bromoform (Fisher Scientific), phenylsilane (Alfa Aesar), trimethylsilyl isocyanate (Alfa Aesar), and dimethylzinc (Strem Chemicals). Trimethylsilanol was obtained by the literature method.⁷¹ PhSiD_3 was prepared by using a method analogous to that reported in the literature method for PhSiH_3 ,⁷² but employing LiAlD_4 (Aldrich) in place of LiAlH_4 .

2.9.2 Computational details

Calculations were carried out using DFT as implemented in the Jaguar 7.5 (release 207) suite of *ab initio* quantum chemistry programs.⁷³ Geometry optimizations were performed with the B3LYP density functional⁷⁴ using the 6-31G** (C, H, N, O, Si, S, F, Cl) and LAV3P (Br, I and Zn) basis sets.⁷⁵ The energies of the optimized structures were reevaluated by additional single point calculations on each optimized geometry using cc-pVTZ(-f)⁷⁶ correlation consistent triple- ζ (C, H, N, O, Si, S, F, Cl) and LAV3P (Br, I, Zn) basis sets.

2.9.3 X-ray structure determinations

X-ray diffraction data were collected on a Bruker Apex II diffractometer. Crystal data, data collection and refinement parameters are summarized in Table 6. The structures were solved using direct methods and standard difference map techniques, and were refined by full-matrix least-squares procedures on F^2 with SHELXTL (Version 6.1).⁷⁷

2.9.4 Synthesis of [Tp^{Bu^t,Me}]ZnNO₃

A filtered solution of [Tp^{Bu^t,Me}]Tl (70 mg, 0.11 mmol) in THF (*ca.* 1 mL) was treated with a solution of Zn(NO₃)₂·6H₂O (33 mg, 0.11 mmol) in H₂O (*ca.* 1 mL) and the resulting suspension was stirred for 1 hour. After this period, the precipitate was dried *in vacuo* to give [Tp^{Bu^t,Me}]ZnNO₃ as a white solid (32 mg, 52%). ¹H NMR (C₆D₆): 1.40 [s, 27H, κ^3 -HB{(C₃N₂H(Me)CMe₃)₃}, 2.04 [s, 9H, κ^3 -HB{(C₃N₂H(Me)CMe₃)₃}, 4.1-5.1 [vb, 1H, κ^3 -HB{(C₃N₂H(Me)CMe₃)₃}, 5.61 [s, 3H, κ^3 -HB{(C₃N₂H(Me)CMe₃)₃].

2.9.5 Measurement of the equilibrium constant for the formation of [Tp^{Bu^t,Me}]ZnOCO₂H via reaction of [Tp^{Bu^t,Me}]ZnOH with CO₂

A solution of [Tp^{Bu^t,Me}]ZnOH (38 mg, 0.08 mmol) in CD₂Cl₂ (0.6 mL) containing

mesitylene (10 μL , 0.07 mmol) as an internal standard was placed in an NMR tube equipped with a J. Young valve. The solution was frozen, degassed, allowed to warm to room temperature and then treated with $^{13}\text{CO}_2$ (600 mm Hg). The sample was placed in the probe of an NMR spectrometer pre-cooled to 217 K and monitored by ^1H NMR spectroscopy, until the conversion of $[\text{Tp}^{\text{Bu}^t, \text{Me}}]\text{ZnOH}$ to $[\text{Tp}^{\text{Bu}^t, \text{Me}}]\text{ZnOCO}_2\text{H}$ reached equilibrium. The concentrations of $[\text{Tp}^{\text{Bu}^t, \text{Me}}]\text{ZnOH}$, $[\text{Tp}^{\text{Bu}^t, \text{Me}}]\text{ZnOCO}_2\text{H}$ and CO_2 were determined relative to that of mesitylene by using $^{13}\text{C}\{^1\text{H}\}$ NMR spectroscopy (with an inverse-gated sequence employing a pulse delay of 150 seconds),⁷⁸ and taking into account statistical factors resulting from the fact that the CO_2 contains 99 % ^{13}C , as compared to a value of 1.11 % for natural abundance. The experiment was repeated with a different concentration of $^{13}\text{CO}_2$, resulting in an average value of $K = 6 \pm 2 \times 10^3 \text{ M}^{-1}$.⁷⁹

2.9.6 Synthesis of $[\text{Tp}^{\text{Bu}^t, \text{Me}}]\text{ZnOH}$

$[\text{Tp}^{\text{Bu}^t, \text{Me}}]\text{ZnOH}$ was prepared by a method analogous to that previously reported.⁸⁰ A solution of $[\text{Tp}^{\text{Bu}^t, \text{Me}}]\text{Li}$ (1.868 g, 4.34 mmol) in MeOH (*ca.* 40 mL) was treated with $\text{Zn}(\text{ClO}_4)_2 \cdot 6\text{H}_2\text{O}$ (1.864 g, 5.01 mmol) and the resulting suspension was stirred for 15 minutes, during which period most of the solid dissolved. KOH (268 mg, 4.78 mmol) was added and the suspension was stirred for 1 hour, after which the volatile components were removed *in vacuo*. Benzene (*ca.* 50 mL) was added and the mixture was washed with several portions of H_2O (300 mL total). The benzene layer was filtered and then lyophilized to give $[\text{Tp}^{\text{Bu}^t, \text{Me}}]\text{ZnOH}$ (1.73 g, 79 %) as a white solid of sufficient purity for further reactions. Large colorless crystals of $[\text{Tp}^{\text{Bu}^t, \text{Me}}]\text{ZnOH}$ can be obtained from vapor diffusion of ether into a saturated benzene solution.

2.9.7 Structural characterization of $[\text{Tp}^{\text{Bu}^t, \text{Me}}]\text{ZnOCO}_2\text{H}$

Crystals of $[\text{Tp}^{\text{Bu}^t, \text{Me}}]\text{ZnOCO}_2\text{H}$ suitable for X-ray diffraction were obtained by treatment of $[\text{Tp}^{\text{Bu}^t, \text{Me}}]\text{ZnOH}$ with CO_2 . A solution of $[\text{Tp}^{\text{Bu}^t, \text{Me}}]\text{ZnOH}$ (*ca.* 10 mg) in benzene (*ca.* 0.5 mL) was placed in a small vial that was located inside a larger vial that contained pentane and dry ice. The larger vial was lightly stoppered until the dry ice had sublimed and then sealed completely. The sample was allowed to stand at room temperature, thereby depositing colorless crystals of $[\text{Tp}^{\text{Bu}^t, \text{Me}}]\text{ZnOCO}_2\text{H}$ that were suitable for X-ray diffraction. IR Data (KBr disk, cm^{-1}): 3424 (w), 2962 (s), 2930 (m), 2868 (m), 2548 (m), 1651 (m), 1636 (m), 1588 (m), 1545 (s), 1479 (m), 1405 (m), 1425 (s), 1383 (w), 1364 (s), 1309 (s), 1245 (w), 1192 (s), 1068 (s), 1029 (w), 852 (w), 795 (w), 771 (m), 649 (m). Upon dissolving in C_6D_6 , solutions of $[\text{Tp}^{\text{Bu}^t, \text{Me}}]\text{ZnOCO}_2\text{H}$ immediately release CO_2 and regenerate $[\text{Tp}^{\text{Bu}^t, \text{Me}}]\text{ZnOH}$, as indicated by ^1H NMR spectroscopy.

2.9.8 Synthesis of $\{[\kappa^3\text{-Tp}^t\text{m}]\text{Zn}(\mu\text{-OH})\}_2$

A suspension of $[\kappa^3\text{-Tp}^t\text{m}]\text{ZnH}$ (28 mg, 0.07 mmol) in pentane (*ca.* 4 mL) was treated with H_2O (50 μL , 2.78 mmol) and ethanol (10 μL , 0.16 mmol) *via* syringe. Evolution of H_2 was observed, and the reaction was left open to the nitrogen manifold at room temperature for 2 days. After this period, much of the pentane has evaporated and the residue was dried *in vacuo* to give $\{[\kappa^3\text{-Tp}^t\text{m}]\text{Zn}(\mu\text{-OH})\}_2$ as an off-white solid (23 mg, 79%). Colorless crystals of $\{[\kappa^3\text{-Tp}^t\text{m}]\text{Zn}(\mu\text{-OH})\}_2 \cdot (\text{C}_6\text{H}_6)$ suitable for X-ray diffraction were obtained from a concentrated solution in benzene, but it should be noted that $\{[\kappa^3\text{-Tp}^t\text{m}]\text{Zn}(\mu\text{-OH})\}_2$ decomposes to $[\text{Tp}^t\text{m}]\text{H}$ and unidentified zinc products over several hours at room temperature. In addition, crystals of composition $\{[\kappa^3\text{-Tp}^t\text{m}]\text{Zn}(\mu\text{-OH})\}_2 \cdot (\text{C}_7\text{H}_8)$ were obtained by the slow hydrolysis of a solution of $[\kappa^4\text{-Tp}^t\text{m}]\text{ZnN}(\text{SiMe}_3)_2$ in toluene with adventitious water over a period of two months at -15°C . Anal. Calcd. for $\{[\kappa^3\text{-Tp}^t\text{m}]\text{Zn}(\mu\text{-OH})\}_2 \cdot 0.30(\text{C}_7\text{H}_8)$: C, 48.0%; H, 3.4%; N, 9.3%.

Found: C, 48.1%; H, 3.1%; N, 9.1%. IR Data (KBr disk, cm^{-1}): 3402 (w), 3078 (w), 3047 (w), 1589 (s), 1555 (s), 1453 (s), 1416 (s), 1280 (m), 1131 (s), 1090 (m), 1045 (m), 1006 (m), 759 (s), 723 (m), 637 (w). ^1H NMR (C_6D_6): Not observed [$(\text{SC}_5\text{H}_4\text{N})_3\text{CZnOH}$], 6.20 [t, $^3J_{\text{H-H}} = 6$ Hz, 3H, $(\text{SC}_5\text{H}_4\text{N})_3\text{CZnOH}$], 6.61 [t, $^3J_{\text{H-H}} = 7$ Hz, 3H, $(\text{SC}_5\text{H}_4\text{N})_3\text{CZnO}_2\text{H}$], 6.74 [d, $^3J_{\text{H-H}} = 7$ Hz, 3H, $(\text{SC}_5\text{H}_4\text{N})_3\text{CZnOH}$], 8.95 [s, 3H, $(\text{SC}_5\text{H}_4\text{N})_3\text{CZnOH}$]. $^{13}\text{C}\{^1\text{H}\}$ NMR (C_6D_6): Not observed, [$(\text{SC}_5\text{H}_4\text{N})_3\text{CZnOH}$], 118.7 [s, 3C, $(\text{SC}_5\text{H}_4\text{N})_3\text{CZnOH}$], 120.7 [s, 3C, $(\text{SC}_5\text{H}_4\text{N})_3\text{CZnOH}$], 137.0 [s, 3C, $(\text{SC}_5\text{H}_4\text{N})_3\text{CZnOH}$], 149.2 [s, 3C, $(\text{SC}_5\text{H}_4\text{N})_3\text{CZnOH}$], not observed [s, 3H, $(\text{SC}_5\text{H}_4\text{N})_3\text{CZnOH}$].

2.9.9 Synthesis of $[\kappa^4\text{-Tptm}]\text{ZnOCO}_2\text{H}$

(a) A solution of $[\kappa^4\text{-Tptm}]\text{ZnOSiMe}_3$ (30 mg, 0.06 mmol) in C_6H_6 (*ca.* 2 mL) in a small Schlenk tube was treated with H_2O (40 μL , 40 mg, 2.22 mmol). The sample was frozen, degassed and allowed to warm to room temperature. The suspension was then treated with CO_2 (1 atm) while being shaken vigorously for a brief period. The mixture was allowed to stand at room temperature, thereby depositing colorless crystals of $[\kappa^4\text{-Tptm}]\text{ZnOCO}_2\text{H}\cdot(\text{C}_6\text{H}_6)$ over a period of 30 minutes. The mother liquor was decanted, and the precipitate was washed with benzene (*ca.* 1 mL). The precipitate was dried *in vacuo* giving $[\kappa^4\text{-Tptm}]\text{ZnOCO}_2\text{H}\cdot(\text{C}_6\text{H}_6)$ (12 mg, 36 %) as an off white powder. Colorless crystals of $[\kappa^4\text{-Tptm}]\text{ZnOCO}_2\text{H}$ suitable for X-ray diffraction were obtained directly from the reaction mixture before drying *in vacuo*. IR Data (KBr disk, cm^{-1}): 3078 (w), 3018 (w), 2633 (w), 1628 (s)/1621 (s) [$\nu(\text{CO}_3)$], 1591 (s), 1558 (s), 1477 (m), 1459 (s), 1416 (s), 1363 (s) [$\nu_{\text{sym}}(\text{CO}_2)$], 1283 (s), 1155 (w), 1094 (m), 1047 (m), 1032 (m), 1007 (m), 975 (w), 834 (w), 757 (s), 723 (m), 692 (s), 642 (m), 611 (w). Anal. calcd. for $[\kappa^4\text{-Tptm}]\text{ZnOCO}_2\text{H}\cdot 0.9(\text{C}_6\text{H}_6)$: C, 49.9%; H, 3.4%; N, 7.8%. Found: C, 49.7%; H, 3.3%; N, 7.4%. Crystals of $[\kappa^4\text{-Tptm}]\text{ZnOCO}_2\text{H}$ were also obtained *via* the analogous reactions employing $[\kappa^3\text{-Tptm}]\text{ZnN}(\text{SiMe}_3)_2$ and $[\kappa^3\text{-Tptm}]\text{ZnH}$ instead of $[\kappa^4\text{-Tptm}]\text{ZnOSiMe}_3$.

(b) A solution of $\{[\kappa^3\text{-Tptm}]\text{Zn}(\mu\text{-OH})\}_2$ (8 mg, 0.01 mmol) in benzene (ca. 2 mL) was treated with H_2O (50 μL , 2.78 mmol). The sample was frozen, degassed, and allowed to warm to room temperature. The resulting suspension was treated with CO_2 (1 atm) while being shaken vigorously, thereby resulting in the formation of colorless crystals. The mixture was allowed to stand at room temperature for 30 minutes and lyophilized to give $[\kappa^4\text{-Tptm}]\text{ZnOCO}_2\text{H}\cdot(\text{C}_6\text{H}_6)$ (7 mg, 70%) as a white solid.

2.9.10 Synthesis of $[\kappa^4\text{-Tptm}]\text{ZnO}^{13}\text{CO}_2\text{H}$

A degassed solution of $[\kappa^4\text{-Tptm}]\text{ZnOSiMe}_3$ (103 mg, 0.21 mmol) in benzene (ca. 2.0 mL) was treated with $^{13}\text{CO}_2$ (1 atm). H_2O (30 mg, 1.67 mmol) was added and the sample was shaken. The sample was allowed to stand at room temperature for 1 hour, over which period colorless crystals of $[\kappa^4\text{-Tptm}]\text{ZnO}^{13}\text{CO}_2\text{H}\cdot(\text{C}_6\text{H}_6)$ were deposited. The mixture was filtered and the precipitate was dried *in vacuo* giving $[\kappa^4\text{-Tptm}]\text{ZnO}^{13}\text{CO}_2\text{H}\cdot(\text{C}_6\text{H}_6)$ (75 mg, 66%) as an off-white powder. IR Data (KBr disk, cm^{-1}): 3085 (w), 3014 (w), 2908 (w), 1591 (s), 1580 (s) [$\nu(\text{CO}_3)$], 1556 (s), 1459 (s), 1417 (s), 1389 (w), 1352 (s) [$\nu_{\text{sym}}(\text{CO}_2)$], 1282 (w), 1132 (s), 1095 (w), 1047 (m), 1007 (m), 808 (w), 757 (s), 724 (m), 697 (m).

$^{13}\text{C}\{^1\text{H}\}$ NMR (Solid state): 165.0, $[(\text{SC}_5\text{H}_4\text{N})_3\text{CZn}^{13}\text{CO}_2\text{H}]$.

2.9.11 Synthesis of $[\kappa^4\text{-Tptm}]\text{ZnO}^{13}\text{CO}_2\text{D}$

A degassed solution of $[\kappa^4\text{-Tptm}]\text{ZnOSiMe}_3$ (103 mg, 0.21 mmol) in benzene (ca. 2 mL) was treated with $^{13}\text{CO}_2$ (1 atm). D_2O (20 mg, 1.00 mmol) was added and the sample was shaken. The mixture was allowed to stand at room temperature for 1 hour, during which period colorless crystals of $[\kappa^4\text{-Tptm}]\text{ZnO}^{13}\text{CO}_2\text{D}\cdot(\text{C}_6\text{H}_6)$ were deposited. The mixture was filtered, and the precipitate was dried *in vacuo* giving $[\kappa^4\text{-Tptm}]\text{ZnO}^{13}\text{CO}_2\text{D}\cdot(\text{C}_6\text{H}_6)$ (29 mg, 25%) as an off-white powder. IR Data (KBr disk, cm^{-1}): 3085 (w), 3014 (w), 2362 (w), 2339 (w), 1590 (s) [$\nu(\text{CO}_3)$] (overlapping), 1556 (s), 1479

(w), 1458 (s), 1417 (s), 1370 (m), 1355 (s) [$\nu_{\text{asym}}(\text{CO}_2)$], 1282 (m), 1252 (m), 1131 (s), 1094 (w), 1066 (w), 1047 (m), 1007 (m), 809 (w), 758 (s), 724 (m), 693 (m), 642 (w).

2.9.12 Synthesis of [Tptm]Zn(μ -CO₃)Zn[Tptm]

(a) A solution of [κ^4 -Tptm]ZnOSiMe₃ (18 mg, 0.04 mmol) in benzene (*ca.* 1 mL) was treated with H₂O (10 mg, 0.56 mmol). The sample was exposed to air for 14 hours, during which period colorless crystals were deposited. The crystals were isolated, washed with benzene (3 × 1 mL) and dried *in vacuo* to give [κ^3 -Tptm]Zn(μ - κ^2, κ^1 -OCO₂)Zn[κ^4 -Tptm]·(C₆H₆) (12 mg, 70 %). IR Data (KBr disk, cm⁻¹): 3055 (w), 2384(w), 2293 (w), 2221 (w), 1589 (s), 1554 (s), 1480 (s) [$\nu(\text{CO}_3)$], 1454 (s), 1418 (s), 1407 (s) [$\nu(\text{CO}_3)$], 1278 (m), 1131 (s), 1091 (w), 1044 (m), 1011 (m), 848 (w), 765 (m), 747 (s), 721 (m), 642 (w), 610 (w). Anal. calcd. for [κ^3 -Tptm]Zn(μ - κ^2, κ^1 -OCO₂)Zn[κ^4 -Tptm]·0.9(C₆H₆): C, 48.6%; H, 2.7%; N, 8.6%. Found: C, 48.8%; H, 3.1%; N, 8.9%. Crystals of composition [κ^3 -Tptm]Zn(μ - κ^2, κ^1 -OCO₂)Zn[κ^4 -Tptm]·(THF) were obtained by performing the reaction in THF, whereas [κ^4 -Tptm]Zn(μ - κ^2, κ^2 -OCO₂)Zn[κ^4 -Tptm] was obtained by performing the reaction in toluene. IR data (KBr disk, cm⁻¹): 3043 (w), 3002 (w), 2360(w), 2341 (w), 1585 (s), 1557 (s), 1492 (m) [$\nu(\text{CO}_3)$], 1453 (s), 1417 (s), 1385 (m) [$\nu(\text{CO}_3)$], 1280 (m), 1129 (s), 1090 (w), 1044 (m), 1010 (m), 845 (w), 756 (m), 721 (m), 638 (w), 617 (m), 485 (m). ¹H NMR (CD₂Cl₂): 6.91 [s, 6H, {(SC₅H₄N)₃CZn}₂CO₃], 7.09 [d, ³J_{H-H} = 8 Hz, 6H, {(SC₅H₄N)₃CZn}₂CO₃], 7.53 [t, ³J_{H-H} = 8 Hz, 6H, {(SC₅H₄N)₃CZn}₂CO₃], 8.70 [s, 6H, {(SC₅H₄N)₃CZn}₂CO₃]. See below for ¹³C NMR data.

(b) A solution of {[κ^3 -Tptm]Zn(μ -OH)}₂ (8 mg, 0.01 mmol) in C₆H₆ (*ca.* 2 mL) was frozen, degassed and allowed to warm to room temperature. CO₂ (1 atm) was added and the mixture was shaken, thereby resulting in the formation of a colorless precipitate over a period of 20 minutes. The sample was lyophilized to give [κ^4 -Tptm]Zn(CO₃)Zn[κ^3 -Tptm] (6 mg, 70 %) as a white solid.

(c) A solution of $\{[\kappa^3\text{-Tptm}]\text{Zn}(\mu\text{-OH})\}_2$ (2 mg, 0.002 mmol) in C_6H_6 (ca. 1 mL) was exposed to air for two hours, during which period colorless crystals were deposited. The mother liquor was decanted to give $[\text{Tptm}]\text{Zn}(\mu\text{-CO}_3)\text{Zn}[\text{Tptm}]$ (1 mg, 50%) as colorless crystals that was dried *in vacuo*.

2.9.13 Synthesis of $[\text{Tptm}]\text{Zn}(\mu\text{-}^{13}\text{CO}_3)\text{Zn}[\text{Tptm}]$

A solution of $[\kappa^4\text{-Tptm}]\text{ZnOSiMe}_3$ (52 mg, 0.10 mmol) in benzene (ca. 1.0 mL) was treated with H_2O (30 mg, 1.67 mmol). The sample was shaken, then frozen, and degassed. The sample was allowed to warm to room temperature, at which point the sample was filled with a mixture of $^{13}\text{CO}_2$ (100 mm Hg) and N_2 (660 mm Hg). Colorless crystals of $[\kappa^3\text{-Tptm}]\text{Zn}(\mu\text{-}\kappa^2, \kappa^1\text{-O}^{13}\text{CO}_2)\text{Zn}[\kappa^4\text{-Tptm}]\cdot(\text{C}_6\text{H}_6)$ formed slowly over a period of 5 hours. The mixture was filtered, and the precipitate was dried *in vacuo* giving $[\kappa^3\text{-Tptm}]\text{Zn}(\mu\text{-}\kappa^2, \kappa^1\text{-O}^{13}\text{CO}_2)\text{Zn}[\kappa^4\text{-Tptm}]\cdot(\text{C}_6\text{H}_6)$ (31 mg, 62%) as an off white powder. IR Data (KBr disk, cm^{-1}): 3061 (w), 2949 (w), 1587 (s), 1561 (s), 1557 (s), 1556 (s), 1457 (s) $[\nu(\text{CO}_3)]$ (overlapping), 1419 (s), 1347 (w) $[\nu(\text{CO}_3)]$, 1282 (w), 1248 (w), 1131 (s), 1093 (w), 1044 (m), 1006 (m), 905 (w), 837 (w), 758 (s), 722 (m), 640 (w). ^1H NMR (CD_2Cl_2): 6.91 [s, 6H, $\{(\text{SC}_5\text{H}_4\text{N})_3\text{CZn}\}_2\text{CO}_3$], 7.09 [d, $^3J_{\text{H-H}} = 8$ Hz, 6H, $\{(\text{SC}_5\text{H}_4\text{N})_3\text{CZn}\}_2\text{CO}_3$], 7.53 [t, $^3J_{\text{H-H}} = 7$ Hz, 6H, $\{(\text{SC}_5\text{H}_4\text{N})_3\text{CZn}\}_2\text{CO}_3$], 8.70 [s, 6H, $\{(\text{SC}_5\text{H}_4\text{N})_3\text{CZn}\}_2\text{CO}_3$]. $^{13}\text{C}\{^1\text{H}\}$ NMR (Solid state): 171.6 and 172.1 (two isomers). $^{13}\text{C}\{^1\text{H}\}$ NMR (CD_2Cl_2 , 298 K): 170.5 [s, 1C, $\{(\text{SC}_5\text{H}_4\text{N})_3\text{CZn}\}_2\text{CO}_3$]. $^{13}\text{C}\{^1\text{H}\}$ NMR (CD_2Cl_2 , 228 K): 168.8 and 170.5 [s, 1C, $\{(\text{SC}_5\text{H}_4\text{N})_3\text{CZn}\}_2\text{CO}_3$].

2.9.14 Synthesis of $[\kappa^4\text{-Tptm}]\text{ZnO}_2\text{CH}$ by reduction of $[\kappa^4\text{-Tptm}]\text{ZnOCO}_2\text{H}$ with PhSiH_3

A suspension of $[\kappa^4\text{-Tptm}]\text{ZnOCO}_2\text{H}$ (4 mg, 0.01 mmol) in C_6D_6 (ca. 0.7 mL) was treated with PhSiH_3 (5 mg, 0.05 mmol). The reaction was monitored by ^1H NMR spectroscopy,

thereby demonstrating the formation of $[\kappa^4\text{-Tptm}]\text{ZnO}_2\text{CH}$ over a period of 2 hours at room temperature.

2.9.15 Synthesis of $[\kappa^4\text{-Tptm}]\text{ZnO}_2^{13}\text{CH}$ by reduction of $[\kappa^4\text{-Tptm}]\text{ZnO}^{13}\text{CO}_2\text{H}$ with PhSiH_3

A suspension of $[\kappa^4\text{-Tptm}]\text{ZnO}^{13}\text{CO}_2\text{H}$ (5 mg, 0.01 mmol) in C_6D_6 (ca. 0.7mL) was treated with PhSiH_3 (8 mg, 0.07 mmol). The reaction was monitored by ^1H and ^{13}C NMR spectroscopy, thereby demonstrating the formation of $[\kappa^4\text{-Tptm}]\text{ZnO}_2^{13}\text{CH}$ over a period of 2 hours at room temperature.

2.9.16 Reduction of $[\kappa^4\text{-Tptm}]\text{ZnO}^{13}\text{CO}_2\text{H}$ with PhSiH_3 in the presence of CO_2

A suspension of $[\kappa^4\text{-Tptm}]\text{ZnO}^{13}\text{CO}_2\text{H}$ (3 mg, 0.01 mmol) in C_6D_6 (ca. 0.7mL) was treated with PhSiH_3 (20 mg, 0.18 mmol) in the presence of CO_2 (1 atm). The reaction was monitored by ^1H and ^{13}C NMR spectroscopy, thereby demonstrating the formation of $[\kappa^4\text{-Tptm}]\text{ZnO}_2\text{CH}$ (*i.e.* loss of the ^{13}C label) over a period of 2 hours at room temperature.

2.9.17 Reduction of $[\kappa^4\text{-Tptm}]\text{ZnO}^{13}\text{CO}_2\text{D}$ with PhSiH_3

A suspension of $[\kappa^4\text{-Tptm}]\text{ZnO}^{13}\text{CO}_2\text{D}$ (3 mg, 0.01 mmol) in C_6D_6 (ca. 0.7mL) was treated with PhSiH_3 (20 mg, 0.18 mmol). The reaction was monitored by ^1H and ^{13}C NMR spectroscopy, thereby demonstrating the formation of $[\kappa^4\text{-Tptm}]\text{ZnO}_2^{13}\text{CH}$ and HD over a period of 2 hours at room temperature.

2.9.18 H/D Exchange in the reaction of $[\kappa^4\text{-Tptm}]\text{ZnD}$ with PhSiH_3

A suspension of $[\kappa^3\text{-Tptm}]\text{ZnD}$ (4 mg, 0.01 mmol) in C_6D_6 (ca. 0.7mL) was treated with PhSiH_3 (5 mg, 0.05 mmol). The reaction was monitored by ^1H NMR spectroscopy,

thereby demonstrating the formation of $[\kappa^4\text{-Tptm}]\text{ZnH}$ over a period of 20 minutes at room temperature.

2.9.19 H/D Exchange in the reaction of $[\kappa^4\text{-Tptm}]\text{ZnH}$ with PhSiD_3

A suspension of $[\kappa^3\text{-Tptm}]\text{ZnH}$ (4 mg, 0.01 mmol) in C_6D_6 (ca. 0.7mL) was treated with PhSiD_3 (5 mg, 0.05 mmol). The reaction was monitored by ^1H NMR spectroscopy, thereby demonstrating the formation of $[\kappa^4\text{-Tptm}]\text{ZnD}$ and PhSiH_3 over a period of 20 minutes at room temperature.

2.9.20 Reaction of $[\kappa^4\text{-Tptm}]\text{ZnO}^{13}\text{CO}_2\text{H}$ with Me_3SiCl : Formation of $[\kappa^4\text{-Tptm}]\text{ZnCl}$

A suspension of $[\kappa^4\text{-Tptm}]\text{ZnO}^{13}\text{CO}_2\text{H}$ (5 mg, 0.01 mmol) in C_6D_6 (ca. 0.7mL) was treated with Me_3SiCl (5 μL , 0.04 mmol). The reaction was monitored by ^1H and ^{13}C NMR spectroscopy, thereby demonstrating the formation of $[\kappa^4\text{-Tptm}]\text{ZnCl}$, Me_3SiOH and $^{13}\text{CO}_2$ over a period of 1 hour at room temperature.

2.9.21 Reaction of $[\text{Tptm}]\text{Zn}(\mu\text{-CO}_3)\text{Zn}[\text{Tptm}]$ with PhSiH_3 : Formation of $[\kappa^3\text{-Tptm}]\text{ZnH}$ and $[\kappa^4\text{-Tptm}]\text{ZnO}_2\text{CH}$

A suspension of $[\kappa^3\text{-Tptm}]\text{Zn}(\mu\text{-}\kappa^2,\kappa^1\text{-OCO}_2)\text{Zn}[\kappa^4\text{-Tptm}]$ (4 mg, 0.005 mmol) in C_6D_6 (ca. 0.7mL) was treated with PhSiH_3 (15 mg, 0.14 mmol). The reaction was monitored by ^1H NMR spectroscopy, thereby demonstrating the formation of $[\kappa^3\text{-Tptm}]\text{ZnH}$ and $[\kappa^4\text{-Tptm}]\text{ZnO}_2\text{CH}$. It should be noted that $[\kappa^3\text{-Tptm}]\text{ZnH}$ and $[\kappa^4\text{-Tptm}]\text{ZnO}_2\text{CH}$ undergo exchange with each other on the NMR timescale, which was confirmed in an independent experiment in which a 1:1 mixture of $[\kappa^3\text{-Tptm}]\text{ZnH}$ and $[\kappa^4\text{-Tptm}]\text{ZnO}_2\text{CH}$ in C_6D_6 was examined by ^1H NMR spectroscopy. Specifically, at 228 K, no exchange is observed, and both $[\kappa^3\text{-Tptm}]\text{ZnH}$ and $[\kappa^4\text{-Tptm}]\text{ZnO}_2\text{CH}$ are observed.

**2.9.22 Reaction of [Tptm]Zn(μ -CO₃)Zn[Tptm] with PhSiH₃ in the presence of CO₂:
Formation of [κ^4 -Tptm]ZnO₂CH**

A suspension of [κ^3 -Tptm]Zn(μ - κ^2 , κ^1 -OCO₂)Zn[κ^4 -Tptm] (4 mg, 0.005 mmol) in C₆D₆ (ca. 0.7 mL) was treated with PhSiH₃ (15 mg, 0.14 mmol). The mixture was frozen, degassed, allowed to warm to room temperature, and treated with CO₂ (1 atm). The reaction was monitored by ¹H NMR spectroscopy, thereby demonstrating the formation of [κ^4 -Tptm]ZnO₂CH.

2.9.23 Reaction of [κ^4 -Tptm]ZnO₂¹³CH with CO₂: Exchange of CO₂

A solution of [κ^4 -Tptm]ZnO₂¹³CH (3 mg, 0.01 mmol) in C₆D₆ (ca. 0.7 mL) was frozen, degassed, allowed to warm to room temperature, and treated with CO₂ (1 atm). The sample was monitored by ¹H NMR spectroscopy, thereby demonstrating the formation of [κ^4 -Tptm]ZnO₂CH. After 40 hours, the ratio of [κ^4 -Tptm]ZnO₂CH : [κ^4 -Tptm]ZnO₂¹³CH was *ca.* 1:9.

2.9.24 Synthesis of [κ^4 -Tptm]ZnO₂CH by reduction of [κ^4 -Tptm]ZnOCO₂H with Et₂SiH₂

A suspension of [κ^4 -Tptm]ZnOCO₂H (1 mg, 0.002 mmol) in C₆D₆ (*ca.* 0.7 mL) was treated with Et₂SiH₂ (10 mg, 0.11 mmol). The reaction was monitored by ¹H NMR spectroscopy, thereby demonstrating the formation of [κ^4 -Tptm]ZnO₂CH along with other unidentified products over a period of 2 hours at room temperature.

2.9.25 Absence of H/D Exchange in the reaction of [κ^4 -Tptm]ZnD with Et₂SiH₂

A suspension of [κ^3 -Tptm]ZnD (1 mg, 0.002 mmol) in C₆D₆ (ca. 0.7 mL) was treated with Et₂SiH₂ (7 mg, 0.08 mmol). The reaction was monitored by ¹H NMR spectroscopy, thereby demonstrating that no H/D exchange occurs over a period of 2 hours at room

temperature.

2.9.26 Synthesis of $[\kappa^4\text{-Tptm}]\text{ZnO}_2\text{CD}$ by reduction of $[\kappa^4\text{-Tptm}]\text{ZnOCO}_2\text{H}$ with Et_2SiH_2

A suspension of $[\kappa^4\text{-Tptm}]\text{ZnOCO}_2\text{H}$ (3 mg, 0.01 mmol) and $[\kappa^3\text{-Tptm}]\text{ZnD}$ (3 mg, 0.01 mmol) in C_6D_6 (ca. 0.7 mL) was treated with Et_2SiH_2 (5 mg, 0.06 mmol). The reaction was monitored by ^1H NMR spectroscopy, thereby demonstrating the formation of $[\kappa^4\text{-Tptm}]\text{ZnO}_2\text{CH}$ along with other unidentified products over a period of 2 hours at room temperature. The mixture was lyophilized and the mixture dissolved in C_6H_6 (ca. 0.7 mL) and analyzed by ^2D NMR spectroscopy, thereby showing the presence of $[\kappa^4\text{-Tptm}]\text{ZnO}_2\text{CD}$. A separate experiment where $[\kappa^4\text{-Tptm}]\text{ZnOCO}_2\text{H}$ and $[\kappa^3\text{-Tptm}]\text{ZnH}$ are mixed in C_6D_6 showed no formation of $[\kappa^4\text{-Tptm}]\text{ZnO}_2\text{CH}$.

2.10 Crystallographic data

Table 6. Crystal, intensity collection and refinement data.

	$[\kappa^4\text{-Tp}^{\text{tm}}]\text{ZnOCO}_2\text{H}\cdot(\text{C}_6\text{H}_6)$	$[\text{Tp}^{\text{Bu}^{\text{t}},\text{Me}}]\text{ZnOCO}_2\text{H}\cdot(\text{C}_6\text{H}_6)$
lattice	Monoclinic	Monoclinic
formula	$\text{C}_{23}\text{H}_{19}\text{N}_3\text{O}_3\text{S}_3\text{Zn}$	$\text{C}_{31}\text{H}_{47}\text{BN}_6\text{O}_3\text{Zn}$
formula weight	546.96	627.93
space group	$P2_1/n$	$P2_1/n$
$a/\text{\AA}$	8.9280(7)	10.750(4)
$b/\text{\AA}$	14.6268(12)	19.725(7)
$c/\text{\AA}$	18.4948(15)	15.634(5)
$\alpha/^\circ$	90	90
$\beta/^\circ$	103.8610(10)	91.283(6)
$\gamma/^\circ$	90	90
$V/\text{\AA}^3$	2344.9(3)	3314(2)
Z	4	4
temperature (K)	150(2)	150(2)
radiation (λ , \AA)	0.71073	0.71073
ρ (calcd.), g cm^{-3}	1.549	1.258
μ (Mo $\text{K}\alpha$), mm^{-1}	1.346	0.781
θ max, deg.	30.51	24.41
no. of data collected	37376	33541
no. of data used	7148	5450
no. of parameters	302	397
$R_1 [I > 2\sigma(I)]$	0.0412	0.0490
$wR_2 [I > 2\sigma(I)]$	0.0799	0.0867
R_1 [all data]	0.0778	0.1079
wR_2 [all data]	0.0924	0.1067
GOF	1.011	1.012

Table 6 (cont). Crystal, intensity collection and refinement data.

	$[\kappa^3\text{-Tptm}]\text{Zn}(\mu\text{-}\kappa^2,\kappa^1\text{-}\text{OCO}_2)\text{Zn}[\kappa^4\text{-Tptm}]\cdot(\text{C}_6\text{H}_6)$	$[\kappa^3\text{-Tptm}]\text{Zn}(\mu\text{-}\kappa^2,\kappa^1\text{-}\text{OCO}_2)\text{Zn}[\kappa^4\text{-Tptm}]\cdot(\text{THF})$
lattice	Monoclinic	Monoclinic
formula	$\text{C}_{39}\text{H}_{30}\text{N}_6\text{O}_3\text{S}_6\text{Zn}_2$	$\text{C}_{35}\text{H}_{28}\text{N}_6\text{O}_{3.5}\text{S}_6\text{Zn}_2$
formula weight	953.79	911.73
space group	$P2_1/c$	$C2/c$
$a/\text{\AA}$	22.3176(17)	31.669(6)
$b/\text{\AA}$	10.4067(8)	8.7545(18)
$c/\text{\AA}$	17.2733(14)	28.505(6)
$\alpha/^\circ$	90	90
$\beta/^\circ$	99.2290(10)	108.802(3)
$\gamma/^\circ$	90	90
$V/\text{\AA}^3$	3959.8(5)	7481(3)
Z	4	8
temperature (K)	125(2)	150(2)
radiation (λ , \AA)	0.71073	0.71073
ρ (calcd.), g cm^{-3}	1.600	1.619
μ (Mo $K\alpha$), mm^{-1}	1.575	1.664
θ max, deg.	30.58	31.36
no. of data collected	60665	61941
no. of data used	12104	12294
no. of parameters	505	472
$R_1 [I > 2\sigma(I)]$	0.0659	0.0451
$wR_2 [I > 2\sigma(I)]$	0.1536	0.1053
R_1 [all data]	0.1231	0.0855
wR_2 [all data]	0.1801	0.1219
GOF	1.128	1.021

Table 6 (cont). Crystal, intensity collection and refinement data.

	$[\kappa^4\text{-Tptm}]\text{Zn}(\mu\text{-}\kappa^2,\kappa^2\text{-}\text{OCO}_2)\text{Zn}[\kappa^4\text{-Tptm}]$	$\{[\kappa^3\text{-Tptm}]\text{Zn}(\mu\text{-}\text{OH})\}_2\cdot(\text{Toluene})$
lattice	Monoclinic	Triclinic
formula	$\text{C}_{33}\text{H}_{24}\text{N}_6\text{O}_3\text{S}_6\text{Zn}_2$	$\text{C}_{40.75}\text{H}_{36}\text{N}_6\text{O}_2\text{S}_6\text{Zn}_2$
formula weight	875.68	964.86
space group	$P2_1/n$	$P-1$
$a/\text{\AA}$	8.8656(9)	12.632(3)
$b/\text{\AA}$	28.048(3)	15.474(3)
$c/\text{\AA}$	14.4431(15)	22.903(5)
$\alpha/^\circ$	90	93.590(3)
$\beta/^\circ$	102.816(2)	96.263(3)
$\gamma/^\circ$	90	107.390(3)
$V/\text{\AA}^3$	3501.9(6)	4225.4(14)
Z	4	4
temperature (K)	150(2)	150(2)
radiation (λ , \AA)	0.71073	0.71073
ρ (calcd.), g cm^{-3}	1.661	1.517
μ (Mo $K\alpha$), mm^{-1}	1.773	1.475
θ max, deg.	28.28	30.62
no. of data collected	48636	67413
no. of data used	8686	25729
no. of parameters	451	1066
$R_1 [I > 2\sigma(I)]$	0.0559	0.0631
$wR_2 [I > 2\sigma(I)]$	0.0879	0.1477
R_1 [all data]	0.1413	0.1762
wR_2 [all data]	0.1129	0.1867
GOF	1.002	1.039

Table 6 (cont). Crystal, intensity collection and refinement data.

{[κ³-Tptm]Zn(μ-OH)}₂·(C₆H₆)	
lattice	Triclinic
formula	C _{40.75} H ₃₆ N ₆ O ₂ S ₆ Zn ₂
formula weight	1005.90
space group	<i>P</i> -1
<i>a</i> /Å	12.575(2)
<i>b</i> /Å	13.205(3)
<i>c</i> /Å	14.031(3)
α/°	112.044(3)
β/°	95.622(3)
γ/°	104.585(3)
<i>V</i> /Å ³	2041.4(7)
<i>Z</i>	2
temperature (K)	150(2)
radiation (λ, Å)	0.71073
ρ (calcd.), g cm ⁻³	1.636
μ (Mo Kα), mm ⁻¹	1.531
θ max, deg.	30.74
no. of data collected	12639
no. of data used	12639
no. of parameters	439
<i>R</i> ₁ [<i>I</i> > 2σ(<i>I</i>)]	0.0548
<i>wR</i> ₂ [<i>I</i> > 2σ(<i>I</i>)]	0.0878
<i>R</i> ₁ [all data]	0.1127
<i>wR</i> ₂ [all data]	0.0957
GOF	1.026

2.11 References and notes

- (1) (a) Lindskog, S. *Pharmacol. Ther.* **1997**, 74, 1-20.
(b) Kumar, V.; Kannan, K. K. *Indian J. Biochem. Biophys.* **1994**, 31, 377-386.
(c) Silverman, D. N. *Can. J. Bot.* **1991**, 69, 1070-1078.
(d) Christianson, D. W.; Fierke, C. A. *Acc. Chem. Res.* **1996**, 29, 331-339.
(e) Liljas, A.; Håkansson, K.; Jonsson, B. H.; Xue, Y. *Eur. J. Biochem.* **1994**, 219, 1-10.
(f) Christianson, D. W.; Cox, J. D. *Annu. Rev. Biochem.* **1999**, 68, 33-57.
(g) Lindskog, S. *Met. Ions Biol.* **1983**, 5, 77-121.
(h) Tripp, B. C.; Smith, K.; Ferry, J. G. *J. Biol. Chem.* **2001**, 276, 48615-48618.
(i) Khalifah, R. G. *Biophys. Chem.* **2003**, 100, 159-170.
- (2) (a) Meldrum, N. M.; Roughton, F. J. *Nature (London)* **1933**, 80, 113-142.
(b) Keilin, D.; Mann, T. *Biochem J.* **1940**, 34, 1163-1176.
- (3) (a) Vaughan-Jones, R. D.; Spitzer, K. W. *Biochem. Cell Biol.* **2002**, 80, 579-596.
(b) Vaughan-Jones, R. D.; Spitzer, K. W.; Swietach, P. *J. Mol. Cell. Cardiol.* **2009**, 46, 318-331.
- (4) (a) Kumar, V.; Kannan, K. K. *J. Mol. Biol.* **1994**, 241, 226-232.
(b) Huang, S.; Sjöblom, B.; Sauer-Eriksson, A. E.; Jonsson, B. H. *Biochemistry* **2002**, 41, 7628-7635.

- (c) Xue, Y.; Vidgren, J.; Svensson, L. A.; Liljas, A.; Jonsson, B.-H.; Lindskog, S. *Proteins* **1993**, *15*, 80-87.
- (d) Xue, Y. F.; Liljas, A.; Jonsson, B. H.; Lindskog, S. *Proteins* **1993**, *17*, 93-106.
- (e) Iverson, T. M.; Alber, B. E.; Kisker, C.; Ferry, J. G.; Rees, D. C. *Biochemistry* **2000**, *39*, 9222-9231.
- (5) (a) Merz, K. M., Jr.; Banci, L. *J. Am. Chem. Soc.* **1997**, *119*, 863-871.
- (b) Hartmann, M.; Merz, K. M.; van Eldik, R.; Clark, T. *J. Mol. Model.* **1998**, *4*, 355-365.
- (c) Miscione, G. P.; Stenta, M.; Spinelli, D.; Anders, E.; Bottoni, A. *Theor. Chem. Acc.* **2007**, *118*, 193-201.
- (d) Amata, O.; Marino, T.; Russo, N.; Toscano, M. *Phys. Chem. Chem. Phys.* **2011**, *13*, 3468-3477.
- (e) Bottoni, A.; Lanza, C. Z.; Miscione, G. P.; Spinelli, D. *J. Am. Chem. Soc.* **2004**, *126*, 1542-1550.
- (f) Tautermann, C. S.; Loferer, M. J.; Voegele, A. F.; Liedl, K. R. *J. Phys. Chem. B* **2003**, *107*, 12013-12020.
- (g) Bräuer, M.; Pérez-Lustres, J. L.; Weston, J.; Anders, E. *Inorg. Chem.* **2002**, *41*, 1454-1463.
- (6) (a) Parkin, G. *Chem. Rev.* **2004**, *104*, 699-767.
- (b) Parkin, G. *Chem. Commun.* **2000**, 1971-1985.

- (c) Parkin, G. *Met. Ions Biol. Syst.*, Vol. 38, Chapter 14, pp 411-460; A. Sigel and H. Sigel, eds., M. Dekker, New York, 2001.
- (d) Vahrenkamp, H. *Acc. Chem. Res.* **1999**, 32, 589-596.
- (e) Vahrenkamp, H. *Dalton Trans.* **2007**, 4751-4759.
- (7) (a) Parkin, G. *Chem. Rev.* **2004**, 104, 699-767.
- (b) Parkin, G. *Chem. Commun.* **2000**, 1971-1985.
- (c) Parkin, G. *Met. Ions Biol. Syst.*, Vol. 38, Chapter 14, pp 411-460; A. Sigel and H. Sigel, eds., M. Dekker, New York, 2001.
- (d) Parkin, G. *Adv. Inorg. Chem.* **1995**, 42, 291-393.
- (8) (a) Vahrenkamp, H. *Dalton Trans.* **2007**, 4751-4759.
- (b) Vahrenkamp, H. *Acc. Chem. Res.* **1999**, 32, 589-596.
- (9) Kimura, E.; Koike, T.; Shionoya, M. *Structure and Bonding* **1997**, 89, 1-28.
- (10) Acharya, A. N.; Das, A.; Dash, A. C. *Adv. Inorg. Chem.* **2004**, 55, 127-199.
- (11) Kitajima, N.; Tolman, W. B. *Prog. Inorg. Chem.* **1995**, 43, 419-531.
- (12) (a) Ichikawa, K.; Nakata, K.; Ibrahim, M. M.; Kawabata, S. *Stud. Surf. Sci. Catal. (Advances in Chemical Conversions For Mitigating Carbon Dioxide)* **1998**, 114, 309-314.
- (b) Echizen, T.; Ibrahim, M. M.; Nakata, K.; Izumi, M.; Ichikawa, K.; Shiro, M. *J. Inorg. Biochem.* **2004**, 98, 1347-1360.

- (13) (a) Alsfasser, R.; Trofimenko, S.; Looney, A.; Parkin, G.; Vahrenkamp, H. *Inorg. Chem.* **1991**, *30*, 4098-4100.
- (b) Alsfasser, R.; Ruf, M.; Trofimenko, S.; Vahrenkamp, H. *Chem. Ber. Recl.* **1993**, *126*, 703-710.
- (c) Looney, A.; Han, R.; McNeill, K.; Parkin, G. *J. Am. Chem. Soc.* **1993**, *115*, 4690-4697.
- (d) Kitajima, N.; Hikichi, S.; Tanaka, M.; Moro-oka, Y. *J. Am. Chem. Soc.* **1993**, *115*, 5496-5508.
- (e) Ruf, M.; Vahrenkamp, H. *Inorg. Chem.* **1996**, *35*, 6571-6578.
- (f) Looney, A.; Parkin, G.; Alsfasser, R.; Ruf, M.; Vahrenkamp, H. *Angew. Chem. Int. Edit. Engl.* **1992**, *31*, 92-93.
- (14) For catalytic dehydration of bicarbonate by $\{\text{Tp}^{\text{RR}'}\text{M}\}$ complexes, see:
- (a) Sun, Y.-J.; Zhang, L. Z.; Cheng, P.; Lin, H.-K.; Yan, S.-P.; Liao, D.-Z.; Jiang, Z.-H.; Shen, P.-W. *Biophys. Chem.* **2004**, *109*, 281-293.
- (b) Guo, S. L.; Li, X. J.; Xia, C. G.; Yin, Y. Q. *Acta Chim. Sin.* **1999**, *57*, 289-297.
- (15) Deacon, G. B.; Phillips, R. J. *Coord. Chem. Rev.* **1980**, *33*, 227-250.
- (16) The $\nu_{\text{sym}}\text{CO}_2$ band will shift to lower frequency, while the $\nu_{\text{asym}}\text{CO}_2$ band will shift to higher frequency.
- (17) While no $^2J_{\text{C-H}}$ coupling was observed for $[\text{Tp}^{\text{Bu}^t, \text{Me}}]\text{ZnOCO}_2\text{H}$, $^2J_{\text{C-H}}$ coupling constant of 15 Hz was reported for $[\text{W}(\text{CO})_5\text{O}_2\text{COH}]^-$. See reference 18.
- (18) Darensbourg, D. J.; Jones, M. L. M.; Reibenspies, J. H. *Inorg. Chem.* **1996**, *35*, 4406-4413.

- (19) See, for example: Ghosh, P.; Parkin, G. *J. Chem. Soc., Dalton Trans.* **1998**, 2281-2283.
- (20) Darensbourg, D. J.; Jones, M. L. M.; Reibenspies, J. H. *Inorg. Chem.* **1993**, 32, 4675-4676.
- (21) (a) Nakata, K.; Uddin, M. K.; Ogawa, K.; Ichikawa, K. *Chem. Lett.* **1997**, 991-992.
(b) Ibrahim, M. M.; Amin, M. A.; Ichikawa, K. *J. Mol. Struct.* **2011**, 985, 191-201.
- (22) Yamaguchi, S.; Tokairin, I.; Wakita, Y.; Funahashi, Y.; Jitsukawa, K.; Masuda, H. *Chem. Lett.* **2003**, 32, 406-407.
- (23) Ito, M.; Ebihara, M.; Kawamura, T. *Inorg. Chim. Acta* **1994**, 218, 199-202.
- (24) Johansson, R.; Wendt, O. F. *Organometallics* **2007**, 26, 2426-2430.
- (25) Jazzar, R. F. R.; Bhatia, P. H.; Mahon, M. F.; Whittlesey, M. K. *Organometallics* **2003**, 22, 670-683.
- (26) The bicarbonate compound $[\text{Zn}(\text{tapa})(\text{HCO}_3)]^+$ has also been reported but ^1H and ^{13}C NMR data were not listed. See: Yamaguchi, S.; Takahashi, T.; Wada, A.; Funahashi, Y.; Ozawa, T.; Jitsukawa, K.; Masuda, H. *Chem. Lett.* **2007**, 36, 842-843.
- (27) Erras-Hanauer, H.; Mao, Z.-W.; Liehr, G.; Clark, T.; van Eldik, R. *Eur. J. Inorg. Chem.* **2003**, 1562-1569.
- (28) The reason for the difference in the temperature is due to each NMR spectrometer having different temperature calibrations.
- (29) 1 entropy unit (e.u.) is equal to $\text{cal mol}^{-1} \text{K}^{-1}$.

- (30) Watson, L. A.; Eisenstein, O. *J. Chem. Educ.* **2002**, *79*, 1269-1277.
- (31) For an example of a zinc compound that features a bridging bicarbonate ligand, see: Meyer, F.; Rutsch, P. *Chem. Commun.* **1998**, 1037-1038.
- (32) The oxygen atoms that are not coordinated to zinc participate in centrosymmetric hydrogen bonding interactions with a second molecule of [Tp^{But,Me}]ZnOCO₂H, [$d(\text{O}\cdots\text{O}) = 2.678(4) \text{ \AA}$]. This type of interaction is observed for many metal bicarbonate complexes.
- (33) Cambridge Structural Database (Version 5.32). *3D Search and Research Using the Cambridge Structural Database*, Allen, F. H.; Kennard, O. *Chemical Design Automation News* **1993**, *8* (1), pp 1 & 31-37.
- (34) For selected examples of other structurally characterized bicarbonate compounds, see:
- (a) Huang, D.; Makhlynets, O. V.; Tan, L. L.; Lee, S. C.; Rybak-Akimova, E. V.; Holm, R. H. *Inorg. Chem.* **2011**, *50*, 10070-10081.
- (b) Darensbourg, D. J.; Jones, M. L. M.; Reibenspies, J. H. *Inorg. Chem.* **1996**, *35*, 4406-4413.
- (d) Huang, D.; Holm, R. H. *J. Am. Chem. Soc.* **2010**, *132*, 4693-4701.
- (e) McClintock, L. F.; Cavigliasso, G.; Stranger, R.; Blackman, A. G. *Dalton Trans.* **2008**, 4984-4992.
- (f) Yoshida, T.; Thorn, D. L.; Okano, T.; Ibers, J. A.; Otsuka, S. *J. Am. Chem. Soc.* **1979**, *101*, 4212-4221.
- (35) For an interesting pair of isomeric bidentate and unidentate bicarbonate complexes, see: Mao, Z. W.; Liehr, G.; van Eldik, R. *J. Am. Chem. Soc.* **2000**, *122*, 4839-4840.

- (36) Baxter, K. E.; Hanton, L. R.; Simpson, J.; Vincent, B. R.; Blackman, A. G. *Inorg. Chem.* **1995**, *34*, 2795-2796.
- (37) Ito, M.; Ebihara, M.; Kawamura, T. *Inorg. Chim. Acta* **1994**, *218*, 199-202.
- (38) The oxygen atoms of the bicarbonate ligand within the carbonic anhydrase that are not involved in the primary Zn–O interactions participate in hydrogen bonding interactions, akin to that of $[\text{Tp}^{\text{Bu}^\dagger, \text{Me}}]\text{ZnOCO}_2\text{H}$, with either other protein residues or water (reference 4).
- (39) Sattler, W.; Parkin, G. *J. Am. Chem. Soc.* **2011**, *133*, 9708–9711.
- (40) These Zn•••O interactions are described as “secondary” on the basis that the Zn•••O distances are less than the value of 3.65 Å, *i.e.* the sum of the crystallographic van der Waals radii of Zn (2.1 Å) and O (1.55 Å) is 3.65 Å.^a The use of the label “secondary” is not intended to imply that the interactions are significant.^b
- (a) Batsanov, S. S. *Inorg. Mater.* **2001**, *37*, 871-885.
- (b) Schiemenz, G. P. *Z.Naturforsch.(B)* **2007**, *62*, 235-243.
- (41) (a) Weinhold, F.; Landis, C. *Valency and Bonding*, Cambridge University Press, New York, **2005**; pp. 275-306.
- (b) Ramsden, C. A. *Chem. Soc. Rev.* **1994**, *23*, 111-118.
- (42) For example, the highest energy ν_{CO} IR absorption of bicarbonate compounds span a range of at least 1513 – 1700 cm^{-1} ,^{a,b} with compounds having values ≥ 1605 cm^{-1} possessing unidentate ligands.^{c,d}
- (a) Cook, D. F.; Curtis, N. F.; Gladkikh, O. P.; Weatherburn, D. C. *Inorg. Chim. Acta* **2003**, *355*, 15-24.

- (b) Ganguly, S.; Mague, J. T.; Roundhill, D. M. *Inorg. Chem.* **1992**, *31*, 3831-3835.
- (c) Kim, J. C.; Cho, J.; Kim, H.; Lough, A. J. *Chem. Commun.* **2004**, 1796-1797.
- (d) Jazzar, R. F. R.; Bhatia, P. H.; Mahon, M. F.; Whittlesey, M. K. *Organometallics* **2003**, *22*, 670-683.
- (43) (a) Hienerwadel, R.; Berthomieu, C. *Biochemistry* **1995**, *34*, 16288-16297.
- (b) Bernitt, D. L.; Hartman, K. O.; Hisatsune, I.C. *J. Chem. Phys.* **1965**, *42*, 3553-3558.
- (c) Quinn, R.; Appleby, J. B.; Pez, G. P. *J. Am. Chem. Soc.* **1995**, *117*, 329-335.
- (d) Hage, W.; Hallbrucker, A.; Mayer, E. *J. Chem. Soc. Faraday Trans.* **1996**, *92*, 3183-3195.
- (e) Hage, W.; Hallbrucker, A.; Mayer, E. *J. Chem. Soc. Faraday Trans.* **1996**, *92*, 3197-3209.
- (f) Berthomieu, C.; Hienerwadel, R. *Photosynth. Res.* **2009**, *101*, 157-170.
- (g) Loerting, T.; Bernard, J. *ChemPhysChem* **2010**, *11*, 2305-2309.
- (h) Bernard, J.; Seidl, M.; Kohl, I.; Liedl, K. R.; Mayer, E.; Gálvez, O.; Grothe, H.; Loerting, T. *Angew. Chem. Int. Edit.* **2011**, *50*, 1939-1943.
- (44) In view of the facile conversion of $[\kappa^4\text{-Tptm}]\text{ZnOCO}_2\text{H}$ to $[\text{Tptm}]\text{Zn}(\mu\text{-CO}_3)\text{Zn}[\text{Tptm}]$ in solution, the successful isolation of the bicarbonate complex from the reaction with CO_2 in the presence of water may be attributed to its low solubility in benzene, such that the bicarbonate complex precipitates during the course of its synthesis.

- (45) For other examples of zinc carbonate formation by fixation of atmospheric CO₂, see:
- (a) Kitajima, N.; Hikichi, S.; Tanaka, M.; Moro-oka, Y. *J. Am. Chem. Soc.* **1993**, *115*, 5496-5508.
 - (b) Bazzicalupi, C.; Bencini, A.; Bianchi, A.; Corana, F.; Fusi, V.; Giorgi, C.; Paoli, P.; Paoletti, P.; Valtancoli, B.; Zanchini, C. *Inorg. Chem.* **1996**, *35*, 5540-5548.
 - (c) Calvo, J. A. M.; Vahrenkamp, H. *Z. Anorg. Allg. Chem.* **2006**, *632*, 1776-1780.
 - (d) Kong, L. Y.; Zhang, Z. H.; Zhu, H. F.; Kawaguchi, H.; Okamura, T.; Doi, M.; Chu, Q.; Sun, W. Y.; Ueyama, N. *Angew. Chem. Int. Edit.* **2005**, *44*, 4352-4355.
 - (e) Qi, Z.-P.; Li, S.-A.; Huang, Y.-Q.; Xu, G.-C.; Liu, G.-X.; Kong, L.-Y.; Sun, W.-Y. *Inorg. Chem. Commun.* **2008**, *11*, 929-934.
 - (f) Murthy, N. N.; Karlin, K. D. *Chem. Commun.* **1993**, 1236-1238.
 - (g) Bauer-Siebenlist, B.; Meyer, F.; Vidovic, D.; Pritzkow, H. *Z. Anorg. Allg. Chem.* **2003**, *629*, 2152-2156.
 - (h) Doring, M.; Ciesielski, M.; Walter, O.; Gorls, H. *Eur. J. Inorg. Chem.* **2002**, 1615-1621.
- (46) For other examples of structurally characterized zinc carbonate complexes, see reference 45 and:
- (a) Han, R.; Looney, A.; McNeill, K.; Parkin, G.; Rheingold, A. L.; Haggerty, B. S. *J. Inorg. Biochem.* **1993**, *49*, 105-121.
 - (b) Mao, Z.-W.; Heinemann, F. W.; Liehr, G.; van Eldik, R. *J. Chem. Soc. Dalton Trans.* **2001**, 3652-3662.

- (c) Acharya, A. N.; Das, A.; Dash, A. C. *Adv. Inorg. Chem.* **2004**, *55*, 127-199.
- (d) Dussart, Y.; Harding, C.; Dalgaard, P.; McKenzie, C.; Kadirvelraj, R.; McKee, V.; Nelson, J. *J. Chem. Soc., Dalton Trans.* **2002**, 1704-1713.
- (e) Erras-Hanauer, H.; Mao, Z. W.; Liehr, G.; Clark, T.; van Eldik, R. *Eur. J. Inorg. Chem.* **2003**, 1562-1569.
- (f) Fondo, M.; Garcia-Deibe, A. M.; Ocampo, N.; Sanmartin, J.; Bermejo, M. R. *Dalton Trans.* **2004**, 2135-2141.
- (g) Halder, G. J.; Park, H.; Funk, R. J.; Chapman, K. W.; Engerer, L. K.; Geiser, U.; Schlueter, J. A. *Crystal Growth & Design* **2009**, *9*, 3609-3614.
- (h) Harrison, W. T. A.; Phillips, M. L. F.; Nenoff, T. M.; MacLean, E. J.; Teat, S. J.; Maxwell, R. S. *J. Chem. Soc., Dalton Trans.* **2001**, 546-549.
- (i) Kajiwara, T.; Yamaguchi, T.; Kido, H.; Kawabata, S.; Kuroda, R.; Ito, T. *Inorg. Chem.* **1993**, *32*, 4990-4991.
- (j) Mann, K. L. V.; Jeffery, J. C.; McCleverty, J. A.; Ward, M. D. *J. Chem. Soc., Dalton Trans.* **1998**, 3029-3035.
- (k) Mao, Z. W.; Heinemann, F. W.; Liehr, G.; van Eldik, R. *J. Chem. Soc., Dalton Trans.* **2001**, 3652-3662.
- (l) Mao, Z. W.; Liehr, G.; van Eldik, R. *J. Chem. Soc., Dalton Trans.* **2001**, 1593-1600.
- (m) Schrodtr, A.; Neubrand, A.; van Eldik, R. *Inorg. Chem.* **1997**, *36*, 4579-4584.
- (n) Trosch, A.; Vahrenkamp, H. *Inorg. Chem.* **2001**, *40*, 2305-2311.

- (o) Zheng, Y. Q.; Lin, J. L.; Wei, D. Y. *Z. Kristallogr.* **2002**, *217*, 191-192.
- (47) Kumar, V.; Kannan, K. K. *J. Mol. Biol.* **1994**, *241*, 226-232.
- (48) Xue, Y.; Vidgren, J.; Svensson, L. A.; Liljas, A.; Jonsson, B.-H.; Lindskog, S. *Proteins* **1993**, *15*, 80-87.
- (49) (a) Merz, K. M., Jr.; Banci, L. *J. Am. Chem. Soc.* **1997**, *119*, 863-871.
- (b) Hartmann, M.; Merz, K. M.; van Eldik, R.; Clark, T. *J. Mol. Model.* **1998**, *4*, 355-365.
- (50) (a) Miscione, G. P.; Stenta, M.; Spinelli, D.; Anders, E.; Bottoni, A. *Theor. Chem. Acc.* **2007**, *118*, 193-201.
- (b) Amata, O.; Marino, T.; Russo, N.; Toscano, M. *Phys. Chem. Chem. Phys.* **2011**, *13*, 3468-3477.
- (c) Bottoni, A.; Lanza, C. Z.; Miscione, G. P.; Spinelli, D. *J. Am. Chem. Soc.* **2004**, *126*, 1542-1550.
- (e) Tautermann, C. S.; Loferer, M. J.; Voegele, A. F.; Liedl, K. R. *J. Phys. Chem. B* **2003**, *107*, 12013-12020.
- (51) Bräuer, M.; Pérez-Lustres, J. L.; Weston, J.; Anders, E. *Inorg. Chem.* **2002**, *41*, 1454-1463.
- (52) The energy difference is 3.7 kcal mol⁻¹ for the cc-pVTZ(-f) (C, H, N, O, B) and LAV3P (Zn) basis sets.
- (53) CSD deposition code: WAJWUZ.

- (54) Addison, C. C.; Logan, N.; Wallwork, S. C.; Garner, C. D. *Quart. Rev. Chem. Soc.* **1971**, *25*, 289-322.
- (55) Kleywegt, G. J.; Wiesmeijer, W. G. R.; van Driel, G. J.; Driessen, W. L.; Reedijk, J.; Noordik, J. H. *J. Chem. Soc. Dalton Trans.* **1985**, 2177-2184.
- (56) For other reviews of nitrate structures, see:
- (a) Morozov, I. V.; Serezhkin, V. N.; Troyanov, S. I. *Russ. Chem. Bull.* **2008**, *57*, 439-450.
- (b) Morozov, I. V.; Serezhkin, V. N.; Troyanov, S. I. *Russ. Chem. Bull.* **2009**, *58*, 2407-2417.
- (57) (a) Han, R.; Parkin, G. *J. Am. Chem. Soc.* **1991**, *113*, 9707-9708.
- (b) Han, R.; Looney, A.; McNeill, K.; Parkin, G.; Rheingold, A. L.; Haggerty, B. S. *J. Inorg. Biochem.* **1993**, *49*, 105-121.
- (58) Yang, K.-W.; Wang, Y.-Z.; Huang, Z.-X.; Sun, J. *Polyhedron* **1997**, *16*, 109-112.
- (59) Hammes, B. S.; Luo, X.; Carrano, M. W.; Carrano, C. J. *Inorg. Chim. Acta* **2002**, *341*, 33-38.
- (60) Varonka, M. S.; Warren, T. H. *Inorg. Chem.* **2009**, *48*, 5605-5607.
- (61) Alsfasser, R.; Powell, A. K.; Trofimenko, S.; Vahrenkamp, H. *Chem. Ber. Recl.* **1993**, *126*, 685-694.
- (62) Looney, A.; Parkin, G. *Inorg. Chem.* **1994**, *33*, 1234-1237.
- (63) King, W. A.; Yap, G. P. A.; Incarvito, C. D.; Rheingold, A. L.; Theopold, K. H. *Inorg. Chim. Acta* **2009**, *362*, 4493-4499.

- (64) For related structures on nitrate complexes, see:
- (a) Kimblin, C.; Allen, W. E.; Parkin, G. *Main Group Chem.* **1996**, *1*, 297-300.
 - (b) Kimblin, C.; Murphy, V. J.; Hascall, T.; Bridgewater, B. M.; Bonanno, J. B.; Parkin, G. *Inorg. Chem.* **2000**, *39*, 967-974.
 - (c) Cronin, L.; Foxon, S. P.; Lusby, P. J.; Walton, P. H. *J. Biol. Inorg. Chem.* **2001**, *6*, 367-377.
- (65) For other calculations which indicate the flexibility of the nitrate ligand, see: Kumar, P. N. V. P.; Marynick, D. S. *Inorg. Chem.* **1993**, *32*, 1857-1859.
- (66) (a) Peters, M.; Kohler, B.; Kuckshinrichs, W.; Leitner, W.; Markewitz, P.; Muller, T. E. *ChemSusChem* **2011**, *4*, 1216-1240.
- (b) Federsel, C.; Jackstell, R.; Beller, M. *Angew. Chem. Int. Edit.* **2010**, *49*, 6254-6257.
 - (c) Himeda, Y. *Eur. J. Inorg. Chem.* **2007**, 3927-3941.
 - (d) Wang, W.; Wang, S. P.; Ma, X. B.; Gong, J. L. *Chem. Soc. Rev.* **2011**, *40*, 3703-3727.
- (67) (a) Laurenczy, G. *Chimia* **2011**, *65*, 663-666.
- (b) Federsel, C.; Jackstell, R.; Boddien, A.; Laurenczy, G.; Beller, M. *ChemSusChem* **2010**, *3*, 1048-1050.
 - (c) Joó, F.; Laurenczy, G.; Karády, P.; Elek, J.; Nádasdi, L.; Roulet, R. *Appl. Organomet. Chem.* **2000**, *14*, 857-859.
 - (d) Laurenczy, G.; Joó, F.; Nádasdi, L. *Inorg. Chem.* **2000**, *39*, 5083-5088.

- (e) Elek, J.; Nadasdi, L.; Papp, G.; Laurenczy, G.; Joo, F. *Appl. Catal. A-Gen.* **2003**, *255*, 59-67.
- (f) Boddien, A.; Gartner, F.; Federsel, C.; Sponholz, P.; Mellmann, D.; Jackstell, R.; Junge, H.; Beller, M. *Angew. Chem. Int. Edit.* **2011**, *50*, 6411-6414.
- (68) Support for this suggestion is provided by the facts that (i) $\{[\kappa^3\text{-Tptm}]\text{Zn}(\mu\text{-OH})\}_2$ reacts with PhSiH_3 to give $[\kappa^3\text{-Tptm}]\text{ZnH}$ (Scheme 2) and (ii) $[\kappa^4\text{-Tptm}]\text{ZnH}$ reacts with CO_2 to give $[\kappa^4\text{-Tptm}]\text{ZnO}_2\text{CH}$ (reference 39).
- (69) (a) McNally, J. P.; Leong, V. S.; Cooper, N. J. in *Experimental Organometallic Chemistry*, Wayda, A. L.; Darensbourg, M. Y., Eds.; American Chemical Society: Washington, DC, 1987; Chapter 2, pp 6-23.
- (b) Burger, B.J.; Bercaw, J. E. in *Experimental Organometallic Chemistry*; Wayda, A. L.; Darensbourg, M. Y., Eds.; American Chemical Society: Washington, DC, 1987; Chapter 4, pp 79-98.
- (c) Shriver, D. F.; Drezdson, M. A.; *The Manipulation of Air-Sensitive Compounds*, 2nd Edition; Wiley-Interscience: New York, 1986.
- (70) Gottlieb, H. E.; Kotlyar, V.; Nudelman, A. *J. Org. Chem.* **1997**, *62*, 7512-7515.
- (71) Cella, J. A.; Carpenter, J. C. *J. Organomet. Chem.* **1994**, *480*, 23-26.
- (72) Banovetz, J. P.; Suzuki, H.; Waymouth, R. M. *Organometallics* **1993**, *12*, 4700-4703.
- (73) Jaguar 7.5, Schrödinger, LLC, New York, NY 2008.
- (74) (a) Becke, A. D. *J. Chem. Phys.* **1993**, *98*, 5648-5652.
- (b) Becke, A. D. *Phys. Rev. A* **1988**, *38*, 3098-3100.

- (c) Lee, C. T.; Yang, W. T.; Parr, R. G. *Phys. Rev. B* **1988**, *37*, 785-789.
- (d) Vosko, S. H.; Wilk, L.; Nusair, M. *Can. J. Phys.* **1980**, *58*, 1200-1211.
- (e) Slater, J. C. *Quantum Theory of Molecules and Solids, Vol. 4: The Self-Consistent Field for Molecules and Solids*; McGraw-Hill: New York, 1974.
- (75) (a) Hay, P. J.; Wadt, W. R. *J. Chem. Phys.* **1985**, *82*, 270-283.
- (b) Wadt, W. R.; Hay, P. J. *J. Chem. Phys.* **1985**, *82*, 284-298.
- (c) Hay, P. J.; Wadt, W. R. *J. Chem. Phys.* **1985**, *82*, 299-310.
- (76) Dunning, T. H. *J. Chem. Phys.* **1989**, *90*, 1007-1023.
- (77) (a) Sheldrick, G. M. *SHELXTL, An Integrated System for Solving, Refining and Displaying Crystal Structures from Diffraction Data*; University of Göttingen, Göttingen, Federal Republic of Germany, 1981.
- (b) Sheldrick, G. M. *Acta Cryst.* **2008**, *A64*, 112-122.
- (78) All carbon atoms of $[\text{Tp}^{\text{Bu}^t, \text{Me}}]\text{ZnOH}$ and $[\text{Tp}^{\text{Bu}^t, \text{Me}}]\text{ZnOCO}_2\text{H}$, including quaternary carbons and the bicarbonate carbon, integrate correctly using this inverse-gated mode procedure.
- (79) This value assumes that the bicarbonate is a monomer in solution. Alternatively, if the bicarbonate complex were to exist as a hydrogen bonded dimer, the equilibrium constant would be $1.4 \times 10^4 \text{ M}^{-1.5}$.
- (80) Alsfasser, R.; Trofimenko, S.; Looney, A.; Parkin, G.; Vahrenkamp, H. *Inorg. Chem.* **1991**, *30*, 4098-4100.

CHAPTER 3

Zinc Catalysts for On Demand Hydrogen Generation and the Hydrosilylation of Aldehydes, Ketones and CO₂

Table of Contents

3.1	Introduction	189
3.2	Zinc catalyzed H ₂ production	192
3.2.1	[κ ³ -Tptm]ZnH catalyzed hydrolysis of PhSiH ₃ for H ₂ production	192
3.2.2	[κ ³ -Tptm]ZnH catalyzed alcoholysis of PhSiH ₃ for H ₂ production	198
3.3	[κ ³ -Tptm]ZnH catalyzed hydrosilylation of aldehydes and ketones with PhSiH ₃	205
3.4	[κ ³ -Tptm]ZnH catalyzed hydrosilylation of CO ₂ with (EtO) ₃ SiH	212
3.5	Synthesis of κ ³ enforced compounds: [Bptm*]H	218
3.6	Summary and conclusions	224
3.7	Experimental details	225
3.7.1	General considerations	225
3.7.2	Computational details	226
3.7.3	X-ray structure determinations	226
3.7.4	[κ ³ -Tptm]ZnH catalyzed hydrolysis of PhSiH ₃	226
3.7.5	[κ ⁴ -Tptm]ZnOSiMe ₃ as a precatalyst for the hydrolysis of PhSiH ₃	227
3.7.6	{[κ ³ -Tptm]Zn(μ-OH)} ₂ catalyzed hydrolysis of PhSiH ₃	228
3.7.7	Reaction of {[κ ³ -Tptm]Zn(μ-OH)} ₂ with PhSiH ₃ to give [κ ³ -Tptm]ZnH	228
3.7.8	[κ ³ -Tptm]ZnH catalyzed methanolysis of PhSiH ₃ to give PhSi(OMe) ₃	228
3.7.9	[κ ⁴ -Tptm]ZnOSiMe ₃ as a precatalyst for the methanolysis of PhSiH ₃ to give PhSi(OMe) ₃	229
3.7.10	[κ ⁴ -Tptm]ZnOSiMe ₃ as a precatalyst for the stepwise methanolysis of PhSiH ₃	230

- 3.7.11 $[\kappa^4\text{-Tptm}]\text{ZnOSiMe}_3$ as a precatalyst for the methanolysis of PhSiH_3 to give $\text{PhSi}(\text{OMe})_3$ at 0 °C 230
- 3.7.12 $[\kappa^4\text{-Tptm}]\text{ZnOSiMe}_3$ as a precatalyst for the methanolysis of PhSiH_3 to give $\text{PhSiH}(\text{OMe})_2$ 230
- 3.7.13 $[\kappa^3\text{-Tptm}]\text{ZnH}$ catalyzed methanolysis of PhMeSiH_2 to give $\text{PhMeSiH}(\text{OMe})_2$ 231
- 3.7.14 $[\kappa^3\text{-Tptm}]\text{ZnH}$ catalyzed methanolysis of PhMeSiH_2 to give $\text{PhMeSi}(\text{OMe})_2$ 231
- 3.7.15 $[\kappa^3\text{-Tptm}]\text{ZnH}$ catalyzed alcoholysis of PhSiH_3 with EtOH to give $\text{PhSi}(\text{OEt})_3$ 232
- 3.7.16 $[\kappa^3\text{-Tptm}]\text{ZnH}$ catalyzed alcoholysis of PhSiH_3 with Pr^iOH to give $\text{PhSi}(\text{OPr}^i)_3$ 232
- 3.7.17 $[\kappa^3\text{-Tptm}]\text{ZnH}$ catalyzed alcoholysis of PhSiH_3 with PhCH_2OH to give $\text{PhSi}(\text{OCH}_2\text{Ph})_3$ 233
- 3.7.18 $[\kappa^3\text{-Tptm}]\text{ZnH}$ catalyzed alcoholysis of PhSiH_3 with racemic 1-phenylethanol to give $\text{PhSi}[\text{OCH}(\text{Me})\text{Ph}]_3$ 233
- 3.7.19 $[\kappa^3\text{-Tptm}]\text{ZnH}$ catalyzed alcoholysis of PhSiH_3 with (*R*)-(+)-1-phenylethanol to give *RRR*- $\text{PhSi}[\text{OCH}(\text{Me})\text{Ph}]_3$ 235
- 3.7.20 $[\kappa^3\text{-Tptm}]\text{ZnH}$ catalyzed hydrosilylation of MeCHO with PhSiH_3 to give $\text{PhSi}(\text{OEt})_3$ 236
- 3.7.21 $[\kappa^3\text{-Tptm}]\text{ZnH}$ catalyzed hydrosilylation of Me_2CO with PhSiH_3 to give $\text{PhSi}(\text{OPr}^i)_3$ 237
- 3.7.22 $[\kappa^3\text{-Tptm}]\text{ZnH}$ catalyzed hydrosilylation of PhCHO with PhSiH_3 to give $\text{PhSi}(\text{OCH}_2\text{Ph})_3$ 237
- 3.7.23 $[\kappa^3\text{-Tptm}]\text{ZnH}$ catalyzed hydrosilylation of $\text{MeC}(\text{O})\text{Ph}$ with PhSiH_3 to give $\text{PhSi}[\text{OCH}(\text{Me})\text{Ph}]_3$ 237
- 3.7.24 $[\kappa^3\text{-Tptm}]\text{ZnH}$ catalyzed hydrosilylation of CO_2 with $(\text{EtO})_3\text{SiH}$ to give $(\text{EtO})_3\text{SiO}_2\text{CH}$ 238
- 3.7.25 $[\kappa^4\text{-Tptm}]\text{ZnO}_2\text{CH}$ catalyzed hydrosilylation of CO_2 with $(\text{EtO})_3\text{SiH}$ to give $(\text{EtO})_3\text{SiO}_2\text{CH}$ 239

3.7.26	$[\kappa^4\text{-Tptm}]\text{ZnOSiMe}_3$ as a precatalyst for the hydrosilylation of CO_2 with $(\text{EtO})_3\text{SiH}$ to give $(\text{EtO})_3\text{SiO}_2\text{CH}$	239
3.7.27	$[\kappa^4\text{-Tptm}]\text{ZnOSiMe}_3$ as a precatalyst for the hydrosilylation of $^{13}\text{CO}_2$ with $(\text{EtO})_3\text{SiH}$ to give $(\text{EtO})_3\text{SiO}_2^{13}\text{CH}$	240
3.7.28	Reaction of $(\text{EtO})_3\text{SiO}_2\text{CH}$ with HCl (aq) to give ethylformate	241
3.7.29	Reaction of $(\text{EtO})_3\text{SiO}_2\text{CH}$ with HNMe_2 to give dimethylformamide (DMF)	241
3.7.30	Synthesis of $[\text{Bptm}^*]\text{H}$	242
3.7.31	Synthesis of $[\kappa^3\text{-Bptm}^*]\text{ZnN}(\text{SiMe}_3)_2$	243
3.7.32	Synthesis of $[\kappa^3\text{-Bptm}^*]\text{ZnO}_2\text{CH}$	244
3.8	Crystallographic data	246
3.9	References and notes	248

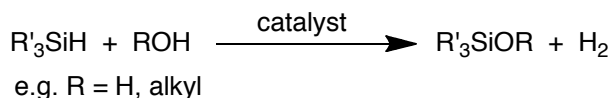
Reproduced in part from:

W. Sattler and G. Parkin, *J. Am. Chem. Soc.* **2011**, *133*, 9708-9711.

3.1 Introduction

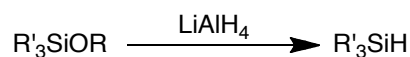
There is currently much effort being directed towards the implementation of a “hydrogen economy”, in which dihydrogen (H₂) serves as a fuel, which when oxidized either by direct combustion or in a fuel cell produces water (H₂O), with no other chemical byproducts.¹ Part of the interest in the implementation of a hydrogen economy is to reduce the production of carbon dioxide (CO₂) that is formed when carbon based fuels are combusted. Additionally, there has been a great research effort aimed to functionalize carbon dioxide, specifically to use it as a C₁ source for the synthesis of useful commodity chemicals.² However, in order to accomplish these objectives in an economical and scalable fashion, new and efficient catalytic processes must be developed that rely on inexpensive and abundant materials.³

One of the greatest challenges associated in implementing a hydrogen economy is the large-scale storage of hydrogen.⁴ For example, the storage of liquid hydrogen has high safety risks. Additionally, the condensation of gaseous hydrogen to liquid hydrogen along with the latter’s cryogenic storage requires considerable energy. Therefore, research has been directed towards compounds with the ability to produce hydrogen *via* a chemical reaction or a physical process.⁵ Compounds that have the capacity to produce hydrogen include ammonia-borane,⁶ organic heterocycles,⁷ formic acid,⁸ and organosilanes.⁹ It should be noted that none of these compounds are ideal, with each having limitations.^{4,10} Organosilanes are, however, an attractive choice (*vide infra*) of the aforementioned options, and as such, will be the focus of this chapter. Firstly, many organosilanes are storable *liquids* that are thermodynamically capable of generating hydrogen by protolytic cleavage of their Si–H bonds with either water or alcohols (Scheme 1).



Scheme 1. Hydrogen generation *via* protolytic cleavage of silanes by water or alcohols.

Secondly, organosilanes can be rich in Si–H groups,¹¹ such that they have high hydrogen storage capabilities in the range 5.0 – 6.9 wt. % upon cleavage with water.¹² Thirdly, organosilanes are readily available since they are already produced on an industrial scale.¹³ Finally, the products of hydrolysis and alcoholysis of organosilanes have commercial value, with applications in materials chemistry and organic synthesis.^{14,15} It should be noted that alkoxy silanes can be regenerated to their respective hydrosilane *via* treatment with suitable hydride reagents (*e.g.* LiAlH₄).¹⁶

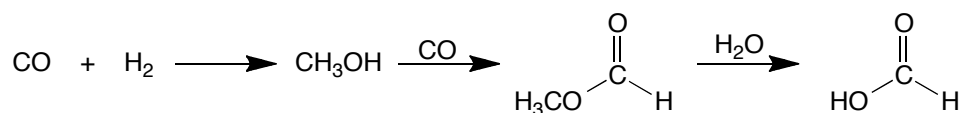


Scheme 2. Regeneration of hydrosilane from alkoxy silane *via* treatment with LiAlH₄.

In order for silanes to provide H₂ at an appreciable rate, catalysts need to be used because the reaction of silanes with water or alcohols do not occur at significant rates, despite the fact that these reactions are thermodynamically favorable. Currently, catalysts for this reaction are not optimal; *i.e.* they are slow, sensitive to air, or expensive. In this vein, both homogeneous^{9a,b,17} and heterogeneous¹⁸ catalysts have already been discovered for the hydrolysis and alcoholysis of silanes. However, the majority of these catalysts rely on precious transition metals such as rhenium, ruthenium, silver and gold; these metals are expensive and are in short supply. For this reason, the development of effective catalysts (*i.e.* high turnover frequencies and high turnover numbers) that are based on more abundant, inexpensive, non-precious metals is desirable.¹⁹

A factor in the desire to switch to a hydrogen economy is to reduce the amount of CO₂ in the atmosphere. CO₂ is a renewable C₁ resource that has been used as a building block for commodity chemicals such as urea²⁰ and salicylic acid.²¹ An

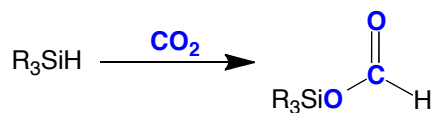
additional example is the metal-catalyzed formation of polycarbonates by copolymerization of CO₂ with epoxides.²² Formic acid is a commodity chemical that could be formed *via* the hydrogenation of CO₂.²³ However, the formation of formic acid using CO₂ is thermodynamically unfavorable under standard conditions unless the reaction is performed in the presence of a base, creating formate instead of formic acid itself in order to drive the equilibrium.²⁴ Therefore, the principal industrial method to synthesize formic acid relies on carbon monoxide (CO) as the carbon source, which involves a multistep sequence as follows: (i) hydrogenation of carbon monoxide to produce methanol, (ii) carbonylation of methanol to produce methyl formate, and finally (iii) hydrolysis of methyl formate to give the desired product, formic acid (Scheme 3).²⁵



Scheme 3. Current industrial synthesis of formic acid.

This process is inefficient and requires multiple steps and additionally, there is no efficient method for recycling the precious metal catalysts that are currently used for formic acid synthesis.²⁶

As an alternative to hydrogenation, the hydrosilylation of CO₂ is thermodynamically favorable and has been used as a method for obtaining silyl-formate derivatives (Scheme 4). The first report of catalytic hydrosilylation of CO₂ appeared in 1981,²⁷ which used RuCl₂(PPh₃)₃ as the catalyst. While many developments have been made since 1981,^{28,29,30,31} the synthesis of formates *via* hydrosilylation has focused almost exclusively on the use of ruthenium catalysts.^{27,32} Therefore, we wished to develop a catalyst that does not use a precious metal.¹⁹



Scheme 4. Hydrosilylation of CO₂.

This chapter will detail the development of zinc compounds using the [Tptm] (Tptm = *tris*(2-pyridylthio)methyl) and [Bptm*] (Bptm* = *bis*(2-pyridylthio)(*p*-tolylthio)methyl) ligands as catalysts for (i) the rapid generation of hydrogen on demand from silanes and alcohols or water, (ii) the hydrosilylation of aldehydes and ketones and, (iii) the hydrosilylation of CO₂.

3.2 Zinc catalyzed H₂ production

3.2.1 [κ³-Tptm]ZnH catalyzed hydrolysis of PhSiH₃ for H₂ production

The [*tris*(2-pyridylthio)methyl]zinc hydride complex, [κ³-Tptm]ZnH (Figure 1), is an effective catalyst for the dehydrocoupling of silanes with alcohols or water (Scheme 5).

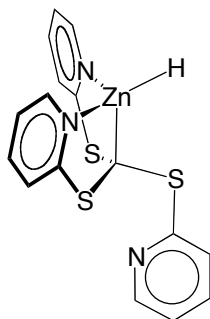
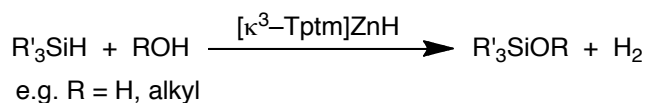
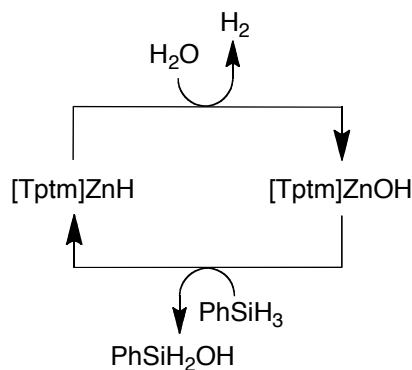


Figure 1. [κ³-Tptm]ZnH.



Scheme 5. [κ³-Tptm]ZnH catalyzed dehydrocoupling of silanes with alcohols or water.

For example, the reaction of PhSiH_3 , a commercially available trihydrosilane, with H_2O produces three equivalents of H_2 (*i.e.* every Si–H bond is utilized in the reaction) to generate an ill-defined siloxane gel.³³ Previously, a heterogeneous catalyst was used for the hydrolysis of PhSiH_3 ,^{18g,h} but in contrast to our result, the authors reported that the product obtained was the silanetriol compound, $\text{PhSi}(\text{OH})_3$.



Scheme 6. Proposed mechanism for the first cycle of H_2 elimination.

The proposed mechanism for the first cycle of H_2 elimination is illustrated in Scheme 6, which involves an initial reaction of the hydride complex, $[\kappa^3\text{-Tptm}]\text{ZnH}$, with H_2O , to release H_2 and form a hydroxide derivative. While the hydroxide complex, $\{[\kappa^3\text{-Tptm}]\text{Zn}(\mu\text{-OH})\}_2$ (Chapter 4) has been structurally characterized as a dimer bridged by hydroxide ligands, it is possible that the dimer does not form in the catalytic reaction. Regardless of whether it is the monomer or dimer, the next step is the reaction with PhSiH_3 with the hydroxide complex to regenerate $[\kappa^3\text{-Tptm}]\text{ZnH}$, producing the hydroxysilane derivative. After the first cycle, PhSiH_2OR ($\text{R} = \text{H}$ or silyl group) continues to react *via* the same process; each cycle releases one equivalent of H_2 .

It is the rate enhancement compared to the background reaction by $[\kappa^3\text{-Tptm}]\text{ZnH}$ that is most notable, allowing for rapid H_2 evolution. Depicted in Figure

2 and Figure 3 are plots of the release of H_2 (mL)³⁴ versus time (seconds) for the $[\kappa^3\text{-Tptm}]\text{ZnH}$ (1.0 mol %) catalyzed hydrolysis of PhSiH_3 . Figure 2 shows a plot for the entire reaction, whereas Figure 3 shows only the first 4 minutes. The first equivalent is released after 14 seconds, corresponding to a turnover frequency (TOF) of $8.58 \times 10^3 \text{ h}^{-1}$, while the second equivalent was released in 58 seconds, corresponding to a TOF of $4.14 \times 10^3 \text{ h}^{-1}$. For comparison, in the absence of a catalyst, only 18 % of H_2 evolution is observed after 115 hours (414,000 seconds).

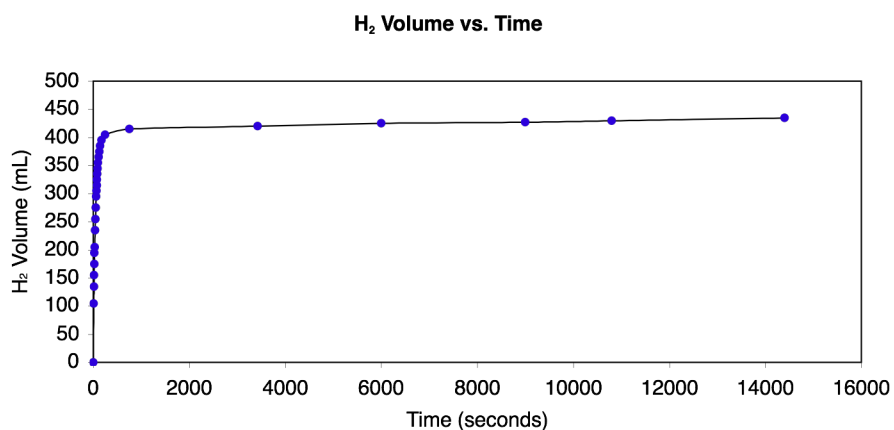


Figure 2. Release of H_2 as a function of time for the $[\kappa^3\text{-Tptm}]\text{ZnH}$ catalyzed hydrolysis of PhSiH_3 .

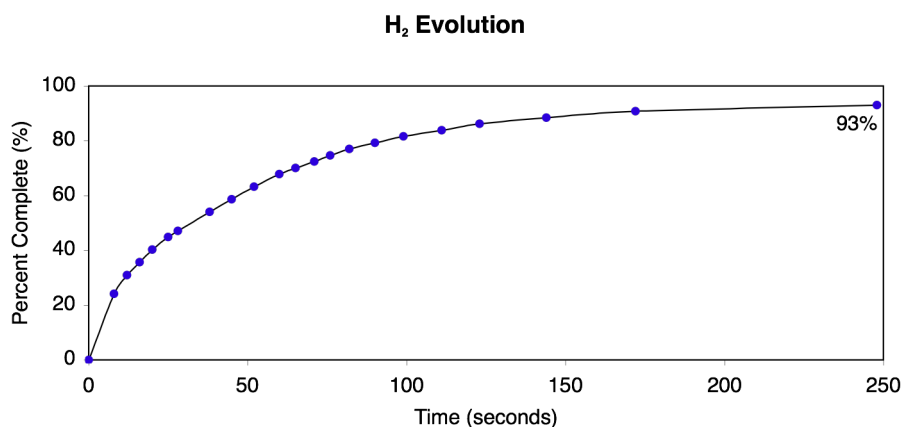


Figure 3. Release of H_2 as a function of time for the $[\kappa^3\text{-Tptm}]\text{ZnH}$ catalyzed hydrolysis of PhSiH_3 for the first 4 minutes.

In addition to $[\kappa^3\text{-Tptm}]\text{ZnH}$ serving as a catalyst for the hydrolysis of Si–H bonds, the trimethylsiloxide complex $[\kappa^4\text{-Tptm}]\text{ZnOSiMe}_3$ (Figure 4, left) and the hydroxide dimer $\{[\kappa^3\text{-Tptm}]\text{Zn}(\mu\text{-OH})\}_2$ (Figure 4, right) may be employed as effective precatalysts because they react with PhSiH_3 to generate the hydride complex (Scheme 7).

The H_2 evolution plots for the $\{[\kappa^3\text{-Tptm}]\text{Zn}(\mu\text{-OH})\}_2$ (1.9 mol %) and $[\kappa^4\text{-Tptm}]\text{ZnOSiMe}_3$ (1.0 mol %) catalyzed hydrolysis reactions of PhSiH_3 are depicted in Figure 5, Figure 6 and Figure 7. It is evident that both $[\kappa^4\text{-Tptm}]\text{ZnOSiMe}_3$ and $\{[\kappa^3\text{-Tptm}]\text{Zn}(\mu\text{-OH})\}_2$ are active for rapid generation of H_2 , with TOFs greater than $1.00 \times 10^4 \text{ h}^{-1}$. These TOF data are summarized in Table 1.

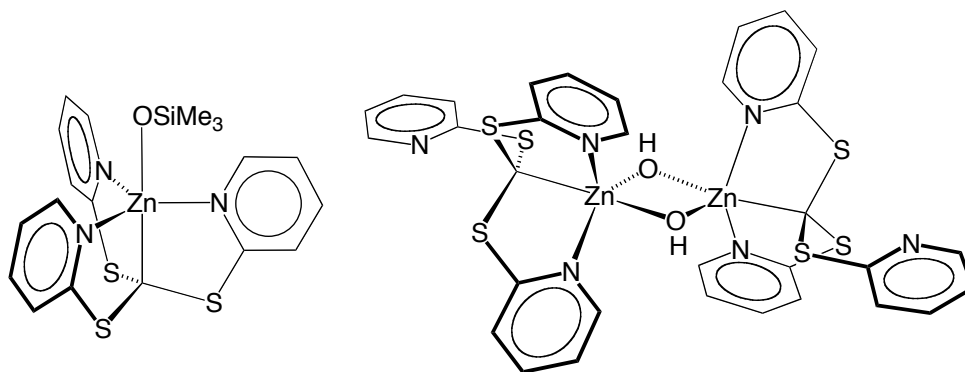


Figure 4. $[\kappa^4\text{-Tptm}]\text{ZnOSiMe}_3$ (left) and $\{[\kappa^3\text{-Tptm}]\text{Zn}(\mu\text{-OH})\}_2$ (right).



Scheme 7. Generation of $[\kappa^3\text{-Tptm}]\text{ZnH}$ *via* treatment of $[\kappa^4\text{-Tptm}]\text{ZnOSiMe}_3$ or $\{[\kappa^3\text{-Tptm}]\text{Zn}(\mu\text{-OH})\}_2$ with PhSiH_3 .

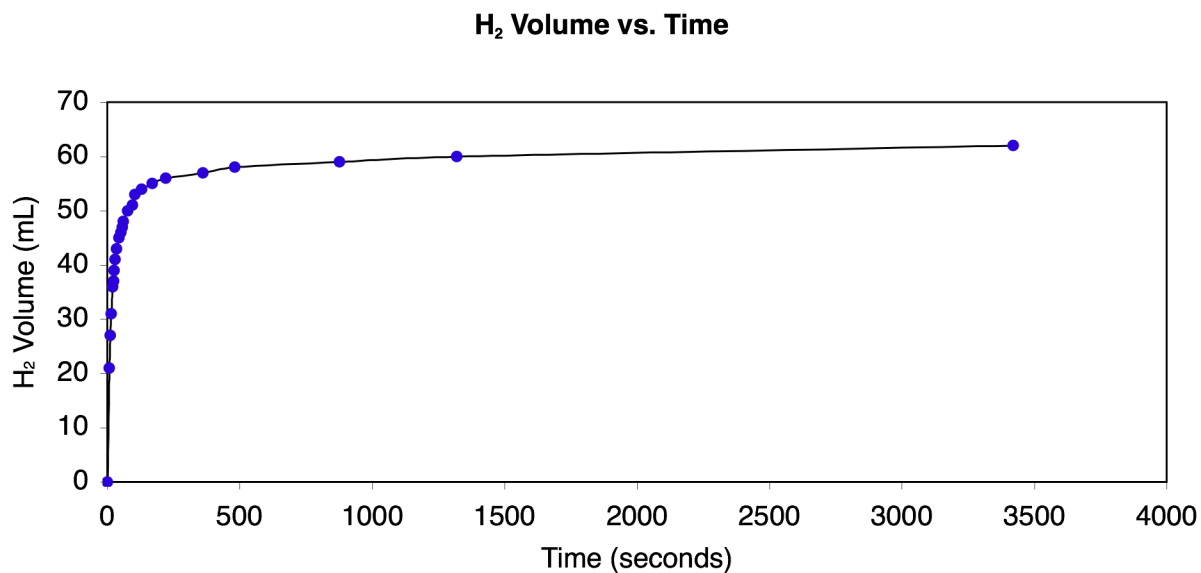


Figure 5. Release of 3 equivalents of H₂ as a function of time for the $[\kappa^3\text{-Tptm}]\text{Zn}(\mu\text{-OH})_2$ catalyzed hydrolysis of PhSiH₃.

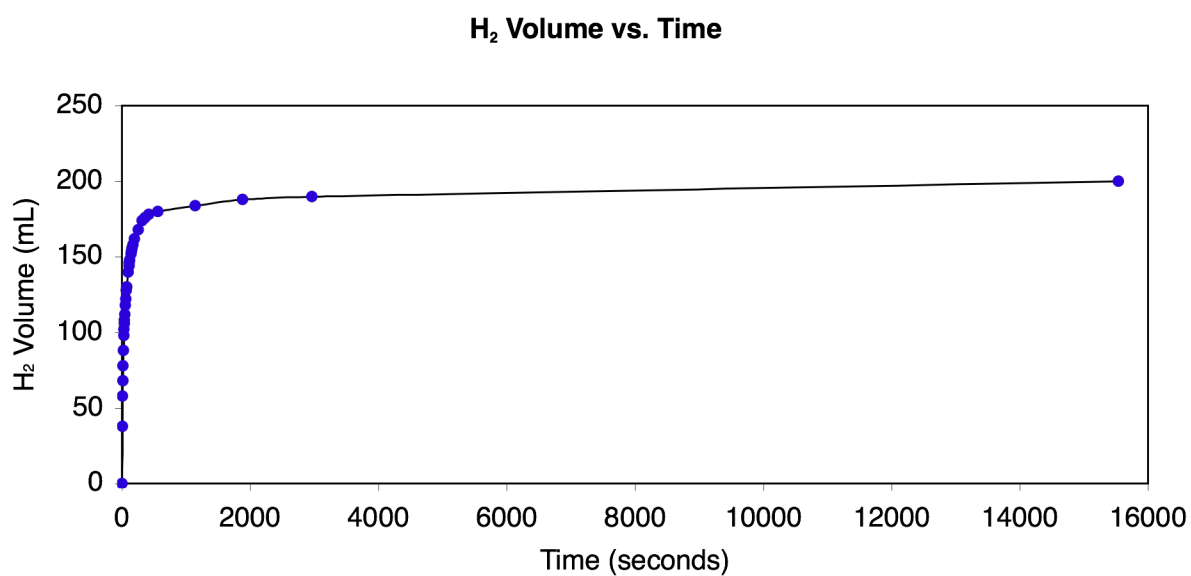


Figure 6. Release of H₂ as a function of time for the $[\kappa^4\text{-Tptm}]\text{ZnOSiMe}_3$ catalyzed hydrolysis of PhSiH₃.

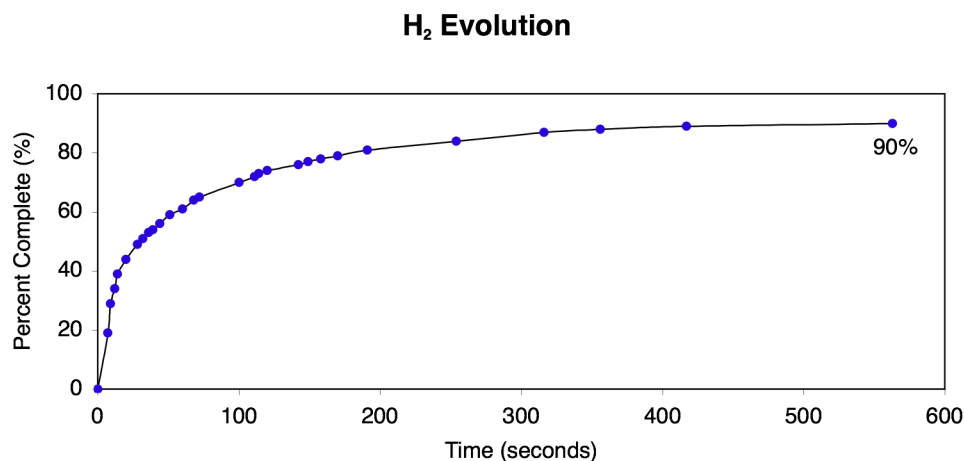


Figure 7. Release of H₂ as a function of time for the [κ⁴-Tptm]ZnOSiMe₃ catalyzed hydrolysis of PhSiH₃ for the first 10 minutes.

Table 1. Turnover frequencies for the 1st and 2nd equivalent of H₂.

Catalyst	Mole percent	T.O.F. (1 st equiv.) h ⁻¹	T.O.F. (2 nd equiv.) h ⁻¹
[κ ³ -Tptm]ZnH	1.0	8.58 × 10 ³	4.14 × 10 ³
[κ ⁴ -Tptm]ZnOSiMe ₃	1.0	1.00 × 10 ⁴	2.67 × 10 ³
{[κ ³ -Tptm]Zn(μ-OH)} ₂	1.9	8.88 × 10 ³	3.89 × 10 ³
Re catalyst ^a	1.0	No data	1.65 – 3.30 × 10 ¹

^a [2-(2'-hydroxyphenyl)-2-oxazolinato]oxorhenium(V) (See Figure 8)

There is only one other homogeneous catalyst for which quantitative data for the hydrolysis of PhSiH₃ has been reported. Abu-Omar and co-workers have reported that 1.0 mol % of [2-(2'-hydroxyphenyl)-2-oxazolinato]oxorhenium(V) (Figure 8), releases only two equivalents of H₂ over a period of 2 – 4 hours, corresponding to a TOF of 16.5 – 33 h⁻¹.^{9a,b} This can be compared to 1.0 mol % of [κ³-Tptm]ZnH, which liberates two equivalents of H₂ in less than two minutes corresponding to a TOF of 4.14 × 10³ h⁻¹.

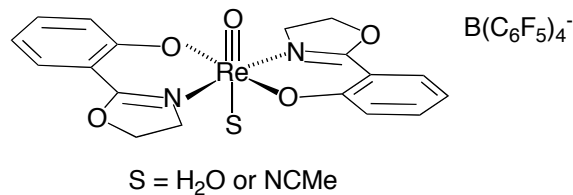


Figure 8. [2-(2'-hydroxyphenyl)-2-oxazolinato]oxorhenium(V) catalyst used by Abu-Omar and co-workers.

The zinc catalysts are also more stable to the reaction conditions compared to the oxorhenium catalyst, the latter being reduced to an inactive form when excess silane is used;^{9a,b} the zinc catalysts operate effectively in the presence of a large excess of silane. These results demonstrate that the zinc catalysts are more effective than is the rhenium catalyst.³⁵

3.2.2 [κ^3 -Tptm]ZnH catalyzed alcoholysis of PhSiH₃ for H₂ production

As described in the previous section, [κ^3 -Tptm]ZnH is an efficient catalyst for the hydrolysis of PhSiH₃. The ability for [κ^3 -Tptm]ZnH to catalyze the alcoholysis of silanes was also tested, as this also provides a means to generate H₂.^{9,36} [κ^3 -Tptm]ZnH does catalyze this reaction, and is the most efficient catalyst for methanolysis in the literature to date (Table 2). The fastest, and most efficient catalyst in the literature for the methanolysis of silanes prior to [κ^3 -Tptm]ZnH was [RuCl₂(*p*-cymene)]₂.^{36c} Specifically, 0.1 mole % of [RuCl₂(*p*-cymene)]₂ achieved a TOF of $3.67 \times 10^5 \text{ h}^{-1}$, accomplishing 1,000 turnovers when using PhMe₂SiH as the silane; this TOF was determined by the initial rate, which gives a higher TOF than ones recorded at later reaction times. Additionally, lowering the catalyst loading to 0.0013 mole %, [RuCl₂(*p*-cymene)]₂ achieves 6.00×10^4 turnovers, which corresponding to a reaction that achieves only 78% completion, which was the greatest TON prior to [κ^3 -Tptm]ZnH. Another factor to note is the fact that the ruthenium catalyst is dimeric, relying on two metal atoms per catalyst, compared to

$[\kappa^3\text{-Tptm}]\text{ZnH}$, which only relies on one zinc atom. As can be seen in Table 2, excluding $[\kappa^3\text{-Tptm}]\text{ZnH}$, the best catalysts in the literature rely on precious transition metals. Thus, the discovery of a highly reactive zinc catalyst is thus particularly exciting.

Table 2. Catalysts for the methanolysis of silanes.

Catalyst	mol %	Silane	TON	TOF (h^{-1}) ^a	Ref.
$[\kappa^4\text{-Tptm}]\text{ZnOSiMe}_3$	0.001	PhSiH ₃	1.00×10^5	1.63×10^6	---
$[\kappa^4\text{-Tptm}]\text{ZnOSiMe}_3^{\text{b}}$	0.025	PhSiH ₃	4.00×10^3	1.21×10^5	---
$[\text{To}^{\text{M}}]\text{ZnH}^{\text{c}}$	10.0	BnMe ₂ SiH	1.00×10^1	1.00×10^1	36a
$[\text{RuCl}_2(p\text{-cymene})]_2^{\text{d}}$	1.0	PhMe ₂ SiH	1.00×10^2	3.67×10^5	36c
[Au]-SMAP-Rh	0.001	PhMe ₂ SiH	6.00×10^4	3.75×10^3	36x
$[\text{IrH}_2(\text{THF})_2(\text{PPh}_3)_2]\text{SbF}_6$	0.4	Et ₃ SiH	2.50×10^2	5.30×10^4	36h
$\text{Bu}_4\text{NF} \cdot \text{H}_2\text{O}^{\text{e}}$	4.0	PhSiH ₃	2.40×10^1	8.73×10^3	9c

^a The TOFs listed in the table are the highest numbers reported for each catalyst system.

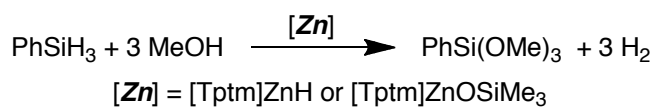
^b Reaction was performed at 0 °C.

^c Reaction was performed at 60 °C.

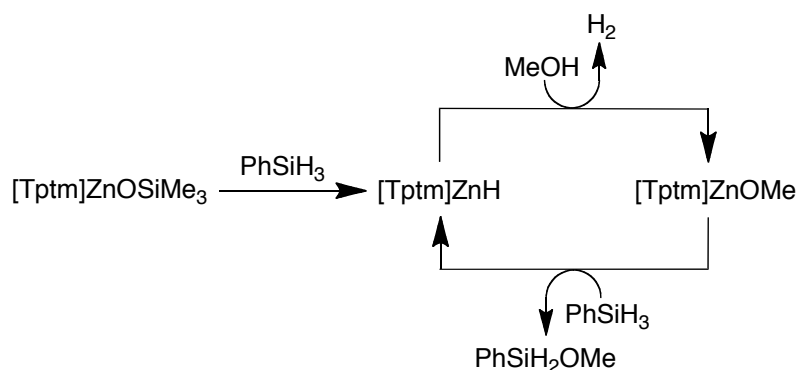
^d Reaction was performed at 0 °C in neat methanol.

^e Reaction performed in neat methanol.

In this vein, $[\kappa^4\text{-Tptm}]\text{ZnOSiMe}_3$, which is used as a precatalyst for the methanolysis reaction (Scheme 7 and Scheme 9), outperforms the ruthenium catalyst described above. For example, only 0.001 mol % of $[\kappa^4\text{-Tptm}]\text{ZnOSiMe}_3$ achieves quantitative liberation of three equivalents of H₂ (Scheme 8) from a mixture of PhSiH₃ and MeOH in toluene, corresponding to a TON of 10⁵. The resulting TON is *not* a limit, but is the value obtained due to depletion of the PhSiH₃ (*i.e.* when more PhSiH₃ is added, more H₂ is liberated).



Scheme 8. Catalyzed methanolysis of PhSiH₃ to give PhSi(OMe)₃ + 3H₂.



Scheme 9. [κ^4 -Tptm]ZnOSiMe₃ as precatalyst for methanolysis of PhSiH₃.

The evolution of H₂ from the methanolysis reaction is also very rapid, with release of the first equivalent occurring in less than two minutes, corresponding to an impressive TOF of $1.63 \times 10^6 \text{ h}^{-1}$. The second equivalent was also released with a TOF greater than one million per hour (TOF = $1.43 \times 10^6 \text{ h}^{-1}$), and the reaction went to completion with a final TOF of $1.02 \times 10^5 \text{ h}^{-1}$. The H₂ evolution is depicted in Figure 9. While the reaction between PhSiH₃ and MeOH occurs without a catalyst, it is slow; 48 % of the H₂ is released over a period of 123 hours (442,800 seconds).

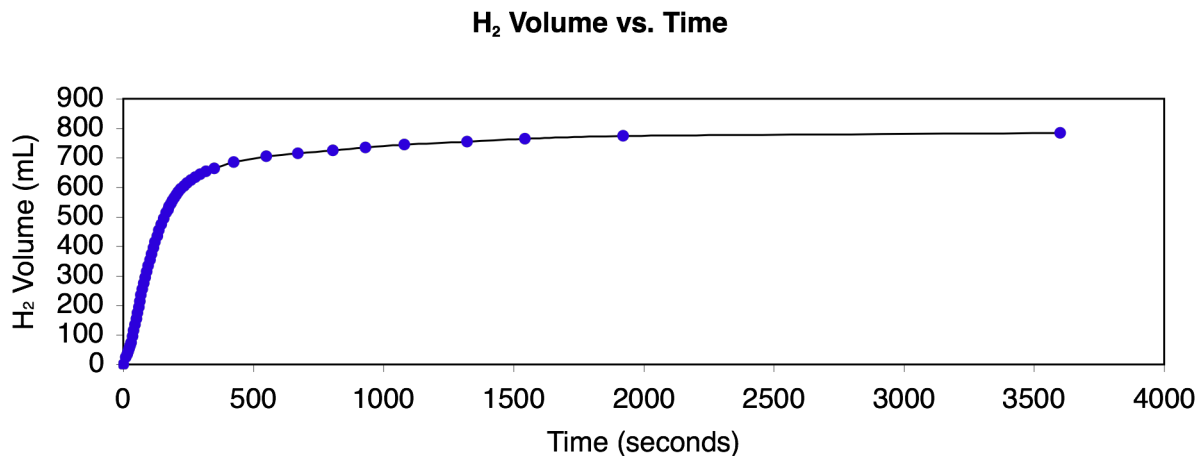


Figure 9. Release of H₂ as a function of time for the [κ^4 -Tptm]ZnOSiMe₃ (0.001 mol %) catalyzed methanolysis of PhSiH₃.

As would be expected, the reaction is faster with higher catalyst loadings. For example, using a catalyst loading of 0.1 mol % [κ^4 -Tptm]ZnOSiMe₃, the reaction is 85 % complete within 5 seconds, and 100 % within 5 minutes (Figure 10).

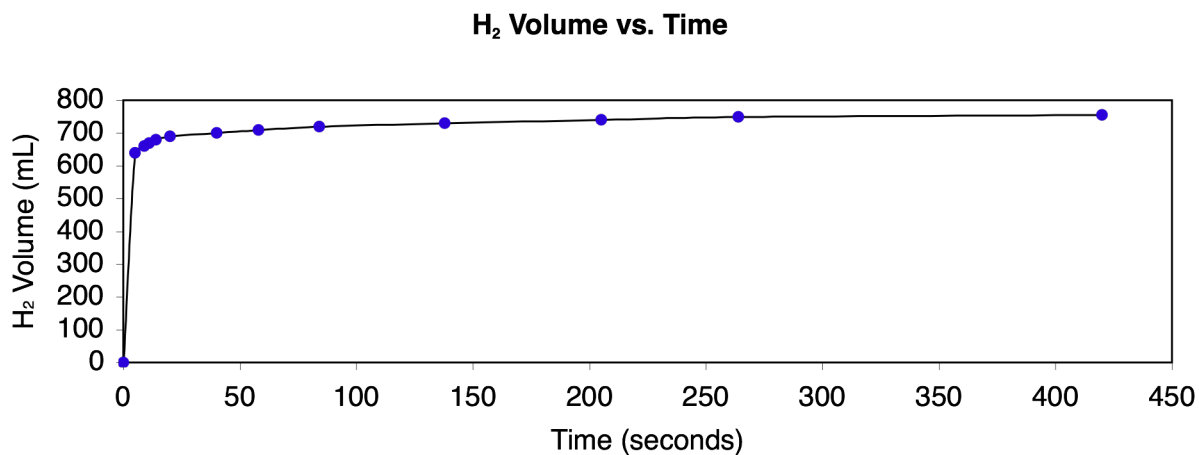


Figure 10. Release of H₂ as a function of time for the [κ^4 -Tptm]ZnOSiMe₃ (0.1 mol %) catalyzed methanolysis of PhSiH₃.

Catalytic methanolysis of PhSiH_3 using the zinc complexes also occurs at $0\text{ }^\circ\text{C}$, although the reaction rate decreases resulting in reduction of the TOFs (Table 2). Quantitative methanolysis of PhSiH_3 may be achieved using 0.025 mol % of $[\kappa^4\text{-Tptm}]\text{ZnOSiMe}_3$ at $0\text{ }^\circ\text{C}$, with the first equivalent of H_2 being released with a TOF of $1.21 \times 10^5\text{ h}^{-1}$ and the second equivalent having a TOF = $4.90 \times 10^4\text{ h}^{-1}$ (Figure 11).

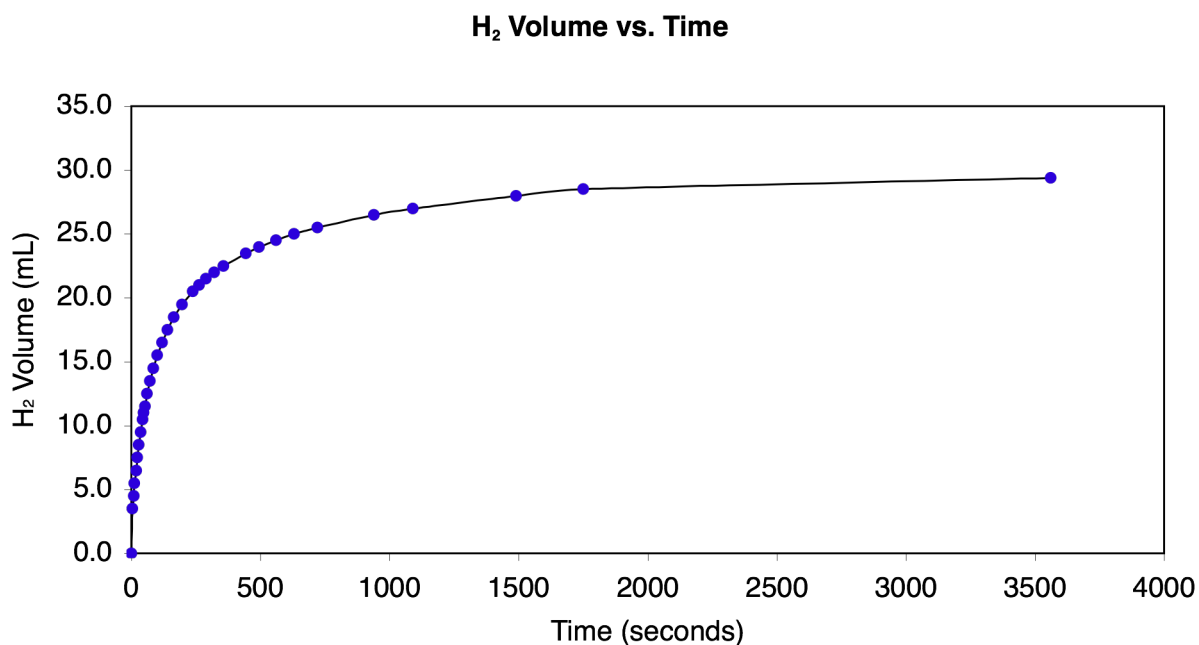


Figure 11. Release of H_2 as a function of time for the $[\kappa^4\text{-Tptm}]\text{ZnOSiMe}_3$ (0.025 mol %) catalyzed methanolysis of PhSiH_3 at $0\text{ }^\circ\text{C}$.

It has been demonstrated that $[\kappa^4\text{-Tptm}]\text{ZnOSiMe}_3$ is a highly effective precatalyst for the methanolysis of PhSiH_3 , with catalyst loadings that are orders of magnitude lower than have previously been employed for this transformation, and turnover frequencies that are orders of magnitude greater.^{9c} Additionally, it was important to determine if the catalyst was stable to the reaction conditions for long periods of time, such that H_2 could be generated on demand with methanol additions. In this vein, $[\kappa^3\text{-Tptm}]\text{ZnH}$ remains an active catalyst for an extended period of time, as

shown in Figure 12. The release of H₂ was monitored upon sequential injections of methanol into a reaction mixture containing [κ³-Tptm]ZnH, PhSiH₃ and toluene, thereby depleting the silane.

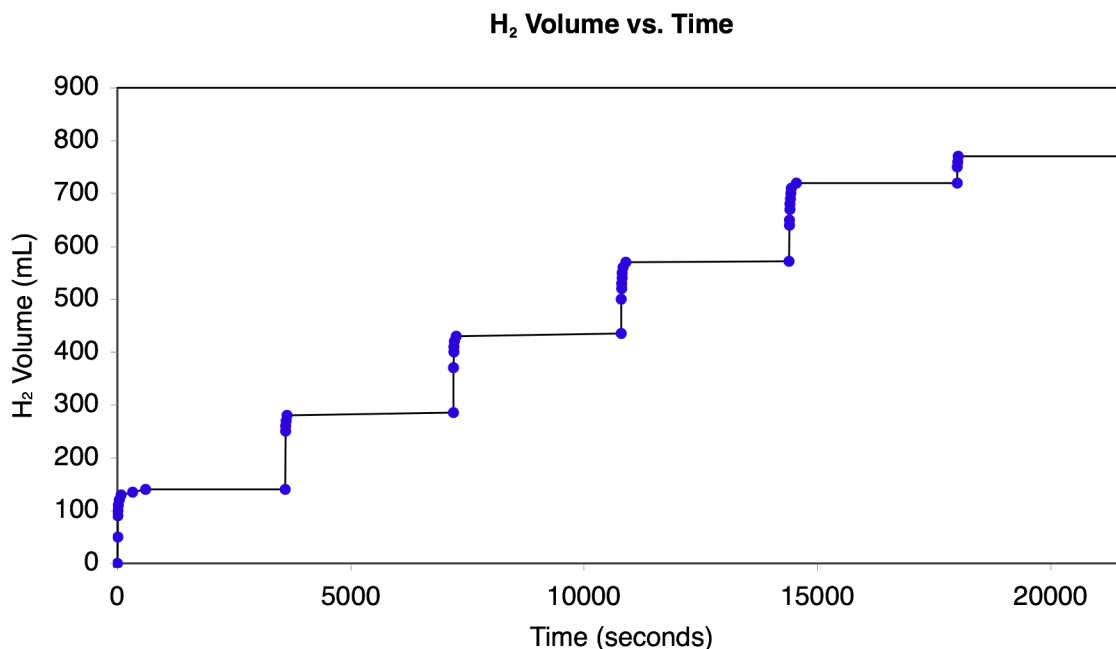


Figure 12. Stepwise release of H₂ as a function of time for zinc catalyzed methanolysis of PhSiH₃.

Finally, it should be noted that the reaction product, PhSi(OMe)₃, can be reconverted to PhSiH₃ by treatment with LiAlH₄,¹⁶ thereby providing a means to recycle the spent fuel (Scheme 2).

To provide a direct comparison to the only other zinc catalyst for which quantitative data is known, the activity of the [κ³-Tptm]ZnH catalyst was compared to that of the *tris*(4,4-dimethyl-2-oxazoliny)phenylborate zinc hydride catalyst ([To^M]ZnH)^{36a,37} (Figure 13) for the methanolysis of PhMeSiH₂ to PhMeSiH(OMe) (Scheme 10).

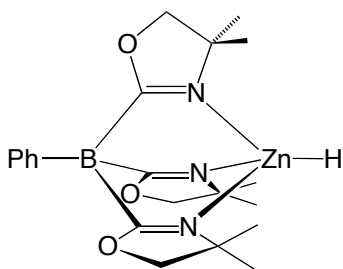
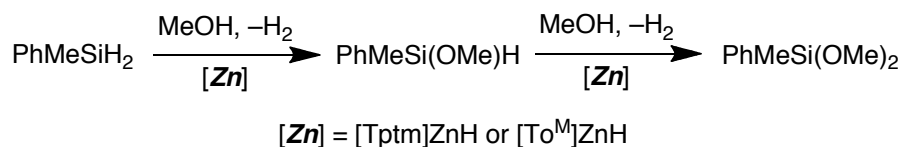


Figure 13. *Tris*(4,4-dimethyl-2-oxazoliny)phenylborate zinc hydride catalyst ($[To^M]ZnH$).

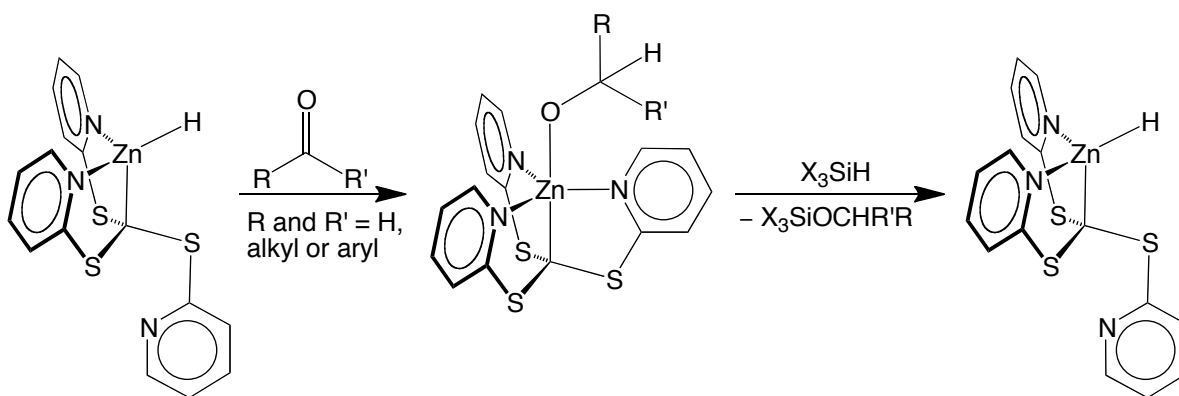


Scheme 10. Catalyzed methanolysis of PhMeSiH_2 to PhMeSiH(OMe) and then to PhMeSi(OMe)_2 .

Sadow and co-workers reported that 10 mol % of $[To^M]ZnH$ converted a 1:1 mixture of PhMeSiH_2 and MeOH to an approximately 9:1 ratio of mono and disubstituted products, PhMeSiH(OMe) and PhMeSi(OMe)_2 over 10 hours at 45°C (Scheme 10). This reaction rate corresponds to a TOF of only 1 h^{-1} , based on the PhMeSiH_2 consumed.^{36a} The corresponding reaction employing only 0.3 mol % $[\kappa^3\text{-Tptm}]ZnH$ also converts a 1:1 mixture of PhMeSiH_2 and MeOH to an approximately 9:1 ratio of mono and disubstituted products, however, this occurs within only 30 minutes at room temperature, which corresponds to a TOF of 258 h^{-1} (Scheme 10). When using $[\kappa^3\text{-Tptm}]ZnH$ with an excess of methanol, the disubstituted product, PhMeSi(OMe)_2 , is obtained exclusively within 6 minutes at room temperature, corresponding to a TOF of $2.98 \times 10^3 \text{ h}^{-1}$. Overall, it is evident that $[\kappa^3\text{-Tptm}]ZnH$ is an effective catalyst for the methanolysis of silanes, especially, PhSiH_3 .

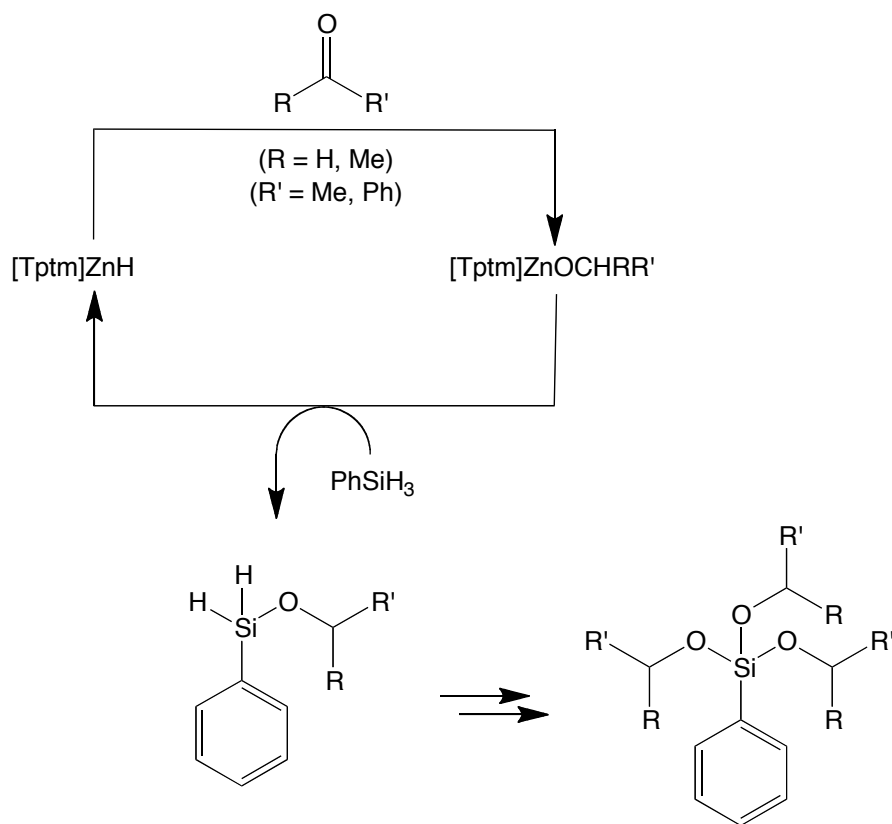
3.3 $[\kappa^3\text{-Tptm}]\text{ZnH}$ catalyzed hydrosilylation of aldehydes and ketones with PhSiH_3

$[\kappa^3\text{-Tptm}]\text{ZnH}$ has been demonstrated to be a reactive nucleophilic metal-hydride (see chapter 1). Therefore, the reactivity of $[\kappa^3\text{-Tptm}]\text{ZnH}$ was explored towards carbonyl compounds, such as aldehydes and ketones. If an aldehyde or ketone inserts into the Zn–H bond, the product is presumably the corresponding zinc-alkoxide (i.e. formal reduction of the carbonyl compound). As described above, zinc-alkoxides are reactive towards silanes to regenerate $[\kappa^3\text{-Tptm}]\text{ZnH}$ (Scheme 11).



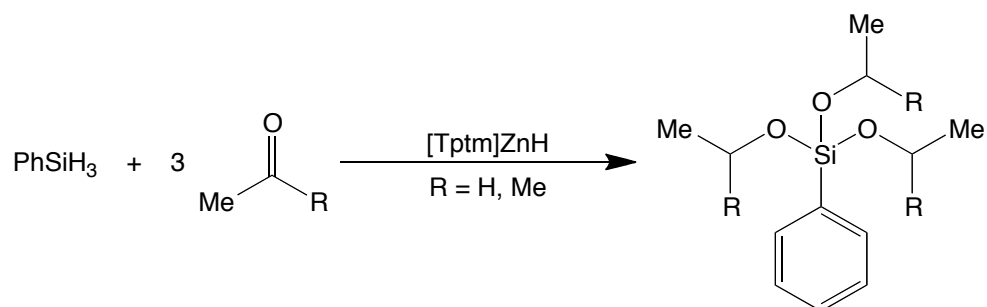
Scheme 11. Reaction of $[\kappa^3\text{-Tptm}]\text{ZnH}$ with aldehyde or ketone followed by reaction of the resulting alkoxide derivative, $[\kappa^4\text{-Tptm}]\text{ZnOCHR}'\text{R}$ with a silane to regenerate $[\kappa^3\text{-Tptm}]\text{ZnH}$.

Thus, the resulting catalytic hydrosilylation of aldehydes and ketones would produce siloxanes,³⁸ which are also the products of alcoholysis of silanes. A key difference is that there are two fewer hydrogen atoms for the hydrosilylation, such that no H_2 is produced in this reaction. The proposed catalytic cycle involving PhSiH_3 is depicted in Scheme 12.

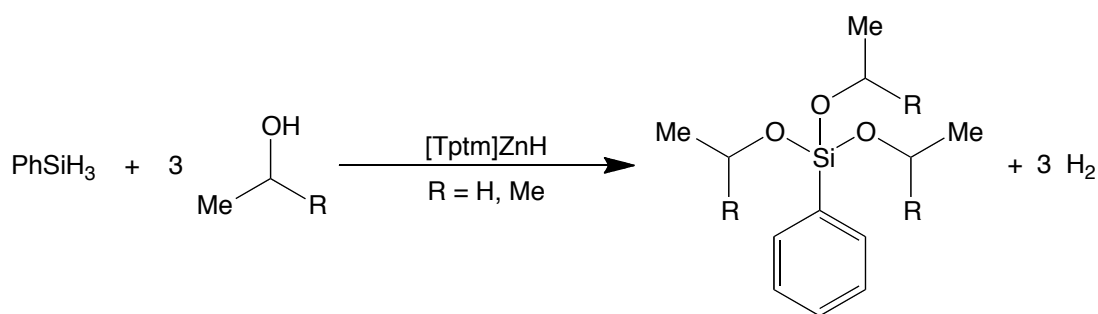


Scheme 12. $[\kappa^3\text{-Tptm}]\text{ZnH}$ catalyzed hydrosilylation of aldehydes and ketones by PhSiH_3 .

In this vein, $[\kappa^3\text{-Tptm}]\text{ZnH}$ reacts with both aldehydes and ketones to produce the corresponding zinc-alkoxide products that are reactive towards PhSiH_3 ; therefore, $[\kappa^3\text{-Tptm}]\text{ZnH}$ is a hydrosilylation catalyst for aldehydes and ketones (Scheme 12). For example, $[\kappa^3\text{-Tptm}]\text{ZnH}$ catalyzes the insertion of aliphatic aldehydes and ketones, namely acetaldehyde and acetone, into all three Si–H bonds of PhSiH_3 to give $\text{PhSi}(\text{OEt})_3$ and $\text{PhSi}(\text{OPr}^i)_3$, respectively (Scheme 13). $\text{PhSi}(\text{OEt})_3$ and $\text{PhSi}(\text{OPr}^i)_3$ have been prepared independently by the $[\kappa^3\text{-Tptm}]\text{ZnH}$ catalyzed alcoholysis of PhSiH_3 with ethanol and *iso*-propanol, respectively (Scheme 14).



Scheme 13. $[\kappa^3\text{-Tptm}]\text{ZnH}$ catalyzed hydrosilylation of acetaldehyde and acetone to give PhSi(OEt)_3 and $\text{PhSi(OPr}^i)_3$, respectively.

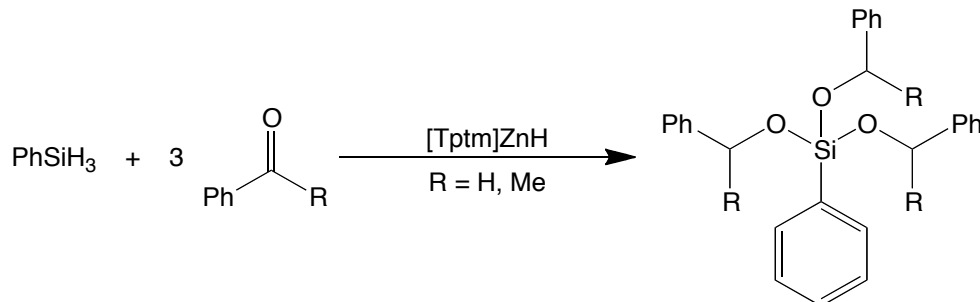


Scheme 14. $[\kappa^3\text{-Tptm}]\text{ZnH}$ catalyzed alcoholysis of PhSiH_3 to give PhSi(OEt)_3 and $\text{PhSi(OPr}^i)_3$.

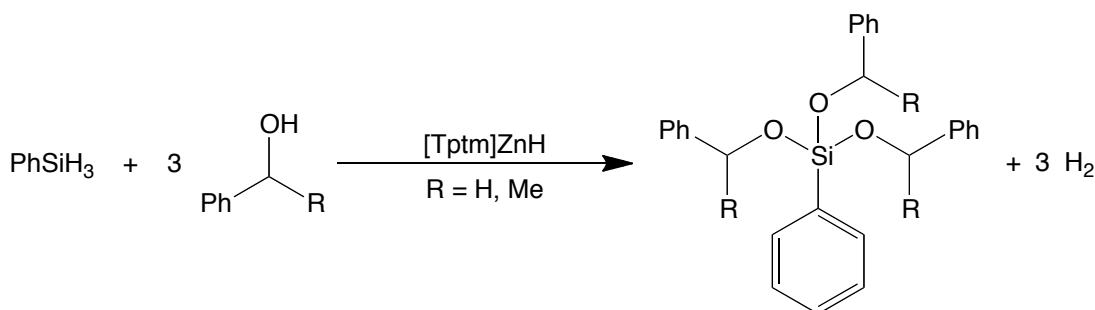
$[\kappa^3\text{-Tptm}]\text{ZnH}$ is an effective catalyst and the reaction occurs with low catalyst loadings. Less than 1.0 mol % is required when using PhSiH_3 , with TOFs of $9.96 \times 10^2 \text{ h}^{-1}$ and $1.25 \times 10^2 \text{ h}^{-1}$ for acetaldehyde and acetone, respectively. It should be noted that the TOF for the acetaldehyde reaction is a lower limit, as by the time analysis is taken the reaction has already gone to completion.

In addition to aliphatic aldehydes and ketones, catalysis also occurs when aromatic carbonyl compounds. For example, benzaldehyde and acetophenone are both catalytically hydrosilylated by PhSiH_3 to give $\text{PhSi(OCH}_2\text{Ph)}_3$ and PhSi[OCH(Me)Ph]_3 , respectively (Scheme 15). Low catalyst loadings have been employed (1.6 mol %), resulting in TOFs of 2.48×10^2 and $1.87 \times 10^2 \text{ h}^{-1}$ for the aldehyde and ketone, respectively. $\text{PhSi(OCH}_2\text{Ph)}_3$ can also be prepared by the alcoholysis of PhSiH_3 using

benzyl alcohol while $\text{PhSi}[\text{OCH}(\text{Me})\text{Ph}]_3$ can be prepared by alcoholysis using 1-phenylethanol (Scheme 16).



Scheme 15. $[\kappa^3\text{-Tptm}]\text{ZnH}$ catalyzed hydrosilylation of benzaldehyde and acetophenone to give $\text{PhSi}(\text{OCH}_2\text{Ph})_3$ and $\text{PhSi}[\text{OCH}(\text{Me})\text{Ph}]_3$.



Scheme 16. $[\kappa^3\text{-Tptm}]\text{ZnH}$ catalyzed alcoholysis of PhSiH_3 to give $\text{PhSi}(\text{OCH}_2\text{Ph})_3$ and $\text{PhSi}[\text{OCH}(\text{Me})\text{Ph}]_3$.

The product of catalytic hydrosilylation of acetophenone by PhSiH_3 does *not* give one product. $\text{PhSi}[\text{OCH}(\text{Me})\text{Ph}]_3$ exists as two different diastereomers, due to the molecule containing three chiral centers (Figure 14). The two molecules on the left in Figure 14, $\text{SSS-PhSi}[\text{OCH}(\text{Me})\text{Ph}]_3$ and $\text{RRR-PhSi}[\text{OCH}(\text{Me})\text{Ph}]_3$, comprise one diastereomer as they are enantiomers of each other, while the six other compounds comprise only one other diastereomer (two enantiomers), due to the presence of a C_3 symmetry axis. In order to help clarify the product distribution, RRR-

$\text{PhSi}[\text{OCH}(\text{Me})\text{Ph}]_3$ was synthesized as an enantiopure compound by the $[\kappa^3\text{-Tptm}]\text{ZnH}$ catalyzed alcoholysis of PhSiH_3 with (*R*)-(+)-1-phenylethanol (Scheme 17).

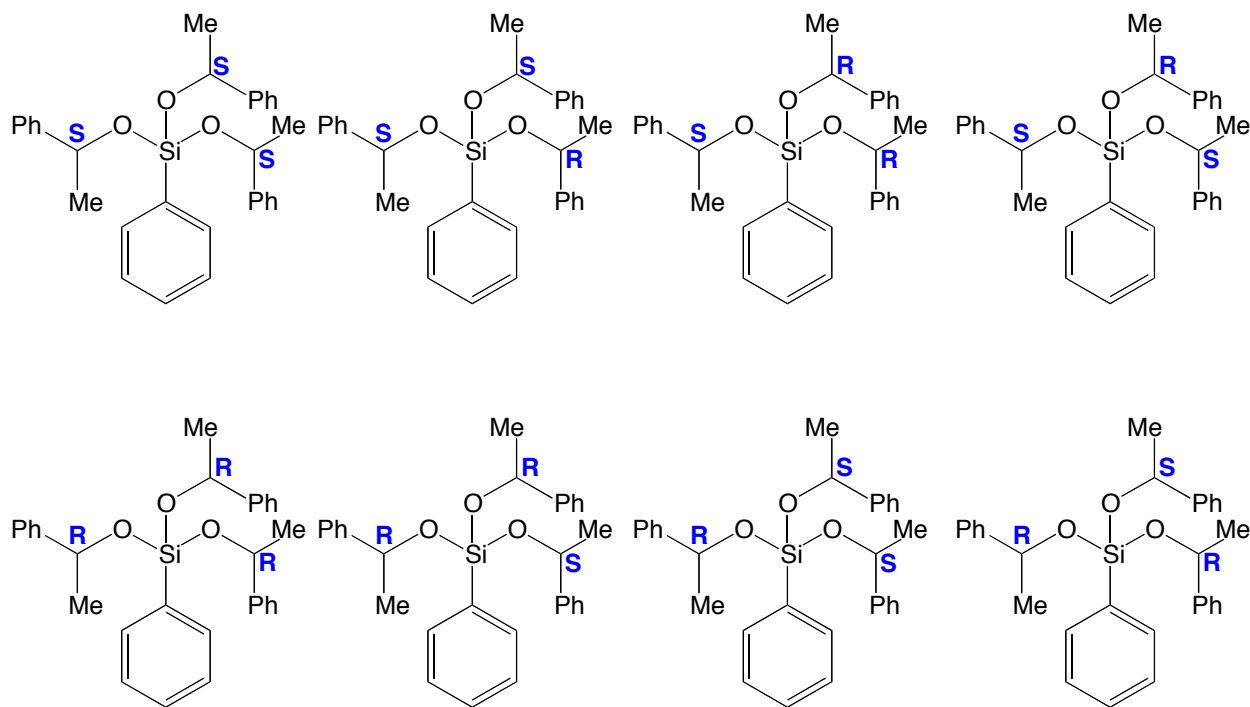
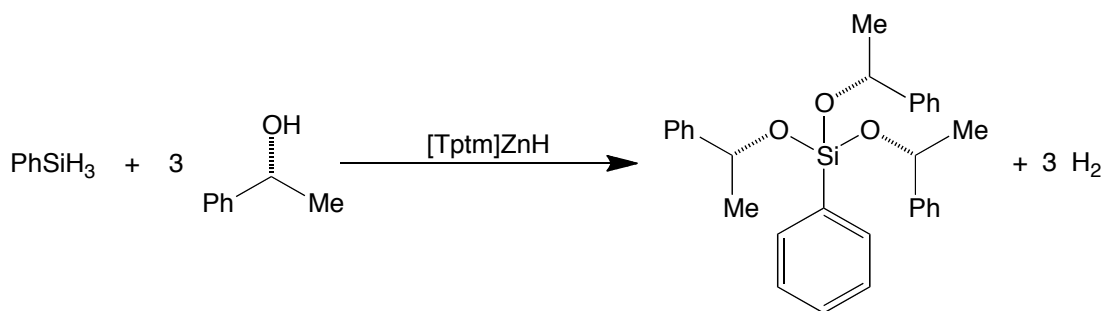


Figure 14. Possible stereoisomers of $\text{PhSi}[\text{OCH}(\text{Me})\text{Ph}]_3$ produced by the hydrosilylation of acetophenone.



Scheme 17. Synthesis of $\text{RRR-PhSi}[\text{OCH}(\text{Me})\text{Ph}]_3$.

The ^1H NMR spectrum of a mixture of diastereomers produced from the reaction of acetophenone and PhSiH_3 shows four doublets for the methyl signal and four

overlapping quartets for the methine signal of $\text{PhSi}[\text{OCH}(\text{Me})\text{Ph}]_3$ (Figure 15). Of note is the fact that there are four signals and only two diastereomers. The enantiopure compounds, $\text{SSS-PhSi}[\text{OCH}(\text{Me})\text{Ph}]_3$ and $\text{RRR-PhSi}[\text{OCH}(\text{Me})\text{Ph}]_3$ display only one signal for methyl and methine protons (Figure 16). The other diastereomer shows three methine and methyl signals, because they are all chemically inequivalent due to the chiral carbon centers. For clarity, the two separate spectra are stacked in Figure 17.

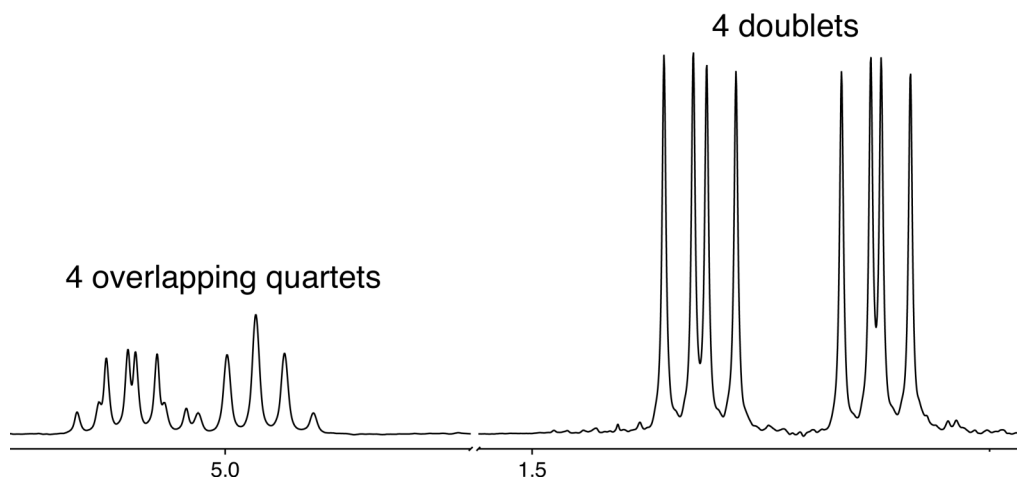


Figure 15. ^1H NMR spectrum of methine (left) and methyl (right) signals for the two diastereomers of $\text{PhSi}[\text{OCH}(\text{Me})\text{Ph}]_3$.

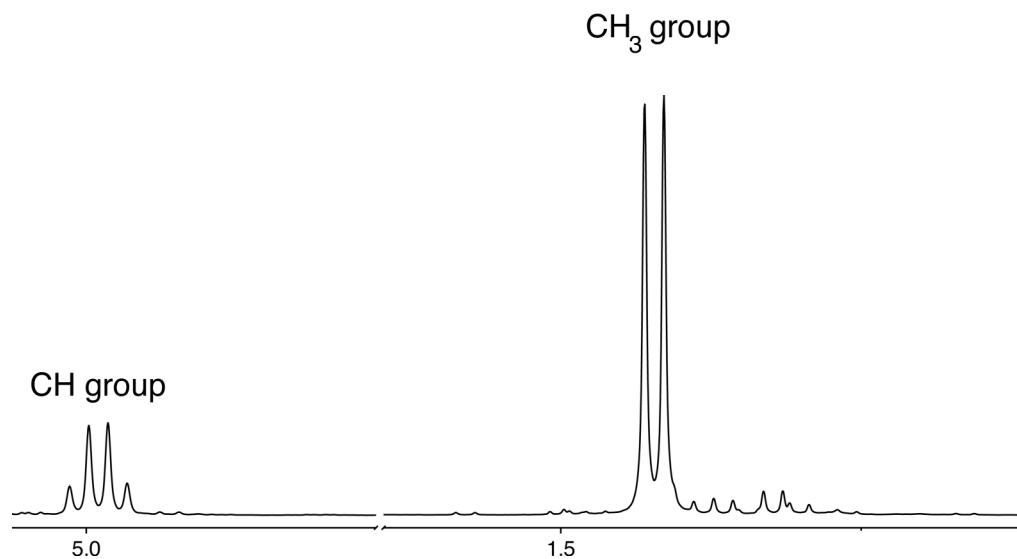


Figure 16. ^1H NMR spectrum of methine (left) and methyl (right) signals for $\text{RRR-PhSi}[\text{OCH}(\text{Me})\text{Ph}]_3$.

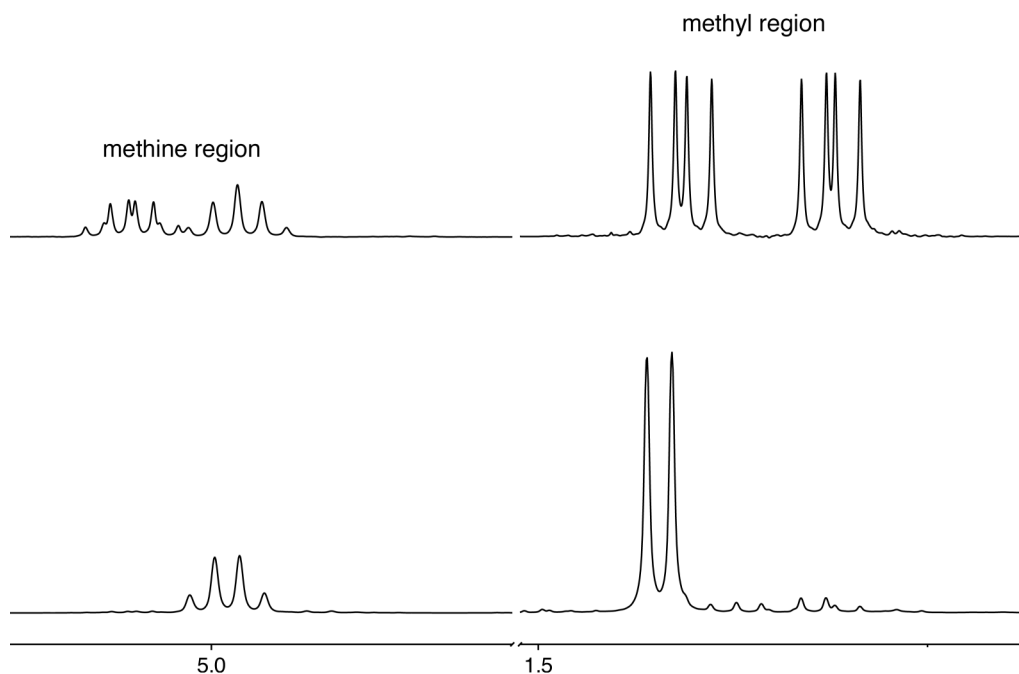


Figure 17. Stacked ^1H NMR spectra of methine (left) and methyl (right) signals for enantiopure, RRR- $\text{PhSi}[\text{OCH}(\text{Me})\text{Ph}]_3$ (bottom) and the mixture of diastereomers of $\text{PhSi}[\text{OCH}(\text{Me})\text{Ph}]_3$ (top).

The same trend is also observed in the $^{13}\text{C}\{^1\text{H}\}$ NMR spectra, which is depicted in Figure 18. While the methine signals (at *ca.* 71 ppm) overlap, the methyl signals (at *ca.* 26 ppm) and one group of signals for a phenyl carbon (at *ca.* 146 ppm) clearly show how the mixture of diastereomers have four signals, while the enantiopure/diastereopure compound has only one signal.

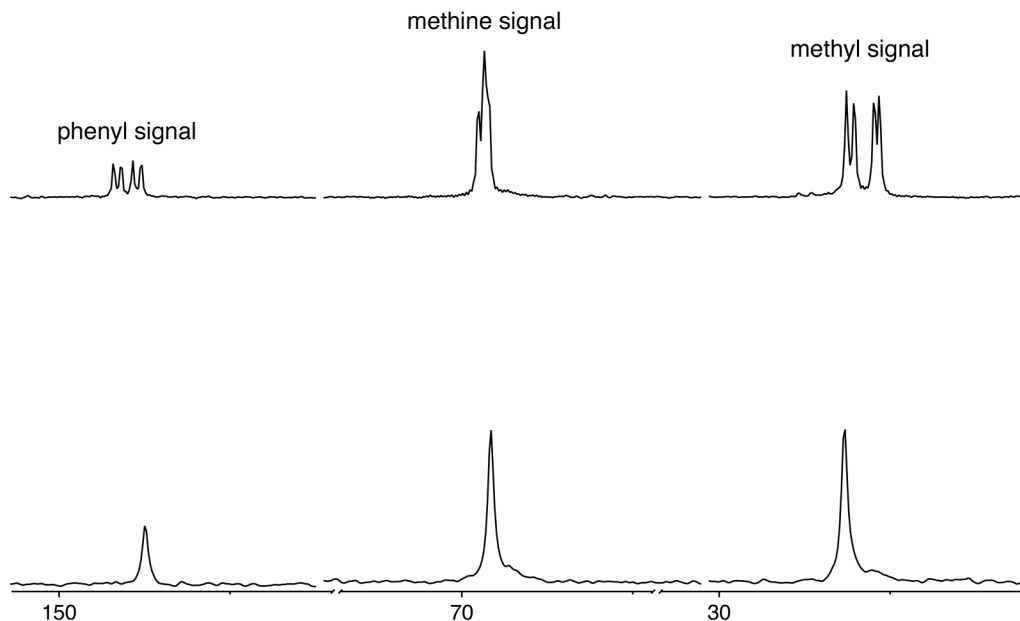


Figure 18. Stacked $^{13}\text{C}\{^1\text{H}\}$ NMR spectra of phenyl (left), methine (middle) and methyl (right) signals for enantiopure, $\text{RRR-PhSi}[\text{OCH}(\text{Me})\text{Ph}]_3$ (bottom) and the mixture of diastereomers of $\text{PhSi}[\text{OCH}(\text{Me})\text{Ph}]_3$ (top).

Finally, ^{29}Si NMR spectroscopy demonstrates how there are only *two* diastereomers. Specifically, the mixture of diastereomers shows two signals in the ^{29}Si spectrum at -60.06 and -59.99 while the enantiopure compound shows only one signal at -60.06 .³⁹

3.4 $[\kappa^3\text{-Tptm}]\text{ZnH}$ catalyzed hydrosilylation of CO_2 with $(\text{EtO})_3\text{SiH}$

Another carbonyl compound that is of interest to hydrosilylate is carbon dioxide. As mentioned earlier, catalytic hydrosilylation of CO_2 was first realized in 1981, using ruthenium complexes.²⁷ There has been few developments in the past 30 years, with most catalysts still relying on precious transition metals. One recent advance is a copper catalyzed hydrosilylation of CO_2 with a relatively unreactive hydrosilane, namely poly(methylhydrosiloxane), (PMHS). In this report, a copper(I) hydride chelated by 1,2-bis(diphenylphosphino)benzene (Figure 19) is presumed to be the active

catalyst for the production of formic acid upon hydrolysis of the reaction mixture. The presumed copper(I) hydride has been previously reported and dubbed as a “Hot” Stryker’s Reagent by Lipshutz and co-workers,⁴⁰ although there is no structural characterization of the compound. It is noteworthy that the copper complex is the most efficient catalyst for the hydrosilylation of CO₂ to date, with a TON of 8100 and a TOF of 1350 h⁻¹.⁴²

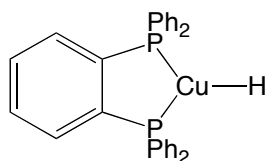


Figure 19. 1,2-bis(diphenylphosphino)benzene copper(I) hydride.

While the majority of CO₂ hydrosilylations result in formic acid derivatives, there are some examples of further reduction to the methanol level and even to methane. For example, one notable accomplishment was the metal free hydrosilylation of CO₂ using an N-heterocyclic carbene (NHC) catalyst.^{30a} In this example, CO₂ is reduced down to the methanol level, achieving 1840 turnovers with a TOF of 25.5 h⁻¹. There have been only two examples of methane produced *via* hydrosilylation, one using a zirconium-borane system²⁹ and the other using a frustrated Lewis pair.³¹ For clarity, Table 3 lists the catalysts that have been developed for the hydrosilylation of CO₂ since this transformation's initial discovery.

Although there have been improvements in the catalytic hydrosilylation of CO₂, there have been no catalysts utilizing main group metals such as zinc. It is, therefore, noteworthy, that [κ³-Tptm]ZnH catalyzes this reaction, providing the first example of zinc-catalyzed hydrosilylation of CO₂. Specifically, we first discovered that triethoxysilane, (EtO)₃SiH, reacts with [κ⁴-Tptm]ZnO₂CH to produce [κ³-Tptm]ZnH at elevated temperatures, albeit with low yield due to [κ³-Tptm]ZnH decomposing at high

temperatures. However, if this reaction is performed in the presence of CO₂, the [κ³-Tptm]ZnH that is generated rapidly reacts with CO₂ to regenerate [κ⁴-Tptm]ZnO₂CH (see Scheme 18 for the proposed catalytic cycle).

Table 3. Catalysts for the hydrosilylation of CO₂.

Catalyst	Ox. State ^a	Temp (°C)	TON	TOF (h ⁻¹)	Ref
[κ ³ -Tptm]ZnH	Formic	100	1000	2.9	this work
[κ ⁴ -Tptm]ZnOSiMe ₃ ^b	Formic	100	400	4.2	this work
[κ ³ -Bptm*]ZnO ₂ CH	Formic	25	c	c	this work
RuX ₂ (PPh ₃) ₄ (X = H, Cl)	Formic	100	1-14	0.7	27
RuX ₃ (MeCN) ₃ (X = Br, Cl)	Formic	85	d	d	32d
RuH ₂ (PMe ₃) ₂	Formic	90	62	1	32e
RuCl ₃ •nH ₂ O	Formic	100	980	49	32c
RuCl ₃ •nH ₂ O	Formic	40	465	233	32b
Ru ₂ Cl ₅ (MeCN) ₇	Formic	100	4619 ^f	^f	32c
RhCl(PPh ₃) ₃	CO	25	d	d	41
HRu ₃ (CO) ₁₁ ⁻	Formic	60	292	12	32a
Ir(CN)(CO)dppe	Methanol	40	d	d	28
Zirconium complex	Methane	25	225	150	29
"[0-C ₆ H ₄ (PPh ₂) ₂]CuH" ^e	Formic	60	8100	1350	42
N-heterocyclic carbene	Methanol	25	1840	25.5	30a
Frustrated Lewis pair	Methane	56	d	d	31

^a Ox. State refers to the formal oxidation level of carbon derived from CO₂, not necessarily the specific compound formed.

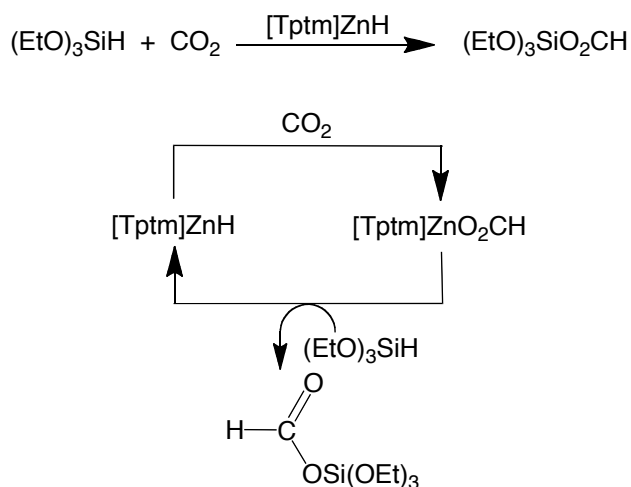
^b [κ⁴-Tptm]ZnOSiMe₃ is a precatalyst.

^c Not yet determined.

^d The TON and TOF are not explicitly stated.

^e No copper complex is isolated. A mixture of Cu(OAc)₂•H₂O and 1,2-bis(diphenylphosphino) benzene is mixed in the presence of PMHS.

^f The TON is the value reported for 10 consecutive experiments with recycled catalyst.



Scheme 18. $[\kappa^3\text{-Tptm}]\text{ZnH}$ catalyzed hydrosilylation of CO_2 by $(\text{EtO})_3\text{SiH}$ to give $(\text{EtO})_3\text{SiO}_2\text{CH}$.

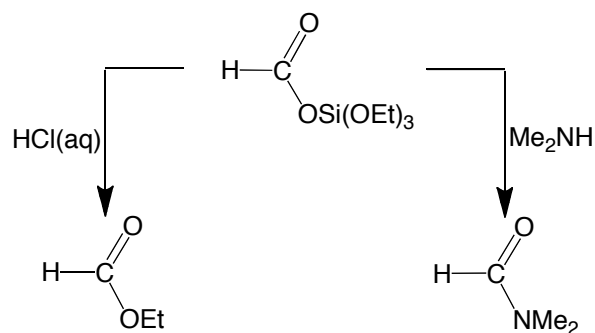
Under catalytic conditions, the product, triethoxysilyl formate, $\text{HCO}_2\text{Si}(\text{OEt})_3$ (Scheme 18),⁴³ is formed in high yield with quantitative conversion of $(\text{EtO})_3\text{SiH}$ and no noticeable decomposition of the catalyst. $\text{HCO}_2\text{Si}(\text{OEt})_3$ is moisture sensitive, and it has been isolated from the reaction mixture *via* vacuum distillation.

Only 0.1 mol % of $[\kappa^3\text{-Tptm}]\text{ZnH}$ catalyzes the hydrosilylation of CO_2 at 100°C , with a TON of 10^3 and a TOF of 2.9 h^{-1} . The TOF has been determined for the entire reaction (*i.e.* determined by the time it takes for all $(\text{EtO})_3\text{SiH}$ to be consumed). It is important to note that the TOF changes throughout the reaction, decreasing as the concentration of silane diminishes, due to the slow step of the catalytic cycle being reaction of the formate complex, $[\kappa^4\text{-Tptm}]\text{ZnO}_2\text{CH}$, with $(\text{EtO})_3\text{SiH}$. The trimethylsiloxide complex, $[\kappa^4\text{-Tptm}]\text{ZnOSiMe}_3$, can be used as an effective precatalyst with very low catalyst loadings. For example, employing 0.25 mol % of $[\kappa^4\text{-Tptm}]\text{ZnOSiMe}_3$, quantitative conversion of $(\text{EtO})_3\text{SiH}$ is achieved, corresponding to a TON of 400 with a TOF of 4.2 h^{-1} . While this is not a high TOF, it is within the range observed for ruthenium-catalyzed hydrosilylation of CO_2 .^{30,32b,44}

A possible mechanism for the catalytic cycle is illustrated in Scheme 18, with support for this mechanism as follows: (i) $[\kappa^3\text{-Tptm}]\text{ZnH}$ reacts rapidly with CO_2 to give the formate complex $[\kappa^4\text{-Tptm}]\text{ZnO}_2\text{CH}$, (ii) $[\kappa^4\text{-Tptm}]\text{ZnO}_2\text{CH}$ reacts with $(\text{EtO})_3\text{SiH}$ at elevated temperatures to regenerate $[\kappa^3\text{-Tptm}]\text{ZnH}$, (iii) $[\kappa^4\text{-Tptm}]\text{ZnO}_2\text{CH}$ may be employed as the initial catalyst, (iv) $[\kappa^4\text{-Tptm}]\text{ZnO}_2\text{CH}$ has been identified by ^1H NMR spectroscopy as the resting state of the catalyst and (v) the catalyst can be recovered as $[\kappa^4\text{-Tptm}]\text{ZnO}_2\text{CH}$ at the end of the reaction. The ability of zinc to effect the hydrosilylation of CO_2 provides fundamental evidence that it is possible that inexpensive, abundant metals can replace precious transition metals that are currently used in these catalytic processes.

The synthesis of silyl formates by the catalyzed hydrosilylation of CO_2 is fully atom efficient and environmentally benign, in contrast to other synthetic methods involving the reaction of silyl halides or triflates with formic acid in the presence of a base (*e.g.* pyridine or Et_3N).⁴⁵ Also of significance is that the zinc-catalyzed hydrosilylation can be performed without the use of solvent (*i.e.* neat reaction). This is in contrast to the ruthenium-catalyzed reaction between Et_3SiH and CO_2 , which gives $\text{HCO}_2\text{SiEt}_3$ in acetonitrile solution, but the siloxane $\text{Et}_3\text{SiOSiEt}_3$ in the absence of a solvent.^{32c}

Silyl formates are of interest because they have the potential for serving as formylating agents.⁴⁶ This overall transformation would provide a means to convert CO_2 into other useful compounds. In this vein, the product of hydrosilylation, $\text{HCO}_2\text{Si}(\text{OEt})_3$, is a reactive formylation agent. For example, treatment with aqueous HCl results in an immediate, exothermic reaction producing ethyl formate, HCO_2Et (Scheme 19). Addition of amines result in formyl transfer to generate the formamide; reaction with Me_2NH results in an immediate, exothermic reaction to give *N,N*-dimethylformamide, Me_2NCHO (Scheme 19). By comparison, amines do not react with simple alkyl esters under these conditions in the absence of a catalyst.⁴⁷



Scheme 19. Formyl transfer from $\text{HCO}_2\text{Si}(\text{OEt})_3$ to give HCO_2Et and Me_2NCHO .

3.5 Synthesis of κ^3 enforced compounds: $[\text{Bptm}^*]\text{H}$

As described previously (chapter 1), the $[\text{Tptm}]$ ligand has the ability to bind to zinc in two different coordination modes, namely κ^3 or κ^4 . We have demonstrated that $[\kappa^3\text{-Tptm}]\text{ZnH}$ is capable of catalyzing the hydrosilylation of CO_2 . However, a negative aspect of this system is that catalysis does not occur at room temperature. Due to the fact that the slow step (*i.e.* the turnover limiting step) is the reaction between $[\kappa^4\text{-Tptm}]\text{ZnO}_2\text{CH}$ and $(\text{EtO})_3\text{SiH}$, we hypothesized that destabilization of $[\kappa^4\text{-Tptm}]\text{ZnO}_2\text{CH}$ would result in a faster reaction. Since $[\kappa^4\text{-Tptm}]\text{ZnO}_2\text{CH}$ exists with the $[\text{Tptm}]$ ligand binding with a κ^4 -coordination, it may be presumed that the κ^3 -isomer, $[\kappa^3\text{-Tptm}]\text{ZnO}_2\text{CH}$, would be higher in energy, and thus more reactive (DFT calculations predict that the κ^4 -isomer is lower in energy by $3.81 \text{ kcal mol}^{-1}$).

$[\kappa^3\text{-Tptm}]\text{ZnO}_2\text{CH}$ presumably cannot be synthesized, so modification of the ligand was necessary. One idea was to replace one of the 2-mercaptopyridine arms with an isomer, namely 4-mercaptopyridine; the nitrogen atom of the pyridine ring is at the 4 position relative to the mercapto group and could not coordinate to the metal center (Figure 20). An alternative idea was to use an aromatic ring that did not possess a coordinating atom; specifically, *para*-thiocresol (*i.e.* 4-methylbenzenethiol) was

selected because the methyl group would provide a distinct ^1H NMR spectroscopic signal (Figure 20).

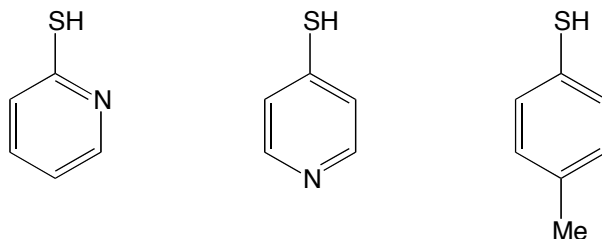
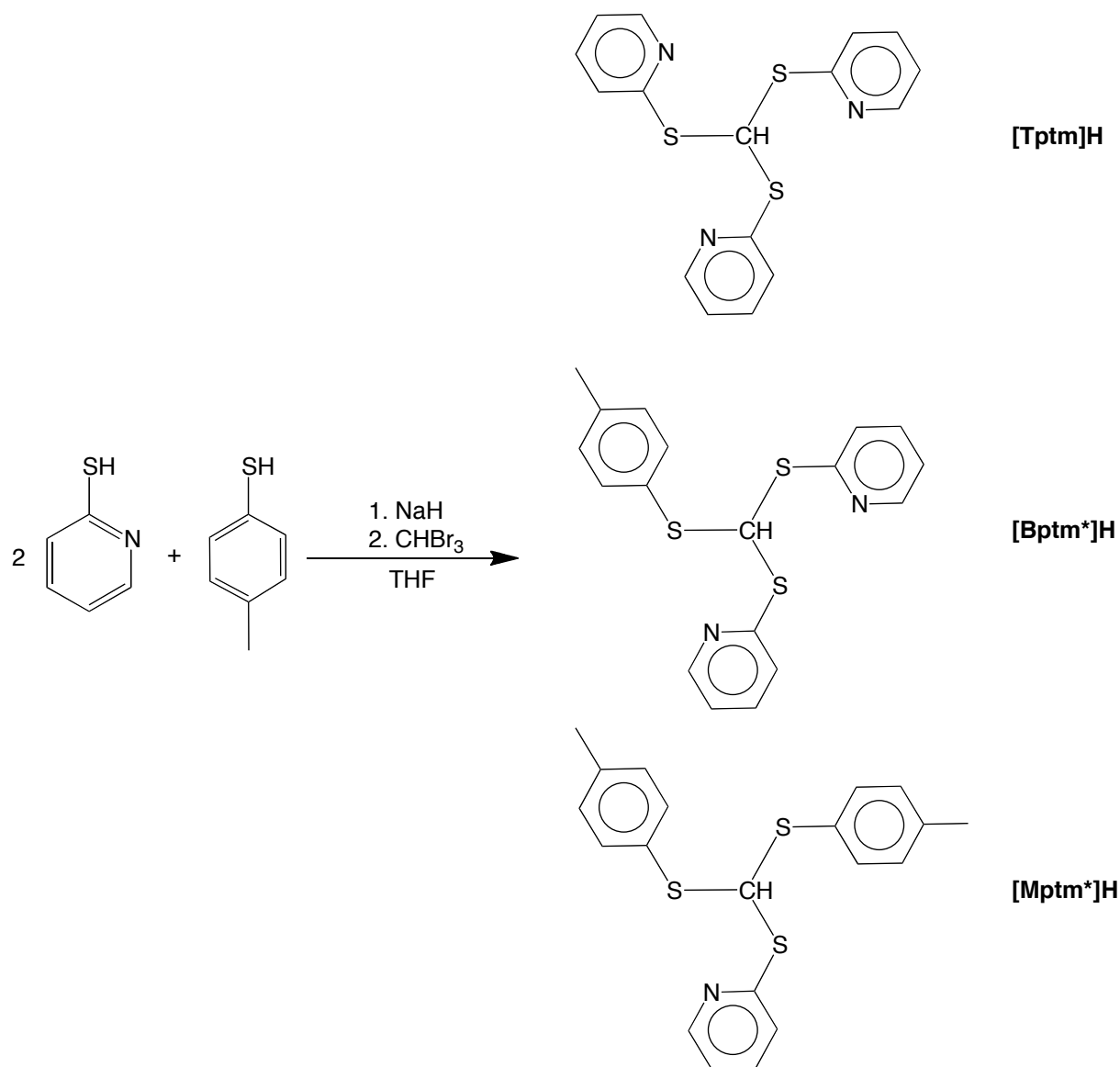


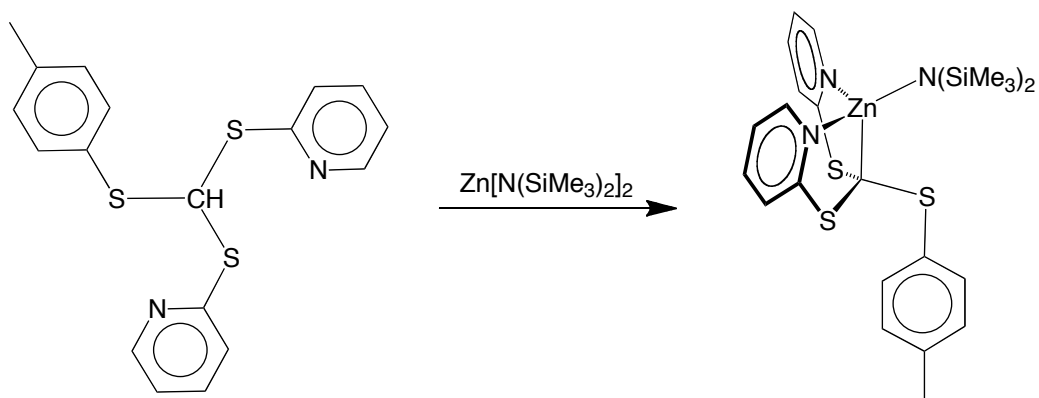
Figure 20. 2-mercaptopyridine (left), 4-mercaptopyridine (middle) and *para*-thiocresol (right).

In order to synthesize the desired κ^3 -enforced ligand, namely, $[\text{Bptm}^*]\text{H}$ ($\text{Bptm}^* = \text{bis}(2\text{-pyridylthio})(p\text{-tolylthio)methyl}$), a two to one ratio of 2-mercaptopyridine and *para*-thiocresol were deprotonated using sodium hydride, to which bromoform was then added. The reaction generated a statistical mixture of compounds that were separable *via* flash column chromatography (Scheme 20). Summarized in Scheme 20, $[\text{Tptm}]\text{H}$, $[\text{Bptm}^*]\text{H}$ and $[\text{Mptm}^*]\text{H}$ are produced in the reaction, with only trace amounts of $\text{HC}(p\text{-thiocresolate})_3$ (not shown in Scheme 20). When isolated as a pure compound, $[\text{Bptm}^*]\text{H}$ is an orange viscous oil.



Scheme 20. Synthesis of [Bptm*]H.

[Bptm*]H reacts readily with $\text{Zn}[\text{N}(\text{SiMe}_3)_2]_2$ in benzene to produce the *bis*(trimethylsilyl)amide complex, $[\kappa^3\text{-Bptm}^*]\text{ZnN}(\text{SiMe}_3)_2$ (Scheme 21). The molecular structure of $[\kappa^3\text{-Bptm}^*]\text{ZnN}(\text{SiMe}_3)_2$ has been determined by single crystal X-ray diffraction, which is shown in Figure 21. As expected, the [Bptm*] ligand binds in a $\kappa^3\text{-CN}_2$ fashion.



Scheme 21. Synthesis of $[\kappa^3\text{-Bptm}^*]\text{ZnN}(\text{SiMe}_3)_2$.

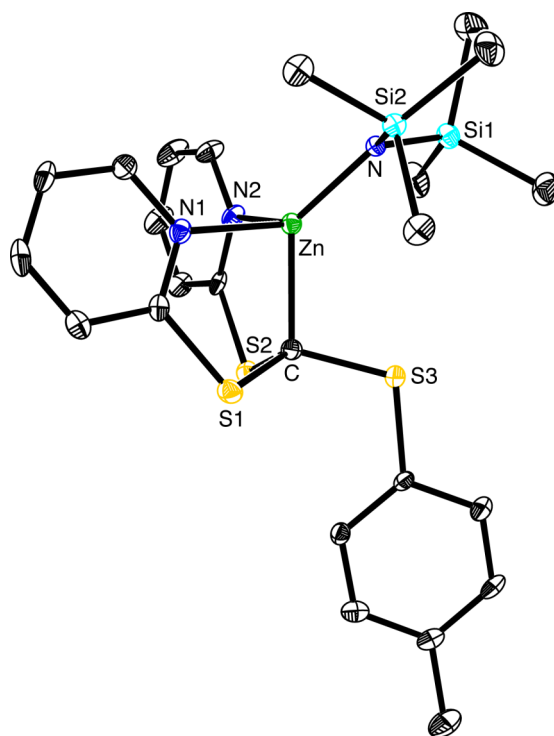
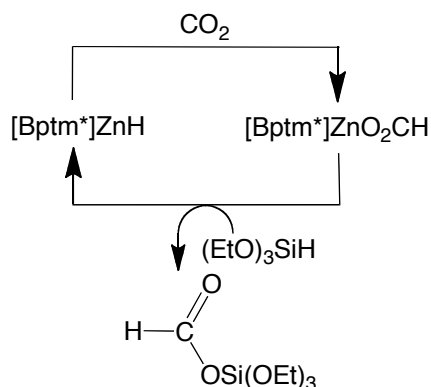


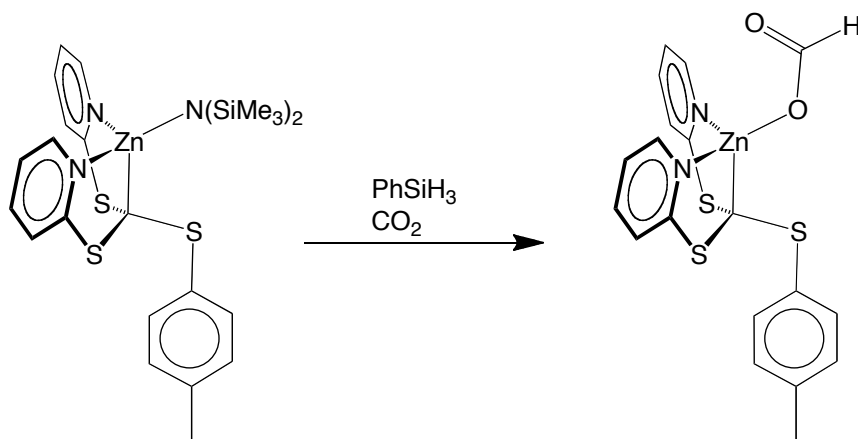
Figure 21. Molecular structure of $[\kappa^3\text{-Bptm}^*]\text{ZnN}(\text{SiMe}_3)_2$.

While $[\kappa^3\text{-Bptm}^*]\text{ZnH}$ is the desired compound for use as a CO_2 hydrosilylation catalyst, to date, the hydride complex has not yet been isolated. If $[\kappa^3\text{-Bptm}^*]\text{ZnH}$ were to be an active catalyst, then the formate complex should presumably also be active, as it is the product of the reaction between $[\kappa^3\text{-Bptm}^*]\text{ZnH}$ and CO_2 . This anticipated

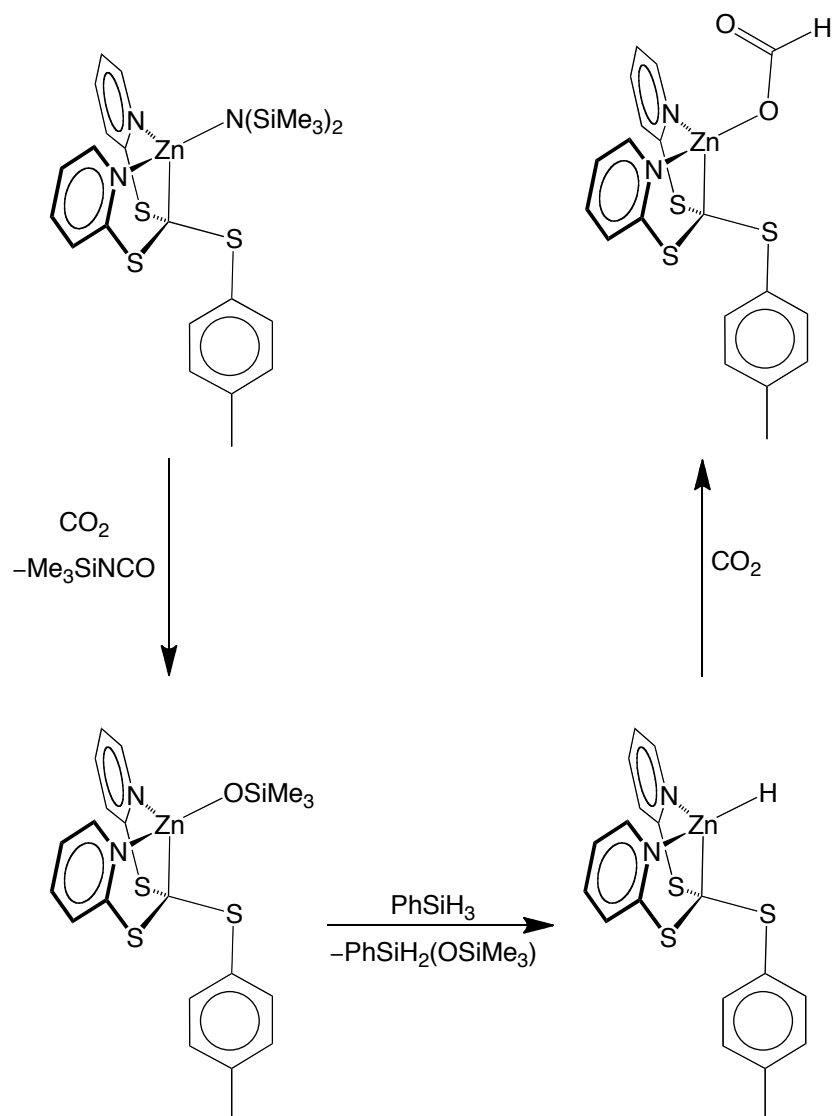
catalytic cycle is depicted in Scheme 22. $[\kappa^3\text{-Bptm}^*]\text{ZnO}_2\text{CH}$ has been synthesized *via* treatment of $[\kappa^3\text{-Bptm}^*]\text{ZnN}(\text{SiMe}_3)_2$ with CO_2 in the presence of PhSiH_3 (Scheme 23). This synthetic method was based on the reactivity observed between $[\kappa^3\text{-Tptm}]\text{ZnN}(\text{SiMe}_3)_2$ and CO_2 (*i.e.* $[\kappa^4\text{-Tptm}]\text{ZnOSiMe}_3$ is first generated, which we have demonstrated reacts with various silanes to produce $[\kappa^3\text{-Tptm}]\text{ZnH}$). A proposed mechanism for the formation of $[\kappa^3\text{-Bptm}^*]\text{ZnO}_2\text{CH}$ from $[\kappa^3\text{-Bptm}^*]\text{ZnN}(\text{SiMe}_3)_2$ is depicted in Scheme 24. The molecular structure of $[\kappa^3\text{-Bptm}^*]\text{ZnO}_2\text{CH}$ has also been determined by single crystal X-ray diffraction, and is depicted in Figure 22.



Scheme 22. $[\kappa^3\text{-Bptm}^*]\text{ZnH}$ catalyzed hydrosilylation of CO_2 by $(\text{EtO})_3\text{SiH}$.



Scheme 23. Synthesis of $[\kappa^3\text{-Bptm}^*]\text{ZnO}_2\text{CH}$.



Scheme 24. Proposed mechanism of formation for $[\kappa^3\text{-Bptm}^*]\text{ZnO}_2\text{CH}$.

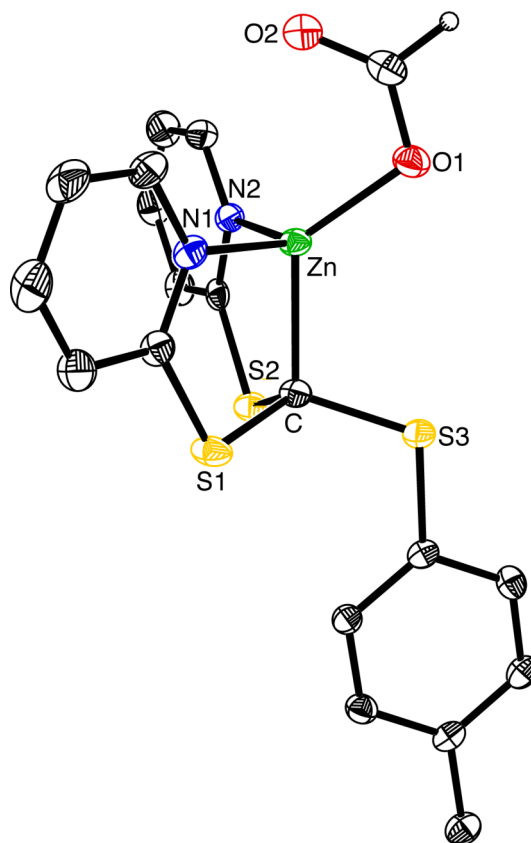


Figure 22. Molecular structure of $[\kappa^3\text{-Bptm}^*]\text{ZnO}_2\text{CH}$.

It is exciting that $[\kappa^3\text{-Bptm}^*]\text{ZnO}_2\text{CH}$ is an active, room-temperature catalyst for the hydrosilylation of CO_2 (Scheme 22). For example, 0.8 mol % of $[\kappa^3\text{-Bptm}^*]\text{ZnO}_2\text{CH}$ in benzene solvent achieves 13 turnovers at room temperature in 68 hours, corresponding to a TOF of 0.2 h^{-1} .⁴⁸ This is different than the [Tptm] system, which shows no catalysis at room temperature. The silylformate derivative, $\text{HCO}_2\text{Si}(\text{OEt})_3$ is the product of this catalysis.

3.6 Summary and conclusions

In summary, the zinc hydride complex, $[\kappa^3\text{-Tptm}]\text{ZnH}$, is an effective and robust catalyst for (i) rapid generation of hydrogen on demand, (ii) hydrosilylation of aldehydes and ketones producing siloxanes and (iii) the functionalization of CO_2 that

produces a useful formylating agent. Additionally, $[\kappa^3\text{-Bptm}^*]\text{ZnO}_2\text{CH}$ has been synthesized, which serves as a room temperature catalyst for the hydrosilylation of CO_2 . These results provide further evidence that, in suitable ligand environments, cheap and abundant non-transition metals can perform reactions that are typically catalyzed by compounds that contain precious metals.

3.7 Experimental details

3.7.1 General considerations

All manipulations were performed using a combination of glovebox, high vacuum, and Schlenk techniques under a nitrogen or argon atmosphere.⁴⁹ Solvents were purified and degassed by standard procedures. ^1H NMR spectra were measured on Bruker 300 DRX, Bruker 400 DRX, and Bruker Avance 500 DMX spectrometers. ^1H NMR chemical shifts are reported in ppm relative to SiMe_4 ($\delta = 0$) and were referenced internally with respect to the protio solvent impurity (δ 7.16 for $\text{C}_6\text{D}_5\text{H}$, 7.26 for CHCl_3).⁵⁰ ^{13}C NMR spectra are reported in ppm relative to SiMe_4 ($\delta = 0$) and were referenced internally with respect to the solvent (δ 128.06 for C_6D_6 and δ 77.16 for CDCl_3).⁵⁰ ^{29}Si NMR are reported in ppm relative to internal SiMe_4 ($\delta = 0$). Coupling constants are given in hertz. Infrared spectra were recorded on Nicolet Avatar 370 DTGS spectrometer and are reported in cm^{-1} . Mass spectra were obtained on a Micromass Quadrupole-Time-of-Flight mass spectrometer using fast atom bombardment (FAB). All chemicals were obtained from Aldrich, with the exception of phenylsilane (97 %, Alfa Aesar), triethoxysilane (Alfa Aesar) and methanol (Fisher Scientific). $[\kappa^4\text{-Tptm}]\text{ZnOSiMe}_3$,⁵¹ $[\kappa^3\text{-Tptm}]\text{ZnH}$,⁵¹ and $[\kappa^4\text{-Tptm}]\text{ZnO}_2\text{CH}$ ⁵¹ were prepared by the literature methods.

3.7.2 Computational details

Calculations were carried out using DFT as implemented in the Jaguar 7.5 (release 207) suite of *ab initio* quantum chemistry programs.⁵² Geometry optimizations were performed with the B3LYP density functional⁵³ using the 6-31G** (C, H, N, O, S) and LAV3P (Zn) basis sets.⁵⁴ The energies of the optimized structures were reevaluated by additional single point calculations on each optimized geometry using cc-pVTZ(-f)⁵⁵ correlation consistent triple- ζ (C, H, N, O, Si, S,) and LAV3P (Zn) basis sets.

3.7.3 X-ray structure determinations

X-ray diffraction data were collected on a Bruker Apex II diffractometer. Crystal data, data collection and refinement parameters are summarized in Table 4. The structures were solved using direct methods and standard difference map techniques, and were refined by full-matrix least-squares procedures on F^2 with SHELXTL (Version 6.1).⁵⁶

3.7.4 [κ^3 -Tptm]ZnH catalyzed hydrolysis of PhSiH₃

(i) A mixture of PhSiH₃ (10 μ L, 0.08 mmol) and [κ^3 -Tptm]ZnH (5 mg, 0.01 mmol, 5.0 mol % per SiH bond) in THF-*d*₈ (*ca.* 0.7 mL) was treated with H₂O (10 μ L, 0.56 mmol) resulting in the rapid generation of H₂. The mixture was monitored by ¹H NMR spectroscopy which demonstrated the evolution of H₂ over a period of 1 hour.

(ii) A mixture of PhSiH₃ (700 μ L, 5.67 mmol) and [κ^3 -Tptm]ZnH (69 mg, 0.17 mmol, 1.0 mol % per SiH bond) in THF (2.0 mL) was treated with H₂O (500 μ L, 27.75 mmol), thereby resulting in the rapid evolution of H₂, which was measured volumetrically. One equivalent of H₂ was released after 14 seconds (TOF = 8.58×10^3 h⁻¹) and two equivalents after 58 seconds (TOF = 4.14×10^3 h⁻¹). Release of the third equivalent occurred over *ca.* 4 hours (TOF = 25 h⁻¹ for the overall reaction). The volatile

components were then removed *in vacuo* to give a yellowish sticky solid. ^1H NMR (CDCl_3): δ 7.0 – 8.1 (broad and ill defined). $^{13}\text{C}\{^1\text{H}\}$ NMR (CDCl_3): 127.8, 130.3, 131.4 and 134.2 (broad). In the absence of a catalyst, a mixture of PhSiH_3 (480 mg, 4.44 mmol) and H_2O (400 μL , 22.20 mmol) in THF (2.0 mL) releases only 59 mL (18 %) of H_2 over a period of 115 hours; 115 mL of H_2 were released after 364 hours.

3.7.5 $[\kappa^4\text{-Tptm}]\text{ZnOSiMe}_3$ as a precatalyst for the hydrolysis of PhSiH_3

(i) A mixture of PhSiH_3 (10 μL , 0.08 mmol) and $[\kappa^4\text{-Tptm}]\text{ZnOSiMe}_3$ (5 mg, 0.01 mmol, 4.1 mol % per SiH bond) in THF- d_8 (*ca.* 0.7 mL) was treated with H_2O (10 μL , 0.55 mmol) resulting in the rapid generation of H_2 . The mixture was monitored by ^1H NMR spectroscopy which demonstrated the evolution of H_2 over a period of 1 hour.

(ii) A solution of $[\kappa^4\text{-Tptm}]\text{ZnOSiMe}_3$ (40 mg, 0.08 mmol, 1.0 mol % per SiH bond) and PhSiH_3 (290 mg, 2.68 mmol) in THF (1.20 mL) was treated with H_2O (160 μL , 8.88 mmol) and the hydrogen released was measured volumetrically. One equivalent of H_2 was released after 12 seconds ($\text{TOF} = 1.00 \times 10^4 \text{ h}^{-1}$) and two equivalents after 90 seconds ($\text{TOF} = 2.67 \times 10^3 \text{ h}^{-1}$). Release of the third equivalent occurred over *ca.* 4 hours ($\text{TOF} = 25 \text{ h}^{-1}$ for the overall reaction).

(iii) A suspension of $[\kappa^4\text{-Tptm}]\text{ZnOSiMe}_3$ (1 mg, 0.002 mmol) and PhSiH_3 (35 mg, 0.32 mmol) in THF (*ca.* 0.5 mL) in a small vial was treated with H_2O (50 μL , 2.77 mmol). The vial was closed with a rubber septum that was pierced with a cannula. The gas released was bubbled for two minutes *via* the cannula into C_6D_6 (*ca.* 1 mL) in a small vial. The solution in C_6D_6 was transferred to an NMR tube equipped with a J. Young valve and analyzed by ^1H NMR spectroscopy, thereby indicating the presence of H_2 .

3.7.6 $\{[\kappa^3\text{-Tptm}]\text{Zn}(\mu\text{-OH})\}_2$ catalyzed hydrolysis of PhSiH_3

(i) A solution of $\{[\kappa^3\text{-Tptm}]\text{Zn}(\mu\text{-OH})\}_2$ (8 mg, 0.01 mmol) in C_6D_6 (ca. 0.7 mL) in an NMR tube equipped with a J. Young valve was treated with PhSiH_3 (20 mg, 0.18 mmol) and H_2O (50 μL , 2.77 mmol). The reaction was monitored by ^1H NMR spectroscopy, thereby providing evidence for evolution of H_2 over a period of 1 day.

(ii) A solution of PhSiH_3 (88 mg, 0.81 mmol) and H_2O (75 μL , 4.16 mmol) in THF (1.0 mL) was added to $\{[\kappa^3\text{-Tptm}]\text{Zn}(\mu\text{-OH})\}_2$ (20 mg, 0.02 mmol, 1.9 mol % of monomeric $[\text{Tptm}]\text{ZnOH}$ per SiH bond), resulting in the rapid evolution of H_2 , which was measured volumetrically. One equivalent of H_2 was released after 7 seconds (TOF = $8.88 \times 10^3 \text{ h}^{-1}$) and two equivalents after 32 seconds (TOF = $3.89 \times 10^3 \text{ h}^{-1}$). Release of the third equivalent occurred over ca. 1 hour (TOF = 52 h^{-1} for the overall reaction).

3.7.7 Reaction of $\{[\kappa^3\text{-Tptm}]\text{Zn}(\mu\text{-OH})\}_2$ with PhSiH_3 to give $[\kappa^3\text{-Tptm}]\text{ZnH}$

A solution of $\{[\kappa^3\text{-Tptm}]\text{Zn}(\mu\text{-OH})\}_2$ (3 mg, 0.004 mmol) in C_6D_6 (ca. 0.7 mL) in an NMR tube equipped with a J. Young valve was treated with PhSiH_3 (20 mg, 0.18 mmol). The reaction was monitored by ^1H NMR spectroscopy, thereby indicating the conversion to $[\kappa^3\text{-Tptm}]\text{ZnH}$ after a period of 15 minutes at room temperature.

3.7.8 $[\kappa^3\text{-Tptm}]\text{ZnH}$ catalyzed methanolysis of PhSiH_3 to give $\text{PhSi}(\text{OMe})_3$

A mixture of PhSiH_3 (25 mg, 0.23 mmol) and $[\kappa^3\text{-Tptm}]\text{ZnH}$ (2 mg, 0.005 mmol) in C_6D_6 (ca. 0.7 mL) was treated with MeOH (9.0 μL , 0.22 mmol). The mixture was monitored by ^1H NMR spectroscopy which demonstrated the evolution of H_2 and a reaction mixture with the composition of PhSiH_3 , $\text{PhSiH}(\text{OMe})_2$, $\text{PhSi}(\text{OMe})_3$ in a 10:5:1 ratio after 20 minutes. The mixture was then treated with MeOH (9.0 μL , 0.22 mmol), and monitored by ^1H NMR spectroscopy which demonstrated the evolution of H_2 and a

reaction mixture with the composition of PhSiH_3 , $\text{PhSiH}(\text{OMe})_2$, and $\text{PhSi}(\text{OMe})_3$ in a 1:5:1 ratio after 20 minutes. The mixture was then treated with MeOH (15.0 μL , 0.37 mmol), and monitored by ^1H NMR spectroscopy which demonstrated the evolution of H_2 and the clean formation of $\text{PhSi}(\text{OMe})_3$ after 20 minutes. The mixture was then passed through a small plug of silica, and the volatiles were evaporated *in vacuo* giving $\text{PhSi}(\text{OMe})_3$ as a colorless oil, as identified by comparison of the NMR data to the literature data.⁵⁷

^1H NMR (CDCl_3): 3.65 [s, 9H, $\text{PhSi}(\text{OCH}_3)_3$], 7.39-7.49 [m, 3H, $\text{PhSi}(\text{OCH}_3)_3$], 7.66-7.69 [m, 2H, $\text{PhSi}(\text{OCH}_3)_3$]. $^{13}\text{C}\{^1\text{H}\}$ NMR (CDCl_3): 51.0 [s, 3C, $\text{PhSi}(\text{OCH}_3)_3$], 128.1 [s, 2C, $\text{PhSi}(\text{OCH}_3)_3$], 129.5 [s, 1C, $\text{PhSi}(\text{OCH}_3)_3$], 130.8 [s, 1C, $\text{PhSi}(\text{OCH}_3)_3$], 134.9 [s, 2C, $\text{PhSi}(\text{OCH}_3)_3$].

3.7.9 $[\kappa^4\text{-Tptm}]\text{ZnOSiMe}_3$ as a precatalyst for the methanolysis of PhSiH_3 to give $\text{PhSi}(\text{OMe})_3$

(i) A solution of $[\kappa^4\text{-Tptm}]\text{ZnOSiMe}_3$ (40.0 μL of 0.008 M in toluene, 3.2×10^{-4} mmol, 0.001 mol % per SiH bond) and PhSiH_3 (1350 μL , 10.94 mmol) in toluene (1.00 mL) was treated with MeOH (1.60 mL, 39.50 mmol). The rapid evolution of hydrogen was measured volumetrically. One equivalent of H_2 was released after 75 seconds (TOF = $1.63 \times 10^6 \text{ h}^{-1}$) and two equivalents after 171 seconds (TOF = $1.43 \times 10^6 \text{ h}^{-1}$). Release of the third equivalent occurred over *ca.* 1 hour (TOF = $1.02 \times 10^5 \text{ h}^{-1}$ for the overall reaction). In the absence of a catalyst, a mixture of PhSiH_3 (1154 mg, 10.66 mmol) and MeOH (1.60 mL, 39.50 mmol) in toluene (1.0 mL) releases only 380 mL of H_2 (48 %) over a period of 123 hours.

(ii) A solution of $[\kappa^4\text{-Tptm}]\text{ZnOSiMe}_3$ (16 mg, 0.03 mmol, 0.1 mol % per SiH bond) and PhSiH_3 (1300 μL , 10.54 mmol) in toluene (1.00 mL) was treated with MeOH (1.60 mL,

39.50 mmol). The rapid evolution of hydrogen was measured volumetrically, thereby demonstrating that 85 % of the H₂ was released after 5 seconds (TOF = $6.11 \times 10^5 \text{ h}^{-1}$). Complete release of 3 equivalents was observed after 420 seconds.

3.7.10 [κ^4 -Tptm]ZnOSiMe₃ as a precatalyst for the stepwise methanolysis of PhSiH₃

A solution of [κ^4 -Tptm]ZnOSiMe₃ (16.0 mg, 0.03 mmol) and PhSiH₃ (1154 mg, 10.66 mmol) in toluene (1.0 mL) was treated with MeOH (250 μL , 6.17 mmol) and the hydrogen released was measured volumetrically. Additional portions of MeOH were added on an hourly basis until the PhSiH₃ was fully consumed (6 times total).

3.7.11 [κ^4 -Tptm]ZnOSiMe₃ as a precatalyst for the methanolysis of PhSiH₃ to give PhSi(OMe)₃ at 0 °C

A solution of [κ^4 -Tptm]ZnOSiMe₃ (30.0 μL of 0.01 M in toluene, 3.0×10^{-4} mmol, 0.025 mol % per SiH bond) and PhSiH₃ (50 μL , 0.41 mmol) in toluene (1.00 mL) was placed in an ice-bath and treated with MeOH (1.00 mL, 24.69 mmol). The evolution of hydrogen was measured volumetrically. One equivalent of H₂ was released after 40 seconds (TOF = $1.21 \times 10^5 \text{ h}^{-1}$) and two equivalents after 197 seconds (TOF = $4.90 \times 10^4 \text{ h}^{-1}$). Release of the third equivalent was much slower, requiring *ca.* 1 hour (TOF = $4.03 \times 10^3 \text{ h}^{-1}$).

3.7.12 [κ^4 -Tptm]ZnOSiMe₃ as a precatalyst for the methanolysis of PhSiH₃ to give PhSiH(OMe)₂

A solution of [κ^4 -Tptm]ZnOSiMe₃ (1.0 mg, 0.002 mmol) in toluene (2.0 mL) was placed in an ice bath and was treated with PhSiH₃ (1140 μL , 9.24 mmol). The mixture was stirred for 2 minutes and then treated with MeOH (0.8 mL, 19.75 mmol), thereby resulting in the rapid evolution of H₂. The volatile components were removed *in vacuo* after 15 minutes and the colorless liquid obtained was distilled *in vacuo* at 40 °C to give PhSi(OMe)₂H (940 mg, 57%) which contained a 6 mole percent impurity of PhSi(OMe)₃.

^1H NMR (C_6D_6): 3.40 [s, 6H, $\text{PhSiH}(\text{OCH}_3)_2$], 5.14 [s, 1H, $\text{PhSiH}(\text{OCH}_3)_2$], 7.16-7.19 [m, 3H, $\text{PhSiH}(\text{OCH}_3)_2$], 7.70-7.72 [m, 2H, $\text{PhSiH}(\text{OCH}_3)_2$]. $^{13}\text{C}\{^1\text{H}\}$ NMR (C_6D_6): 50.91 [s, 2C, $\text{PhSiH}(\text{OCH}_3)_2$], 128.3 [s, 2C, $\text{PhSiH}(\text{OCH}_3)_2$], 131.0 [s, 1C, $\text{PhSiH}(\text{OCH}_3)_2$], 133.1 [s, 1C, $\text{PhSiH}(\text{OCH}_3)_2$], 134.5 [s, 2C, $\text{PhSiH}(\text{OCH}_3)_2$].

3.7.13 [κ^3 -Tptm]ZnH catalyzed methanolysis of PhMeSiH_2 to give $\text{PhMeSiH}(\text{OMe})$

A suspension of [κ^3 -Tptm]ZnH (1.0 mg, 0.002 mmol, 0.3 mol % per SiH bond) in C_6D_6 (0.7 mL) in a small vial was treated with PhMeSiH_2 (50 μL , 0.36 mmol). MeOH (15.0 μL , 0.37 mmol) was then added to the mixture, thereby resulting in the rapid evolution of H_2 over a period of *ca.* 30 minutes. The reaction was then analyzed by ^1H NMR spectroscopy, thereby indicating the presence of PhMeSiH_2 , $\text{PhMeSiH}(\text{OMe})$ and $\text{PhMeSi}(\text{OMe})_2$ in a *ca.* 3:11:1 ratio (TON = 129 and TOF = 258 h^{-1}).

3.7.14 [κ^3 -Tptm]ZnH catalyzed methanolysis of PhMeSiH_2 to give $\text{PhMeSi}(\text{OMe})_2$

A suspension of [κ^3 -Tptm]ZnH (1.0 mg, 0.002 mmol, 0.3 mol % per SiH bond) in C_6D_6 (0.7 mL) in a small vial was treated with PhMeSiH_2 (50 μL , 0.36 mmol). MeOH (40.0 μL , 0.99 mmol) was then added to the mixture, thereby resulting in the rapid evolution of H_2 over a period of *ca.* 6 minutes. The reaction was analyzed by ^1H NMR spectroscopy, thereby indicating the quantitative conversion to $\text{PhMeSi}(\text{OMe})_2$ (TON = 298 and TOF = $2.98 \times 10^3 \text{ h}^{-1}$).

^1H NMR (CDCl_3): 0.36 [s, 3H, $\text{PhMeSi}(\text{OCH}_3)_2$], 3.57 [s, 6H, $\text{PhMeSi}(\text{OCH}_3)_2$], 7.38-7.45 [m, 3H, $\text{PhMeSi}(\text{OCH}_3)_2$], 7.62 [d, $^3J_{\text{H-H}} = 7 \text{ Hz}$, 2H, $\text{PhMeSi}(\text{OCH}_3)_2$]. $^{13}\text{C}\{^1\text{H}\}$ NMR (CDCl_3): -5.0 [s, 1C, $\text{PhMeSi}(\text{OCH}_3)_2$], 50.7 [s, 2C, $\text{PhMeSi}(\text{OCH}_3)_2$], 128.1 [s, 2C, $\text{PhMeSi}(\text{OCH}_3)_2$], 130.3 [s, 1C, $\text{PhMeSi}(\text{OCH}_3)_2$], 133.9 [s, 1C, $\text{PhMeSi}(\text{OCH}_3)_2$], 134.1 [s, 2C, $\text{PhMeSi}(\text{OCH}_3)_2$].

3.7.15 [κ^3 -Tptm]ZnH catalyzed alcoholysis of PhSiH₃ with EtOH to give PhSi(OEt)₃

[κ^3 -Tptm]ZnH (2 mg, 0.005 mmol, 0.4% mole catalyst per SiH bond) was added to a mixture of PhSiH₃ (44 mg, 0.41 mmol) and EtOH (80 mg, 1.74 mmol) in a small vial, thereby resulting in the rapid, exothermic evolution of H₂ over a period of one minute. The product was analyzed by ¹H NMR spectroscopy, thereby showing >99% conversion of PhSiH₃ to PhSi(OEt)₃ (TON = 248, TOF = 1.49 × 10⁴ h⁻¹), as identified by comparison of the NMR data to the literature data.⁵⁸

¹H NMR (CDCl₃): 1.25 [t, ³J_{H-H} = 7 Hz, 9H, PhSi(OCH₂CH₃)₃], 3.87 [q, ³J_{H-H} = 7 Hz, 6H, PhSi(OCH₂CH₃)₃], 7.35-7.43 [m, 3H, PhSi(OCH₂CH₃)₃], 7.66-7.69 [m, 2H, PhSi(OCH₂CH₃)₃]. ¹³C{¹H} NMR (CDCl₃): 18.4 [s, 3C, PhSi(OCH₂CH₃)₃], 58.9 [s, 3C, PhSi(OCH₂CH₃)₃], 128.0 [s, 2C, PhSi(OCH₂CH₃)₃], 130.5 [s, 1C, PhSi(OCH₂CH₃)₃], 131.1 [s, 1C, PhSi(OCH₂CH₃)₃], 135.0 [s, 2C, PhSi(OCH₂CH₃)₃].

3.7.16 [κ^3 -Tptm]ZnH catalyzed alcoholysis of PhSiH₃ with PrⁱOH to give PhSi(OPrⁱ)₃

A suspension of [κ^3 -Tptm]ZnH (4 mg, 0.01 mmol, 0.8 mol % per SiH bond) in C₆D₆ (ca. 0.7 mL) in an NMR tube equipped with a J. Young valve was treated with PhSiH₃ (44 mg, 0.41 mmol). PrⁱOH (108 mg, 1.80 mmol) was added and the reaction was monitored by ¹H NMR spectroscopy, thereby demonstrating the evolution of H₂ and formation of PhSi(OPrⁱ)₃ over a period of 2 hours (TON = 125 and TOF = 62 h⁻¹).

¹H NMR (CDCl₃): 1.24 [d, ³J_{H-H} = 6 Hz, 18H, PhSi(OCH(CH₃)₂)₃], 4.30 [sept, ³J_{H-H} = 6 Hz, 3H, PhSi(OCH(CH₃)₂)₃], 7.36-7.43 [m, 3H, PhSi(OCH(CH₃)₂)₃], 7.70-7.73 [m, 2H, PhSi(OCH(CH₃)₂)₃]. ¹³C{¹H} NMR (CDCl₃): 25.6 [s, 6C, PhSi(OCH(CH₃)₂)₃], 65.5 [s, 3C, PhSi(OCH(CH₃)₂)₃], 127.8 [s, 2C, PhSi(OCH(CH₃)₂)₃], 130.1 [s, 1C, PhSi(OCH(CH₃)₂)₃], 132.9 [s, 1C, PhSi(OCH(CH₃)₂)₃], 135.0 [s, 2C, PhSi(OCH(CH₃)₂)₃]. PhSi(OPrⁱ)₃ has been previously reported.⁵⁹

3.7.17 [κ^3 -Tptm]ZnH catalyzed alcoholysis of PhSiH₃ with PhCH₂OH to give PhSi(OCH₂Ph)₃

[κ^3 -Tptm]ZnH (2 mg, 0.005 mmol, 0.4 mol % per SiH bond) was added to a mixture of PhSiH₃ (44 mg, 0.41 mmol) and PhCH₂OH (160 mg, 1.48 mmol) in a small vial, thereby resulting in the rapid exothermic evolution of H₂ over a period of one minute. The sample was analyzed by ¹H NMR spectroscopy, showing >99% conversion of PhSiH₃ to PhSi(OCH₂Ph)₃ (TON = 248, TOF = 1.49 × 10⁴ h⁻¹). The reaction mixture was then extracted into CH₂Cl₂ (ca. 2 mL), and washed with saturated aqueous Na₂CO₃ (ca. 3 mL). The volatile components were removed *in vacuo* and the colorless oil obtained was dissolved in CHCl₃ and passed through a small plug of silica. The solvent was removed *in vacuo* to give PhSi(OCH₂Ph)₃ as a colorless oil, as identified by comparison of the NMR data to the literature data.⁶⁰ Mass spectrum: *m/z* = 425.2 {M-1}⁺.

¹H NMR (CDCl₃): 4.86 [s, 6H, PhSi(OCH₂Ph)₃], 7.25-7.32 [m, 15H, PhSi(OCH₂Ph)₃], 7.37-7.41 [m, 2H, PhSi(OCH₂Ph)₃], 7.44-7.48 [m, 1H, PhSi(OCH₂Ph)₃], 7.70-7.72 [m, 2H, PhSi(OCH₂Ph)₃]. ¹³C NMR (CDCl₃): 65.2 [s, 3C, PhSi(OCH₂Ph)₃], 126.8 [s, 6C, PhSi(OCH₂Ph)₃], 127.4 [s, 3C, PhSi(OCH₂Ph)₃], 128.1 [s, 3C, PhSi(OCH₂Ph)₃], 128.4 [s, 6C, PhSi(OCH₂Ph)₃], 130.9 [s, 1C, PhSi(OCH₂Ph)₃], 131.0 [s, 1C, PhSi(OCH₂Ph)₃], 135.1 [s, 2C, PhSi(OCH₂Ph)₃], 140.2 [s, 2C, PhSi(OCH₂Ph)₃].

3.7.18 [κ^3 -Tptm]ZnH catalyzed alcoholysis of PhSiH₃ with racemic 1-phenylethanol to give PhSi[OCH(Me)Ph]₃

A suspension of [κ^3 -Tptm]ZnH (8 mg, 0.02 mmol, 0.8 mol % per SiH bond) in C₆D₆ (ca. 0.7 mL) in an NMR tube equipped with a J. Young valve was treated with PhSiH₃ (88 mg, 0.81 mmol). 1-Phenylethanol (393 μ L, 3.26 mmol) was added, thereby resulting in evolution of H₂ over a period of ca. 2.5 hours. The sample was analyzed by ¹H NMR spectroscopy, thereby demonstrating the conversion to PhSi[OCH(Me)Ph]₃ as a

statistical mixture of *RRR/SSS* and *RRS/RSS* diastereomers (TON = 125, TOF = 50 h⁻¹).

Mass spectrum: $m/z = 467.3 \{M-1\}^+$.

¹H NMR (CDCl₃): (RRR) 1.42 [d, ³J_{H-H} = 6 Hz, 9H, PhSi(OCH(CH₃)Ph)₃], 4.99 [q, ³J_{H-H} = 6 Hz, 3H, PhSi(OCH(CH₃)Ph)₃], 7.17-7.37 [m, 18H, PhSi(OCH(CH₃)Ph)₃], 7.57-7.60 [m, 2H, PhSi(OCH(CH₃)Ph)₃].

(RRS): 1.30 [d, ³J_{H-H} = 6 Hz, 3H, PhSi(OCH(CH₃)Ph)₃], 1.32 [d, ³J_{H-H} = 6 Hz, 3H, PhSi(OCH(CH₃)Ph)₃], 1.40 [d, ³J_{H-H} = 6 Hz, 3H, PhSi(OCH(CH₃)Ph)₃], 4.95-5.08 [m (overlapping with RRR diastereomer, 3H, PhSi(OCH(CH₃)Ph)₃), 7.17-7.37 [m (overlapping with RRR diastereomer), 18H, PhSi(OCH(CH₃)Ph)₃], 7.54-7.56 [m, 2H, PhSi(OCH(CH₃)Ph)₃].

¹H NMR (C₆D₆): (RRR) 1.44 [d, ³J_{H-H} = 6 Hz, 9H, PhSi(OCH(CH₃)Ph)₃], 5.12 [q, ³J_{H-H} = 6 Hz, 3H, PhSi(OCH(CH₃)Ph)₃], 7.05-7.30 [m overlapping with RRS diastereomer, 18H, PhSi(OCH(CH₃)Ph)₃], 7.82-7.85 [m, 2H, PhSi(OCH(CH₃)Ph)₃].

(RRS): 1.35 [d, ³J_{H-H} = 6 Hz, 3H, PhSi(OCH(CH₃)Ph)₃], 1.37 [d, ³J_{H-H} = 6 Hz, 3H, PhSi(OCH(CH₃)Ph)₃], 1.43 [d, ³J_{H-H} = 6 Hz, 3H, PhSi(OCH(CH₃)Ph)₃], 5.10-5.21 [m (overlapping with RRR diastereomer, 3H, PhSi(OCH(CH₃)Ph)₃), 7.05-7.30 [m (overlapping with RRR diastereomer), 18H, PhSi(OCH(CH₃)Ph)₃], 7.78-7.80 [m, 2H, PhSi(OCH(CH₃)Ph)₃].

¹³C{¹H} NMR (CDCl₃): (RRR) 26.8 [s, 3C, PhSi(OCH(CH₃)Ph)₃], 71.2 [s, 3C, PhSi(OCH(CH₃)Ph)₃], 125.5 [s, 6C, PhSi(OCH(CH₃)Ph)₃], 127.0 [s, 3C, PhSi(OCH(CH₃)Ph)₃], 127.8 [s, 2C, PhSi(OCH(CH₃)Ph)₃], 128.2 [s, 6C, PhSi(OCH(CH₃)Ph)₃], 130.3 [s, 1C, PhSi(OCH(CH₃)Ph)₃], 131.7 [s, 1C, PhSi(OCH(CH₃)Ph)₃], 135.1 [s, 2C, PhSi(OCH(CH₃)Ph)₃], 145.8 [s, 3C, PhSi(OCH(CH₃)Ph)₃].

¹³C{¹H} NMR (CDCl₃): RRR and RRS together: 26.59 [s, 1C, PhSi(OCH(CH₃)Ph)₃], 26.62 [s, 1C, PhSi(OCH(CH₃)Ph)₃], 26.72 [s, 1C, PhSi(OCH(CH₃)Ph)₃], 26.75 [s, 3C, PhSi(OCH(CH₃)Ph)₃], 71.25 [s, 3C, PhSi(OCH(CH₃)Ph)₃], 71.28 [s, 2C, PhSi(OCH(CH₃)Ph)₃].

PhSi(OCH(CH₃)Ph)₃], 71.3 [s, 1C, PhSi(OCH(CH₃)Ph)₃], 125.48 [s, 6C,
 PhSi(OCH(CH₃)Ph)₃], 125.50 [s, 2C, PhSi(OCH(CH₃)Ph)₃], 125.53 [s, 2C,
 PhSi(OCH(CH₃)Ph)₃], 125.55 [s, 2C, PhSi(OCH(CH₃)Ph)₃], 126.97 [s, 3C,
 PhSi(OCH(CH₃)Ph)₃], 127.05 [s, 3C, PhSi(OCH(CH₃)Ph)₃] 127.79 [s, 2C,
 PhSi(OCH(CH₃)Ph)₃], 127.81 [s, 2C, PhSi(OCH(CH₃)Ph)₃], 128.18 [s, 6C,
 PhSi(OCH(CH₃)Ph)₃], 128.24 [s, 6C, PhSi(OCH(CH₃)Ph)₃], 130.33 [s, 2C,
 PhSi(OCH(CH₃)Ph)₃], 131.56 [s, 1C, PhSi(OCH(CH₃)Ph)₃], 131.72 [s, 1C,
 PhSi(OCH(CH₃)Ph)₃], 135.09 [s, 4C, PhSi(OCH(CH₃)Ph)₃], 145.80 [s, 3C,
 PhSi(OCH(CH₃)Ph)₃], 145.84 [s, 1C, PhSi(OCH(CH₃)Ph)₃], 145.90 [s, 1C,
 PhSi(OCH(CH₃)Ph)₃], 145.94 [s, 1C, PhSi(OCH(CH₃)Ph)₃].

²⁹Si{¹H} NMR (CDCl₃): RRR: -60.75. RRS: -60.66. ²⁹Si{¹H} NMR (C₆D₆): RRR: -
 60.06. RRS: -59.99.

3.7.19 [κ^3 -Tptm]ZnH catalyzed alcoholysis of PhSiH₃ with (R)-(+)-1-phenylethanol to give RRR-PhSi[OCH(Me)Ph]₃

A suspension of [κ^3 -Tptm]ZnH (8 mg, 0.02 mmol, 0.8 mol % per SiH bond) in C₆D₆ (ca. 0.7 mL) in an NMR tube equipped with a J. Young valve was treated with PhSiH₃ (88 mg, 0.81 mmol). (R)-(+)-1-Phenylethanol (393 μ L, 3.26 mmol) was added, thereby resulting in evolution of H₂ over a period of ca. 2.5 hours. The sample was analyzed by ¹H NMR spectroscopy, thereby demonstrating the conversion to RRR-PhSi[OCH(Me)Ph]₃ (TON = 125, TOF = 50 h⁻¹). The volatile components were removed *in vacuo* and the colorless oil obtained was redissolved in CH₂Cl₂ (ca. 1 mL), and purified by flash column chromatography (silica gel, ca. 3 mL) to give RRR-PhSi[OCH(Me)Ph]₃ as a colorless oil after removal of the solvent *in vacuo*.

^1H NMR (CDCl_3): 1.42 [d, $^3J_{\text{H-H}} = 6$ Hz, 9H, $\text{PhSi}(\text{OCH}(\underline{\text{C}}\text{H}_3)\text{Ph})_3$], 4.99 [q, $^3J_{\text{H-H}} = 6$ Hz, 3H, $\text{PhSi}(\text{OCH}(\underline{\text{C}}\text{H}_3)\text{Ph})_3$], 7.17-7.37 [m, 18H, $\underline{\text{P}}\text{hSi}(\text{OCH}(\text{C}\text{H}_3)\underline{\text{P}}\text{h})_3$], 7.57-7.60 [m, 2H, $\underline{\text{P}}\text{hSi}(\text{OCH}(\text{C}\text{H}_3)\underline{\text{P}}\text{h})_3$].

^1H NMR (C_6D_6): 1.44 [d, $^3J_{\text{H-H}} = 6$ Hz, 9H, $\text{PhSi}(\text{OCH}(\underline{\text{C}}\text{H}_3)\text{Ph})_3$], 5.12 [q, $^3J_{\text{H-H}} = 6$ Hz, 3H, $\text{PhSi}(\text{OCH}(\underline{\text{C}}\text{H}_3)\text{Ph})_3$], 7.05-7.23 [m, 18H, $\underline{\text{P}}\text{hSi}(\text{OCH}(\text{C}\text{H}_3)\underline{\text{P}}\text{h})_3$], 7.82-7.84 [m, 2H, $\underline{\text{P}}\text{hSi}(\text{OCH}(\text{C}\text{H}_3)\underline{\text{P}}\text{h})_3$].

$^{13}\text{C}\{^1\text{H}\}$ NMR (CDCl_3): 26.8 [s, 3C, $\text{PhSi}(\text{OCH}(\underline{\text{C}}\text{H}_3)\text{Ph})_3$], 71.2 [s, 3C, $\text{PhSi}(\text{OCH}(\text{C}\text{H}_3)\text{Ph})_3$], 125.5 [s, 6C, $\text{PhSi}(\text{OCH}(\text{C}\text{H}_3)\underline{\text{P}}\text{h})_3$], 127.0 [s, 3C, $\text{PhSi}(\text{OCH}(\text{C}\text{H}_3)\underline{\text{P}}\text{h})_3$], 127.8 [s, 2C, $\underline{\text{P}}\text{hSi}(\text{OCH}(\text{C}\text{H}_3)\text{Ph})_3$], 128.2 [s, 6C, $\text{PhSi}(\text{OCH}(\text{C}\text{H}_3)\underline{\text{P}}\text{h})_3$], 130.3 [s, 1C, $\underline{\text{P}}\text{hSi}(\text{OCH}(\text{C}\text{H}_3)\text{Ph})_3$], 131.7 [s, 1C, $\underline{\text{P}}\text{hSi}(\text{OCH}(\text{C}\text{H}_3)\text{Ph})_3$], 135.1 [s, 2C, $\underline{\text{P}}\text{hSi}(\text{OCH}(\text{C}\text{H}_3)\text{Ph})_3$], 145.8 [s, 3C, $\text{PhSi}(\text{OCH}(\text{C}\text{H}_3)\underline{\text{P}}\text{h})_3$].

$^{29}\text{Si}\{^1\text{H}\}$ NMR (CDCl_3): RRR: -60.75. $^{29}\text{Si}\{^1\text{H}\}$ NMR (C_6D_6): RRR: -60.06.

3.7.20 [κ^3 -Tptm]ZnH catalyzed hydrosilylation of MeCHO with PhSiH_3 to give $\text{PhSi}(\text{OEt})_3$

A suspension of [κ^3 -Tptm]ZnH (2 mg, 0.005 mmol, 0.4 mol % per SiH bond) in C_6D_6 (ca. 0.7 mL) in an NMR tube equipped with a J. Young valve was treated with PhSiH_3 (44 mg, 0.41 mmol). MeCHO (ca. 1.0 mL, 17.89 mmol) was added, thereby resulting in an exothermic reaction to form $\text{PhSi}(\text{OEt})_3$, which was complete within 15 minutes as judged by ^1H NMR spectroscopy (TON = 249, TOF = $9.96 \times 10^2 \text{ h}^{-1}$). The volatile components were removed *in vacuo*, dissolved in CHCl_3 (ca. 1 mL), and passed through a small plug of silica, giving $\text{PhSi}(\text{OEt})_3$ as a colorless oil after removal of the solvent *in vacuo*.

^1H NMR (CDCl_3): 1.25 [t, $^3J_{\text{H-H}} = 7$ Hz, 9H, $\text{PhSi}(\text{OCH}_2\underline{\text{C}}\text{H}_3)_3$], 3.87 [q, $^3J_{\text{H-H}} = 7$ Hz, 6H, $\text{PhSi}(\text{OCH}_2\underline{\text{C}}\text{H}_3)_3$], 7.35-7.43 [m, 3H, $\underline{\text{P}}\text{hSi}(\text{OCH}_2\underline{\text{C}}\text{H}_3)_3$], 7.66-7.69 [m, 2H,

$\text{PhSi}(\text{OCH}_2\text{CH}_3)_3$. $^{13}\text{C}\{^1\text{H}\}$ NMR (CDCl_3): 18.4 [s, 3C, $\text{PhSi}(\text{OCH}_2\text{CH}_3)_3$], 58.9 [s, 3C, $\text{PhSi}(\text{OCH}_2\text{CH}_3)_3$], 128.0 [s, 2C, $\text{PhSi}(\text{OCH}_2\text{CH}_3)_3$], 130.5 [s, 1C, $\text{PhSi}(\text{OCH}_2\text{CH}_3)_3$], 131.1 [s, 1C, $\text{PhSi}(\text{OCH}_2\text{CH}_3)_3$], 135.0 [s, 2C, $\text{PhSi}(\text{OCH}_2\text{CH}_3)_3$].

3.7.21 $[\kappa^3\text{-Tptm}]\text{ZnH}$ catalyzed hydrosilylation of Me_2CO with PhSiH_3 to give $\text{PhSi}(\text{OPr}^i)_3$

A suspension of $[\kappa^3\text{-Tptm}]\text{ZnH}$ (4 mg, 0.01 mmol, 0.8 mol % per SiH bond) in C_6D_6 (ca. 0.7 mL) in an NMR tube equipped with a J. Young valve was treated with PhSiH_3 (44 mg, 0.41 mmol). Me_2CO (120 μL , 1.63 mmol) was added, thereby resulting in an exothermic reaction to form $\text{PhSi}(\text{OPr}^i)_3$, which was complete within 1 hour as judged by ^1H NMR spectroscopy (TON = 125, TOF = $1.25 \times 10^2 \text{ h}^{-1}$). The volatile components were removed *in vacuo*, dissolved in CHCl_3 (ca. 1 mL), and passed through a small plug of silica, giving $\text{PhSi}(\text{OPr}^i)_3$ as a colorless oil after removal of the solvent *in vacuo*.

3.7.22 $[\kappa^3\text{-Tptm}]\text{ZnH}$ catalyzed hydrosilylation of PhCHO with PhSiH_3 to give $\text{PhSi}(\text{OCH}_2\text{Ph})_3$

A suspension of $[\kappa^3\text{-Tptm}]\text{ZnH}$ (8 mg, 0.02 mmol, 1.6 mol % per SiH bond) in C_6D_6 (ca. 0.7 mL) in an NMR tube equipped with a J. Young valve was treated with PhSiH_3 (44 mg, 0.41 mmol). PhCHO (150 μL , 1.47 mmol) was added, thereby resulting in an exothermic reaction to form $\text{PhSi}(\text{OCH}_2\text{Ph})_3$, which was complete within 15 minutes as judged by ^1H NMR spectroscopy (TON = 62, TOF = $2.48 \times 10^2 \text{ h}^{-1}$).

3.7.23 $[\kappa^3\text{-Tptm}]\text{ZnH}$ catalyzed hydrosilylation of $\text{MeC}(\text{O})\text{Ph}$ with PhSiH_3 to give $\text{PhSi}[\text{OCH}(\text{Me})\text{Ph}]_3$

A suspension of $[\kappa^3\text{-Tptm}]\text{ZnH}$ (8 mg, 0.02 mmol, 1.6 mol % per SiH bond) in C_6D_6 (ca. 0.7 mL) in an NMR tube equipped with a J. Young valve was treated with PhSiH_3 (44

mg, 0.41 mmol). Acetophenone (190 μ L, 1.63 mmol) was added thereby resulting in an exothermic reaction to form $\text{PhSi}[\text{OCH}(\text{Me})\text{Ph}]_3$, which was complete within 20 minutes as judged by ^1H NMR spectroscopy (TON = 62, TOF = $1.87 \times 10^2 \text{ h}^{-1}$).

3.7.24 $[\kappa^3\text{-Tptm}]\text{ZnH}$ catalyzed hydrosilylation of CO_2 with $(\text{EtO})_3\text{SiH}$ to give $(\text{EtO})_3\text{SiO}_2\text{CH}$

(i) A mixture of $[\kappa^3\text{-Tptm}]\text{ZnH}$ (6 mg, 0.01 mmol), $(\text{EtO})_3\text{SiH}$ (28 mg, 0.17 mmol) and C_6D_6 (ca. 0.7 mL) in an NMR tube equipped with a J. Young valve was treated with CO_2 (1 atm) and heated at 120 $^\circ\text{C}$. The sample was monitored by ^1H NMR spectroscopy, thereby demonstrating the formation of $(\text{EtO})_3\text{SiO}_2\text{CH}$ over a period of 16 hours (see spectroscopic data below).

(ii) A mixture of $[\kappa^3\text{-Tptm}]\text{ZnH}$ (49 mg, 0.12 mmol, 0.1 mol %) and $(\text{EtO})_3\text{SiH}$ (20.00 g, 99%, 120.53 mmol), distilled prior to use, was placed in a Fischer-Porter bottle (3 oz) containing a stir-bar. The suspension was sealed, purged with CO_2 five times (by pressurizing to ca. 85 psi and releasing the pressure to ca. 10 psi), and then pressurized to 80 psi. The vessel was sealed and heated at 100 $^\circ\text{C}$, thereby resulting in dissolution of the formate $[\kappa^4\text{-Tptm}]\text{ZnO}_2\text{CH}$ that is formed upon addition of the CO_2 . The uptake of CO_2 was monitored and the system was periodically repressurized to 100 psi. The mixture was allowed to cool after 348.5 hours, and the contents were transferred to a distillation apparatus in an argon box and analyzed by ^1H NMR spectroscopy thereby demonstrating that the TON based on $(\text{EtO})_3\text{SiH}$ consumed is 1006, while the TOF is 2.9 hr^{-1} . The mixture was distilled at 40 $^\circ\text{C}$ *in vacuo* to give $(\text{EtO})_3\text{SiO}_2\text{CH}^{61}$ (19.28 g, 89% purity, 68 % yield) as a colorless liquid. The TON based on the yield of isolated $(\text{EtO})_3\text{SiO}_2\text{CH}$ is 681, while the TOF is 2.0 hr^{-1} .

^1H NMR (C_6D_6): 1.09 [t, $^3J_{\text{H-H}} = 7$ Hz, 9H, $(\underline{\text{H}}_3\text{CCH}_2)_3\text{SiO}_2\text{CH}$], 3.81 [q, $^3J_{\text{H-H}} = 7$ Hz, 6H, $(\text{H}_3\text{C}\underline{\text{C}}\text{H}_2)_3\text{SiO}_2\text{CH}$], 7.78 [s, 1H, $(\text{H}_3\text{CCH}_2)_3\text{SiO}_2\text{C}\underline{\text{H}}$]. $^{13}\text{C}\{^1\text{H}\}$ NMR (C_6D_6): 18.0 [s, 3C, $(\text{H}_3\text{C}\underline{\text{C}}\text{H}_2)_3\text{SiO}_2\text{CH}$], 60.1 [s, 3C, $(\text{H}_3\text{C}\underline{\text{C}}\text{H}_2)_3\text{SiO}_2\text{CH}$], 158.2 [s, 1C, $(\text{H}_3\text{CCH}_2)_3\text{SiO}_2\text{C}\underline{\text{H}}$]. ^{13}C NMR (C_6D_6): 18.0 [q, $^1J_{\text{C-H}} = 126$ Hz, 3C, $(\text{H}_3\text{C}\underline{\text{C}}\text{H}_2)_3\text{SiO}_2\text{CH}$], 60.1 [tq, $^1J_{\text{C-H}} = 144$ Hz, $^2J_{\text{C-H}} = 5$ Hz, 3C, $(\text{H}_3\text{C}\underline{\text{C}}\text{H}_2)_3\text{SiO}_2\text{CH}$], 158.2 [d, $^1J_{\text{C-H}} = 227$ Hz, 1C, $(\text{H}_3\text{CCH}_2)_3\text{SiO}_2\text{C}\underline{\text{H}}$]. $^{29}\text{Si}\{^1\text{H}\}$ NMR (C_6D_6): -86.0.

IR Data (NaCl salt disks, cm^{-1}): 3431 (w), 2979 (s), 2930 (m), 2900 (m), 2770 (w), 2742 (w), 1900 (w), 1750 (m), 1726 (s), 1445 (w), 1392 (w), 1297 (w), 1204 (m), 1168 (m), 1104 (s), 1086 (s), 972 (m), 898 (w), 797 (m), 740 (w).

3.7.25 $[\kappa^4\text{-Tptm}]\text{ZnO}_2\text{CH}$ catalyzed hydrosilylation of CO_2 with $(\text{EtO})_3\text{SiH}$ to give $(\text{EtO})_3\text{SiO}_2\text{CH}$

A mixture of $[\kappa^4\text{-Tptm}]\text{ZnO}_2\text{CH}$ (5 mg, 0.01 mmol), $(\text{EtO})_3\text{SiH}$ (35 mg, 0.21 mmol) and C_6D_6 (*ca.* 0.7 mL) were placed in an NMR tube equipped with a J. Young valve. The mixture was treated with CO_2 (1 atm) and heated at 100 °C. The reaction was monitored by ^1H NMR spectroscopy, thereby demonstrating formation of $(\text{EtO})_3\text{SiO}_2\text{CH}$ over a period of 24 hours.

3.7.26 $[\kappa^4\text{-Tptm}]\text{ZnOSiMe}_3$ as a precatalyst for the hydrosilylation of CO_2 with $(\text{EtO})_3\text{SiH}$ to give $(\text{EtO})_3\text{SiO}_2\text{CH}$

A mixture of $[\kappa^4\text{-Tptm}]\text{ZnOSiMe}_3$ (145 mg, 0.29 mmol, 0.25 mol %) and $(\text{EtO})_3\text{SiH}$ (20.00 g, 95%, 115.66 mmol) was placed in a Fischer-Porter bottle (3 oz) containing a stir-bar. The suspension was sealed, purged with CO_2 five times, by pressurizing to *ca.* 85 psi and releasing the pressure to *ca.* 10 psi, and then pressurized to 80 psi. The vessel was sealed and heated at 100 °C, thereby resulting in dissolution of the formate $[\kappa^4\text{-Tptm}]\text{ZnO}_2\text{CH}$ that is formed upon addition of the CO_2 . The uptake of CO_2 was

monitored and the system was periodically repressurized to 100 psi. The mixture was allowed to cool after 85.5 hours and the contents were transferred to a distillation apparatus in an argon glove box and analyzed by ^1H NMR spectroscopy thereby demonstrating that the TON based on the $(\text{EtO})_3\text{SiH}$ consumed is 396, while the TOF is 4.6 hr^{-1} . The mixture was distilled at $40 \text{ }^\circ\text{C}$ *in vacuo* to give $(\text{EtO})_3\text{SiO}_2\text{CH}$ (19.61 g, 88% purity, 72 % yield) as a colorless liquid. The TON based on the yield of isolated $(\text{EtO})_3\text{SiO}_2\text{CH}$ is 258, while the TOF is 3.3 hr^{-1} . The residue of the distillation was placed at -12°C for 24 hours, thereby depositing the catalyst as an off-white solid, which was washed with benzene ($6 \times 1 \text{ mL}$) and was identified by ^1H NMR spectroscopy as predominantly the formate complex $[\kappa^4\text{-Tptm}]\text{ZnO}_2\text{CH}$.

3.7.27 $[\kappa^4\text{-Tptm}]\text{ZnOSiMe}_3$ as a precatalyst for the hydrosilylation of $^{13}\text{CO}_2$ with $(\text{EtO})_3\text{SiH}$ to give $(\text{EtO})_3\text{SiO}_2^{13}\text{CH}$

(i) A solution of $[\kappa^4\text{-Tptm}]\text{ZnOSiMe}_3$ (2 mg, 0.004 mmol) in C_6D_6 (ca. 0.7 mL) in an NMR tube equipped with a J. Young valve was treated with $(\text{EtO})_3\text{SiH}$ (15 mg, 95%, 0.09 mmol), followed by $^{13}\text{CO}_2$ (1 atm). The sample was heated at $100 \text{ }^\circ\text{C}$ for 2 hours, and analyzed by ^1H and ^{13}C NMR spectroscopy, thereby demonstrating the formation of $(\text{EtO})_3\text{SiO}_2^{13}\text{CH}$.

(ii) A mixture of $[\kappa^4\text{-Tptm}]\text{ZnOSiMe}_3$ (6 mg, 0.01 mmol) and $(\text{EtO})_3\text{SiH}$ (90 mg, 0.55 mmol) in an NMR tube equipped with a J. Young valve and was treated with $^{13}\text{CO}_2$ (1 atm). The sample was heated at $120 \text{ }^\circ\text{C}$ for 5 hours, and then dissolved in C_6D_6 (ca. 0.7 mL) and analyzed by ^1H and ^{13}C NMR spectroscopy to demonstrate the formation of $(\text{EtO})_3\text{SiO}_2^{13}\text{CH}$.

3.7.28 Reaction of $(\text{EtO})_3\text{SiO}_2\text{CH}$ with HCl (aq) to give ethylformate

(i) A solution of $(\text{EtO})_3\text{SiO}_2\text{CH}$ (58 mg, 85%, 0.24 mmol) in C_6D_6 (ca. 0.7 mL) was treated with HCl (20 μL , 37 % aqueous), resulting in an exothermic reaction, and the precipitation of a white solid. The reaction mixture was shaken for 2 minutes, and analyzed by ^1H NMR spectroscopy, thereby demonstrating the formation of ethylformate.

(ii) $(\text{EtO})_3\text{SiO}_2\text{CH}$ (4.0 g, 89%, 17.1 mmol) was treated with H_2O (1.23 mL, 68.3 mmol) followed by HCl (100 μL , 37% aqueous), resulting in an exothermic reaction and the deposition of a white solid. The reaction mixture was fractionally distilled giving EtO_2CH (990 mg, 84% by NMR, impurity is EtOH , 66% yield).

(iii) A solution of $(\text{EtO})_3\text{SiO}_2\text{CH}$ (23 mg, 89%, 0.10 mmol) and mesitylene as an internal standard (5 μL , 0.04 mmol) in C_6D_6 (ca. 0.7 mL) was treated with HCl (15 μL , 37 % aqueous), resulting in an exothermic reaction and the precipitation of a white solid. The reaction mixture was shaken for 2 minutes, and analyzed by ^1H NMR spectroscopy, thereby demonstrating the formation of ethylformate in quantitative yield.

3.7.29 Reaction of $(\text{EtO})_3\text{SiO}_2\text{CH}$ with HNMe_2 to give dimethylformamide (DMF)

(i) $(\text{EtO})_3\text{SiO}_2\text{CH}$ (82 mg, 85%, 0.34 mmol) was treated HNMe_2 (1 atm), resulting in an exothermic reaction. The reaction was analyzed by ^1H NMR spectroscopy, thereby demonstrating the formation of Me_2NCHO .

(ii) $(\text{EtO})_3\text{SiO}_2\text{CH}$ (1.00 g, 85%, 4.08 mmol) was treated HNMe_2 (1 atm), resulting in an exothermic reaction. The mixture was stirred for 1 hour, maintaining the pressure of HNMe_2 at 1 atmosphere. H_2O (300 μL , 16.67 mmol) was then added resulting in the

immediate precipitation of a white solid. The solid was extracted with benzene (5 × 2 mL) and the extract was filtered through celite. The volatile components were removed *in vacuo*, giving Me₂NCHO (50 mg, 92% purity, 15.4%).

(iii) A solution of (EtO)₃SiO₂CH (23 mg, 89%, 0.10 mmol) in C₆D₆ (*ca.* 0.7 mL), with mesitylene as an internal standard (5 μL, 0.04 mmol), was treated with HNMe₂ (1 atm), thereby resulting in an exothermic reaction. The reaction mixture was analyzed by ¹H NMR spectroscopy, thereby demonstrating the formation of Me₂NCHO in 91% yield.

3.7.30 Synthesis of [Bptm*]H

A yellow solution of 2-mercaptopyridine (1.0 g, 9.00 mmol) and *p*-thiocresol (550 mg, 4.43 mmol) in THF (*ca.* 20 mL) was added dropwise to a suspension of NaH (380 mg, 15.83 mmol) in THF (*ca.* 30 mL) *via* cannula. Iodoform (1.743 g, 4.43 mmol) was then added to the suspension in 5 portions, resulting in an exothermic reaction. The resulting red solution was then stirred for 20 minutes, at which point EtOH (*ca.* 5 mL) was added to quench the excess NaH. The sample was then evaporated *in vacuo*, leaving a brownish-red residue, which was then purified by flash column chromatography (silica gel, DCM) to give [Bptm*]H as a dark yellow-red oil (850 mg, 53.8%). The first major fraction is [Mptm*]H (Mptm* = *bis*(*p*-tolylthio)(2-pyridylthio)methyl) which is an orangish solid. Anal. Calcd. for [Bptm*]H: C, 60.6%; H, 4.5%; N, 7.9%. Found: C, 60.7%, H, 4.3%, N, 7.8%.

¹H NMR (C₆D₆): 1.95 [s, 3H, (MeC₆H₄S)(C₅H₄NS)₂CH], 6.34 [m, 2H, (MeC₆H₄S)(C₅H₄NS)₂CH], 6.71-6.80 [m, 4H, (MeC₆H₄S)(C₅H₄NS)₂CH], 6.86 [d, ³J_{H-H} = 8 Hz, 2H, (MeC₆H₄S)(C₅H₄NS)₂CH], 7.77 [d, ³J_{H-H} = 8 Hz, 2H, (MeC₆H₄S)(C₅H₄NS)₂CH], 7.89 [s, 1H, (MeC₆H₄S)(C₅H₄NS)₂CH], 8.26 [m, 2H, (MeC₆H₄S)(C₅H₄NS)₂CH]. ¹³C{¹H} NMR (C₆D₆): 21.1 [s, 1C, (MeC₆H₄S)(C₅H₄NS)₂CH], 55.1 [s, 1C, (MeC₆H₄S)(C₅H₄NS)₂CH],

120.1 [s, 2C, (MeC₆H₄S)(C₅H₄NS)₂CH], 122.2 [s, 2C, (MeC₆H₄S)(C₅H₄NS)₂CH], 130.0 [s, 2C, (MeC₆H₄S)(C₅H₄NS)₂CH], 131.5 [s, 1C, (MeC₆H₄S)(C₅H₄NS)₂CH], 134.1 [s, 2C, (MeC₆H₄S)(C₅H₄NS)₂CH], 136.1 [s, 2C, (MeC₆H₄S)(C₅H₄NS)₂CH], 138.6 [s, 1C, (MeC₆H₄S)(C₅H₄NS)₂CH], 150.0 [s, 2C, (MeC₆H₄S)(C₅H₄NS)₂CH], 158.1 [s, 2C, (MeC₆H₄S)(C₅H₄NS)₂CH].

IR Data (NaCl salt disks, cm⁻¹): 3072 (w), 3044 (w), 2917 (w), 2844 (w), 2360 (w), 1574 (s), 1557 (s), 1490 (m), 1451 (s), 1415 (s), 1281 (w), 1147 (w), 1122 (s), 1084 (w), 1043 (w), 986 (w), 811 (m), 756 (s), 721 (m).

3.7.31 Synthesis of [κ³-Bptm*]ZnN(SiMe₃)₂

A solution of [Bptm*]H (1.18 g, 3.31 mmol) in benzene (*ca.* 8 mL) was treated with Zn[N(SiMe₃)₂]₂ (1.28 g, 3.31 mmol) *via* pipette. The reaction mixture was allowed to stand at room temperature overnight and then lyophilized for 24 hours to give [κ³-Bptm*]ZnN(SiMe₃)₂ (1.73 g, 90%) as an off white solid. Large colorless crystals suitable for X-ray diffraction can be obtained by (i) slow evaporation from benzene and (ii) pentane diffusion into a benzene solution of [κ³-Bptm*]ZnN(SiMe₃)₂.

¹H NMR (C₆D₆): 0.46 [s, 18H, (MeC₆H₄S)(C₅H₄NS)₂CZnN(SiMe₃)₂], 2.06 [s, 3H, (MeC₆H₄S)(C₅H₄NS)₂CZnN(SiMe₃)₂], 6.11-6.14 [m, 2H, (MeC₆H₄S)(C₅H₄NS)₂CZnN(SiMe₃)₂], 6.37-6.43 [m, 4H, (MeC₆H₄S)(C₅H₄NS)₂CZnN(SiMe₃)₂], 7.02 [d, ³J_{H-H} = 8 Hz, 2H, (MeC₆H₄S)(C₅H₄NS)₂CZnN(SiMe₃)₂], 7.90 [d, ³J_{H-H} = 8 Hz, 2H, (MeC₆H₄S)(C₅H₄NS)₂CZnN(SiMe₃)₂], 8.10 [m, 2H, (MeC₆H₄S)(C₅H₄NS)₂CZnN(SiMe₃)₂].
¹³C{¹H} NMR (C₆D₆): Not observed [1C, (MeC₆H₄S)(C₅H₄NS)₂CZnN(SiMe₃)₂], 6.6 [s, 6C, (MeC₆H₄S)(C₅H₄NS)₂CZnN(SiMe₃)₂], 21.0 [s, 1C, (MeC₆H₄S)(C₅H₄NS)₂CZnN(SiMe₃)₂], 119.4 [s, 2C, (MeC₆H₄S)(C₅H₄NS)₂CZnN(SiMe₃)₂], 121.5 [s, 2C, (MeC₆H₄S)(C₅H₄NS)₂CZnN(SiMe₃)₂], 130.0 [s, 2C, (MeC₆H₄S)(C₅H₄NS)₂CZnN(SiMe₃)₂].

130.7 [s, 1C, (MeC₆H₄S)(C₅H₄NS)₂CZnN(SiMe₃)₂], 136.5 [s, 1C, (MeC₆H₄S)(C₅H₄NS)₂CZnN(SiMe₃)₂], 137.4 [s, 1C, (MeC₆H₄S)(C₅H₄NS)₂CZnN(SiMe₃)₂], 138.1 [s, 2C, (MeC₆H₄S)(C₅H₄NS)₂CZnN(SiMe₃)₂], 156.6 [s, 2C, (MeC₆H₄S)(C₅H₄NS)₂CZnN(SiMe₃)₂], 164.1 [s, 2C, (MeC₆H₄S)(C₅H₄NS)₂CZnN(SiMe₃)₂].

IR Data (KBr disk, cm⁻¹): 3066 (w), 3014 (w), 2952 (w), 2357 (w), 1590 (s), 1556 (s), 1490 (m), 1455 (s), 1417 (s), 1280 (m), 1250 (m), 1180 (w), 1132 (s), 1091 (w), 1045 (w), 1006 (w), 930 (m), 883 (w), 843 (m), 801 (m), 758 (s), 724 (m), 640 (w), 512 (w), 486 (w), 410 (w).

3.7.32 Synthesis of [κ³-Bptm*]ZnO₂CH

A solution of [κ³-Bptm*]ZnN(SiMe₃)₂ (700 mg, 1.20 mmol) in benzene (*ca.* 10 mL) and PhSiH₃ (150 mg, 1.39 mmol) in a small Schlenk tube was treated with CO₂ (1 atm) resulting in the precipitation of colorless crystals. The reaction mixture was allowed to stand at room temperature for 1 hour, and was then filtered. The precipitate was washed with benzene (*ca.* 3 mL), and then evaporated *in vacuo* giving [κ³-Bptm*]ZnO₂CH as a colorless solid (377 mg, 67%). The combined filtrates were lyophilized, and then washed with benzene (*ca.* 5 mL × 2) to give [κ³-Bptm*]ZnO₂CH as a colorless solid (67 mg). Large colorless crystals suitable for X-ray diffraction can be obtained by slow evaporation from benzene. Anal. Calcd. for [κ³-Bptm*]ZnO₂CH C, 49.0%; H, 3.5%; N, 6.0%. Found: C, 48.1%, H, 3.2%, N, 5.8%.

¹H NMR (C₆D₆): 2.08 [s, 3H, (MeC₆H₄S)(C₅H₄NS)₂CZnO₂CH], 6.09 [dt, ³J_{H-H} = 6 Hz, ⁴J_{H-H} = 2 Hz, 2H, (MeC₆H₄S)(C₅H₄NS)₂CZnO₂CH], 6.39-6.44 [m, 4H, (MeC₆H₄S)(C₅H₄NS)₂CZnO₂CH], 7.05 [d, ³J_{H-H} = 8 Hz, 2H, (MeC₆H₄S)(C₅H₄NS)₂CZnO₂CH], 7.86 [d, ³J_{H-H} = 8 Hz, 2H, (MeC₆H₄S)(C₅H₄NS)₂CZnO₂CH], 8.81 [d, ³J_{H-H} = 5 Hz, (MeC₆H₄S)(C₅H₄NS)₂CZnO₂CH], 8.91 [s, 1H, (MeC₆H₄S)(C₅H₄NS)₂CZnO₂CH]. ¹³C{¹H} NMR (C₆D₆): not observed [1C,

(MeC₆H₄S)(C₅H₄NS)₂CZnO₂CH], 21.0 [s, 1C, (MeC₆H₄S)(C₅H₄NS)₂CZnO₂CH], 119.6 [s, 2C, (MeC₆H₄S)(C₅H₄NS)₂CZnO₂CH], 120.9 [s, 2C, (MeC₆H₄S)(C₅H₄NS)₂CZnO₂CH], 130.0 [s, 2C, (MeC₆H₄S)(C₅H₄NS)₂CZnO₂CH], 130.1 [s, 2C, (MeC₆H₄S)(C₅H₄NS)₂CZnO₂CH], 136.3 [s, 1C, (MeC₆H₄S)(C₅H₄NS)₂CZnO₂CH], 137.2 [s, 1C, (MeC₆H₄S)(C₅H₄NS)₂CZnO₂CH], 138.6 [s, 2C, (MeC₆H₄S)(C₅H₄NS)₂CZnO₂CH], 148.7 [s, 2C, (MeC₆H₄S)(C₅H₄NS)₂CZnO₂CH], 163.8 [s, 2C, (MeC₆H₄S)(C₅H₄NS)₂CZnO₂CH], 171.0 [s, 1C, (MeC₆H₄S)(C₅H₄NS)₂CZnO₂CH].

IR Data (KBr disk, cm⁻¹): 3088 (w), 3053 (w), 3016 (w), 2916 (w), 2840 (w), 2360 (w), 2335 (w), 1608 (s) [$\nu_{\text{asym}}(\text{CO}_2)$], 1593 (s), 1555 (s), 1491 (m), 1459 (s), 1418 (s), 1358 (w), 1309 (m) [$\nu_{\text{sym}}(\text{CO}_2)$], 1286 (m), 1133 (s), 1091 (w), 1046 (m), 1014 (m), 797 (m), 761 (s), 723 (m), 655 (m), 484 (w).

3.8 Crystallographic data

Table 4. Crystal, intensity collection and refinement data.

	[κ^3 -Bptm*]ZnN(SiMe ₃) ₂	[κ^3 -Bptm*]ZnO ₂ CH
lattice	Triclinic	Monoclinic
formula	C ₃₀ H ₃₉ N ₃ S ₃ ZnSi ₂	C ₁₉ H ₁₆ N ₂ S ₃ ZnO ₂
formula weight	659.37	465.89
space group	<i>P</i> -1	<i>P</i> 2 ₁ / <i>c</i>
<i>a</i> /Å	14.748(4)	9.4432(19)
<i>b</i> /Å	15.109(4)	27.166(5)
<i>c</i> /Å	16.841(4)	8.0692(16)
α /°	90.390(4)	90
β /°	108.578(4)	109.715(3)
γ /°	106.831(4)	90
<i>V</i> /Å ³	3384.3(15)	1948.7(7)
<i>Z</i>	4	4
temperature (K)	150 (2)	150(2)
radiation (λ , Å)	0.71073	0.71073
ρ (calcd.), g cm ⁻³	1.294	1.588
μ (Mo K α), mm ⁻¹	1.005	1.599
θ max, deg.	27.10	30.74
no. of data collected	43808	30992
no. of data used	14925	6070
no. of parameters	682	249
R_1 [$I > 2\sigma(I)$]	0.0647	0.0526
wR_2 [$I > 2\sigma(I)$]	0.0946	0.1056
R_1 [all data]	0.1765	0.1221
wR_2 [all data]	0.1204	0.1272
GOF	0.999	1.025

Table 4(cont). Crystal, intensity collection and refinement data.

	[Mptm*]H
lattice	Monoclinic
formula	C ₂₀ H ₁₉ NS ₃
formula weight	369.54
space group	<i>P</i> 2 ₁ / <i>c</i>
<i>a</i> /Å	14.828(4)
<i>b</i> /Å	7.824(2)
<i>c</i> /Å	15.484(4)
α /°	90
β /°	94.571(5)
γ /°	90
<i>V</i> /Å ³	1790.5(9)
<i>Z</i>	4
temperature (K)	150(2)
radiation (λ , Å)	0.71073
ρ (calcd.), g cm ⁻³	1.371
μ (Mo K α), mm ⁻¹	0.415
θ max, deg.	30.77
no. of data collected	28320
no. of data used	5552
no. of parameters	219
R_1 [$I > 2\sigma(I)$]	0.0691
wR_2 [$I > 2\sigma(I)$]	0.1440
R_1 [all data]	0.1659
wR_2 [all data]	0.1808
GOF	1.001

3.9 References and notes

- (1) Lewis, N. S.; Nocera, D. G. *Proc. Natl. Acad. Sci. U.S.A.* **2006**, *103*, 15729-15735.
- (2) *Carbon Dioxide as a Chemical Feedstock*, Aresta, M. (Ed), Wiley-VCH, Weinheim (2010).
- (3) Gray, H. B. *Nature Chem.* **2009**, *1*, 7.
- (4) Schlapbach, L.; Züttel, A. *Nature* **2001**, *414*, 353-358.
- (5) Eberle, U.; Felderhoff, M.; Schüth, F. *Angew. Chem. Int. Edit.* **2009**, *48*, 6608-6630.
- (6) Smythe, N. C.; Gordon, J. C. *Eur. J. Inorg. Chem.* **2010**, 509-521.
- (7) (a) Crabtree, R. H. *Energy Environ. Sci.* **2008**, *1*, 134-138.
(b) Wang, Z. H.; Belli, J.; Jensen, C. M. *Faraday Discuss.* **2011**, *151*, 297-305.
(c) Teichmann, D.; Arlt, W.; Wasserscheid, P.; Freymann, R. *Energy Environ. Sci.* **2011**, *4*, 2767-2773.
- (8) (a) Joó, F. *ChemSusChem* **2008**, *1*, 805-808.
(b) Enthaler, S. *ChemSusChem* **2008**, *1*, 801-804.
(c) Loges, B.; Boddien, A.; Gärtner, F.; Junge, H.; Beller, M. *Top. Catal.* **2010**, *53*, 902-914.
(d) Johnson, T. C.; Morris, D. J.; Wills, M. *Chem. Soc. Rev.* **2010**, *39*, 81-88.
(e) Enthaler, S.; von Langermann, J.; Schmidt, T. *Energy Environ. Sci.* **2010**, *3*, 1207-1217.

- (f) Boddien, A.; Gärtner, F.; Mellmann, D.; Sponholz, P.; Junge, H.; Laurency, G.; Beller, M. *Chimia* **2011**, *65*, 214-218.
- (g) Jiang, H.-L.; Singh, S. K.; Yan, J.-M.; Zhang, X.-B.; Xu, Q. *ChemSusChem* **2010**, *3*, 541-549.
- (h) Fukuzumi, S.; Yamada, Y.; Suenobu, T.; Ohkubo, K.; Kotani, H. *Energy Environ. Sci.* **2011**, *4*, 2754-2766.
- (i) Laurency, G. *Chimia* **2011**, *65*, 663-666.
- (j) Boddien, A.; Gärtner, F.; Federsel, C.; Sponholz, P.; Mellmann, D.; Jackstell, R.; Junge, H.; Beller, M. *Angew. Chem. Int. Edit.* **2011**, *50*, 6411-6414.
- (9) (a) Ison, E. A.; Corbin, R. A.; Abu-Omar, M. M. *J. Am. Chem. Soc.* **2005**, *127*, 11938-11939.
- (b) Corbin, R. A.; Ison, E. A.; Abu-Omar, M. M. *Dalton Trans.* **2009**, 2850-2855.
- (c) Brunel, J. M. *Int. J. Hydrog. Energy* **2010**, *35*, 3401-3405.
- (d) Han, W.-S.; Kim, T.-J.; Kim, S.-K.; Kim, Y.; Kim, Y.; Nam, S.-W.; Kang, S. O. *Int. J. Hydrog. Energy* **2011**, *36*, 12305-12312.
- (10) Makowski, P.; Thomas, A.; Kuhn, P.; Goettmann, F. *Energy Environ. Sci.* **2009**, *2*, 480-490.
- (11) Examples include *cyclo*-(CH₂SiH₂)₃, *cyclo*-(CH₂SiH₂CHSiH₃)₂, H₃SiCH₂SiH₂CH₂SiH₃, H₃SiCH₂CH(SiH₃)₂, H₃SiCH₂CH(SiH₃)CH₂SiH₃, and C(SiH₃)₄. See reference 9d and
- (a) Schmidbaur, H.; Zech, J. *Eur. J. Solid State Inorg. Chem.* **1992**, *29*, 5-21.

- (b) Hager, R.; Steigelmann, O.; Müller, G.; Schmidbaur, H.; Robertson, H. E.; Rankin, D. W. H. *Angew. Chem. Int. Edit. Engl.* **1990**, *29*, 201-203.
- (12) For reference, the U.S. Department of Energy target for onboard hydrogen storage systems for light-duty vehicles was 4.5 wt % for 2010 and is 5.5 wt % for 2017. See: *DOE Targets for Onboard Hydrogen Storage Systems for Light-Duty Vehicles*.
http://www1.eere.energy.gov/hydrogenandfuelcells/storage/pdfs/targets_onboard_hydro_storage.pdf.
- (13) Jacquet, O.; Gomes, C. D. N.; Ephritikhine, M.; Cantat, T. *J. Am. Chem. Soc.* **2012**, *134*, 2934-2937.
- (14) (a) Chandrasekhar, V.; Boomishankar, R.; Nagendran, S. *Chem. Rev.* **2004**, *104*, 5847-5910.
- (b) Cordes, D. B.; Lickiss, P. D.; Rataboul, F. *Chem. Rev.* **2010**, *110*, 2081-2173.
- (c) Nakao, Y.; Hiyama, T. *Chem. Soc. Rev.* **2011**, *40*, 4893-4901.
- (d) Lukevics, E.; Dzintara, M. *J. Organomet. Chem.* **1985**, *295*, 265-315.
- (15) (a) Liebhafsky, H. A. *Silicones under the Monogram*; Wiley-Interscience: New York, **1978**.
- (b) Rochow, E. G. *Silicon and Silicones*; Springer: Berlin, Heidelberg, **1987**.
- (c) McGregor, R. R. *Silicones and Their Uses*; McGraw-Hill: New York, **1954**.
- (d) Warrick, E. *Forty Years of Firsts*; McGraw-Hill: New York, **1990**.
- (16) (a) Shishigin, E. A.; Avrorin, V. V.; Kochina, T. A.; Sinotova, E. N. *Russ. J. Gen. Chem.* **2004**, *74*, 973-974.

- (b) Westermarck, H. *Acta Chem. Scand.* **1954**, *8*, 1830-1834.
- (17) (a) Matarasso-Tchiroukhine, E. *J. Chem. Soc. Chem. Commun.* **1990**, 681-682.
- (b) Lee, T. Y.; Dang, L.; Zhou, Z.; Yeung, C. H.; Lin, Z.; Lau, C. P. *Eur. J. Inorg. Chem.* **2010**, 5675-5684.
- (c) Lee, M.; Ko, S.; Chang, S. *J. Am. Chem. Soc.* **2000**, *122*, 12011-12012.
- (d) Tan, S. T.; Kee, J. W.; Fan, W. Y. *Organometallics* **2011**, *30*, 4008-4013.
- (e) Na, Y.; Lee, C.; Pak, J. Y.; Lee, K. H.; Chang, S. *Tetrahedron Lett.* **2004**, *45*, 7863-7865.
- (f) Shi, M.; Nicholas, K. M. *J. Chem. Res.-S* **1997**, 400-401.
- (g) Lee, Y.; Seomoon, D.; Kim, S.; Han, H.; Chang, S.; Lee, P. H. *J. Org. Chem.* **2004**, *69*, 1741-1743.
- (h) Schubert, U.; Lorenz, C. *Inorg. Chem.* **1997**, *36*, 1258-1259.
- (i) Chang, S.; Scharrer, E.; Brookhart, M. *J. Mol. Catal. A Chem.* **1998**, *130*, 107-119.
- (j) Gutsulyak, D. V.; Vyboishchikov, S. F.; Nikonov, G. I. *J. Am. Chem. Soc.* **2010**, *132*, 5950-5951.
- (k) Peterson, E.; Khalimon, A. Y.; Simionescu, R.; Kuzmina, L. G.; Howard, J. A. K.; Nikonov, G. I. *J. Am. Chem. Soc.* **2009**, *131*, 908-909.
- (18) (a) Mori, K.; Tano, M.; Mizugaki, T.; Ebitani, K.; Kaneda, K. *New J. Chem.* **2002**, *26*, 1536-1538.

- (b) Mitsudome, T.; Noujima, A.; Mizugaki, T.; Jitsukawa, K.; Kaneda, K. *Chem. Commun.* **2009**, 5302-5304.
- (c) Mitsudome, T.; Arita, S.; Mori, H.; Mizugaki, T.; Jitsukawa, K.; Kaneda, K. *Angew. Chem. Int. Edit.* **2008**, *47*, 7938-7940.
- (d) Barnes Jr., G. H.; Daughenbaugh, N. E. *J. Org. Chem.* **1966**, *31*, 885-887.
- (e) Sommer, L. H.; Lyons, J. E. *J. Am. Chem. Soc.* **1967**, *89*, 1521-1522.
- (f) Choi, E.; Lee, C.; Na, Y.; Chang, S. *Org. Lett.* **2002**, *4*, 2369-2371.
- (g) Chauhan, B. P. S.; Sarkar, A.; Chauhan, M.; Roka, A. *Appl. Organomet. Chem.* **2009**, *23*, 385-390.
- (h) John, J.; Gravel, E.; Hagège, A.; Li, H. Y.; Gacoin, T.; Doris, E. *Angew. Chem. Int. Edit.* **2011**, *50*, 7533-7536.
- (19) *Catalysis without Precious Metals*, Bullock, R. M. (Ed), Wiley-VCH, Weinheim, Germany (2010).
- (20) Fromm, D.; Lutzov, D. *Chem. Unserer Zeit.* **1979**, *13*, 78.
- (21) (a) Kolbe, H.; Lautemann, E. *Ann.* **1869**, *113*, 125.
- (b) Schmitt, R.; Burkard, E. *Ber.* 1877, *20*, 2699.
- (22) (a) Darensbourg, D. J.; Mackiewicz, R. M.; Phelps, A. L.; Billodeaux, D. R. *Acc. Chem. Res.* **2004**, *37*, 836-844.
- (b) Coates, G. W.; Moore, D. R. *Angew. Chem. Int. Edit.* **2004**, *43*, 6618-6639.
- (c) Chisholm, M. H.; Zhou, Z. *J. Mater. Chem.* **2004**, *14*, 3081-3092.

- (23) (a) Wang, W.; Wang, S.; Ma, X.; Gong, J. *Chem. Soc. Rev.* **2011**, *40*, 3703-3727.
- (b) Federsel, C.; Jackstell, R.; Beller, M. *Angew. Chem. Int. Edit.* **2010**, *49*, 6254-6257.
- (c) Himeda, Y. *Eur. J. Inorg. Chem.* **2007**, 3927-3941.
- (b) Jessop, P. G.; Joó, F.; Tai, C.-C. *Coord. Chem. Rev.* **2004**, *248*, 2425-2442.
- (c) Jessop, P. G.; Ikariya, T.; Noyori, R. *Chem. Rev.* **1995**, *95*, 259-272.
- (e) Omae, I. *Catal. Today* **2006**, *115*, 33-52.
- (f) Jessop, P. G.; Ikariya, T.; Noyori, R. *Chem. Rev.* **1999**, *99*, 475-493.
- (g) Leitner, W. *Angew. Chem. Int. Edit. Engl.* **1995**, *34*, 2207-2221.
- (i) Reference 8e.
- (24) (a) Wang, W.; Wang, S.; Ma, X.; Gong, J. *Chem. Soc. Rev.* **2011**, *40*, 3703-3727.
- (b) Federsel, C.; Jackstell, R.; Beller, M. *Angew. Chem. Int. Edit.* **2010**, *49*, 6254-6257.
- (c) Himeda, Y. *Eur. J. Inorg. Chem.* **2007**, 3927-3941.
- (b) Jessop, P. G.; Joó, F.; Tai, C.-C. *Coord. Chem. Rev.* **2004**, *248*, 2425-2442.
- (c) Jessop, P. G.; Ikariya, T.; Noyori, R. *Chem. Rev.* **1995**, *95*, 259-272.
- (e) Omae, I. *Catal. Today* **2006**, *115*, 33-52.
- (f) Jessop, P. G.; Ikariya, T.; Noyori, R. *Chem. Rev.* **1999**, *99*, 475-493.

- (g) Leitner, W. *Angew. Chem. Int. Edit. Engl.* **1995**, *34*, 2207-2221.
- (i) Reference 7e.
- (25) Reutemann, W.; Kieczka, H. *Ullmann's Encyclopedia of Industrial Chemistry* (2011).
- (26) Schaub, T.; Paciello, R. A. *Angew. Chem. Int. Edit.* **2011**, *50*, 7278-7282.
- (27) Koinuma, H.; Kawakami, F.; Kato, H.; Hirai, H. *J. Chem. Soc. Chem. Commun.* **1981**, 213-214.
- (28) Eisenschmid, T. C.; Eisenberg, R. *Organometallics* **1989**, *8*, 1822-1824.
- (29) Matsuo, T.; Kawaguchi, H. *J. Am. Chem. Soc.* **2006**, *128*, 12362-12363.
- (30) (a) Riduan, S. N.; Zhang, Y.; Ying, J. Y. *Angew. Chem. Int. Edit.* **2009**, *48*, 3322-3325.
- (b) Huang, F.; Zhang, C.; Jiang, J.; Wang, Z.-X.; Guan, H. *Inorg. Chem.* **2011**, *50*, 3816-3825.
- (31) Berkefeld, A.; Piers, W. E.; Parvez, M. *J. Am. Chem. Soc.* **2010**, *132*, 10660-10661.
- (32) (a) Süß-Fink, G.; Reiner, J. *J. Organomet. Chem.* **1981**, *221*, C36-C38.
- (b) Jansen, A.; Görls, H.; Pitter, S. *Organometallics* **2000**, *19*, 135-138.
- (c) Jansen, A.; Pitter, S. *J. Mol. Catal. A: Chem.* **2004**, *217*, 41-45.
- (d) Deglmann, P.; Ember, E.; Hofmann, P.; Pitter, S.; Walter, O. *Chem. Eur. J.* **2007**, *13*, 2864-2879.
- (e) Jessop, P. G. *Top. Catal.* **1998**, *5*, 95-103.

- (33) See reference 18g and h. Multiple silicon containing products have been formed under homogeneous conditions (reference 9a,b).
- (34) All volumes are recorded approximately at atmospheric pressure using an apparatus that displaces water in an inverted graduated cylinder.
- (35) $[(C_6H_3Pr^i)_2N]Mo(PMe_3)_3(Cl)H$ has also been reported to catalyze hydrolysis of $PhSiH_3$, but the amount of hydrogen released was not quantified and redistribution of $PhSiH_3$ to Ph_2SiH_2 and SiH_4 was also noted. See reference 17k.
- (36) (a) Mukherjee, D.; Thompson, R. R.; Ellern, A.; Sadow, A. D. *ACS Catal.* **2011**, *1*, 698-702 and references therein.
- (b) Mimoun, H. *J. Org. Chem.* **1999**, *64*, 2582–2589.
- (c) Ojima, Y.; Yamaguchi, K.; Mizuno, N. *Adv. Synth. Catal.* **2009**, *351*, 1405-1411 and references therein.
- (d) Sridhar, M.; Raveendra, J.; Ramanaiah, B. C.; Narsaiah, C. *Tetrahedron Lett.* **2011**, *52*, 5980-5982.
- (e) Weickgenannt, A.; Mewald, M.; Oestreich, M. *Org. Biomol. Chem.* **2010**, *8*, 1497-1504.
- (f) Ito, H.; Saito, T.; Miyahara, T.; Zhong, C.; Sawamura, M. *Organometallics* **2009**, *28*, 4829-4840.
- (g) Lorenz, C.; Schubert, U. *Chem. Berichte* **1995**, *128*, 1267-1269.
- (h) Luo, X.-L.; Crabtree, R. H. *J. Am. Chem. Soc.* **1989**, *111*, 2527-2535.
- (i) Barber, D. E.; Lu, Z.; Richardson, T.; Crabtree, R. H. *Inorg. Chem.* **2002**, *31*, 4709–4711.

- (j) Fang, X.; Huhmann-Vincent, J.; Scott, B. L.; Kubas, G. J. *J. Organomet. Chem.* **2000**, *609*, 95-103.
- (k) Burn, M. J.; Bergman, R. G. *J. Organomet. Chem.* **1994**, *472*, 43-54.
- (l) Yun, S. S.; Lee, J.; Lee, S. *Bull. Korean Chem. Soc.* **2001**, *22*, 623-625.
- (m) Purkayashtha, A.; Baruah, J. B. *Silicon Chem.* **2002**, *1*, 229-232.
- (n) Doyle, M. P.; High, K. G.; Bagheri, V.; Pieters, R. J.; Lewis, P. J.; Pearson, M. M. *J. Org. Chem.* **1990**, *55*, 6082-6086.
- (o) Ito, H.; Watanabe, A.; Sawamura, M. *Org. Lett.* **2005**, *7*, 1869-1871.
- (p) Gevorgyan, V.; Rubin, M.; Benson, S.; Liu, J. X.; Yamamoto, Y. *J. Org. Chem.* **2000**, *65*, 6179-6186.
- (q) Biffis, A.; Braga, M.; Basato, M. *Adv. Synth. Catal.* **2004**, *346*, 451-458.
- (r) Biffis, A.; Zecca, M.; Basato, M. *Green Chem.* **2003**, *5*, 170-173.
- (s) Purkayashtha, A.; Baruah, J. B. *J. Mol. Catal. A-Chem.* **2003**, *198*, 47-55.
- (t) Le Bideau, F.; Coradin, T.; Henique, J.; Samuel, E. *Chem. Commun.* **2001**, 1408-1409.
- (u) Grajewska, A.; Oestreich, M. *Synlett* **2010**, 2482-2484.
- (v) Kim, S.; Kwon, M. S.; Park, J. *Tetrahedron Lett.* **2010**, *51*, 4573-4575.
- (w) Weickgenannt, A.; Oestreich, M. *Chem. Asian J.* **2009**, *4*, 406-410.

- (x) Hara, K.; Akiyama, R.; Takakusagi, S.; Uosaki, K.; Yoshino, T.; Kagi, H.; Sawamura, M. *Angew. Chem. Int. Ed.* **2008**, *47*, 5627-5630.
- (37) Mukherjee, D.; Ellern, A.; Sadow, A. D. *J. Am. Chem. Soc.* **2010**, *132*, 7582-7583.
- (38) For recent examples of catalytic hydrosilylation of aldehydes and ketones as a means to achieve reduction to alcohols, see:
- (a) Junge, K.; Schroder, K.; Beller, M. *Chem. Commun.* **2011**, *47*, 4849-4859.
- (b) Le Bailly, B. A. F.; Thomas, S. P. *RSC Adv.* **2011**, *1*, 1435-1445.
- (c) Morris, R. H. *Chem. Soc. Rev.* **2009**, *38*, 2282-2291.
- (d) Chakraborty, S.; Guan, H. R. *Dalton Trans.* **2010**, *39*, 7427-7436.
- (e) Zhang, M.; Zhang, A. *Appl. Organomet. Chem.* **2010**, *24*, 751-757.
- (f) Yang, J. A.; Tilley, T. D. *Angew. Chem. Int. Edit.* **2010**, *49*, 10186-10188.
- (g) Tondreau, A. M.; Darmon, J. M.; Wile, B. M.; Floyd, S. K.; Lobkovsky, E.; Chirik, P. J. *Organometallics* **2009**, *28*, 3928-3940.
- (h) Tondreau, A. M.; Lobkovsky, E.; Chirik, P. J. *Org. Lett.* **2008**, *10*, 2789-2792.
- (i) Lipshutz, B. H.; Frieman, B. A. *Angew. Chem. Int. Edit.* **2005**, *44*, 6345-6348.
- (j) Lipshutz, B. H.; Noson, K.; Chrisman, W.; Lower, A. *J. Am. Chem. Soc.* **2003**, *125*, 8779-8789.
- (k) Berk, S. C.; Kreutzer, K. A.; Buchwald, S. L. *J. Am. Chem. Soc.* **1991**, *113*, 5093-5095.
- (l) Marinos, N. A.; Enthaler, S.; Driess, M. *ChemCatChem* **2010**, *2*, 846-853.

- (m) Inagaki, T.; Yamada, Y.; Phong, L. T.; Furuta, A.; Ito, J.-I.; Nishiyama, H. *Synlett* **2009**, 253-256.
- (n) Das, S.; Moller, K.; Junge, K.; Beller, M. *Chem. Eur. J.* **2011**, *17*, 7414-7417.
- (o) Carpentier, J.-F.; Bette, V. *Curr. Org. Chem.* **2002**, *6*, 913-936.
- (39) These values are for solutions in C₆D₆.
- (40) Baker, B. A.; Boskovic, Z. V.; Lipshutz, B. H. *Org. Lett.* **2008**, *10*, 289-292.
- (41) Svoboda, P.; Belopota, Ts; Hetflejs, J. Catalysis by Metal-Complexes .23. Formation of Transition Metal-Carbonyl Complexes from Carbon-Dioxide. *J. Organomet. Chem.* **1974**, *65*, C37-C38.
- (42) Motokura, K.; Kashiwame, D.; Miyaji, A.; Baba, R. *Org. Lett.* **2012**, *14*, 2642-2645.
- (43) Sheludyakov, V. D.; Khatuntsev, G. D.; Mironov, V. F. *J. Gen. Chem. U.S.S.R. (Engl. trans)*. **1972**, *42*, 2205-2209.
- (44) Furthermore, the ruthenium complex Ru(PPh₃)₃Cl₂ was reported to achieve only one turnover for the addition of the alkoxy silane (MeO)₂MeSiH to CO₂.
- (45) (a) McFarlane, W.; Seaby, J. M. *J. Chem. Soc. Perkin Trans. 2* **1972**, 1561-1564.
- (b) Trommer, M.; Sander, W.; Patyk, A. *J. Am. Chem. Soc.* **1993**, *115*, 11775-11783.
- (46) (a) Olah, G. A.; Ohannesian, L.; Arvanaghi, M. *Chem. Rev.* **1987**, *87*, 671-686.
- (b) Cochet, T.; Bellosta, V.; Greiner, A.; Roche, D.; Cossy, J. *Synlett* **2011**, 1920-1922.
- (47) (a) Allen, C. L.; Williams, J. M. J. *Chem. Soc. Rev.* **2011**, *40*, 3405-3415.

- (b) De Luca, L.; Giacomelli, G.; Porcheddu, A.; Salaris, M. *Synlett* **2004**, 2570-2572.
- (c) Deutsch, J.; Eckelt, R.; Köckritz, A.; Martin, A. *Tetrahedron* **2009**, *65*, 10365-10369.
- (d) Shekhar, A. C.; Kumar, A. R.; Sathaiah, G.; Paul, V. L.; Sridhar, M.; Rao, P. S. *Tetrahedron Lett.* **2009**, *50*, 7099-7101.
- (48) More experimental work is currently underway for direct comparison to the [Tptm] system.
- (49) (a) McNally, J. P.; Leong, V. S.; Cooper, N. J. in *Experimental Organometallic Chemistry*, Wayda, A. L.; Darensbourg, M. Y., Eds.; American Chemical Society: Washington, DC, 1987; Chapter 2, pp 6-23.
- (b) Burger, B.J.; Bercaw, J. E. in *Experimental Organometallic Chemistry*; Wayda, A. L.; Darensbourg, M. Y., Eds.; American Chemical Society: Washington, DC, 1987; Chapter 4, pp 79-98.
- (c) Shriver, D. F.; Drezdson, M. A.; *The Manipulation of Air-Sensitive Compounds*, 2nd Edition; Wiley-Interscience: New York, 1986.
- (50) Gottlieb, H. E.; Kotlyar, V.; Nudelman, A. J. *Org. Chem.* **1997**, *62*, 7512-7515.
- (51) Sattler, W.; Parkin, G. *J. Am. Chem. Soc.* **2011**, *133*, 9708-9711.
- (52) Jaguar 7.5, Schrödinger, LLC, New York, NY 2008.
- (53) (a) Becke, A. D. *J. Chem. Phys.* **1993**, *98*, 5648-5652.
- (b) Becke, A. D. *Phys. Rev. A* **1988**, *38*, 3098-3100.
- (c) Lee, C. T.; Yang, W. T.; Parr, R. G. *Phys. Rev. B* **1988**, *37*, 785-789.

- (d) Vosko, S. H.; Wilk, L.; Nusair, M. *Can. J. Phys.* **1980**, *58*, 1200-1211.
- (e) Slater, J. C. *Quantum Theory of Molecules and Solids, Vol. 4: The Self-Consistent Field for Molecules and Solids*; McGraw-Hill: New York, 1974.
- (54) (a) Hay, P. J.; Wadt, W. R. *J. Chem. Phys.* **1985**, *82*, 270-283.
- (b) Wadt, W. R.; Hay, P. J. *J. Chem. Phys.* **1985**, *82*, 284-298.
- (c) Hay, P. J.; Wadt, W. R. *J. Chem. Phys.* **1985**, *82*, 299-310.
- (55) Dunning, T. H. *J. Chem. Phys.* **1989**, *90*, 1007-1023.
- (56) (a) Sheldrick, G. M. *SHELXTL, An Integrated System for Solving, Refining and Displaying Crystal Structures from Diffraction Data*; University of Göttingen, Göttingen, Federal Republic of Germany, 1981.
- (b) Sheldrick, G. M. *Acta Cryst.* **2008**, *A64*, 112-122.
- (57) Wakabayashi, R.; Sugiura, Y.; Shibue, T.; Kuroda, K. *Angew. Chem. Int. Ed.* **2011**, *50*, 10708-10711.
- (58) Manoso, A. S.; Ahn, C.; Soheili, A.; Handy, C. J.; Correia, R.; Seganiash, W. M.; DeShong, P. *J. Org. Chem.* **2004**, *69*, 8305-8314.
- (59) Chappelow, C. C.; Elliott, R. L.; Goodwin, J. T. *J. Org. Chem.* **1960**, *25*, 435-439.
- (60) Onozawa, S.; Sakakura, T.; Tanaka, M.; Shiro, M. *Tetrahedron* **1996**, *52*, 4291-4302.
- (61) Sheludiyakov, V. D.; Khatuntsev, G. D.; Mironov, V. F. *J. Gen. Chem. U.S.S.R. (Engl. trans)*. **1972**, *42*, 2205-2209.

CHAPTER 4

Synthesis of Transition Metal Isocyanide Compounds from Carbonyl Complexes *via* Reaction with Li[Me₃SiNR]

Table of Contents

4.1 Introduction	263
4.2 Li[Me ₃ SiNR] as a reagent for the conversion of metal carbonyl complexes to metal isocyanide complexes	266
4.3 Synthesis of CNBu ^t complexes using Li[Me ₃ SiNBu ^t] with L _n MCO	268
4.3.1 Group 6: Cr, Mo and W	268
4.3.2 Group 8: Fe	272
4.4 Synthesis of aryl, sterically hindered, and enantiopure metal isocyanide complexes using Li[Me ₃ SiNR].	275
4.5 Proposed mechanism for the isocyanide formation	281
4.6 Summary and conclusions	283
4.7 Experimental details	284
4.7.1 General considerations	284
4.7.2 X-ray structure determinations	285
4.7.3 Synthesis of Li[Me ₃ SiNBu ^t]	285
4.7.4 Synthesis of Cr(CO) ₅ (CNBu ^t)	285
4.7.5 Synthesis of Mo(CO) ₅ (CNBu ^t)	286
4.7.6 Synthesis of W(CO) ₅ (CNBu ^t)	286
4.7.7 Synthesis of <i>cis</i> -Cr(CO) ₄ (CNBu ^t) ₂	287
4.7.8 Synthesis of <i>cis</i> -Mo(CO) ₄ (CNBu ^t) ₂	287
4.7.9 Synthesis of <i>cis</i> -W(CO) ₄ (CNBu ^t) ₂	288
4.7.10 Synthesis of <i>fac</i> -Cr(CO) ₃ (CNBu ^t) ₃	289

	262
4.7.11 Synthesis of <i>fac</i> -Mo(CO) ₃ (CNBu ^t) ₃ and <i>cis</i> -Mo(CO) ₂ (CNBu ^t) ₄	289
4.7.12 Synthesis of <i>fac</i> -W(CO) ₃ (CNBu ^t) ₃	290
4.7.13 Synthesis of <i>axial</i> -Fe(CO) ₄ (CNBu ^t)	291
4.7.14 Synthesis of <i>trans</i> -Fe(CO) ₃ (CNBu ^t) ₂	291
4.7.15 Synthesis of Mo(CO) ₅ (CN-1-Np ^{H4})	292
4.7.16 Synthesis of Mo(CO) ₅ (CN-1-Adamantyl) and <i>cis</i> -Mo(CO) ₄ (CN-1-Adamantyl) ₂	293
4.7.17 Synthesis of Mo(CO) ₅ (CN- <i>p</i> -C ₆ H ₄ Me)	294
4.7.18 Synthesis of Mo(CO) ₅ (CN- <i>p</i> -C ₆ H ₄ OMe)	295
4.7.19 Synthesis of <i>cis</i> -Mo(CO) ₄ (CN-2,4,6-C ₆ H ₂ Me ₃) ₂	295
4.8 Crystallographic data	297
4.9 References and notes	303

Reproduced in part from:

W. Sattler and G. Parkin *Chem. Commun.* **2009**, 7566-7568.

4.1 Introduction

Isocyanides (RNC), also known as isonitriles, are common ligands in transition metal chemistry that are isoelectronic to the ubiquitous carbonyl ligand, CO (Figure 1). While isocyanides are typically classified as L-type ligands according to the covalent bond classification (CBC) system, they are more specifically regarded to as LZ' ligands where Z' refers to a variable amount of back-bonding.¹



Figure 1. Lewis structures of isocyanides (left) and carbon monoxide (right).

The L component corresponds to the ligands σ -donating character while the Z' component corresponds to the ligands π -accepting character.^{2,3,4} Significant back-bonding formally results in a metal-carbon double bond, due to the interaction being more akin to that of an X_2 -type (Figure 2). While this dual feature of the bonding is common to CO (Figure 2), an important distinction between RNC and CO is that the steric and electronic properties of isocyanides may be effectively tuned by modifying the substituent on the nitrogen atom.

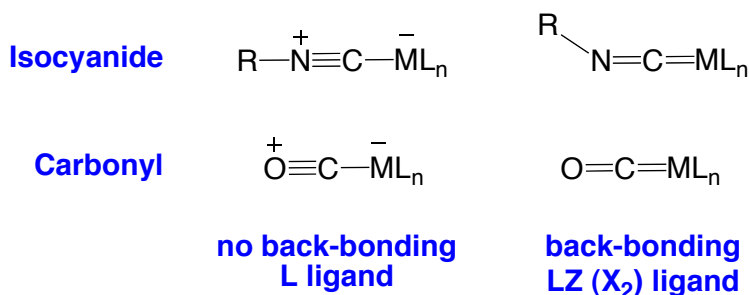
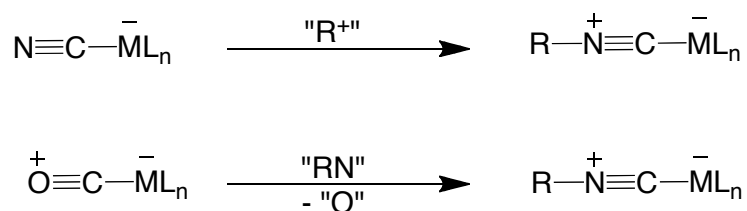


Figure 2. Resonance structures for the interaction of an isocyanide and carbon monoxide with a metal complex, ML_n .

Although the ability to modify an isocyanide ligand has been utilized in the application of transition metal–isocyanide complexes as catalysts for organic transformations,^{5,6,7,8} the majority of transition metal isocyanide complexes feature rather simple substituents on nitrogen. This is presumably a reflection of the paucity of readily available (*i.e.* commercially available) isocyanide compounds. In this regard, it is possible that progress in transition metal isocyanide chemistry would be facilitated by the development of new synthetic methods that do not require the use of the isocyanide as a reagent.

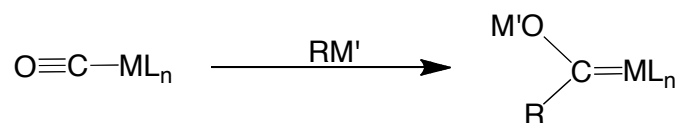
Two approaches to generating an isocyanide ligand without the use of the free isocyanide as a reagent include (*i*) the addition of R^+ to the nitrogen atom of a metal cyanide ligand^{2b,c,f} and (*ii*) the replacement of the oxygen atom of a metal carbonyl ligand by the isoelectronic NR group (Scheme 1).^{9,10,11} Although both approaches are practical and appealing in view of the availability of both cyanide^{12,13} and carbonyl^{12,14} complexes, the latter approach is the more attractive one because there are tens of thousands¹⁴ of transition metal carbonyl compounds.



Scheme 1. Synthesis of metal isocyanides without using the free isocyanide.

The carbon atom within a metal carbonyl moiety, L_nMCO , is well known to be susceptible to nucleophilic attack by external reagents.¹⁵ For example, attack by carbon nucleophiles (*e.g.* a lithium alkyl or a lithium aryl) has been employed in the syntheses of carbene complexes (Scheme 2).¹⁶ This was the method used by E. O. Fischer to synthesize the first transition metal carbene complex, which he prepared on

tungsten.^{17,18} Attack by oxygen nucleophiles is prominently featured in the mechanisms of (i) the water-gas shift reaction (WGS) (Scheme 3),¹⁹ (ii) the exchange of oxygen atoms between a carbonyl ligand and H₂O,²⁰ and (iii) the Me₃NO induced dissociation of a carbonyl ligand as CO₂.²¹

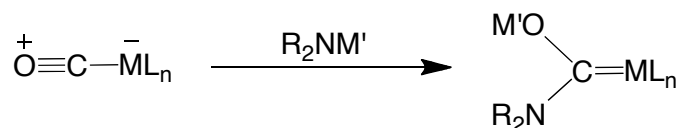


Scheme 2. Reaction of a metal carbonyl complex with a nucleophilic organometallic reagent to give a Fischer carbene complex.



Scheme 3. Water-gas shift reaction.

The carbon atom of L_nMCO is also susceptible to attack by amine based nucleophiles.^{22,23} In principle, this is the first step for converting a carbonyl ligand to an isocyanide ligand (Scheme 4). For example, if after an initial attack by a deprotonated amine (*i.e.* a metal amide) on a metal carbonyl complex, L_nMCO, a substituent (R) on the nitrogen atom of the amine can transfer to the oxygen atom of the carbonyl, with subsequent expulsion of RO⁻, this conversion would result in the formation of an isocyanide complex, L_nMCNR.



Scheme 4. Reaction of a metal carbonyl complex with a nucleophilic metal amide reagent.

This chapter will describe a new general method that utilizes lithium trimethylsilylamides, $\text{Li}[\text{Me}_3\text{SiNR}]$, as reagents for converting transition metal carbonyl compounds L_nMCO into their isocyanide counterparts L_nMCNR .

4.2 $\text{Li}[\text{Me}_3\text{SiNR}]$ as a reagent for the conversion of metal carbonyl complexes to metal isocyanide complexes

As mentioned earlier, attack by an amine nucleophile on a metal carbonyl complex, followed by removal of the oxygen atom *via* a group transfer from N to O, would result in metal isocyanide formation. In this regard, we have discovered that having a silyl group on a lithiated amide, specifically, the ubiquitous trimethylsilyl group (Me_3Si), provided the driving force for N to O transfer followed by subsequent Me_3SiO^- expulsion. This reagent, namely $\text{Li}[\text{Me}_3\text{SiNR}]$, has been used to convert metal carbonyl compounds into their isocyanide counterparts (Figure 3).

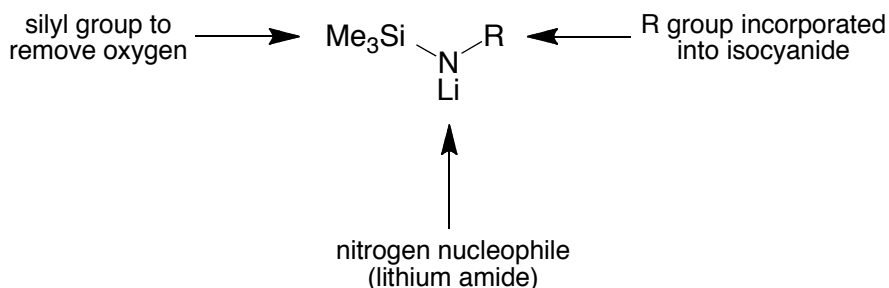


Figure 3. $\text{Li}[\text{Me}_3\text{SiNR}]$ used for nucleophilic attack on a metal carbonyl complex to give a metal isocyanide complex.

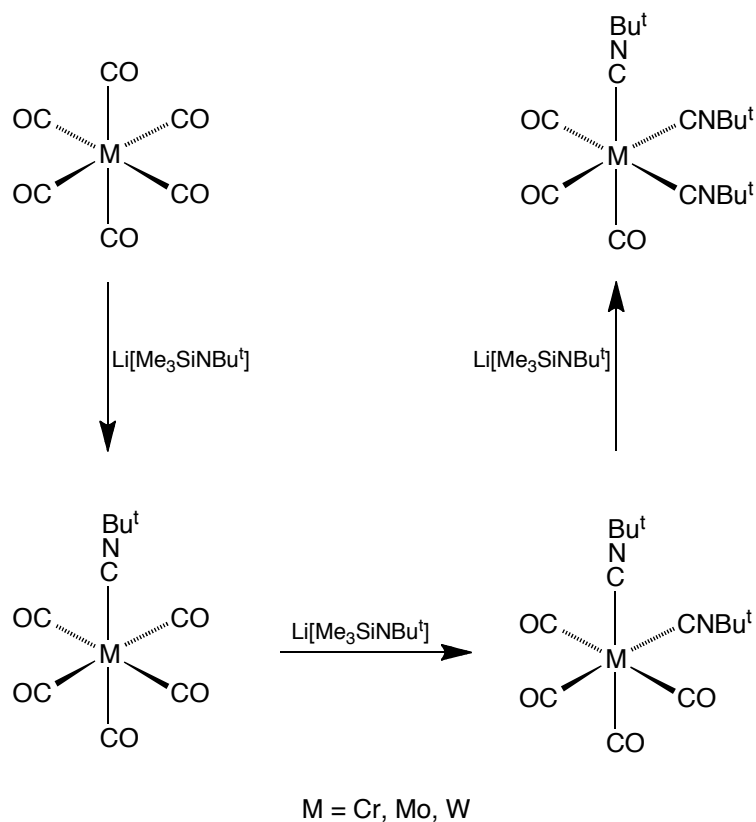
The synthesis of $\text{Li}[\text{Me}_3\text{SiNR}]$ was accomplished by either one of two methods, as depicted in Scheme 5. For more nucleophilic amines (Scheme 5A), the amine was directly treated with trimethylsilyl chloride (Me_3SiCl) to give the ammonium salt, which was then treated with two equivalents of *n*-butyllithium (Bu^nLi) to give $\text{Li}[\text{Me}_3\text{SiNR}]$. Less nucleophilic amines (Scheme 5B), were first treated with one equivalent of Bu^nLi to

4.3 Synthesis of CNBu^t complexes using Li[Me₃SiNBu^t] with L_nMCO

4.3.1 Group 6: Cr, Mo and W

Recently, the molybdenum compounds Mo(CO)_{6-n}(CNBu^t)_n (n = 2, 3, 4) have been used as catalysts for some organic transformations.⁶ For example, Trost and co-workers have used a series of Mo(CO)_{6-n}(CNBu^t)_n (n = 2, 3, 4) compounds as catalysts for different alkylation reactions, while Kazmaier and co-workers have used the same compounds as catalysts for the hydrostannation and distannation of alkynes.⁶ While these isocyanide complexes M(CO)_{6-n}(CNBu^t)_n (n = 1, 2, 3, 4) have been previously synthesized, their syntheses utilized the free isocyanide, Bu^tNC, as a reagent.²⁶

In contrast to using the free isocyanide, the compounds, Mo(CO)_{6-n}(CNBu^t)_n (n = 1, 2, 3, 4) have been synthesized *via* treatment of the group 6 homoleptic carbonyl, Mo(CO)₆ with Li[Me₃SiNBu^t]²⁴. Additionally, the chromium and tungsten compounds may also be prepared *via* the analogous reaction with M(CO)₆ (M = Cr, W). For example, M(CO)₅(CNBu^t) (M = Cr, Mo, W), *cis*-M(CO)₄(CNBu^t)₂ (M = Cr, Mo, W), *fac*-M(CO)₃(CNBu^t)₃ (M = Cr, Mo, W), and *cis*-M(CO)₂(CNBu^t)₄ (M = Mo) are obtained by treatment of M(CO)₆ with the appropriate number of equivalents of Li[Me₃SiNBu^t] (Scheme 6). The compounds were purified by flash column chromatography using silica gel, followed by crystallization in air. It is interesting to note the stereochemistry of the resulting isocyanide complexes. Specifically, the *bis*-isocyanide compounds have the isocyanide ligands displaced in a *cis*-disposition, while the *tris*-isocyanide compounds have a *fac*-stereochemistry. The stereochemistry was determined by IR spectroscopy, and in some cases, confirmed by single crystal X-ray diffraction.



Scheme 6. Reaction of $\text{Li}[\text{Me}_3\text{SiNBu}^t]$ with group 6 carbonyl compounds.

The molecular structures have been determined by using single crystal X-ray diffraction for the following compounds: $\text{Cr}(\text{CO})_5(\text{CNBu}^t)$ (Figure 4), *cis*- $\text{Cr}(\text{CO})_4(\text{CNBu}^t)_2$ (Figure 5), *cis*- $\text{Mo}(\text{CO})_4(\text{CNBu}^t)_2$ (Figure 6), *cis*- $\text{W}(\text{CO})_4(\text{CNBu}^t)_2$ (Figure 7), and *fac*- $\text{W}(\text{CO})_3(\text{CNBu}^t)_3$ ²⁷ (Figure 8).

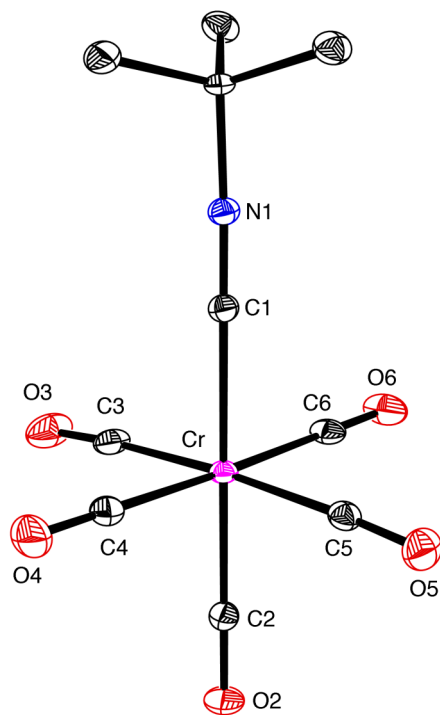


Figure 4. Molecular structure of $\text{Cr}(\text{CO})_5(\text{CNBu}^t)$.

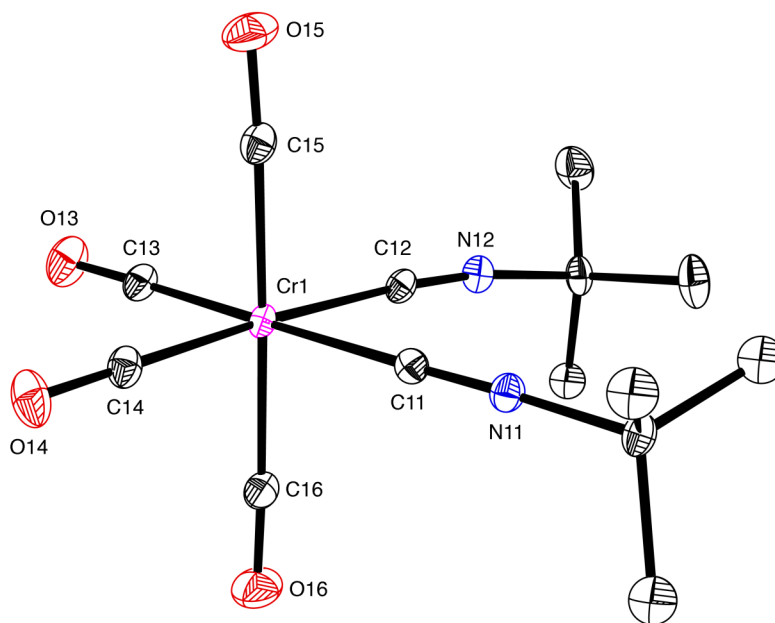


Figure 5. Molecular structure of $\text{cis-Cr}(\text{CO})_4(\text{CNBu}^t)_2$.

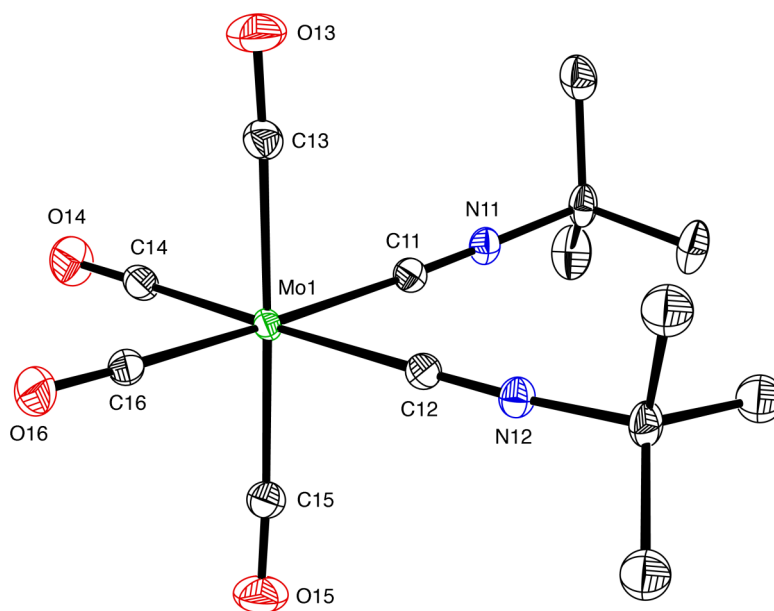


Figure 6. Molecular structure of *cis*-Mo(CO)₄(CNBu)₂.

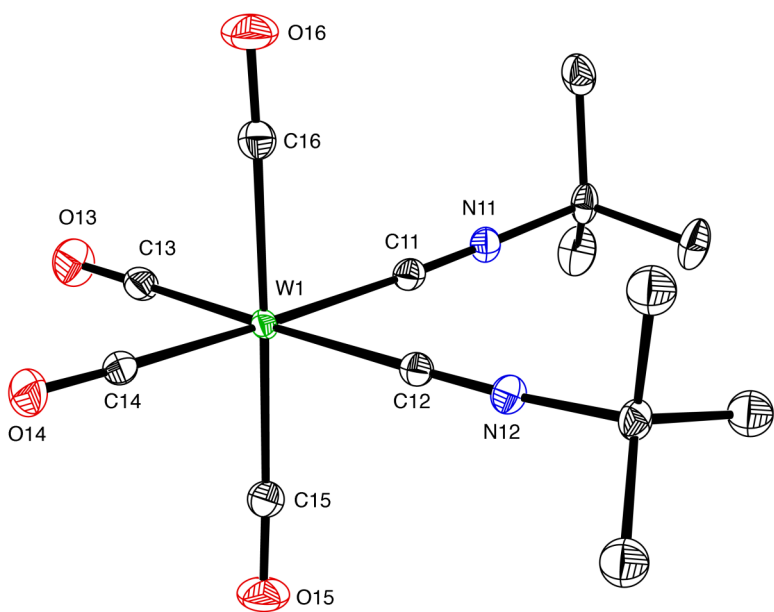


Figure 7. Molecular structure of *cis*-W(CO)₄(CNBu)₂.

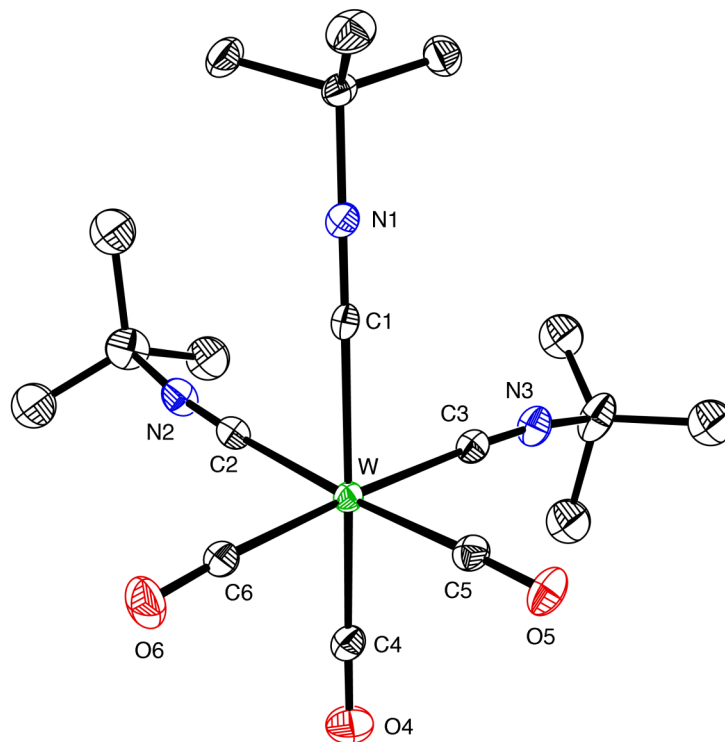
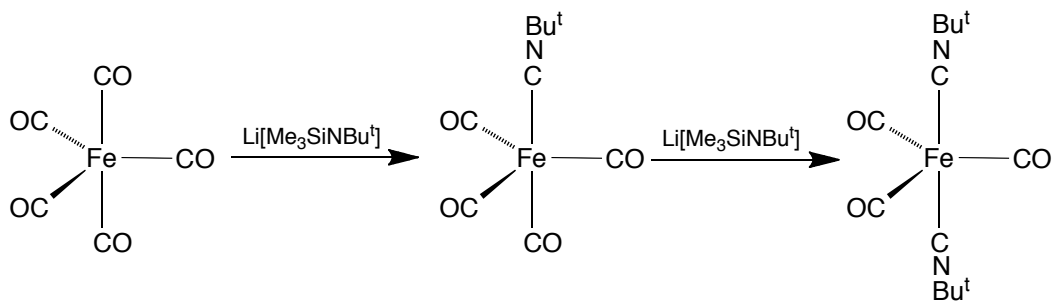


Figure 8. Molecular structure of *fac*-W(CO)₃(CNBu^t)₃.

4.3.2 Group 8: Fe

In addition to the Group 6 metal carbonyl compounds, the reactivity of the Group 8 homoleptic carbonyl complex, Fe(CO)₅, was explored. Li[Me₃SiNBu^t] reacts with Fe(CO)₅ to give *axial*-Fe(CO)₄(CNBu^t) (Scheme 7), while addition of a second equivalent of Li[Me₃SiNBu^t] yields *trans*-Fe(CO)₃(CNBu^t)₂ (Scheme 7).



Scheme 7. Reaction of Li[Me₃SiNBu^t] with Fe(CO)₅.

The molecular structure of both the monosubstituted derivative, *axial*-Fe(CO)₄(CNBu^t) (Figure 9) and the disubstituted derivative, *trans*-Fe(CO)₃(CNBu^t)₂ (Figure 10) have been determined by using single crystal X-ray diffraction. As depicted in Figure 9, the isocyanide ligand adopts an axial position, with an Fe–CNBu^t distance of 1.89 Å which is significantly longer than the Fe–CO bond distances that range from 1.79 – 1.81 Å. While a variety of Fe(CO)_{5-x}(CNR)_x are known,²⁸ the only structurally characterized heteroleptic examples of which we are aware of are the disubstituted derivatives *trans*-Fe(CO)₃(CNMe)₂²⁹ and *trans*-Fe(CO)₃(CNBu^t)₂.³⁰

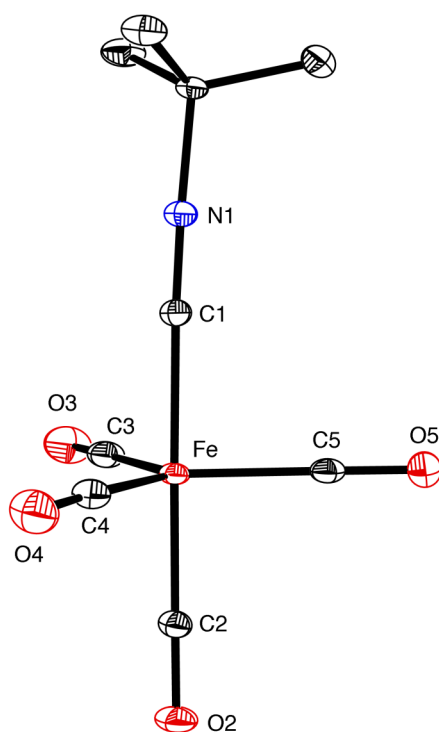


Figure 9. Molecular structure of *axial*-Fe(CO)₄(CNBu^t).

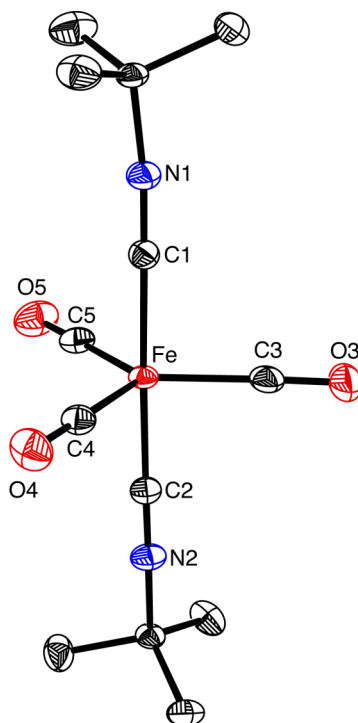


Figure 10. Molecular structure of *trans*-Fe(CO)₃(CNBu^t)₂. The molecular structure of *trans*-Fe(CO)₃(CNBu^t)₂ has previously been determined, see reference 30.

While the FeL₅ complexes have a trigonal-bipyramidal geometry, and the ML₆ (M = Cr, Mo or W) complexes have an octahedral geometry, it is still interesting to briefly compare the stereochemistry of the isocyanide complexes. For the Group 6 metals, the isocyanides are *cis* to each other as mentioned above.³¹ However, *trans*-Fe(CO)₃(CNBu^t)₂ exhibits the opposite tendency, where the isocyanide ligands are displaced from each other in a *trans*-diaxial disposition. DFT calculations on the different geometry optimized stereoisomers of Fe(CO)₃(CNMe)₂ suggests *trans*-Fe(CO)₃(CNBu^t)₂ is the thermodynamically favored product (Figure 11).³²

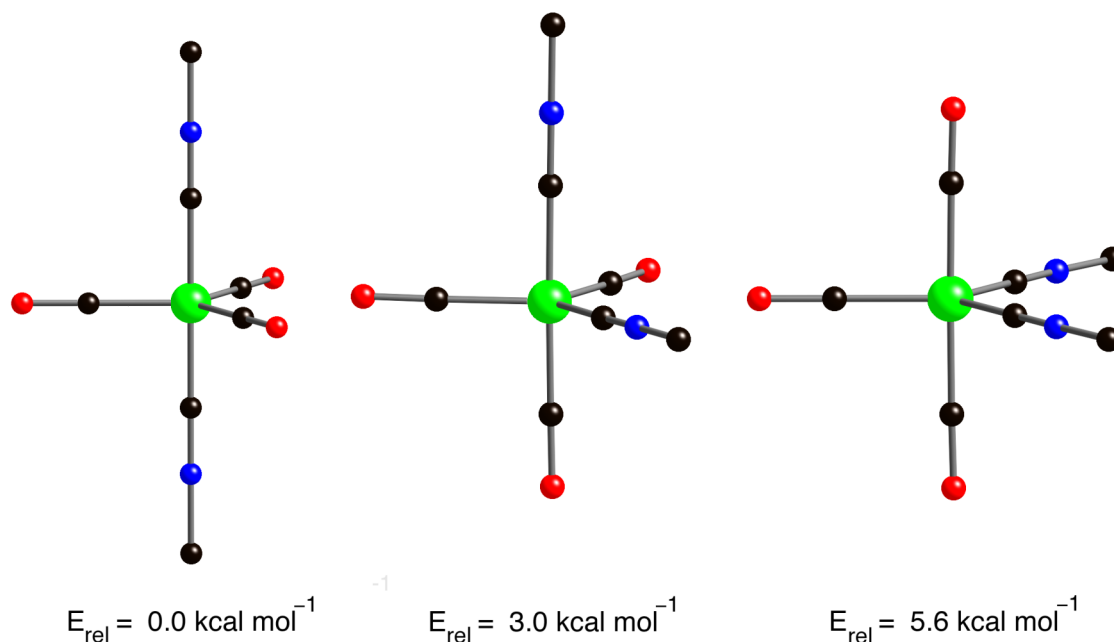
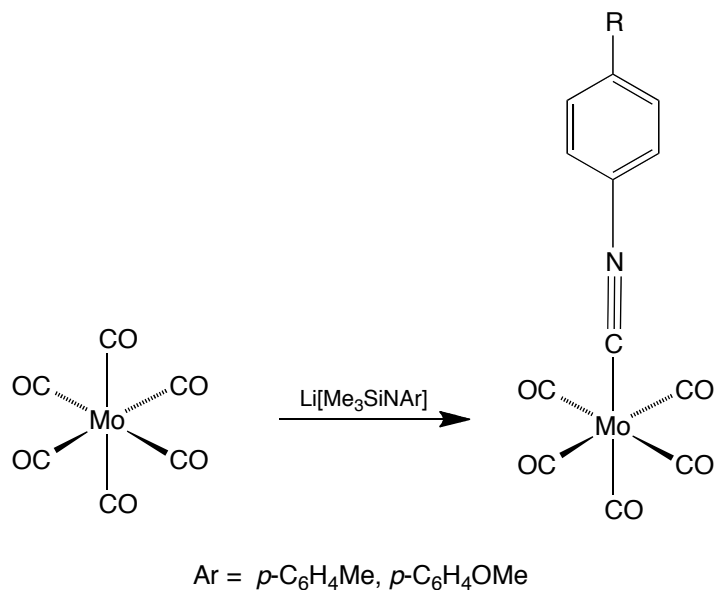


Figure 11. Geometry optimized structures for the different stereoisomers of $\text{Fe}(\text{CO})_3(\text{CNMe})_2$ (hydrogen atoms not shown for clarity). Color code: Green = Fe, red = O, blue = nitrogen and black = carbon.

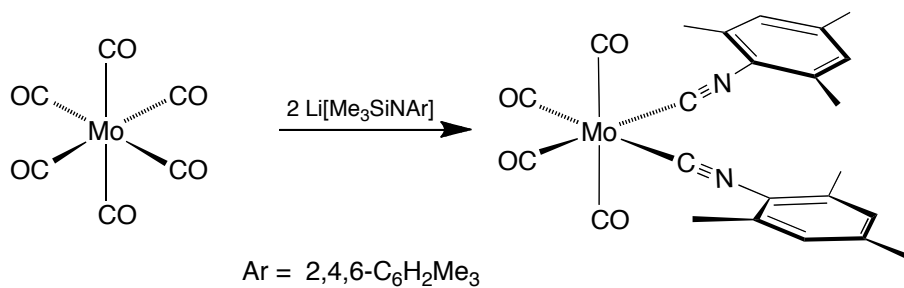
4.4 Synthesis of aryl, sterically hindered, and enantiopure metal isocyanide complexes using $\text{Li}[\text{Me}_3\text{SiNR}]$.

In addition to the synthesis of numerous Bu^tNC complexes, a variety of alkyl and aryl amines have been employed with this synthetic method to generate other isocyanide ligands. For example, the previously reported mono arylisocyanide derivatives $\text{Mo}(\text{CO})_5(\text{CNAr})$ ($\text{Ar} = p\text{-C}_6\text{H}_4\text{Me}$,³³ $p\text{-C}_6\text{H}_4\text{OMe}$ ⁴) have been synthesized as shown in Scheme 8.



Scheme 8. Synthesis of Mo(CO)₅(CNAr) (Ar = *p*-C₆H₄Me, *p*-C₆H₄OMe).

Additionally, the *bis*-arylisocyanide compound, *cis*-Mo(CO)₄(CNAr)₂ (Ar = 2,4,6-C₆H₂Me₃) has been synthesized as depicted in Scheme 9. The molecular structures of Mo(CO)₅(CN-*p*-C₆H₄OMe) and Mo(CO)₄(CN-2,4,6-C₆H₂Me₃)₂ are presented in Figure 12 and Figure 13, respectively.



Scheme 9. Synthesis of Mo(CO)₄(CN-2,4,6-C₆H₂Me₃)₂.

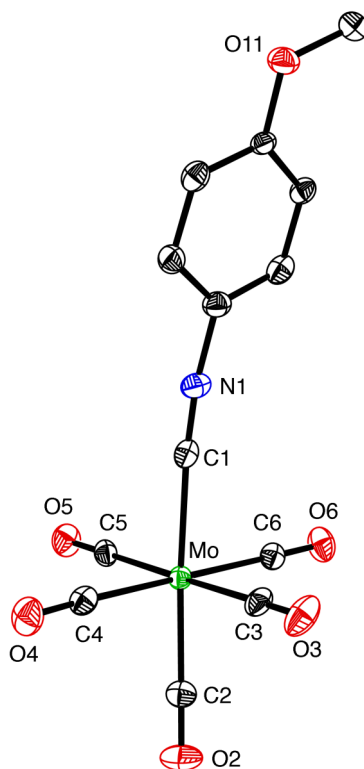


Figure 12. Molecular structure of $\text{Mo}(\text{CO})_5(\text{CN-}p\text{-C}_6\text{H}_4\text{OMe})$.

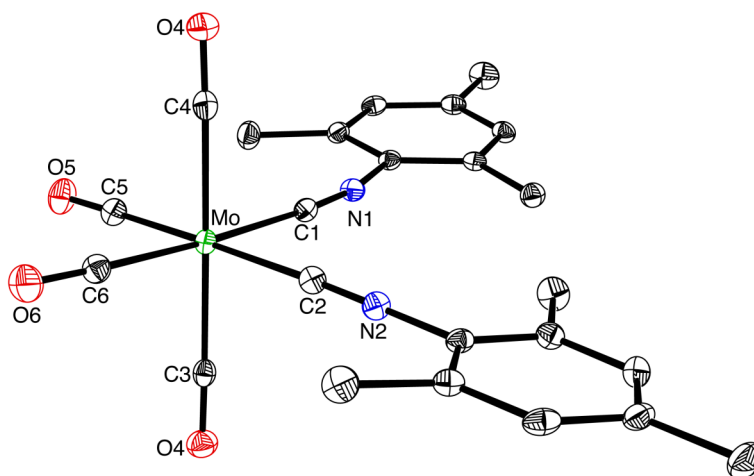
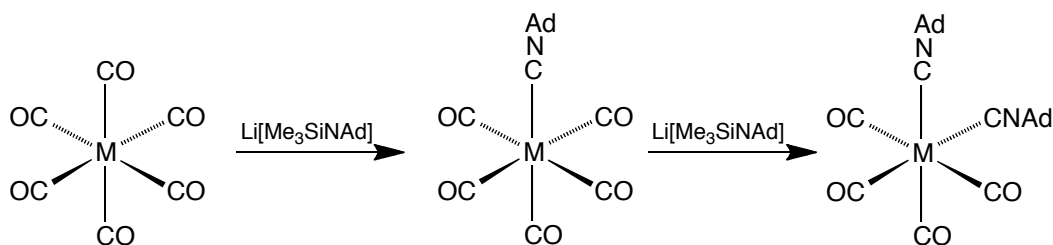


Figure 13. Molecular structure of $\text{Mo}(\text{CO})_4(\text{CN-}2,4,6\text{-C}_6\text{H}_2\text{Me}_3)_2$.

There has recently been interest in utilizing metal complexes with bulky isocyanide ligands in order to isolate low-coordinate, low-valent metal complexes, most

notably by Figueroa^{7,34,35} who has utilized terphenyl isocyanides. Figueroa's metal complexes were generated using the free isocyanide as a reagent.³⁶ In this vein, $\text{Li}[\text{Me}_3\text{SiNAd}]$ (Ad = adamantyl) has been prepared in two steps from the commercially available amine, 1-adamantamine, which was used to synthesize the bulky *mono*- and *bis*-adamantyl isocyanide complexes (Scheme 10).



Scheme 10. Synthesis of $\text{Mo}(\text{CO})_5(\text{CN-1-Ad})$ and *cis*- $\text{Mo}(\text{CO})_4(\text{CN-1-Ad})_2$.

The molecular structures of $\text{Mo}(\text{CO})_5(\text{CN-1-Ad})$ and *cis*- $\text{Mo}(\text{CO})_4(\text{CN-1-Ad})_2$ are shown in Figure 14 and Figure 15, respectively.

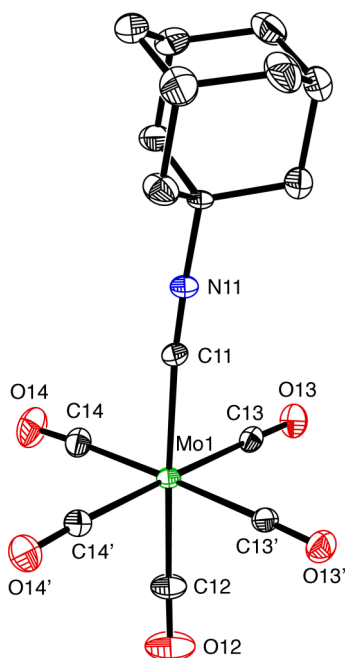


Figure 14. Molecular structure of $\text{Mo}(\text{CO})_5(\text{CN-1-Ad})$.

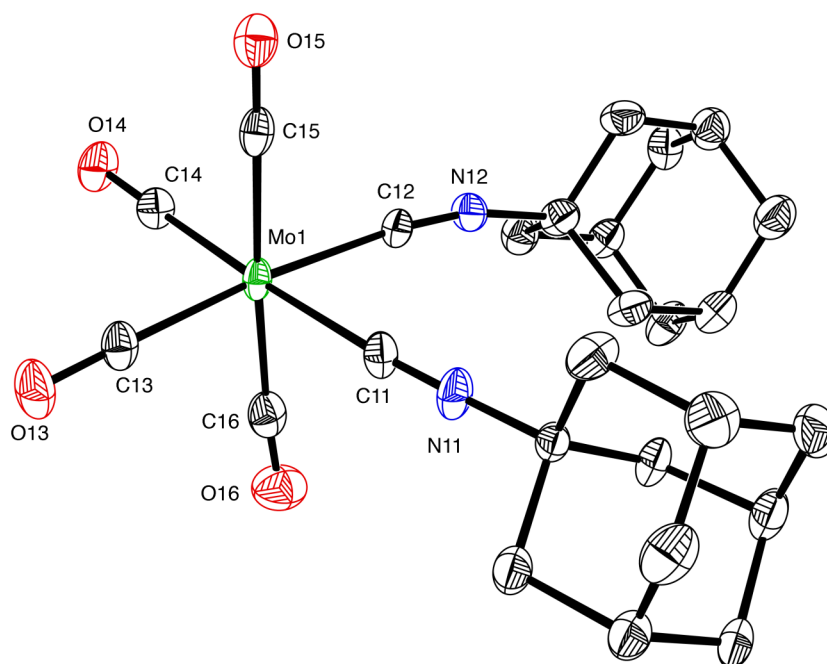
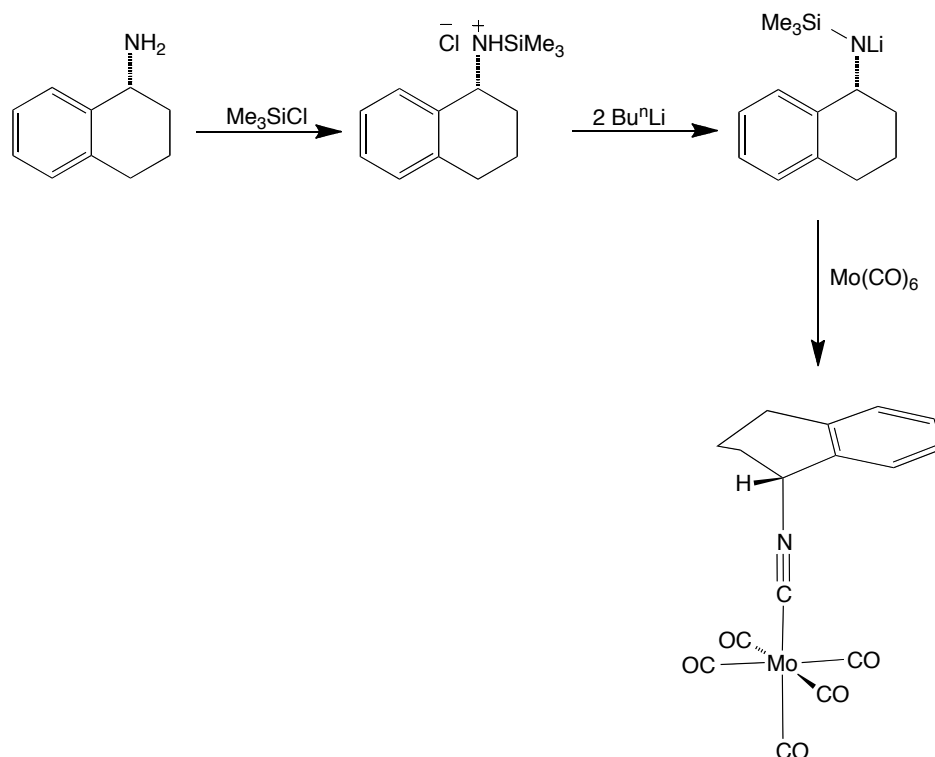


Figure 15. Molecular structure of *cis*-Mo(CO)₄(CN-1-Ad)₂.

Finally, as mentioned earlier, enantiopure isocyanides are of interest for asymmetric catalysts. Using chiral primary amines, an enantiopure isocyanide complex can be formed in three steps. Specifically, (*R*)-1,2,3,4-tetrahydro-1-naphthyl derivative, Mo(CO)₅(CN-1-Np^{H4}), has been synthesized and structurally characterized by single crystal X-ray diffraction (Figure 16). The synthesis was accomplished in a one-pot reaction with sequential additions of (*R*)-1,2,3,4-tetrahydro-1-naphthylamine, Me₃SiCl, BuⁿLi and then Mo(CO)₆ (Scheme 11).



Scheme 11. Synthesis of $\text{Mo(CO)}_5(\text{CN-1-Np}^{\text{H}_4})$.

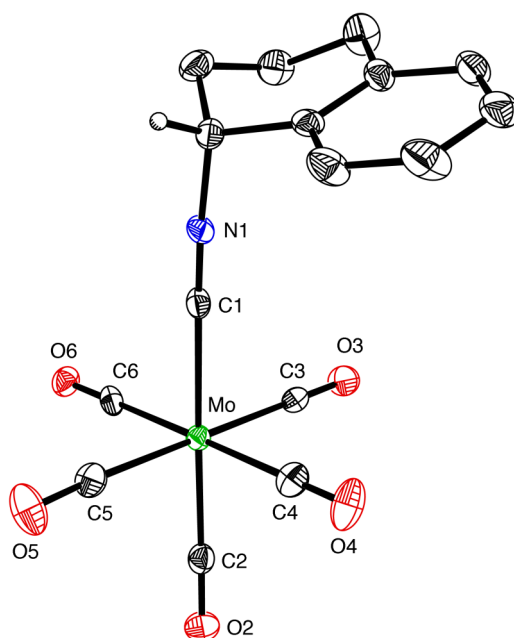
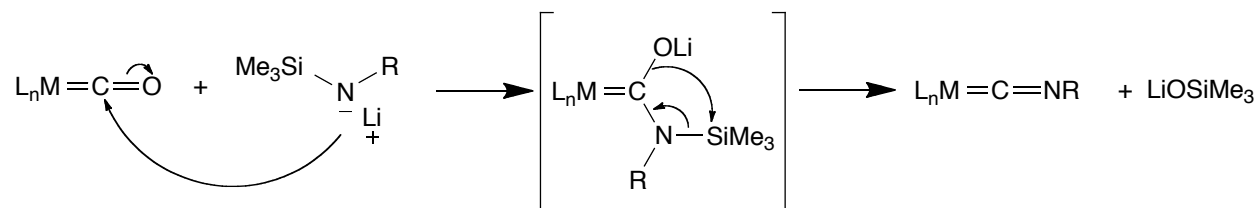


Figure 16. Molecular structure of $\text{Mo(CO)}_5(\text{CN-1-Np}^{\text{H}_4})$ (space group is $P2_12_12_1$).³⁷

Compared to tertiary phosphines, which are commonplace in asymmetric catalysis, enantiomerically pure isocyanide ligands have not been employed much in transition metal chemistry.⁹ It is possible that this simple synthetic method could pave the way to new asymmetric catalysts, thereby replacing some of the expensive phosphine based catalyst systems.

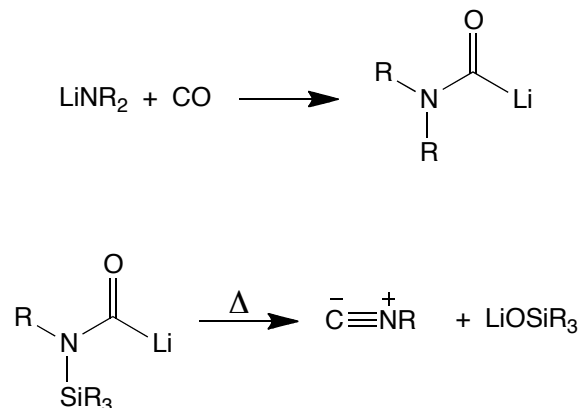
4.5 Proposed mechanism for the isocyanide formation

The mechanism proposed for the conversion of the carbonyl ligand to an isocyanide ligand is illustrated in Scheme 12. The elementary steps are as follows: (i) initial attack of the amide nitrogen on the carbon of the metal carbonyl, which generates a carbamoyl anion intermediate, namely $L_nM[C(O)N(R)SiMe_3]^-$ and (ii) rearrangement *via* trimethylsilyl migration to extrude $LiOSiMe_3$ and thereby generating the new isocyanide ligand.^{38,39}



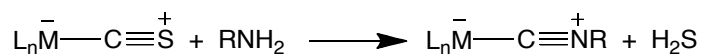
Scheme 12. Proposed mechanism for carbonyl/isocyanide conversion.

Precedent for this mechanism is provided by the fact that lithium amides are known to react with CO to generate $[R_2NC(O)Li]^{40}$ and that silyl derivatives of the type $[(R_3Si)N(R)C(O)Li]$ decompose to give RNC and R_3SiOLi at elevated temperatures (Scheme 13).⁴¹



Scheme 13. Attack of lithium amide on carbon monoxide (top). Decomposition of $[(\text{R}_3\text{Si})\text{N}(\text{R})\text{C}(\text{O})\text{Li}]$ to give RNC and R_3SiOLi (bottom).

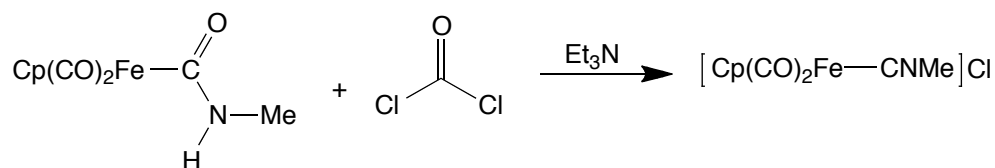
Also of relevance to the conversion of metal carbonyl complexes to metal isocyanide complexes is the fact that primary amines, RNH_2 , react with thiocarbonyl complexes to give the isocyanide derivative with loss of hydrogen sulfide as depicted in Scheme 14.⁴²



Scheme 14. Reaction of a primary amine with a metal thiocarbonyl complex to give the corresponding isocyanide derivative.

One difference between the thiocarbonyl and carbonyl ligands is the higher electrophilicity of the thiocarbonyl.^{42a,b,43,44} For example, Angelici demonstrated that in mixed carbonyl/thiocarbonyl complexes, primary amines react at the carbon of the thiocarbonyl ligand preferentially to give isocyanide derivatives.^{42b} Additionally, in isocyanide preparations from thiocarbonyl complexes, elimination of H_2S is a more facile process compared to the elimination of H_2O .²² The demanding elimination of H_2O is demonstrated by the fact that metal carbonyl compounds react with primary amines (only aliphatic amines) to make the carbamoyl derivative, $\{\text{L}_n\text{M}[\text{C}(\text{O})\text{NHR}]\}[\text{RNH}_3]$ but

do not eliminate H₂O to make the isocyanide derivative.²² However, conversion of this intermediate to the isocyanide derivative can be accomplished by using dehydrating agents such as phosgene (C(O)Cl₂) or oxalyl chloride ([C(O)Cl]₂).¹¹ One example of a metal carbamoyl dehydration yielding an isocyanide compound is the reaction of CpFe(CO)₂[C(O)NHMe] with C(O)Cl₂ in the presence of Et₃N to give [CpFe(CNMe)]Cl.^{11a} A key improvement concerning the use of Li[Me₃SiNR] compared to these methodologies is the fact that highly toxic, undesirable chemicals such as phosgene are not required.



Scheme 15. Reaction of CpFe(CO)₂[C(O)NHMe] with C(O)Cl₂ in the presence of Et₃N to give [CpFe(CNMe)]Cl.

The ability of Li[Me₃SiNR] to achieve deoxygenation of the carbonyl ligand may be attributed to the formation of the strong Si–O bond which provides a driving force for the reaction. This is in comparison to the formation of an O–H bond when a primary amine is used. Along the same lines as using Li[Me₃SiNR] to convert carbonyl compounds to their isocyanide counterparts, there are analogous reactions using phosphorimidates, Li[(EtO)₂(O)PNR],⁹ and phosphinimines, R₃PNR',¹⁰ for which P–O bond formation presumably provides the driving force.

4.6 Summary and conclusions

In summary, the reaction of metal carbonyl compounds, L_nMCO, with Li[Me₃SiNR] yields the corresponding isocyanide derivatives, L_nMCNR. Since metal isocyanide compounds are most commonly synthesized using the free isocyanide, this

new approach provides a convenient synthetic method that circumvents the use of the free isocyanide, which has the advantage of eliminating problems associated with the putrid smell of the free isocyanides.^{25b} While the formation of isocyanide complexes by reaction of thiocarbonyl complexes with RNH_2 may be considered a more appealing, direct method, a downside to this route is the fact that compounds which feature thiocarbonyl ligands are much less common than carbonyl derivatives.⁴⁵ The reaction of a carbonyl derivative with $\text{Li}[\text{Me}_3\text{SiNR}]$ provides a convenient alternative for the synthesis of isocyanide compounds from carbonyl derivatives.

4.7 Experimental details

4.7.1 General considerations

All manipulations were performed using a combination of dry glovebox, high vacuum, and Schlenk techniques under a nitrogen or argon atmosphere,⁴⁶ with the exception of chromatography that was performed in air. Solvents were purified and degassed by standard procedures. ^1H NMR spectra were measured on Bruker 300 DRX, Bruker 400 DRX, and Bruker Avance 500 DMX spectrometers. ^1H chemical shifts are reported in ppm relative to SiMe_4 ($\delta = 0$) and were referenced internally with respect to the protio solvent impurity (δ 7.16 for $\text{C}_6\text{D}_5\text{H}$).⁴⁷ Coupling constants are given in hertz. Infrared spectra were recorded on Nicolet Avatar 370 DTGS spectrometer and are reported in cm^{-1} . Mass spectra were obtained on a Micromass Quadrupole-Time-of-Flight mass spectrometer using fast atom bombardment (FAB). All chemicals were obtained from Aldrich, with the exception of $\text{Cr}(\text{CO})_6$ and $\text{W}(\text{CO})_6$ which were obtained from Strem.

4.7.2 X-ray structure determinations

X-ray diffraction data were collected on a Bruker Apex II diffractometer. Crystal data, data collection and refinement parameters are summarized in Table 1. The structures were solved using direct methods and standard difference map techniques, and were refined by full-matrix least-squares procedures on F^2 with SHELXTL (Version 6.1).⁴⁸

4.7.3 Synthesis of Li[Me₃SiNBu^t]

Li[Me₃SiNBu^t] was prepared by an adaption of a literature method. A solution of BuⁿLi in hexanes (2.5 M, 3.2 mL, 8.0 mmol) was added dropwise to a solution of Me₃SiN(Bu^t)H (1.32 mL, 6.9 mmol) in Et₂O (*ca.* 10 mL) at -78 °C. The mixture was stirred for 20 minutes at -78 °C, allowed to warm to room temperature, and then stirred for 6 hours. After this period, the solution was concentrated to a volume of *ca.* 1 mL, thereby inducing the deposition of a white precipitate. *n*-Hexane (*ca.* 5 mL) was added and the mixture was filtered and the precipitate was dried *in vacuo* overnight, giving Li[Me₃SiNBu^t] as a fine white powder (0.94 g, 90 %).

¹H NMR (C₆D₆): 0.2 – 0.4 [bm, 9H, (CH₃)₃SiNBut], 1.2 – 1.4 [bm, 9H, Me₃SiNC(CH₃)₃].

4.7.4 Synthesis of Cr(CO)₅(CNBu^t)

A mixture of Cr(CO)₆ (12 mg, 0.05 mmol) and Li[Me₃SiNBu^t] (9 mg, 0.06 mmol) placed in an NMR tube equipped with a J. Young valve was treated with C₆D₆ (0.7 mL). The sample was heated at 60 °C, shaken periodically, and monitored by ¹H NMR spectroscopy, thereby indicating the formation of Cr(CO)₅(CNBu^t) after a period of 150 minutes. The resulting mixture was purified by flash column chromatography (silica gel, hexanes) in air to give Cr(CO)₅(CNBu^t) as a microcrystalline solid (9 mg, 60 %) after

removal of the solvent *in vacuo*. Crystals suitable for X-ray diffraction were obtained from hexanes.

$^1\text{H NMR}$ (C_6D_6): 0.68 [s, $\text{CNC}(\underline{\text{CH}}_3)_3$]. IR data (hexanes, cm^{-1}): $\nu_{\text{CN}} = 2151$ (m); $\nu_{\text{CO}} = 2060$ (m), 1958 (s) and 1930 (w).⁴⁹

4.7.5 Synthesis of $\text{Mo}(\text{CO})_5(\text{CNBu}^t)$

A mixture of $\text{Mo}(\text{CO})_6$ (15 mg, 0.06 mmol) and $\text{Li}[\text{Me}_3\text{SiNBu}^t]$ (9 mg, 0.06 mmol) placed in an NMR tube equipped with a J. Young valve was treated with C_6D_6 (0.7 mL). The sample was heated at 60 °C, shaken periodically, and monitored by $^1\text{H NMR}$ spectroscopy, thereby indicating the formation of $\text{Mo}(\text{CO})_5(\text{CNBu}^t)$ after a period of 30 minutes. The resulting mixture was purified by flash column chromatography (silica gel, hexanes) to give $\text{Mo}(\text{CO})_5(\text{CNBu}^t)$ as a microcrystalline solid (13 mg, 71 %) after removal of the solvent *in vacuo*.

$^1\text{H NMR}$ (C_6D_6): 0.68 [1:1:1 t, $^3J_{\text{N-H}} = 2$, $\text{CN}(\underline{\text{CH}}_3)_3$]. IR data (hexanes, cm^{-1}): $\nu_{\text{CN}} = 2152$ (m); $\nu_{\text{CO}} = 2066$ (m), 1959 (s) and 1928 (w).⁴⁹

4.7.6 Synthesis of $\text{W}(\text{CO})_5(\text{CNBu}^t)$

A mixture of $\text{W}(\text{CO})_6$ (20 mg, 0.06 mmol) and $\text{Li}[\text{Me}_3\text{SiNBu}^t]$ (9 mg, 0.06 mmol) placed in an NMR tube equipped with a J. Young valve was treated with C_6D_6 (0.7 mL). The sample was heated at 60 °C, shaken periodically, and monitored by $^1\text{H NMR}$ spectroscopy, thereby indicating the formation of $\text{W}(\text{CO})_5(\text{CNBu}^t)$ after a period of 30 minutes. The resulting mixture was purified by flash column chromatography (silica gel, hexanes) to give $\text{W}(\text{CO})_5(\text{CNBu}^t)$ as a microcrystalline solid (13 mg, 56 %) after removal of the solvent *in vacuo*.

$^1\text{H NMR}$ (C_6D_6): 0.66 [s, $\text{CNC}(\underline{\text{CH}}_3)_3$]. IR data (hexanes, cm^{-1}): $\nu_{\text{CN}} = 2153$ (m); $\nu_{\text{CO}} = 2062$ (m), 1954 (s) and 1923 (w).⁴⁹

4.7.7 Synthesis of *cis*-Cr(CO)₄(CNBu^t)₂

A mixture of Cr(CO)₆ (12 mg, 0.05 mmol) and Li[Me₃SiNBu^t] (17 mg, 0.11 mmol) placed in an NMR tube equipped with a J. Young valve was treated with C₆D₆ (0.7 mL). The sample was heated at 60 °C, shaken periodically, and monitored by ¹H NMR spectroscopy, thereby indicating the formation of *cis*-Cr(CO)₄(CNBu^t)₂ after a period of 20 hours. The mixture was filtered through silica gel (*ca.* 1 mL) and eluted with hexanes (*ca.* 10 mL) and dichloromethane (*ca.* 5 mL). The combined filtrate was concentrated to a volume of *ca.* 3 mL and placed at -15 °C, thereby depositing colorless crystals of *cis*-Cr(CO)₄(CNBu^t)₂ which were isolated by decanting and dried *in vacuo* (6 mg, 33 %). The mother liquor was placed at -15 °C, thereby depositing a second crop of colorless crystals (7 mg), composed of a *ca.* 1:1 mixture of *cis*-Cr(CO)₄(CNBu^t)₂ and Cr(CO)₅(CNBu^t). Crystals suitable for X-ray diffraction were obtained from hexanes at -15°C.

¹H NMR (C₆D₆): 0.85 [s, CNC(CH₃)₃]. IR data (hexanes, cm⁻¹): ν_{CN} = 2145 (w) and 2107 (m); ν_{CO} = 2010 (m) and 1926 (s).⁴⁹

4.7.8 Synthesis of *cis*-Mo(CO)₄(CNBu^t)₂

(i) A mixture of Mo(CO)₆ (36 mg, 0.14 mmol) and Li[Me₃SiNBu^t] (50 mg, 0.33 mmol) placed in an NMR tube equipped with a J. Young valve was treated with C₆D₆ (0.7 mL). The sample was shaken periodically and monitored by ¹H NMR spectroscopy, thereby indicating the formation of *cis*-Mo(CO)₄(CNBu^t)₂ after a period of 37 hours at room temperature.⁵⁰ The mixture was filtered through silica gel (*ca.* 1 mL) and eluted with hexanes (*ca.* 10 mL). The combined filtrate was concentrated to a volume of *ca.* 3 mL and placed at -15 °C, thereby depositing colorless crystals of *cis*-Mo(CO)₄(CNBu^t)₂ which were isolated and dried *in vacuo* (41 mg, 81 %). Crystals suitable for X-ray diffraction

were obtained from hexanes at $-15\text{ }^{\circ}\text{C}$.

^1H NMR (C_6D_6): 0.82 [s, $\text{CNC}(\underline{\text{C}}\text{H}_3)_3$]. IR data (hexanes, cm^{-1}): $\nu_{\text{CN}} = 2146$ (w) and 2109 (m); $\nu_{\text{CO}} = 2014$ (m) and 1928 (s).⁴⁹

(ii) A mixture of $\text{Mo}(\text{CO})_6$ (1.00 g, 3.79 mmol) and $\text{Li}[\text{Me}_3\text{SiNBu}^t]$ (1.26 g, 8.33 mmol) was treated with Et_2O (45 mL) at $-78\text{ }^{\circ}\text{C}$, and then allowed to warm to room temperature with stirring. After a period of 1 day, an additional quantity of $\text{Li}[\text{Me}_3\text{SiNBu}^t]$ (600 mg, 3.97 mmol) was added at $-78\text{ }^{\circ}\text{C}$. The mixture was stirred for an additional 12 hours. After this period, the volatile components were removed *in vacuo*. Hexanes (*ca.* 10 mL) were added and the mixture was filtered through silica gel (*ca.* 25 mL) and eluted with hexanes (*ca.* 350 mL). The filtrate was placed at $-15\text{ }^{\circ}\text{C}$, thereby depositing colorless crystals of *cis*- $\text{Mo}(\text{CO})_4(\text{CNBu}^t)_2$ which were isolated and dried *in vacuo* (506 mg). The mother liquor was then concentrated to *ca.* 50 mL and placed at $-15\text{ }^{\circ}\text{C}$, thereby depositing a second batch of colorless crystals of a 4:1 mixture of *cis*- $\text{Mo}(\text{CO})_4(\text{CNBu}^t)_2$ and $\text{Mo}(\text{CO})_5(\text{CNBu}^t)$ which were isolated and dried *in vacuo* (151 mg).

4.7.9 Synthesis of *cis*- $\text{W}(\text{CO})_4(\text{CNBu}^t)_2$

A mixture of $\text{W}(\text{CO})_6$ (20 mg, 0.06 mmol) and $\text{Li}[\text{Me}_3\text{SiNBu}^t]$ (17 mg, 0.11 mmol) placed in an NMR tube equipped with a J. Young valve was treated with C_6D_6 (0.7 mL). The sample was heated at $60\text{ }^{\circ}\text{C}$, shaken periodically, and monitored by ^1H NMR spectroscopy, thereby indicating the formation of *cis*- $\text{W}(\text{CO})_4(\text{CNBu}^t)_2$ after a period of 5 hours. The mixture was filtered through silica gel (*ca.* 1 mL) and eluted with hexanes (*ca.* 10 mL). The combined filtrate was concentrated to a volume of *ca.* 3 mL and placed at $-15\text{ }^{\circ}\text{C}$, thereby depositing colorless crystals of *cis*- $\text{W}(\text{CO})_4(\text{CNBu}^t)_2$ which were isolated and dried *in vacuo* (11 mg, 42 %). The mother liquor was placed at $-15\text{ }^{\circ}\text{C}$, thereby depositing a second crop of colorless crystals (6 mg) composed of a *ca.* 1:3

mixture of *cis*-W(CO)₄(CNBu^t)₂ and W(CO)₅(CNBu^t). Crystals suitable for X-ray diffraction were obtained from hexanes at -15 °C.

¹H NMR (C₆D₆): 0.82 [s, CNC(CH₃)₃]. IR data (hexanes, cm⁻¹): ν_{CN} = 2148 (w) and 2104 (w); ν_{CO} = 2009 (m) and 1922 (s).⁴⁹

4.7.10 Synthesis of *fac*-Cr(CO)₃(CNBu^t)₃

A mixture of Cr(CO)₆ (12 mg, 0.05 mmol) and Li[Me₃SiNBu^t] (43 mg, 0.28 mmol) placed in an NMR tube equipped with a J. Young valve was treated with C₆D₆ (0.7 mL). The sample was heated at 60 °C, shaken periodically, and monitored by ¹H NMR spectroscopy, thereby indicating the formation of *fac*-Cr(CO)₃(CNBu^t)₃ after a period of 69 hours. The mixture was filtered through silica gel (*ca.* 1 mL) and eluted with hexanes (*ca.* 10 mL). The combined filtrate was concentrated to a volume of *ca.* 3 mL and placed at -15 °C, thereby depositing pale yellow crystals of *fac*-Cr(CO)₃(CNBu^t)₃ which were isolated and dried *in vacuo* (3 mg, 14 %).

¹H NMR (C₆D₆): 1.00 [s, CNC(CH₃)₃]. IR data (CH₂Cl₂, cm⁻¹): ν_{CN} = 2150 (w) and 2109 (m); ν_{CO} = 1932 (s) and 1863 (s).⁴⁹

4.7.11 Synthesis of *fac*-Mo(CO)₃(CNBu^t)₃ and *cis*-Mo(CO)₂(CNBu^t)₄

A mixture of Mo(CO)₆ (36 mg, 0.14 mmol) and Li[Me₃SiNBu^t] (70 mg, 0.46 mmol) placed in an NMR tube equipped with a J. Young valve was treated with C₆D₆ (0.7 mL). The sample was heated at 60 °C, shaken periodically, and monitored by ¹H NMR spectroscopy, thereby indicating the formation of *fac*-Mo(CO)₃(CNBu^t)₃ after a period of 3 hours, together with a small amount of *cis*-Mo(CO)₄(CNBu^t)₂. An additional quantity of Li[Me₃SiNBu^t] (70 mg, 0.46 mmol) was added, and the mixture was heated at 60 °C for 1 day. The mixture was filtered through silica gel (*ca.* 1 mL) and eluted with hexanes (*ca.* 10 mL). The combined filtrate was concentrated to a volume of *ca.* 3 mL

and placed at $-15\text{ }^{\circ}\text{C}$, thereby depositing pale yellow crystals of *fac*-Mo(CO)₃(CNBu^t)₃ which were isolated and dried *in vacuo* (17 mg, 28 %) contaminated with a small amount (*ca.* 2 %) of *cis*-Mo(CO)₂(CNBu^t)₄. The mother liquor was placed at $-15\text{ }^{\circ}\text{C}$, thereby depositing a second crop of pale yellow crystals (9 mg) composed of a *ca.* 3:1 mixture of *fac*-Mo(CO)₄(CNBu^t)₂ and *cis*-Mo(CO)₂(CNBu^t)₄.

Data for fac-Mo(CO)₃(CNBu^t)₃.

¹H NMR (C₆D₆): 0.95 [s, CNC(CH₃)₃]. IR Data (dichloromethane, cm⁻¹): ν_{CN} = 2154 (w) and 2114 (m); ν_{CO} = 1935 (s) and 1861 (s).⁴⁹

Data for cis-Mo(CO)₂(CNBu^t)₄.

¹H NMR (C₆D₆): 1.04 [s, CNC(CH₃)₃], 1.15 [s, CNC(CH₃)₃].

4.7.12 Synthesis of *fac*-W(CO)₃(CNBu^t)₃

A mixture of W(CO)₆ (20 mg, 0.06 mmol) and Li[Me₃SiNBu^t] (43 mg, 0.28 mmol) placed in an NMR tube equipped with a J. Young valve was treated with C₆D₆ (0.7 mL). The sample was heated at $60\text{ }^{\circ}\text{C}$, shaken periodically, and monitored by ¹H NMR spectroscopy, thereby indicating the formation of *fac*-W(CO)₃(CNBu^t)₃ after a period of 22 hours. The mixture was filtered through silica gel (*ca.* 1 mL) and eluted with hexanes (*ca.* 10 mL). The combined filtrate was concentrated to a volume of *ca.* 3 mL and placed at $-15\text{ }^{\circ}\text{C}$, thereby depositing pale yellow crystals of *fac*-W(CO)₃(CNBu^t)₃ which were isolated and dried *in vacuo* (21 mg, 66 %) contaminated with a small amount of *cis*-W(CO)₂(CNBu^t)₄ (3 %). The mother liquor was placed at $-15\text{ }^{\circ}\text{C}$, thereby depositing a second batch of pale yellow crystals (3 mg); total yield 24 mg, 80 %). Crystals suitable for X-ray diffraction were obtained from hexanes at $-15\text{ }^{\circ}\text{C}$.

¹H NMR (C₆D₆): 0.95 [s, CNC(CH₃)₃]. IR Data (CH₂Cl₂, cm⁻¹): ν_{CN} = 2155 (w) and

2108 (m); $\nu_{\text{CO}} = 1929$ (s) and 1857 (s).⁴⁹

4.7.13 Synthesis of *axial*-Fe(CO)₄(CNBu^t)

A mixture of Fe(CO)₅ (10 μ L, 0.07 mmol) and Li[Me₃SiNBu^t] (11 mg, 0.07 mmol) placed in an NMR tube equipped with a J. Young valve was treated with C₆D₆ (0.7 mL). The sample was heated at 60 °C and monitored by ¹H NMR spectroscopy, thereby indicating the formation of *axial*-Fe(CO)₄(CNBu^t) after a period of 20 minutes. The mixture was filtered through silica gel (*ca.* 1 mL) and eluted with hexanes (*ca.* 10 mL). The combined filtrate was concentrated to a volume of *ca.* 3 mL and placed at -15 °C, thereby depositing colorless crystals of *axial*-Fe(CO)₄(CNBu^t) which were isolated and dried *in vacuo* (9 mg, 48 %) contaminated with a small amount of *trans*-Fe(CO)₃(CNBu^t)₂ (< 2 %). Crystals suitable for X-ray diffraction were obtained from hexanes at -15 °C.

¹H NMR (C₆D₆): 0.66 [s, CNC(CH₃)₃]. IR data (hexanes, cm⁻¹): $\nu_{\text{CN}} = 2171$ (w); $\nu_{\text{CO}} = 2055$ (m), 1993 (m) and 1967 (s).⁵¹

4.7.14 Synthesis of *trans*-Fe(CO)₃(CNBu^t)₂

(i) A mixture of Fe(CO)₅ (10 μ L, 0.07 mmol) and Li[Me₃SiNBu^t] (25 mg, 0.16 mmol) placed in an NMR tube equipped with a J. Young valve was treated with C₆D₆ (0.7 mL). The sample was heated at 60 °C and monitored by ¹H NMR spectroscopy. The sample was monitored by ¹H NMR spectroscopy, thereby indicating the formation of *trans*-Fe(CO)₃(CNBu^t)₂ after a period of 16 hours. The mixture was filtered through silica gel (*ca.* 1 mL) and eluted with hexanes (*ca.* 10 mL) and then dichloromethane (*ca.* 5 mL). The combined filtrate was concentrated to a volume of *ca.* 3 mL and placed at -15 °C, thereby depositing colorless crystals of *trans*-Fe(CO)₃(CNBu^t)₂ which were isolated and dried *in vacuo* (14 mg, 62 %). Crystals suitable for X-ray diffraction were obtained from hexanes at -15 °C.⁵²

^1H NMR (C_6D_6): 0.82 [s, $\text{CNC}(\underline{\text{C}}\text{H}_3)_3$]. IR data (hexanes, cm^{-1}): $\nu_{\text{CN}} = 2116$ (m); $\nu_{\text{CO}} = 1996$ (w) and 1933 (s).⁵¹

(ii) A suspension of $\text{Li}[\text{Me}_3\text{SiNBu}^t]$ (2.00 g, 13.22 mmol) in Et_2O (30 mL) was treated with $\text{Fe}(\text{CO})_5$ (0.812 mL, 1.177 g, 6.01 mmol) at -78 °C. The mixture was stirred and allowed to warm to room temperature. After 16 hours, an additional quantity of $\text{Li}[\text{Me}_3\text{SiNBu}^t]$ (600 mg, 3.97 mmol) was added at -78 °C. The mixture was allowed to warm to room temperature and stirred for 16 hours. After this period, the volatile components were removed *in vacuo*. Hexanes (*ca.* 10 mL) were added and the mixture was filtered through silica gel (*ca.* 25 mL) and eluted with hexanes (*ca.* 200 mL); *caution* – the dry residue on the column may be pyrophoric. The filtrate was placed at -78 °C, thereby depositing pale yellow crystals of *trans*- $\text{Fe}(\text{CO})_3(\text{CNBu}^t)_2$ which were isolated and dried *in vacuo* (906 mg, 49 %).

4.7.15 Synthesis of $\text{Mo}(\text{CO})_5(\text{CN-1-Np}^{\text{H}_4})$

Me_3SiCl (190 μL , 1.5 mmol) was added to a solution of (*R*)-1,2,3,4-tetrahydro-1-naphthylamine (200 μL , 1.36 mmol) in Et_2O (*ca.* 10 mL) and the resulting suspension was stirred for 30 minutes at room temperature, and then treated in a dropwise manner with a solution of Bu^nLi in hexanes (1.6 M, 1.9 mL, 3.0 mmol). The suspension was stirred overnight at room temperature, cooled to -78 °C, and treated with $\text{Mo}(\text{CO})_6$ (180 mg, 0.68 mmol). The suspension was allowed to warm to room temperature and stirred for 6 hours. After this period, the volatile components were removed *in vacuo* and the residue obtained was extracted into hexanes (*ca.* 20 mL), filtered through silica gel (*ca.* 8 mL) and eluted with hexanes (*ca.* 75 mL) to give $\text{Mo}(\text{CO})_5(\text{CN-1-Np}^{\text{H}_4})$ as a microcrystalline solid (105 mg, 39 %). Crystals suitable for X-ray diffraction were obtained from hexanes at -15 °C.

^1H NMR (C_6D_6): 1.07 – 1.44 [several multiplets, 4H, $\text{C}_6\text{H}_4\text{C}_3\text{H}_6\text{CH}(\text{NC})$], 2.09 – 2.27 [m, 2H $\text{C}_6\text{H}_4\text{C}_3\text{H}_6\text{CH}(\text{NC})$], 3.98 [t, $^3J_{\text{H-H}} = 5$, 1H, $\text{C}_6\text{H}_4\text{C}_3\text{H}_6\text{CH}(\text{NC})$], 6.69 [m, 1H, $\text{C}_6\text{H}_4\text{C}_3\text{H}_6\text{CH}(\text{NC})$], 6.92 [m, 2H, $\text{C}_6\text{H}_4\text{C}_3\text{H}_6\text{CH}(\text{NC})$], 7.05 [m, 1H, $\text{C}_6\text{H}_4\text{C}_3\text{H}_6\text{CH}(\text{NC})$]. $^{13}\text{C}\{^1\text{H}\}$ NMR (C_6D_6): 19.3 [s, 1C, $\text{C}_6\text{H}_4\text{C}_3\text{H}_6\text{CH}(\text{NC})$], 28.2 [s, 1C, $\text{C}_6\text{H}_4\text{C}_3\text{H}_6\text{CH}(\text{NC})$], 30.2 [s, 1C, $\text{C}_6\text{H}_4\text{C}_3\text{H}_6\text{CH}(\text{NC})$], 55.1 [s, 1C, $\text{C}_6\text{H}_4\text{C}_3\text{H}_6\text{CH}(\text{NC})$], 126.9 [s, 1C, $\text{C}_6\text{H}_4\text{C}_3\text{H}_6\text{CH}(\text{NC})$], 128.0 [s, 1C, $\text{C}_6\text{H}_4\text{C}_3\text{H}_6\text{CH}(\text{NC})$], 128.8 [s, 1C, $\text{C}_6\text{H}_4\text{C}_3\text{H}_6\text{CH}(\text{NC})$], 129.7 [s, 1C, $\text{C}_6\text{H}_4\text{C}_3\text{H}_6\text{CH}(\text{NC})$], 131.6 [s, 1C, $\text{C}_6\text{H}_4\text{C}_3\text{H}_6\text{CH}(\text{NC})$], 136.3 [s, 1C, $\text{C}_6\text{H}_4\text{C}_3\text{H}_6\text{CH}(\text{NC})$], 152.9 [s, 1C, $\text{C}_6\text{H}_4\text{C}_3\text{H}_6\text{CH}(\text{NC})$], 204.4 [s, 4C $\text{Mo}(\text{CO})_5$], 207.1 [s, 1C $\text{Mo}(\text{CO})_5$]. IR data (Hexanes, cm^{-1}): $\nu_{\text{CN}} = 2154$ (m); $\nu_{\text{CO}} = 2066$ (m), 1960 (s) and 1929 (w).

4.7.16 Synthesis of $\text{Mo}(\text{CO})_5(\text{CN-1-Adamantyl})$ and $\text{cis-Mo}(\text{CO})_4(\text{CN-1-Adamantyl})_2$

Me_3SiCl (100 μL , 0.79 mmol) was added to a suspension of 1-adamantamine, AdNH_2 , (70 mg, 0.46 mmol) in Et_2O (ca. 10 mL). The suspension was stirred for 30 minutes, cooled to $-78\text{ }^\circ\text{C}$, and treated in a dropwise manner with a solution of Bu^nLi in hexanes (2.5 M, 0.40 mL, 1.00 mmol). The resulting solution was allowed to warm to room temperature, thereby depositing a white precipitate. The mixture was stirred for 3 hours at room temperature, cooled to $-78\text{ }^\circ\text{C}$, and was treated with $\text{Mo}(\text{CO})_6$ (50 mg, 0.19 mmol). The suspension was allowed to warm to room temperature and was stirred overnight. After this period, the volatile components were removed *in vacuo* and the residue obtained was extracted into hexanes (ca. 3 mL) and purified by flash chromatography (silica, hexanes, Et_2O gradient). $\text{Mo}(\text{CO})_5(\text{CN-1-Ad})$ was the first fraction (24 mg, 32 % based on $\text{Mo}(\text{CO})_6$) and $\text{cis-Mo}(\text{CO})_4(\text{CN-1-Ad})_2$ (43 mg, 43 %) was obtained as the second fraction. Crystals of $\text{Mo}(\text{CO})_5(\text{CN-1-Ad})$ and $\text{Mo}(\text{CO})_4(\text{CN-1-Ad})_2$ suitable for X-ray diffraction were obtained from hexanes at $-15\text{ }^\circ\text{C}$.

Data for Mo(CO)₅(CN-1-Ad)

¹H NMR (C₆D₆): 1.12 [m, 6H of Ad], 1.40 [s, 6H of Ad], 1.50 [s, 3H of Ad]. IR data (hexanes, cm⁻¹): ν_{CN} = 2147 (m); ν_{CO} = 2065 (m), 1958 (s), and 1930 (w). Mass spectrum (FAB+): *m/z* = 399.0 {M}⁺.

Data for cis-Mo(CO)₄(CN-1-Ad)₂

¹H NMR (C₆D₆): 1.18 [m, 6H of Ad], 1.57 [s, 3H of Ad], 1.60 [s, 6H of Ad]. IR data (Et₂O, cm⁻¹): ν_{CN} = 2147 (w) and ν_{CN} = 2115 (m); ν_{CO} = 2016 (m) and 1928 (s). Mass spectrum (FAB+): *m/z* = 532.2 {M}⁺.

4.7.17 Synthesis of Mo(CO)₅(CN-*p*-C₆H₄Me)

Me₃SiCl (100 μL, 0.79 mmol) was added to a solution of *p*-MeC₆H₄NH₂ (20 mg, 0.19 mmol) in Et₂O (*ca.* 10 mL) giving a suspension that was stirred for 2 hours, cooled to -78 °C, and treated in a dropwise manner with a solution of BuⁿLi in hexanes (2.5 M, 0.17 mL, 0.42 mmol). The resulting solution was allowed to warm to room temperature, thereby depositing a white precipitate. The mixture was stirred for 4 hours at room temperature, cooled to -78 °C, and treated with Mo(CO)₆ (50 mg, 0.19 mmol). The mixture was allowed to warm to room temperature and was stirred for 2 days. The volatile components were removed *in vacuo* and the residue obtained was extracted into hexanes (*ca.* 5 mL) and purified by flash column chromatography (silica gel, hexanes), to give Mo(CO)₅(CN-*p*-C₆H₄Me) as a white microcrystalline solid (47 mg, 70 %).

¹H NMR (C₆D₆): 1.79 [s, 3H, CN-*p*-C₆H₄CH₃], 6.46 [s, 4H, CN-*p*-C₆H₄Me]. IR data (hexanes, cm⁻¹): ν_{CN} = 2137 (w); ν_{CO} = 2059 (m), 1965 (s) and 1930 (w). Mass spectrum (FAB+): *m/z* = 355.0 {M}⁺.

4.7.18 Synthesis of $\text{Mo(CO)}_5(\text{CN-}p\text{-C}_6\text{H}_4\text{OMe})$

Me_3SiCl (100 μL , 0.79 mmol) was added to a solution of $p\text{-MeOC}_6\text{H}_4\text{NH}_2$ (23 mg, 0.19 mmol) in Et_2O (ca. 10 mL) and stirred for 30 minutes at room temperature. The mixture was cooled to $-78\text{ }^\circ\text{C}$ and treated in a dropwise manner with a solution of Bu^nLi in hexanes (2.5 M, 0.17 mL, 0.42 mmol). The resulting solution was allowed to warm to room temperature, thereby depositing a white precipitate. The mixture was stirred for 2 hours at room temperature, cooled to $-78\text{ }^\circ\text{C}$, and treated with Mo(CO)_6 (50 mg, 0.19 mmol). The mixture was allowed to warm to room temperature and was stirred overnight. After this period, the volatile components were removed *in vacuo* and the residue obtained was extracted into hexanes (ca. 5 mL) and purified by flash column chromatography (silica gel, hexanes) to give $\text{Mo(CO)}_5(\text{CN-}p\text{-C}_6\text{H}_4\text{OMe})$ as a microcrystalline solid (56 mg, 80 %). Crystals suitable for X-ray diffraction were obtained from hexanes at $-15\text{ }^\circ\text{C}$.

$^1\text{H NMR}$ (C_6D_6): 3.03 [s, 3H, $\text{CN-}p\text{-C}_6\text{H}_4\text{OCH}_3$], 6.24 [d, $^3J_{\text{H-H}} = 9\text{ Hz}$, 2H, $\text{CN-}p\text{-C}_6\text{H}_4\text{OCH}_3$], 6.49 [d, $^3J_{\text{H-H}} = 9\text{ Hz}$, 2H, $\text{CN-}p\text{-C}_6\text{H}_4\text{OCH}_3$]. IR data (hexanes, cm^{-1}): $\nu_{\text{CN}} = 2137$ (m); $\nu_{\text{CO}} = 2059$ (m), 1964 (s) and 1942 (w). Mass spectrum (FAB+): $m/z = 371.0$ $\{\text{M}\}^+$.

4.7.19 Synthesis of $\text{cis-Mo(CO)}_4(\text{CN-}2,4,6\text{-C}_6\text{H}_2\text{Me}_3)_2$

A solution of Bu^nLi in hexanes (2.5 M, 0.2 mL, 0.5 mmol) was added to a solution of 2,4,6-trimethylaniline (60 μL , 0.43 mmol) in Et_2O (ca. 10 mL). The solution was stirred at room temperature for 2 hours and then cooled to $-78\text{ }^\circ\text{C}$, thereby depositing a white precipitate. Me_3SiCl was added dropwise and the mixture was allowed to warm to room temperature, during which period it became a solution and then a suspension. The resulting suspension was allowed to stir for 1 hour at room temperature. After this period, the mixture was treated with a solution of Bu^nLi in hexanes (2.5 M, 0.2 mL, 0.5

mmol). The suspension was stirred for 1 hour, cooled to $-78\text{ }^{\circ}\text{C}$ and then treated with $\text{Mo}(\text{CO})_6$ (50 mg, 0.19 mmol). The mixture was allowed to warm to room temperature and then stirred for 2 days at $60\text{ }^{\circ}\text{C}$. After this period, the volatile components were removed *in vacuo* and the residue obtained was extracted into hexanes (*ca.* 3 mL) and purified by flash chromatography (silica, hexanes, Et_2O gradient) to give $\text{Mo}(\text{CO})_4(\text{CN}-2,4,6\text{-C}_6\text{H}_2\text{Me}_3)_2$ (46 mg, 49 %) as a white microcrystalline solid. Crystals suitable for X-ray diffraction were obtained from hexanes at $-15\text{ }^{\circ}\text{C}$.

^1H NMR (C_6D_6): 1.90 [s, 3H, $\text{CN}-2,4,6\text{-C}_6\text{H}_2(\underline{\text{C}}\text{H}_3)_3$], 2.09 [s, 6H, $\text{CN}-2,4,6\text{-C}_6\text{H}_2(\underline{\text{C}}\text{H}_3)_3$], 6.39 [s, 2H, $\text{CN}-2,4,6\text{-C}_6\text{H}_2\text{Me}_3$]. IR data (hexanes, cm^{-1}): $\nu_{\text{CN}} = 2131$ (w) and $\nu_{\text{CN}} = 2079$ (m); $\nu_{\text{CO}} = 2013$ (m) and 1940 (s). Mass spectrum (FAB+): $m/z = 500.1$ {M} $^+$.

4.8 Crystallographic data

Table 1. Crystal, intensity collection and refinement data.

	Cr(CO) ₅ (CNBu ^t)	Cr(CO) ₄ (CNBu ^t) ₂
lattice	Monoclinic	Monoclinic
formula	C ₁₀ H ₉ CrNO ₅	C ₁₄ H ₁₈ CrN ₂ O ₄
formula weight	275.18	330.30
space group	<i>P</i> 2 ₁ / <i>c</i>	<i>P</i> 2 ₁ / <i>c</i>
<i>a</i> /Å	9.1589(12)	17.0086(16)
<i>b</i> /Å	15.059(2)	11.1264(10)
<i>c</i> /Å	9.3824(12)	18.3223(17)
α /°	90	90
β /°	103.357(2)	101.7850(10)
γ /°	90	90
<i>V</i> /Å ³	1259.1(3)	3394.3(5)
<i>Z</i>	4	8
temperature (K)	125(2)	125(2)
radiation (λ , Å)	0.71073	0.71073
ρ (calcd.), g cm ⁻³	1.452	1.293
μ (Mo K α), mm ⁻¹	0.916	0.689
θ max, deg.	30.49	30.53
no. of data collected	20007	53504
no. of data used	3833	10369
no. of parameters	157	401
R_1 [$I > 2\sigma(I)$]	0.0403	0.0400
wR_2 [$I > 2\sigma(I)$]	0.0811	0.0849
R_1 [all data]	0.0738	0.0746
wR_2 [all data]	0.0926	0.0849
GOF	1.009	1.004

Table 1 (cont). Crystal, intensity collection and refinement data.

	Mo(CO) ₄ (CNBu ^t) ₂	W(CO) ₄ (CNBu ^t) ₂
lattice	Monoclinic	Monoclinic
formula	C ₁₄ H ₁₈ MoN ₂ O ₄	C ₁₄ H ₁₈ WN ₂ O ₄
formula weight	374.24	462.15
space group	<i>P</i> 2 ₁ / <i>c</i>	<i>P</i> 2 ₁ / <i>c</i>
<i>a</i> /Å	17.2165(10)	17.109(10)
<i>b</i> /Å	11.2053(7)	11.131(7)
<i>c</i> /Å	18.6121(11)	18.487(11)
α /°	90	90
β /°	101.2930(10)	101.259(8)
γ /°	90	90
<i>V</i> /Å ³	3521.1(4)	3453(4)
<i>Z</i>	8	8
temperature (K)	125(2)	125(2)
radiation (λ , Å)	0.71073	0.71073
ρ (calcd.), g cm ⁻³	1.412	1.778
μ (Mo K α), mm ⁻¹	0.759	6.706
θ max, deg.	30.35	32.94
no. of data collected	55011	59772
no. of data used	10593	12348
no. of parameters	401	401
R_1 [$I > 2\sigma(I)$]	0.0393	0.0239
wR_2 [$I > 2\sigma(I)$]	0.0696	0.0437
R_1 [all data]	0.0741	0.0373
wR_2 [all data]	0.0806	0.0471
GOF	1.001	1.008

Table 1 (cont). Crystal, intensity collection and refinement data.

	W(CO)₃(CNBu^t)₃	Fe(CO)₄(CNBu^t)
lattice	Monoclinic	Monoclinic
formula	C ₁₈ H ₂₇ WN ₃ O ₃	C ₉ H ₉ FeNO ₄
formula weight	517.28	251.02
space group	<i>P</i> 2 ₁ / <i>c</i>	<i>P</i> 2 ₁ / <i>c</i>
<i>a</i> /Å	9.2308(12)	8.9045(4)
<i>b</i> /Å	14.955(2)	14.4203(6)
<i>c</i> /Å	16.648(2)	9.0702(4)
α /°	90	90
β /°	94.987(2)	102.7840(10)
γ /°	90	90
<i>V</i> /Å ³	2289.6(5)	1135.79(9)
<i>Z</i>	4	4
temperature (K)	125(2)	125(2)
radiation (λ , Å)	0.71073	0.71073
ρ (calcd.), g cm ⁻³	1.501	1.468
μ (Mo K α), mm ⁻¹	5.063	1.320
θ max, deg.	30.85	32.60
no. of data collected	37064	18983
no. of data used	7183	3954
no. of parameters	227	139
R_1 [$I > 2\sigma(I)$]	0.0390	0.0236
wR_2 [$I > 2\sigma(I)$]	0.0711	0.0618
R_1 [all data]	0.0764	0.0282
wR_2 [all data]	0.0815	0.0651
GOF	0.992	1.052

Table 1 (cont). Crystal, intensity collection and refinement data.

	$\text{Fe}(\text{CO})_3(\text{CNBu}^t)_2$	$\text{Mo}(\text{CO})_5-$ $(\text{CN-}p\text{-C}_6\text{H}_4\text{OMe})$
lattice	Orthorhombic	Monoclinic
formula	$\text{C}_{13}\text{H}_{18}\text{FeN}_2\text{O}_3$	$\text{C}_{13}\text{H}_7\text{MoNO}_6$
formula weight	306.14	369.14
space group	<i>Pbca</i>	<i>P2</i> ₁
<i>a</i> /Å	11.6817(9)	10.8089(18)
<i>b</i> /Å	16.0996(13)	5.8009(10)
<i>c</i> /Å	16.4104(13)	11.831(2)
α /°	90	90
β /°	90	107.521(2)
γ /°	90	90
<i>V</i> /Å ³	3086.3(4)	707.4(2)
<i>Z</i>	8	2
temperature (K)	125(2)	125(2)
radiation (λ , Å)	0.71073	0.71073
ρ (calcd.), g cm ⁻³	1.318	1.733
μ (Mo K α), mm ⁻¹	0.982	0.952
θ max, deg.	32.65	32.51
no. of data collected	50292	11852
no. of data used	5476	4735
no. of parameters	178	192
R_1 [$I > 2\sigma(I)$]	0.0226	0.0359
wR_2 [$I > 2\sigma(I)$]	0.0611	0.0751
R_1 [all data]	0.0280	0.0463
wR_2 [all data]	0.0652	0.0789
GOF	1.045	1.005

Table 1 (cont). Crystal, intensity collection and refinement data.

	Mo(CO) ₄ (CN-2,4,6- C ₆ H ₂ Me ₃) ₂	Mo(CO) ₅ (CN-1-Np ^{H4})
lattice	Triclinic	Orthorhombic
formula	C ₂₄ H ₂₂ MoN ₂ O ₄	C ₁₆ H ₁₁ MoNO ₅
formula weight	498.38	393.20
space group	<i>P</i> -1	<i>P</i> 2 ₁ 2 ₁ 2 ₁
<i>a</i> /Å	10.3163(11)	23.215(17)
<i>b</i> /Å	10.5038(11)	12.599(9)
<i>c</i> /Å	11.9238(12)	5.648(4)
α /°	87.101(2)	90
β /°	82.733(2)	90
γ /°	63.7150(10)	90
<i>V</i> /Å ³	1149.1(2)	1652(2)
<i>Z</i>	2	4
temperature (K)	125(2)	200(2)
radiation (λ , Å)	0.71073	0.71073
ρ (calcd.), g cm ⁻³	1.440	1.581
μ (Mo K α), mm ⁻¹	0.602	0.817
θ max, deg.	32.65	28.28
no. of data collected	19899	15546
no. of data used	7821	4090
no. of parameters	286	209
R_1 [$I > 2\sigma(I)$]	0.0367	0.0411
wR_2 [$I > 2\sigma(I)$]	0.0839	0.0674
R_1 [all data]	0.0518	0.1018
wR_2 [all data]	0.0907	0.0912
GOF	1.027	1.037

Table 1 (cont). Crystal, intensity collection and refinement data.

	Mo(CO) ₅ (CN-1-Ad)	Mo(CO) ₄ (CN-1-A) ₂
lattice	Orthorhombic	Triclinic
formula	C ₁₆ H ₁₄ MoNO ₅	C ₂₆ H ₃₀ MoN ₂ O ₄
formula weight	396.22	530.46
space group	<i>Pnma</i>	<i>P-1</i>
<i>a</i> /Å	23.3043(9)	12.833(8)
<i>b</i> /Å	10.5340(4)	13.248(9)
<i>c</i> /Å	14.0154(5)	16.906(11)
α /°	90	94.485(10)
β /°	90	107.173(10)
γ /°	90	112.316(10)
<i>V</i> /Å ³	3440.6(2)	2481(3)
<i>Z</i>	8	4
temperature (K)	200(2)	200(2)
radiation (λ , Å)	0.71073	0.71073
ρ (calcd.), g cm ⁻³	1.530	1.420
μ (Mo K α), mm ⁻¹	0.785	0.562
θ max, deg.	30.51	25.35
no. of data collected	53927	27609
no. of data used	5510	9079
no. of parameters	235	959
R_1 [$I > 2\sigma(I)$]	0.0349	0.0580
wR_2 [$I > 2\sigma(I)$]	0.0911	0.0971
R_1 [all data]	0.0454	0.1567
wR_2 [all data]	0.0984	0.1273
GOF	1.053	0.956

4.9 References and notes

- (1) For the definition of L, X and Z donor functions, see:
 - (a) M. L. H. Green, *J. Organomet. Chem.*, **1995**, 500, 127–148.
 - (b) G. Parkin, in *Comprehensive Organometallic Chemistry III*, ed. R. H. Crabtree and D. M. P. Mingos, vol. 1, ch. 1, Elsevier, Oxford, **2006**.
- (2)
 - (a) Kuznetsov, M. L. *Russ. Chem. Rev.* **2002**, 71, 265-282.
 - (b) Werner, H. *Angew. Chem. Int. Ed. Engl.* **1990**, 29, 1077-1089.
 - (c) Crociani, B. in “Reactions of Coordinated Ligands” Braterman, P. S. ,Ed.; Plenum Press: New York, 1986, Vol. 1, p 553.
 - (d) Singleton, E.; Oosthuizen, H. E. *Adv. Organomet. Chem.* **1983**, 22, 209-310.
 - (e) Yamamoto, Y. *Coord. Chem. Rev.* **1980**, 32, 193-233.
 - (f) Bonati, F.; Minghetti, G. *Inorg. Chim. Acta* **1974**, 9, 95-112.
- (3)
 - (a) Csonka, I. P.; Szepes, U.; Modelli, A. *J. Mass. Spect.* **2004**, 1456-1466.
 - (b) Károlyi, B.; Gengeliczki, Z.; Vass, G.; Szepes, L. *J. Organomet. Chem.* **2009**, 694, 2923-2926.
- (4) Cotton, F. A.; Zingales, F. *J. Am. Chem. Soc.*, **1961**, 83, 351-355.
- (5)
 - (a) Adams, K. P.; Joyce, J. A.; Nile, T. A.; Patel, A. I.; Reid, C. D.; Walters, J. M. *J. Mol. Catal.* **1985**, 29, 201-208.
 - (b) Saegusa, T.; Ito, Y. *Synthesis* **1975**, 291-300.

- (6) (a) Trost, B. M.; Merlic, C. A. *J. Am. Chem. Soc.* **1990**, *112*, 9590-9600.
- (b) Braune, S.; Kazmaier, U. *J. Organomet. Chem.* **2002**, *641*, 26-29.
- (c) Braune, S.; Kazmaier, U. *Angew. Chem. Int. Ed. Engl.* **2003**, *42*, 306-308.
- (d) Kazmaier, U.; Pohlman, M.; Schauss, D. *Eur. J. Org. Chem.* **2000**, 2761-2766.
- (e) Kazmaier, U.; Schauss, D.; Pohlman, M. *Org. Lett.* **1999**, *1*, 1017-1019.
- (7) (a) Ito, H.; Kato, T.; Sawamura, M. *Chem. Asian J.* **2007**, *2*, 1436-1446.
- (b) Ito, H.; Kato, T.; Sawamura, M. *Chem. Lett.* **2006**, *35*, 1038-1039.
- (c) Hagiwara, T.; Taya, K.; Yamamoto, Y.; Yamazaki, H. *J. Mol. Catal.* **1989**, *54*, 165-170.
- (d) Tanabiki, M.; Tsuchiya, K.; Kumanomido, Y.; Matsubara, K.; Motoyama, Y.; Nagashima, H. *Organometallics* **2004**, *23*, 3976-3981.
- (8) (a) Ito, Y.; Suginome, M.; Murakami, M. *J. Org. Chem.* **1991**, *56*, 1948-1951.
- (b) Suginome, M.; Iwanami, T.; Ohmori, Y.; Matsumoto, A.; Ito, Y. *Chem. Eur. J.* **2005**, *11*, 2954-2965.
- (c) Suginome, M.; Matsuda, T.; Ito, Y. *J. Am. Chem. Soc.* **2000**, *122*, 11015-11016.
- (d) Yoshida, H.; Ikadai, J.; Shudo, M.; Ohshita, J.; Kunai, A. *Organometallics* **2005**, *24*, 156-162.
- (9) (a) Gibson, S. E.; Ibrahim, H.; Pasquier, C.; Peplow, M. A.; Rushton, J. M.; Steed, J. W.; Sur, S. *Chem. Eur. J.* **2002**, *8*, 269-276.

- (b) Gibson, S. E.; Hinkamp, T. W.; Peplow, M. A.; Ward, M. F. *Chem. Commun.* **1998**, 1671-1672.
- (10) (a) Alper, H.; Partis, R. A. *J. Organomet. Chem.* **1972**, 35, C40-C42.
- (d) Kiji, J.; Matsumura, A.; Haishi, T.; Okazaki, S.; Furukawa, J. *Bull. Chem. Soc. Jpn.* **1977**, 50, 2731-2733.
- (c) Chen, L.-C.; Chen, M.-Y.; Chen, J.-H.; Wen, Y.-S.; Lu, K.-L. *J. Organomet. Chem.* **1992**, 425, 99-111.
- (b) Lu, K.-L.; Chen, C.-C.; Lin, Y.-W.; Hong, F.-E.; Gau, H.-M.; Gan, L.-L.; Luoh, H.-D. *J. Organomet. Chem.* **1993**, 453, 263-267.
- (11) (a) Fehlhammer, W. P.; Mayr, A. *Angew. Chem. Int. Ed. Engl.* **1975**, 14, 757-758.
- (b) Luart, D.; Salaün, J.-Y.; Patinec, W.; Rumin, R.; des Abbayes, H. *Inorg. Chim. Acta* **2003**, 350, 656-660.
- (12) Cambridge Structural Database, Version 5.33. Allen, F. H.; Kennard, O. *Chemical Design Automation News* **1993**, 8, 31-37.
- (13) For example, according to the Cambridge Structural Database, there are 4,063 examples of terminal metal cyanide complexes.
- (14) For example, according to the Cambridge Structural Database, there are 41,415 examples of terminal metal carbonyl complexes.
- (15) *Current Methods in Inorganic Chemistry, Vol. 3: Fundamentals of Molecular Catalysis*, Kurosawa, H.; Yamamoto, A. (Eds.) Elsevier, New York (2007).

- (16) de Frémont, P.; Marion, N.; Nolan, S. P. *Coord. Chem. Rev.* **2009**, *253*, 862–892.
- (17) Fischer, E. O.; Maasböl, D.-C. A. *Angew. Chem. Int. Ed. Engl.* **1964**, *3*, 580-581.
- (18) Today, this type of carbene complex is most commonly referred to as a Fischer carbene, named in his honor.
- (19) (a) Ford, P. C.; Rokicki, A. *Adv. Organomet. Chem.* **1988**, *28*, 139-217.
- (b) Torrent, M.; Sola, M.; Frenking, G. *Organometallics* **1999**, *18*, 2801-2812.
- (20) Darensbourg, D. J.; Froelich, J. A. *J. Am. Chem. Soc.* **1977**, *99*, 4726-4729.
- (21) Albers, M. O.; Coville, N. J. *Coord. Chem. Rev.* **1984**, *53*, 227-259.
- (22) (a) Angelici, R. J. *Acc. Chem. Res.* **1972**, *5*, 335-341.
- (b) Behrens, H. *Adv. Organomet. Chem.* **1980**, *18*, 1-53.
- (23) (a) Ovchinnikov, M. V.; Wang, X. P.; Schultz, A. J.; Guzei, I. A.; Angelici, R. J. *Organometallics* **2002**, *21*, 3292-3296.
- (b) Anderson, S.; Cook, D. J.; Hill, A. F. *Organometallics* **1997**, *16*, 5595-5597.
- (24) (a) Bush, R. P.; Lloyd, N. C.; Pearce, C. A. *Chem. Commun.* **1967**, 1270.
- (b) Rees, W. S., Jr.; Green, D. M.; Hesse, W. *Polyhedron* **1992**, *11*, 1697-1699.
- (c) Harris, D. H.; Lappert, M. F. *J. Organomet. Chem. Library* **1976**, *2*, 13-102.
- (25) (a) Suginome, M.; Ito, Y. *Science of Synthesis* **2004**, *19*, 445-530.
- (b) Ugi, I.; Fetzer, U.; Eholzer, U.; Knapfer, H.; Offermann, K. *Angew. Chem. Int. Ed. Engl.* **1965**, *4*, 472-484.

- (26) (a) King, R. B.; Saran, M. S. *Inorg. Chem.* **1974**, 13, 74-78.
- (b) Imhof, W.; Halbauer, K.; Dönnecke, D.; Görls, H. *Acta Crystallogr. Sect. E* **2006**, 62, M462-M464.
- (c) Coville, N. J.; Albers, M. O. *Inorg. Chim. Acta* **1982**, 65, L7-L8.
- (27) The molecular structure of *fac*-M(CO)₃(CNBu^t)₃ has been reported. See reference 26b.
- (28) (a) Albers, M. O.; Coville, N. J.; Singleton, E. J. *Chem. Soc., Dalton Trans.* **1982**, 1069-1079.
- (b) Cotton, F. A.; Parish, R. V. *J. Chem. Soc.* **1960**, 1440-1446.
- (29) Harris, G. W.; Boeyens, J. C. A.; Coville, N. J. *Acta Crystallogr. Sect. C* **1983**, C39, 1180-1182.
- (30) Halbauer, K.; Dönnecke, D.; Görls, H.; Imhof, W. *Z. Anorg. Allg. Chemie* **2006**, 632, 1477-1482.
- (31) The *fac*-isomer is the result of an addition in which the isocyanide ligand is *cis* to both isocyanide ligands, whereas the *mer*-isomer would result from addition *cis* to only one isocyanide ligand.
- (32) The energy differences calculated for the chromium system are very small: *cis*-Cr(CO)₄(CNMe)₂ is 0.30 kcal mol⁻¹ lower in energy *trans*-Cr(CO)₄(CNMe)₂. *fac*-Cr(CO)₃(CNMe)₃ is 0.32 kcal mol⁻¹ lower in energy *mer*-Cr(CO)₃(CNMe)₃.
- (33) Al-Jibori, S. A.; Shaw, B. J. *Organometal. Chem.* **1980**, 192, 83-85.

- (34) (a) Stephens, F. H.; Figueroa, J. S.; Cummins, C. C.; Kryatova, O. P.; Kryatov, S. V.; Rybak-Akimova, E. V.; McDonough, J. E.; Hoff, C. D. *Organometallics* **2004**, *23*, 3126-3138.
- (b) Suginome, M.; Oike, H.; Shuff, P. H.; Ito, Y. *Organometallics* **1996**, *15*, 2170-2178.
- (35) (a) Fox, B. J.; Sun, Q. Y.; DiPasquale, A. G.; Fox, A. R.; Rheingold, A. L.; Figueroa, J. S. *Inorg. Chem.* **2008**, *47*, 9010-9020.
- (b) Fox, B. J.; Millard, M. D.; DiPasquale, A. G.; Rheingold, A. L.; Figueroa, J. S. *Angew. Chem. Int. Ed. Engl.* **2009**, *48*, 3473–3477.
- (c) Labios, L. A.; Millard, M. D.; Rheingold, A. L.; Figueroa, J. S. *J. Am. Chem. Soc.* **2009**, *131*, 11318-11319.
- (d) Ditri, T. B.; Fox, B. J.; Moore, C. E.; Rheingold, A. L.; Figueroa, J. S. *Inorg. Chem.* **2009**, *48*, 8362-8375.
- (36) The free isocyanide is synthesized from the primary amine, *via* formylation followed by dehydration.
- (37) The Flack parameter is equal to 0.01 with an ESD of 9 [*i.e.* 0.01(9)].
- (38) For other examples of reactions that involve cleavage of a Si–N bond and formation of a Si–O bond, see: Pike, R. M. *J. Org. Chem.* **1961**, *26*, 232-236.
- (39) It is worth noting that metal carbonyl compounds also react with *bis*(trimethylsilyl)amide derivatives, $M[N(\text{SiMe}_3)_2]$, but the products obtained are typically cyanide compounds ($L_n\text{MCN}$) resulting from cleavage of both N–SiMe₃ bonds or products derived from deprotonation of a ligand. See:
- (a) Wannagat, U.; Seyffert, H. *Angew. Chem. Int. Ed. Engl.* **1965**, *4*, 438-439.

- (b) King, R. B. *Inorg. Chem.* **1967**, *6*, 25-29.
- (c) Brunner, H. *Chem. Ber.* **1969**, *102*, 305-30.
- (d) Moll, M.; Behrens, H.; Kellner, R.; Knöchel, H.; Würstl, P. *Z. Naturforsch.* **1976**, *31b*, 1019-1020.
- (40) For an early example, see: Jutzi, P.; Schröder, F. W. *Angew. Chem. Int. Ed. Engl.* **1971**, *10*, 339.
- (41) (a) Orita, A.; Ohe, K.; Murai, S. *Organometallics* **1994**, *13*, 1533-1536.
- (b) Baldwin, J. E.; Derome, A. E.; Riordan, P. D. *Tetrahedron* **1983**, *39*, 2989-2994.
- (42) (a) Dombeck, B. D.; Angelici, R. J. *J. Am. Chem. Soc.* **1973**, *95*, 7516-7518.
- (b) Dombek, B. D.; Angelici, R. J. *Inorg. Chem.* **1976**, *15*, 2403-2408.
- (c) Dombek, B. D.; Angelici, R. J. *J. Am. Chem. Soc.* **1976**, *98*, 4110-4115.
- (d) Quick, M. H.; Angelici, R. J. *J. Organomet. Chem.* **1978**, *160*, 231-239.
- (e) Greaves, W. W.; Angelici, R. J. *Inorg. Chem.* **1981**, *20*, 2983-2988.
- (f) Busetto, L.; Palazzi, A. *Inorg. Chim. Acta* **1976**, *19*, 233-240.
- (g) Faraone, F.; Piraino, P.; Marsala, V.; Sergi, S. *J. Chem. Soc., Dalton Trans.* **1977**, 859-861.
- (43) Angelici notes in reference 42a that the $\nu(\text{CO})$ bands for $\text{M}(\text{CO})_5(\text{CS})$ ($\text{M} = \text{Cr}, \text{Mo}, \text{W}$) complexes are at significantly higher frequencies than most $\text{LM}(\text{CO})_5$ complexes; they are close to the bands for the complexes $\text{M}(\text{CO})_5(\text{PF}_3)$, which is considered to be one of the best π -accepting ligands known. Additionally, he

mentions molecular orbital calculations⁴⁴ that indicate that the LUMO of $\text{M}(\text{CO})_5(\text{CS})$ is the CS π -antibonding orbital which is concentrated on the thiocarbonyl atom.

- (44) Lichtenberger, D. L.; Fenske, R. F. *Inorg. Chem.* **1976**, *15*, 2015-2022.
- (45) (a) Petz, W. *Coord. Chem. Rev.* **2008**, *252*, 1689-1733.
- (b) Moltzen, E. K.; Klabunde, K. J.; Senning, A. *Chem. Rev.* **1988**, *88*, 391-406.
- (46) (a) McNally, J. P.; Leong, V. S.; Cooper, N. J. in *Experimental Organometallic Chemistry*, Wayda, A. L.; Darensbourg, M. Y., Eds.; American Chemical Society: Washington, DC, 1987; Chapter 2, pp 6-23.
- (b) Burger, B.J.; Bercaw, J. E. in *Experimental Organometallic Chemistry*; Wayda, A. L.; Darensbourg, M. Y., Eds.; American Chemical Society: Washington, DC, 1987; Chapter 4, pp 79-98.
- (c) Shriver, D. F.; Drezdson, M. A.; *The Manipulation of Air-Sensitive Compounds*, 2nd Edition; Wiley-Interscience: New York, 1986.
- (47) Gottlieb, H. E.; Kotlyar, V.; Nudelman, A. J. *Org. Chem.* **1997**, *62*, 7512-7515.
- (48) (a) Sheldrick, G. M. SHELXTL, An Integrated System for Solving, Refining and Displaying Crystal Structures from Diffraction Data; University of Göttingen, Göttingen, Federal Republic of Germany, 1981.
- (b) Sheldrick, G. M. *Acta Cryst.* **2008**, *A64*, 112-122.
- (49) For literature data, see: King, R. B.; Saran, M. S. *Inorg. Chem.* **1974**, *13*, 74-78.
- (50) The reaction was performed at room temperature to minimize formation of $\text{Mo}(\text{CO})_3(\text{CNBu}^t)_3$.

- (51) For literature data, see: Albers, M. O.; Coville, N. J.; Singleton, E. J. *Chem. Soc., Dalton Trans.* **1982**, 1069-1079.
- (52) For a previous report, see: Halbauer, K.; Dönnecke, D.; Görls, H.; Imhof, W. Z. *Anorg. Allg. Chemie* **2006**, 632, 1477-1482.

CHAPTER 5

Structure and Reactivity of Thimerosal: Studies Towards Mercury Detoxification**Table of Contents**

5.1	Introduction	314
5.1.1	Mercury toxicity and previous studies in the Parkin Group	314
5.1.2	Thimerosal	317
5.2	Structural characterization of thimerosal	318
5.3	Spectroscopic characterization of thimerosal	320
5.4	Protonation of thimerosal	330
5.5	Stability of $(\text{Ar}^{\text{CO}_2\text{H}})\text{SHgEt}$ with respect to protolytic cleavage of the Hg–C bond	338
5.6	Mercuration of thimerosal	339
5.7	Synthesis of thiol based chelating agents for mercury detoxification.	341
5.8	Summary and conclusions	349
5.9	Experimental details	349
5.9.1	General considerations	350
5.9.2	X-ray structure determinations	350
5.9.3	Spectroscopic Data for Thimerosal	351
5.9.4	Synthesis of $(\text{Ar}^{\text{CO}_2\text{H}})\text{SHgEt}$	352
5.9.5	Deprotonation of $(\text{Ar}^{\text{CO}_2\text{H}})\text{SHgEt}$	352
5.9.6	Thermal stability of $(\text{Ar}^{\text{CO}_2\text{H}})\text{SHgEt}$	353
5.9.7	Synthesis of $[(\text{Ar}^{\text{CO}_2\text{HgEt}})\text{SHgEt}]_2$	353
5.9.8	Synthesis of 2-Carboxy-1,3-propanedithiol	354
5.9.9	2,4-Dibromoglutaric acid	354
5.9.10	Dimethyl-2,4-dibromoglutarate	355

	313
5.9.11 Dimethyl-2,4-bis(acetylthio)glutarate	355
5.9.12 1,2-Dithiolane-3,5-dicarboxylic acids	356
5.9.13 (\pm) 2,4-Dimercaptoglutaric acid	357
5.9.14 <i>Meso</i> - 2,4-Dimercaptoglutaric acid	357
5.10 Crystallographic data	359
5.11 References and notes	364

Reproduced in part from:

J. G. Melnick, K. Yurkerwich, D. Buccella, W. Sattler and G. Parkin *Inorg. Chem.* **2008**, *47*, 6421-6426.

W. Sattler, K. Yurkerwich and G. Parkin *Dalton Trans.* **2009**, 4327-4333.

5.1 Introduction

5.1.1 Mercury toxicity and previous studies in the Parkin Group

Mercury has become infamous in popular culture due to its potent toxicity.¹ Of the different mercury species, alkylmercurials and inorganic mercury trump elemental mercury in their relative toxicities. Specifically, methylmercury compounds are of the highest toxicity known. As such, investigations of the nature of these compounds, and mechanisms of their detoxification are relevant to both human health and environmental concerns.

Methylmercury compounds are produced by the natural biomethylation of inorganic mercury, Hg(II), in aqueous media.^{2,3,4} This process is performed by microorganisms, particularly sulfate-reducing bacteria, which live in or close to the sediments in aqueous ecosystems.⁵ Most notably, methylcobalamin (Figure 1), a derivative of vitamin B₁₂, methylates Hg(II) in methylcobalamin-utilizing methanogenic bacteria.⁶

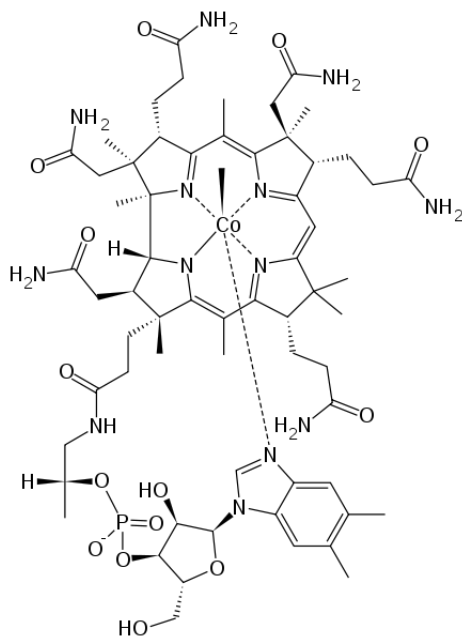
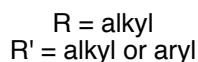


Figure 1. Methylcobalamin.

The methylmercury species that is generated is exceedingly kinetically stable (*i.e.* the mercury carbon bond is resistant to cleavage), resulting in its biomagnification upon ascending the food chain.⁷ Methylmercury is found in a copious number of seafoods, with the highest concentrations found in long-lived, large, predatory fish. The methylmercury is transferred to the human, when these fish are consumed.

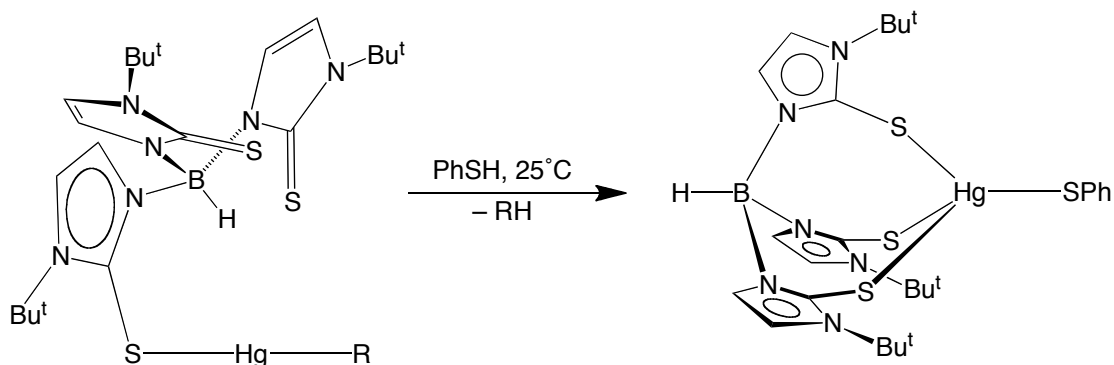
The thiophilicity of mercury is well established.⁸ Thiols, also termed mercaptans due to their high affinity for mercury, have been demonstrated to protolytically cleave mercury carbon bonds in mercury alkyl compounds, producing the corresponding alkane and the mercury thiolate derivative (Scheme 1).^{2,8} This process is thermodynamically favorable, with both experimental and computational data providing evidence that the products (*i.e.* the mercury-thiolate and alkane) are the energetically more stable species.⁹ However, this process has a large activation barrier, such that the mercury alkyl compounds are kinetically inert at ambient temperatures and neutral pH (Scheme 1).^{1,3} In this vein, it has recently been demonstrated that increasing the number of sulfur donors available for the mercury atom significantly lowers the activation energy needed for this protolytic process, resulting in room temperature cleavage (*vide infra*).²



Scheme 1. Reaction of alkylmercurial with thiol.

Organomercurial lyase, MerB, is a bacterial enzyme that cleaves mercury-carbon bonds under physiological conditions.¹⁰ MerB has three cysteine residues (Cys-96, Cys-159 and Cys-160) in its active site, of which only two (Cys-96 and Cys-159) are

essential for enzymatic activity.^{11,12} In the mercurated state of MerB, only the two essential cysteine residues are bound to the mercury atom, along with a water molecule that forms a trigonal-planar geometry around mercury. A former member of the Parkin research group, Jonathan Melnick, used the sulfur rich *tris*(2-mercapto-1-*tert*-butylimidazolyl)hydroborato ligand, [Tm^{Bu^t}], to mimic the enzyme, MerB.² Specifically, the [Tm^{Bu^t}] ligand has three sulfur donors, analogous to the three active-site cysteine residues in MerB.^{11,12} Upon addition of benzene thiol to the two-coordinate mercury alkyl complex, [κ^1 -Tm^{Bu^t}]HgR (R = Me, Et), alkane (methane or ethane) was eliminated rapidly at room temperature, presumably *via* access to higher coordinate mercury complexes, namely the κ^2 -S₂ isomer or the κ^3 -S₃ isomer (Scheme 2). It was postulated that the susceptibility of the Hg–R bond towards protolytic cleavage, in comparison to the notorious inertness of other two-coordinate mercury alkyl compounds, was a consequence of the availability of the additional sulfur donors.¹³ To reinforce the importance of increased sulfur coordination, the cationic complex, [[Hmim^{Bu^t}]HgR][BF₄], (Hmim^{Bu^t} = 2-mercapto-1-*tert*-butylimidazole) does not react rapidly with PhSH at room temperature, whereas addition of excess Hmim^{Bu^t} causes rapid elimination of RH. This observation is consistent with the formation of higher coordinate mercury species resulting in faster protolytic cleavage.²



Scheme 2. Protolytic cleavage of [κ^1 -Tm^{Bu^t}]HgR (R = Me, Et) by benzene thiol.

5.1.2 Thimerosal

Sodium ethylmercury thiosalicylate, $[(Ar^{CO_2})SHgEt]Na$, which is commonly known as thimerosal (Figure 2),^{14,15} was first introduced as a pharmaceutical ingredient in the early 1930s under the trade name Merthiolate.¹⁶ Thimerosal is an alkylmercurial compound, as it has an ethyl mercury bond. Additionally, the sodium carboxylate functionality allows thimerosal to be water soluble, as the protonated derivative is not soluble in water (*vide infra*). Thimerosal was often used as a vaccine preservative and as an antiseptic for the topical treatment of cuts and wounds.¹⁷ In addition to its use and antiseptic, there are many other applications of thimerosal that result from its antimicrobial properties. Some of these include contact lens cleaners, soap-free cleansers, eye, nose and ear drops and skin test antigens.^{18,19,20} Recently, there has been controversy concerning thimerosal due to it being linked to autism in children due to its use as a vaccine preservative.^{21,22,23,24,25} However, there is currently no strong scientific evidence that supports this claim.²⁶

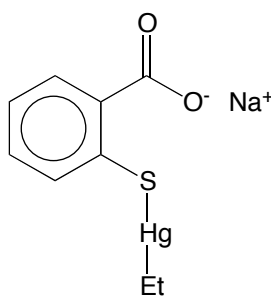


Figure 2. Thimerosal.

Organomercurials have also found use as fungicides, contraceptive spermicides and disinfectants.²⁷ One infamous example was the use of a fungicide containing methylmercury that resulted in the death of approximately 500 people in Iraq in the early 1970s, when wheat seeds treated with these pesticides were used for making bread rather than for growing wheat.²⁸

Considering the widespread applications of thimerosal, the structure, spectroscopic properties and reactivity were examined.²⁹ This chapter will detail the molecular structures and spectroscopic properties of thimerosal and some related derivatives. Additionally, some reactivity of thimerosal will be discussed, and then selected attempts to design chelating agents for mercury detoxification will be mentioned.

5.2 Structural characterization of thimerosal

Thimerosal was first reported in 1928;^{30,31,32} however, there are almost no reports discussing its structure, spectroscopic properties and reactivity. In this vein, single crystal X-ray diffraction has been used to determine the molecular structure of thimerosal. Crystals of thimerosal suitable for analysis were obtained by slow evaporation from methanol; the molecular structure is illustrated in Figure 3 and Figure 4. Figure 3 shows the entire asymmetric unit, which has six independent thimerosal molecules, while Figure 4 shows only one of the ethylmercury thiosalicylate groups for clarity.

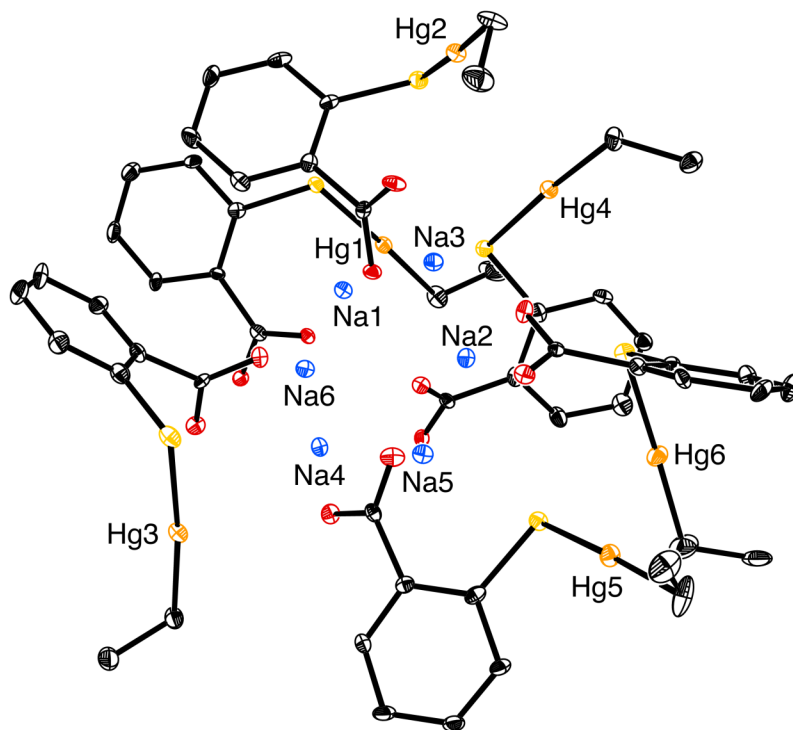


Figure 3. Asymmetric unit of thimerosal containing six independent molecules of thimerosal.

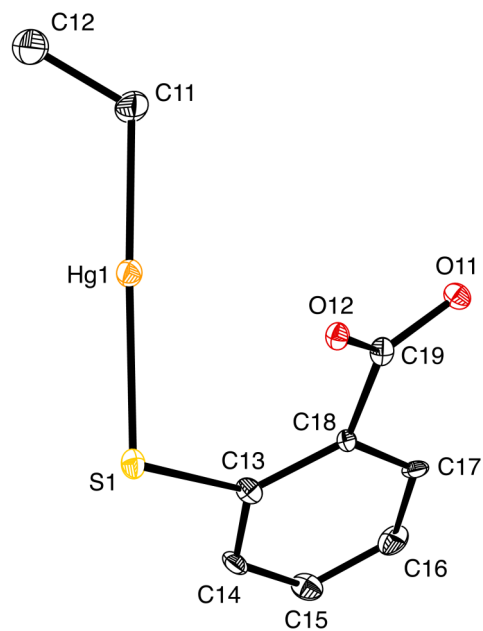


Figure 4. Molecular structure of one of the anions of thimerosal in the asymmetric unit.

The asymmetric unit shows that the Na⁺ cations are coordinated to both the oxygen and sulfur atoms of the thiosalicylate ligand. Some of the Na⁺ cations coordinate only to the carboxylate oxygen atoms, while other Na⁺ cations also coordinate to the sulfur atom. The structures of each of the [(Ar^{CO₂})SHgEt]⁻ units are similar, with all mercury atoms having the linear two-coordinate geometry that is common for alkyl and thiolate compounds.^{33,34,35,36} The main difference among the anions are the torsion angles involving the (Ar^{CO₂}) ligand. Selected metrical data for the [(Ar^{CO₂})SHgEt]⁻ moieties are summarized in Table 1.

Table 1. Comparison of bond length (Å) and bond angle (°) data for the six independent molecules of [(Ar^{CO₂})SHgEt]Na in the asymmetric unit.

	$d(\text{Hg-C})/\text{Å}$	$d(\text{Hg-S})/\text{Å}$	$\text{C-Hg-S}/^\circ$
molecule #1	2.075(13)	2.383(3)	178.0(4)
molecule #2	2.081(13)	2.364(3)	176.9(4)
molecule #3	2.129(12)	2.391(3)	173.3(4)
molecule #4	2.094(11)	2.376(3)	176.5(4)
molecule #5	2.100(12)	2.371(3)	175.0(5)
molecule #6	2.075(16)	2.363(3)	176.8(7)
Average	2.07(1)	2.383(3)	178.0(4)

5.3 Spectroscopic characterization of thimerosal

In addition to structurally characterizing thimerosal in the solid state, multinuclear NMR studies have been performed in order to characterize thimerosal in solution. ¹⁹⁹Hg NMR spectroscopic studies are consistent with thimerosal possessing a linear two-coordinate geometry in solution. Specifically, the ¹⁹⁹Hg{¹H} NMR chemical shift of thimerosal is -784 ppm relative to HgMe₂ (δ = 0) (referenced externally to 1.0 M

HgI_2 in d^6 -DMSO, $\delta = -3106$), which is within the range (-1200 to -600 ppm) observed for two-coordinate mercury thiolate compounds.^{37,38} In the ^{199}Hg spectrum, the signal is a well-resolved triplet of quartets, which is the expected coupling pattern based on previously reported $^2J_{\text{H-H}}$ and $^3J_{\text{H-H}}$ coupling constants for ethyl mercury compounds (Figure 5). The $^2J_{\text{H-H}}$ and $^3J_{\text{H-H}}$ coupling constants correspond to the hydrogen atoms on the methylene (CH_2) and methyl (CH_3) groups, respectively, which are $^2J_{\text{Hg-H}} = 176$ Hz and $^3J_{\text{Hg-H}} = 250$ Hz. It is interesting to note that the three-bond coupling constant is larger than the two-bond coupling constant. A similar trend in $^2J_{\text{Hg-H}}$ and $^3J_{\text{Hg-H}}$ coupling constants is also observed for other EtHgX derivatives.³⁹ The simulated ^{199}Hg spectrum and the predicted coupling pattern based on mercury-hydrogen coupling constants are depicted in Figure 6 and Figure 7, respectively.

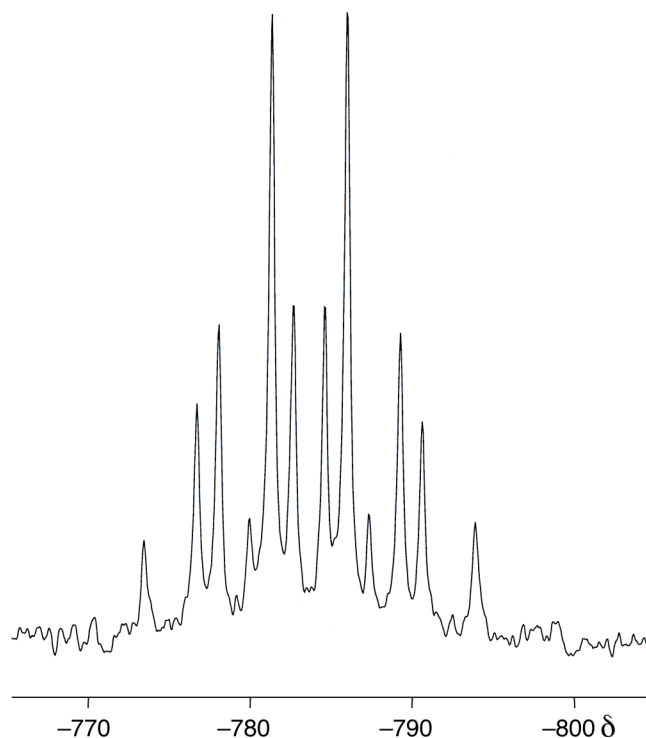


Figure 5. ^{199}Hg NMR spectrum (53.75 MHz) of thimerosal in D_2O .

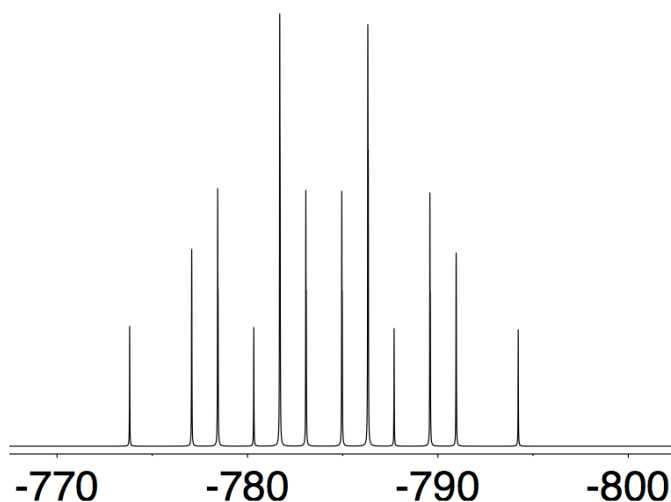


Figure 6. Simulated ^{199}Hg NMR spectrum with $^2J_{\text{Hg-H}} = |176|$ Hz and $^3J_{\text{Hg-H}} = |250|$ Hz.

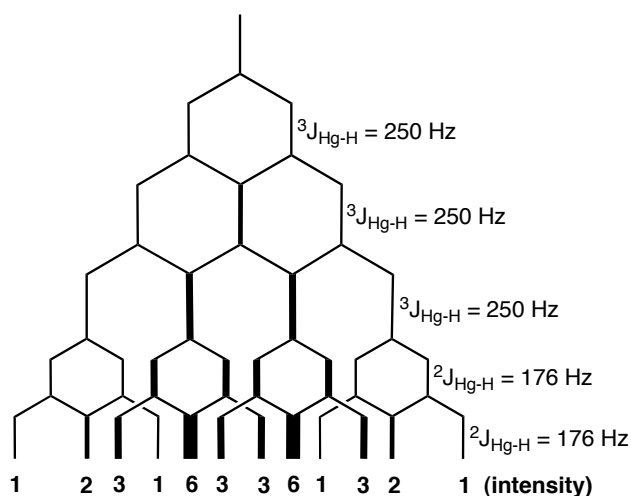


Figure 7. Predicted ^{199}Hg NMR coupling pattern with $^2J_{\text{Hg-H}} = |176|$ Hz and $^3J_{\text{Hg-H}} = |250|$ Hz (the line thickness represents the intensity of the signal).

The corresponding ^1H and $^{13}\text{C}\{^1\text{H}\}$ NMR spectra exhibit ^{199}Hg satellites (16.9 % abundance), as illustrated in Figure 8 and Figure 9. Note that in Figure 8, the ^{199}Hg satellites in the ^1H spectra have different appearances based on the magnetic field strength (*vide infra*). Specifically, the $J_{\text{H-H}}$ coupling resolution decreases at higher magnetic field strengths for the satellite signals (*vide infra*). $J_{\text{Hg-C}}$ and $J_{\text{Hg-H}}$ coupling

constant data are listed in Table 2. The one-bond mercury-carbon coupling constant ($^1J_{\text{Hg-C}} = |1316|$ Hz) is considerably larger than is the two-bond mercury-carbon coupling constant ($^2J_{\text{Hg-C}} = |74|$ Hz). The opposite trend is observed for the mercury-proton coupling constants (*i.e.* for the corresponding two-bond and three-bond $J_{\text{Hg-H}}$ coupling constants).

Table 2. ^1H and ^{13}C NMR spectroscopic data for the ethyl ligand of thimerosal in D_2O .

^1H	^{13}C
$\delta(\underline{\text{CH}}_2) = 1.65$	$\delta(\underline{\text{C}}\text{H}_2) = 28.3$
$^3J_{\text{H-H}} = 8$	$^1J_{\text{C-H}} = 136$
$^2J_{\text{Hg-H}} = 176$	$^1J_{\text{Hg-C}} = 1316$
$\delta(\underline{\text{CH}}_3) = 1.26$	$\delta(\underline{\text{C}}\text{H}_3) = 15.9$
$^3J_{\text{H-H}} = 8$	$^1J_{\text{C-H}} = 126$
$^3J_{\text{Hg-H}} = 250$	$^2J_{\text{Hg-C}} = 74$

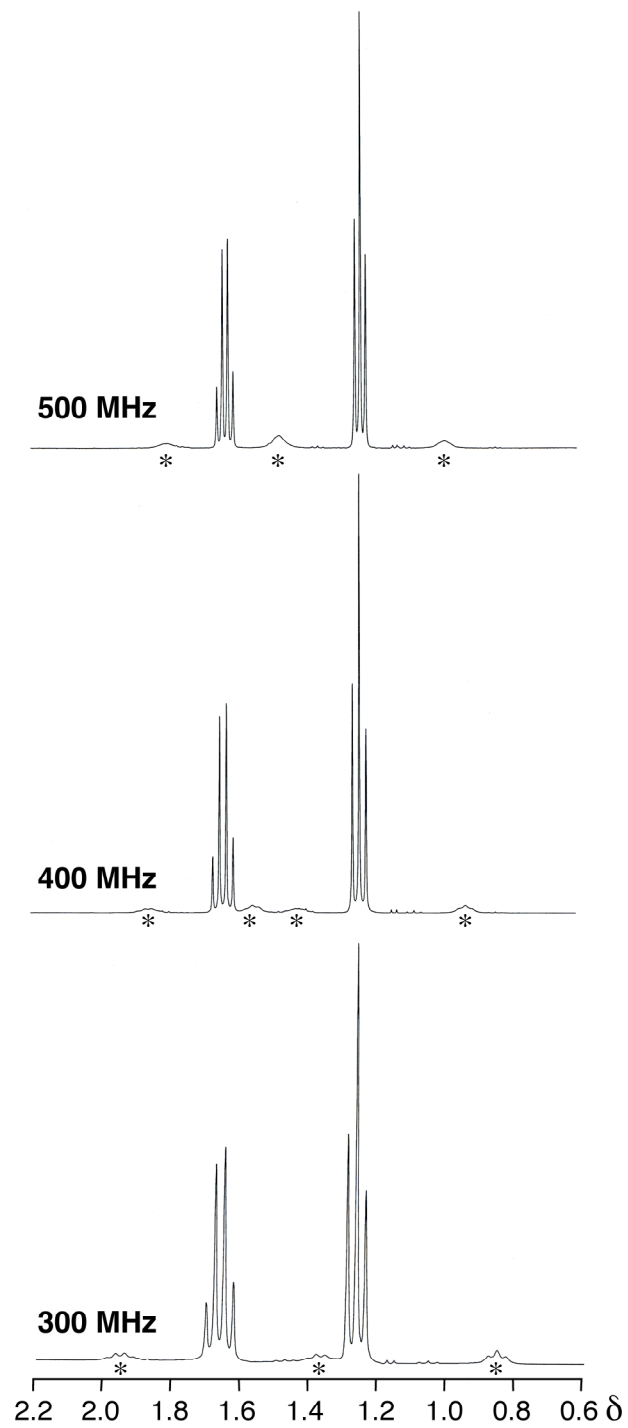


Figure 8. ^1H NMR spectra of Thimerosal in D_2O at different magnetic field strength (^{199}Hg satellites are marked with a *).

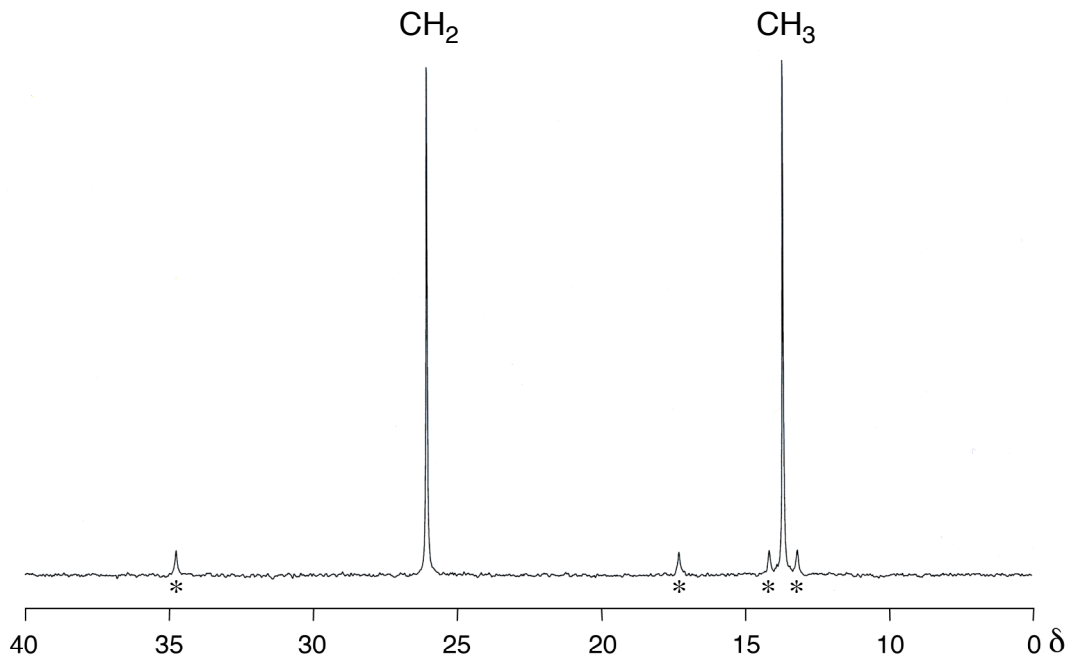


Figure 9. $^{13}\text{C}\{^1\text{H}\}$ NMR spectrum (75.4677 MHz) of thimerosal in D_2O (^{199}Hg satellites are marked with *).

Interestingly, the ^1H chemical shift of the CH_2 group of thimerosal is *downfield* of the CH_3 group (Figure 8), an order that is in accord with that reported for other EtHgX derivatives ($\text{X} = \text{CN}, \text{Br}, \text{Cl}, \text{NO}_3, \text{I}, \text{ClO}_4$), but opposite to that of Et_2Hg ⁴⁰ (*vide infra*).^{41,42}

For clarity, listed in

Table 3 is a compiled list of the chemical shifts of the CH₂ and CH₃ groups for various EtHgX compounds. It should be noted, however, that according to reference 39 and 43, the CH₂ group of Et₂Hg is *downfield* of the CH₃ group, while the other EtHgX derivatives have the CH₂ group *upfield* of the CH₃ group. It is postulated that this discrepancy is a result of the chemical shifts reported in reference 39 and 43 being based on a different sign convention to the current δ chemical shift scale.

Table 3. ^1H chemical shifts for CH_2 and CH_3 groups for various EtHgX compounds.

Compound	δ CH_2	δ CH_3	Solvent	Reference
Et_2Hg	+1.00	+1.29	CH_2Cl_2	42
EtHgBr	+2.02	+1.37	CH_2Cl_2	42
EtHgI	+2.10	+1.44	CH_2Cl_2	42
$\text{EtHgClO}_4^{\text{a}}$	+2.29	+1.04	D_2O	42
EtHgCl	+1.97	+1.35	CH_2Cl_2	42
EtHgCl	+1.65	+1.25	DMSO	our work
EtHgCl	+1.98	+1.35	CD_2Cl_2	our work
$[(\text{Ar}^{\text{CO}_2})\text{SHgEt}]\text{Na}$	+1.65	+1.26	D_2O	our work
$(\text{Ar}^{\text{CO}_2\text{H}})\text{SHgEt}$	+1.89	+1.35	CDCl_3	our work
$[(\text{Ar}^{\text{CO}_2\text{HgEt}})\text{SHgEt}]_2$	+1.83	+1.32	CD_2Cl_2	our work

^a Based on Me_3COH in water = 1.31 ppm.

Finally, it is also of interest to discuss the appearance of the ^{199}Hg satellites in the ^1H NMR spectra. Whereas the main signals associated with the ethyl group consist of a well-defined triplet and quartet for the CH_3 and CH_2 groups respectively, the satellites are broad such that the proton-proton coupling ($^3J_{\text{H-H}}$) is not well resolved. The appearance of the ^{199}Hg satellites is dependent on the magnetic field with stronger magnetic fields resulting in broader ^{199}Hg satellites (*i.e.* the resolution is inversely dependent on magnetic field strength). This can be seen in Figure 8. The magnetic field dependence of the satellites is due to relaxation by chemical shift anisotropy (CSA).⁴⁴ CSA does not apply only to ^{199}Hg ,⁴⁵ but also to other nuclei such as ^{31}P ,⁴⁶ ^{77}Se ,^{46b,47} ^{57}Fe ,⁴⁸ ^{103}Rh ,⁴⁹ ^{195}Pt ,⁵⁰ ^{207}Pb ,⁵¹ and ^{205}Tl .^{52,53} CSA is defined as the chemical shift difference between the isotropic and anisotropic states. The difference in chemical shift is due to the fact that the chemical shift is dependent on the local magnetic field and therefore,

the orientation of the molecule (*i.e.* depending on the direction of the molecule, the chemical shift of the nuclei of interest will vary). This anisotropy modifies the effective magnetic field, thus providing a means to relax the neighboring nuclei. In a situation where $\omega_0\tau_c \ll 1$ (ω_0 = Larmor frequency and τ_c = rotational correlation time) is satisfied, the relaxation component due to chemical shift anisotropy is directly proportional to B_0^2 ; as such, relaxation will become faster with stronger magnetic fields (Equations 1).⁴⁴ Thus, as the strength of the magnetic field increases, the linewidth at half-height ($w_{1/2}$) of the satellites increases such that it is not possible to resolve the $^3J_{\text{H-H}}$ coupling.

$$R(\text{CSA}) = (2/15)\gamma^2 B_0^2 (\sigma_{\parallel} - \sigma_{\perp})^2 \{\tau_c / (1 + \omega_0^2 \tau_c^2)\}$$

$$R(\text{CSA}) = (2/15)\gamma^2 B_0^2 (\sigma_{\parallel} - \sigma_{\perp})^2 \tau_c \quad \text{for } \omega_0 \tau_c \ll 1$$

$$(\omega_0 = -\gamma B_0)$$

Equations 1. $R(\text{CSA})$ = spin-lattice relaxation due to chemical shift anisotropy; γ = gyromagnetic ratio; B_0 = applied magnetic field; σ_{\parallel} and σ_{\perp} = parallel and perpendicular components of the shielding tensor; τ_c = rotational correlation time; ω_0 = Larmor frequency.

As stated above, relaxation *via* CSA is influenced by the rotational correlation time (τ_c). Therefore, the line width of the satellites is a function of the viscosity of the solvent. For situations where $\omega_0\tau_c \ll 1$, relaxation due to CSA is proportional to the rotational correlation time which is dependent on the viscosity.⁴⁴ For this reason, the multiplet structure of the mercury satellites of the ethyl group of thimerosal are much better resolved in methanol (Figure 10) and acetone solvents that have lower viscosities compared to water.⁵⁴

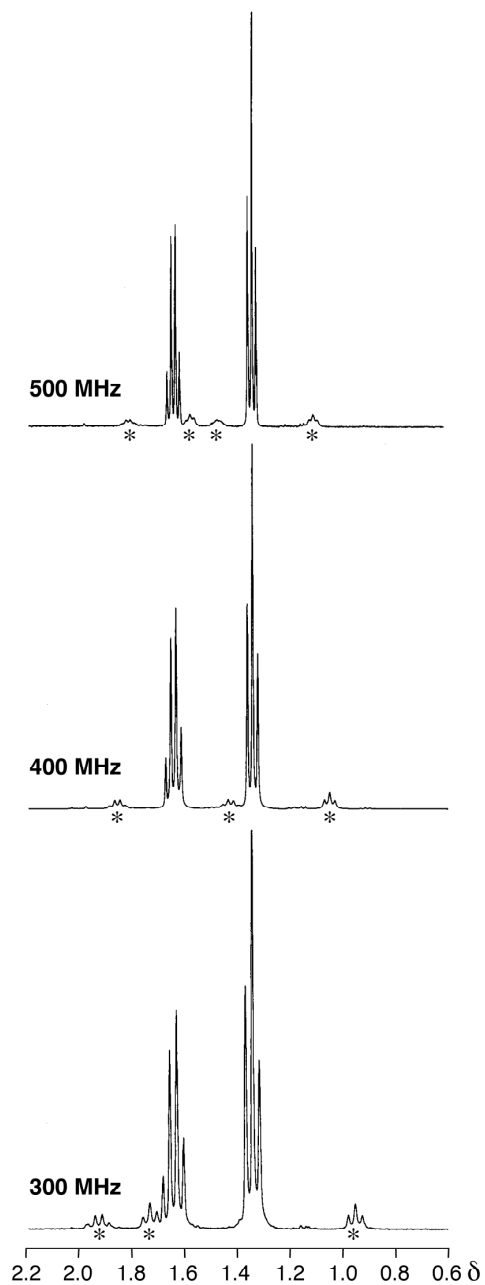


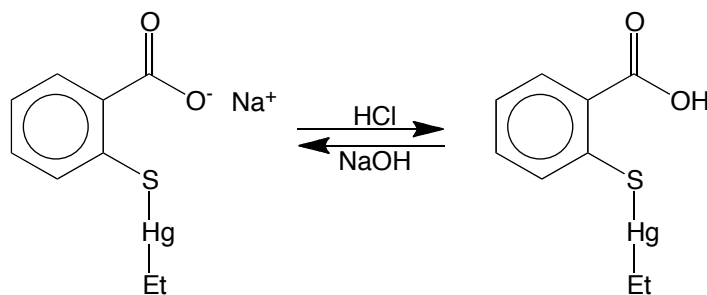
Figure 10. ^1H NMR spectra of thimerosal in CD_3OD at different magnetic field strength (^{199}Hg satellites are marked with a *).

As depicted in Figure 8 and Figure 10, the ^{199}Hg satellites suffer from relaxation due to CSA, because the ^{199}Hg chemical shift range is quite large. The relaxation due to

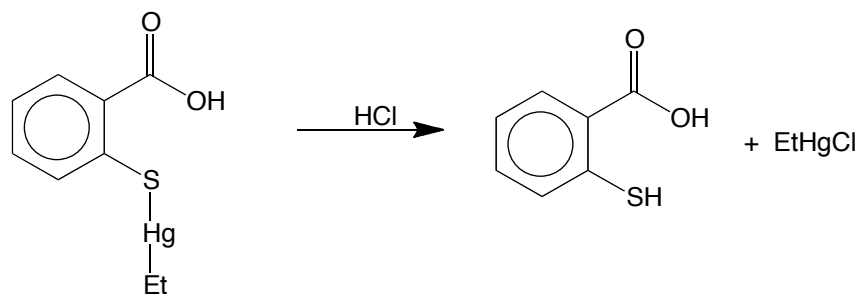
CSA is verified by the fact that the resolution of the ^{199}Hg satellites is dependent on both applied magnetic field and solvent viscosity (Equations 1).

5.4 Protonation of thimerosal

Thimerosal has multiple sites that may be subject to electrophilic attack. The two most apparent sites are the carboxylate oxygen and the mercury–carbon bond. In the latter case, it is the carbon that acts as the nucleophile, similar to the reactivity of the more common Grignard reagent. The most common and straightforward electrophile is the proton (H^+), and therefore, the reactivity of thimerosal with a proton source was explored. Treatment of an aqueous solution of thimerosal with aqueous HCl results in the selective protonation of the carboxylate oxygen. This results in the precipitation of the carboxylic acid derivative $(\text{Ar}^{\text{CO}_2\text{H}})\text{SHgEt}$ (Scheme 3),⁵⁵ with the mercury–carbon bond remaining intact. It should be noted that over time, mercury–sulfur bond cleavage occurs, to give the corresponding thiol, thiosalicylic acid and EtHgCl (Scheme 4).



Scheme 3. Protonation of thimerosal with HCl (forward reaction) and deprotonation of $(\text{Ar}^{\text{CO}_2\text{H}})\text{SHgEt}$ using NaOH (reverse reaction).



Scheme 4. Protonation of $(\text{Ar}^{\text{CO}_2\text{H}})\text{SHgEt}$ by HCl to give thiosalicylic acid and EtHgCl .

The protonated derivative is of interest due to the fact that thimerosal is believed to enter cells *via* its protonated form.⁵⁶ The molecular structure of $(\text{Ar}^{\text{CO}_2\text{H}})\text{SHgEt}$ has been determined using single crystal X-ray diffraction. These studies, on two different crystalline forms of $(\text{Ar}^{\text{CO}_2\text{H}})\text{SHgEt}$ (both are in the monoclinic crystal system, one in space group $P2_1/n$ and one in $P2/c$) indicate that the compound exists as a centrosymmetric dimer involving hydrogen bonding interactions between the carboxylic acid groups, as illustrated in Figure 11.

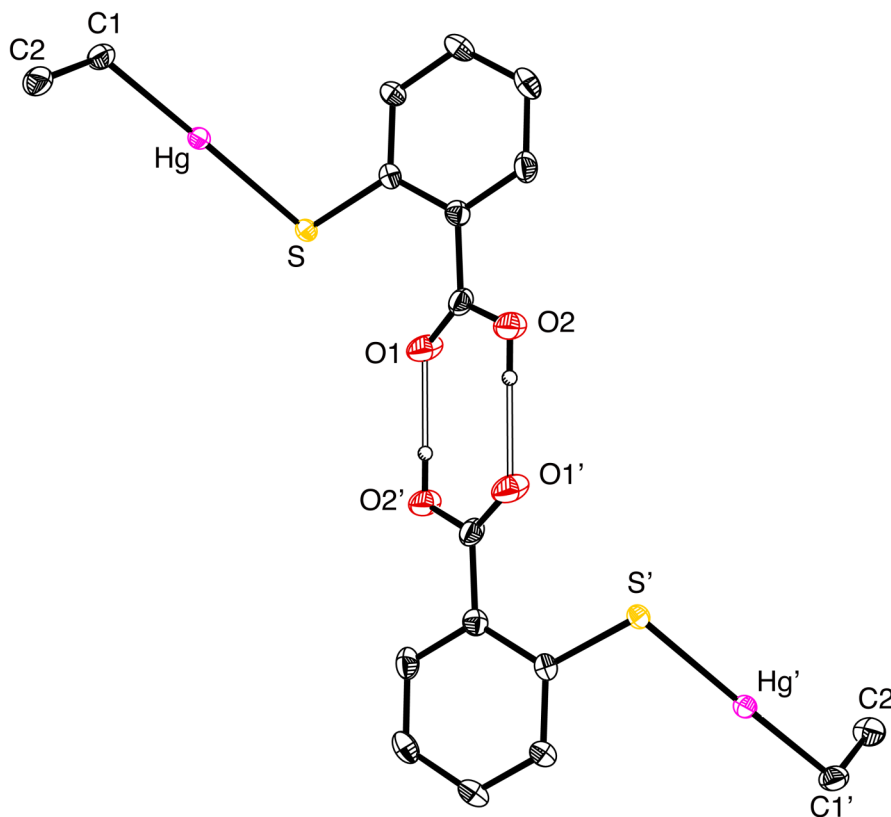


Figure 11. Molecular structure of $(\text{Ar}^{\text{CO}_2\text{H}})\text{SHgEt}$ (hydrogen bonded dimer is shown).

This dimeric structure provides an interesting contrast to the complex network observed for thimerosal, where $[(\text{Ar}^{\text{CO}_2})\text{SHgEt}]^-$ anions are connected to Na^+ cations *via* both the oxygen and sulfur atoms of the thiosalicylate ligand (Figure 3). The centrosymmetric dimer is somewhat expected, as this is a very common motif for molecules containing one carboxylic acid moiety. However, the geometrical features at mercury in both crystalline forms of $(\text{Ar}^{\text{CO}_2\text{H}})\text{SHgEt}$ are similar to those of thimerosal, and are summarized in Table 4.

Table 4. Comparison of the mercury coordination geometries in (Ar^{CO₂H})SHgEt and [(Ar^{CO₂})SHgEt]Na.

	(Ar ^{CO₂H})SHgEt modification #1	(Ar ^{CO₂H})SHgEt ^a modification #2	[(Ar ^{CO₂})SHgEt]Na ^b
Hg–C/Å	2.086(5)	2.093	2.092
Hg–S/Å	2.380(1)	2.383	2.375
C–Hg–S/°	175.4(1)	173.0	176.1

^a average values for 4 crystallographically independent molecules.

^b average values for 6 crystallographically independent molecules.

In addition to the solid-state structure of (Ar^{CO₂H})SHgEt, we have also characterized (Ar^{CO₂H})SHgEt in solution by using ¹H NMR spectroscopy. This provides evidence for both the mercury ethyl moiety and the carboxylic acid proton. With respect to the mercury-ethyl group, the ¹H NMR chemical shift for the CH₂ group is downfield of the CH₃ group, the same trend as for thimerosal itself. Like thimerosal, the ¹⁹⁹Hg satellites of (Ar^{CO₂H})SHgEt are particularly interesting in the ¹H NMR spectrum. Specifically, while the outermost satellites for the CH₂ and CH₃ groups have the expected coupling pattern, a quartet and triplet, respectively, the innermost satellites appear as a *singlet* when acquiring the spectrum at 400 MHz (Figure 12).

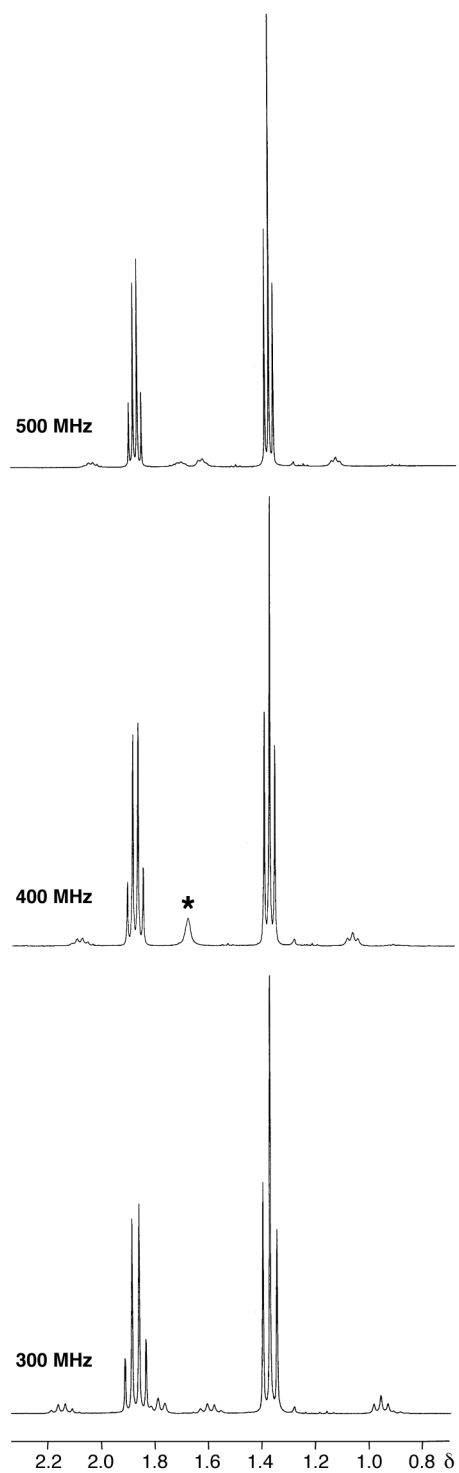


Figure 12. ^1H NMR spectra of $(\text{Ar}^{\text{CO}_2\text{H}})\text{SHgEt}$ at different magnetic field strengths. At 400 MHz, the central pair of ^{199}Hg satellites appear as a singlet (*).

The singlet stems from the fact that the satellites correspond to the A_2B_3 portion of an A_2B_3X spin system. Therefore, their appearance depends on the J_{A-X} (i.e. ${}^2J_{\text{Hg-H}}$) and J_{B-X} (i.e. ${}^3J_{\text{Hg-H}}$) coupling constants. If $\Delta\delta$ is the absolute chemical shift difference ($|\delta_A - \delta_B|$) of the CH_2 and CH_3 groups for molecules devoid of magnetically active ${}^{199}\text{Hg}$ nuclei, the "effective" chemical shift difference ($\Delta\delta'$) for those with the two spin states of ${}^{199}\text{Hg}$ is $|\Delta\delta \pm \frac{1}{2}(J_{A-X} - J_{B-X})|$.^{57,58} For clarity, this is illustrated in Figure 13, where $A = \text{CH}_2$ and $B = \text{CH}_3$. Thus, the satellites will only have a first-order appearance if $|\Delta\delta \pm \frac{1}{2}(J_{A-X} - J_{B-X})| \gg |J_{AB}|$, and complex spectra for the satellites will result if this inequality is not maintained.^{57,58}

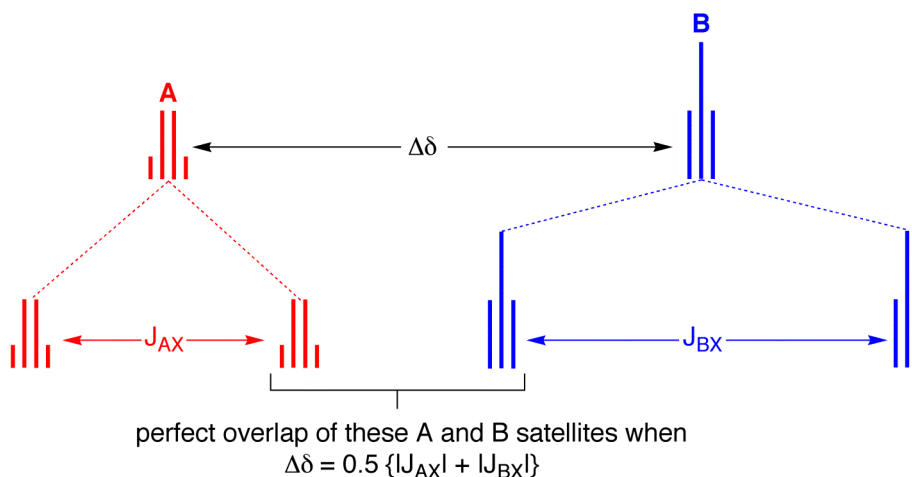


Figure 13. Schematic illustration of the ${}^{199}\text{Hg}$ satellites for a mercury ethyl group. The two inner satellites overlap if $\Delta\delta = \frac{1}{2} \{ |J_{A-X}| + |J_{B-X}| \}$. If J_{A-X} and J_{B-X} have opposite signs, the two satellites correspond to the same molecule and so a singlet results.

In the case that $|\Delta\delta \pm \frac{1}{2}(J_{A-X} - J_{B-X})|$ is zero, (i.e. $\Delta\delta = \frac{1}{2}|J_{A-X} - J_{B-X}|$) the corresponding A_2B_3 subspectra will become a *singlet*. While this is not common, such situations have arisen when the CH_2 and CH_3 groups *coincidentally* have the same chemical shift. For example, the silicon ethyl groups of $[\text{Tp}^{\text{Me}_2}]_2\text{Pt}(\text{H})_2\text{Si}(\text{CH}_2\text{CH}_3)_3$

([Tp^{Me2}] = *tris*(3,5-dimethylpyrazolyl)hydroborato) appear as a singlet in the ¹H NMR spectrum due to the CH₂ and CH₃ groups having the same chemical shift.^{59,60} Meanwhile, the ²⁹Si satellites for the CH₃ and CH₂ groups appear as triplets and quartets, respectively, because the different ²J_{Si-H} and ³J_{Si-H} coupling constants remove the coincidental chemical shift degeneracy for molecules having the magnetically active nucleus ²⁹Si.⁶¹ Another example of lifted degeneracy is in the ³¹P{¹H} NMR spectrum of Pt[(*R,R*)-Me-Duphos][CH₂CH(CO₂Bu^t)] (Duphos = diphosphine ligand) due to the ¹⁹⁵Pt satellite signals, where the central signal is observed as a singlet, but coupling is observed in the satellite signals.^{62,63}

The fact that the “inner” pair of satellites exhibits the second-order behavior gives information about the sign of the Hg-H coupling constants. Specifically, ²J_{Hg-H} and ³J_{Hg-H} must have opposite signs.^{57,58,64} If ²J_{Hg-H} and ³J_{Hg-H} were to have the same sign, the “outer” pair of satellites would exhibit the second-order behavior if the requirement $\Delta\delta = \frac{1}{2}|J_{A-X} - J_{B-X}|$ were satisfied. This has been observed for the ¹⁹⁵Pt satellites in the ³¹P{¹H} NMR spectrum of [{Pt(OP(OMe)₂)₂dppe}₂Zn]²⁺ (dppe = 1,2-*bis*(diphenylphosphino)ethane) because the two J_{Pt-P} coupling constants have the same sign.⁶⁵ The conclusion that ²J_{Hg-H} and ³J_{Hg-H} for (Ar^{CO₂H})SHgEt have opposite signs is consistent with previous studies that suggest that ²J_{Hg-H} is negative, while ³J_{Hg-H} is positive.⁶⁴

As a consequence of the fact that the chemical shift difference (in terms of Hz) of the CH₂ and CH₃ groups is a function of the applied magnetic field, the chemical shifts of the ¹⁹⁹Hg satellites are also field dependent. Thus, while the signals of the CH₂ and CH₃ inner satellites of (Ar^{CO₂H})SHgEt overlap at 400 MHz to give a singlet, more complex spectra are observed at both lower field strength (300 MHz) and higher field strength (500 MHz) which can be seen in Figure 12. In addition to (Ar^{CO₂H})SHgEt, we also studied the ¹H NMR spectra of the commercially available ethylmercury compound EtHgCl. Coincidentally, for EtHgCl, a singlet is also observed for the inner

satellites at 400 MHz (Figure 14). The coupling constants for thimerosal, $(\text{Ar}^{\text{CO}_2\text{H}})\text{SHgEt}$ and EtHgCl ⁶⁶ are summarized in Table 5. In each case, the magnitude of ${}^2J_{\text{Hg-H}}$ is smaller than ${}^3J_{\text{Hg-H}}$, consistent with other EtHgX derivatives.³⁹

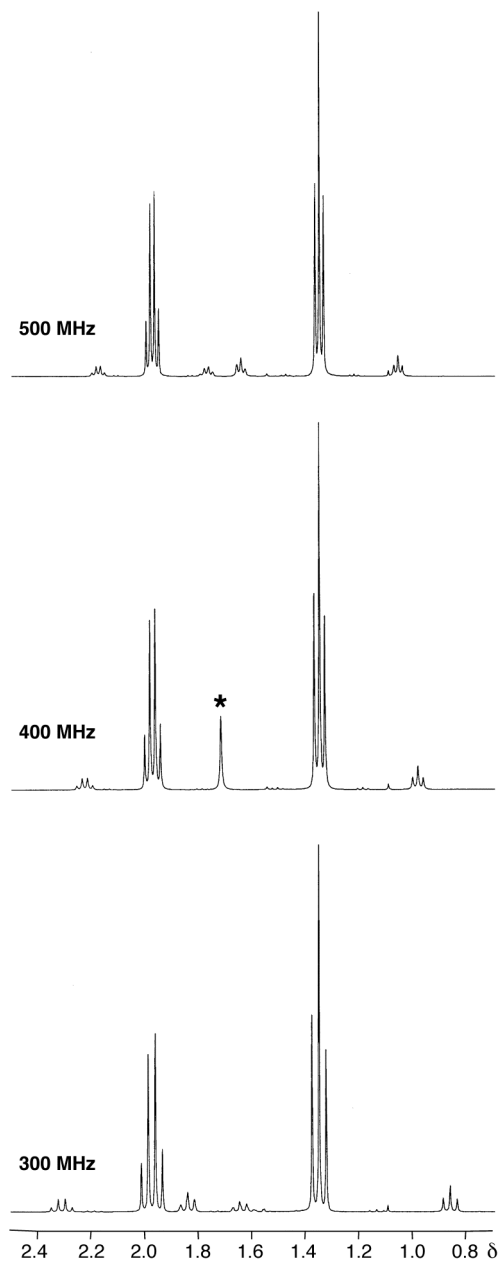


Figure 14. ${}^1\text{H}$ NMR spectra of EtHgCl at different magnetic field strengths. At 400 MHz, the central pair of ${}^{199}\text{Hg}$ satellites appear as a singlet (*).

Table 5. ^1H NMR Chemical shift and coupling constant data for mercury ethyl complexes.

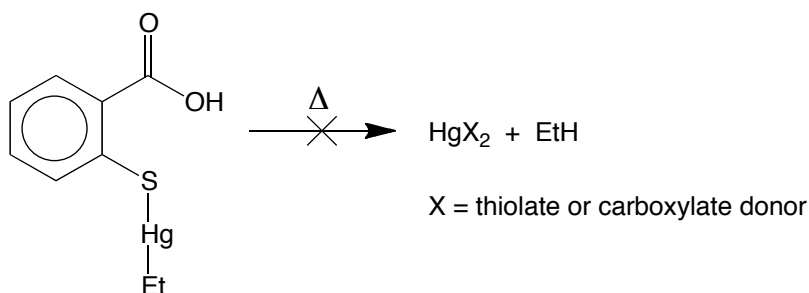
	solvent	$\delta(\underline{\text{CH}}_2)$	$\delta(\underline{\text{CH}}_3)$	$^2J_{\text{Hg-H}}/\text{Hz}^a$	$^3J_{\text{Hg-H}}/\text{Hz}^a$
$(\text{Ar}^{\text{CO}_2\text{H}})\text{SHgEt}$	CDCl_3	1.89 $^3J_{\text{H-H}} = 8$	1.35 $^3J_{\text{H-H}} = 8$	-168	+252
$[(\text{Ar}^{\text{CO}_2\text{HgEt}})\text{SHgEt}]_2$	CD_2Cl_2	1.83 $^3J_{\text{H-H}} = 8$	1.32 $^3J_{\text{H-H}} = 8$	-193	+273
$[(\text{Ar}^{\text{CO}_2})\text{SHgEt}]\text{Na}$	D_2O	1.65 $^3J_{\text{H-H}} = 8$	1.26 $^3J_{\text{H-H}} = 8$	-176	+250
EtHgCl	CD_2Cl_2	1.98 $^3J_{\text{H-H}} = 8$	1.35 $^3J_{\text{H-H}} = 8$	-202	+292

^a Where indicated, the relative signs are determined by analysis of the data, but the absolute sign is based on comparison with the literature (reference 64).

5.5 Stability of $(\text{Ar}^{\text{CO}_2\text{H}})\text{SHgEt}$ with respect to protolytic cleavage of the Hg–C bond

While treatment of thimerosal with $\text{HCl}(\text{aq})$ results in the protonation of the carboxylate oxygen, this is presumably a kinetic product, and not the lowest energy product(s). The expected thermodynamic product(s) would result from the protolytic cleavage of the Hg–C bond to give the alkane in addition to the corresponding mercury complex.⁶⁷ As protonation of the carboxylate oxygen is reversible (Scheme 3), there must be a significant kinetic barrier for protolytically cleaving the Hg–C bond. It should be noted that it is possible that the Hg–C bond of $(\text{Ar}^{\text{CO}_2\text{H}})\text{SHgEt}$ could be cleaved in an intermolecular manner by the carboxylic acid group of another molecule of $(\text{Ar}^{\text{CO}_2\text{H}})\text{SHgEt}$; however, this is not observed even at elevated temperatures. For example, heating $(\text{Ar}^{\text{CO}_2\text{H}})\text{SHgEt}$ at 150°C over a period of 10 days does not result in any observable elimination of ethane. The kinetic stability of $(\text{Ar}^{\text{CO}_2\text{H}})\text{SHgEt}$ towards protolytic cleavage is consistent with the notion that two-coordinate mercury alkyl

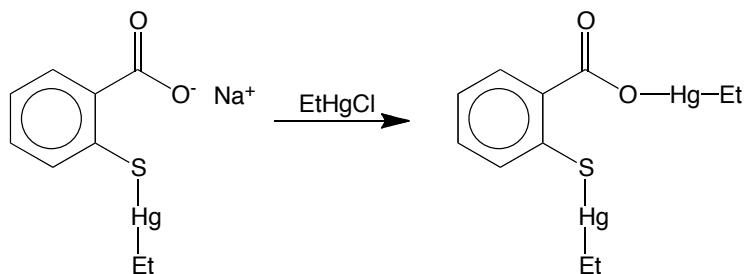
compounds are generally not susceptible to protolytic cleavage.² However, while these observations indicate that the Hg–C bonds of both thimerosal and its protonated derivative are not subject to facile protolytic cleavage, the correct coordination environments around mercury, and different Brønsted acids promote the cleavage as seen previously by using the [Tm^{Bu^t}] ligand.²



Scheme 5. Kinetic stability of (Ar^{CO₂H})SHgEt.

5.6 Mercuration of thimerosal

In addition to electrophilic attack by a proton, we also explored the reaction of thimerosal with the mercury-based electrophile, EtHgCl. Like the protonation reaction described above, the carboxylate oxygen may be mercured by addition of EtHgCl to give [(Ar^{CO₂HgEt})SHgEt]₂ (Scheme 6), which exists as a dimer in the solid state as depicted in Figure 15.⁶⁸ The synthesis of this complex is significant because a compound with its empirical formula has been reported to be an impurity in the synthesis of thimerosal.⁶⁹



Scheme 6. Mercuration of thimerosal to give [(Ar^{CO₂HgEt})SHgEt]₂ (only the monomer is shown in the scheme for clarity).

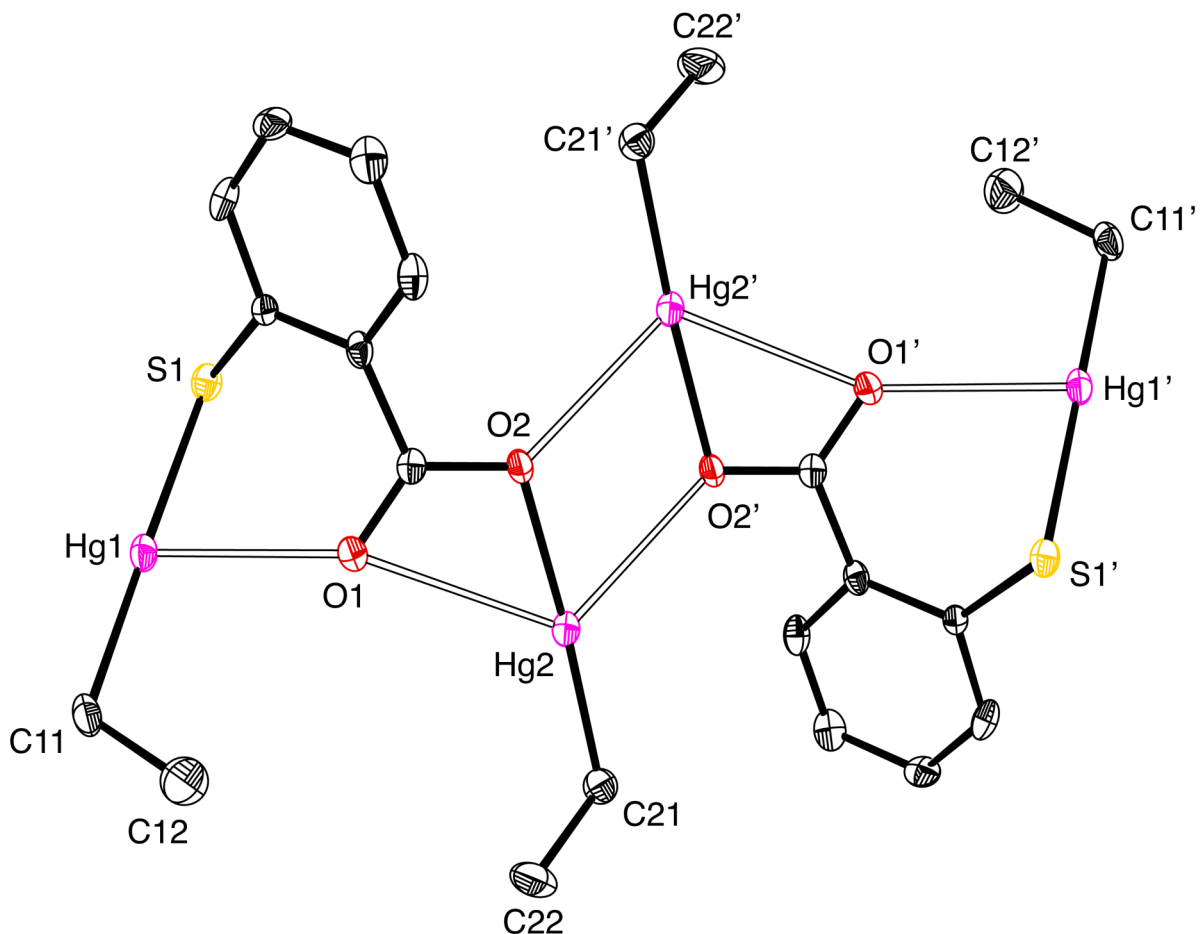


Figure 15. Molecular structure of $[(\text{Ar}^{\text{CO}_2\text{HgEt}})\text{SHgEt}]_2$.

Single crystal X-ray diffraction demonstrates that $[(\text{Ar}^{\text{CO}_2\text{HgEt}})\text{SHgEt}]_2$ has a tetranuclear structure where the mercury atoms are both three- and four-coordinate due to coordination to the carboxylate oxygens. The Hg–O distances span a substantial range from 2.13 to 2.80 Å (Table 6), with the shortest Hg–O interactions being *trans* to the ethyl group.

Table 6. Selected bond lengths for $[(\text{Ar}^{\text{CO}_2\text{HgEt}})\text{SHgEt}]_2$.

	$d(\text{Hg-X})/\text{\AA}$
Hg1–C11	2.099(10)
Hg2–C21	2.074(9)
Hg1–S1	2.382(2)
Hg1–O1	2.596(6)
Hg2–O2'	2.751(6)
Hg2–O1	2.799(6)
Hg2–O2	2.132(6)

The mercury coordination environments are best described as being two-coordinate linear centers supplemented by secondary oxygen interactions.⁷⁰ ¹H NMR spectroscopy indicates the presence of only one chemically distinct mercury ethyl group even though $[(\text{Ar}^{\text{CO}_2\text{HgEt}})\text{SHgEt}]_2$ possesses two chemically distinct [HgEt] moieties. It is possible that the equivalence is coincidental; however, the most plausible explanation is chemical exchange involving dissociation of $[\text{HgEt}]^+$.

5.7 Synthesis of thiol based chelating agents for mercury detoxification.

In order to remove mercury from the body, new chelating agents need to be synthesized for more selective, efficient chelation of mercury. These chelating agents should bind selectively to the metal of interest (mercury), such that it is mobilized for excretion. Currently, *meso*-dimercaptosuccinic acid (DMSA)^{71,72} is most commonly used to detoxify the body in the event of mercury poisoning; it is also used for other metals such as lead (Figure 16). One metric that is important to note is the S—C—C—S torsion angle, which is 180.00° due to the two thiols being orientated in an anti-staggered conformation (Table 7). Other chelating agents that have been used are also depicted in

Figure 16. These include the R-(+) isomer of lipoic acid (LA),^{71a,73} 2,3-dimercapto-1-propanesulfonic acid (DMPS)^{71a,74} and dimercaprol (BAL) (Figure 16). It is interesting to note why dimercaprol is abbreviated BAL,⁷⁵ which is short for British anti-Lewisite. BAL was developed by British biochemists at Oxford University during World War II, to combat the arsenic based chemical warfare agent, lewisite, but has since been used medically to treat heavy metal poisoning.⁷⁵

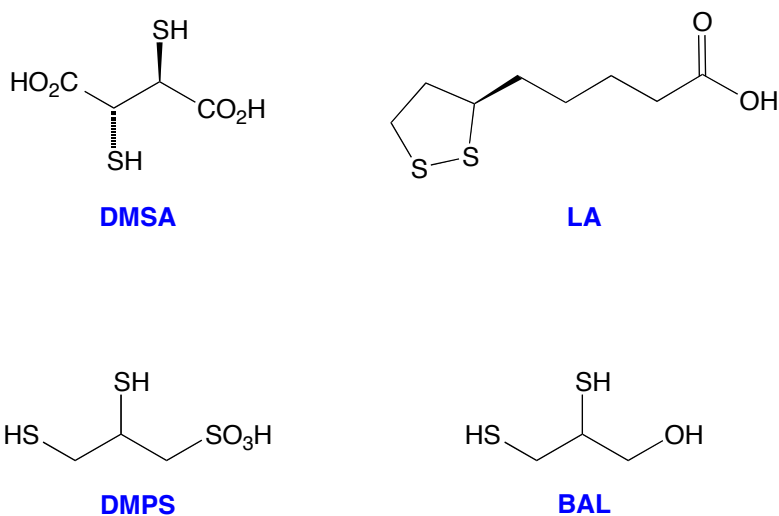


Figure 16. Chelating agents used presently and in the past.

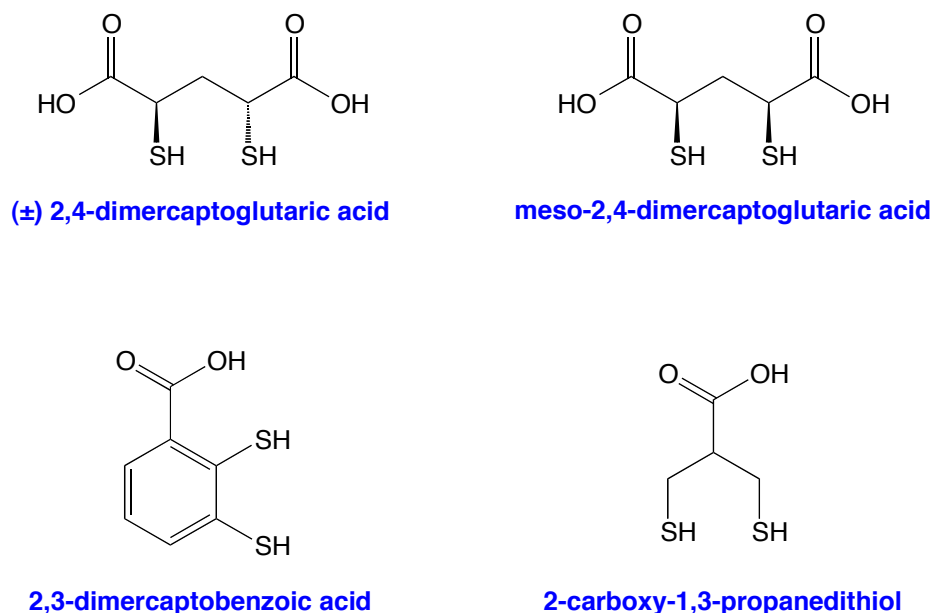
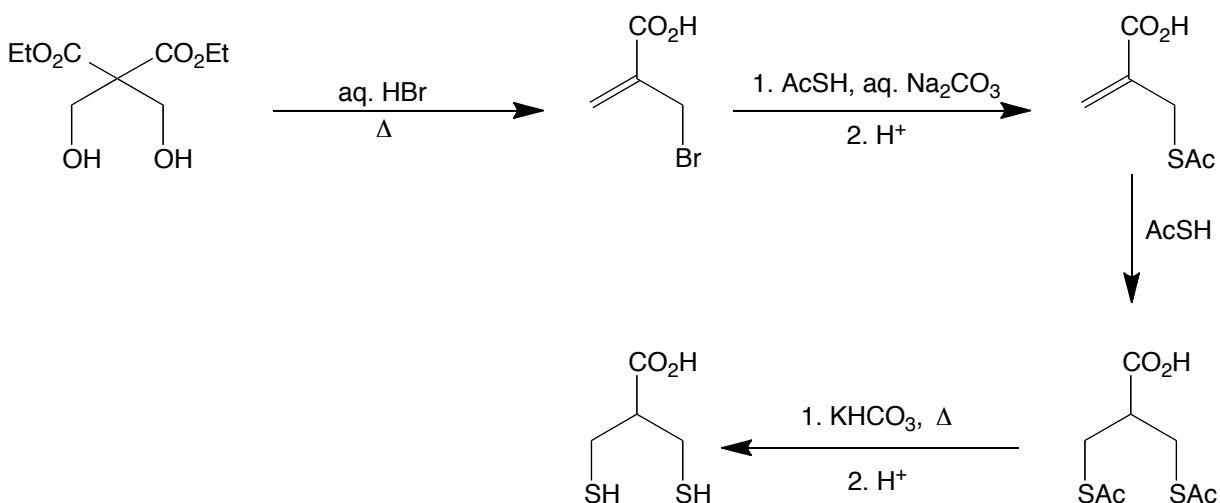


Figure 17. Dithiol compounds synthesized for use as mercury chelating agents.

Based on the fact that these known chelating agents rely on a dithiol motif, a variety of published dithiol compounds that are depicted in Figure 17 were synthesized. Each compound also contains either one or two carboxylic acid moieties such that the molecules should have high water solubility.

2-carboxy-1,3-propanedithiol was prepared by a method published by Whitesides and co-workers and is depicted in Scheme 7.⁷⁶ The molecular structure of 2-carboxy-1,3-propanedithiol was determined by single crystal X-ray diffraction, and is depicted in Figure 18 as its hydrogen bonded dimer. The S—C—C—S torsion angle is 125.98°, which is distinctly less than that of DMSA (Table 7). This is due to two sequential staggered interactions, with the two thiol groups pointed away from each other presumably to reduce steric repulsion. It should be noted that the S—C—C—S torsion angle in DMSA is *via* three direct bonds, while the torsion angle in 2-carboxy-1,3-propanedithiol is *via* two carbons that are not bonded to each other.



Scheme 7. Synthesis of 2-carboxy-1,3-propanedithiol.

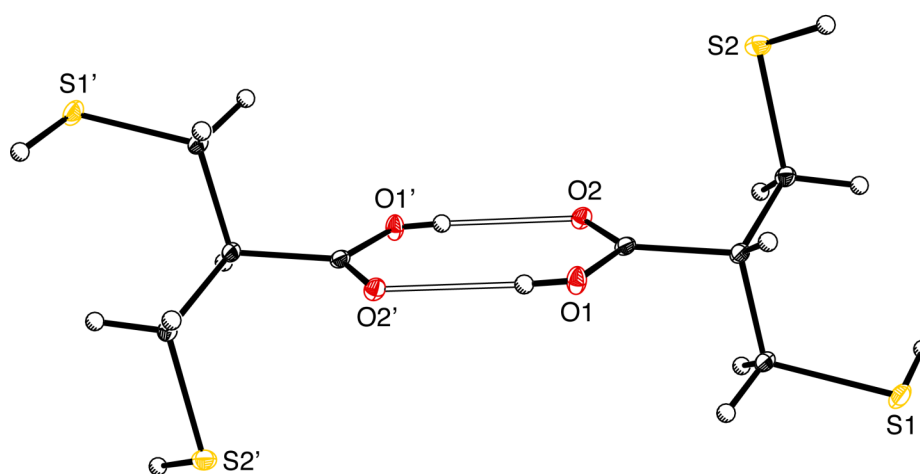
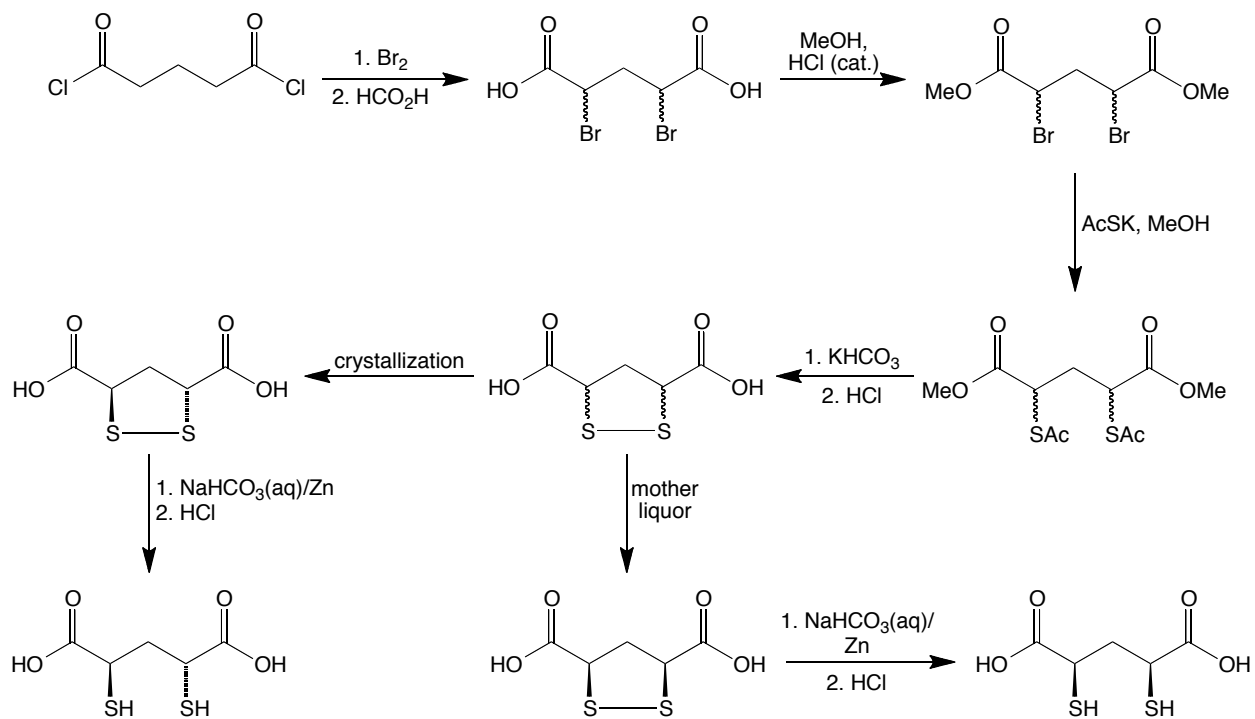


Figure 18. Molecular structure of 2-carboxy-1,3-propanedithiol (hydrogen bonded dimer shown).

Two similar dithiols (diastereomers of each other), each having a geminal carboxyl group with respect to the thiol group, namely (\pm)-2,4-dimercaptoglutaric acid and *meso*-2,4-dimercaptoglutaric acid (Figure 17) were then prepared. These compounds were much more difficult to prepare compared to 2-carboxy-1,3-propanedithiol, and additionally, the synthetic intermediates smell quite putrid! The

syntheses of the glutaric acid derivatives are summarized in Scheme 8. Starting with glutaryl chloride, a Hell-Volhard-Zelinsky halogenation reaction was performed using elemental bromine in order to α -brominate both positions. This was followed by treatment with formic acid to give 2,4-dibromoglutaric acid (both diastereomers) *via* a decarbonylation reaction (this occurs *via* the initial synthesis of the mixed formic anhydride, which decomposes to give the acid derivative and carbon monoxide). Fischer esterification of 2,4-dibromoglutaric acid using MeOH with a catalytic amount of HCl gives dimethyl 2,4-dibromoglutarate, which was subsequently treated with potassium thioacetate to give dimethyl 2,4-bis(acetylthio)glutarate as a dark yellow oil. At this point, the literature procedure cleaved the thioacetate groups by treatment with KOH, followed by oxidative quenching using iodine and ammonia.⁷⁷ This did not work well, giving a low yield of the disulfide compounds, and therefore, a new procedure was adopted as follows: Dimethyl 2,4-bis(acetylthio)glutarate was treated with aqueous potassium bicarbonate (KHCO_3), and refluxed for six hours, followed by an acidic workup *in air*, to give an approximate 1:1 ratio of meso:racemic isomers, together with other impurities. At this point, (\pm)-1,2-dithiolane-3,5-dicarboxylic acid could be isolated *via* low temperature crystallization, while the meso-isomer was enriched in the mother liquor (but never fully purified). Now that each diastereomer was separated to a substantial purity, each disulfide was treated with zinc powder in aqueous sodium bicarbonate (NaHCO_3) followed by acidic work-up to give the corresponding reduced dithiol compounds. Both dithiol compounds are rapidly oxidized to their disulfide derivatives when dissolved in basic water.



Scheme 8. Synthesis of (±)- and *meso*-2,4-dimercaptoglutaric acid.

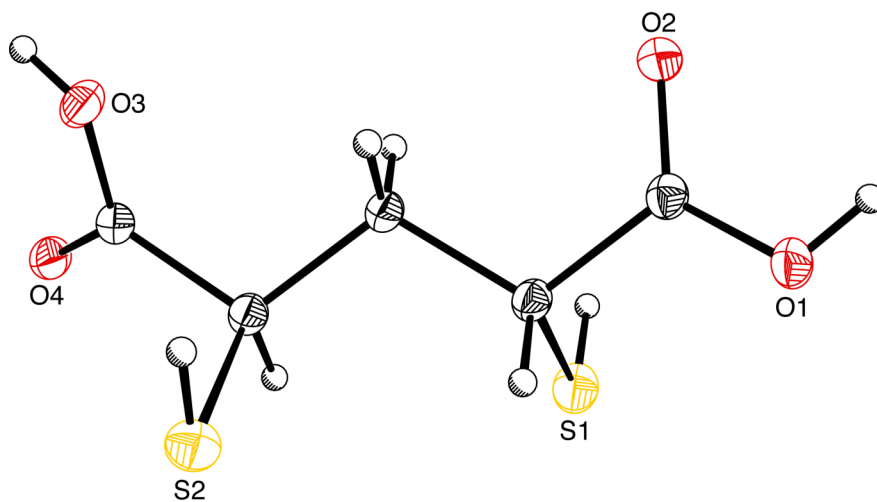


Figure 19. Molecular structure of (±)-2,4-dimercaptoglutaric acid.

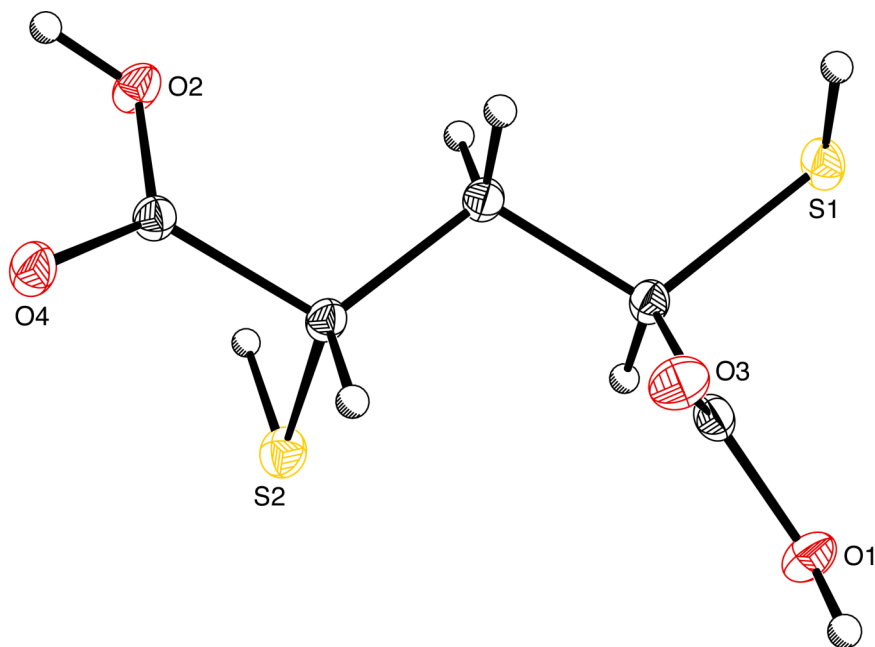


Figure 20. Molecular structure of *meso*-2,4-dimercaptoglutaric acid.

The molecular structures of the (\pm) isomer and the *meso* isomer are shown in Figure 19 and Figure 20, respectively. Due to the fact that both isomers of 2,4-dimercaptoglutaric acid have two carboxylic acid functionalities, the solid-state structures exist as extended hydrogen bonded networks involving the normal “dimeric” carboxylic acid groups. However, there are additional intermolecular interactions involved in the packing network, which include S-H \cdots S hydrogen bonding, S-H \cdots O hydrogen bonding and S \cdots S close contacts (3.494 Å). While there are S-H \cdots O hydrogen bonding interactions in the solid-state structure of 2-carboxy-1,3-propanedithiol, there are no S-H \cdots S hydrogen bonding interactions or S \cdots S close contacts. Furthermore, like 2-carboxy-1,3-propanedithiol, the S—C—C—S torsion angles for the 2,4-dimercaptoglutaric acids are close to 120°. Specifically, the racemic and *meso* derivatives have S—C—C—S torsion angles of 116.20° and 119.69°, respectively (Table 7). Depicted in Figure 21 is an overlay of the (\pm) and *meso* diastereomers of 2,4-dimercaptoglutaric acid. Whereas the (\pm) isomer has the two sulfur

atoms 4.301 Å away from each other due to all of the carbon atoms being part of a straight chain, the S...S distance in the *meso* isomer is 4.935 Å (Table 7).

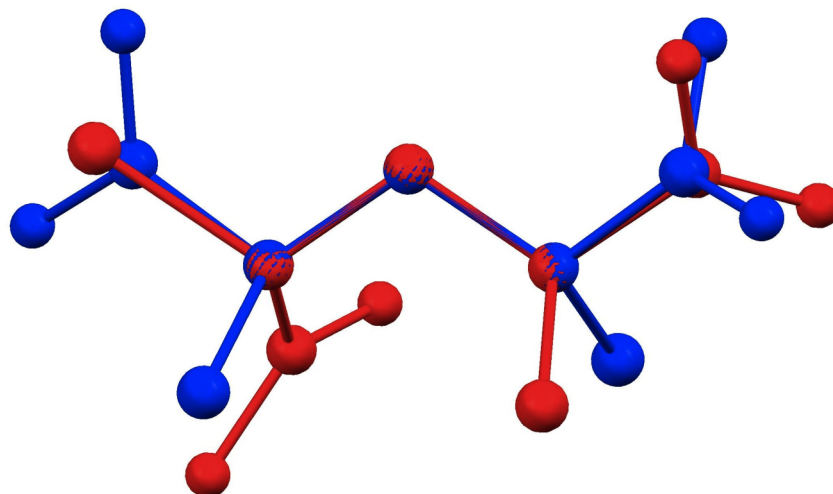


Figure 21. Overlay of (±)-2,4-dimercaptoglutaric acid (blue) and *meso*-2,4-dimercaptoglutaric acid (red).

Table 7. Metrics for selected dithiol compounds.

Compound	S—C—C—S torsion angle	S...S distance
DMSA ⁷²	180.00°	4.437 Å
2-carboxy-1,3-propanedithiol	125.98°	4.969 Å
(±)-2,4-dimercaptoglutaric acid	116.20°	4.301 Å
<i>meso</i> -2,4-dimercaptoglutaric acid	119.59°	4.935 Å

Finally, 2,3-dimercaptobenzoic acid was prepared according to the literature method as follows. Benzene thiol is ortho-lithiated using BuⁿLi and TMEDA (TMEDA = tetramethylethylenediamine). The resulting di-lithium compound is treated with sulfur and then LiAlH₄ to give 1,2-dimercaptobenzene upon acidic workup. 1,2-dimercaptobenzene is ortho-lithiated using BuⁿLi and TMEDA to give the tri-lithium compound, which is then treated with CO₂ to give the benzoic acid derivative, 2,3-

dimercaptobenzoic acid, upon acid workup.⁷⁸ This yellow compound is putrid, even as a solid.

2-carboxy-1,3-propanedithiol, (\pm)-2,4-dimercaptoglutaric acid and *meso*-2,4-dimercaptoglutaric acid were all sent out for animal testing. Rats were treated with these compounds and tested for mercury chelation. While initial testing did show mercury chelation and mobilization, unfortunately, the compounds proved to be too toxic, resulting in animal death, and therefore the testing was discontinued.

5.8 Summary and conclusions

Single crystal X-ray diffraction studies have been performed on thimerosal, its protonated derivative, $(\text{Ar}^{\text{CO}_2\text{H}})\text{SHgEt}$, and its mercurated derivative, $[(\text{Ar}^{\text{CO}_2\text{HgEt}})\text{SHgEt}]_2$. ^1H NMR spectroscopic studies indicate that the appearance of the ^{199}Hg mercury satellites of the ethyl group of these organomercury compounds is highly dependent on the magnetic field and the viscosity of the solvent, an observation that is attributed to relaxation due to chemical shift anisotropy (CSA). Additionally, we have been able to determine the relative signs of the $J_{\text{Hg-H}}$ coupling constants due to the fact that the inner pair of satellites appears as a singlet at 400 MHz. The protonated derivative provides evidence, in line with literature precedent, that the Hg-C bond is quite kinetically stable with respect to protolytic cleavage. Finally, we have synthesized a series of dithiol compounds to be used for mercury chelation. However, these compounds proved to be too toxic for further studies.

5.9 Experimental details

5.9.1 General considerations

All manipulations were performed using a combination of glovebox, high-vacuum and Schlenk techniques under a nitrogen or argon atmosphere, except where otherwise stated. Solvents were purified and degassed by standard procedures. NMR spectra were measured on Bruker 300 DRX, Bruker 400 DRX and Bruker Avance 500 DMX spectrometers. ^1H NMR spectra are reported in ppm relative to SiMe_4 ($\delta = 0$) and were referenced internally with respect to the protio solvent impurity (δ 7.26 for CHCl_3 ⁷⁹ and 5.32 for CDHCl_2 ⁸⁰). ^{13}C NMR spectra are reported in ppm relative to SiMe_4 ($\delta = 0$) and were referenced internally with respect to the solvent ($\delta = 39.52$ for d^6 -DMSO).⁷⁹ ^{199}Hg NMR chemical shifts are reported relative to neat HgMe_2 ($\delta = 0$) but in view of the toxicity of the latter compound, the spectra were referenced externally with respect to HgI_2 (1 M in d^6 -DMSO, $\delta = -3106$).⁸¹ Coupling constants are given in hertz. IR spectra were recorded as KBr pellets on a Nicolet Avatar DTGS spectrometer, and the data are reported in reciprocal centimeters. All reagents were obtained from Aldrich, with the exception of thimerosal and potassium thioacetate, which was obtained from Acros Organics, formic acid and hydrobromic acid, which were obtained from Fluka, and EtHgCl which was obtained from Strem.

5.9.2 X-ray structure determinations

X-ray diffraction data were collected on a Bruker Apex II diffractometer. Crystal data, data collection and refinement parameters are summarized in Table 8. The structures were solved using direct methods and standard difference map techniques, and were refined by full-matrix least-squares procedures on F^2 with SHELXTL (Version 6.1).⁸²

5.9.3 Spectroscopic Data for Thimerosal

^1H NMR (D_2O): 1.26 [t, $^3J_{\text{H-H}} = 8$, $^3J_{\text{H-Hg}} = 249$, 3 H of $\text{NaO}_2\text{CC}_6\text{H}_4\text{SHgCH}_2\text{CH}_3$], 1.65 [q, $^3J_{\text{H-H}} = 8$, $^3J_{\text{H-Hg}} = 173$, 2 H of $\text{NaO}_2\text{CC}_6\text{H}_4\text{SHgCH}_2\text{CH}_3$], 7.13-7.23 [m, 3H of $\text{NaO}_2\text{CC}_6\text{H}_4\text{SHgCH}_2\text{CH}_3$], 7.49 [m, 1 H of $\text{NaO}_2\text{CC}_6\text{H}_4\text{SHgCH}_2\text{CH}_3$].

^1H NMR (CD_3OD): 1.35 [t, $^3J_{\text{H-H}} = 8$, $^3J_{\text{H-Hg}} = 232$, 3 H of $\text{NaO}_2\text{CC}_6\text{H}_4\text{SHgCH}_2\text{CH}_3$], 1.65 [q, $^3J_{\text{H-H}} = 8$, $^3J_{\text{H-Hg}} = 173$, 2 H of $\text{NaO}_2\text{CC}_6\text{H}_4\text{SHgCH}_2\text{CH}_3$], 7.00-7.07 [m, 2 H of $\text{NaO}_2\text{CC}_6\text{H}_4\text{SHgCH}_2\text{CH}_3$], 7.24 [m, 1H of $\text{NaO}_2\text{CC}_6\text{H}_4\text{SHgCH}_2\text{CH}_3$], 7.41 [m, 1 H of $\text{NaO}_2\text{CC}_6\text{H}_4\text{SHgCH}_2\text{CH}_3$].

^1H NMR ($(\text{CD}_3)_2\text{CO}$): 1.29 [t, $^3J_{\text{H-H}} = 8$, $^3J_{\text{H-Hg}} = 230$, 3 H of $\text{NaO}_2\text{CC}_6\text{H}_4\text{SHgCH}_2\text{CH}_3$], 1.47 [q, $^3J_{\text{H-H}} = 8$, $^3J_{\text{H-Hg}} = 173$, 2 H of $\text{NaO}_2\text{CC}_6\text{H}_4\text{SHgCH}_2\text{CH}_3$], 6.91-7.01 [m, 2 H of $\text{NaO}_2\text{CC}_6\text{H}_4\text{SHgCH}_2\text{CH}_3$], 7.37-7.42 [m, 2 H of $\text{NaO}_2\text{CC}_6\text{H}_4\text{SHgCH}_2\text{CH}_3$].

^{13}C NMR (D_2O): 15.9 [q, $^1J_{\text{C-H}} = 126$, $^2J_{\text{Hg-C}} = 74$, 1 C of $\text{NaO}_2\text{CC}_6\text{H}_4\text{SHgCH}_2\text{CH}_3$], 28.3 [t, $^1J_{\text{C-H}} = 136$, $^1J_{\text{Hg-C}} = 1316$, 1 C of $\text{NaO}_2\text{CC}_6\text{H}_4\text{SHgCH}_2\text{CH}_3$], 128.0 [d, $^1J_{\text{C-H}} = 163$, 1 C of $\text{NaO}_2\text{CC}_6\text{H}_4\text{SHgCH}_2\text{CH}_3$], 128.2 [d, $^1J_{\text{C-H}} = 163$, 1 C of $\text{NaO}_2\text{CC}_6\text{H}_4\text{SHgCH}_2\text{CH}_3$], 130.5 [d, $^1J_{\text{C-H}} = 160$, 1 C of $\text{NaO}_2\text{CC}_6\text{H}_4\text{SHgCH}_2\text{CH}_3$], 132.5 [s, 1 C of $\text{NaO}_2\text{CC}_6\text{H}_4\text{SHgCH}_2\text{CH}_3$], 137.6 [d, $^1J_{\text{C-H}} = 162$, 1 C of $\text{NaO}_2\text{CC}_6\text{H}_4\text{SHgCH}_2\text{CH}_3$], 147.0 [s, 1 C of $\text{NaO}_2\text{CC}_6\text{H}_4\text{SHgCH}_2\text{CH}_3$], 181.4 [s, 1 C of $\text{NaO}_2\text{CC}_6\text{H}_4\text{SHgCH}_2\text{CH}_3$].

^{199}Hg NMR (D_2O): -784 [tq, $^2J_{\text{Hg-H}} = 176$, $^3J_{\text{Hg-H}} = 250$].

IR Data (KBr, cm^{-1}): 3042 (w), 2962 (w), 2917 (w), 2862 (w), 1610 (m), 1586 (s), 1569 (vs), 1547 (s), 1464 (w), 1454 (m), 1425 (m), 1410 (m), 1394 (s), 1387 (vs), 1373 (s), 1260 (m), 1246 (w), 1233 (w), 1177 (m), 1098 (br), 1054 (m), 1035 (m), 837 (m), 802 (m), 745 (s), 714 (m), 704 (m), 677 (m), 649 (m).

5.9.4 Synthesis of (Ar^{CO₂H})SHgEt

A solution of thimerosal (200 mg, 0.49 mmol) in water (5 mL) was treated with HCl_{aq} (0.040 mL of 12.2 M, 0.49 mmol), resulting in the immediate formation of a white precipitate, which was extracted into CH₂Cl₂ (7 mL). The dichloromethane extract was washed with water (3 × 3 mL) and the volatile components were then removed *in vacuo* to give (Ar^{CO₂H})SHgEt as a white solid (147 mg, 79 %).

¹H NMR (CDCl₃): 1.35 [t, ³J_{H-H} = 8, ³J_{H-Hg} = 252, 3 H of HO₂CC₆H₄SHgCH₂CH₃], 1.89 [q, ³J_{H-H} = 8, ²J_{H-Hg} = 168, 2 H of HO₂CC₆H₄SHgCH₂CH₃], 7.30 [t, ³J_{H-H} = 8, 1 H of HO₂CC₆H₄SHgCH₂CH₃], 7.39 [t, ³J_{H-H} = 8, 1 H of HO₂CC₆H₄SHgCH₂CH₃], 7.61 [d, ³J_{H-H} = 8, 1 H of HO₂CC₆H₄SHgCH₂CH₃], 8.25 [d, ³J_{H-H} = 8, 1 H of HO₂CC₆H₄SHgCH₂CH₃], 11.79 [s, 1 H of HO₂CC₆H₄SHgCH₂CH₃]. ¹³C NMR (DMSO): 13.7 [q, ¹J_{C-H} = 124, ²J_{Hg-C} = 73, 1 C of HO₂CC₆H₄SHgCH₂CH₃], 25.4 [t, ¹J_{C-H} = 132, ¹J_{Hg-C} = 1362, 1 C of HO₂CC₆H₄SHgCH₂CH₃], 124.4 [d, ¹J_{C-H} = 163, 1 C of HO₂CC₆H₄SHgCH₂CH₃], 128.6 [d, ¹J_{C-H} = 161, 1 C of HO₂CC₆H₄SHgCH₂CH₃], 129.9 [d, ¹J_{C-H} = 160, 1 C of HO₂CC₆H₄SHgCH₂CH₃], 135.4 [d, ¹J_{C-H} = 161, 1 C of HO₂CC₆H₄SHgCH₂CH₃], 136.2 [s, 1 C of HO₂CC₆H₄SHgCH₂CH₃], 137.3 [s, 1 C of HO₂CC₆H₄SHgCH₂CH₃], 170.2 [s, 1 C of HO₂CC₆H₄SHgCH₂CH₃]. ¹⁹⁹Hg{¹H} NMR (DMSO): -788 [tq].

IR Data (KBr, cm⁻¹): 3066 (s), 2963 (s), 2942 (s), 2909 (s), 2856 (s), 2725 (m), 2638 (m), 2544 (m), 1921 (w), 1692 (vs), 1589 (m), 1556 (m), 1468 (s), 1424 (m), 1403 (vs), 1302 (s), 1282 (s), 1251 (vs), 1172 (m), 1138 (m), 1109 (w), 1049 (s), 1032 (m), 946 (w), 902 (m), 809 (m), 787 (w), 732 (vs), 708 (m), 696 (m), 643 (m).

5.9.5 Deprotonation of (Ar^{CO₂H})SHgEt

A suspension of (Ar^{CO₂H})SHgEt (20 mg, 0.052 mmol) in D₂O was treated with NaOH (0.28 mL of 0.225 M NaOH in D₂O, 0.063 mmol), thereby resulting in the formation of a

solution. The sample was monitored by ^1H NMR spectroscopy which demonstrated the formation of $[(\text{Ar}^{\text{CO}_2})\text{SHgEt}]\text{Na}$.

5.9.6 Thermal stability of $(\text{Ar}^{\text{CO}_2\text{H}})\text{SHgEt}$

A solution of $(\text{Ar}^{\text{CO}_2\text{H}})\text{SHgEt}$ (ca. 20 mg) in CD_3OD was heated at 140°C . The sample was monitored by ^1H NMR spectroscopy which demonstrated that $(\text{Ar}^{\text{CO}_2\text{H}})\text{SHgEt}$ is stable with respect to elimination of ethane over a period of 12 hours.

5.9.7 Synthesis of $[(\text{Ar}^{\text{CO}_2\text{HgEt}})\text{SHgEt}]_2$

A mixture of thimerosal (100 mg, 0.247 mmol) and EtHgCl (59 mg, 0.223 mmol) in water (1 mL) and methanol (2 mL) was stirred for 5 minutes. After this period, the mixture was filtered and the precipitate was washed sequentially with water (3×1 mL) and methanol (2×2 mL) and dried *in vacuo* to give $[(\text{Ar}^{\text{CO}_2\text{HgEt}})\text{SHgEt}]_2$ as a white solid (47 mg, 35 %).

^1H NMR (CD_2Cl_2): 1.32 [t, $^3J_{\text{H-H}} = 8$, $^3J_{\text{H-Hg}} = 273$, 6 H of $\text{H}_3\text{CCH}_2\text{HgO}_2\text{CC}_6\text{H}_4\text{SHgCH}_2\text{CH}_3$], 1.83 [q, $^3J_{\text{H-H}} = 8$, $^2J_{\text{H-Hg}} = 193$, 4 H of $\text{H}_3\text{CCH}_2\text{HgO}_2\text{CC}_6\text{H}_4\text{SHgCH}_2\text{CH}_3$], 7.12 [t, $^3J_{\text{H-H}} = 8$, 1 H of $\text{H}_3\text{CCH}_2\text{HgO}_2\text{CC}_6\text{H}_4\text{SHgCH}_2\text{CH}_3$], 7.21 [t, $^3J_{\text{H-H}} = 8$, 1 H of $\text{H}_3\text{CCH}_2\text{HgO}_2\text{CC}_6\text{H}_4\text{SHgCH}_2\text{CH}_3$], 7.54 [m, 2 H of $\text{H}_3\text{CCH}_2\text{HgO}_2\text{CC}_6\text{H}_4\text{SHgCH}_2\text{CH}_3$]. ^{13}C NMR (DMSO): 13.9 [q, $^1J_{\text{C-H}} = 126$, $^2J_{\text{Hg-C}} = 91$, 2 C of $\text{H}_3\text{CCH}_2\text{HgO}_2\text{CC}_6\text{H}_4\text{SHgCH}_2\text{CH}_3$], 20.7 [t, $^1J_{\text{C-H}} = 133$, $^1J_{\text{Hg-C}} = 1570$, 2 C of $\text{H}_3\text{CCH}_2\text{HgO}_2\text{CC}_6\text{H}_4\text{SHgCH}_2\text{CH}_3$], 124.4 [d, $^1J_{\text{C-H}} = 162$, 1 C of $\text{H}_3\text{CCH}_2\text{HgO}_2\text{CC}_6\text{H}_4\text{SHgCH}_2\text{CH}_3$], 127.9 [d, $^1J_{\text{C-H}} = 160$, 1 C of $\text{H}_3\text{CCH}_2\text{HgO}_2\text{CC}_6\text{H}_4\text{SHgCH}_2\text{CH}_3$], 128.6 [d, $^1J_{\text{C-H}} = 158$, 1 C of $\text{H}_3\text{CCH}_2\text{HgO}_2\text{CC}_6\text{H}_4\text{SHgCH}_2\text{CH}_3$], 135.3 [d, $^1J_{\text{C-H}} = 162$, 1 C of $\text{H}_3\text{CCH}_2\text{HgO}_2\text{CC}_6\text{H}_4\text{SHgCH}_2\text{CH}_3$], 135.5 [s, 1 C of $\text{H}_3\text{CCH}_2\text{HgO}_2\text{CC}_6\text{H}_4\text{SHgCH}_2\text{CH}_3$],

141.2 [s, 1 C of $\text{H}_3\text{CCH}_2\text{HgO}_2\text{CC}_6\text{H}_4\text{SHgCH}_2\text{CH}_3$], 173.7 [s, 1 C of $\text{H}_3\text{CCH}_2\text{HgO}_2\text{CC}_6\text{H}_4\text{SHgCH}_2\text{CH}_3$].

IR Data (KBr, cm^{-1}): 3056 (w), 3043 (w), 2973 (m), 2946 (m), 2913 (m), 2858 (m), 1600 (vs), 1577 (s), 1460 (m), 1425 (m), 1338 (vs), 1271 (m), 1254 (m), 1231 (w), 1183 (m), 1142 (m), 1115 (w), 1048 (m), 1033 (w), 960 (w), 949 (w), 857 (m), 792 (w), 752 (vs), 732 (m), 711 (m), 689 (m), 651 (m).

5.9.8 Synthesis of 2-Carboxy-1,3-propanedithiol

2-Carboxy-1,3-propanedithiol was prepared by the literature method,⁷⁶ and the molecular structure was determined by X-ray diffraction.

5.9.9 2,4-Dibromoglutaric acid

2,4-Dibromoglutaric acid was prepared by an adaptation of the literature method.⁸³ Glutaryl chloride (11.2 mL, 87.14 mmol) was heated at 100 °C and treated with bromine (2 mL). The solution was stirred at 100 °C until the deep red color dissipated. This procedure was repeated four more times (10 mL Br_2 total, 195.17 mmol). Caution should be employed to vent the HBr that is eliminated. When the reaction is complete (*ca.* 8 hours), the solution was allowed to cool, and then poured into formic acid (*ca.* 20 mL). Evolution of gas was observed (*CARE!* Carbon monoxide is generated), with the production of crystals of 2,4-dibromoglutaric acid. The mother liquor was decanted, and the crystals were washed with chloroform. The crystals were dried *in vacuo*, giving 2,4-dibromoglutaric acid (20.5 g, 36.2%, racemic:meso, 1.42:1).

(±) isomer ^1H NMR (d_6 -acetone): 2.71 [t, $^3J_{\text{H-H}} = 7$ Hz, 2H, $[\text{HOOC}(\text{CHBr})_2\text{CH}_2]$], 4.57 [t, $^3J_{\text{H-H}} = 7$ Hz, 2H, $[\text{HOOC}(\text{CHBr})_2\text{CH}_2]$].

Meso isomer ^1H NMR (d_6 -acetone): 2.58 [m, 1H, $[\text{HOOC}(\text{CHBr})_2\text{CH}_2]$], 2.92 [m, 1H, $[\text{HOOC}(\text{CHBr})_2\text{CH}_2]$], 4.52 [t, $^3J_{\text{H-H}} = 8$ Hz, 2H, $[\text{HOOC}(\text{CHBr})_2\text{CH}_2]$].

5.9.10 Dimethyl-2,4-dibromoglutarate

HCl (1.0 M in Et_2O , 10.0 mL, 10.0 mmol) was added to a solution of 2,4-dibromoglutaric acid (mixture of diastereomers, 10.3 g, 35.53 mmol) in methanol (*ca.* 70 mL) and the solution was stirred for 2 days at room temperature. After this period, the volatile components were removed *in vacuo* and the residue obtained was diluted with Et_2O and washed with a saturated aqueous solution of NaHCO_3 . The organic layer was dried with MgSO_4 , and the solvent was removed *in vacuo* to give dimethyl 2,4-dibromoglutarate (9.77 g, 86.5%).

(±) isomer ^1H NMR (d_6 -acetone): 2.72 [m, 2H, $[\text{MeOOC}(\text{CHBr})_2\text{CH}_2]$], 3.78 [s, 6H, $[\text{MeOOC}(\text{CHBr})_2\text{CH}_2]$], 4.59 [t, $^3J_{\text{H-H}} = 7$ Hz, 2H, $[\text{MeOOC}(\text{CHBr})_2\text{CH}_2]$].

Meso isomer ^1H NMR (d_6 -acetone): 2.60 [m, 1H, $[\text{MeOOC}(\text{CHBr})_2\text{CH}_2]$], 2.95 [m, 1H, $[\text{MeOOC}(\text{CHBr})_2\text{CH}_2]$], 3.78 [s, 6H, $[\text{MeOOC}(\text{CHBr})_2\text{CH}_2]$], 4.54 [t, $^3J_{\text{H-H}} = 7$ Hz, 2H, $[\text{MeOOC}(\text{CHBr})_2\text{CH}_2]$].

5.9.11 Dimethyl-2,4-bis(acetylthio)glutarate Dimethyl 2,4-bis(acetylthio)glutarate was prepared by an adaptation of the literature method.⁷⁷ A solution of potassium thioacetate (11.85 g, 103.76 mmol) in methanol (*ca.* 50 mL) was added slowly to a solution of dimethyl-2,4-dibromoglutarate in methanol (*ca.* 50 mL) at 0 °C, thereby resulting in a color change from red to yellow, with precipitation of KBr. After the addition was complete, the reaction was allowed to warm to room temperature, and the mixture was stirred overnight. The mixture was filtered and the volatile components were removed from the filtrate *in vacuo*. The residue obtained was extracted into Et_2O and washed with H_2O . The organic layer was isolated and dried with MgSO_4 . The

volatile components were removed *in vacuo* to give impure dimethyl 2,4-bis(acetylthio)glutarate as a dark yellow oil (12.58 g, 85.0%) that was not purified, but used directly for the synthesis of the 1,2-dithiolane-3,5-dicarboxylic acids.

5.9.12 1,2-Dithiolane-3,5-dicarboxylic acids

1,2-dithiolane-3,5-dicarboxylic acids have been previously reported,⁷⁷ but an alternative route was used here. Dimethyl-2,4-bis(acetylthio)glutarate (3.05 g, 9.89 mmol) was added to a solution of KHCO₃ (10.0 g, 99.90 mmol) in H₂O (*ca.* 100 mL). The biphasic mixture was refluxed for 6 hours, over which period the yellow oil reacted and a single yellow aqueous phase was obtained. The solution was allowed to cool to room temperature and then placed in an ice bath. HCl (1M) was added until a pH of 1 was obtained (*caution: stench!*). The solution was extracted with ethyl acetate and the extract was dried with MgSO₄ and concentrated *in vacuo* to give 1,2-dithiolane-3,5-dicarboxylic acids as a *ca.*1:1 ratio of meso:racemic isomers, together with other impurities. The solution was placed at -15 °C, thereby depositing crystals of (±)-1,2-dithiolane-3,5-dicarboxylic acid (270 mg, 14.1%). The mother liquor contained both racemic and meso isomers, and repeated crystallizations gave more (±)-1,2-dithiolane-3,5-dicarboxylic acid, enriching the mother liquor in meso-1,2-Dithiolane-3,5-dicarboxylic acid. Although neither isomer was obtained in 100% purity, the purity was sufficient for the synthesis of the dithiol compounds, which could be purified *via* crystallization.

(±) isomer ¹H NMR (d₆-acetone): 2.74 [t, ³J_{H-H} = 6 Hz, 2H, [HOOC(CHS-)]₂CH₂], 4.55 [t, ³J_{H-H} = 6 Hz, 2H, [HOOC(CH₂S-)]₂CH₂].

Meso isomer ¹H NMR (d₆-acetone): 2.83 [t, ³J_{H-H} = 7 Hz, 2H, [HOOC(CHS-)]₂CH₂], 4.44 [t, ³J_{H-H} = 7 Hz, 2H, [HOOC(CH₂S-)]₂CH₂].

5.9.13 (±) 2,4-Dimercaptoglutaric acid

(±) 2,4-Dimercaptoglutaric acid was prepared by an adaptation of the literature method.⁷⁷ A suspension of (±)-1,2-dithiolane-3,5-dicarboxylic acid (555 mg, 2.86 mmol) in water (*ca.* 10 mL) was treated with NaHCO₃ (264 mg, 3.14 mmol), thereby resulting in evolution of CO₂. Zn powder (1.00 g, 15.3 mmol) was added, and the mixture was stirred for 30 minutes. After this period, HCl(aq) (1.0 M, 32.0 mL, 32.0 mmol) was added and the mixture was filtered into a flask containing HCl(aq) (1.0M, 8.0 mL, 8.0 mmol). The solution was extracted with ethyl acetate and the extract was dried with Na₂SO₄. The solution was evaporated *in vacuo* to give crystals of (±) 2,4-dimercaptoglutaric acid, which was recrystallized from Et₂O (400 mg, 71.3%).

¹H NMR d₆-acetone: 2.28 [t, ³J_{H-H} = 8 Hz, 2H, [HOOC(CHSH)]₂CH₂], 3.60 [t, ³J_{H-H} = 8 Hz, 2H, [HOOC(CH₂SH)]₂CH₂].

5.9.14 Meso- 2,4-Dimercaptoglutaric acid

Meso-2,4-dimercaptoglutaric acid was prepared by an adaptation of the literature method.⁷⁷ A suspension of meso 1,2-dithiolane-3,5-dicarboxylic acid (525 mg, 2.70 mmol, *ca.* 90% meso) in water (*ca.* 10 mL) was treated with NaHCO₃ (250 mg, 2.98 mmol), thereby resulting in evolution of CO₂. Zn powder (900 mg, 13.76 mmol) was added, and the mixture was stirred for 2 hours. After this period, HCl(aq) (1.0 M, 32.0 mL, 32.0 mmol) was added and the mixture was filtered into a flask containing HCl(aq) (1.0M, 8.0 mL, 8.0 mmol). The solution was extracted with Et₂O and the extract was dried with Na₂SO₄. The solution was evaporated *in vacuo* to give crystals that were washed with cold Et₂O to afford meso-2,4-dimercaptoglutaric acid (150 mg, 28.3%), accompanied by small amount of the (±) isomer (*ca.* 5 %).

¹H NMR (D₂O): Meso: 2.17 [m, 1H, [HOOC(CHSH)]₂CH₂], 2.56 [m, 1H, [HOOC(CHSH)]₂CH₂], 3.69 [t, ³J_{H-H} = 7 Hz, 2H, [HOOC(CH₂SH)]₂CH₂].

5.10 Crystallographic data

Table 8. Crystal, intensity collection and refinement data.

	Thimerosal	$[(Ar^{CO_2HgEt})SHgEt]_2$
lattice	Monoclinic	Monoclinic
formula	$C_9H_9O_2SHgNa$	$C_{22}H_{28}Hg_4O_4S_2$
formula weight	404.8	1222.92
space group	$P2_1/c$	$C2/c$
$a/\text{\AA}$	14.653(1)	22.943(3)
$b/\text{\AA}$	25.455(2)	7.7108(9)
$c/\text{\AA}$	17.730(1)	15.0681(16)
$\alpha/^\circ$	90	90
$\beta/^\circ$	103.418(1)	94.551(2)
$\gamma/^\circ$	90	90
$V/\text{\AA}^3$	6432.7(8)	2657.2(5)
Z	24	8
temperature (K)	125(2)	125(2)
radiation (λ , \AA)	0.71073	0.71073
ρ (calcd.), g cm^{-3}	2.508	3.057
μ (Mo $K\alpha$), mm^{-1}	14.559	23.222
θ max, deg.	31.69	32.46
no. of data	21546	4547
no. of parameters	758	145
$R_1 [I > 2\sigma(I)]$	0.0611	0.0509
$wR_2 [I > 2\sigma(I)]$	0.1126	0.0655
GOF	1.037	1.104

Table 8 (cont). Crystal, intensity collection and refinement data.

	(Ar ^{CO₂H})SHgEt	(Ar ^{CO₂H})SHgEt
	#1	#2
lattice	Monoclinic	Monoclinic
formula	C ₉ H ₁₀ HgO ₂ S	C ₉ H ₁₀ HgO ₂ S
formula weight	382.82	382.82
space group	<i>P</i> 2 ₁ / <i>n</i>	<i>P</i> 2/ <i>c</i>
<i>a</i> /Å	9.1662(8)	30.096(3)
<i>b</i> /Å	5.3545(5)	4.0444(4)
<i>c</i> /Å	20.5095(17)	33.472(4)
α /°	90	90
β /°	93.666(1)	91.153(1)
γ /°	90	90
<i>V</i> /Å ³	1004.6(2)	4073.4(7)
<i>Z</i>	4	16
temperature (K)	125(2)	125(2)
radiation (λ , Å)	0.71073	0.71073
ρ (calcd.), g cm ⁻³	2.531	2.497
μ (Mo K α), mm ⁻¹	15.492	15.282
θ max, deg.	32.37	31.29
no. of data	3436	13211
no. of parameters	118	469
R_1 [$I > 2\sigma(I)$]	0.0291	0.0354
wR_2 [$I > 2\sigma(I)$]	0.0835	0.0598
GOF	1.038	1.020

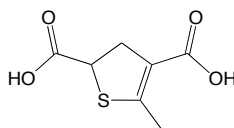
Table 8 (cont). Crystal, intensity collection and refinement data.

	(±) 2,4-Dimercaptoglutaric acid (Low Temp.)	(±) 2,4-Dimercaptoglutaric acid (Room Temp.)
lattice	Monoclinic	Monoclinic
formula	C ₅ H ₈ O ₄ S ₂	C ₅ H ₈ O ₄ S ₂
formula weight	196.23	196.23
space group	<i>P2₁/n</i>	<i>P2₁/n</i>
<i>a</i> /Å	6.8561(8)	7.009(4)
<i>b</i> /Å	12.4153(15)	12.378(7)
<i>c</i> /Å	10.0971(12)	10.248(6)
α /°	90	90
β /°	106.796(2)	107.496(9)
γ /°	90	90
<i>V</i> /Å ³	822.81(17)	847.9(9)
<i>Z</i>	4	4
temperature (K)	125(2)	296(2)
radiation (λ , Å)	0.71073	0.71073
ρ (calcd.), g cm ⁻³	1.584	1.537
μ (Mo K α), mm ⁻¹	0.611	0.593
θ max, deg.	32.43	30.42
no. of data	2867	2555
no. of parameters	110	110
R_1 [$I > 2\sigma(I)$]	0.0482	0.0545
wR_2 [$I > 2\sigma(I)$]	0.1343	0.1570
GOF	1.058	1.056

Table 8 (cont). Crystal, intensity collection and refinement data.

	2-Carboxy-1,3- propanedithiol	Meso-2,4- dimercaptoglutaric acid
lattice	Monoclinic	Monoclinic
formula	C ₄ H ₈ O ₂ S ₂	C ₅ H ₈ O ₄ S ₂
formula weight	152.22	196.23
space group	<i>P</i> 2 ₁ / <i>n</i>	<i>P</i> -1
<i>a</i> /Å	9.719(5)	6.8623(5)
<i>b</i> /Å	6.930(3)	7.8506(5)
<i>c</i> /Å	10.475(5)	8.5151(10)
α /°	90	97.5080(10)
β /°	110.663(7)	91.8010(10)
γ /°	90	114.5930(10)
<i>V</i> /Å ³	660.1(6)	411.67(6)
<i>Z</i>	4	2
temperature (K)	125(2)	125(2)
radiation (λ , Å)	0.71073	0.71073
ρ (calcd.), g cm ⁻³	1.532	1.583
μ (Mo K α), mm ⁻¹	0.715	0.610
θ max, deg.	32.25	32.66
no. of data	2258	2807
no. of parameters	85	110
R_1 [$I > 2\sigma(I)$]	0.0457	0.0400
wR_2 [$I > 2\sigma(I)$]	0.1085	0.1031
GOF	1.023	1.038

Table 8 (cont). Crystal, intensity collection and refinement data.



lattice	Monoclinic
formula	$C_7H_8O_4S$
formula weight	188.19
space group	$C2/C$
$a/\text{\AA}$	27.79(4)
$b/\text{\AA}$	7.514(10)
$c/\text{\AA}$	7.684(10)
$\alpha/^\circ$	90
$\beta/^\circ$	96.32(2)
$\gamma/^\circ$	90
$V/\text{\AA}^3$	1595(4)
Z	8
temperature (K)	125(2)
radiation (λ , \AA)	0.71073
ρ (calcd.), g cm^{-3}	1.568
μ (Mo $K\alpha$), mm^{-1}	0.375
θ max, deg.	30.39
no. of data	2389
no. of parameters	112
$R_1[I > 2\sigma(I)]$	0.0603
$wR_2[I > 2\sigma(I)]$	0.1356
GOF	1.018

5.11 References and notes

- (1) Clarkson, T. W.; Magos, L. *Crit. Rev. Toxicol.* **2006**, *36*, 609–662.
- (2) Melnick, J. G.; Parkin, G. *Science* **2007**, *317*, 225-227.
- (3) Fitzgerald, W. F.; Lamborg, C. H.; Hammerschmidt, C. R. *Chem. Rev.* **2007**, *107*, 641-662.
- (4) Barkay, T.; Miller, S. M.; Summers, A. O. *FEMS Microbiol. Rev.* **2003**, *27*, 355.
- (5) Compeau, G. C.; Bartha, R. *Appl. Environ. Microbiol.* **1985**, *50*, 498-502.
- (6) Wood, J. M.; Kennedy, F. S.; Rosen, C. G. *Nature* **1968**, *220*, 173-174.
- (7) (a) Clifton, C. C. *Pediatr. Clin. N. Am.* **2007**, *54*, 237-269.

(b) Baeyens, W.; Leermakers, M.; Papina, T.; Saprykin, A.; Brion, N.; Noyen, J.; De Gieter M.; Elskens, M.; Goeyens, L. *Arch. Environ. Contam. Toxicol.* **2003**, *45*, 498-508.

(c) Mergler, D.; Anderson, H. A.; Chan, L. H.; Mahaffey, K. R.; Murray, M.; Sakamoto, M.; Stern, A. H. *Ambio* **2007**, *36*, 3–11.

(d) Scheuhammer, A. M.; Meyer, M. W.; Sandheinrich, M. B.; Murray, M. W. *Ambio* **2007**, *36*, 12–18.
- (8) Cross, R. J.; Jenkins, M. *Environ. Pollut.* **1975**, *8*, 179-184.
- (9) Cundari, T.; Yoshikawa, A. *J. Comp. Chem.* **1998**, *19*, 902-911.
- (10) Moore, M. J.; Distefano, M. D.; Zydowsky, L. D.; Cummings, R. T.; Walsh, C. T. *Acc. Chem. Res.* **1990**, *23*, 301-308.

- (11) There are four cysteine residues in MerB. Cys-117 is not located near the active site. See: Lafrance-Vanasse, J.; Lefebvre, M.; Di Lello, P.; Sygusch, J.; Omichinski, J. G. *J. Biol. Chem.* **2009**, *284*, 938-944.
- (12) When Cys-160 is replaced with serine (Ser), there is only a moderate reduction of catalytic activity. See: Pitts, K. E.; and Summers, A. O. *Biochemistry* **2002**, *41*, 10287–10296.
- (13) Li, X.; Liao, R.-Z.; Zhou, W.; Chen, G. *Phys. Chem. Chem. Phys.*, **2010**, *12*, 3961–3971.
- (14) Geier, D. A.; Sykes, L. K.; Geier, M. R. *J. Toxicol. Environ. Health – Part B* **2007**, *10*, 575-596.
- (15) In addition to the trade name Methiolate, there are many other synonyms for thimerosal, some of which include: thiomersal, elicide, estivin, mercurothiolate, merfamin, merphol, merseptyl, mertorgan, merzonin, and nosemack.
- (16) Powell, H. M.; Jamieson, W. A. *Am. J. Hygiene* **1931**, *13*, 296-310.
- (17) Ohno, H.; Doi, R.; Kashima, Y.; Murae, S.; Kizaki, T.; Hitomi, Y.; Nakano, N.; Harada, M. *Bull. Environ. Contam. Toxicol.* **2004**, *73*, 777-780.
- (18) Gil, S.; Lavilla, I.; Bendicho, C. *J. Anal. At. Spectrom.* **2007**, *22*, 569–572.
- (19) Fagundes, A.; Marzochi, M. C. A.; Perez, M.; Schubach, A.; Ferreira, A.; Silva, J. P.; Schubach, T.; Marzochi, K. B. F. *Acta Tropica* **2007**, *101*, 25-30.
- (20) Meyer, B. K.; Ni, A.; Hu, B; Shi, L. *J. Pharm. Sci.* **2007**, *96*, 3155-3167.
- (21) (a) Clarkson, T. W.; Magos, L. *Crit. Rev. Toxicol.* **2006**, *36*, 609-662.
- (b) Mutter, J.; Naumann, J.; Guethlin, C. *Crit. Rev. Toxicol.* **2007**, *37*, 537-549.

- (c) Clarkson, T. W. *Env. Health Persp. Suppl.* **2002**, 110, 11-23.
- (d) Clarkson, T. W. *Crit. Rev. Clin. Lab. Sci.* **1997**, 34, 369-403.
- (e) Langford, N. J.; Ferner, R. E. *J. Human Hypertension* **1999**, 13, 651-656.
- (f) Boening, D. W. *Chemosphere* **2000**, 40, 1335-1351.
- (g) Magos, L. *Metal Ions in Biological Systems* **1997**, 34, 321-370.
- (h) Hutchison, A. R.; Atwood, D. A. *J. Chem. Crystallogr.* **2003**, 33, 631-645.
- (i) Alessio, L.; Campagna, M.; Lucchini, R. *Am. J. Ind. Med.* **2007**, 50, 779-787.
- (j) Clarkson, T. W.; Vyas, J. B.; Ballatorl, N. *Am. J. Ind. Med.* **2007**, 50, 757-764.
- (k) Risher, J. F.; De Rosa, C. T. *J. Env. Health* **2007**, 70, 9-16.
- (l) Clifton, J. C. *Ped. Clin. North America* **2007**, 54, 237-269.
- (22) (a) Clements, C. J.; McIntyre, P. B. *Expert Opin. Drug Safety* **2006**, 5, 17-29.
- (b) Blaxill, M. F.; Redwood, L.; Bernard, S. *Med. Hypoth.* **2004**, 62, 788-794.
- (c) Bernard S.; Enayati, A.; Redwood, L.; Roger, H.; Binstock, T. *Med. Hypoth.* **2001**, 56, 462-471.
- (d) Stratton, K.; Gable, A.; McCormick, M. C. eds. *Thimerosal-Containing Vaccines and Neurodevelopmental Disorders*. National Academy Press, Washington, DC, **2001**.
- (e) Geier, D. A.; Geier, M. R. *J. Toxicol. Env. Health Part A* **2007**, 70, 837-851.

- (23) (a) de Stefano, F. *Clin. Pharmacol. Therapeutics* **2007**, *82*, 756-759.
- (b) Offit, P. A. *New Eng. J. Med.* **2007**, *357*, 1278-1279.
- (c) Thompson, W. W.; Price, C.; Goodson, B.; Shay, D. K.; Benson, P.; Hinrichsen, V. L.; Lewis, E.; Eriksen, E.; Ray, P.; Marcy, S. M.; Dunn, J.; Jackson, L. A.; Lieu, T. A.; Black, S.; Stewart, G.; Weintraub, E. S.; Davis, R. L.; DeStefano, F. *New Eng. J. Med.* **2007**, *357*, 1281-1292.
- (24) (a) Bernard, S. *New Eng. J. Med.* **2008**, *358*, 93.
- (b) Rooney, J. P. K. *New Eng. J. Med.* **2008**, *358*, 93-94.
- (c) Thompson, W. W.; Price, C. DeStafano, F. *New Eng. J. Med.* **2008**, *358*, 94.
- (25) Baker, J. P. *Am. J. Public Health* **2008**, *98*, 2-11.
- (26) DeStefano, F. *Clin. Pharmacol. Ther.* **2007**, *82*, 756-759.
- (27) Gotelli, C. A.; Astolfi, E.; Cox, C.; Cernichiari, E.; Clarkson, T. W. *Science*, **1985**, *227*, 638-640.
- (28) (a) Rustam, H.; Hamdi, T. *Brain* **1974**, *97*, 499-510.
- (b) Bakir, F.; Damluji, S. F., Amin-Zaki, L., Murtadha, M.; Khaudi, A.; Al-Rawi, N. Y., Tikrit, S.; Dhahir, H. I.; Clarkson, T. W.; Smith, J. C.; Dohert, R. A. *Science* **1973**, *181*, 230-241.
- (29) For two brief reports pertaining to the chemistry of thimerosal, see:
- (a) Trikojus, V. M. *Nature* **1946**, *158*, 472-473.
- (b) Tan, M.; Parkin, J. E. *Int. J. Pharm.* **2000**, *208*, 23-34.

- (30) Kharasch, M. S. U. S. Patent #1,672,615 (1928).
- (31) For a later synthesis, see: Swirska, A.; Kotler-Brajtburg, J.; Dahlig, W.; Pasynkiewicz, S. *Przemysl Chemiczny* **1960**, *39*, 371-372.
- (32) The name "thimerosal" for sodium ethylmercury thiosalicylate appeared in the literature much later. For an early use of the name "thimerosal", see: Hughes, E. J. *Drug Standards* **1952**, *20*, 121-124.
- (33) (a) Casa, J. S.; García-Tasende, M. S.; Sordo, J. *Coord. Chem. Rev.* **1999**, *193-195*, 283-359.
- (b) Holloway, C. E.; Melník, M. *J. Organomet. Chem.* **1995**, *495*, 1-31.
- (c) Rabenstein, D. L. *Acc. Chem. Res.* **1978**, *11*, 100-107.
- (34) Wright, J. G.; Natan, M. J.; MacDonnell, F. M.; Ralston, D. M.; O'Halloran, T. V. *Prog. Inorg. Chem.* **1990**, *38*, 323-412.
- (35) The propensity of mercury to adopt linear coordination is often attributed to relativistic effects which stabilize the 6s orbital, thereby resulting in a large 6s-6p energy gap which limits the use of the 6p orbitals, and a small 5d-6s energy gap that favors linear sd_{z^2} hybridization. Other factors have also, nevertheless, been considered. See, for example:
- (a) Pyykkö, P.; Desclaux, J.-P. *Acc. Chem. Res.* **1979**, *12*, 276-281.
- (b) Pyykkö, P. *Chem. Rev.* **1988**, *88*, 563-594.
- (c) Kaupp, M.; von Schnering, H. G. *Inorg. Chem.* **1994**, *33*, 2555-2564.
- (d) Tossell, J. A.; Vaughan, D. J. *Inorg. Chem.* **1981**, *20*, 3333-3340.

- (36) As observed for many linear mercury complexes, in addition to the primary interactions, the mercury centers exhibit longer range secondary interactions to the thiolate sulfur atoms of adjacent molecules.
- (37) Wright, J. G.; Natan, M. J.; MacDonnell, F. M.; Ralston, D. M.; O'Halloran, T. V. *Prog. Inorg. Chem.* **1990**, *38*, 323-412.
- (38) (a) Almagro, X.; Clegg, W.; Cucurull-Sánchez, L.; González-Duarte, P.; Traveria, M. *J. Organomet. Chem.* **2001**, *623*, 137-148.
- (b) Carlton, L.; White, D. *Polyhedron* **1990**, *9*, 2717-2720.
- (39) Petrosya, V. S.; Reutov, O. A. *J. Organomet. Chem.* **1974**, *76*, 123-169.
- (40) http://riodb01.ibase.aist.go.jp/sdbs/cgi-bin/cre_index.cgi?lang=eng
- (41) For references that contain the spectrum of Et₂Hg and indicate that the CH₃ group is downfield of the CH₂ group, see:
- (a) Dessy, R. E.; Flautt, T. J.; Jaffé, H. H.; Reynolds, G. F. *J. Chem. Phys.* **1959**, *30*, 1422-1425.
- (b) Narasimhan, P. T.; Rogers, M. T. *J. Am. Chem. Soc.* **1960**, *82*, 34-40.
- (42) Evans, D. F.; Maher, J. P. *J. Chem. Soc.* **1962**, 5125-5128.
- (43) Hatton, J. V.; Schneider, W.G.; Siebrand, W. J. *Chem. Phys.* **1963**, *39*, 1330-1336.
- (44) (a) Farrar, T. C.; Becker, E. D. *Pulse and FT NMR*, Academic Press, New York, 1971.
- (b) Farrar, T. C. *Introduction to Pulse NMR Spectroscopy*, The Farragut Press Chicago, Madison, 1989.

- (c) Thouvenot, R. *L'Actualite Chimique* **1996**, 7, 102-111.
- (d) Kowalewski, J.; Mäler, L. *Nuclear Spin Relaxation in Liquids: Theory, Experiments, and Applications*, Taylor and Francis, New York, 2006.
- (45) (a) Benn, R.; Günther, H.; Maercker, A.; Menger, V.; Schmitt, P. *Angew. Chem. Int. Ed. Engl.* **1982**, 21, 295-296.
- (b) Gillies, D. G.; Blaauw, L. P.; Hays, G. R.; Huis, R.; Clague, A. D. H. *J. Magn. Reson.* **1981**, 42, 420-428.
- (c) Cecconi, F.; Ghilardi, C. A.; Innocenti, P.; Midollini, S.; Orlandini, A.; Ienco, A.; Vacca, A. *J. Chem. Soc., Dalton Trans.* **1996**, 2821-2826.
- (46) (a) Randall, L. H.; Carty, A. J. *Inorg. Chem.* **1989**, 28, 1194-1196.
- (b) Penner, G. H. *Can. J. Chem.* **1991**, 69, 1054-1056.
- (47) Wong, T. C.; Ang, T. T.; Guziec, F. S., Jr.; Moustakis, C. A. *J. Magn. Reson.* **1984**, 57, 463-470.
- (48) Baltzer, L.; Becker, E. D.; Averill, B. A.; Hutchinson, J. M.; Gansow, O. A. *J. Am. Chem. Soc.* **1984**, 106, 2444-2446.
- (49) (a) Socol, S. M.; Meek, D. W. *Inorg. Chim. Acta* **1985**, 101, L45-L46.
- (b) Cocivera, M.; Ferguson, G.; Lenkinski, R. E.; Szczecinski, P.; Lalor, F. J.; O'Sullivan, D. J. *J. Magn. Reson.* **1982**, 46, 168-171.
- (50) (a) Lallemand, J.-Y.; Soulié, J.; Chottard, J.-C. *J. Chem. Soc., Chem. Commun.* **1980**, 436-438.
- (b) Anklin, C. G.; Pregosin, P. S. *Magn. Reson. Chem.* **1985**, 23, 671-675.

- (c) Benn, R.; Büch, H. M.; Reinhardt, R.-D. *Magn. Reson. Chem.* **1985**, *23*, 559-564.
- (d) Dechter, J. J.; Kowaleski, J. J. *Magn. Reson.* **1984**, *59*, 146-149.
- (e) Pregosin, P. S. *Coord. Chem. Rev.* **1982**, *44*, 247-291.
- (e) Ismail, I. M.; Kerrison, S. J. S.; Sadler, P. J. *Polyhedron* **1982**, *1*, 57-59.
- (f) Skvortsov, A. N. *Russ. J. Gen. Chem.* **2000**, *70*, 1023-1027.
- (g) Hughes, R. P.; Sweetser, J. T.; Tawa, M. D.; Williamson, A.; Incarvito, C. D.; Rhatigan, B.; Rheingold, A. L.; Rossi, G. *Organometallics* **2001**, *20*, 3800-3810.
- (h) Reinartz, S.; Baik, M.-H.; White, P. S.; Brookhart, M.; Templeton, J. L. *Inorg. Chem.* **2001**, *40*, 4726-4732.
- (i) Reinartz, S.; White, P. S.; Brookhart, M.; Templeton, J. L. *Organometallics* **2000**, *19*, 3854-3866.
- (51) (a) Hawk, R. M.; Sharp, P. R. *J. Chem. Phys.* **1974**, *60*, 1522-1527.
- (b) Hays, G. R.; Gillies, D. G.; Blaauw, L. P.; Clague, A. D. H. *J. Magn. Reson.* **1981**, *45*, 102-107.
- (52) (a) Brady, F.; Matthews, R. W.; Forster, M. J.; Gillies, D. G. *Inorg. Nucl. Chem. Lett.* **1981**, *17*, 155-159.
- (b) Hinton, J. F.; Ladner, K. H. *J. Magn. Reson.* **1978**, *32*, 303-306.
- (c) Brady, F.; Matthews, R. W.; Forster, M. J.; Gillies, D. G. *J. Chem. Soc., Chem. Commun.* **1981**, 911-912.

- (d) Ghosh, P.; Desrosiers, P. J.; Parkin, G. J. *Am. Chem. Soc.* **1998**, *120*, 10416-10422.
- (53) Benn, R.; Rufinska, A. *Angew. Chem. Int. Ed. Engl.* **1986**, *25*, 861-881.
- (54) Viscosity of water = 0.890 cP; viscosity of methanol = 0.544 cP; viscosity of acetone = 0.306. See: Lide, D. R. ed., *CRC Handbook of Chemistry and Physics, 88th Edition (Internet Version 2008)*, CRC Press/Taylor and Francis, Boca Raton, FL, pp 6-175 – 6-179.
- (55) (Ar^{CO₂H})SHgEt has been previously described without any detailed characterization. See:
- (a) Waldo, J. H. *J. Am. Chem. Soc.* **1931**, *53*, 992-996.
- (b) Kharasch, M. S. US Patent #1,672,615 (1928).
- (56) Elferink, J. G. *Gen. Pharmacol.* **1999**, *33*, 1–6.
- (57) Narasimhan, P. T.; Rogers, M. T. *J. Chem. Phys.* **1959**, *31*, 1430.
- (58) For other examples of second-order satellite subspectra for [XCH₂CH₃] compounds, see reference 57 and:
- (a) Narasimhan, P. T.; Rogers, M. T. *J. Chem. Phys.* **1951**, *34*, 1049-1055.
- (b) Kettle, S. F. A. *J. Chem. Soc.* **1965**, 6664-6665.
- (c) Hamer, G.; Shaver, A. *Can. J. Chem.* **1980**, *58*, 2011-2015.
- (d) Scherr, P. A.; Oliver, J. P. *J. Am. Chem. Soc.* **1972**, *94*, 8026-8031.

- (59) Reinartz, S.; White, P. S.; Brookhart, M.; Templeton, J. L. *Organometallics* **2000**, *19*, 3748-3750.
- (60) For a vinyl compound in which the three hydrogen atoms appear as a singlet, see: Al-Najaar, I. M.; Green, M. *Trans. Met. Chem.* **1978**, *3*, 142-144.
- (61) Brookhart, M. personal communication.
- (62) Glueck, D. S. *Coord. Chem. Rev.* **2008**, *252*, 2171-2179.
- (63) For a related example, see: Kalberer, E. W.; Roddick, D. M. *Organometallics* **2004**, *23*, 4209-4214.
- (64) Anet, F. A. L.; Sudmeier, J. L. *J. Magn. Reson.* **1969**, *1*, 124-138.
- (65) Sperline, R. P.; Beaulieu, W. B.; Roundhill, D. M. *Inorg. Chem.* **1978**, *17*, 2032-2035.
- (66) The coupling constants for EtHgCl are comparable to the values of $^2J_{\text{HH}} = -222$ Hz and $^3J_{\text{HH}} = +300$ Hz measured using a 60 MHz spectrometer. See reference 64.
- (67) See, for example: Cundari, T. R.; Yoshikawa, A. *J. Comp. Chem.* **1998**, *19*, 902-911.
- (68) A zinc derivative of thimerosal has been described, although no spectroscopic or structural data were reported. See: Birner, J.; Garnet, J. R. *J. Pharm. Sci.* **1964**, *53*, 1266-1267.
- (69) Trikojus, V. M. *Nature* **1946**, *158*, 472-473.
- (70) (a) Casa, J. S.; García-Tasende, M. S.; Sordo, J. *Coord. Chem. Rev.* **1999**, *193-195*, 283-359.
- (b) Holloway, C. E.; Melník, M. *J. Organomet. Chem.* **1995**, *495*, 1-31.

- (71) (a) Rooney, J. *Toxicology* **2007**, 234,145–156.
- (b) Frumkin, H.; Manning, C. C.; Williams, P. L.; Sanders, A.; Taylor, B. B.; Pierce, M.; Elon, L.; Hertzberg, V. S. *Environ. Health Perspect.* **2001**, 109, 167–71.
- (72) The molecular structure of DMSA has been determined as the DMF adduct. See:
Pyrka, G. J.; Scott, N.; Fernando, Q. *Acta Cryst.* **1992**, C48, 2007-2009.
- (73) Gregus, Z.; Stein, A. F.; Varga, F.; Klaassen, C. D. *Toxicology and Applied Pharmacology* **1992**, 114, 88–96.
- (74) Van der Linde A.A.; Pillen S.; Gerrits G. P.; Bouwes Bavinck, J. N. *Clin. Toxicol.* **2008**, 46, 479–81.
- (75) Peters, R; Stocken, L; Thompson, R. *Nature* **1945**, 156, 616–619.
- (76) Singh, R.; Whitesides, G.M. *J. Am. Chem. Soc.* **1990**, 112, 1190-1197.
- (77) Hedblom, M., Swedish. *J. Agric. Res.* **1971**, 1, 43-49.
- (78) Seidel, W.; Hahn, F. E.; Lügger, T. *Inorg. Chem.* **1998**, 37, 6587-6596.
- (79) Gottlieb, H. E.; Kotlyar, V.; Nudelman, A. *J. Org. Chem.* **1997**, 62, 7512-7515.
- (80) Cambridge Isotope Laboratories, Inc., NMR Solvent Data Chart (www.isotope.com/cil/products/images/nmrchart.pdf).
- (81) Kidd, R. G.; Goodfellow, R. J. in *NMR and the Periodic Table* Harris, R. K.; Mann, B. E. (Eds.), Academic Press, New York, 1978, p 268.
- (82) (a) Sheldrick, G. M. SHELXTL, An Integrated System for Solving, Refining and Displaying Crystal Structures from Diffraction Data; University of Göttingen, Göttingen, Federal Republic of Germany, 1981.

- (b) Sheldrick, G. M. *Acta Cryst.* **2008**, *A64*, 112-122.
- (83) Ingold, C. K. *J. Chem. Soc., Trans.* **1921**, *119*, 305-329.

Wesley Sattler

Curriculum Vitae

604 west 115th Street, Apartment 6A, New York, NY 10025

wis2102@columbia.edu

914.438.4328

Education

- **Columbia University, Graduate School of Arts and Sciences (2007 – 2012)**
M.A. in Chemistry (2009)
M.Phil. in Chemistry (2011)
Ph.D. in Chemistry (2012)
Area of Concentration: Inorganic/ Organometallic Chemistry
- **State University of New York – Binghamton University (2003 – 2007)**
B.S. with Honors in Chemistry, *Summa Cum Laude* (2007)
Distinguished Independent Work - Honors Thesis (2007)
Areas of Concentration: Inorganic Chemistry, Physical Chemistry. Major GPA: 4.0/4.0

Awards and Honors

- **Louis Hammett Award to Outstanding Ph.D. Student (2012)**
Columbia University
- **Reaxys PhD Prize Finalist (2012)**
Columbia University
- **Presidential Teaching Award Finalist (2011)**
Columbia University
- **Presidential Teaching Award Finalist (2010)**
Columbia University
- **The Jack Miller Award for Excellence in Teaching (2009)**
Columbia University
- **Presidential Teaching Award Finalist (2009)**
Columbia University
- **National Science Foundation (NSF) Graduate Research Fellowship Honorable Mention (2009)**
Columbia University
- **Binghamton Section of the American Chemical Society Outstanding Graduating Senior Award (2007)**
Binghamton University
- **Graduated Summa Cum Laude (2007)**
Binghamton University
- **Graduated with Honors (2007)**
Binghamton University – Distinguished Independent Work in Chemistry
- **Phi Beta Kappa National Honor Society (2006)**
Binghamton University
- **Phi Eta Sigma National Honor Society (2004)**
Binghamton University
- **Dean's List (7 Semesters out of possible 7) (2003 – 2006)**
Binghamton University
- **State of New York Attorney General Triple "C" Award (2003)**
Ardsley High School
- **AP Scholar (2003)**
Ardsley High School

Research Experience

- **Graduate Research (Prof. Gerard Parkin) (2008 – Present)**
 1. Investigation of the structure and reactivity of sodium ethylmercury thiosalicylate (thimerosal).

2. Design and synthesis of dithiol compounds for applications in mercury chelation therapy.
 3. Development of a new method for the conversion of transition metal-carbonyl compounds into their isocyanide derivatives without the use of the free isocyanide ligand.
 4. Study of small molecule reactivity with zinc compounds for applications to biological modeling and catalysis.
 5. Synthesis and study of organozinc compounds as catalysts for the production of dihydrogen, and the functionalization of carbon dioxide.
- **Undergraduate Research (Prof. Wayne E. Jones Jr.) (2005 – 2007)**
 1. Synthesis of conjugated fluorescent polymers serving as chemosensors for toxic metal cations.
 2. Investigated the optoelectronic properties of heterobimetallic layered structures.
 - **Summer Research at Memorial Sloan Kettering (Dr. Raju Chaganti) (2005)**
Research concerning the VHL gene and kidney cancer, DNA sequencing, gel electrophoresis, and PCR (polymerase chain reaction) to determine mutations influencing the effectiveness of chemotherapies.

Teaching Experience

- **Teaching Assistant** – Structural Methods in Inorganic Chemistry with Prof. Gerard Parkin (**Spring 2011**)
Columbia University
- **Teaching Assistant** – General Chemistry I with Prof. Gerard Parkin (**Fall 2009**)
Columbia University
- **Teaching Assistant** – General Chemistry I with Prof. Gerard Parkin (**Fall 2008**)
Columbia University
- **Teaching Assistant** – General Chemistry II with Dr. Stacey Brydges (**Spring 2008**)
Columbia University
- **Teaching Assistant** – General Chemistry I with Prof. Gerard Parkin (**Fall 2007**)
Columbia University
- **Teaching Assistant** – Intro. to Physical Chemistry with Prof. James Dix (**Fall 2006**)
Binghamton University

Publications

1. "Molecular Structures of Thimerosal (Merthiolate) and Other Arylthiolate Mercury Alkyl Compounds." Jonathan G. Melnick, Kevin Yurkerwich, Daniela Buccella, **Wesley Sattler** and Gerard Parkin *Inorg. Chem.* **2008**, *47*, 6421-6426.
2. "Molecular Structures of Protonated and Mercurated Derivatives of Thimerosal." **Wesley Sattler**, Kevin Yurkerwich and Gerard Parkin *Dalton Trans.* **2009**, 4327-4333.
3. "2-Mercapto-1-t-butylimidazolyl as a Bridging Ligand: Synthesis and Structural Characterization of Nickel and Palladium Paddlewheel Complexes." Keliang Pang, Joshua S. Figueroa, Ian A. Tonks, **Wesley Sattler** and Gerard Parkin *Inorg. Chim. Acta*, **2009**, *362*, 4609-4615.
4. "Synthesis of Transition Metal Isocyanide Compounds from Carbonyl Complexes *via* Reaction with Li[Me₃SiNR]." **Wesley Sattler** and Gerard Parkin *Chem. Commun.* **2009**, 7566-7568.
5. "Synthesis of Polynitroxides Based on Nucleophilic Aromatic Substitution." Olaf Zeika, Yongjun Li, Steffen Jockusch, Gerard Parkin, Aaron Sattler, **Wesley Sattler** and Nicholas J. Turro *Org. Lett.* **2010**, *12*, 3696 – 3699.
6. "Reticulated Heterojunctions for Photovoltaic Devices." Alon A. Gorodetsky, Chien-Yang Chiu, Theanne Schiros, Matteo Palma, Marshall Cox, Zhang Jia, **Wesley Sattler**, Ioannis Kymissis, Michael Steigerwald and Colin Nuckolls *Angew. Chem. Int. Ed. Engl.* **2010**, *49*, 7909-7912.
7. "Synthesis and structural characterization of tris(2-oxo-1-*tert*-butylimidazolyl) and tris(2-oxo-1-methylbenzimidazolyl)hydroborato complexes: a new class of tripodal oxygen donor ligand." Ahmed Al-Harbi, **Wesley Sattler**, Aaron Sattler and Gerard Parkin *Chem. Commun.* **2011**, *47*, 3123 – 3125.
8. "Shape-shifting in contorted dibenzotetrathienocoronenes." Chien-Yang Chiu, Bumjung

- Kim, Alon A. Gorodetsky, **Wesley Sattler**, Sujun Wei, Aaron Sattler, Michael Steigerwald and Colin Nuckolls *Chem. Sci.* **2011**, *2*, 1480-1486.
9. "Synthesis, Structure, and Reactivity of a Mononuclear Organozinc Hydride Complex: Facile Insertion of CO₂ into a Zn-H Bond and CO₂-Promoted Displacement of Siloxide Ligands." **Wesley Sattler** and Gerard Parkin *J. Am. Chem. Soc.* **2011**, *133*, 9708-9711.
 10. "A General Strategy for the Stereocontrolled Preparation of Diverse 8- and 9-Membered *Laurencia*-Type Bromoethers." Scott A. Snyder, Daniel S. Treitler, Alexandria P. Brucks and **Wesley Sattler** *J. Am. Chem. Soc.* **2011**, *133*, 15898-15901.
 11. "Low Temperature NMR Spectroscopic Investigation of a Zinc Bicarbonate Compound: Thermodynamics of Bicarbonate Formation by Insertion of CO₂ into the Zinc Hydroxide Bond of [Tp^{Bu^t,Me}]₂ZnOH." **Wesley Sattler** and Gerard Parkin *Polyhedron*, **2012**, *32*, 41-48.
 12. "Structural characterization of zinc bicarbonate compounds relevant to the mechanism of action of carbonic anhydrase." **Wesley Sattler** and Gerard Parkin *Chem. Sci.* **2012**, *3*, 2015-2019.
 13. "Synthesis, Electrochemistry and Reactivity of New Iridium(III) and Rhodium(III) Hydrides." Yue Hue, Ling Li, Anthony P. Shaw, Jack R. Norton, **Wesley Sattler** and Yi Rong *Organometallics*, **2012**, *31*, 5058-5064.
 14. "Mechanisms by which Alkynes React with CpCr(CO)₃H. Application to Radical Cyclization." Deven P. Estes, Jack R. Norton, Steffen Jockusch and **Wesley Sattler** *J. Am. Chem. Soc.* **2012**, *134*, DOI: 10.1021/ja306120n.
 15. "Zinc Catalysts for On Demand Hydrogen Generation and Carbon Dioxide Functionalization." **Wesley Sattler** and Gerard Parkin *Submitted*.

Presentations

- Aaron Sattler, **Wesley Sattler** and Wayne R. Jones Jr. "Conjugated Fluorescent Polymer Chemosensors Based on the Dipyridilquinoxaline Receptor Unit" *Undergraduate Poster Session, Binghamton, NY. 10/6/2006* ACS-NERM 2006 Conference. **(POSTER)**
- **Wesley Sattler** and Daniel Griffith. Thursday Night Organic Problem Solving Session. Columbia University Department of Chemistry. **4/21/2011**.
- **Wesley Sattler** and Gerard Parkin "Synthesis, Structure, and Reactivity of Mononuclear Organozinc Compounds." Gordon Research Conference, Organometallic Chemistry. Salve Regina University, Newport, RI, USA. **7/10/2011. (POSTER)**
- **Wesley Sattler** "Applications of Tridentate and Tetradentate Nitrogen Donor Ligands to Zinc Chemistry: Transformations Relevant to Carbonic Anhydrase." Chemical Synthesis Student Symposium. Columbia University, Department of Chemistry, New York, NY, USA. **10/7/2011**.
- **Wesley Sattler** "Multifunctional Zinc Catalysts." Awards Ceremony, Hammett Award Talk. Columbia University, Department of Chemistry, New York, NY, USA. **4/24/2012**.
- **Wesley Sattler** "Multifunctional Zinc Catalysts and Transformations Relevant to Carbonic Anhydrase." Thesis Defense in Chemistry. Columbia University, Department of Chemistry, New York, NY, USA. **7/24/2012**.

Leadership and Mentoring

- Research Mentor for Undergraduate Student: *Julia Oktawaiec* **(2011-2012)**
- Volunteer for the Women in Science at Columbia, Girls' Science Day **(2011)**
- Volunteer for the Columbia Secondary School Chemistry Day **(2011)**
- Volunteer for the Women in Science at Columbia, Girls' Science Day **(2010)**
- Volunteer for the Columbia Secondary School Chemistry Day **(2010)**
- Volunteer for the Women in Science at Columbia, Girls' Science Day **(2009)**
- Volunteer for the Columbia Secondary School Chemistry Day **(2009)**
- Research Mentor for Undergraduate Student: *Ariel Schapp* **(Spring 2009)**

- Volunteer for the Columbia Secondary School Chemistry Day (2008)
- Volunteer for the Columbia Secondary School Bridge-to-School Day (2008)
- Volunteer for the Women in Science at Columbia, Girls' Science Day (2008)
- Volunteer for the Johns Hopkins University Center for Talented Youth Academic Program "Pathways to College" program (2008)
- Research Mentor for High School Student: *Ned Lieb* (Summer 2008)

Technical Skills

- Single Crystal X-Ray Diffraction
- Homonuclear and Heteronuclear Nuclear Magnetic Resonance (NMR) Spectroscopy
- UV-Visible Spectroscopy (UV-Vis)
- Infrared Spectroscopy (IR)
- DFT Calculations (Jaguar 7.5)

Other Contributions

Papers in which I have been acknowledged for performing single crystal X-ray analysis

1. Wang, Z.; Min, S.-J.; Danishefsky, S. J. *J. Am. Chem. Soc.* **2009**, *131*, 10848 – 10849.
2. Snyder, S. A.; Treitler, D. S. *Angew. Chem. Int. Ed.* **2009**, *48*, 7899 – 7903.
3. Vadola, P. A.; Sames, D. J. *Am. Chem. Soc.* **2009**, *131*, 16525–16528.
4. Zhang, Y.; Danishefsky, S. J. *J. Am. Chem. Soc.* **2010**, *132*, 9567 – 9569.
5. Li, X.; Danishefsky, S. J. *J. Am. Chem. Soc.* **2010**, *132*, 11004 – 11005.
6. Snyder, S. A.; Treitler, D. S.; Brucks, A. P. *J. Am. Chem. Soc.* **2010**, *132*, 14303 – 14314.
7. Lee, J. H.; Zhang, Y.; Danishefsky, S. J. *J. Am. Chem. Soc.* **2010**, *132*, 14330 – 14333.
8. Snyder, S. A.; Sherwood, T. C.; Ross, A. G. *Angew. Chem. Int. Ed.* **2010**, *49*, 5146 – 5150.
9. Loo, Y.-L.; Hiszpanski, A. M.; Kim, B.; Wei, S.; Chiu, C.-Y.; Steigerwald, M. L.; Nuckolls, C. *Org. Lett.* **2010**, *12*, 4840-4843.
10. Yurkerwich, K.; Parkin, G. J. *Cluster Science* **2010**, *21*, 225 – 234.
11. Peng, F.; Danishefsky, S. J. *Tetrahedron Lett.* **2011**, *52*, 2104 – 2106.
12. Zhang, Y.; Lee, J. H.; Danishefsky, S. J. *J. Am. Chem. Soc.* **2011**, *133*, 752 – 755.
13. Snyder, S. A.; Wespe, D. A.; von Hof, J. M. *J. Am. Chem. Soc.* **2011**, *133*, 8850-8853.
14. Baxter Vu, J. M.; Leighton, J. L. *Org. Lett.* **2011**, *13*, 4056-4059.
15. Snyder, S. A.; Wright, N. E.; Pflueger, J. J.; Breazzano, S. P. *Angew. Chem. Int. Ed.* **2011**, *50*, 8629-8633.
16. Snyder, S. A.; Brill, Z. G. *Org. Lett.* **2011**, *13*, 5524 – 5527.
17. Snyder, S. A.; Thomas, S. B.; Mayer, A. C.; Breazzano, S. P. *Angew. Chem. Int. Ed.* **2012**, *51*, 4080-4084.
18. Clalifoux, W. A.; Reznik, S. K.; Leighton, J. L. *Nature*, **2012**, *487*, 86-89.
19. Peng, F.; Dai, M.; Angeles, A. R.; Danishefsky, S. J. *Chem. Sci.* **2012**, *3*, DOI: 10.1039/c2sc20868g.